SYNTHESIS AND ANTIOXIDANT PROPERTIES OF SOME NEW DI-*TERT*-BUTYLPHENOL DERIVATIVES BEARING HETEROCYCLIC RING

RAIED MUSTAFA SHAKIR

THESIS SUBMITTED IN FULFILLMENT OF THE REQUIREMENTS FOR THE DEGREE OF DOCTOR OF PHILOSOPHY

DEPARTMENT OF CHEMISTRY
FACULTY OF SCIENCE
UNIVERSITY OF MALAYA
KUALA LUMPUR

2014

UNIVERSITI MALAYA

ORIGINAL LITERARY WORK DECLARATION

Name of Candidate: **RAIED MUSTAFA SHAKIR** **I**/C/Passport No: **G1686698**

Regisration/Matric No.: **SHC080076**

Name of Degree: **DOCTOR OF PHILOSOPHY**

Title of Project Paper/Research Report/Dissertation/Thesis ("this Work"):

"SYNTHESIS AND ANTIOXIDANT PROPERTIES OF SOME NEW DI-TERT-BUTYLPHENOL DERIVATIVES BEARING HETEROCYCLIC RING"

Field of Study: **ORGANIC CHEMISTRY**

I do solemnly and sincerely declare that:

(1) I am the sole author/writer of this Work,
(2) This Work is original,
(3) Any use of any work in which copyright exists was done by way of fair dealing and for permitted purposes and any excerpt or extract from, or reference to or reproduction of any copyright work has been disclosed expressly and sufficiently and the title of the Work and its authorship have been acknowledged in this Work,
(4) I do not have any actual knowledge nor do I ought reasonably to know that the making of this work constitutes an infringement of any copyright work,
(5) I hereby assign all and every rights in the copyright to this Work to the University of Malaya ("UM"), who henceforth shall be owner of the copyright in this Work and that any reproduction or use in any form or by any means whatsoever is prohibited without the written consent of UM having been first had and obtained,
(6) I am fully aware that if in the course of making this Work I have infringed any copyright whether intentionally or otherwise, I may be subject to legal action or any other action as may be determined by UM.

(Candidate Signature) Date:

Subscribed and solemnly declared before,

Witness's Signature Date:

Name: **ASSOC. PROF. DR AZHAR ARIFFIN**

Designation

Abstract

The hindered phenolic compounds are known as one of the important antioxidants. Eleven new derivatives of aryl 1,3,4-oxadiazoles containing 2,6-di-*tert*-butylphenol were synthesized to increase the antioxidant ability. These oxadiazoles (coded as **2.12-2.22**) were synthesized through the condensation of different aryl hydrazides with 3,5-di-*tert*-butyl-4-hydroxybenzoic acid in the presence of $POCl_3$ as a dehydrating agent. The DPPH and FRAP assays showed that the antioxidant ability of these compounds depends on the type of substituents and their position in the phenyl ring. The sequence of substituents in order of their antioxidant activity are found to be 4-OH > 2-Me > 2,4-di-Me > 4-Me > OMe ≈ OEt >4-Cl > 2-Cl >4-Br ≈ 3,4-di-Cl ≈ 3,5-di-Cl. The second series consists of seven bis-oxadiazole-bis-2,6-di-*tert*-butylphenol (coded as **2.31-2.37**) and were synthesized through the condensation of seven different dihydrazides with 3,5-di-*tert*-butyl-4-hydroxybenzoic acid using $POCl_3$ as the dehydrating agent. Compounds **2.33** and **2.35** showed significant antioxidant ability while the other five compounds recorded low activity.

Increasing the steric hindrance and the resonance of the compunds would lead to increase the antioxidant ability. As the effect of steric hindrance of 2,4-di-*tert*-butylphenol group is less than 2,6-di-*tert*-butylphenol, in order to have hight antioxidant ability, compounds containing 1,3,4-oxadiazole ring (coded as **3.5-3.8**) at position six of 2,4-di-*tert*-butylphenol were synthesized. The formation of oxadiazoles occurred through the synthesis of hydrazones of 2,4-di-*tert*-butyl derivatives (coded as **3.1-3.4**). The cyclization of these hydrazones to oxadiazoles were achieved by using bromine in glacial acetic acid as the oxidising reagent. The antioxidant activity of the hydrazones and oxadiazoles were quite similar. Two bis-hydrazones (coded as **3.9-3.10**) were also synthesized and then cyclized to form bis-oxadiazoles. The bis-oxadiazoles gave low antioxidant activity for both DPPH and FRAP. A new series of 1,3,4-oxadiazole-5-

thione (coded as **3.15**) and their alkyl derivatives (coded as **3.16-3.18**) were synthesized at the sixth position of 2,4-di-*tert*-butylphenol. The 1,3,4-oxadiazole-5-thione (**3.15**) showed 91.53% DPPH inhibition and this value was slightly higher than that of ascorbic acid (90.65%). The compound (**3.15**) also exhibited FRAP value higher than gallic acid. However, the alkylated derivatives of compound (**3.15**) showed lower DPPH and FRAP values. Of these alkylated derivatives, the compound alkylated by 4-bromobenzyl bromide (**3.18**) exhibited the highest value.

The 5-amino-oxadiazole ring (coded as **3.19**) were synthesized from the reaction between 3,5-di-*tert*-butyl-2-hydroxybenzohydrazide and cyanogen bromide. Whereas the 5-amino-1,3,4-thiadiazole ring compounds (coded as **3.21**) was synthesized by two methods: the first was from the cyclization of the corresponding thiosemihydrazones (coded **3.20**) and the second from cyclization of 3,5-di-*tert*-butyl-2-hydroxybenzoic acid with thiosemicarbazide. Both compounds **3.19** and **3.21** gave slightly similar antioxidant activity in DPPH and FRAP. Generally, the DPPH values were lower than that of FRAP when compared to the reference compounds. The last series of compounds synthesized were those containing 1,2,4-triazole ring, namely 4-amino-1,2,4-triazole-5-thione (**3.22**) and 4-substituted-phenyl-1,2,4-triazole-5-thione (**3.26-3.28**). The antioxidant activity of these compounds was higher than BHT. The intermediate compounds (**3.26-3.28**) gave good antioxidant activity quite similar to that of ascorbic acid.

Abstrak

Sebatian fenol terlindung telah dikenalpasti sebagai salah satu antioksida yang penting. Sebelas terbitan baru bagi aril 1,3,4-oxadiazola yang mengandungi 2,6-di-*tert*-butil fenol telah disintesis untuk meningkatkan keupayaan sebagai antioksida. Sebatian oxadiazola ini (dikod sebagai **2.12-2.22**) disintesiskan melalui kondensasi beberapa aril hidrazida yang berlainan dengan asid 3,5-di-*tert*-butil-4-hidroksibenzoik dalam kehadiran $POCl_3$ sebagai agen pendehidratan. Ujian DPPH dan FRAP menunjukkan keupayaan antioksida sebatian-sebatian ini bergantung kepada jenis kumpulan penukarganti dan kedudukan mereka pada gelang fenil. Turutan kumpulan penukarganti dari segi tertib keaktifan antioksida mereka adalah seperti berikut 4-OH > 2-Me > 2,4-di-Me > 4-Me > OMe ≈ OEt >4-Cl > 2-Cl >4-Br ≈ 3,4-di-Cl ≈ 3,5-di-Cl. Siri yang kedua terdiri dari tujuh sebatian bis-oxadiazola-bis-2,6-di-tert-butilfenol (dikod sebagai **2.31-2.37**) dan telah disintesiskan melalui kondensasi tujuh dihidrazida yang berlainan dengan asid 3,5-di-*tert*-butil-4-hidroksibenzoik menggunakan $POCl_3$ sebagai agen pendehidratan. Sebatian **2.33** dan **2.35** menunjukkan keupayaan sebagai antioksida yang tinggi, manakala lima lagi terbitan yang lain menunjukkan keupayaan antioksida yang rendah.

Dengan meningkatkan halangan sterik dan pentaksetempatan elektron sesuatu sebatian akan meningkatkan keupayaan antioksida. Oleh kerana kesan halangan sterik 2,4-di-*tert*-butilfenol adalah kurang berbanding 2,6-di-*tert*-butilfenol, jadi untuk mendapatkan antioksida yang tinggi sebatian yang mengandungi gelang 1,3,4-oxadiazola (dikod sebagai **3.5-3.8**) pada kedudukan enam bagi 2,4-di-*tert*-butilfenol telah disintesiskan. Pembentukan oxadiazola ini berlaku melalui sintesis hidrazon bagi terbitan 2,4-di-*tert*-butil (dikod sebagai **3.1-3.4**). Pensiklikan hidrazon ini kepada oxadiazola terhasil dengan menggunakan bromin dalam asid asetik glasial sebagai reagen pengoksida. Keupayaan antioksida bagi hidrazon dan oxadiazola adalah hampir

sama. Dua sebatian bis-hidrazon (dikod sebagai **3.9-3.10**) juga telah disintesiskan dan seterusnya dijalankan tindak balas pensiklikan untuk membentuk bis-oxadiazola. Sebatian bis-oxadiazola ini menunjukkan keaktifan antioksida yang rendah pada kedua-dua ujian DPPH dan FRAP. Satu siri baru sebatian 1,3,4-oxadiazola-5-thion dan terbitan alkilnya (dikod sebagai **3.15-3.18**) telah disintesiskan pada kedudukan keenam bagi 2,4-di-*tert*-butilfenol. Sebatian 1,3,4-oxadiazola-5-tiona (**3.15)** menunjukkan perencatan DPPH sebanyak 91.53% dan nilai ini adalah lebih tinggi sedikit dari asid askorbik (90.65%). Sebatian (**3.15**) juga mempamerkan nilai FRAP yang lebih tinggi daripada asid galik. Bagaimanapun, terbitan alkil bagi sebatian (**3.15**) menunjukkan nilai DPPH dan FRAP yang lebih rendah. Antara terbitan alkil ini, hanya sebatian yang dialkilkan oleh 4-bromobenzil bromide mempamerkan nilai tertinggi.

Gelang 5-amino-thiadiazola (dikod sebagai **3.21**) telah disintesis daripada tindak balas antara 3,5-di-*tert*-butil-2-hidroksibenzohidrazida dan sianogen bromide. Manakala, sebatian gelang 5-amino-1,3,4-thiadiazole ring (coded as **3.21**) telah disintesis melalui dua kaedah: pertama daripada pensiklikan tiosemihidrazon yang sepadan (dikod sebagai **3.20**) dan yang kedua daripada pensiklikan asid 3,5-di-*tert*-butil-2-hidroksibenzoik dengan tiosemikarbazida. Kedua-dua sebatian, **3.19** dan **3.21** memberi keaktifan antioksida yang hampir setara pada DPPH dan FRAP. Secara umumnya nilai DPPH adalah lebih rendah dari nilai FRAP jika dibandingkan dengan sebatian rujukan. Siri terakhir yang disintesis merupakan sebatian yang mengandungi gelang 1,2,4-triazola iaitu 4-amino-1,2,4-triazola-5-thion (**3.22**) dan 4-tertukarganti-fenil-1,2,4-triazola-5-thion (**3.26-3.28**). Keupayaan antioksida bagi sebatian-sebatian ini adalah lebih tinggi dari BHT. Sebatian perantara (**3.26-3.28)** menunjukkan keupayaan antioksida yang baik yang hampir setara dengan nilai keupayaan antioksida bagi asid askorbik.

.

.

Dedication

To memory of my father Mustafa Shakir Al-Sayab

AKNOWLEDGEMENT

It was impossible to write this thesis without the great help and support of the kind people around me, to only some of whom it is possible to give particular mention here. For those people, who are their names may not appear here, their efforts and help will still be in my mind forever.

With a deep sense of gratitude and respect, I would like to thank my Supervisor Associate Professor Dr. Azhar Ariffin for his guidance, support and encouragement to my work until the end of this research. Special thanks will go to Professor Dr. Amir Auto for all advice, helpful discussions and his successful opinion as well as my grateful to Professor Rosiyah Yahya for her support and encouragement.

I would like to extend my thanks and gratitude to prof. Dr. Kee Chin Hui for the valuable assistance provided for the completion this thesis. Also, I wish to express my appreciation to NMR staff, Miss Norzalida Zakaria, Dara Fiona, Suwing eh Vit, Mr. Fateh Ngaliman and Nordin Mohamad. I would like to acknowledge the financial, academic and technical support of the University of Malaya, especially for the UMRG PS345/2009B. Special thanks to university of Baghdad for giving me the opportunity to do this research and for the financial support.

Furthermore, I would like to thank prof. Dr. Mahmood Amin for doing the antioxidant tests. Also great thanks to Prof. Dr Ng Seik Weng for x-ray analysis. I sincerely thank all my friends for all support they have provided to me during this research, especially Mr. Nassir N. Al-Mohammed, Wisam Naji Al-Mehana, Dr. Wageeh A. Yehye and Dr. Karem J. Sabah. Also, I will remember forever my group members and

my PhD colleagues in the Department of Chemistry, University of Malaya for the real brotherhood and friendship that they had shown to me throughout the period of PhD study.

Love and respect without limits to my mother, my beloved wife Huda, my sweetheart children: Rula, Mustafa, Sadeer,Yousif, Saif and my sisters whose have given me their unequivocal support throughout, as always, for which my mere expression of thanks likewise does not suffice.

Table of contents

List of Figures

List of Schemes

List of Tables

List of Abbreviations

BDE	Bond Dissociation Energy
BHA	**B**utylated hydroxyanisole
BHT	Butylated hydroxyltoluene
BS	Broad Singlet
Calc.	Calculate
d	Doublet
Dec.	Decomposition
DEPT	Distortionless Enhancement by Polarization Transfer
DMF	Dimethylformamide
DPPH	2,2-diphenyl-1-picrylhydrazyl radical
DTBP	di -*tert*-butylphenol
Et	Ethyl
EIMS	Electron ionization mass spectroscopy
EWG	Electron-withdrawing groups
EDG	Electron-donating groups
FCR	Folin-Ciocalteu reagent
FRAP	Ferric ion reducing antioxidant power
HAT	Hydrogen atom transfer
h	Hour
HREIMS	High resolution electron ionization mass spectroscopy
HMBC	Heteronuclear Multiple Bond Correlation
HMQC	Heteronuclear Multiple-Quantum Correlation
HSQC	Heteronuclear Single Quantum Coherence
IC_{50}	Half maximal inhibitory concentration
IP	Ionization potentials
J	Coupling constant
LDBS	locally dense basis sets
m	Multiplet
Me	Methyl
MF	Molecular Formula
Mmol	Millimole
M.p.	Melting point

NMR	Nuclear magnetic resonance
^{o}C	Celsius Degree
OMe	Methoxy group
ORAC	Oxygen radical absorbance capacity
ORTEP	Oak Ridge Thermal Ellipsoid Plot
PG	Propyl Gallate
$POCl_3$	Phosphorus oxychloride
Q	Quartet
RNS	Reactive nitrogen species
R.T	Room Temperature
s	Singlet
SD	Standard deviation
SEM	Standard Error of the mean
SET	Single electron transfer
SOMO	Semi-occupied orbital
t	Triplet
TBHQ	*Tert*-butylhydroquinone
t-Bu	*Tert*-butyl
tert	Tertiary
TEAC	Trolox equivalence antioxidant capacity
TRAP	Total radical trapping antioxidant parameter
µmg	Microgram

Chapter 1 : Introduction and Literature Review

1.1 Introduction

It has been known for more than 60 years that the reactive oxygen species (ROS) and oxidative stress play an important role in the etiology and progression of major human degenerative diseases. This triggered enormous and worldwide interesting endogenous and exogenous antioxidant. The last few decades saw a widening of interest in antioxidants. There is now abundant evidence that the antioxidant substances in fruit and vegetable are preventives of various diseases such as cancer, heart diseases, diabetes and cataracts. Furthermore, a large number of drugs for anti inflammatory, digestive, anti necrotic, neuroprotective, and hepatoprotective have antioxidant ability, and their radical scavenger properties was the part of their activity.[1] In addition to that, the antioxidants are widely used in food and pharmaceutical industries and, it can prevent industrial material from oxidation and damage as a result of exposure to light, heat, and oxygen. For that an antioxidant can be classified as important material due to their many benefits. The hindered phenolic compounds are one of the most important antioxidant. A large number of di-*tert*-butylphenol containing heterocyclic ring shown significant biological activity such as cyclo-oxygenase (COX) inhibitor, 5-lipoxygenase (5-LOX) inhibitor, anti-inflammatory, antitumor and anti-rheumatic. Many di-*tert*-butylphenol derivatives were also used in industrial field as stabilizers in food, oil, pigments, rubber, and plastic.

1.2 Free Radicals and Antioxidant

A free radical is a molecule or atom that has an unpaired electron and symbolized by a radical dot (•). They are highly reactive and unstable when compared to similar ions. It is evidently that the free radicals participate in many biological processes.[2] In

living systems, including humans, the effects of free radicals are considered very normal. The existence of enzyme superoxide dismutase (SOD), for instance, clearly hinted on the existence of the superoxide radical, ($^{-\bullet}O_2$, $^{\bullet}O$, $^{\bullet}OOH$ and $^{\bullet}OH$).[3] Furthermore, the reactive oxygen species (ROS) can be generated during aerobicrespiration.[4] Other species like hydrogen peroxide radical, hypochlorite radical, nitric radical, and different lipid peroxide are considered to be one of the most important radical species in biological functions.[5] The ROS and related species as free radicals are capable to react either directly or indirectly, to damage all biomolecules, including proteins, lipids, DNA, and carbohydrates resulting cell damage.[6] This damage causes many diseases. A large numbers of researches reported the implication of these free radicals in causing several diseases such as inflammatory disease,[7] cancers disease,[8] degenerative disease [9] and chronic diseases.[10] Figure 1.1 summarized the clinical effect of ROS.

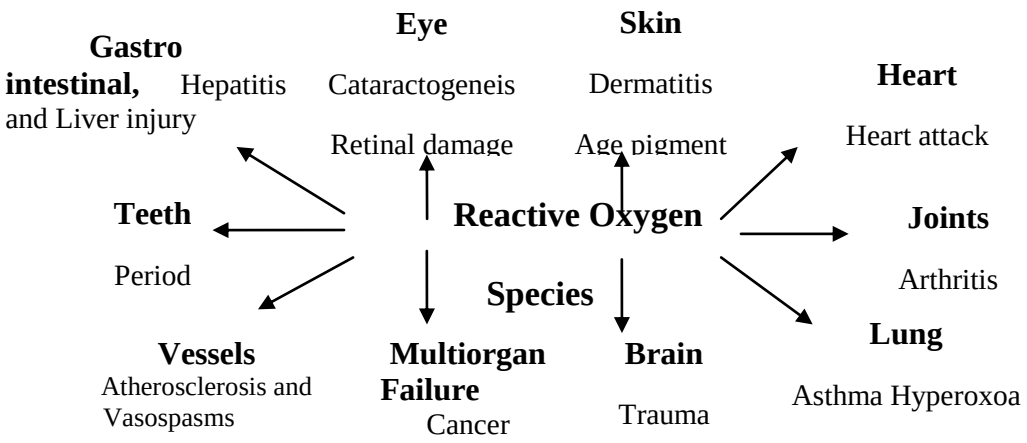

Figure 1.1 : Diseases caused by ROS. [11]

The antioxidant (free radical scavenging), which can be defined as any material or substance when present in low concentration can delay or prevent the oxidation and inhibit the free radical effect.[12] This capability makes the antioxidant an important material especially in medical field. The mechanism of antioxidant can be divided into two pathways, where the antioxidant play a preventive role.[13] The first pathway is

through H-atom transfer (HAT) as in peroxidation of lipid as demonstrated in Scheme 1.1.

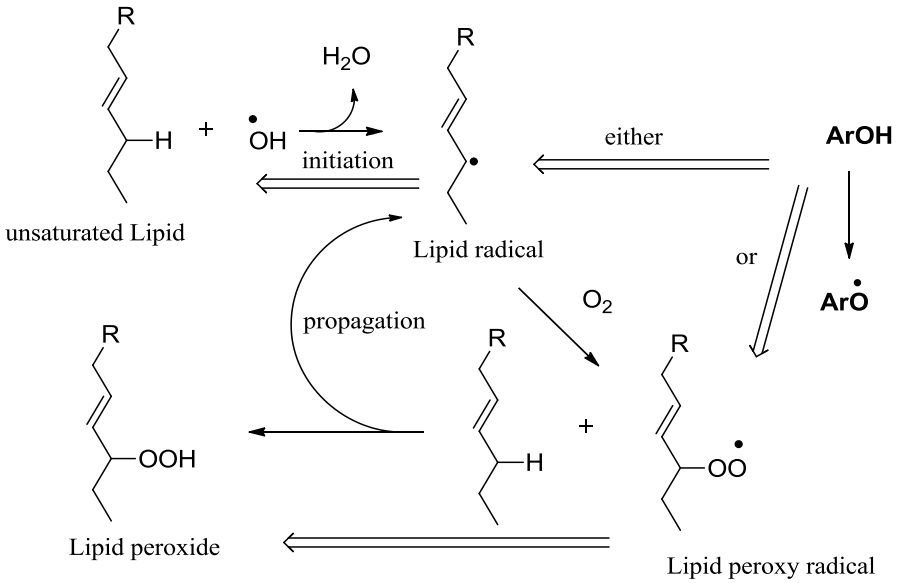

Scheme 1.1: Lipid peroxidation pathway.[14]

The first reaction is the initiation; the reactive hydroxyl radical or any other free radical reacts with the lipids to form a lipid radical and initiate the chain reaction in the propagation step. The free radical reacts with oxygen to form the lipid peroxyl radical. The propagation step is very fast, the rate constant $K_p = 10^{-9}$ $M^{-1}S^{-1}$. Reaction of lipid peroxyl radical with lipid is slow $K_p = 10^{1}$ $M^{-1}S^{-1}$.[13, 15] The function of antioxidant ArOH is to interrupt the initiation reaction or break off the chain reaction and to terminate the lipid peroxyl radical. The antioxidant after donating a proton will be converted to free radical ($ArO^{\bullet}$).The resulting free radical should be stable.[15] In the second pathway, the antioxidant can deactivate the free radical through single electron transfer (SET).[15]

In SET, the radical is formed rapidly and then reversible by de-protonation in solution as demonstrated in Scheme 1.2

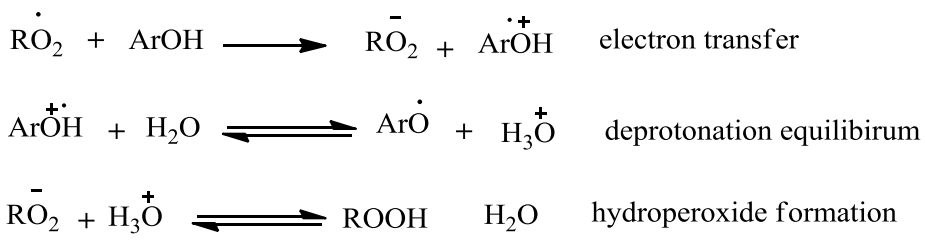

Scheme 1.2 : Electron transfer mechanism

The lipid peroxidation, which involves a series of free radical mediated chain reaction processes, is also associated with several types of biological damage. Therefore, much attention has been focused on the use of antioxidants. There are two sources of antioxidant. From the natural source such as fruits, vegetables, nuts, seeds, leaves, roots and barks[16] which is known as natural antioxidant and the second source is the synthetic antioxidant.

1.2.1 Natural Antioxidants

The antioxidant which existed in plants or their extracts can be classified as natural antioxidant; usually they are phenolic or poly phenolic compounds, such as flavonoids, cinnamic acid derivative, coumarins, tocopherols, and polyfunctional organic acid. A large numbers of literature reported the relationship between our diet habit and health. Vegetables and fruit can reduce the risk of several diseases e.g. cardiovascular,[17] diabetes,[18] cancer,[19] hypertension[20] and inflammatory processes.[21] Vitamins A, E, and C in vegetables and fruit are one of the main constituents responsible for these protective effects beside minerals such as potassium, zinc and selenium as well carotenes, dietary fiber and phenolic compounds.[22] Phenolic compounds are considers to be antioxidant inhibiter of free radicals, antimutagens and metal chelators.[23] Although the vegetable, fruit and lifestyle have the impact to reduce the risk of developing disease, the results are sometimes inconsistent.[24] Some phenolic compounds have been reported to be harmful when consumed in large amounts.[25]

One of the side effects from phenolic compounds are their ability to precipitate proteins from complexes with polysaccharides via lipid metabolism.[26]

The antioxidant capability in the human body can be classified into three types. The first type, is accomplished by enzymes to regulates initial free radical production.[27] When oxygen is taken during the respiration process, hydrogen peroxide, hydroxyl radical and superoxide are usually formed, catalase and glutathione peroxidase assists to quench the formation of ROS.[28] The second type of antioxidant comes from diet. Various vegetables and fruits are rich with antioxidant. Those antioxidants such as α-tocopherol and ascorbate are capable of slowing down or stamp out the chain reaction of free radicals through H–atom transfer or single electron transfer. Boskou Dimitrios[29] reported some of the important phenols in plant and fruits (Figure 1.2).

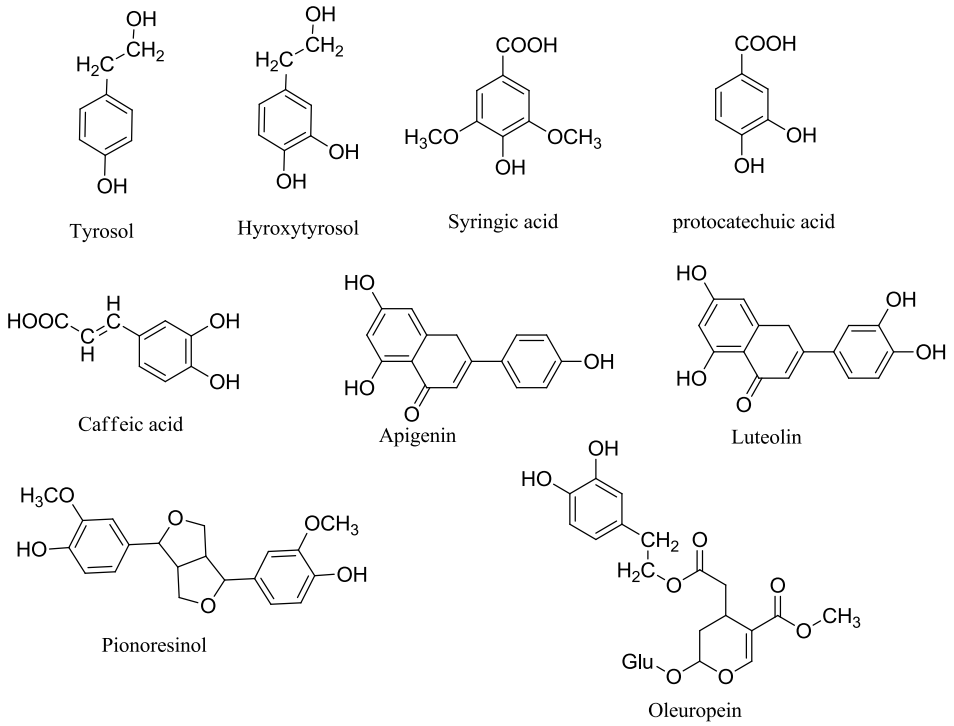

Figure 1.2 : Some natural phenolic compounds

Vitamin E (α-toc) also known as lipophilic antioxidant, plays a significant role in various biological and physiological processes.[30] Vitamin E can donate one or two protons. The first one does not affected the structure of vitamin,[31] while the second proton lead to the breakdown of the chromonal ring and it is irreversible.[32] The products

are reactive quinine methide which can dimerizes or form spirodimer via a benzyl radical [33] as summarized in Scheme 1.3. This dimer has been found as a "natural impurity" in vitamin E and it cause extraordinary kinetic behavior.[34]

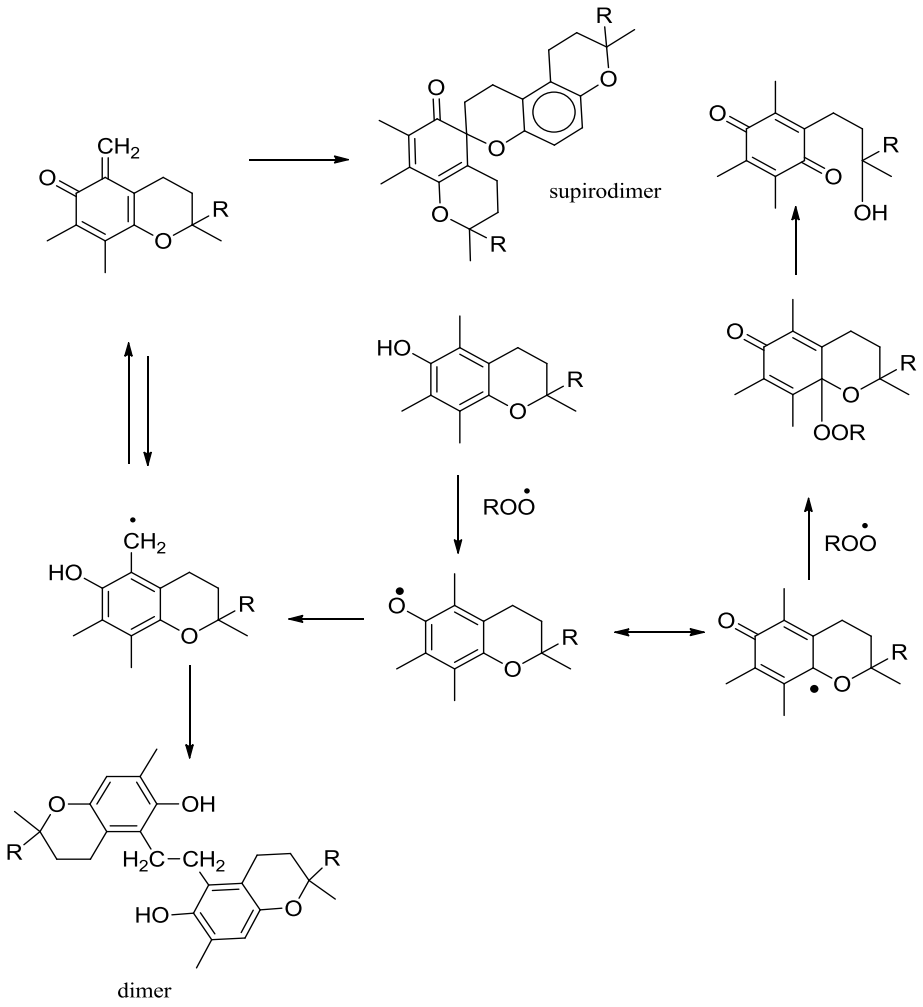

Scheme 1.3 : Oxidation products of Vitamin E with peroxyl radical,[33] R= $C_{16}H_{33}$

The third type of antioxidants is the replenisher. The Carotenoids, Flavonoids, Coenzyme Q and Glutathione are good example of replenishers.[35]

1.2.2 Synthetic Antioxidants

In addition to natural antioxidant, synthetic antioxidants have a wide range of uses in feeding industrial, confectionery and edible oil industry. Butylated hydroxyltoluene (BHT), butylated hydroxyanisole (BHA), propyl gallate (PG) and *tert*-butyl hydroquinone (TBHQ) are commonly used in this field. The synthetic antioxidants are

also used as polymer stabilizer in diverse industrial fields. The effective concentration, the thermal stability and synergism of antioxidant should be taken into account,[36] because some antioxidants have been reported to show potential adverse health effects.[37] Therefore, the synthetic antioxidants should be tested for their safety and approved before using in food at low concentration. Synthetic antioxidant are classified into two classes, primary and secondary antioxidant according to their functional properties.

There are so many synthetic antioxidant compounds that were synthesized to be used as therapy agent or in industry. For example, AO-60 [methylene-3-(3,5-di-*tert*-butyl-4-hydroxyphenyl) propionyloxy] which is known commercial product, it structure is displayed in Figure 1.3. AO-60 is an important chemical substance and is one of the most widely used antioxidants for polyolefin. By addition of hindered phenolic compounds such as AO-60, [38,39] functional rubbery materials could be produced.

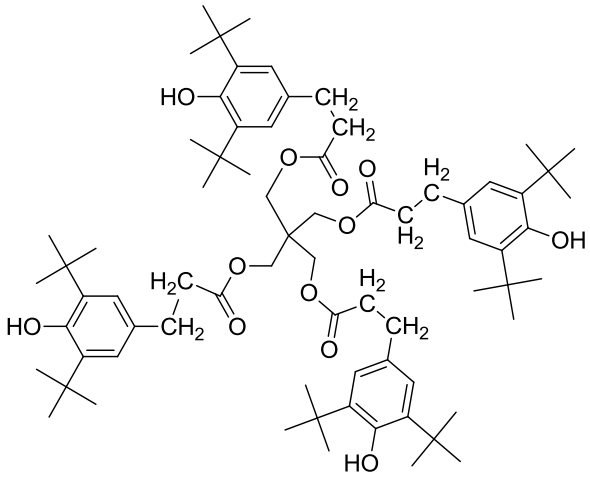

Figure 1.3 : Structure of AO-60.

In addition, many of phenolic compounds have been synthesized for therapeutic purposes and investigated their biological activities.

1.3 The biological activity of hindered Phenols

Various compounds were found to contain hindered phenol; such as di-*tert*-butylphenol (DTBP) that displayed superior biological activity. R-830 (Figure 1.4) was confirmed to be a potent inhibitor of guinea pig lung lipoxygenases and bovine seminal vesicle cyclooxygenase.[40] R-830 also inhibited PGE_2 production by stimulating rat synovial cells with an IC_{50} of 0.003 μM and significantly inhibited LTB4 production by human neutrophils with the calcium ionophore A23187.[40] Furthermore, this compound has been reported as an effective anti-inflammatory drug in several animal models of acute and chronic inflammation such as the carrageenan-induced paw edema and adjuvant arthritis in rats. Finally, its antioxidant properties were demonstrated in *vitro* using several different tests.

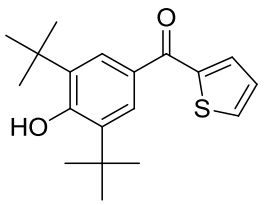

R-830

Figure 1.4 : Structure of R-830 an anti-inflammatory.

Katayama *et al*.[41] reported that the *N*-methoxy-3-(3,5-di-*tert*-butyl-4-hydroxybenzylidene)-2-pyrrolidone (E-5110) (Figure 1.5) is a novel nonsteroidal anti-inflammatory agent and it can inhibited PGE2 generation (PGE2: is the prostaglandin that ultimately induces fever) by cultured rat synovial cells. E-5110 also inhibited the superoxide generation by human (PMN) stimulated with opsonized zymosan, F-Met-Leu-Phe or phorbol myristate acetate (PMA).[42] Furthermore, it exhibited an analgesic profile similar to indomethacin but appeared significantly less ulcerogenic than indomethacin and piroxicam.[43]

Hidaka *et al*. reported that the KME-4 possess an analgesic properties[44] and are able to decrease radiographic bone damage scores in a dose dependent manner.[45]

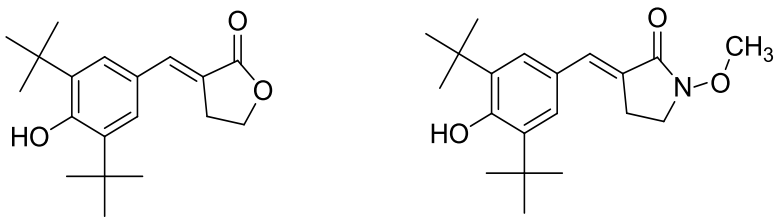

KME-4 E-5110

Figure 1.5 : Structure of KME-4 and E-5110.

Mullincan *et al.*[46] designed new compounds that contained a heterocyclic as derivatives of di-*tert*-butylphenol (Figure 1.6) and studied their oral activity for non ulcerogenic anti inflammatory compound. Most arachidonic acid are non steroidal anti-inflammatory drugs (NSAIDs). They have been widely used for the treatment of inflammatory diseases. However, they have been implicated to possess major side effects which include dyspepsia, gastric ulceration, and nephrotoxicity.[47]

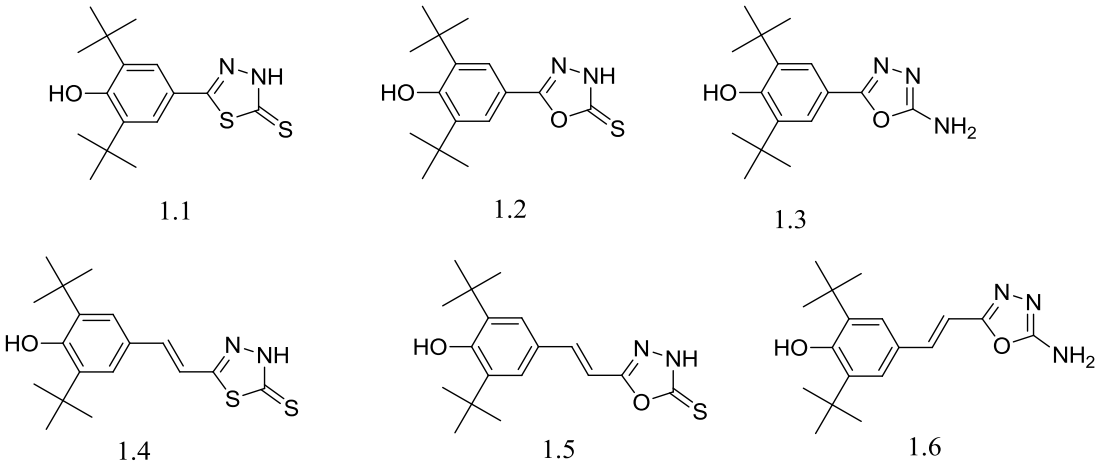

Figure 1.6 : Structures of some heterocyclic compounds containing 2,6-di-*tert*-butylphenol.

In addition to that, Ziakas *et al*.[48] synthesized several heterocyclic compound as di-*tert*-butylphenol derivatives and found that these compounds have anti-inflammatory properties besides the antioxidant activity. (Figure1.7)

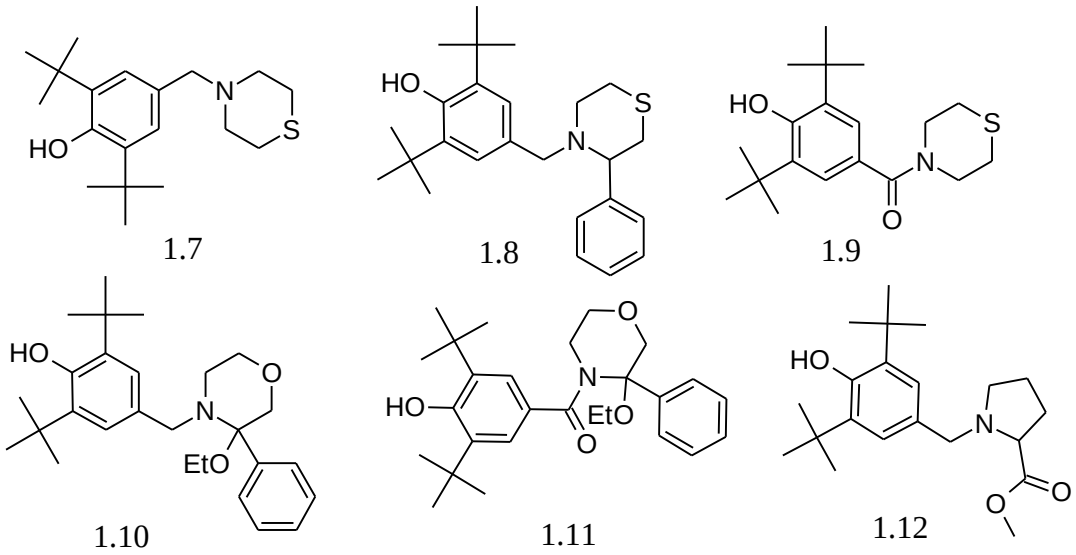

Figure 1.7 : Some phenolic heterocyclic derivative as bio active compounds.

The acyl-CoA and cholesterol acyltransferase (ACAT), are responsible for developing atherosclerosis through catalyzes the formation of cholesterol esters from cholesterol and long chain fatty acyl-coenzyme A.[49] Lee *et al*. [50] reported that two isomers of ACAT in mammals, ACAT-1 and ACAT-2. Furthermore, the selective inhibition of ACAT-1 could be beneficial for atherosclerosis. While, the selective inhibition of ACAT-2 would be useful for treating cholesterol gall stone and hypercholesterole-mia[51]. In 2004 Jeong *et al*.[52] synthesized a series of compounds containing heterocyclic consisted of 2,6-di-*tert*-butylphenol and studied their effect as ACAT inhibitors (Scheme 1.4).

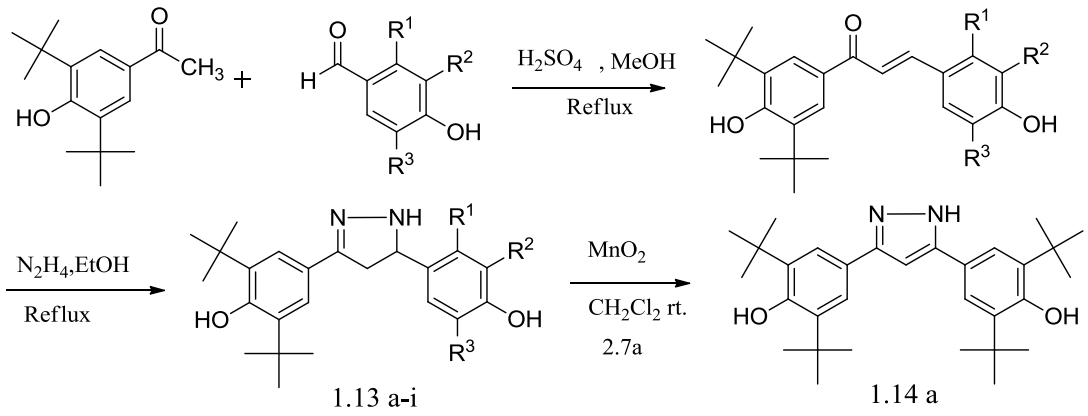

1.13a R^1=H,R^2=R^3=t-Bu 1.13bR1=H,R^2=R^3=i-Pr
1.13c R^1=H,R^2=R^3=Me 1.13d R^1=R^2=R^3=Me
1.13e R^1=H,R^2=R^3=F 1.13f R^1=H,R^2=R^3=Ph
1.13g R^1=R^2=R^3=OMe 1.13h R^1=,R^2=R^3=NO_2
1.13i R^1=H,R^2=R^3=H

Scheme 1.4 : Synthesis of 2,6 di-*tert*-butylphenol derivatives.

Pontiki *et al.* [53]synthesized some of DTBP moiety with acrylic acid derivatives (Figure 1.8). They exhibited good lipoxygenase and cyclooxygenase-1 inhibitors in addition to the antioxidant anti-inflammatory activities.

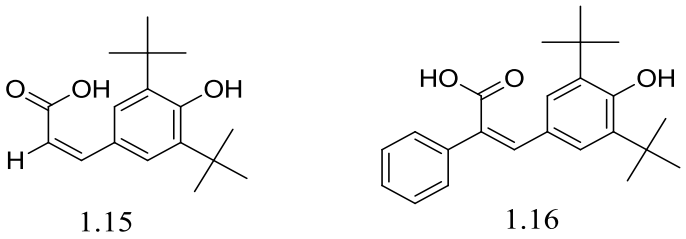

1.15 1.16

Figure 1.8 : Structure of 1.15 and 1.16 as bioactive hindered phenols derivatives.

Duarte *et al.*[54] reported that the compound 1.17 which is coded as LASSBio-881 (Figure 1.9), possess good cannabinoid receptors.[55]

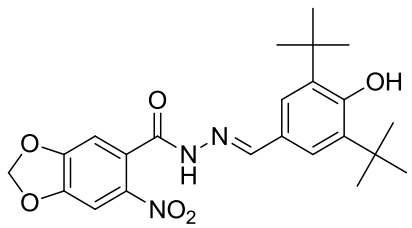

1.17

Figure 1.9 : Structure of 1.17 as good cannabinoid receptors.

Whereas, Marnett *et al.*[56] reported that the 2,6-di *tert*-butylphenol thiadiazole deriveative and thiazolenon derivative such as PD 164387 and PD 138387 are selective COX-2 inhibitors.

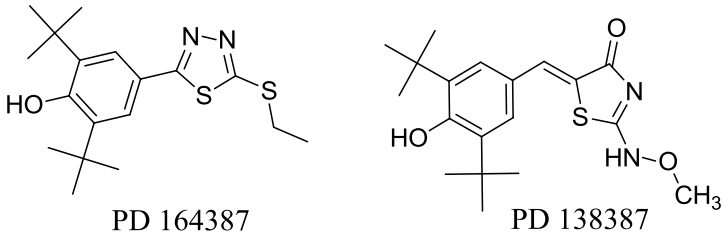

Figure 1.10 : Structures of PD 164387 and PD 138387.

Noguchi and Niki[57] designed new compounds that contained hindered phenol as antioxidant and drug for atherosclerosis.

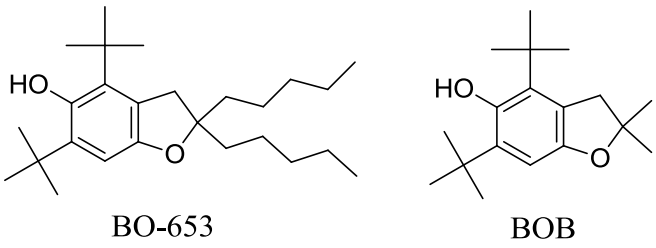

Figure 1.11 : Structures of some antioxidant as drug for atherosclerosis.

2,6-di-*tert*-butylphenol derivatives that contain heterocyclic ring exhibited a wide range of biological activities. Thus synthesis of new compounds that contain hindered phenol and heterocyclic ring and investigation of their biological activity could be somewhat interesting. Table 1-1 demonstrated some of these compounds with their biological activity.

Table 1.1 : Structure, name and bioactivity of some hindered phenol derivatives.

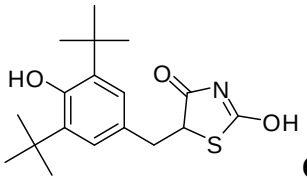 **CI-1004**	Inhibitor of COX & 5-LOX, orally administrated to rats at the dose of 200 mg/kg, did not cause gastric ulceration.[58]
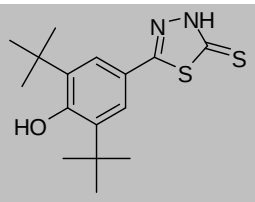 **CI-986**	Inhibitory activity on both 5-LOX and COX also as anti inflammatory agent. [46]
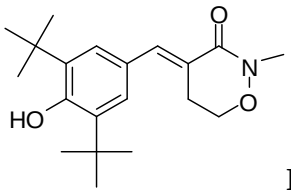 **BF-389**	Potent COX inhibitor *vitro* using human leukocytes. In the same cells, BF-389inhibited *in vitro* LTB4 production. It's, ulcerogenic potential[59] and evaluated as anti-rheumatic agent.[60]
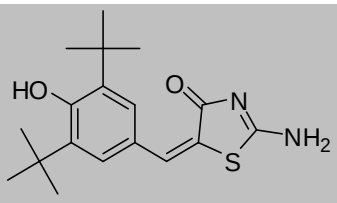 **Darbufelone**	Anti-inflammatory drug induces growth inhibition of lung cancer cells both in vitro and in vivo.[61]
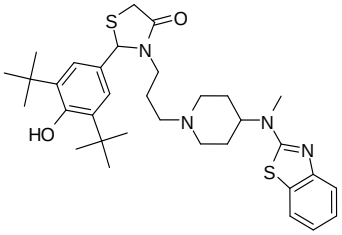 **1.19**	Calcium Overload Inhibition & Antioxidant Activity.[62]

The biological activity and antioxidant activity does not confined to di-*tert*-btyl flanked the hydroxyl group (2,6-DTBP), but also embrace the semi-hindered phenol with one *tert*-butyl group in position two and another one at position four. The compound **1.20** and **1.21** shown in Figure 1.12 have been reported as inhibitors of lipoxygenase, antioxidants, and anti-inflammatory agents.[53, 63]

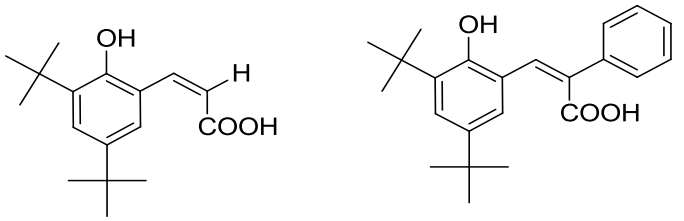

1.20 1.21

Figure 1.12 : Structures of some lipoxygenase antioxidant and anti-inflammatory.

Belostotskaya *et al*.[64] synthesized a few series of some dialkyl aminomethyl 4,6-di-*tert*-butylphenols derivatives (Figure 1.13) and they too exhibited good antioxidant ability.

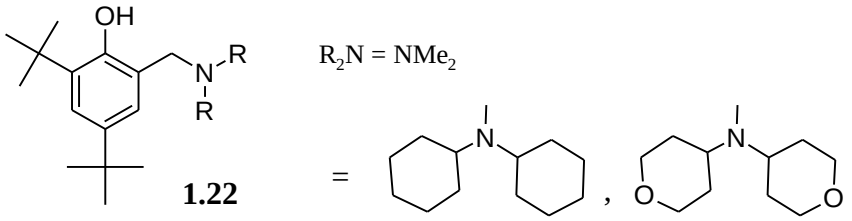

Figure 1.13 : Dialkylaminomethyl-4,6-di-*tert*-butylphenols.

In 2003, Lodyato *et al*.[65] reported that compound **1.23** and the derivatives of **1.24** (Figure 1.14) are an amphiphilic antioxidant. Additionally in 2004, compounds **1.25** had been reported to possess potent antioxidant activity.[66]

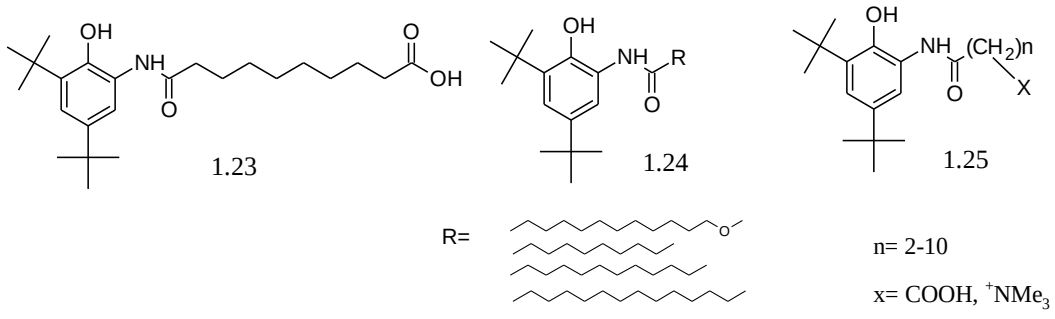

Figure 1.14 : 4,6-di-*tert*-butylphenols derivatives as antioxidant

The compounds which can be classified as a strong antioxidant usually shared common structural features. They often contain bulky phenol like DTBP or multiple phenolic hydroxyl groups like flavonoids [67] as well as full conjugation π system like

carotenoids.[68] It is known that from structure activity relationships (SAR), combination of two or more bioactive group could enhance the pharmacophore, thus in this work we presented new hindered phenol derivatives that contain heterocyclic group.

1.4 The biological activity of 1,3,4-Oxadiazole

The five member ring heterocycles exhibited various biological activities and among them is the 1,3,4-oxadiazole. Furthermore, the 1,3,4-oxadiazole and their 2,5 di substituted derivatives are significant for their development due to their large spectrum of biological activity e.g. anti inflammatory,[69] anticancer,[70] antibacterial,[71] antifungal,[72] anti-HIV[73] and antioxidant activities.[74] A large numbers of oxadiazoles derivatives are known to exhibit antioxidant ability. Table 2.1 depicted some of these compounds.

Table 1.2 : Oxadiazoles derivatives that possess antioxidant properties.

Structure	Ref.	Structure	Ref.
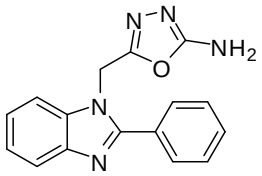	75	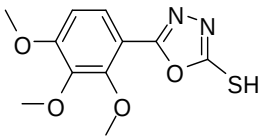	76
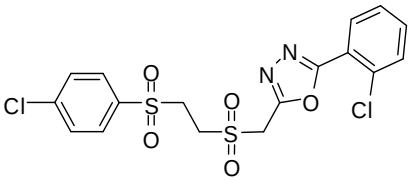	77	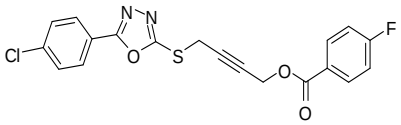	78
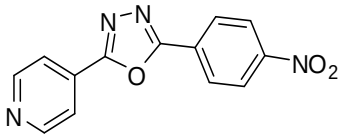	74	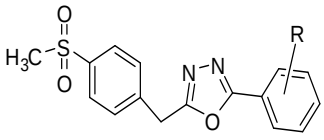	79

In addition to 1,3,4-oxadiazole, the bis-oxadiazole compounds were also reported as a biological active compounds,[80] and it had physical property like electrochemical properties [81], electro-optical properties[82] and Luminescence property.[83] In this research two series of 1,3,4-oxadiazole were synthesized. The first series of oxadiazole contain 2,6-di-*tert*-butylphenol at position four (see Chapter two) and the second series consist

of 2,4-di-*tert*-butylphenol at position six (see Chapter three). The oxadiazole could play an important role in increasing the antioxidant ability through the long range resonance as well the substituted phenyl group at position five of the oxadiazole ring can also be affected. The general structures of the synthesized oxadiazole are shown in Figure 1.15.

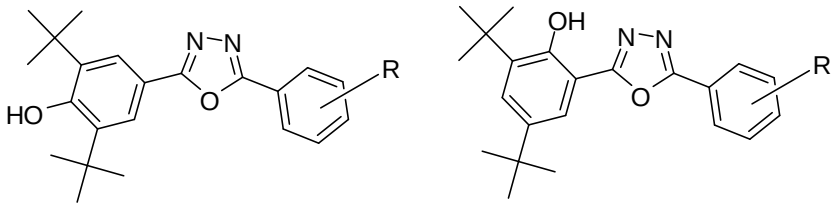

Figure 1.15 : General structures of the synthesized oxadiazoles.

The second series of the synthesized compound include bis-oxadiazole bis-2,6-di-*tert*-butylphenol as shown in Figure 1.16 and will be discussed in Chapter 2.

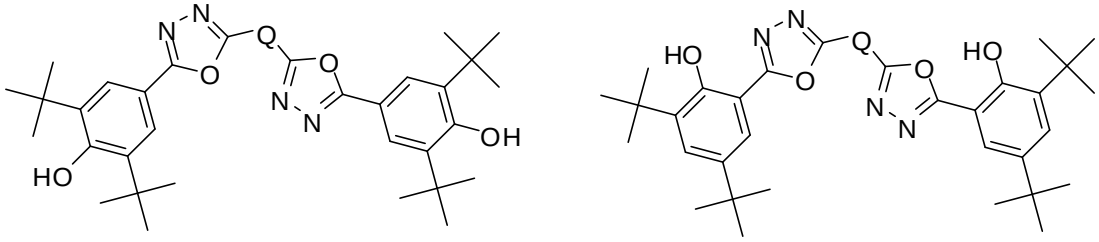

Figure 1.16 : General structure of the synthesized bis-oxadiazoles.

1.5 The biological activity of Triazole and Thiadiazole

The triazole derivatives also exhibited a wide range biological activity such as antiviral,[84] inhibitors of Methionine Aminopeptidase-2,[85] Anhydrase inhibitors,[86] anti-cancer[87], anti-inflammatory,[88] inhibitors of the HIV-1,[89] antibacterial, antifungal[90], analgesic [91] and antioxidant.[92]

The thiadiazole are similar to triazole in terms of the wide diversity of biological activity e.g. anti-tumor,[93] anti-inflammatory,[94] antibacterial,[95] antifungal,[96] antidepressant,[97] anti-oxidant.[98] Khan *et al*. [92] in 2010 synthesized different triazole and thiadiazoles derivatives (Figure 1.17) and their antioxidant activity were evaluated. The synthesized triazoles and thiadiazoles displayed fair antioxidant ability.

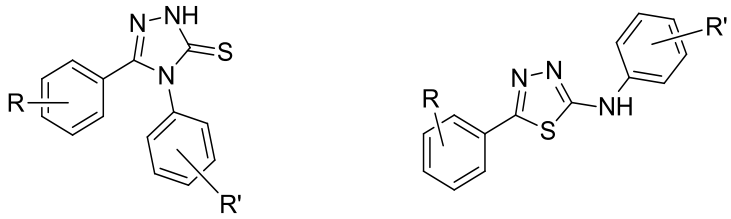

1.26 1.27

R= 4-Cl, 3-Cl, 2-Cl, 4-CH_3, 2-CH_3, 3-NO_2, H.

R'= 2,4-diCH_3, 2,3-di-CH_3, 2,6-di-CH_3

Figure 1.17 : Triazole and Thiadiazoles derivative as antioxidant.

Yehye *et al.*[99] synthesized triazoles derivatives and thiadiazoles derivatives moiety with BHT group (Figure1.18) and they found that these compounds have good antioxidant ability especially when electron withdrawal group is at *meta* position.

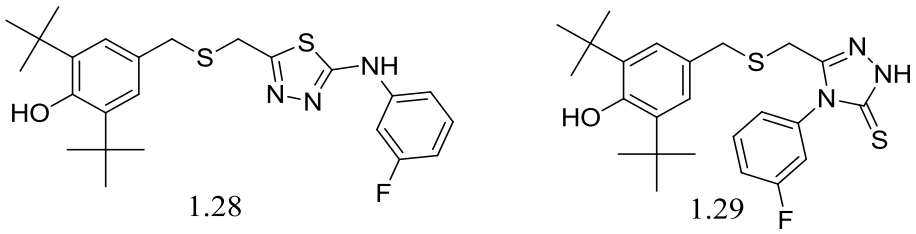

1.28 1.29

Figure 1.18 : Thiadiazole and Triazole contain hindered phenol.

Based on this report, we would synthesized triazole and thiadiazole containing 2,4 DTBP (see Chapter 3). In addition to the antioxidant ability due of hindered phenol we believe that this heterocycles could also enhance the antioxidant ability of the molecule. Furthermore, formation of the five membered heterocyclic at position six could also increase the stability of the free radical through the resonance stabilization, as demonstrated in Scheme 1.5.

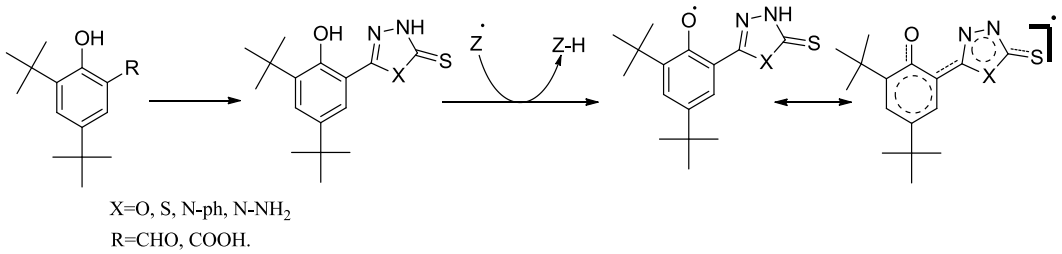

Scheme 1.5 : Possible resonance structures stability with five membered ring heterocyclic at position six.

1.6 The biological activity of Hydrazones

The hydrazones has a wide range of biological activity such as analgesic[100], anti-inflammatory,[101] antibacterial,[102] anticancer[103] and antioxidant.[104] The salicyl hydrazones are one of the important hydrazones. The SHI, HAPI and NHAPI (Figure 1.19) showed good antioxidant ability and they can increase plasma hydrolysis.[105]

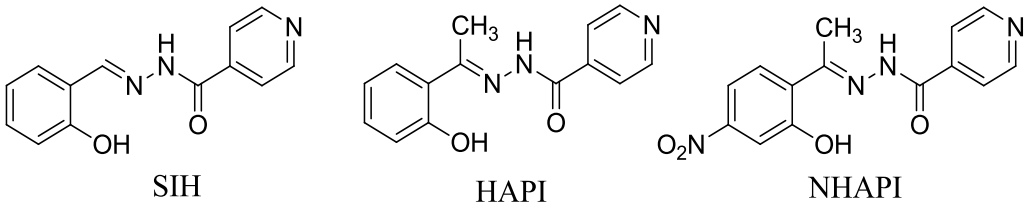

Figure 1.19 : Some hydrazones have antioxidant ability.

In this research the hydrazones were synthesized as an intermediate to the formation of the 1,3,4-oxadiazole ring and bis-oxadiazole rings (see Chapter 3). However, we will also investigate their antioxidant ability and will be discussed further in Chapter 4. Figure 1.20 illustrates the hydrazones and the bis-hydrazones.

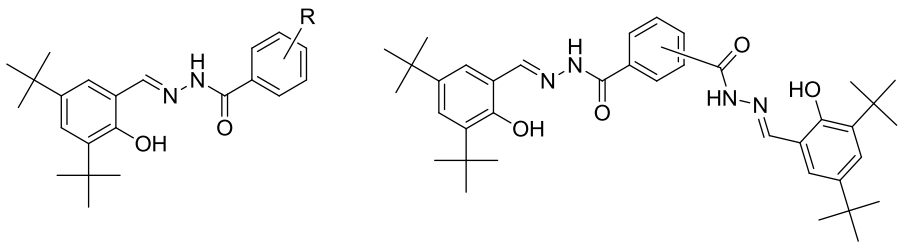

R= 4-CH_3, 4-OCH_3, 4-Cl, 2-Cl

Figure 1.20 : General structure of synthesised hydrazones and bis-hydrazones.

Chapter 2 : Synthesis of 1,3,4-Oxadiazole and Bis-1,3,4-Oxadiazole Containing 2,6-di-*tert*-butylphenol Group

2.1 Introduction

The antioxidant ability of the di-*tert*-butylphenol derivatives and the 1,3,4-oxadiazole derivatives have been discussed in Chapter 1. In this chapter, various methods to synthesized 1,3,4-oxadiazole will be presented and discussed.

2.2 Synthesis

2.2.1 Synthesis of 2,5-disubstituted-1,3,4-oxadiazoles.

In 1955, two literatures reported the first method for synthesizing 1,3,4-oxadiazole.[106] Since then, many literatures reported several methods for synthesizing 1,3,4-oxadiazole derivatives.

a) In 1966, Ainsworth & Hackler synthesized some alkyl 1,3,4-oxadiazole by heating the 1-acyl-2-ethoxymethylene hydrazines at atmospheric pressure.[107]

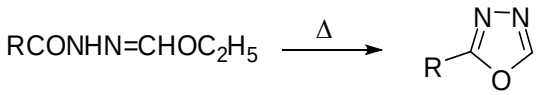

Scheme 2.1 : Synthesis of oxadiazole method **a**.

b) Reaction of 1,2-diacyl and 1,2-diaroyl hydrazines with $BF_3.Et_2O$, as cyclo-dehydration reagent.[108]

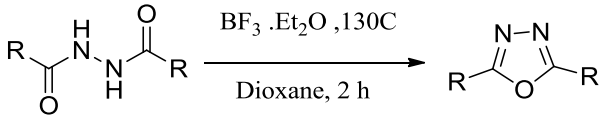

Scheme 2.2 : Synthesis of oxadiazole method **b**.

c) Reaction of two mole of Aryl carboxylic acid with hydrazine dihydrochloride in the presence of phosphorus pentoxide and phosphoric acid, using microwave irradiation.[109]

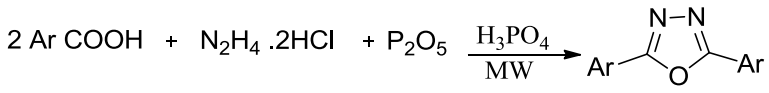

Scheme 2.3 : Synthesis of oxadiazole method **c**.

d) Synthesis of some 2,5-disubstituted-1,3,4-oxadiazoles by condensing mono aryl hydrazides with acid chlorides in the presence of HMPA as a solvent under the microwave heating.[110]

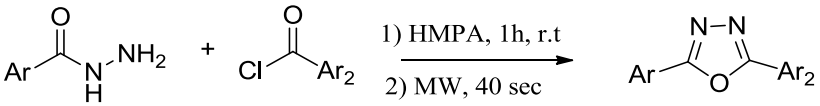

Scheme 2.4 : Synthesis of oxadiazole method **d**.

e) Cyclization of hydrazone using bis (trifluoroacetoxy) iodobenzene as an oxidizing agent in chloroform or DMSO at room temperature.[111]

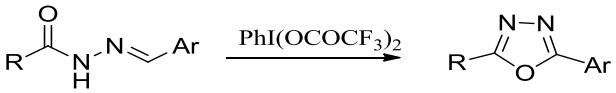

Scheme 2.5 : Synthesis of oxadiazole method **e**.

f) Condensation of different acyl hydrazides with orthoesters in the presence of silica sulphuric acid (solvent free).[112]

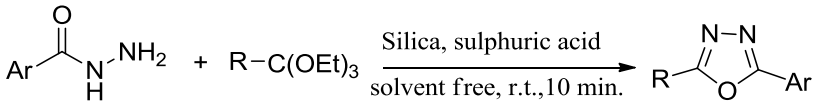

Scheme 2.6 : Synthesis of oxadiazole method **f**.

g) 2,5-di-substituted-1,3,5-oxadiazole prepared by using *N*-chlorosuccinimide/1,8-diazabicyclo[5.4.0]undec-7-ene (DBU) as an effective oxidant for oxidative cyclization of acyl hydrazone.[113]

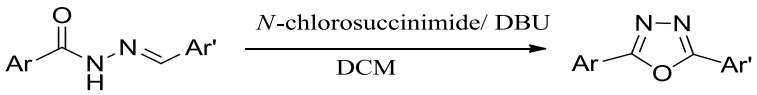

Scheme 2.7 : Synthesis of oxadiazole method **g**.

h) Synthesis of 2,5-disubstituted 1,3,4-oxadiazoles catalyzed by condensation between acid hydrazide and carboxylic acid by Ceric ammonium nitrate (CAN) and polyethylene glycol (PEG) as catalyst.[114]

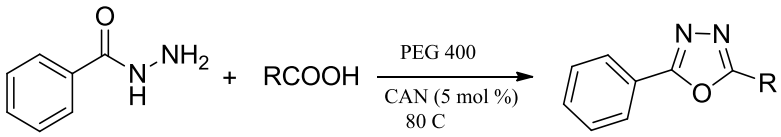

Scheme 2.8 : Synthesis of oxadiazole method **h**.

i) Antibacterial study for synthesized oxadiazole had been reported, and this cyclization proceeded by using Chloramine-T as a cyclising agents.[115]

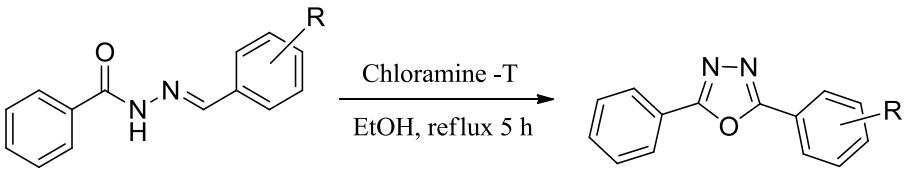

Scheme 2.9 : Synthesis of oxadiazole method **i**.

j) Disubstituted oxadiazoles were synthesized via one pot reaction at room temperature, from reaction of different acid hydrazide and acyl halides in the presence of phosphorus pentoxide in acetonitrile. This method shows excellent yield.[116]

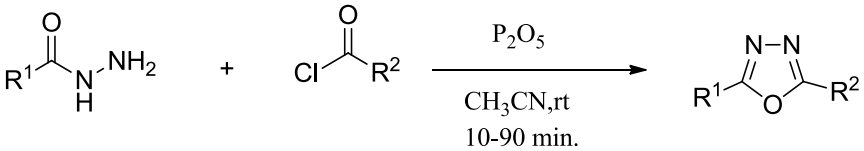

Scheme 2.10 : Synthesis of oxadiazole method **j**.

k) Treatment of aryl hydrazones with potassium permanganate on the surface of SiO_2 with acetone or water under microwave irradiation.[117]

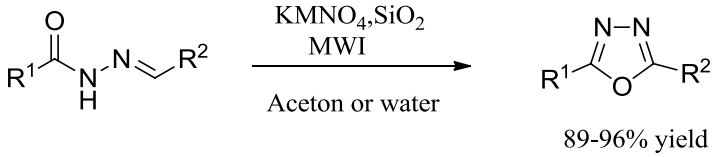

Scheme 2.11 : Synthesis of oxadiazole method **k**.

l) Cyclization of the alkyl or aryl hydrazone by bromine as oxidative agent[118] in glacial acetic acid, in the presence of sodium acetate.

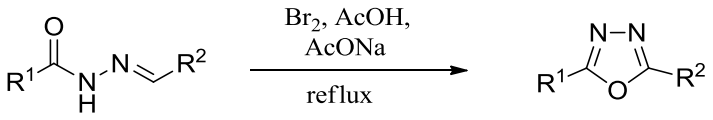

Scheme 2.12 : synthesis oxadiazole using Br_2 as oxidizing agent.

This method was used to synthesize our 1,3,5-oxadiazole in Chapter 3.

m) Formation of the oxadiazole from condensation of carboxylic acid and acid hydrazide or 1,2-diacyl and 1,2-diaroyl hydrazines in the presence of $POCl_3$ as dehydration agent.[77, 119]

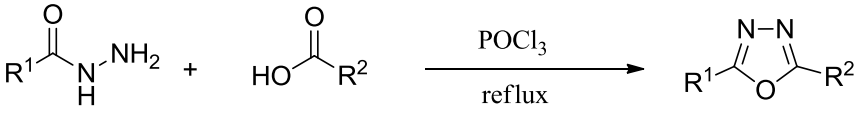

Scheme 2.13 : Synthesis oxadiazole in presence of $POCl_3$ as dehydration agent.

This method was used to achieve our goal; eleven of 2,6-di-*tert*-butyl-4-(5-aryl-1,3,4-oxadiazol-2-yl)phenol **2.12-2.22** and seven of 4,4'-(5,5'-(substitute)bis(1,3,4-oxadiazole-5,2-diyl))bis(2,6-di-*tert*-butylphenol) **2.31-2.37** were synthesized according to this method.

2.3 Results and Discussion

The antioxidant donates a proton to the reactive radical and breaks the chain reaction. The antioxidant after donating a proton were converted to a stable radical; this stability enhances the property of the antioxidant.[120] Two series of oxadiazoles and bis-

oxadiazoles were synthesized and their antioxidant ability were investigated. The conjugated system increases their radical stability.[121] In this section we will discuss the syntheses and characterization of eleven new oxadiazoles and seven new bis-oxadiazoles bearing of 2,6-DTBP.

2.3.1 Synthesis of 2,6-di-*tert*-butyl-4-(5-aryl-1,3,4-oxadiazol-2-yl)phenol

The compounds were prepared in two steps: eleven different aryl acid hydrazides were synthesized followed by a condensation reaction with 3,5-di-*tert*-butyl-4-hydroxybenzoic in the presence of $POCl_3$.

2.3.1.1 Synthesis of acid hydrazide

Eleven acid hydrazides were synthesized from substituted benzoic acid. All the acids were reacted with thionyl chloride to form acid chloride, which was reacted directly without further purification with excess of hydrazine hydrate in dry benzene (see Section 6.1.3) as shown in Scheme 2.14.

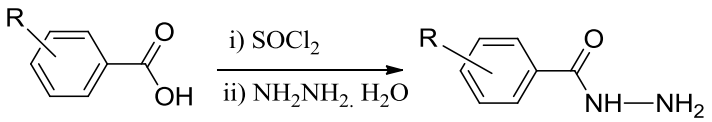

2.1 - 2.11

R= 4-Me, 4-OMe, 4-OEt, 4-Br, 4-Cl, 4-OH, 3,4-di-Cl, 3,5-di-Cl, 2,4-di-Me, 2-Me, 2-Cl

Scheme 2.14 : Synthesis of acid hydrazide.

The aryl hydrazides were characterized by IR and ^{1}H NMR spectrums and by comparing their melting points with literatures. The IR spectrum of (**2.1-2.11**) shows the presence of the NH, NH_2, and amide carbonyl in range 3319-3280, 3225-3176, and 1669-1662 cm^{-1} respectively. Furthermore, the ^{1}H NMR shows the NH peak between 9.9-9.58 and the NH_2 at 4.37-4.58. In addition, the peaks of corresponding aromatic protons and the substitution group for compounds **2.1**, **2.2**, **2.3**, **2.6**, **2.9** and **2.10** were also observed. Table 2.1. summarized some properties of the synthesized hydrazide

Table 2.1 : The structure, m.p and yield of the synthesised acid hydrazides.

No.	Structure	m.p. (°C)	yield (%)
2.1	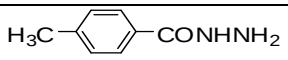	115 -118	95
2.2	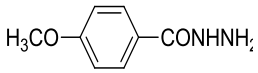	136 -138	86
2.3	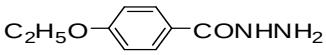	125- 127	79
2.4	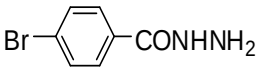	186- 170	82
2.5	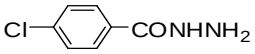	160- 164	91
2.6	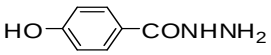	262- 264 dec	89
2.7	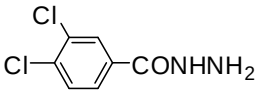	150- 152	80
2.8	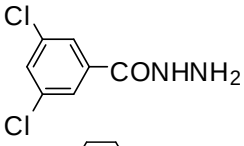	200- 204	87
2.9	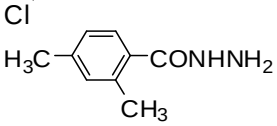	122 -124	88
2.10	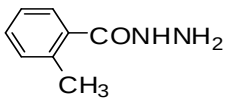	120 – 124	77
2.11	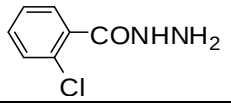	110 – 114	95

2.3.1.2 Formation of 2, 6-di-*tert*-butyl-4-(5-aryl-1,3,4-oxadiazol-2-yl)phenol

Formation of the target oxadiazoles was achieved by cyclization of the hydrazides (**2.1-2.11**) with 3,5-di-*tert*-butyl-4-hydroxybenzoic acid in the presence of $POCl_3$ as dehydrating agent. The mixture was refluxed for three hours in a water bath. Scheme 2.15 depicted the reaction pathway. The resulting oxadiazoles were purified either by recrystallization or column chromatography. The results are summarized in Table 2.2.

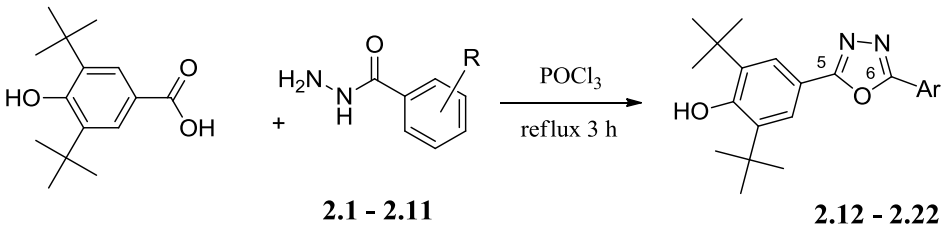

Scheme 2.15 : Cyclization of acid hydrazide with 3,5-di-*tert*-butyl-4-hydroxybenzoic acid.

Table 2.2 : Some experimental data of the synthesized oxadiazoles.

No.	Ar	yield (%)	m.p. (°C)	MF	HREIMS Found
2.12	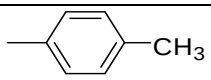	76	196-197	$C_{23}H_{28}N_2O_2$	364.2147
2.13	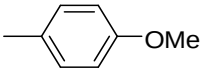	76	176-178	$C_{23}H_{28}N_2O_3$	380.2095
2.14	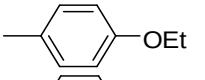	84	168-170	$C_{24}H_{30}N_2O_3$	394.2249
2.15	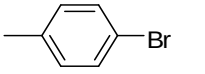	74	179-181	$C_{22}H_{25}BrN_2O_2$	428.1093
2.16	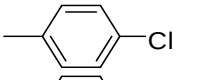	83	162-164	$C_{22}H_{25}ClN_2O_2$	384.1597
2.17	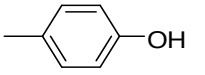	70	144-146	$C_{22}H_{26}N_2O_3$	366.1938
2.18	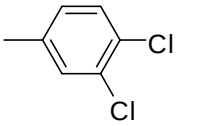	80	222-224	$C_{22}H_{24}Cl_2N_2O_2$	418.1219
2.19	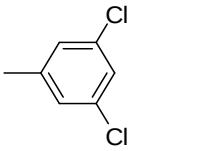	75	195-197	$C_{22}H_{24}Cl_2N_2O_2$	418.1210
2.20	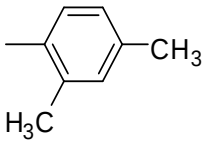	60	170-172	$C_{24}H_{30}N_2O_2$	378.2301
2.21	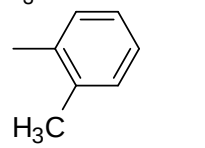	68	132-134	$C_{23}H_{28}N_2O_2$	364.2144
2.22	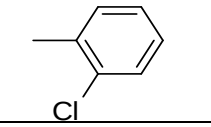	81	113-115	$C_{22}H_{25}ClN_2O_2$	384.1600

2.3.2 Products Characterization

The newly synthesized 1,3,4-oxadiazole derivatives were obtained in moderate to good yield after purification. They were characterized by IR, ^{1}H NMR, ^{13}C NMR and mass spectra (EIMs and HREIMs) and further supported by 2D NMR (DEPT, HSQC and HMBC). The X-ray crystallography was carried out for compound **2.20.** These results were in agreement with the proposed structure, i.e. 1,3,4-oxadiazole.

2.3.2.1 Fourier Transform Infra-red (FTIR)

Significant peaks corresponding to the major functional groups were observed in the IR spectrum. The medium strong band at 1624-1608 cm^{-1} revealed the formation of C=N bond of the oxadiazole ring. The OH of phenol appeared as a medium band at 3658-3525 cm^{-1} due to the non hydrogen bonding for the hindered phenol.[122] Earlier work has shown that the OH group of a highly hindered phenolic was capable of formation hydrogen bonding [123] but only to a small extent and was insignificant. Thus the OH group appeared as a medium strong and not a broad band. The IR spectra for compound **2.12-2.22** showed strong absorption s at 3011-3003 cm^{-1}, 2962-2952 cm^{-1}, 1506-1585 cm^{-1}, 1219-1250 cm^{-1} attributed to (C-H) aromatic, (C-H) aliphatic, and (C=C) aromatic), respectively.

2.3.2.2 Nuclear Magnetic Resonance (NMR)

The ^{1}H NMR spectra of compounds **2.12-2.22** (Appendix A) showed the disappearance of NH and NH_2 signals of the hydrazide. An interesting peak of di-*tert*-butyl group appeared as a singlet at 1.44-1.52 ppm with integration correspond to eighteen protons. A singlet peak for two protons at position 3 of the 2,6-di-*tert*-butylphenol ring appeared in the range 7.90-7.96 ppm. The singlet peak at 5.63-5.69 ppm with integration equals to one belongs to the OH of the hindered phenol.[124] The aromatic protons at 7.02-8.08 ppm is attributed to the aryl oxadiazole at position five. The aromatic ring with a *para* substituent showed two doublet peaks with a coupling constant of J=7.5-8.8 due to 1,2 splitting. The doublet appeared like an AB system (first order) in **2.13** (Figure 2.1). In some cases, the doublet peak appeared to be more complicated and existed as a symmetrical mirror image. However, it cannot be classified as an AA'BB', because the other double peak appeared without any recognizable splitting. A typical spectrum is shown in Figure 2.2 for compound **2.15**.

A small peak at 7.58 ppm and 7.60 ppm indicates the proton neighbouring to the halide. No significant peak was observed for the proton neighbouring next oxadiazole ring. Hence, it is not an AA'BB' system. Thus, we can confirm that the small *J* value belongs to a 1,3 coupling constants.[125] (Section 6.1.4 and Appendix –A2).

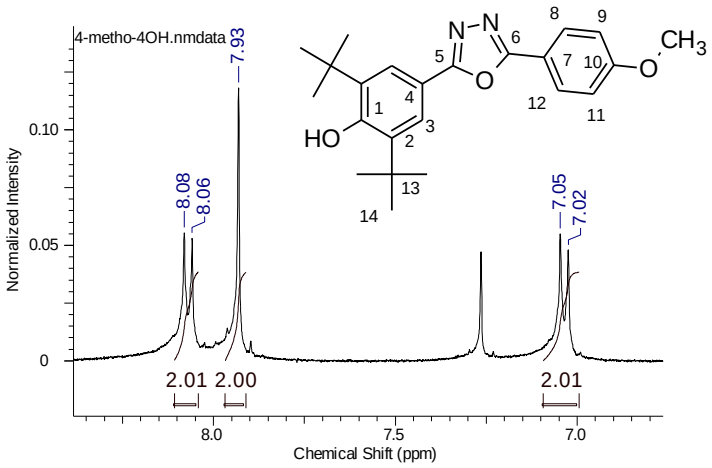

Figure 2.1 : ^{1}H NMR expansion region of **2.13**

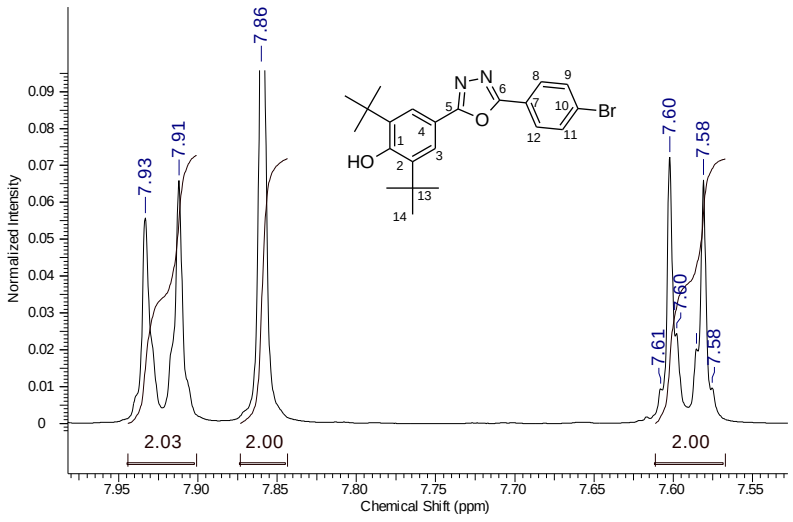

Figure 2.2 : ^{1}H NMR expansion region of **2.15**.

The ^{13}C NMR spectra for compounds **2.12 -2.22** showed a significant peak for six methyl carbons (C_{14}) of 2,6-di-*tert*-butyl group which were located at 30.06-30.13 ppm. The two quaternary carbons of the tertiary butyl group (C_{13}) appeared in the range of 34.45–34.61 ppm and the carbon attached with the hydroxyl group of hindered phenol

(C_1) appeared at 156.93–157.12 ppm. The two C_2 attached to the di-*tert*-butyl appeared at 136.68–136.89 while C_3 appeared at 124.18– 124.35 ppm. The C_4 attached to 1,3,4-oxadiazole ring appeared between 114.89 and 115.53 ppm. The C_7 at position 5 of the oxadiazole ring appeared in a wide range (115.58–126.87 ppm) and this could be due to the effect of a substituted group on the phenyl ring. The substituted group at the *para* position does not have any effect while the *meta* or *ortho* will shift to the high field.

The ^{13}C NMR spectra for the substituted group of the aromatic ring, i.e. 4-methyl, 4-methoxy, 4-ethoxy, 2,4-dimethyl and 2-methyl of compounds **2.12, 2.13, 2.14, 2.20** and **2.21** respectively, appeared in the expected area. The C_5 & C_6 representing the two carbons of 1,3,4-oxadiazole ring and appeared as two separate peaks in the range 161.88-164.33 ppm and 164.75-166.04 ppm respectively.

The 2D NMR spectra (DEPT-135, HSQC and HMBC) were used to distinguish the two carbons of the oxadiazole ring. Compound **2.15** was chosen to illustrate our discussions. In DEPT-135, only three CH were observed Two of the peaks representing the (C_8-H_8, C_{12}-H_{12}) and (C_9-H_9, C_{11}-H_{11}). The third peak is attributed to two carbons of C_3-H_3 (Figure 2.3).

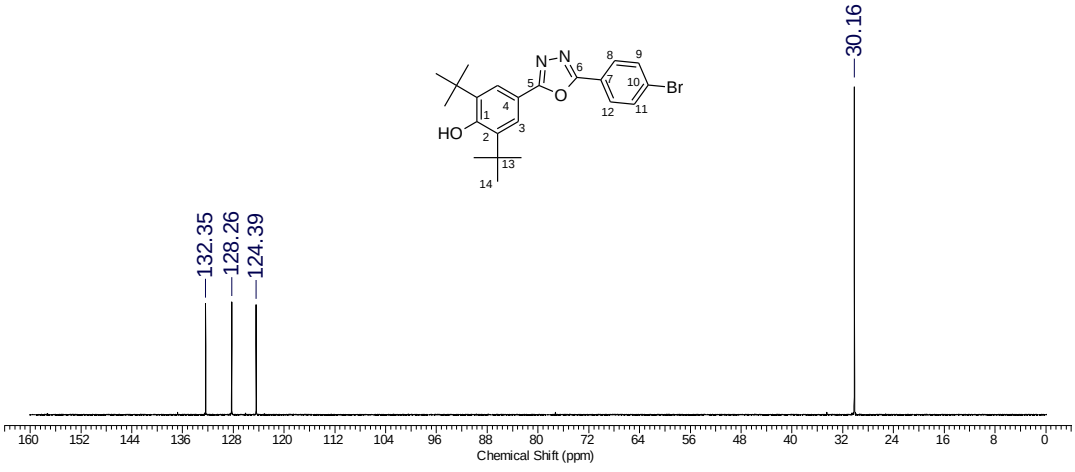

Figure 2.3 : The DEPT-135 spectrum of **2.15**.

The HSQC spectrum showed the correlation between the two mirror image protons for H_9-C_9, H_{11}-C_{11} and the correlation between the doublet peaks due to protons H_8-C_8, H_{12}-C_{12} and H_3-C_3, as depicted in Figure 2.4.

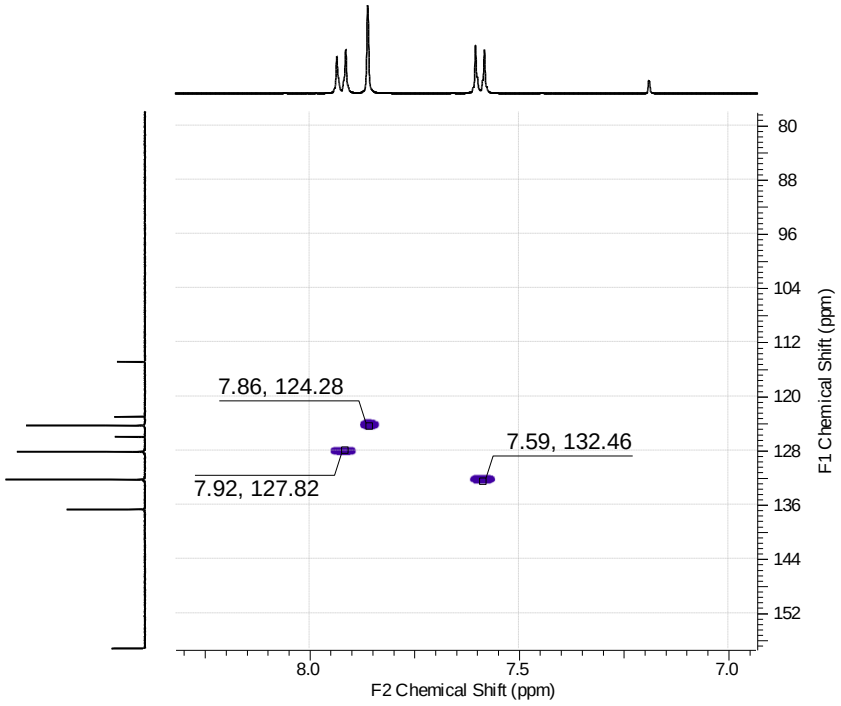

Figure 2.4 : The HSQC, Expansion of the aromatic area for **2.15**.

The HMBC spectrum disclosed the correlation between the long distance coupling of J_3 as well as the weak coupling for J_2. Some of these correlations were very important and were able to illustrate that the C_5 in oxadiazole was connected to C_4 of the 2,6-di-*tert*-butylphenol and not the C_6. In this case, the ^{13}C NMR spectra was unable to distinguish between them. This spectrum illustrated the correlation between H_3 and both of C_1 and C_5. The HMBC also allowed us to distinguish the relationship between H_8 and C_6 and C_{10} and able to determine the C_5 and C_6 of the oxadiazole ring. On top of that, the position of C_7 was also determined by the correlation between H_9 and C_7. The Figure 2.5 shows the expansion of HMBC (see Appendix A).

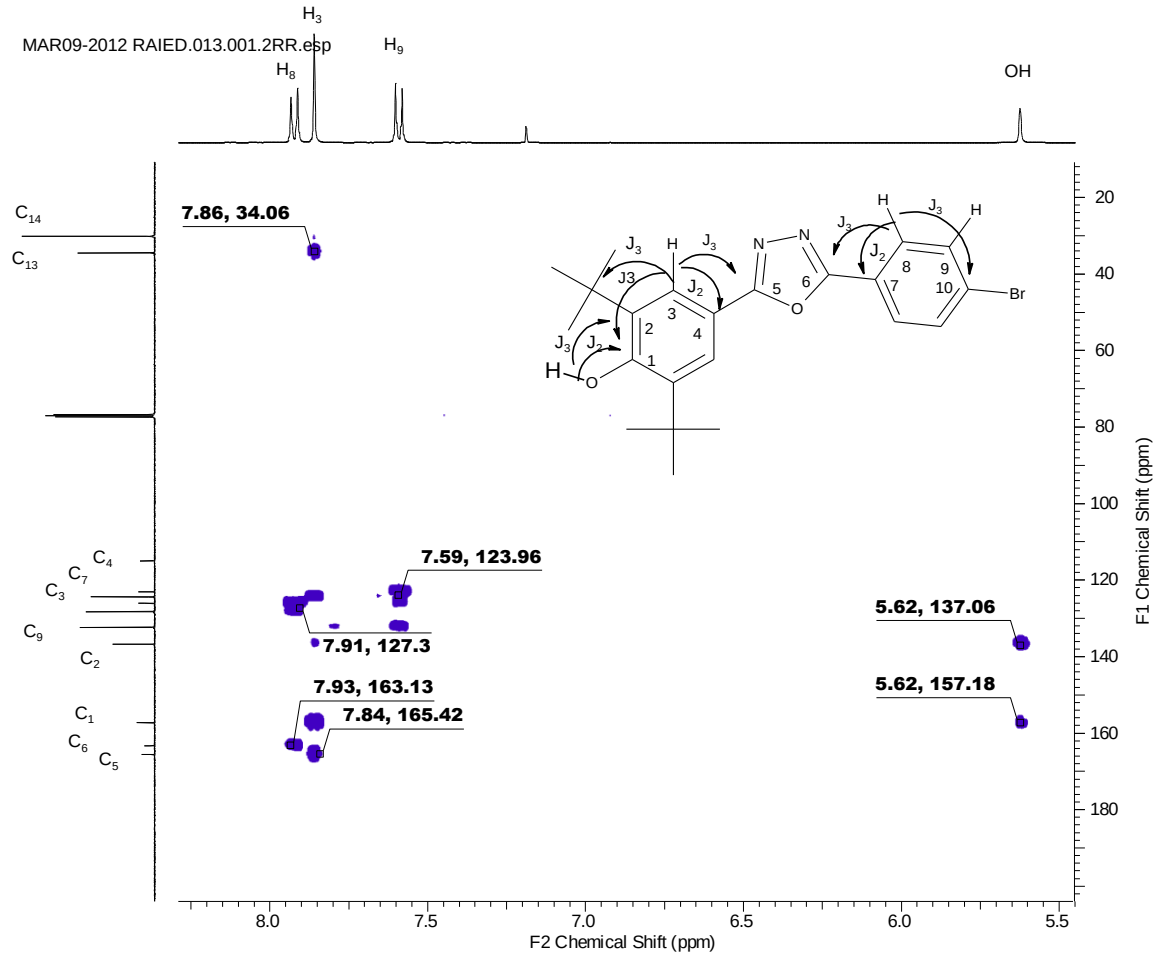

Figure 2.5 : Expansion of HMBC of **2.15**.

2.3.2.3 Mass spectroscopy

The structures of all the eleven compounds were confirmed by using EIMs and HREIMs. EIMS gives the molecular ion $M^{\cdot+}$ peak and the base peak (100%). The m/z value of the base peak was either equal the molecular ion value or the molecular ion minus methyl radical ($M^{\cdot+}$-$^{\cdot}CH_3$). The fragmentations in EIMs confirm of the proposed structures and the HREIMs confirmed the accurate mass and the molecular formula. The results obtained in this work are in agreement with calculated mass.

The interesting fragmentation observed on mass spectrum was the losing of *iso*cyanic acid (HNCO). The same observation was reported in literature.[126] where the fragmentation started from $M^{\cdot+}$+H. However, in our case, the losing of HNCO started

from molecular ion ($M^{\cdot+}$).[127] This could be attributed to proton transfer in $M^{\cdot+}$. The losing of HNCO can be explained through the rearrangement of molecular ion and migration. Compound **2.20** was used as an example to demonstrate the mechanism and was shown in Scheme 2.16 (See Appendix B).

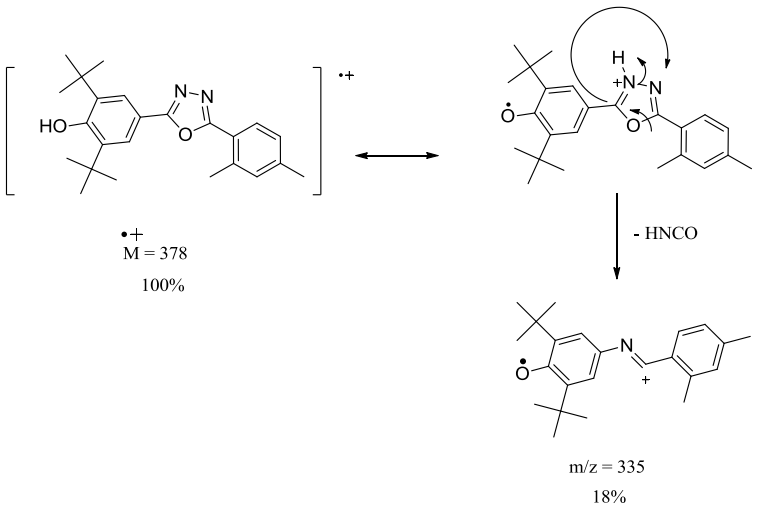

Scheme 2.16 : Suggested pathway for the losing of HNCO

The proposed fragmentation pattern could take place in one step or it could also occur in multistep. For multistep, Two pathways were suggested for the radical migration, path (B) and (C). Both pathways, (B) and (C) have intermediate (A) as their starting point which is formed by intra fragmentation of the molecular ion and migration of 2,6-di-*tert*-butylphenol as displayed in Scheme 2.17 . Path B is similar to the mass fragmentation pathway proposed by Frański *et al.*[126b]

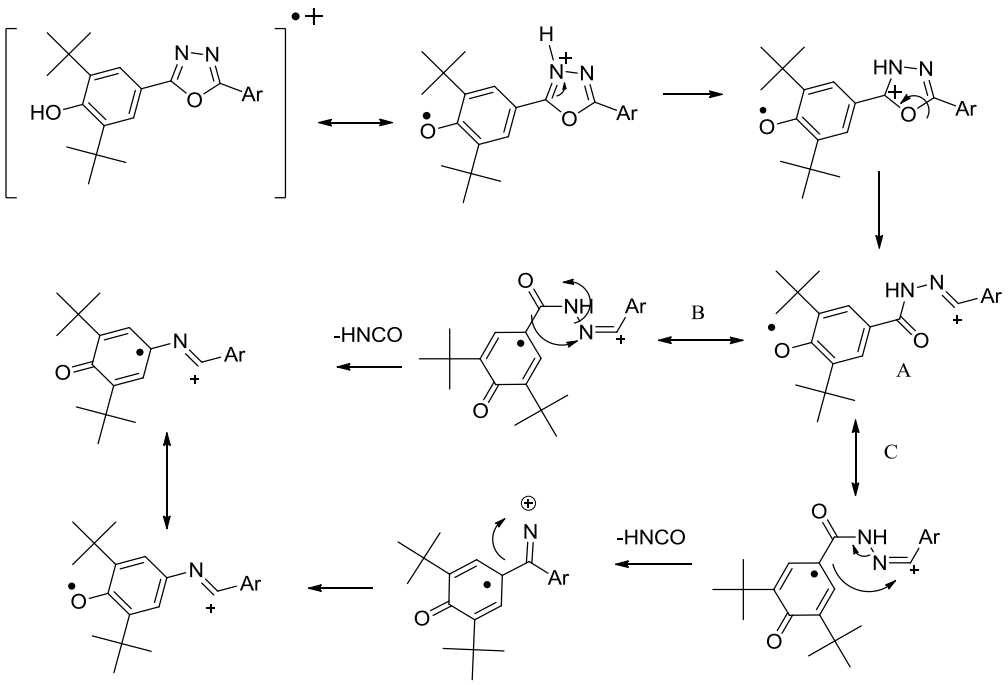

Scheme 2.17 : Proposed pathways of losing HNCO in multistep. [127]

Table 2.3 summarizes the values of the molecular ion, the base peak and values after losing HNCO.

Table 2.3 : Molecular ion observed, calculated, base peak and the m/z after losing HNCO.

No.	$M^{\cdot+}$ found	$M^{\cdot+}$ calculated	m/z of base peak 100%	$M^{\cdot+}$-HNCO
2.12	364.2	364.21	349.2	321.1
2.13	380.2	380.21	380.2	337.1
2.14	394.3	394.22	394.3	351.1
2.15	428.2	428.10	413.1	385.1
2.16	384.2	384.16	369.1	341.1
2.17	366.2	366.19	366.2	323.1
2.18	418.2	418.12	403.1	375.1
2.19	418.2	418.12	403.1	375.0
2.20	378.3	378.23	378.3	335.1
2.21	364.3	364.21	349.2	321.1
2.22	384.2	384.16	369.2	341.1

The other pattern that we observed from EIMs where the usual fragmentation pattern of the 1,3,4- oxadiazole ring, which were reported in some literatures.[126c]

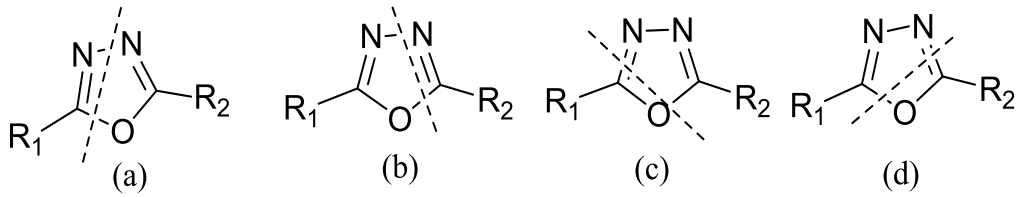

Figure 2.6 : pathway of oxadiazole fragmentations.[126c]

Compound **2.12** was used as an example to illustrate our discussion. The fragmentations of (b) and (c) in Figure 2.6 clearly indicate that all our compounds have a similar fragmentation pattern. The existence of peak 233.1, which belongs to the ion [2,6-di-*tert*-4-hydroxy-C_6H_2-CO]$^+$ appeared in all of the EIMs spectrum. Scheme 2.18 demonstrated the most important fragmentations of compound **2.12**.

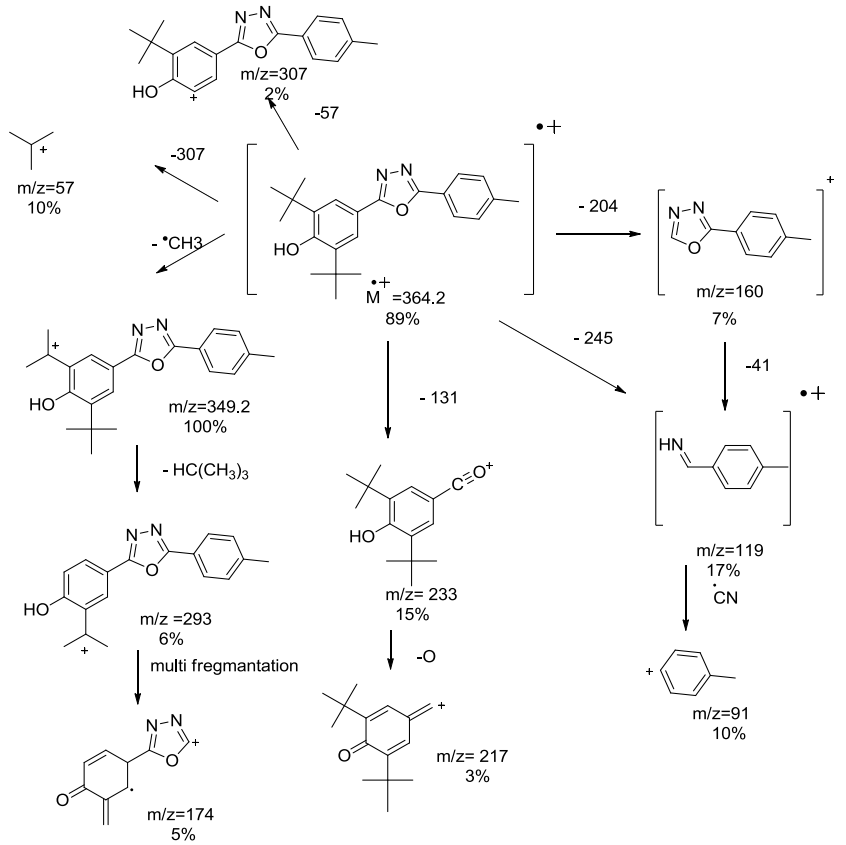

Scheme 2.18 : Some EIMs fragmentation of **2.12**.

2.3.2.4 X-ray Crystallography

The X-ray analysis of single crystal of compound **2.20** was able to confirm our proposed structure and this was in agreement with IR, ^{1}H NMR, ^{13}C NMR, EIMS and HREIMs. Figure 2.7 showed the ORTEP for the crystal and all the data were summarized in Appendix C. The structure has an orthorhombic crystal system.

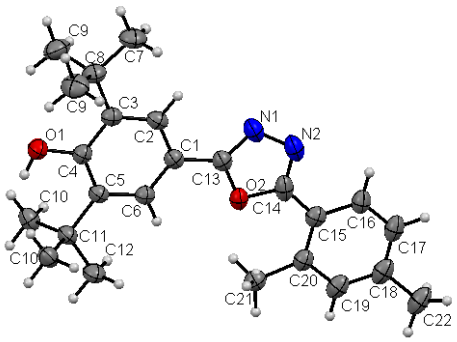

Figure 2.7 : The ORTEP of compound **2.20**.

2.3.2.5 Mechanism of Reaction

Before 1969 the mechanism for cyclization the carboxylic acid and hydrazide or diacyl, aryl hydrazine in presence of phosphorus oxychloride was assumed to take place by the formation of the intermediates II, α,α'-dichloroazines,[128] as shown in Scheme 2.19

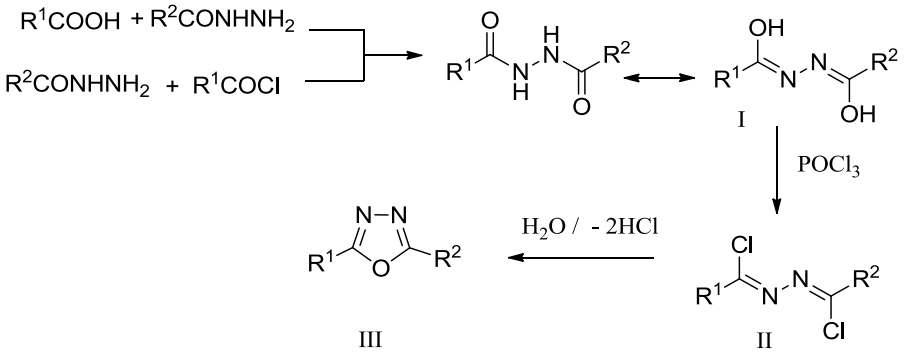

Scheme 2.19 : The suggested mechanism of formation oxadiazole through formation of α,α'-dichloroazines.

In 1969 this mechanism was disproved by Levin *et al*. [129] They proposed that compound (II) were not isolated from (I); instead only compound (I) and the hydrochloride salt were isolated. Secondly, when α,α'-dichloroazines (synthesized from a different method) was dissolved in phosphorus oxychloride, it did not give the corresponding oxadiazole. With these two observations Levin *et al*. proposed a new mechanism which is still in used until today.[130] Scheme 2.20 demonstrates Levin *et al* proposed mechanism.

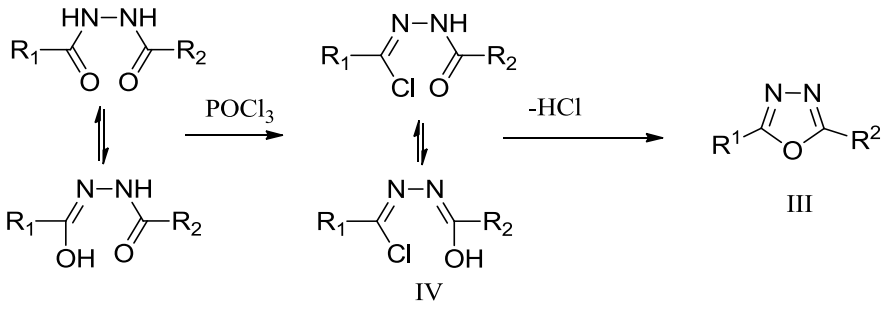

Scheme 2.20 : Levin *et al* suggested mechanism of reaction $POCl_3$.

Although the new suggested mechanism has some weak points as mentioned above, cyclization of the carboxylic acid with hydrazide or diacyl, aryl hydrazine to form the oxadiazole usually employed dehydrating agents. As $POCl_3$ is a better dehydrating agent rather than a chlorinating agent, [131] the cyclization could also take place in the presence of an alternative dehydrating agent such as concentrated H_2SO_4 or PPA, P_2O_5 and trifluroacetic acid.[123] This shows that the intermediate α-chloro-alkylideneacyl hydrazine is not a requirement to complete the cyclization. On the other hand, the behavior of $POCl_3$ in most reactions is different from the other chlorinating agents. For example, thionyl chloride could react with alcohols to obtain alkyl chloride, while $POCl_3$ gives an alkene in elimination reaction (E2)[131b]. $SOCl_2$ or PCl_3 could react with carboxylic acid to form acid chloride, while $POCl_3$ will not produce the acid chloride and only the sodium salt of carboxylic acid can form acyl chloride.[132] In

addition to that, the dehydration of amides to nitriles in the presence of $POCl_3$ is well known in the literature and it is not included in the chlorination.[133]

Bentiss and Lagrenée[134] synthesized symmetrical 2,5-disubstituted 1,3,4-oxadiazole by reacting carboxylic acid with hydrazine dihydrochloride. They proposed a different mechanism as shown in Scheme 2.21

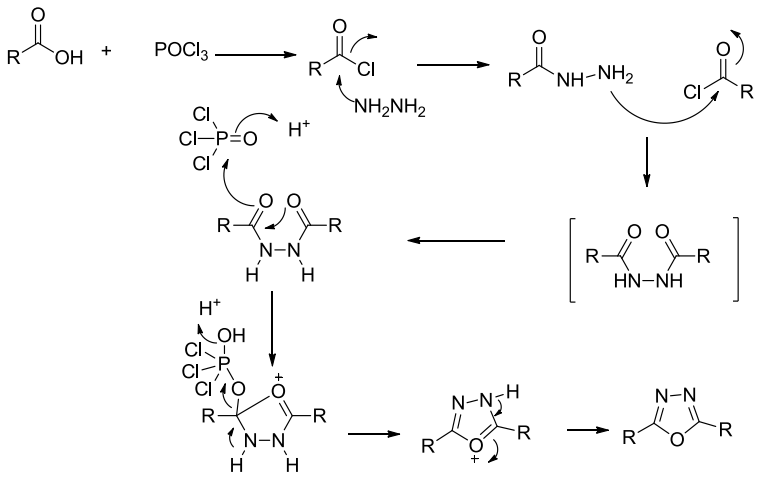

Scheme 2.21 : Proposed mechanism for 1,3,4-oxadiazole formation. [134]

This suggested mechanism was even better, and it did not include the α-chloro-alkylideneacyl hydrazine. However, the reaction of carboxylic acid with $POCl_3$ did not lead to acetyl chloride as mentioned earlier. Furthermore, Effenberger *et al.*[135] isolated the intermediates of dichlorophosphates and it can react with sodium fluoride to give acid fluoride, whereas reaction of the acid chloride with NaF did not give the acid fluoride as demonstrated in Scheme 2.22.

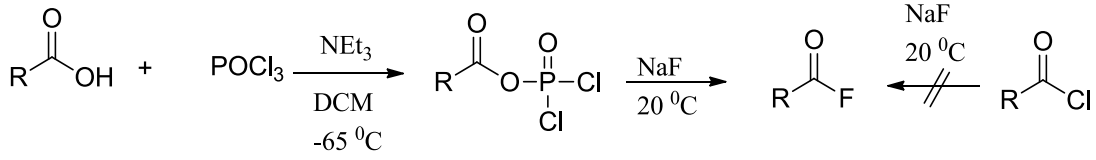

Scheme 2.22 : Reaction of $POCl_3$ with carboxylic acid.

Based on the previously reported mechanisms, we suggested our own mechanism as demonstrated in Scheme 2.23.

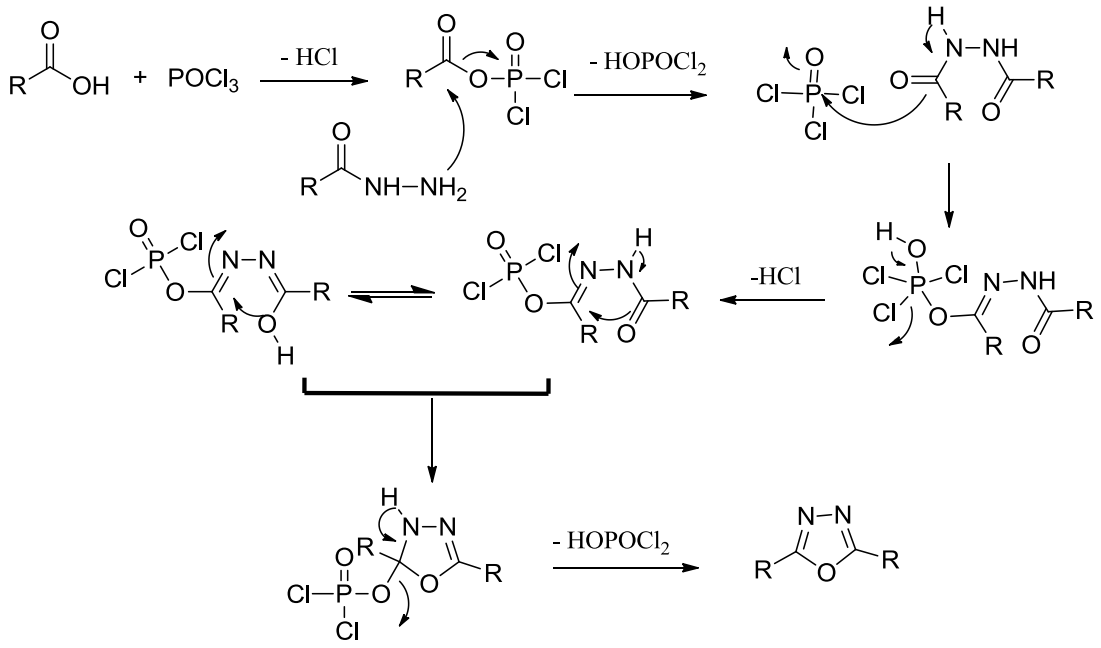

Scheme 2.23 : New suggested mechanism of cyclization in the presence of $POCl_3$.

From our observations the oxadiazole was not formed when one equivalent of $POCl_3$ was used. This reaction needs at least two equivalents of $POCl_3$ to obtain the oxadiazole. Furthermore, when an excess of $POCl_3$ was used (four or more equivalents) it did not affect the yield. On the other hand, we agree with Bentiss and Lagrenéeinone, that dichlorophosphate ion ($^{-}OPOCl_2$) will be a better leaving group than chloride ion Cl^{-}. However, we assume that the cleavage of $^{-}OPOCl_2$ from carbon sp^3 was more acceptable than sp^2; which is known to be inefficient when compared to a leaving group on sp^3 hybridized carbon.[136]

2.3.3 Synthesis of 4,4'-(5,5'-(Substituted)bis(1,3,4-oxadiazole-5,2diyl))bis(2,6-di-*tert*-butylphenol)

Seven bis-oxadiazoles bis 2,6-di-*tert*-butyl-phenol (**2.31-2.37**) were synthesized from reaction of two equivalents of 3,5-di-*tert*-butyl-4-hydroxybenzoic acid with seven different dihydrazide in the presence of $POCl_3$.

2.3.3.1 Synthesis of Dihydrazide

Seven dihydrazides (**2.24-2.30)** were synthesized by reacting diethyl esters with hydrazine hydrate. Six of the diethylesters are commercially only diethylester **2.23** was synthesized in the lab. The diesters were refluxed with an excess of hydrazine hydrate in ethanol to obtain the dihydrazide as shown in Scheme 2.24.

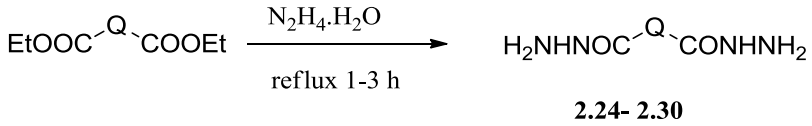

Scheme 2.24 : Synthesis of the dihydrazide.

The dihydrazides were characterized by IR, ^{1}H NMR spectrums and their melting point were compared with the melting point mentioned in literatures. The results were tabulated in Table 2.4

Table 2.4 : Structures, m.p. and the yield of the synthesized dihydrazide.

No.	NH_2NH-Q-$NHNH_2$	m.p. (°C)	Yield (%)
2.24	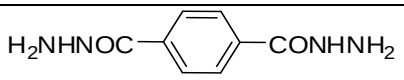	342-344 (lit.360)	92
2.25	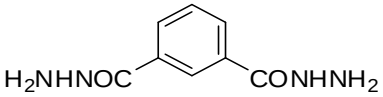	302-304 dec. (lit.>300).	87
2.26	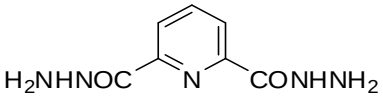	384-286 (lit. 285-286)	93
2.27	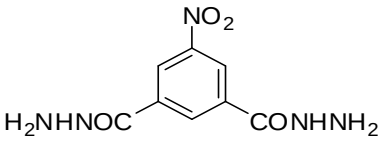	246-250 (lit.250)	90
2.28	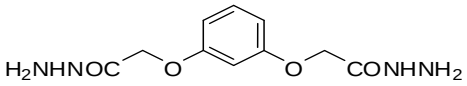	220-224 (lit. 223-224)	94
2.29	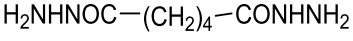	176-178 (lit. 180-182)	88
2.30	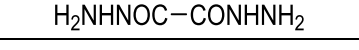	234-238 (lit. 232)	81

2.3.3.2 Formation of Bis-Oxadiazole

The bis-oxadiazoles were formed from cyclization reaction of one equivalent of dihydrazide with two equivalent of 3,5-di-*tert*-butyl-4-hydroxybenzoic acid in the

presence of $POCl_3$ as depicted in Scheme 2-25. All seven bis-oxadiazole bis-2,6-di-*tert*-butylphenol were characterized by IR,^{1}H NMR,^{13}C NMR. For further characterizations 2D NMR (DEPT-135, HSQC and HMBC) were used with compound **2.36.** Furthermore, the X-ray crystallography confirmed the molecular structure of **2.33** and **2.35.**

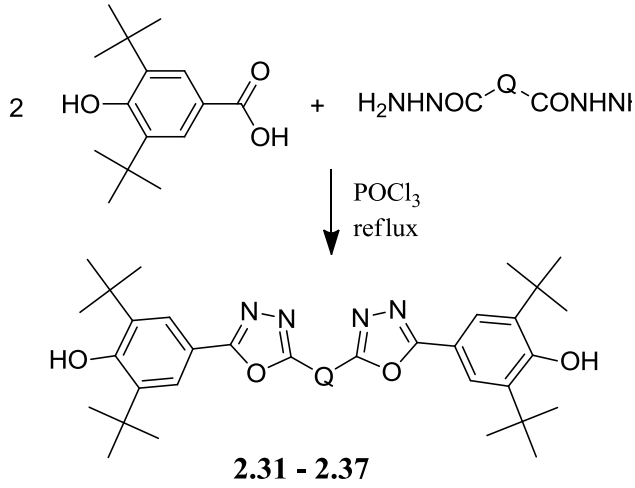

2.31 - 2.37

Scheme 2.25 : Synthesised of bis phenol bis oxadiazole.

Table 2.5: The Q group, yield, m.p., MF and the HREIMs of the bis-phenol bis-oxadiazole.

No.	Q	Yield (%)	m.p. (°C)	MF	HREIMs Found	HREIMs Calc.
2.31	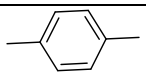	74	335-336	$C_{38}H_{46}N_4O_4$	622.3532	622.3519
2.32	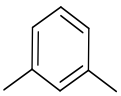	78	274-276	$C_{38}H_{46}N_4O_4$	622.3527	622.3519
2.33	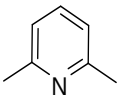	71	300-302	$C_{37}H_{35}N_5O_4$	623.3478	623.3472
2.34	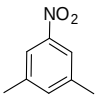	81	286-288	$C_{38}H_{45}N_5O_6$	667.3372	667.3370
2.35	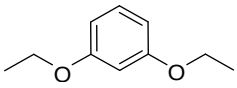	70	98-100	$C_{40}H_{50}N_4O_6$	682.3706	682.3730
2.36	$-(CH_2)_4-$	63	163-165	$C_{36}H_{50}N_4O_4$	602.3840	602.3832
2.37	$-(CH_2)_0-$	79	272-276	$C_{32}H_{42}N_4O_4$	546.3207	546.3206

2.3.3.3 Characterization of the bis-oxadiazole

All seven bis-oxdiazoles bis di-*tert*-butylphenol were characterized by IR, ^{1}H NMR, ^{13}C NMR, EIMs, HREIMs and 2D NMR was used to elucidate compound **2.36.** Two crystal structures were confirmed by the X-ray analysis. The reaction mechanism was similar with previous mono oxadiazole as discussed in Section 2.3.2.5. The only exception was that this compound needed at least four equivalents of $POCl_3$ while, the earlier mono oxadiazoles needed only two equivalents. Increasing the $POCl_3$ did not affect the yield.

2.3.3.3.1 Fourier Transform Infra-red (FTIR)

The IR spectra of compounds **2.31-2.37** showed two sharp absorption bands. One of them appeared as medium strong band at 3658-3525 cm^{-1} which is attributed to the hydroxyl of hindered phenolic group. The other observed at 1625-1610 cm^{-1} is assigned to the imine group of 1,3,4-oxadiazole ring. All the other compounds also showed stretching absorption bands at 3100–3047 cm^{-1}, 2975–2855 cm^{-1}, 1590–1457 cm^{-1} which are attributed to (C-H) aromatic, (C-H) aliphatic, (C=C) aromatic. These compounds also showed characteristic stretching absorption band at 1234-1239 cm^{-1} which was assigned to C-O. Compound **2.34** showed stretching absorption band at 1347 cm^{-1} which is assigned to Ar-NO2.

2.3.3.3.2 Nuclear Magnetic Resonance (NMR)

^{1}H NMR spectra of compounds **2.31-2.37** were carried out in $CDCl_3$. The appearance of singlet peak at δ 1.43-1.53 ppm with integration of 36 H confirmed the presence of four di-*tert*-butyl groups. In addition, the presence of the singlet peak at δ 7.8-8.03 ppm with integration of 4H and presence of OH phenol at 5.61-5.78 ppm with an integration of two protons confirmed the presence of two groups of 2,6-di-*tert*-butyl phenol.

The ^{1}H NMR spectra of group Q appeared clearly in the expected region. The appearance of a singlet at 8.3 ppm for the four protons indicates the presence of 1,4-phenylene group. Meanwhile, the appearance of three protons in compound **3.32** at 7.70 (t, *J*=7.78), 8.31(d, *J*=8.02), 8.82 (s) indicates the presence of 1,3-phenylene group identified as Q.

All the carbons of DTBP and Q groups in the bis-oxadiazole ring were clearly seen in the ^{13}C NMR. The ^{13}C-NMR spectra of the bis-oxadiazole showed characteristic peaks of 2,6-di-*tert*-butylphenol group in δ 30.17-30.27 ppm, 34.52-34.58 ppm, 113.95-115.08 ppm, 152.71-158.19 which were assigned to 4×-C($\underline{CH_3}$)$_3$, 4×$\underline{C}$(CH_3)$_3$, 2×C_4 and 2×C_1 respectively. The peaks recorded at δ 158.163.25 ppm and 165.79-167.15 ppm are attributed to the 2×C_5 and 2×C_6 for bis-oxadiazole, respectively.

The 2D NMR experiment was used in elucidating compound **2.36.** All bis-oxadiazole and the oxadiazole mentioned in Section 2.3.3.2 showed two peaks in ^{13}C NMR. For compound **2.36,** one peak with a small shoulder was observed at 165 ppm. The DEPT-135, HSQC and HMBC were able to prove that the two peaks of C=N in oxadiazole ring in compound **2.36** has the same value. The DEPT confirmed that the two peaks in ^{13}C NMR 25.04 ppm and 25.93 ppm represented the CH_2 and the peak at 30.14 ppm belonged to CH_3. Furthermore, the 124.14 ppm is for C-H_3, as demonstrated in Figure 2.8. The HSQC gave the correlation between C_7-H_7, C_8-H_8, C_{10}-H_{10} and C_3-H_3 (See Appendix A)

The HMBC allowed us to determine the correlation through long distance coupling J_3 between H_8 and C_6 in 165 and H_3 with C_5 in 165. These observations are consistent with the appearance of C=N in oxadiazole ring. A week J_2 due to 1,2 coupling in HMBC was also displayed in Figure 2.8.

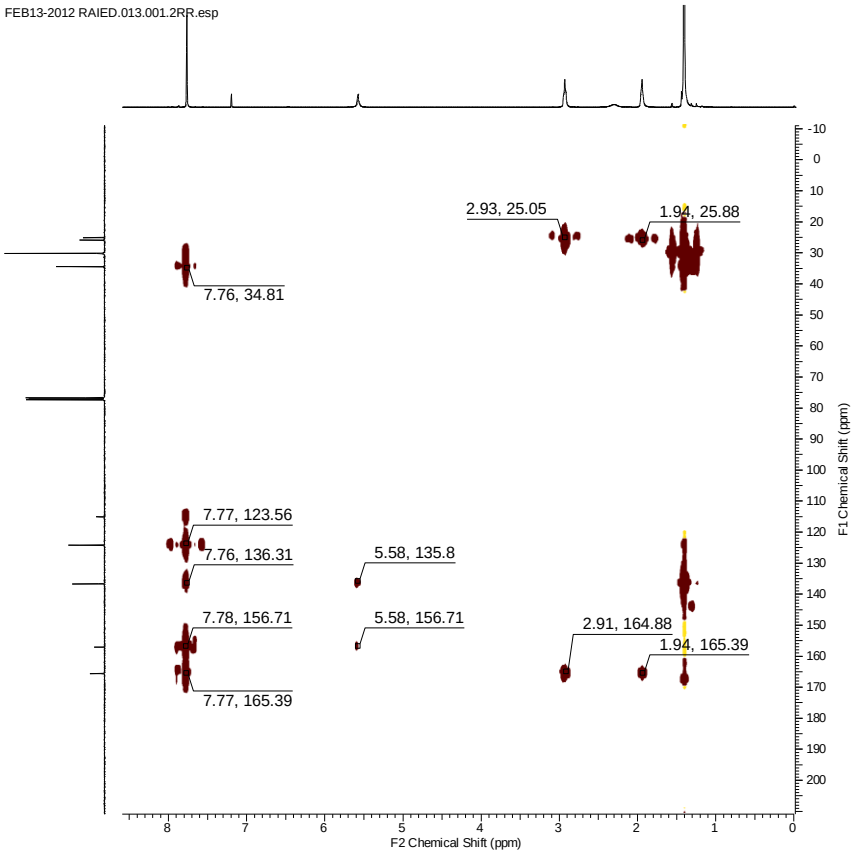

Figure 2.8 : HMBC spectrum of **2.36** shows that the C_5 and C_6 have the same value.

2.3.3.3.3 The mass spectroscopy

The EIMs and HREIMs were in agreement with the structure and the molecular formula for the new bis-oxadiazoles (See Section 6.1.7 and Appendix B).

The EIMs gave the molecular ions, whereas the base peak appeared to be the same value of molecular ions or the molecular ion minus methyl radical as mentioned earlier with 2,6-di-*tert*-butyl-4-(5-aryl-1,3,4-oxadiazol-2-yl)phenol. For example **2.31**, **2.32** and **2.37** have identical base peak value of $[M^{\cdot+}]$**,** while compound **2.34** gave the base peak as $[M^{\cdot+}\text{-}^{\bullet}CH_3]$. It is interesting to note that compound **2.33** has two base peak, m/z = 623 and 608 (see Appendix B), due to $[M^{\cdot+}]$ and $[M^{\cdot+}\text{-}^{\bullet}CH_3]$. Compounds **2.35** and **2.36** have base peak value of 233.1 which is related to the ion [2,6-di-*tert*-4-hydroxy-C_6H_2-CO]$^+$ as mention in Section 2.3.3.2. In these seven bis-oxadiazoles the losses of *iso*cyanic acid were not observed at all.

2.3.3.3.4 The X-ray Crystallography

The single crystal of compounds **2.33** and **2.35** were analyzed by X-ray crystallography. The results obtained confirmed the structures of **2.33** and **2.35**. Both compounds exhibited intermolecular hydrogen bonding between the hindered hydroxyl and the nitrogen of the oxadiazole ring. Figures 2.9 and 2.10 depicted the ORTEP structure of **2.33**, **2.35** respectively.

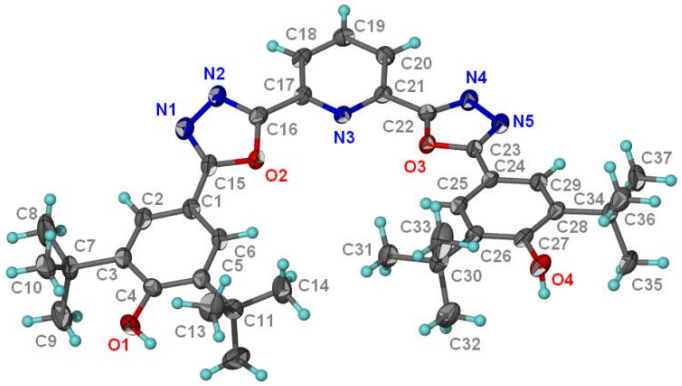

Figure 2.9 : The ORTEP of compound **2.33**.

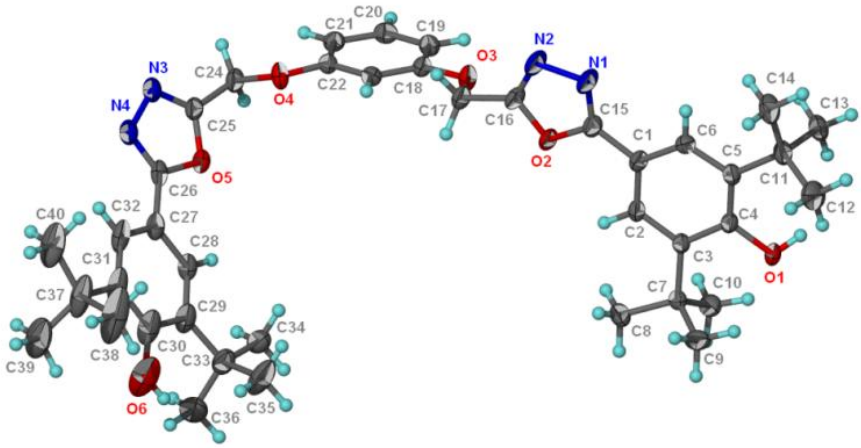

Figure 2.10 : The ORTEP of compound **2.35**.

Eleven derivatives of the substituted 1,3,4-oxadiazole attached with 2,6-di-*tert*-butylphenol and seven derivatives of bis-oxadiazole bis-2,6-di-*tert*-butylphenol were successfully synthesized. The antioxidant properties of these compounds were evaluated using both the DPPH and FRAP assay. The antioxidant results will be discussed in Chapter 4.

Chapter 3 : Synthesis of 2,4-di-*tert*-butylphenols containing different heterocyclic rings at position six

3.1 Introduction

Recently, many reports emphasized that phenol derivatives have important function in human health and therapeutic fields,[137] and also in the industry where it is used as a stabilizer [138] via their antioxidant activity. The 2,4-di *tert*-butylphenol (2,4-DTBP) is a known antioxidant and has been reported for having antioxidant ability less than BHT and BHA.[139] Khorasani *et al*.[140] have reported sequences of antioxidant activity for some hindered phenol as shown in the figure below:

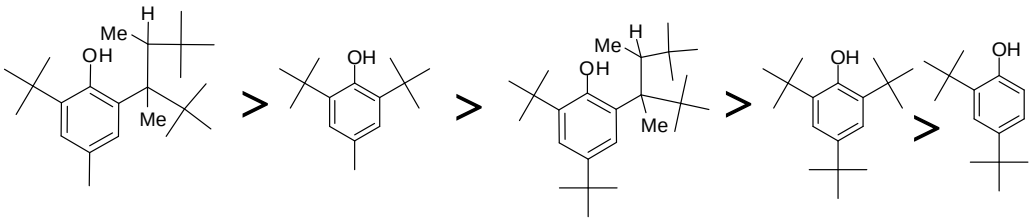

Figure 3.1 : The relation between increasing hindrance and antioxidant ability

The results published by Rosenwald in 1950[139] clearly stated that a *t*-Bu group at position *para* reduce the antioxidant ability. In this study, we aim to synthesize new 2,4-DTBP derivatives with the intention of improving their antioxidant properties. There are two challenges in this work, i.e. to increase the steric hindrance around hydroxyl group and overcome of the negative effect of the *t*-Bu group in position *para*. Therefore, we proposed to form a heterocyclic ring on position six. By doing so, this ring could improve the antioxidant activity of our targeted compounds by increasing the steric hindrance around the hydroxyl group of phenol. Furthermore, the antioxidant ability could be increased by the long term resonance due to the participation of the

heterocyclic ring in the resonance structures, which in return could increase the stability of phenoxyl radical. These two reasons inspire us to prepare different kind of heterocyclic ring at position six and then evaluate their antioxidant activity to confirm our hypothesis. By combining the biological activity for salicyl derivatives (which are known as bioactive material) a good antioxidant properties could be a promising bioactive compounds. Therefore, these synthesized compounds could have potential as a good therapeutic application in the near future.

3.2 Results and Discussion

Twenty six new compounds were synthesized, including sixteen heterocyclic rings, which were formed at position six of 2,4-DTBP. These compounds have steric hindrance phenol which can lead to higher antioxidants activity.[141] These rings could be responsible for promoting the antioxidant activity by increasing the steric hindrance around the hydroxyl of phenol. Involvement of these rings in the resonance structure could play an important role in enhancing the antioxidant ability. The 2,4-DTBP recorded a less antioxidant abilities than BHT. Clearly, there are two factors involved in decreasing their antioxidant properties. 2,4-DTBP is less sterical henderance than BHT since it did not have a methyl group in *para* position (which is important in antioxidant radical stability). However, it has a *t*-Bu in *para* position which is inoperative for antioxidant properties. For that, our aims are to synthesize derivatives of 2,4-DTBP that have a higher antioxidants ability than 2,4 di-*tert*-butylphenol or nearer to BHT.

3.2.1 Synthesis of 2,4 di-*tert*-butylphenols derivatives.

New heterocyclic compounds were synthesized consisting of a five membered ring. The sixth position of 2,4-DTBP was attached to 5-aryl-1,3,4-oxadiazole, 1,3,4-oxadiazole-5-thione and their thioalkyl, 5-amino-1,3,4-oxadiazole, 5-amino-1,3,4-

thiadiazole, 4-amino-1,2,4-triazole-3-thione and 4-aryl-1,2,4-triazole-5thione as demonstrated in Scheme 3.1.

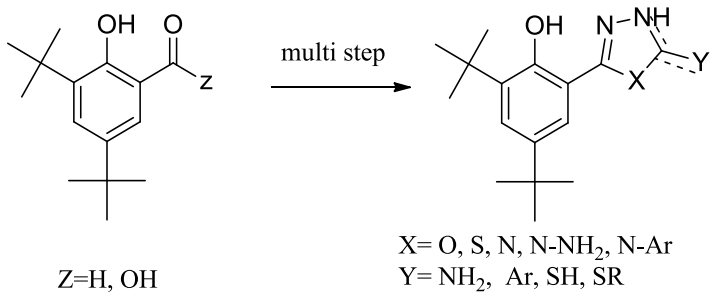

Scheme 3.1 : Schematic route for the formation of five membered heterocyclic ring

3.2.1.1 Synthesis of 2,4-di-*tert*-butyl-6-(5-aryl-1,3,4-oxadiazol-2-yl)phenol (3.5-3.8)

Four compounds of 2,4-di-*tert*-butyl-6-(5-(substituted)-1,3,4-oxadiazol-2-yl) phenol (**3.5-3.8**) were synthesized in a two step reaction. First, four new hydrazones were synthesized (**3.1-3.4**) from reaction of 3,5-di-*tert*-butyl-2-hydroxybenzaldehyde with hydrazide in ethanol (Scheme 3.2).

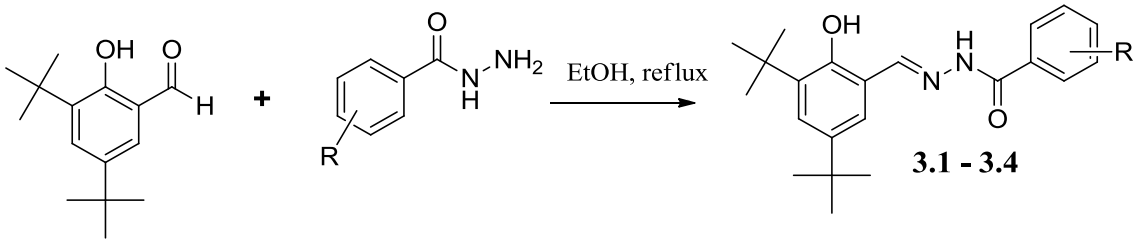

Scheme 3.2 : Synthesis of the hydrazones.

The hydrazone formation is one of the known reactions that came from condensation of amine group with aldehyde and losing H_2O to form imine (which is also known as Schiff base or azomethine). If acid hydrazide is used instead of aliphatic or aromatic amine, those compounds are called hydrazones. These four compounds were characterized by IR, 1D NMR, 2D NMR, EIMS and HREIMs. Table 3.1 demonstrated some properties of the hydrazones

Table 3.1: Experimental data of the synthesized hydrazones.

No.	R	Yield (%)	m.p. (°C)	FW	HREIMS Found	HREIMS calculate
3.1	4-CH_3	87	314-316	$C_{23}H_{30}N_2O_2$	366.2310	366.2307
3.2	4-OCH_3	95	258-260	$C_{23}H_{30}N_2O_3$	382.2250	382.2256
3.3	4-Br	95	276-278	$C_{22}H_{27}BrN_2O_2$	430.1084	430.1256
3.4	2-Cl	90	228-230	$C_{22}H_{27}ClN_2O_2$	386.1763	386.1761

In the second step, the synthesized hydrazones were cyclized in the presence of equivalent bromine (as oxidative agent) in glacial acetic acid and two equivalents of anhydrous sodium acetate. This method was modified from literature[142] to offer good yield and all oxadiazoles were recrystallized from suitable solvent. The following Scheme 3.3 demonstrated the reaction pathway:

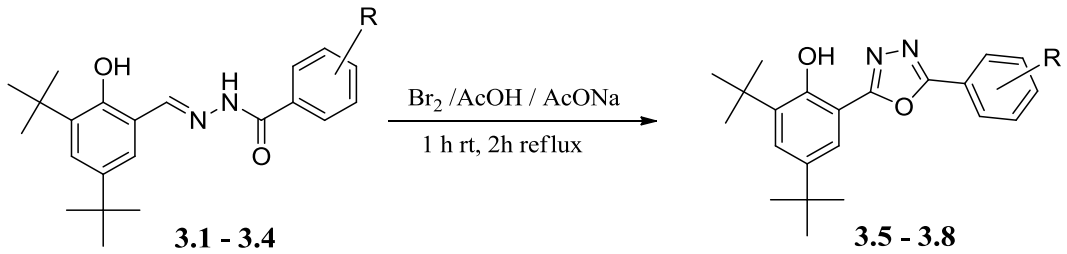

3.1 - 3.4 **3.5 - 3.8**

R= 4-CH_3, 4-OCH_3, 4-Br, 2-Cl

Scheme 3.3 : Formation the 1,3,4-oxadiazole from the hydrazone.

The oxadiazole were characterized by IR, ^{1}H NMR, ^{13}C NMR, EIMs, HREIMs and compound **3.6** was studied further by DEPT-135, HMQC and HMBC to determine the structure. The single crystal X-ray was used to confirm the structure of compounds **3.5** and **3.8**. Table 3.2 shows some experimental data of the synthesized compounds.

Table 3.2 : Experimental data of the synthesized oxadiazole.

No.	R	Yield (%)	m.p. (°C)	FW	HREIMS Found	HREIMS Calculate
3.5	4-CH_3	70	184-186	$C_{23}H_{28}N_2O_2$	364.2162	364.2151
3.6	4-OCH_3	74	170-172	$C_{23}H_{28}N_2O_3$	380.2102	380.2100
3.7	4-Br	79	158-162	$C_{22}H_{25}Br^{79}N_2O_2$	428.1102	428.1099
3.8	2-Cl	80	138-140	$C_{22}H_{25}Cl^{35}N_2O_2$	384.1605	384.1605

3.2.1.2 Synthesis of 6,6'-(5,5'-(1,3 or 1,4-phenylene)bis(1,3,4-oxadiazole-5,2 diyl))bis(2,4-di-*tert*-butylphenol)

Two bis-oxadiazole bis (2,4-di-*tert*-butylphenol) were synthesized from their dihydrazones. The dihydrazone was synthesized from the reaction of two equivalents of 3,5-di-*tert*-butyl-2-hydroxybenzaldehyde and dihydrazide. The reaction proceeded using glacial acetic acid as the solvent to give good yield (see Section 6.2.2). The products were recrystallized from ethanol. The pathway of reaction can be described in Scheme 3.4

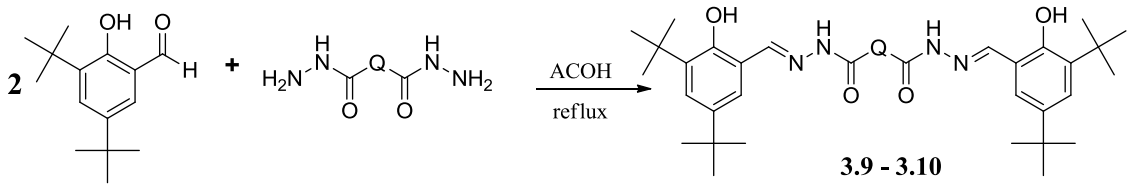

Scheme 3.4 : Formation of the bis-hydrazones.

The bis-hydrazones were characterized by IR, ^{1}H NMR, ^{13}C NMR, EIMs and HREIMS spectrums. The structures were confirmed by spectroscopic technique and the data are summarized in Table 3.3

Table 3.3 : Experimental data of bis-hydrazones

No	Q	Yield (%)	m.p. (°C)	FW	HREIMS Found	HREIMS Calc.
3.9	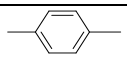	89	344-348 dec.	$C_{38}H_{50}N_4O_4$	626.3833	626.3832
3.10		85	320-324 dec.	$C_{38}H_{50}N_4O_4$	626.3826	626.3832

Bis-oxadiazoles were obtained from their respective dihydrazone through the same procedure reported in Section 6.2.3. The dihydrazone were treated with two equivalents of bromine and four equivalents of anhydrous sodium acetate (Scheme 3.5).

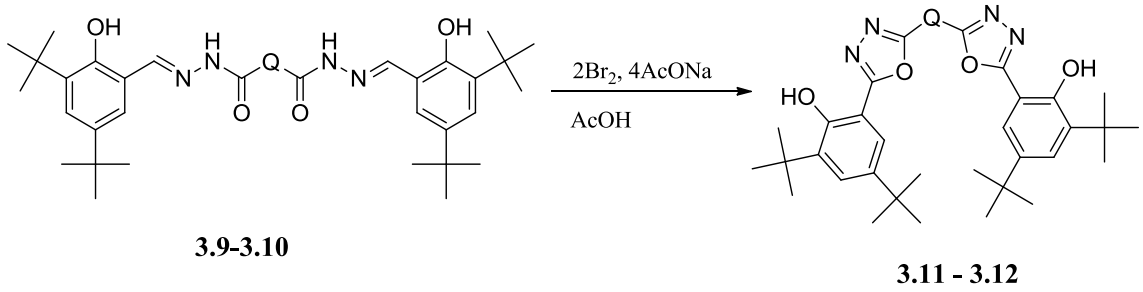

3.9-3.10 **3.11 - 3.12**

Scheme 3.5 : Synthesis of bis-oxadiazole from their bis-hydrazones

The bis-oxadiazoles structures were confirmed by IR, ^{1}H NMR, ^{13}C NMR, EIMs and HREIMS.

Table 3.4: Experimental data of bis-oxadiazole

No	Q	Yield (%)	m.p. (°C)	FW	HREIMS Found	HREIMS Calc.
3.11	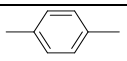	70	288-290	$C_{38}H_{46}N_4O_4$	622.3516	622.3519
3.12	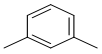	78	172-174	$C_{38}H_{46}N_4O_4$	622.3506	622.3519

3.2.1.3 Synthesis of 2,4-di-*tert*-butyl-6-(5-thio-4-hydro-1,3,4-oxadiazol-2-yl) phenol.and their derivatives

The 2,4-di-*tert*-butyl-6-(5-thio-4-hydro-1,3,4-oxadiazol-2-yl)phenol.was synthesized in three steps. In the first step, 3,5-di-*tert*-butylsalicylic acid was converted to methyl ester **3.13**. The esterification was carried out by reacting the targeted acid with methyl iodide in the presence of sodium hydrogen carbonate by refluxing for nine hours to obtain a good yield. The second step was to synthesize the acid hydrazide from the corresponding ester. By using normal hydrazinztion procedure, hydrazide **3.14** was obtained in low yield. On the other hand, by using melt method, **3.14** was isolated in excellent yield (96%). This hydrazide can also be considered as a good substance to

form many different types of heterocyclic ring at position six. This will increase steric hindrance, and could also increase the antioxidant activity. In the Final step, the acid hydrazide will react with carbon disulfide in the presence potassium hydroxide to give high yield of the desired product. The outline of these three steps is described in Scheme 3.6.

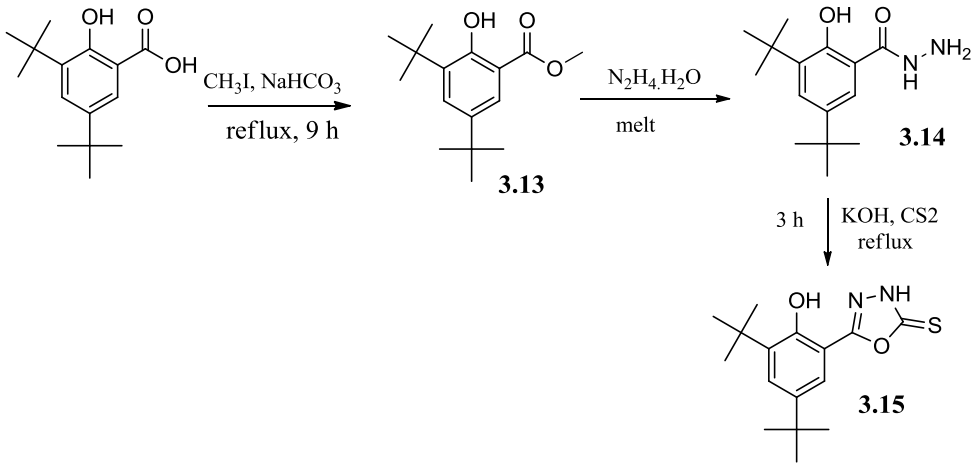

Scheme 3.6 : Synthesis of 2,4-di-*tert*-butyl-6-(5-thio-4-hydro-1,3,4-oxadiazol-2-yl) phenol

The 2,4-di-*tert*-butyl-6-(5-thio-4-hydro-1,3,4-oxadiazol-2-yl)phenol. **3.15** was characterized by IR, ^{1}H NMR, ^{13}C NMR, EIMs and HREIMs. The collected data was in agreement with the suggested structure. Three derivatives of 2,4-di-*tert*-butyl-6-(5-(alkylthio)-1,3,4-oxadiazol-2-yl)phenol (**3.16-3.18**) were synthesized from alkylation reaction of **3.15** in acetone. Three alkyl halide was used in the presence of anhydrous potassium carbonate as base at room temperature. Scheme 3.7 describes the reaction pathway.

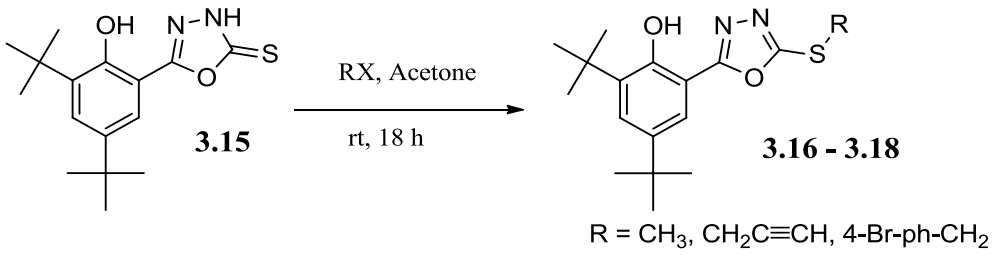

Scheme 3.7 : Alkylation of **3.15**.

These compounds were characterized by IR, 1D, 2D NMR, EIMs and HREIMs. The results were tabulated in Table 3.5.

Table 3.5 Experimental data of **3.16 - 3.18**.

No.	R	Yield (%)	m.p. (°C)	FW	HREIMS Found	HREIMS Calculate
3.16	$-CH_3$	83	100-102	$C_{17}H_{24}N_2O_2S$	320.1562	320.1558
3.17	$-CH_2C{\equiv}CH$	86	108-110	$C_{19}H_{24}N_2O_2S$	344.1558	344.1558
3.18	$-CH_2C_6H_4$-4-Br	78	118-120	$C_{23}H_{27}BrN_2O_2S$	474.0960	474.0956

3.2.1.4 Synthesis of 2,4-di-*tert*-butyl-6-(5-amino-1,3,4-oxadiazol-2-yl)phenol (3.19)

This compound was synthesized by reacting 3,5-di-*tert*-butyl-2-hydroxybenzo-hydrazide, **3.14** with cyanogen bromide at room temperature (in methanol) in the presence of sodium hydrogen carbonate as scavenger. The product was characterized by using IR, ^{1}H NMR, ^{13}C NMR and EIMs, HREIMs spectra. The DEPT-135 was used to distinguish between the aromatic protons and the amine. The reaction was shown in Scheme 3.8. Further explanation on the characterization is given in Section 3.2.2.6.

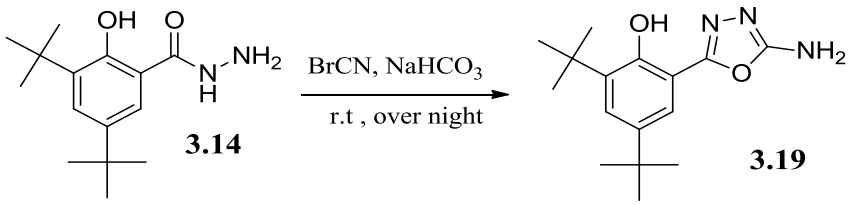

Scheme 3.8 : Synthesis of 2,4-di-*tert*-butyl-6-(5-amino-1,3,4-oxadiazol-2-yl)phenol.

3.2.1.5 Synthesis of 2,4-di-*tert*-butyl-6-(5-amino-1,3,4-thiadiazol-2-yl)phenol

The thiadiazole which is known for their pharmacological effects (as mentioned earlier) was formed at position six of 2,4-DTBP by two different methods. The first one was from its hydrazinecarbothioamide. The 2-(3,5-di-*tert*-butyl-2-hydroxybenzylidene) hydrazinecarbothioamide **3.20** was synthesized via condensation of the 3,5-di-*tert*-

butyl-2-hydroxybenzaldehyde with thiosemicarbazide in ethanol and glacial acetic acid (Scheme 3.9)

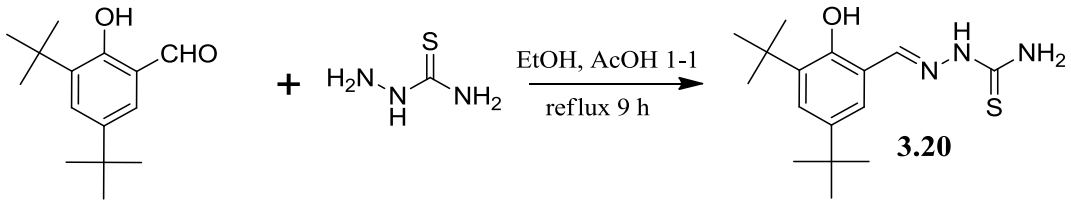

Scheme 3.9 : Synthesis of thiosemihydrazone **3.20**.

The synthesized product reacted with bromine in the same reaction conditions described in Section 3.2.1.1 to produce compound **3.21** in 81% yield after purification; the reaction path was described in Scheme 3.10.

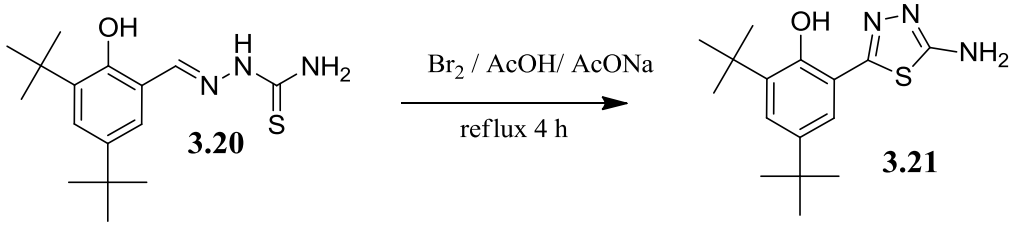

Scheme 3.10 : Synthesis of thiadiazole **3.21**, method A.

In the second method, 3,5-di-*tert*-butyl-2-hydroxybenzoic acid was reacted with thiosemi-carbazide in the presence of $POCl_3$ and this reaction is similar to the reactions described in Chapter 2. Scheme 3.11 explained the reaction path:

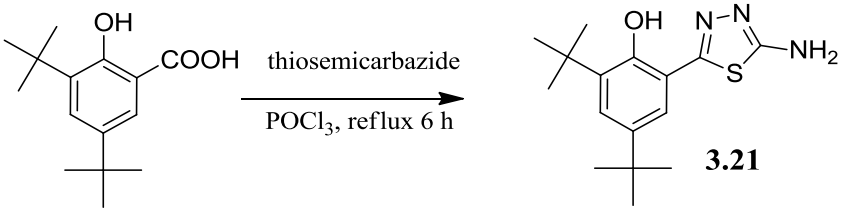

Scheme 3.11 : Synthesis of thiadiazole **3.21**, method B.

The yield of this reaction was unsatisfactory (less 50%) and we decided to go ahead with the first method.

3.2.1.6 Synthesis of 2,4-di-*tert*-butyl-6-(4-amino-1,2,4-triazol-3-yl-5-thione) phenol

As mentioned earlier, hydrazide **3.14** is considered as a good starting material to formed different types of heterocyclic ring at position six. Therefore, we would like to design 4-amino-1,2,4-triazole at position six starting from hydrazide **3.14.** The hydrazide was stirred with carbon disulfide and potassium hydroxide at room temperature in absolute ethanol to produce the potassium salt of hydrazine carbodithioate. After washing the salt with diethyl ether and cyclized with hydrazine hydrate it give rise to the target **3.22** in good yield. The following Scheme 3.12 described the reaction pathway:

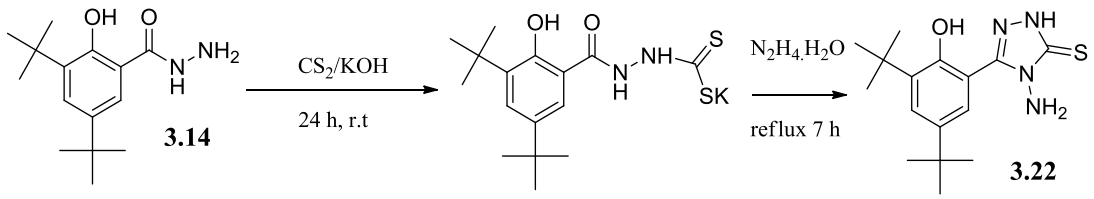

Scheme 3.12 : synthesis of 2,4-di-*tert*-butyl-6-(4-amino-1,2,4-triazol-3-yl-5-thione)phenol

3.2.1.7 Synthesis of 2,4-di-*tert*-butyl-6-(4-aryl-1,2,4-triazol-3-yl-5-thione)phenol

The target compounds (**3.26-3.28**) were prepared in two stages. The first stage was the formation of N-(aryl) hydrazinecarbothioamide (**3.23-3.25**) from the reaction of hydrazide with three different substituted phenyl isothiocynate in ethanol at 50 ºC for 3h. The product was then treated with 4N sodium hydroxide solution and refluxed for 3h to give the target compound. The reaction was demonstrated in Scheme 3.13 The compounds were characterized by IR, ^{1}H NMR, ^{13}C NMR, EIMs and HREIMs. 2D NMR was also used to clarify the ^{1}H NMR spectrum of **3.2** and **3.4**. The X-ray analysis was used to confirm the structures of **3.26.**

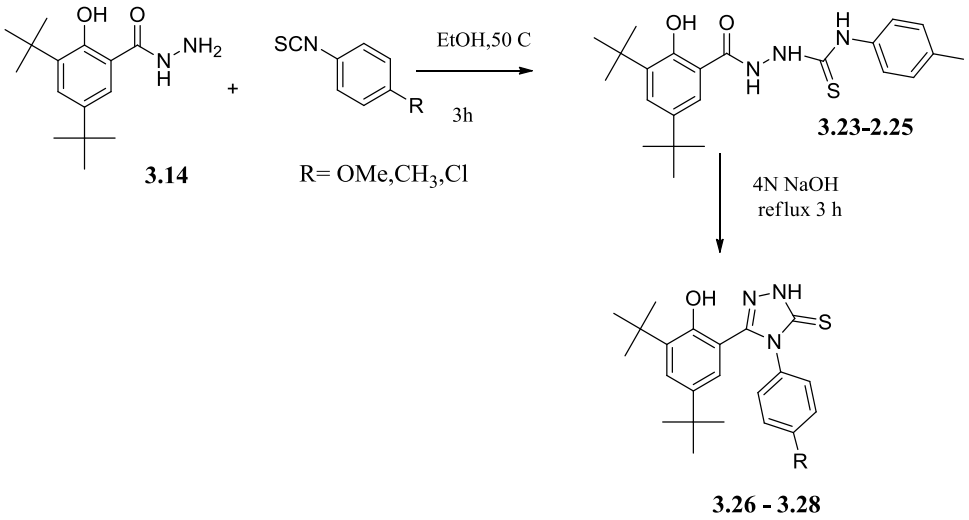

Scheme 3.13 : Pathway of synthesis the triazoles.

The experimental data are summarized in Table 3.6.

Table 3.6 : Experimental data of **3.23-3.28**.

No	R	Yield (%)	m.p. (°C)	FW	HREIMS Found	HREIMS Calculate
3.23	-OCH_3	94	168-170	$C_{23}H_{31}N_3O_3S$	429.2096	429.2086
3.24	-Cl	95	196-198	$C_{22}H_{28}ClN_3O_2S$	433.1595	433.1591
3.25	-CH_3	95	162-164	$C_{23}H_{31}N_3O_2S$	413.2122	413.2110
3.26	-OCH_3	70	300-302 dec	$C_{23}H_{29}N_3O_2S$	411.1987	411.1980
3.27	-Cl	66	238-240	$C_{22}H_{26}ClN_3OS$	415.1488	415.1485
3.28	-CH_3	72	236-238 dec	$C_{23}H_{29}N_3OS$	395.2030	395.2031

3.2.2 Product characterization

3.2.2.1 Characterization of *N'*-[(3,5-di-*tert*-butyl-2-hydroxyphenyl)methylidene] -substituted benzohydrazide (hydrazones 3.1-3.4)

The disappearance of the aldehyde and the primary amine peaks from the IR spectrum indicates that the reaction was successful. The secondary amide at 3160-3174 cm^{-1}, the carbonyl at 1651-1664 cm^{-1} and a new peak in the range of 1611-1613cm^{-1} for imine group (CH=N) further assured that the reaction was successful.

The ^{1}H NMR spectra also confirmed the formation of hydrazones. The two peaks at 1.24-1.42 ppm (with integration value of nine protons) indicate that there were two groups of di-*tert*-butyl at position 2 and 4 of phenol group. The two hydrogens of position three and five for phenol appeared in 7.16-7.23 ppm and 7.26-7.32 ppm respectively as a doublet peak with a coupling constant of 2.2-2.38 Hz due to the *meta* splitting.[122] In addition, the proton of the imine has an integration equals to one at 8.42-8.56 ppm. Finally, both protons of OH and NH appeared at 12.05-12.28 ppm and in the range of 12.15-12.23 ppm. Two peaks of NH and OH were difficult to be resolved because they appeared in a close range. By utilizing 2D NMR, we able to resolve this problem and we will discuss it in the following section.

The ^{13}C NMR spectra are able to identify the skeleton structure of the hydrazones. The spectrum showed the two peaks for the *t*-Bu (29.26-31.49 ppm) and the two quaternary carbons (31.26-35.19 ppm). The imine group appeared at 150-155 ppm and the carbonyl of hydrazones was at 162-163 ppm. (Section 6.2 and Appendix A) Although it was difficult to distinguish between the carbons that is attached to phenol hydroxide and the carbon of an imine group, the HMQC and HMBC were able to allow us to distinguish between NH and OH, as well as between C-OH and CH=N. Compound **3.2** was used as example to illustrate this problem.

From HMQC spectrum we are able to distinguish the carbon of imine through the correlation between the hydrogen of imine and its carbon. The correlation between hydrogen and carbon for the two groups of di-*tert*-butyl at position two and four, showed the correlation between H_3, C_3 and H_5, C_5. Figure 3.2 showed an expansion of HMQC and correlations between H_7-C_7 for the imine group are at 8.54- 150.55.

The HMBC spectrum disclosed the correlation for long distance coupling J_3 and weak for J_2. The most important correlation is the hydrogen of phenol hydroxyl at 12.27

ppm with C_6, C_2 and C_1. The NH at 12.04 ppm shows correlation with a carbonyl group C_8. The proton of imine group shows correlation with C_1. H_{10} exhibited correlation with C_{12} and C_8 while, H_{11} show correlation with H_9. Figure 3.3 showed an expansion of the HMBC mentioned.

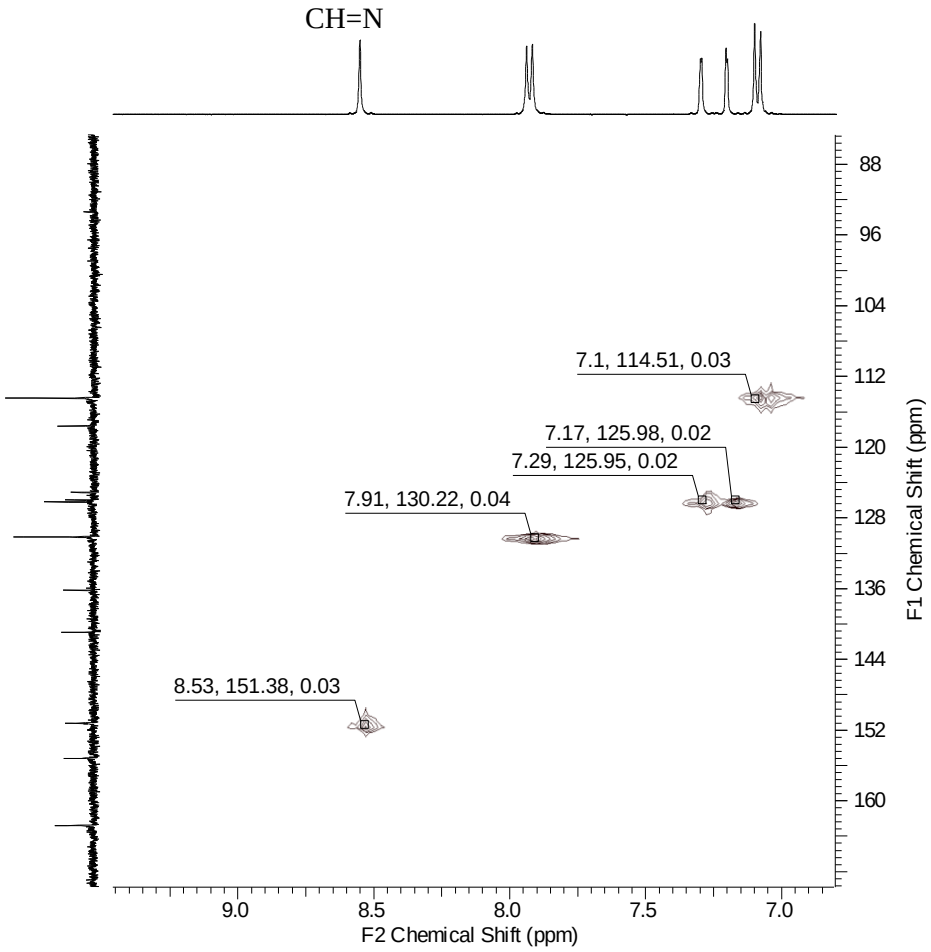

Figure 3.2:: The HMQC expansion of **3.2**.

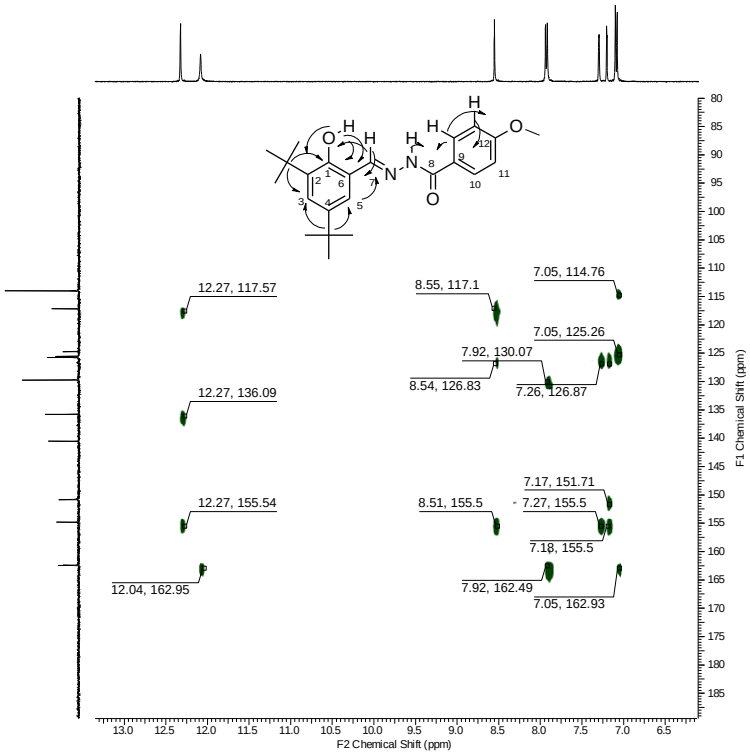

Figure 3.3: HMBC expansion of **3.2**.

The EI-mass showed the molecular ion as $M^{\bullet+}$ for all hydrazones. These fragmentations for compound **3.2** were explained in Scheme 3.14. The observed HREIMs values were in agreement with the calculated value.

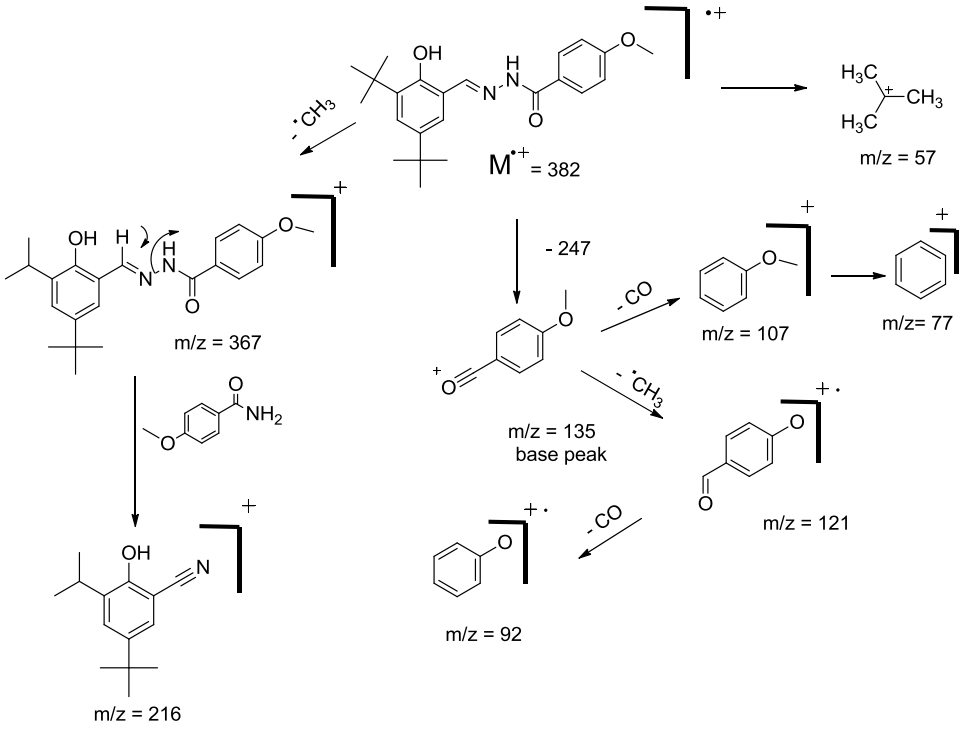

Scheme 3.14 : Mass fragmentation of **3.2**.

3.2.2.2 Characterizations of 2,4-di-*tert*-butyl-6-(5-aryl-1,3,4-oxadiazol-2-yl) phenol. (3.5-3.8)

The four oxadiazoles were characterized by IR, ^{1}H NMR, ^{13}C NMR, 2D NMR, HREIMs and EIMs. The disappearance of the carbonyl group (1651-1664 cm^{-1}) in hydrazones, the NH (3160-3175 cm^{-1}) and the shift in the value for C=N (in the oxadiazole) were some of the indicators that the cyclization has occurred.

The ^{1}H NMR spectra displayed all expected peaks in oxadiazole structure (see Section 6.2.1 and Appendix A). Two peaks at 165.39-165.85 ppm and 161.45-164.24 ppm indicated the two C_7 and C_8 of C=N in oxadiazole ring. We also observed the disappearance of CH=N (for the hydrazone) at 150-152 ppm and the carbon of carbonyl at 162-163 ppm. 2D NMR was used to determine the success of the acyclization and to help in structure elucidation (Figure 3.4).

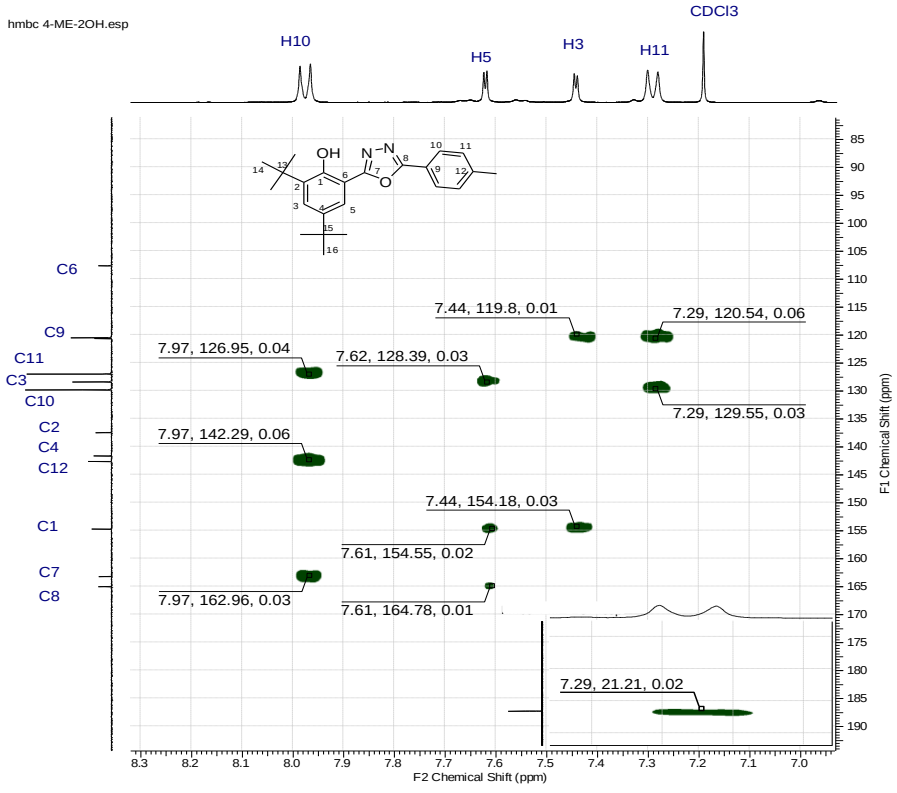

Figure 3.4 : HMBC expansion of aromatic region of **3.5**.

For compound **3.5** (Figure 3.3), the correlation between H_{10} with C_{11}, C_{12} and C_8 and the correlation of H_5 with C_3, C_1 and C_7 were extremely useful in distinguishing between the two carbons in the oxadiazole ring. Furthermore, through the long coupling of H_{11} with the carbon of 4-methyl group H_{11} and H_{10} were easily distinguished.

The HREIMs were in agreement with the calculated exact mass value. Moreover, the EIMs fragmentations matched with the proposed structure. The loosing of *iso*cyanic acid was also observed in the oxadiazoles. The next steps of losing *iso*cyanic acid (HNCO) further strengthen our proposed structure. Scheme 3.15 demonstrated the proposed pathway of losing HNCO from compound **3.6.**

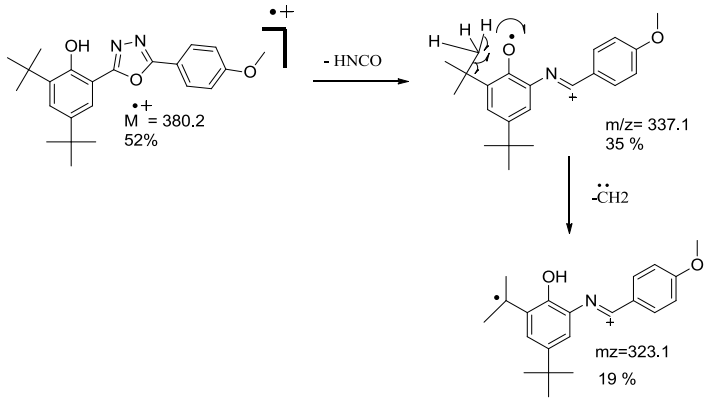

Scheme 3.15 : Proposed pathway of losing HNCO from the oxadiazole and their next step.

Table 3.7 tabulated the molecular ions, base peak, losing *iso*cyanic acid and the next step for losing HNCO.

Table 3.7 : The EI mass for the oxadiazoles and the losing HNCO value with next step.

No.	**M $^{\bullet+}$**	**%**	**Base peak 100%**	**-HNCO**	**%**	**Next step**	**%**
3.5	364.2	52	349.1(-CH_3radical)	321.1	2	307.1(- **:**CH_2)	20
3.6	380.2	52	366.1(-CH_3radical)	337.1	5	323.1(- **:**C H_2)	9
3.7	428.1	50	413.1(-CH_3radical)	387.0	1	371.0(- **:**C H_2)	20
3.8	384.1	40	369.1(-CH_3radical)	341.1	2	327.0(- **:**C H_2)	5

From this table we can conclude that these compounds behaved similarly in mass spectroscopy. Besides losing the HNCO, the other pattern can also be described in the following scheme.

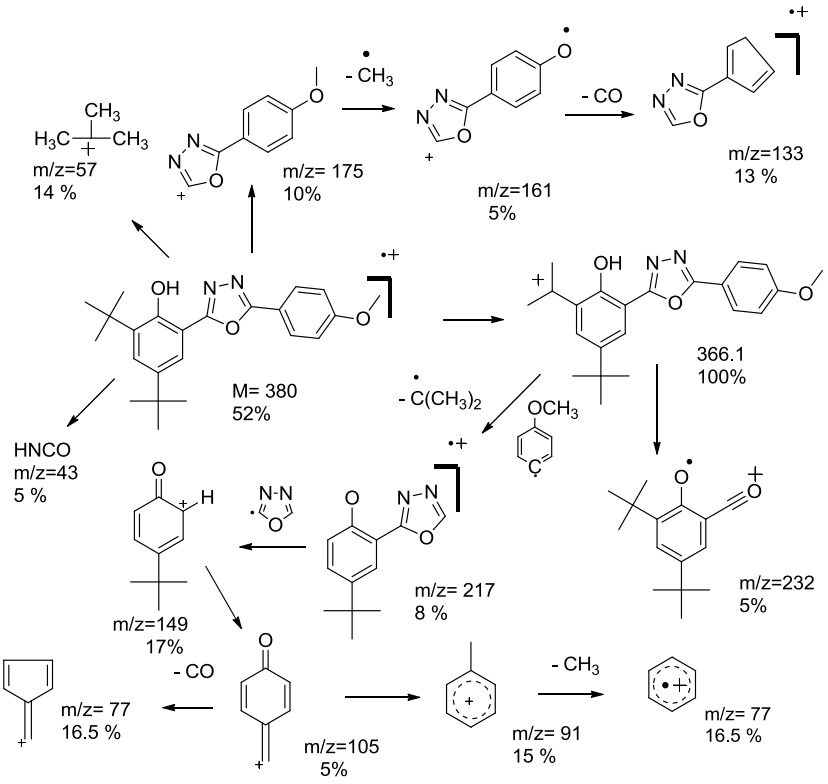

Scheme 3.16 : EI mass fragmentations of 3.6.

The structure of **3.5** was confirmed by X-ray analysis; the crystal system was formed as monoclinic and the refinement data was shown in Appendix C. Figure 3.5 showed the ORTEP diagram.

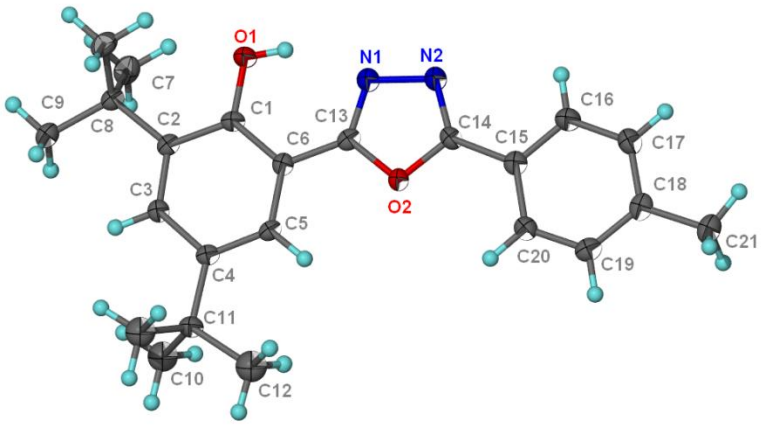

Figure 3.5 : The molecular structure of **3.5**.

The X-ray showed the hydrogen bonding between the protons of hydroxyl in phenol with N_1 in oxadiazole ring (see Appendix C). In addition to that, the crystal system of **3.8** was confirmed and the ORTEP diagram displayed the structure of **3.8** in Figure 3.6 (for more detail see Appendix C).

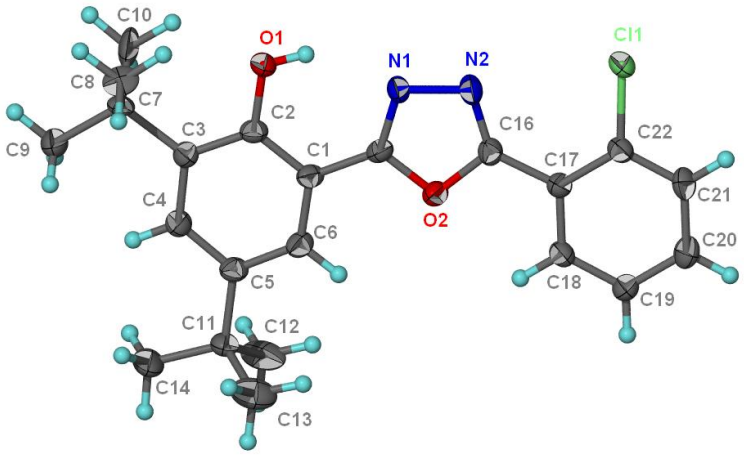

Figure 3.6 : The ORTEP diagram of **3.8**.

3.2.2.3 Characterizations of 1-*N'*-[(3,5-di-*tert*-butyl-2-hydroxyphenyl)methyl]-X-*N'*-[(3,5-di-*tert*-butyl-2-hydroxyphenyl)methylidene]substituted-dicarbohydrazide and butylphenol). (3.9-3.10)

The bis-hydrazones were characterized by IR, ^{1}H NMR, ^{13}C NMR, HREIMs and EIMs. The IR spectra for these compounds exhibited the OH of phenol, both C-H aliphatic and aromatic, the C=O and the C=N of bishydrazones. ^{1}H NMR displayed all the expected protons for example, the two group of di-*tert*-butyl and the aromatics proton besides the proton of imine the NH and OH phenol in high field. Compounds **3.9** and **3.10** were difficult to dissolve in deuterated solvent and the best solvent was DMSO-d_6 : $CDCl_3$ (4:1) at 70 ºC. We are able to get a clear ^{1}H NMR spectrum, but not a good ^{13}C NMR for those compounds. However, the HREIMs were able to confirm the accurate mass value, and the EIMs fragmentations give us a good picture of the proposed structure. Furthermore, these compounds were identified from the next step

(formation the bis-oxadiazole rings). The bis-oxadiazoles **3.11** and **3.12** cannot be formed from this reaction unless the structure of compounds **3.9** and **3.10** were correct. The ^{13}C NMR spectra for compound **3.11** and **3.12** have all the significant peaks e.g. two group of di-*tert*-butyl group peaks, the peaks of 1,4 phenylene as well as the two peaks for the oxadiazole rings.

The HREMs provide the accurate mass for the bishydrazones. The EIMs show the $M^{\cdot+}$and the other fragmentations which match with the hydrazones structure. The Scheme 3.17 showed some of these fragmentions.

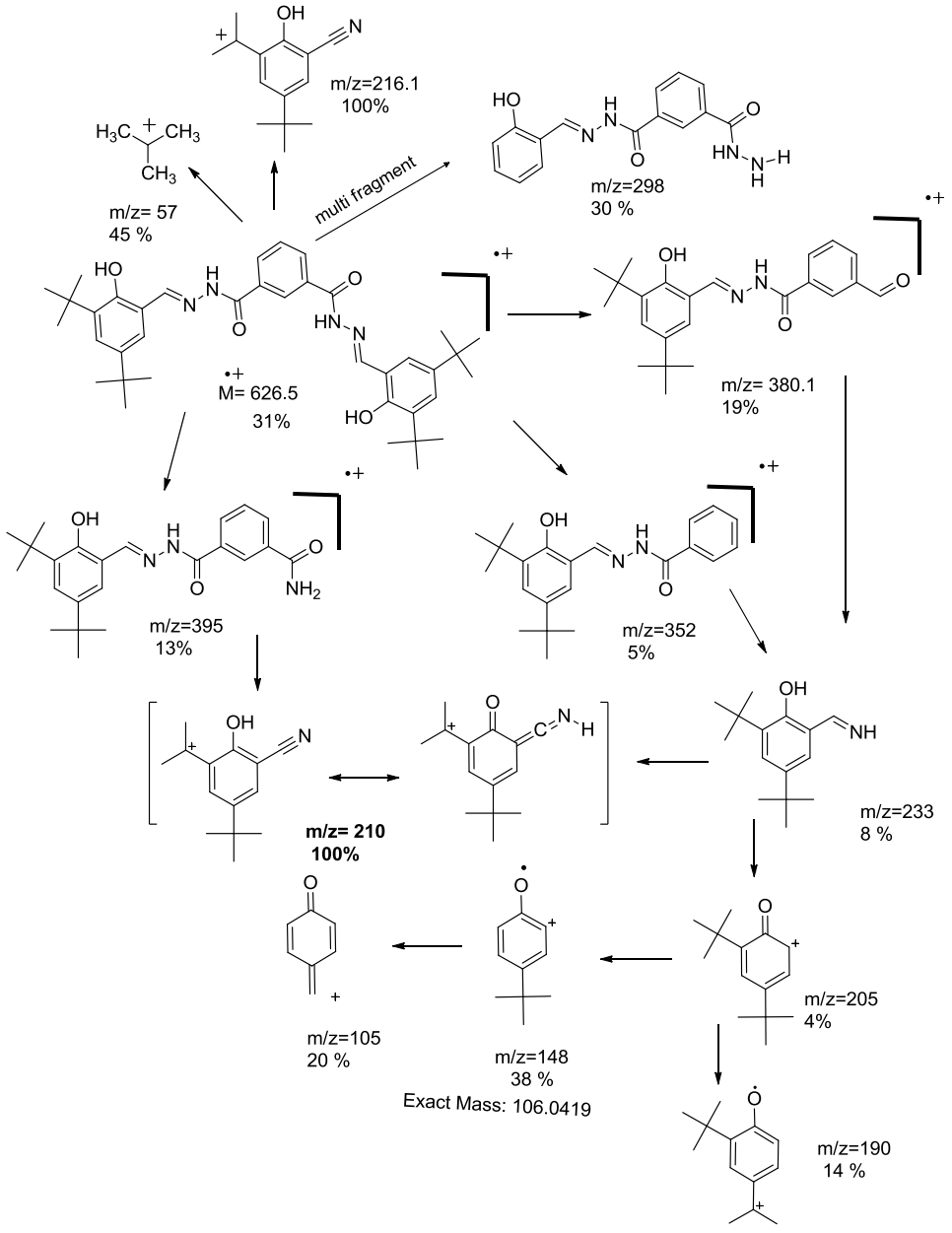

Scheme 3.17 : EI mass fragmentations of **3.10**.

3.2.2.4 Characterizations of 6,6'-(5,5'-(1,3 or 1,4-phenylene)bis(1,3,4-oxadiazole-5,2-diyl))bis(2,4-di-*tert*-butylphenol)

IR spectrum were able to give a rough picture for the bis-oxadiazoles through the disappearance of NH and C=O from the starting material. This is shown in a shift of wavenumber for C=N of the hydrazones to oxadiazoles which corresponds to the cyclization reaction.

The expected peaks in an oxadiazole structure were observed in the ^{1}H NMR. In addition to that, the disappearance of proton of the imine group and the NH proton gives good evidence that the cyclization was successful. Furthermore, the ^{13}C NMR in agreement to the IR and ^{1}H NMR. For more details, see Section 6.2.3 and Appendix A.

The HREIMs afforded the accurate mass in relative to the calculated mass of the synthesized bis-oxadiazole. The EIMs spectrum offered the molecular ion mass and their fragmentations, which corresponded to the bis-oxadiazole structures (See Appendix B). Table 3-8 below displayes the losing HNCO. The pattern of fragmentation was similar to mono oxadiazole discussed earlier.

Table 3.8 : Molecular ion and base peak for the bis- oxadiazoles.

No.	$M^{\cdot+}$	%	Base peak 100%	$M^{\cdot+}$- HNCO	%
3.11	622.4	96	607.4(- $^{\cdot}CH_3$)	579.5	21
3.12	622.5	98	607.4(- $^{\cdot}CH_3$)	579.4	28

3.2.2.5 Characteristic of 2,4-di-*tert*-butyl-6-(5-thio-4-hydro-1,3,4-oxadiazol-2-yl) phenol.and their derivative's

As mentioned earlier the 2,4-di-*tert*-butyl-2 hydroxybenzoic acid was converted to the corresponding methyl ester. This ester **3.13** was characterized by IR, ^{1}H NMR, ^{13}C NMR, HREIMS and EIMs. Then the ester was converted to the corresponding hydrazide **3.14** and this hydrazide was characterized by the same methods (Appendix A & B). The 2,4-di-*tert*-butyl-6-(5-thio-4-hydro-1,3,4-oxadiazol-2-yl)phenol.**3.15** was

identified from its IR spectrum through the disappearance of some peaks. This indicated that the cyclization between the acid hydrazide with CS_2 was successful. The peaks of NH_2, NH and C=O disappeared and considered as an initial indicator that the cyclization have proceeded. The C=S bond has been observed at 1246 $cm^{-1}$and the C=N at 1618 cm^{-1}. A week peak for NH at 3167 cm^{-1} was also observed. In the ^1H NMR, NH_2 of hydrazide disappeared and a weak NH peak was observed at 9.1 ppm. Furthermore, the oxadiazole-5-thione is known with this tautomerism[143] as shown in Figure 3.7 below:

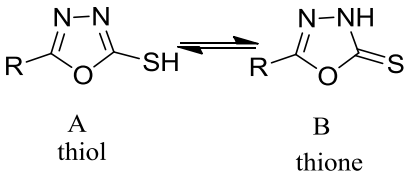

Figure 3.7 : Tautomerism structure of oxadiazole (thiol-thione).

In solution, both of these structures might be existent. However, based on the NMR data, we believed that it exists as the thione form (B) in DMSO-d_6. We observed the appearance of NH proton and no signal for the thiol proton. This suggestion was further strengthened with ^{13}C NMR. The ^{13}C NMR, in Figure 3.8 displayed the peaks at 177.11 ppm and are more compatible with thione form (B) than thiol form (A). In the solid state, the form A could be the more stable and this corresponded to the IR spectrum and is in agreement with literatures.[143b, 144]

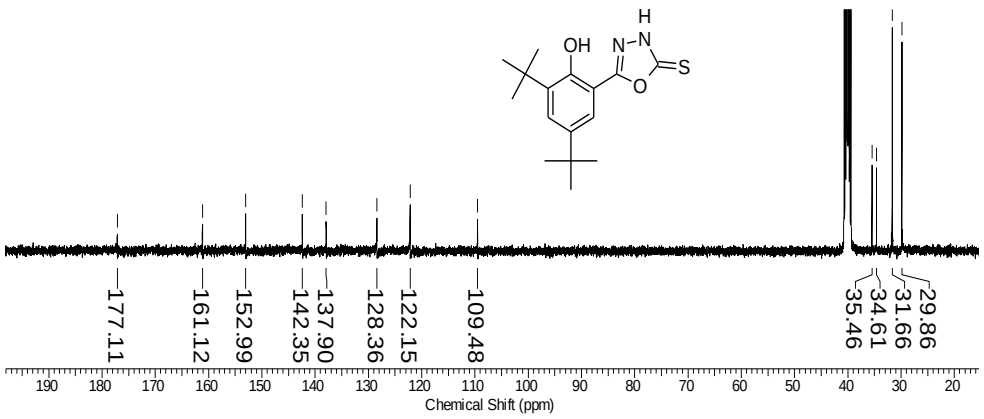

Figure 3.8 : ^{13}C NMR of **3.15** in DMSO-d_6.

The HREIMs and EIMs confirmed the structures through the determination of accurate mass and the fragmentation pattern. The pattern of this fragmentation is described in Scheme 3.18.

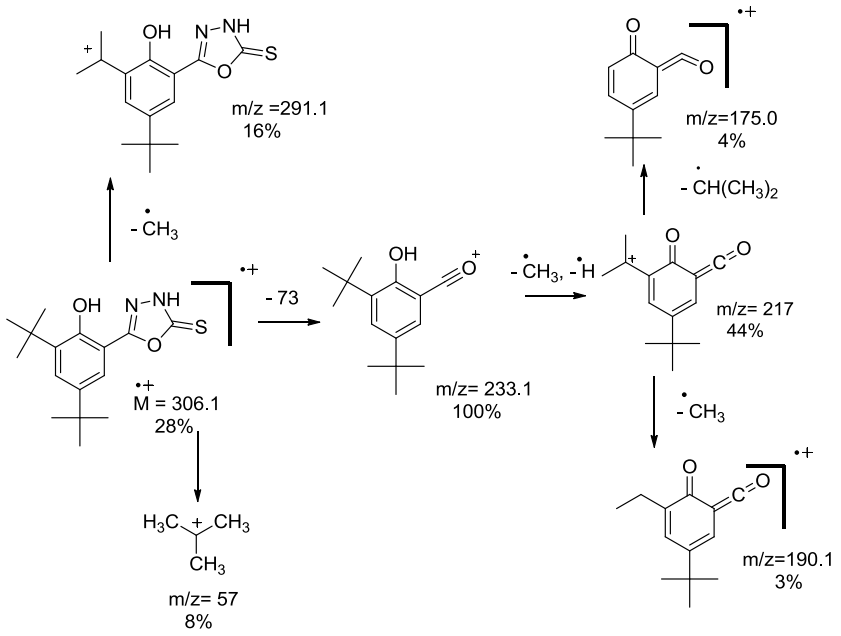

Scheme 3.18 : Some mass fragmentations of **3.15**.

The three derivatives **3.16, 3.17** and **3.18** were characterized by the same methods. Generally, in IR spectrum recorded the disappearance of NH band and a shift in the value of band C=N. For compound **3.17**, C≡C and ≡C-H appeared at 3276 and 2164 cm^{-1} respectively. The ^{1}H NMR spectrum for **3.16** displayed all the expected peaks, including the peaks of thiomethyl which appeared at 2.78 ppm (in addition of the disappearance of the weak NH peak). For **3.17**, protons ($\underline{CH_2}C\equiv$) of propargyl group ($S\underline{CH_2}C\equiv CH$) appeared at 4.22 ppm as doublet with *J*=2.68 while the proton (≡CH) appeared as triplet at 3.37 ppm with *J*=2.67 due to the long range proton-proton coupling.[145] The ^{13}C NMR, EIMs and HREIMs confirmed the structure.of the compounds.

^{13}C NMR spectra displayed all the expected peaks including the addition of thiomethyl carbon at 14.77 ppm and also the disappearance of the thiocarbonyl group at 177.11 ppm. A new peak at 166.35 ppm was observed for **3.16**. ^{13}C NMR, of **3.17**

showed the presence of thio propargyl group and gave three peaks for their carbons at 20.95 ppm for SCH_2, 75.16 and 78.92 for the two carbon of C≡CH respectively. Even though the ^{13}C NMR spectrum of **3.18** gave all expected carbons, we cannot distinguish between the SCH_2 carbon from the three similar peaks at 34.38 ppm, 35.32 ppm and 36.16 ppm. Two of them are the quaternary carbon at the di-*tert*-butyl group and the HSQC was able to distinguish them. The HSQC spectrum display the correlation between proton of SCH_2 group and their carbon's (H_9-C_9) at 4.44-36.16, therefore the other two carbons were for C_{14} and C_{16} (Section 3.2.7 and Appendix A). Correlation between H_{11} and C_{11} confirmed that the multiplate peaks at 7.37 - 7.50 ppm belongs to H_3, H_5 and H_{12}

The HREIMs values were given earlier in Table 3.5 and EIMs confirmed the structure (Scheme 3.19). The alklyted derivatives of **3.15**, **3.16**, **3.17** and **3.18,** showed a similar mass fragmentation pattern, where the base peak appeared as the molecular ion minus the methyl radical. The following scheme showed some significant fragmentations for **3.16**.

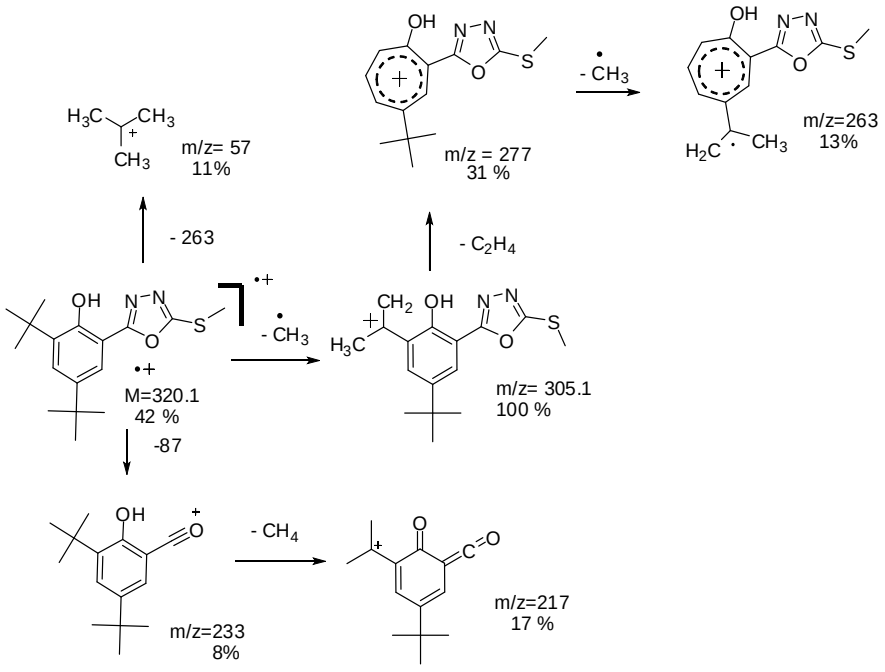

Scheme 3.19 : Mass fragmentations of **3.16**.

The interesting fragmentation was from the base peak m/z = 305 to m/z = 277 which was consistent with the removal of an ethylene unit. Fragmentation to m/z = 263 further strengthen our proposed pathway as proposed in Scheme 3.20.

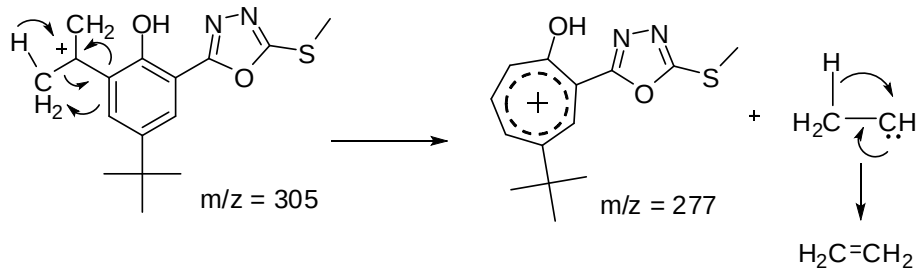

Scheme 3.20 : Proposed pathway for losing ethylene from base peak.

The structure of **3.16** was determined by X-ray analysis; the crystal system was monoclinic and the refinement data were shown in Appendix C. Figure 3.9 represented the ORTEP diagram of **3.16**.

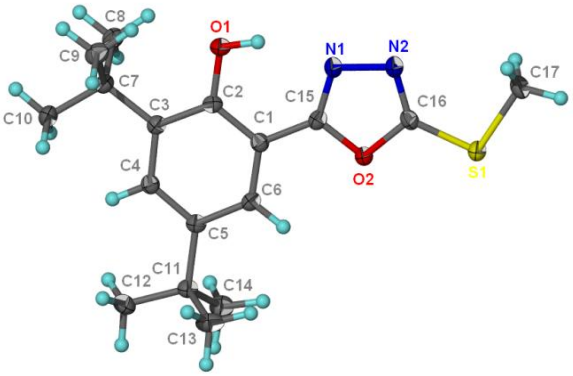

Figure 3.9 : The ORTEP digram for molecular structure of **3.16**.

3.2.2.6 Characterizations of 2,4-di-*tert*-butyl-6-(5-amino-1,3,4-oxadiazol-2-yl) phenol (3.19)

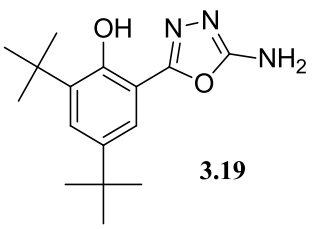

3.19

The IR spectrum of compound **3.19** exhibited bands at 3300, 3266, and 3196 cm^{-1} which shows the presence of NH_2 and OH bands (with intramolecular hydrogen bonding)[122] The C=N and the C=C appeared at 1630 and 1605,1515 cm^{-1}, 1240 cm^{-1} for C-O-C oxadiazole and 1361 cm^{-1} for C-N stretchings.

The ^1H NMR spectrum showed the two aromatic hydrogens appears as doublet with J = 1.95-2.2 Hz for the 1,3 coupling as mentioned earlier in this chapter. The NH_2 peak at 7.46 ppm with the integration of two protons, and OH appear at 10.50 p.m.. The DEPT-135 show four positive peaks; two in high filed represented the two di-*tert*-butyl groups at 28.79, 30.85 ppm and 119.27 and 126.71 ppm in low field for the two aromatic protons. This result confirmed that the proton at 7.46 ppm is for NH_2 and not C-H aromatic proton.

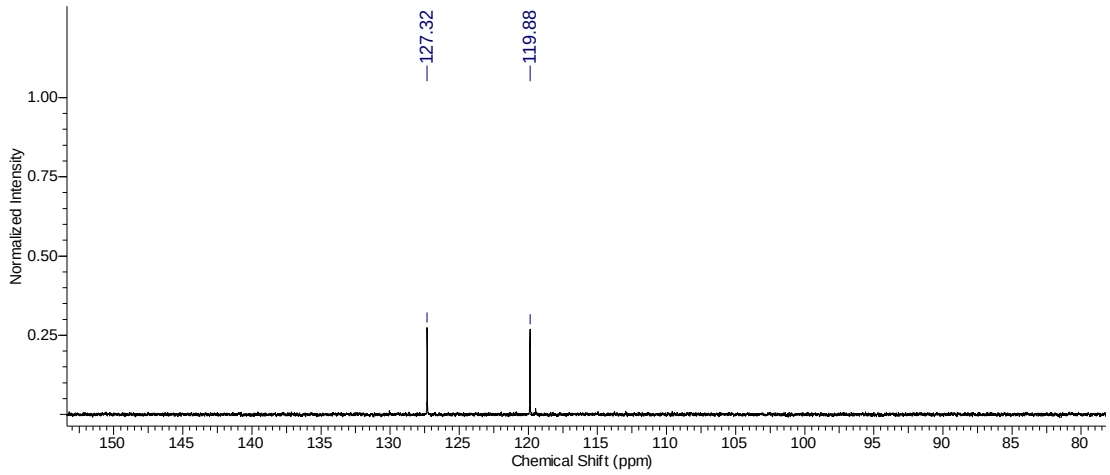

Figure 3.10 : DEPT-135 expansion of aromatic region of **3.19**.

The ^{13}C NMR spectrum was in agreement with IR and ^1H NMR spectrum results. EIMs and HREIMs gave accurate mass and are compatible with the proposed structure (See Table 3.9 and Appendix B).

3.2.2.7 Characterization of 2,4-di-*tert*-butyl-6-(5-amino-1,3,4-thiadiazol-2-yl) phenol (3.21)

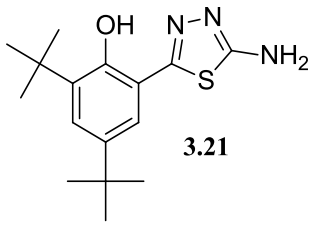

3.21

This compound was synthesized by two methods. In the first method, thiosemicarbazone **3.20** was synthesized followed by cyclization in the presence of bromine. **3.20** was characterized by IR, ^{1}H NMR, ^{13}C NMR, EIMs and HREIMs. The IR spectrum indicated the presence of OH, NH, NH_2 and C=S at 3455, 3266, 3161, 3158 and 1284 cm^{-1} respectively. In addition of the Schiff base beak, C=C was accounted for by the peak at 1608 and 1579 cm^{-1}.

^{1}H NMR spectrum showed the NH_2, CH=N, NH proton at 4.59, 8.16 and 10.05 ppm respectively. ^{13}C NMR spectrum indicated the formation of new peaks for C=N at 149.59 ppm and C=S at 177.79ppm. EIMs and HREIMs gave accurate mass and are in agreement with the proposed structure (See Table 3.9).

The IR spectrum of **3.21** indicated the disappearance of the NH peak and C=S and shifting of C=N value from 1608 to 1617 cm^{-1}. ^{1}H NMR spectrum displayed the two *t*-Bu protons as two singlets appear at 1.29 ppm and 1.41 ppm with an integration equal to 18H. Two single protons at 11.82 ppm indicated the presence the hydroxyl of phenol and the new broad peak at 7.71 ppm (with integration equal two) belonged to the amine group in thiadiazole.

Additionally, the disappearance of the imine proton gave the clue that the cyclization had proceeded successfully. The ^{13}C NMR displayed all expected peaks, including the two carbons for thiadiazole ring at 162.82 and 166.31 ppm. (See Appendix

A and Section 6.2.10). The HREIMs confirmed the structure. For more detail see Table 3.9 and Appendix B.

3.2.2.8 Characterizations of 2,4-di-*tert*-butyl-6-(4-amino-1,2,4-triazol-3-yl-5-thione)phenol (3.22)

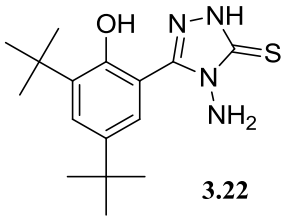

3.22

The IR spectrum indicated the presence of C=N at 1624 cm^{-1} and C=S at 1252 cm^{-1}. Broad peak was due to the intramolecular hydrogen bonding of OH phenol. The ^{1}H NMR spectrum showed the aromatic proton and the two groups of di-*tert*-butyl groups. Broad peak at 6.21 ppm indicated the presence of NH_2. A small broad peak of NH had been observed at 10.91 ppm. For ^{13}C NMR spectrum, C=N appeared at 149.78 ppm and C=S appeared at 165.94 ppm. Accurate mass obtained from HREIMs confirmed the structure (Table 3.9).

Table 3.9: EIMS and HREIMS for **3.19**, **3.20**, **3.21**, and **3.22**.

No	$M^{\bullet+}$	**Base peak**	**Theoretical mass**	**HREIMs found**	**FW**
3.19	289.2	274.2	289.1790	289.1797	$C_{16}H_{23}N_3O_2$
3.20	307.2	216.1	307.1718	307.1727	$C_{16}H_{25}N_3O_1S$
3.21	305.2	290.2	305.1562	305.1563	$C_{16}H_{23}N_3O_1S$
3.22	320.2	305.2	320.1671	320.1668	$C_{16}H_{24}N_4O_1S$

We can take note that the amino-oxadiazole **3.19,** amino-thiadiazole **3.21** and amino-triazole **3.22** have a similar pattern in fragmentation and all the base peak indicated that a methyl radical (m/z = -15) was lost during fragmentation.

3.2.2.9 Characterizations of 2-(3,5-di-*tert*-buthyl-2-hydroxybenzoyl)-*N*-(Aryl) hydrazinecarbothioamide (3.23-3.25).

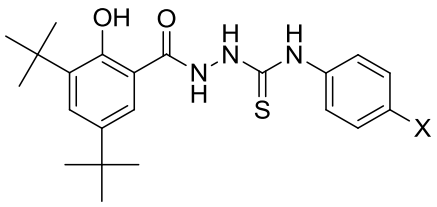

x= OMe, Cl, CH_3

Three compounds were synthesized to be used as starting material for the formation of 1,2,4 triazole ring at position six. These compounds were characterized by IR, 1D NMR, 2D NMR, EIMs and HREIMs. IR spectrum indicated the presence of OH in phenol and aliphatic C-H, C=O group and some new peak, e.g. C=S at1221-1250 cm^{-1}. ^{1}H NMR spectra showed the aryl *iso*thiocyanate peaks in aromatic ring emerged at low field as new two broad peaks indicated the presence of the two NH group. In this structure, there were three NH groups and one OH group appeared in high field (>9.5 ppm). ^{13}C NMR spectrum was in agreement with the IR where the carbons of aryl *iso*thiocyanate have been observed and the carbon of thione was also observed at 181.08-181.25 ppm. HMBC of compound **3.23-3.25** showed the last peak in low field belonging to the hydroxyl proton and the second one for the PhNHCSNH proton. The other peaks are belong to the PhNH, CONH groups. The protons peaks at 12.97, 12.96 and 12.95 for compounds **3.23**, **3.24** and **3.25** showed correlation with C_6 and C_2 through J_3 coupling and showed a correlation with C_1 as J_2 coupling. However the second peak at 10.93-10.99 ppm displayed a correlation with C=O. The other two nitrogens did not show any significant correlation. The following Figure 3.11showed an expansion for HMBC (for **3.23**). HMBC allowed us to distinguish between the two peaks in ^{13}C NMR at 156 ppm and 157 ppm (which are belonged to C_1-OH and C_{12}-OCH_3). Also the C_1-OH appeared at higher field than C_{12}-OCH_3.

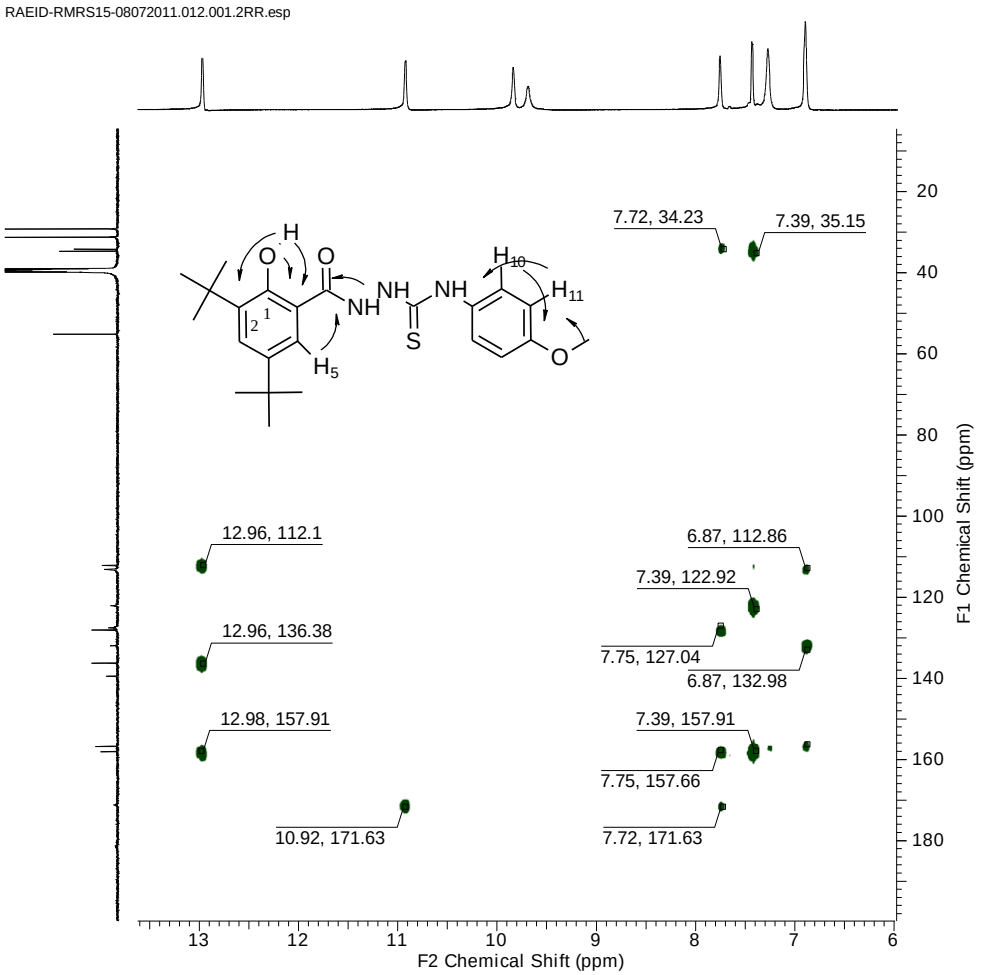

Figure 3.11 : HMBC expansion of aromatic region of **3.23**.

3.2.2.10 Characterizations 2,4-di-*tert*-butyl-6-(4-aryl-1,2,4-triazol-3-yl-5-thione) phenol.(3.26-3.28)

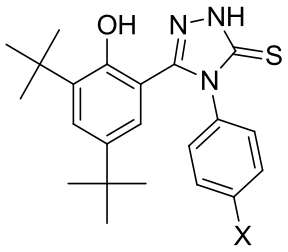

X= OMe, Cl, CH_3

The three triazoles were characterized from their IR, ^{1}H NMR, ^{13}C NMR, 2D NMR, EIMS and HREIMS. The IR spectrum indicated the disappearance of the carbonyl group, thus proving that the cyclization had been successful. With disappearance of two peaks (in ^{1}H NMR), the two NH groups have cyclized. HSQC and

HMBC have been used to assist in structure elucidation. A shift in C=S value and the disappearance of C=O (in ^{13}C NMR) indicated that cyclization had occurred and thus confirming the proposed structure. The HSQC of **3.26** was used to assist in structure elucidation (see Appendix A). The HMBC spectrum (Figure 3.12) showed that the peak at 14 ppm has two correlations with C_7 and C_8 while, the peak at 9.18 ppm displayed three correlations with C_6, C_2 and C_1. This indicates clearly that the peak at 14 ppm belonged to the NH, while the 9.8 ppm belonged to the OH group. In addition to that, the correlation between H_{10} and H_{11} with carbon at 159 ppm refers to C_{12} and the correlations between the proton of hydroxyl and H_3 with C_7 refer to that the C_1 which appeared in a lower field than the C_7.

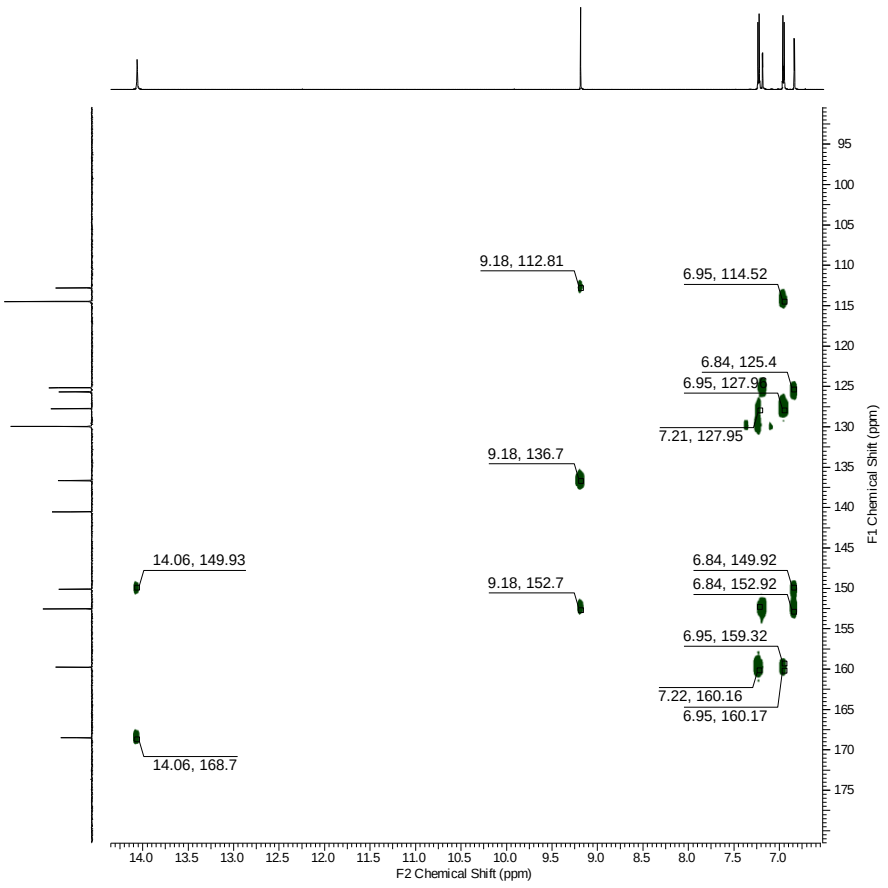

Figure 3.12 : HMBC expansion of **3.26.**

The HREIMs and EI mass results were tabulated in Table 3.6.and Scheme 3.21 showed the most significant mass fragmentations.

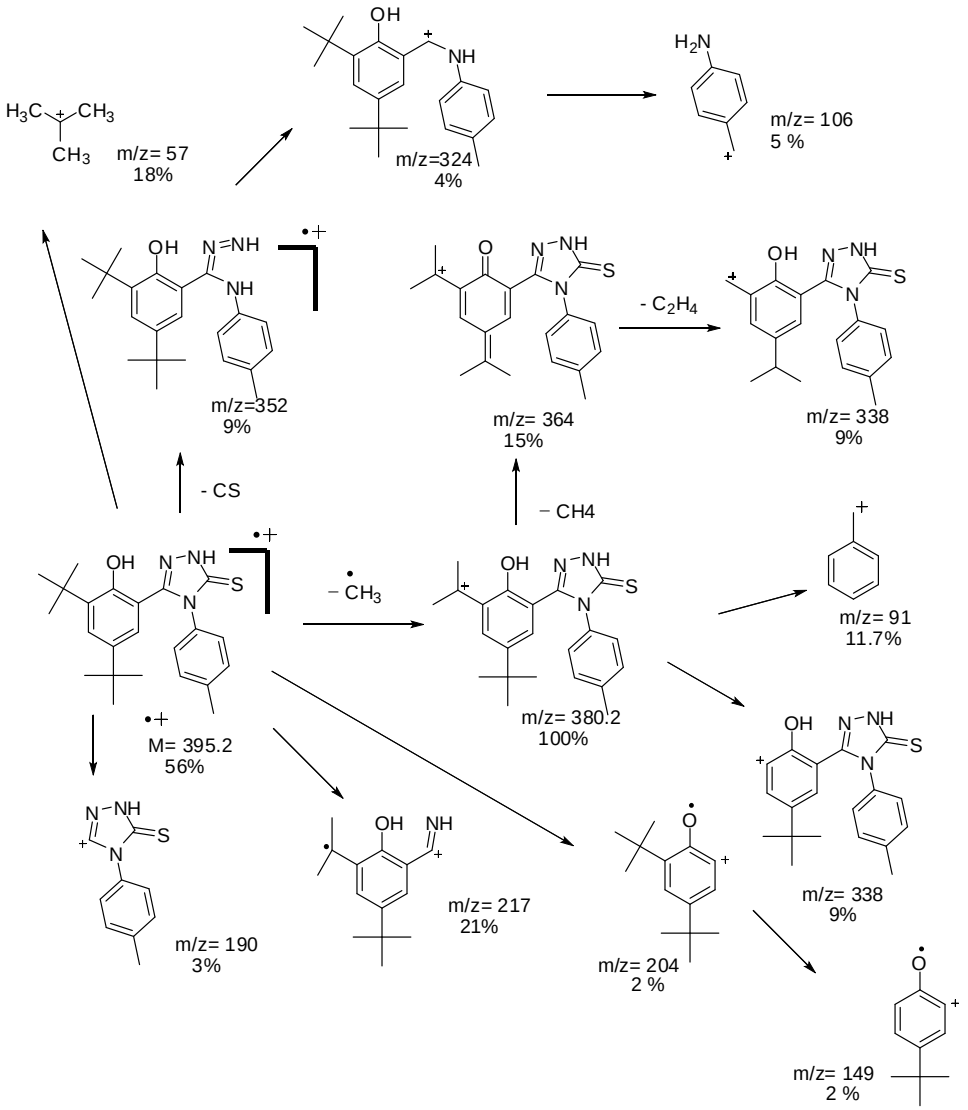

Scheme 3.21 : The EIMs fragmentations of **3.28**.

The EI mass fragmentations were able to give us a clear picture of all the structures. In addition to that, the triazoles base peak has been noted as a molecular ion losing a methyl radical. This pattern was found to be similar for all the synthesized oxadiazoles and bis-oxdiazoles in Chapter 2 as well in oxadiazole and triazole in this chapter. The X-ray analysis was able to confirm the molecular structure of **3.26** (Figure 3.13). For more detail, see Appendix C.

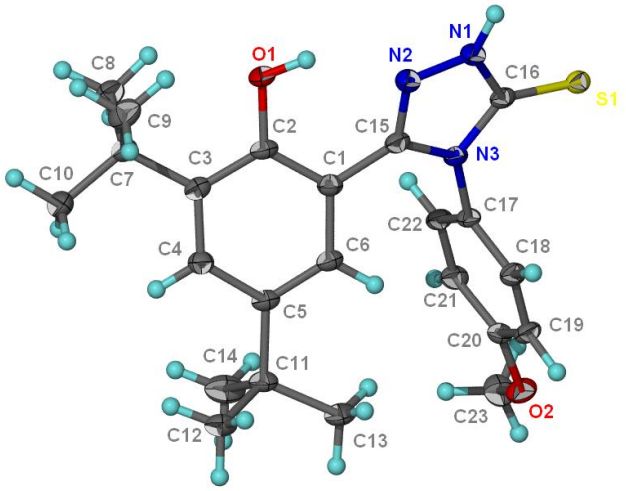

Figure 3.13 : Moleculer structure for **3.26.**

3.2.3 Mechanism for the formation of the heterocyclic ring

The mechanism for the formation of 2,5-substituted oxadiazole and the other ring will be described in the following Section.

3.2.3.1 Mechanism of the formation the 2,4-di-*tert*-butyl-6-(5-(substituted)-1,3,4-oxadiazol-2-yl)phenol

The suggested mechanism for this cyclization could be summarized in two steps. The first step, was bromination of the imines group in hydrazone. The bromination of arylidene aryl hydrazones have been extensively investigated by Chattaway and Walker [146] and many researcher reported similar investigation in the literatures.[147] The second step, is the cyclization, where sodium acetate plays an important role. Scheme 3.22 demonstrated the suggested mechanism.

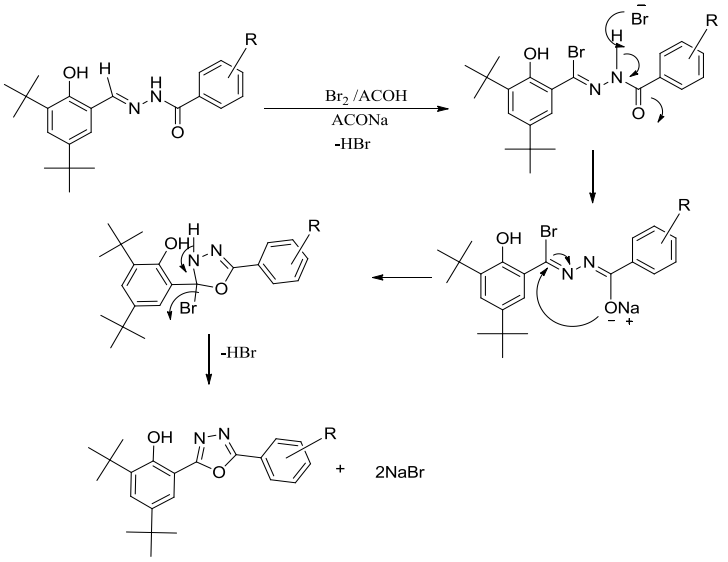

Scheme 3.22 : Proposed mechanism of cyclization of the hydrazone.

3.2.3.2 Mechanism of formation of 2,4-di-tert-butyl-6-(5-thio-4-hydro-1,3,4-oxadiazol-2-yl)phenol..

The 1,3,4-oxadiazole 5-thiol was synthesized by reacting the acid hydrazide with CS_2. As mentioned in Section 1.4, these compounds are known to have a wide range of biological activity. The suggested mechanism could take place as described in Scheme 3.23.

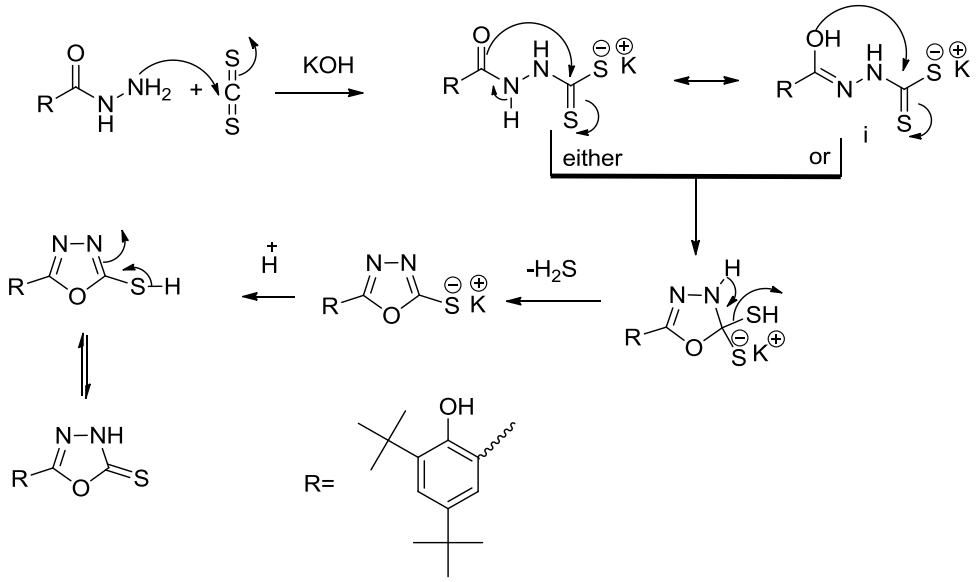

Scheme 3.23 : Suggested mechanism of formation of 2,4-di-*tert*-butyl-6-(5-thio-4-hydro-1,3,4-oxadiazol-2-yl)phenol.

This mechanism was quite similar to Ainsworth et al.[148] and Young et al.[149] where they emphasized that the formation of the intermediate (i) is more acceptable than formation the "xanthate-type" (ii). (Scheme 3.24)

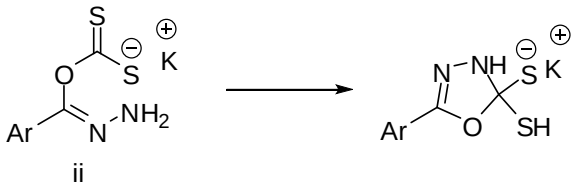

Scheme 3.24 : Formation oxadiazole from xanthate type.

The cyclization of 4-amino-1,2,4-triazol take place through the potassium salt of hydrazine-carbodithioate salt (which was isolated in solid form by reacting the acid hydrazide with CS_2 in the presence of KOH at room temperature). This could complement the suggested intermediate where it will go from intermediate (i) and not from (ii).

Furthermore, in our proposed mechanism, we put two possibilities of cyclization of the intermediate (i). Firstly, it could undergo through keto form of hydrazide carbonyl. It is more acceptable if it is done in a step where we convert to enol and attached simultaneously. The second possibility is that the cyclization will form the Enol and then the hydroxyl group will attach to the thiocarbonyl. Both are possible, but the cyclization from enol is the preferred explanation. Aqueous alkaline solution in ethanol could enhance the stability of enol form than the keto form during the intramolecular hydrogen bonding and thus the formation of seven membered ring as depicted in Figure 3.14.

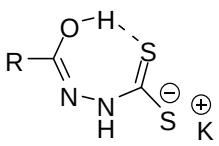

Figure 3.14 : Intramolecular hydrogen bonding could stabilize the enol form.

The alkylation of the mentioned oxadiazole was an S_N2 mechanism. The different between the reactivity of hydroxyl of phenol and thiol group enabled us to successfully force a selective alkylation on thiol to get thioalkyl. Furthermore, this could indicate that the phenolic hydroxide becomes more hindrances due to the ring formation on position six. No alkylation has been observed on hydroxyl group at room temperature.

3.2.3.3 Mechanism of formation of 2,4-di-*tert*-butyl-6-(5-amino-1,3,4-oxadiazol-2-yl)phenol

This ring was formed by reacting the hydrazide with bromocyanogen in the presence of sodium hydrogen carbonate as scavengers. We proposed two mechanisms as shown in Scheme 3.25.

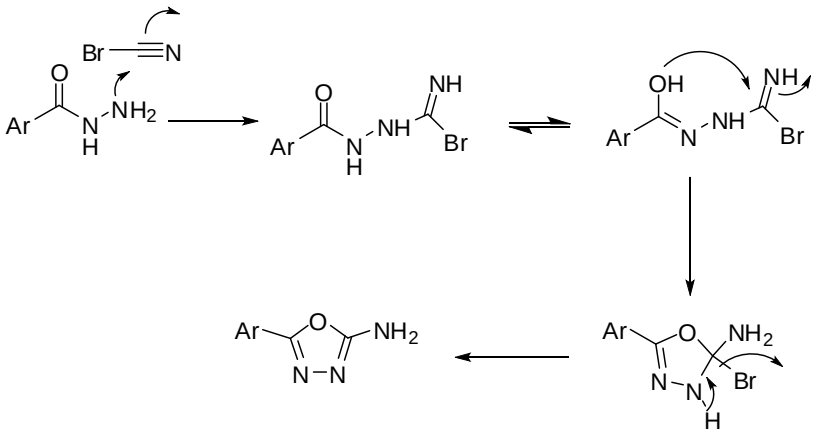

Scheme 3.25 : Suggested mechanism of formation 5-amino-1,3,4-oxadiazole.

The bromine is known as a good leaving group but complication arises when it tries to leave directly from a carbon with two π bonds. No literature has yet been reported about this mechanism. As such, more studies are needed to confirm this proposed mechanism. The second mechanism was shown in Scheme 3.26.

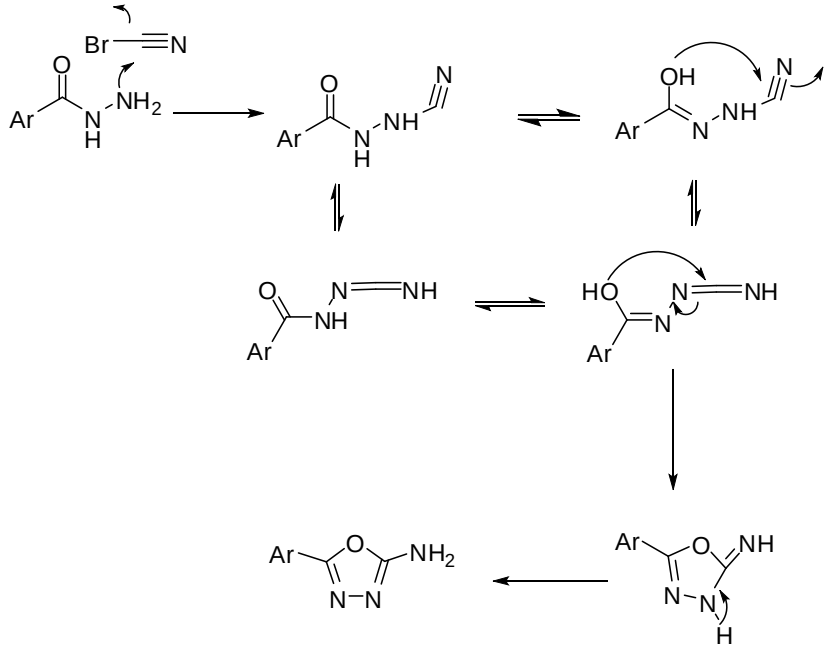

Scheme 3.26 : The second suggested mechanism of formation 5-amino-1,3,5-oxadiazole.

In peptide bond cleavage, Gross and Witkop[150] suggested that the nucleophile would attack the cyanide group and consequently the bromine cation will be expelled. Shaw and Adams.[151] reported the same observation. Vinod[152] synthesized cyanamide and dicyanamides by reacting BrCN with primary and secondary amines. However, other researchers reported different behaviors for reaction involving cyanogen bromide. For example, in 1953, Arnold *et al.*[153] reported that a double bond in the presence of BrCN will involved in iodination reaction and cyclization reaction as illustrated in the following Scheme 2.27.

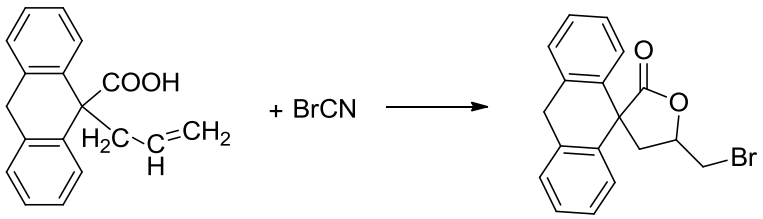

Scheme 3.27 : Different behaviors for reaction cyanogen bromide.

Whereas, Parfitt[154] reported that the reaction of BrCN with 2-tetralone gave two products and that did not include the addition of cyanide ion and bromide cation as leaving group (Scheme 3.28)

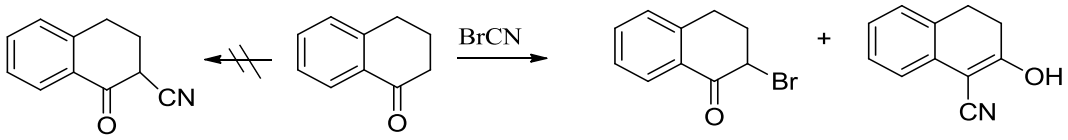

Scheme 3.28 : Reaction of cyanogen bromide.

Finally, Kandeel *et al.*[155] reported the cyclization of cyanogen bromide could not include a direct addition CN ion. For these observations, two mechanisms were proposed for formation of 5-amino-oxadiazole ring.

3.2.3.4 Mechanism of formation 2,4-di-*tert*-butyl-6-(5-amino-1,3,4-thiadiazol-2-yl)phenol

This ring was formed in two methods. In the first method, the thiosemicarbazide hydrazone is involved in cyclization reaction with bromine. This mechanism was similar to the one described earlier in Section 3.2.3.1. The second method, with $POCl_{3,}$ was discussed in Chapter two, Section 2.3.2.5.

3.2.3.5 Mechanism of formation 2,4-di-*tert*-butyl-6-(4-amino-1,2,4-triazol-3-yl-5-thione)phenol

The ring was formed by refluxing potassium salt of hydrazinecarbodithioate with hydrazine hydrate in aqueous solution. Scheme 3.29 display the suggested mechanism

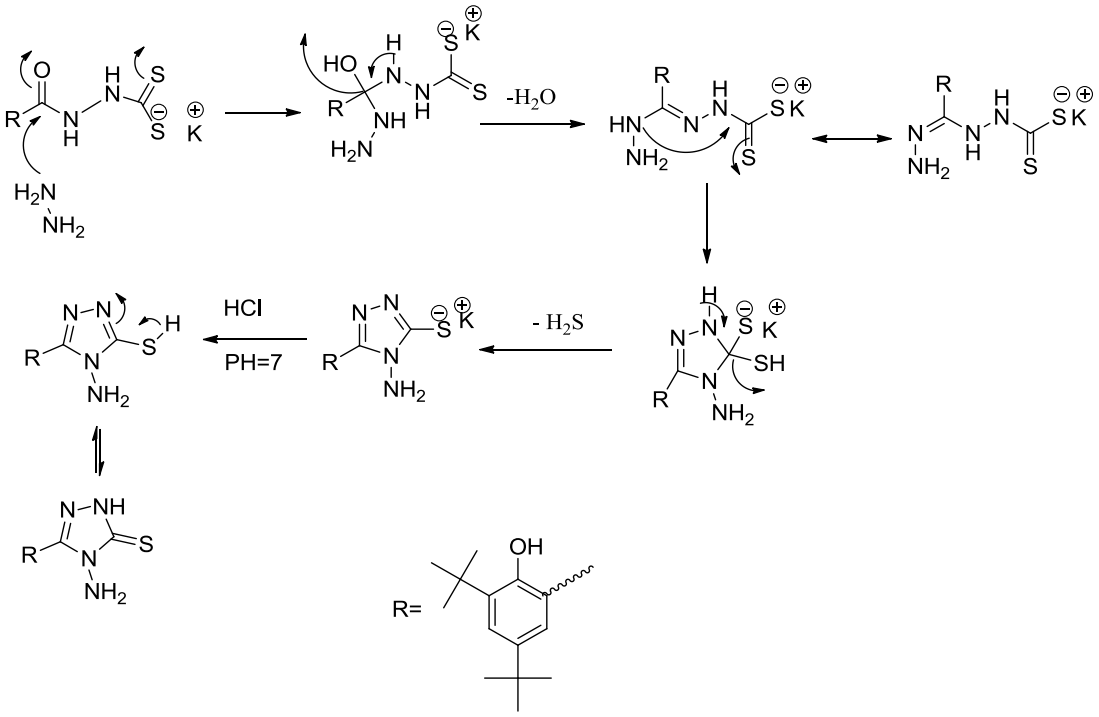

Scheme 3.29 : Suggested mechanism of 2,4-di-*tert*-butyl-6-(4-amino-1,2,4-triazol-3-yl-5-thione)phenol

The carbonyl group in this salt was considered more electrophilic than the thio carbonyl group. The negative charge on a sulfur atom is known as a good electron donor[156] and would decrease the electrophilicity of C=S, thus facilitating the attachment of the carbonyl much more easily. On the other hand, losing H_2S was commonly reported in the literature.[157] The completion of the reaction was indicated by the H_2S. H_2S will cease to evolve once the reaction is completed. Furthermore, if the hydrazine attached to the thionyl group, it will loose hydrogen sulfide before losing H_2O. Completion of the reaction will not be able to be monitored accordingly.

3.2.3.6 Mechanism of 2,4-di-*tert*-butyl-6-(4-aryl-1,2,4-triazol-3-yl-5-thione) phenol

The ring was formed by refluxing the 2- (3,5-di-*tert*-butyl-2-hydroxy-benzoyl)-N-(4-substitiuted phenyl)-hydrazine carbothioamide in a solution of sodium hydroxide (4N) to form the 1,2,4- triazole. The mechanism described in Scheme 3.30.[158]

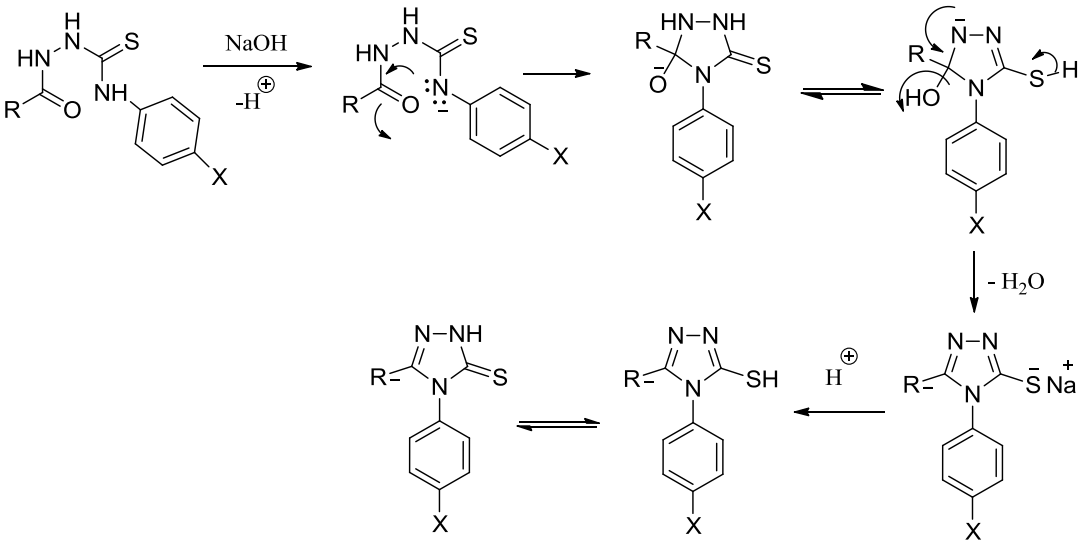

Scheme 3.30 : Proposed mechanism of formation triazole -5-thione.

Chapter 4 : Results and Discussion of the Antioxidant Activity

4.1 Introduction

Reactive oxygen species (ROS) and reactive nitrogen species (RNS) are known to take part in biochemical reactions and physiological processes and have the potential to cause oxidative stress leading to harmful oxidative reactions in organisms. These free radical reactions are the cause of indisputable human diseases, including cardiovascular disease,[159] cancer,[160] inflammations,[161] and brain dysfunction.[162] Antioxidants play important role in preventing oxidative stress that may cause several degenerative diseases. The primary sources of antioxidants are plants; the preservative effect of plant spices and herbs suggests the existence of antioxidative and antimicrobial constituents in their tissues.[163] In 1968, Harmanin put forward the hypothesis that at least some of the degenerations of aging arose through the same processes as those of radiation damage; highly reactive chemicals (were created by our normal metabolism rather than radiation).[164] A corollary of this hypothesis would be that drugs which protected against radiation would also protect against aging; antioxidants are a large class of such substances, well known to protect against radiation damage, and therefore against aging as well.[165] Furthermore, in 1955 Deichmann studied the toxicity of BHT at concentrations of 0.1 percent by weight of diet and found no effect on any of the parameters studied.[166] Therefore, we would like to synthesize heterocyclic compound which have wide bioactivity containing antioxidant group that could lead to be good drugs in future.

4.2 Structure Effect on qualification of antioxidant

Most of the literature reviews emphasized strongly at the relationship between the structure and increase / decrease of the antioxidant efficiency in both hydrogen transfer mechanism and electron transfer mechanism. There are various factors that play

important role in enhancing the antioxidant ability or to reduce it. Therefore, when designing new antioxidant, we should take into consideration the following parameters. These parameters may direct or indirectly arise or enfeeble the antioxidant ability.

4.2.1 Effect of Steric Hindrance and Alkyl group

In the middle of last century, hindered phenol has attracted many researchers due to some desirable properties, e.g. superior antioxidant. Many literatures reported the relationship between increasing the alkyl group and antioxidant properties. In 1950, Rosenwald *et al.*[139] attempted to determine the structure factors involved in affecting maximum potency of the alkyl phenol. In this section, the impact of the steric hindrance on the properties of antioxidants will be discussed. It is found that the addition of a second methyl group on *ortho* position to *para* cresol increased the potency of phenol, e.g 2,4-dimethyl phenol is more potent than *ortho* cresol and *para* cresol.

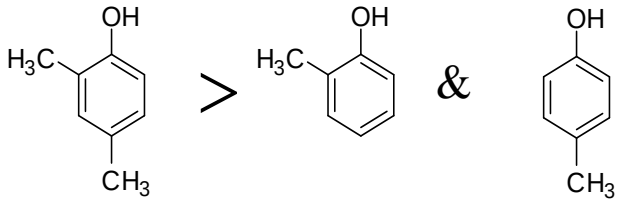

Figure 4.1 : Methylation of phenol increases the antioxidant properties.

This effect is also observed in the butylated phenols. For example, the effectiveness of a 2-*tert*-butyl-4-methylphenol is more potent than 2-*tert*-butylphenol and *p*-cresol.

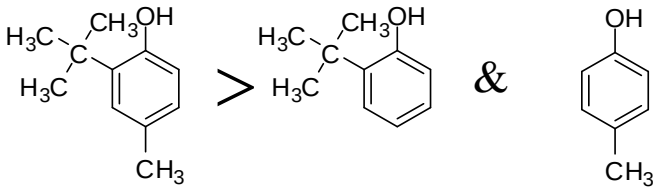

Figure 4.2 : Steric hindrance increases the antioxidant properties.

Increasing the alkyl group at the *para* position does not increase the antioxidant properties, e.g. 2-*tert*-butyl-4-methylphenol and 2-*tert*-butyl-4-butyl phenol.

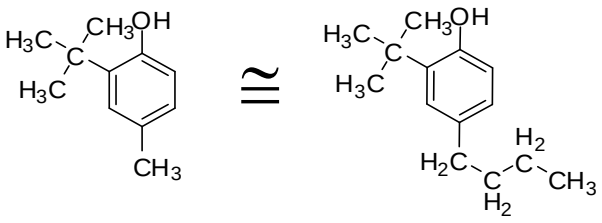

Figure 4.3 : Inceasing the size of carbon chain at *para* position does not improve the antioxidant properties.

Instead, they illustrated that the position of substituted group are very important. The *ortho* alkyl phenols are more potent than *para* alkyl phenols. An increase in the branching of the *ortho* substituent in the monoalkyl phenols increases the antioxidant properties. They concluded that *tert*-butyl in *para* position has a detrimental effect on the properties. Whereas, the potency of 2,4-di-*tert*-butyl-6-methylphenol is about one half that of its position isomer, 2,6-di-*tert*-butyl-4-methylphenol and the 2,6- dimethyl-4-*tert*-butylphenol is about one eighth that of its isomer, 2,4-dimethyl-6-*tert*-butylphenol. These observations are summarized in Figure 4.4.

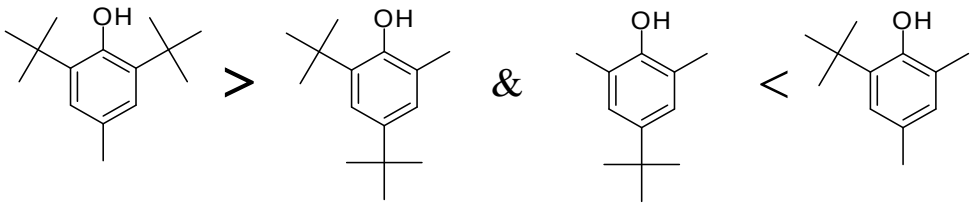

Figure 4.4 : *Tert*-butyl in *para* position decreases the antioxidant properties.

On the other hand, Wasson and Smith[167] studied the effect of alkyl substitution on antioxidant properties of phenols. Different alkyl phenols were studied and the antioxidant ability were evaluated in petroleum-base lubricating oil. A good antioxidant can delay the oxidation of oil. Table 4.1 show the first group substituted on position 6 and life hours of oil without any oxidation.

Table 4.1 : Relation of R with antioxidant.

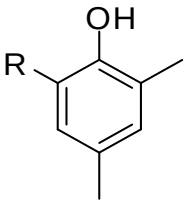

R substituted on position 6	life hours
H	72
Methyl	72
*Iso*propyl	72
sec-butyl	150
tert-butyl	250

The results showed that the *tert*-butyl increase the antioxidant more than other substituted in position 6. However, the next groups in this study are more evident about the steric hindrance effect.

Table 4.2 : Effect of *o*-alkyl.

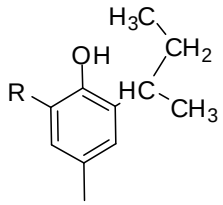

R substituted on position 6	life hours
H	72
*Iso*propyl	150
n-propyl	150
sec-butyl	350
tert-butyl	300

Even though, the *tert*-butyl are more hinderd the secondary butyl in this group showed the greater antioxidant properties. The last group in this study clarified that a more steric group lead to more antioxidant ability. Two group of *tert*-butyl (in position 2 and 6) have greater antioxidant and oil oxidation is 400 h. Another investigation have been done to clarify the effect of methyl group on tocopherol by Burton *et al*.[168] and the result were summarized in Table 4.3.

Table 4.3 : Effect of methyl group at tocopherol on antioxidant activities.

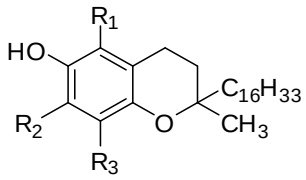

Name	R_1	R_2	R_3	K_{inh} ($M^{-1}S^{-1}\times10^{-4}$)
α-Toc	CH_3	CH_3	CH_3	320
BMT	CH_3	CH_3	H	180
β -Toc	CH_3	H	CH_3	130
γ- Toc	H	CH_3	CH_3	140
δ- Toc	H	H	CH_3	44

The final contrast in Table 4.4 gave the comprehensive pictures the role of methyl and steric effect in increasing the antioxidant ability.[169]

Table 4.4 : Alkylation effect.

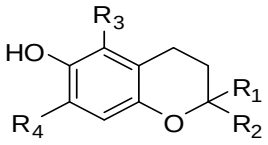

R_1	R_2	R_3	R_4	K_{inh} ($M^{-1}S^{-1}\times10^{-4}$)
CH_3	CH_3	$(CH_3)_2CH$	$(CH_3)_2CH$	238
CH_3	CH_3	CH_3	$(CH_3)_3C$	199

We can conclude that methyl group can significantly enhance the antioxidant activity in all positions (*ortho*, *meta* and *para*), where *ortho* is the better position. Furthermore, the *sec*-butyl and the *tert*-butyl groups enhance the antioxidant more than the methyl group. Finally, increasing the steric hindrance around the phenolic group would increase the antioxidant properties especially in *ortho* position.

4.2.2 Effect of Bond Dissociation Energy (BDE) of O-H

BDE value is one of the essential physical parameters that can be used to determine antioxidant ability. The weaker the OH bond, the faster will be the reaction with the free radicals. In another word, by decreasing the BDE value, we will be able to increase the antioxidant activity.[170] The bond dissociation energies (BDE) of phenolic O-H, the bonds ionization potentials (IP) of phenols or one-electron reduction potentials, *E*° and overall molecular geometry are useful for evaluating or predicting antioxidant activities of phenols. The BDE values are influenced by electron-donating

and electron-withdrawing substituent effects, steric effects and hydrogen bonding of the OH group.[171]

Various strategies have been used to obtain useful BDE values, including theoretical calculations using full basis methodology, and locally dense basis sets (LDBS) as described by Wright and coworkers.[15] Many investigations have been carried out to determine the effect of substitution as electron-withdrawing groups (EWG) and electron-donating groups (EDG) on O–H BDE. The BDE value of *para* substituted phenols has been found to be depend on the nature of substitutes and it is connected with the Hammett σ^+ values as reported by Jovanovic *et al.*[172] They developed a photoacoustic method for measuring BDE of phenols and showed for the first time that a linear relationship existed between the Hammett σ+ *para*-substituent constant and BDEs. Wayner *et al.*[173] also reported a correlation between experimental ΔBDE values for a series of substituted phenols. The studies suggested that the EWG substituent stimulate an increasing of bond dissociation enthalpy value of the O-H bond. Table 4.5 summarized the effect of the EWG and EDG substituent on BDE value.

Table 4.5 : Effect the *para* substituted on BDE value [174]

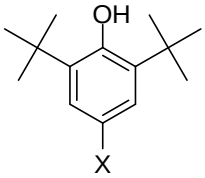

Substituent	**BDE (kcal/mol)**	**Substituent**	**BDE (kcal/mol)**
NO_2	84.94	Ph	81.24
COOH	84.27	Me_3C	81.24
CO_2Me	84.1	Me	81.02
CHO	84.23	RS	81.03
CN	84.24	PhCH=CH	78.9
H	82.8	OMe	78.31
Cl	82.41		

This table depicted that the EWG increased the BDE value and lower the antioxidant properties. This could be due to stabilization of the phenol by polar structure as demonstrated in Scheme 4.1

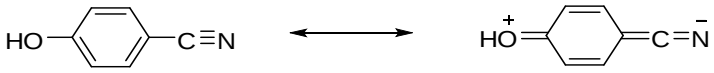

Scheme 4.1 : Stabilization of *p*-cyanophenol.

On the other hand, EDG reduce the BDE due to the stabilization of the phenoxyl radical by mesomeric structures bearing a positive charge on the substituent Scheme 4.2.[174b]

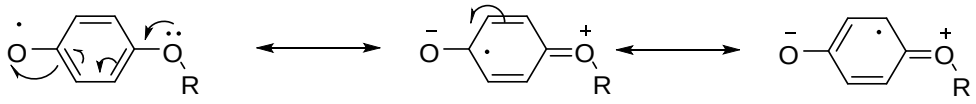

Scheme 4.2 : Mesomeric structure of *p*-alkyloxyphenol.

The *meta* and *ortho* substituent have been noted to have an effect on BDE value. This is demonstrated in Table 4.6.

Table 4.6 : Effect *ortho* and *meta* substituted on BDE value.[174c]

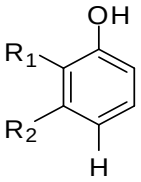

R1	R2	BDE (kcal/mol)	R1	R2	BDE (kcal/mol)
H	H	87.6	OMe	H	83.7
Me	H	84.1	H	CMe_3	86.6
CMe_3	H	82.8	H	Me	86.7

4.2.3 Effect of position of substitute.

There is large interaction between all factors, e.g. we could not separate the effect of position and ignore or omit factors such as, electronic behaviors of the substituent, EWG or EDG in inductive effect and the intramolecular hydrogen bonding. As mentioned earlier in Section 4.2.1 the alkyl group increases the antioxidant in the following order *o*->*p*->*m*-, especially when hydroxyl group flanked by two *ortho*-

methyl or branched alkyl groups. The alkylsubstituent stabilizes the phenoxyl radical by inductive and hyper conjugative effects. *Ortho* groups also provide steric hindrance. It indicates that the EWG groups decrease the antioxidant ability at *para* position and vise versa. Stereoelectronic effects of *para*-methoxy are important in controlling the antioxidant activities of methoxy phenols (Table 4.7).[168]

Table 4.7 : Effect of substituted in position 3, 4 and 5.

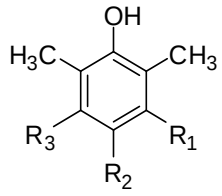

No.	R_1	R_2	R_3	K_{inh} $M^{-1}s\times10^{-4}$
4.1	H	CH_3	H	8.5
4.2	H	OCH_3	H	94
4.3	H	OCH_3	CH_3	130
4.4	OCH_3	OCH_3	CH_3	39
4.5	CH_3	CH_3	CH_3	36
4.6	CH_3	CH_3	H	11
4.7	CH_3	H	CH_3	7.5
4.8	H	H	H	2.5

From this table we can observe that the *para*-methoxy stabilizes a phenoxyl radical by conjugative electron delocalization with the oxygen. This stabilization required the oxygen lone pair at orbital p and must overlap with the semi-occupied orbital (SOMO) of the radical. The extent of overlap depends on the dihedral angle, θ, between the oxygen lone pair and the SOMO (which is perpendicular to the atoms of the aromatic plane) and the angle θ should be the same as the angle θ' between the $O_1{-}C_2$ bond. This plane is demonstrated in Figure 4.7. Therefore, the stabilization of the radical will be at a maximum when θ = 0◦ and at a minimum when θ =90°.[168, 175]

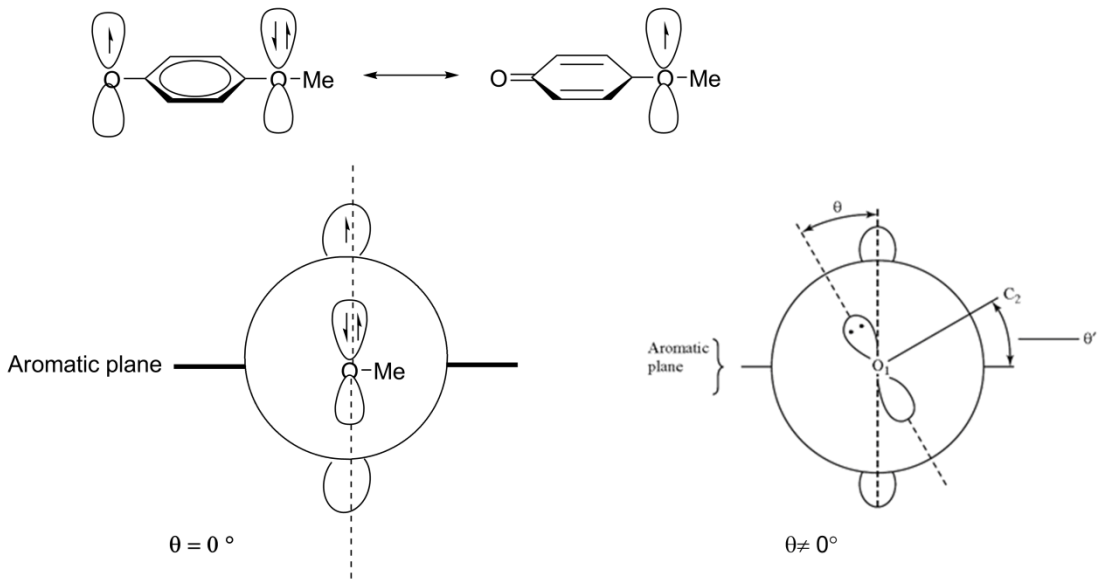

Figure 4.5 : Stereoelectronic effects of heteroatoms on stabilization of free radical.

The free radical scavenging for compound **4.4** (39×10^{-4} M^{-1} s^{-1}) is higher than **4.5** (36×10^{-4} M^{-1} s^{-1}) with *p*-methyl and 4.7 (7.5×10^{-4} M^{-1} s^{-1}) without any *p*-substituent, this enhancement could be due to a perpendicular *para*-methoxyl in **4.4** where the activity is reduced by the withdrawal inductive effect of oxygen. Another possibility is that the 'effective' θ for **4.4** in solution is less than 90° or, as suggested, the withdrawal inductive effect of a perpendicular methoxy group is outweighed by a residual donating mesomeric effect attributed to a resonance contribution from the other lone pair on the oxygen.[168] Furthermore, it has been found that the *p*-SMe is more effective in increasing the antioxidant ability wheras the sulfur atom decrease the BDE value.

4.2.4 Effect of intramolecular hydrogen bonding

The intramolecular hydrogen bonding have been reported to reduce antioxidant activity.[176] Generally, the electron donating substitute at position 2,4,6 of phenol can increase the free radical scavenging ability.[176] While Lawandy *et al.*[177] found that the antioxidant ability depends on the position of substituent where *p*>*o*>*m* and is attributed to an intramolecular hydrogen bonding.[178] The interest in *ortho*-methoxy phenols as antioxidants is driven by their frequent occurrence and importance in various natural

products including ubiquinols, curcumin, lignin model compounds and others. An *ortho*-methoxy group could offer stabilization of the phenoxyl radical formed by the resonance of the type (Figure 4.8).[179]

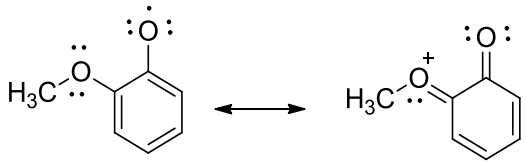

Figure 4.6 : Stabilizing phenoxyl radical by resonance.

The intramolecular hydrogen bonding of *o*-methoxy phenol was depicted in Figure 4.9. In a non-polar solvents, less than 0.1% , it exists as a free phenol.[180]

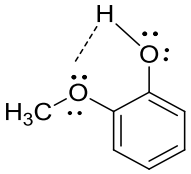

Figure 4.7 : Intramolecular hydrogen bonding of *o*-methoxy phenol.

This intramolecular hydrogen bond is able to stabilize the parent compound by 4 kcal mol^{-1}. The opposing electronic effect of the methoxy group[15] decreases the reactivity when compared to the *para*-methoxyphenol. The non-linearity of the intramolecular hydrogen bond in the *ortho*-methoxy isomer leaves the phenolic hydrogen atom available for abstraction.[181] Thus, the opposing effects and the activating effect of the *ortho*-methoxy against the stabilizing effect of H-bonding will be able to decreased the reactivity of the *o*-methoxy isomer compared to the *p*-methoxy.

Even though, intramolecular hydrogen bonding may decrease the antioxidant activity for *o*-methoxy, it have been reported that the 1,2-dihydroxybenzene (and it derivatives) are remarkably active antioxidants compared to most of *ortho*-methoxyphenols. The 1,2-dihydroxybenzene derivatives are widely available in nature, especially as the flavonoids. This increasing activity could be due to increased

stabilization of the semiquinone radical formed from catechol, and of the corresponding transition state, through strong hydrogen bonding in resonance canonical structures (a) and (b)[182] as demonstrated below:

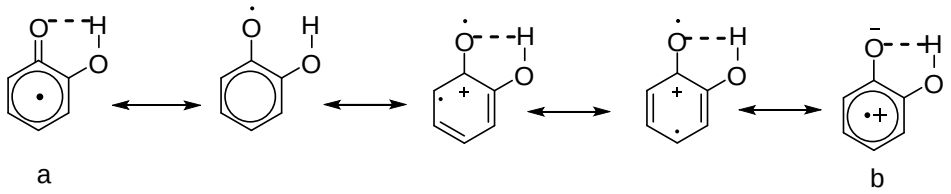

Figure 4.8 : Effect of hydrogen bonding on stability of free radical.

Increased stabilization of the 1,2-dihydroxybenzene radical, (due to hydrogen bonding) was confirmed by calculations. The catechol is stabilized by a moderately strong hydrogen bond of (4 kcal mol^{-1}) while, the respective radical has a much stronger hydrogen bond (8 kcal mol^{-1}).[15] As mention earlier, the electron donating substituent group can increase the antioxidant property by increasing the electron density of phenolic oxygen due to the localization of a radical electron of the phenoxyl radical at *p*-position.[176] Most literatures reported that the *meta* position play limited role in increasing the antioxidant properties. Kajiyama *et al.*[183] have evaluated the antioxidant activity of different groups in *meta* position of phenol like NH_2, OCH_3 CMe_3, Et and OCH_2Ph. They found that the *meta* position does not enhance the antioxidant activity.

4.2.5 The Solvent effect

Hydrogen abstraction of alkoxyl radicals from phenols is the main exception due to their lower rate constants in polar (and especially hydrogen-bond-donating) solvents.[184] This has been attributed to the involvement of the reactive O-H in a hydrogen-bond network, which offers protection against the attack of the reactive alkoxyl radical. In line with this argument, conceptually advanced by Litwinienko *et al.*,[185] hydrogen donors with C-H bonds displayed no detectable kinetic solvent effects

in their reaction with cumyloxyl, [186] peroxyl[187] and 1,1- diphenyl-2-picrylhyrazyl (DPPH) radicals.[188] From the current understanding in radical chemistry that only hydrogen abstractions from O-H bonds, but not those from C-H bonds, are expected to be slower in polar solvents.[185] In another study, Koner *et al*.[189] emphasized that the polar solvent possess effect on a transition state of antioxidant kinetic and also on abstract C-H as demonstrated in Figure 4.9.

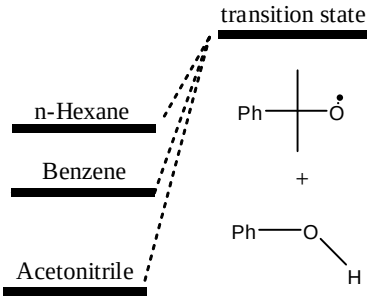

Figure 4.9 : Solvent effect on hydrogen abstraction.

The effect of the solvents on the rate constant of the antioxidants (with the radical species) is dependent on how the solvent interacts with reactants and also on the mechanism of the antioxidant action. Table 4.8 presented an example on the effect of solvent on the rate constant for abstraction of O-H phenol with DPPH and α-TOC (TOH).

Table 4.8 : Solvent effect on rate of constant of abstraction O-H.

Solvent	$K \times 10^{-3}$ **PhOH+DPPH**	$K \times 10^{-2}$ **TOH+DPPH**
n-pentane	-	74
n-octane	160	74
carbon tetrachloride	93	36
chlorobenzene	59	27
benzene	31	18
anisole	7.2	14
Acetonitrile	-	4.9
Acetic acid	3.1	6.2
tert-butyl alcohol	2.9	5.7

4.3 Methods for Evaluation of Antioxidant Activity.

Several methods have been used to estimate the activity of natural and synthetic antioxidant.[190] The antioxidant assays can be divided into two classes depending on the antioxidant mechanism, either H-atom transfer reaction (HAT) or base on electron transfers (ET).[191] Majority of HAT-based assays apply a competitive reaction scheme, in which antioxidant and substrate compete for thermally generated peroxyl radicals through the decomposition of azo compounds. These assays include the inhibition of inducing the autoxidation of low-density lipoprotein, oxygen radical absorbance capacity (ORAC), total radical trapping antioxidant parameter (TRAP), DPPH assay and crocin bleaching assays. ET-based assays measure the capacity of an antioxidant in the reduction of an oxidant where the color changes when reduced.

The degree of color change is correlated with the sample's antioxidant concentrations. ET-based assays include the total phenols assay by Folin-Ciocalteu reagent (FCR), Trolox equivalence antioxidant capacity (TEAC), ferric ion reducing antioxidant power (FRAP) and "total antioxidant potential" assay using a Cu (II) complex as an oxidant. On the basis of this analysis, it is suggested that the total phenols assay by FCR can be applied to quantify an antioxidant's reducing capacity and the ORAC assay can be used to quantify peroxyl radical scavenging capacity.[192] We will focus on these two methods in determining the antioxidant activity of the synthesized compounds. In this work we used DPPH assay and FRAP assay to evaluate the antioxidant abilities of the synthesized compounds.

4.3.1 2,2-Diphenyl-1-picrylhydrazyl (DPPH) Radical Scavenging Capacity Assay.

The DPPH is a stable and commercially available free radicals and was used for estimating antioxidant activity. The DPPH is a nitrogen centered radical having maximum absorbance at 515 nm, which was converted to 1,1-diphenyl-2-picryl hydrazine on reacting with hydrogen donating species.[193] In 1954, Braude *et al.*[194]

observed that DPPH• undergoes a HAT mechanism with antioxidant according to the following scheme.

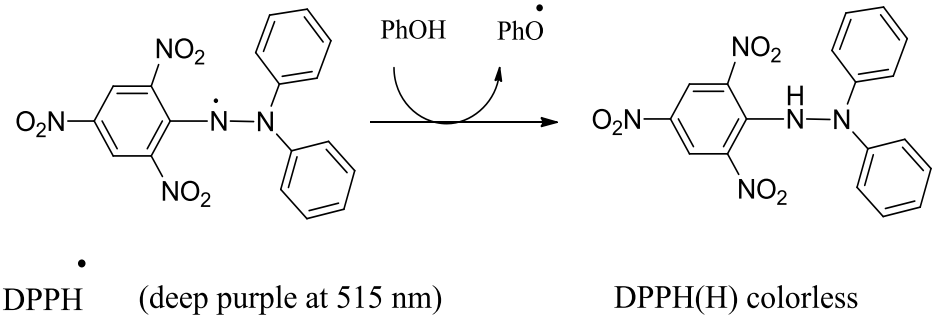

Scheme 4.3 : Reaction of DPPH radical in presence of phenol under HAT mechanism.

In 1958, Blois [195] showed that if a phenolic compound contains more than one phenolic hydroxy functional group, the resultant ArO• formed is sufficiently stable enough to undergo a second simultaneous HAT reaction with another molecule of DPPH•, thereby preserving the stoichiometry of the reaction. Over the past two decades the DPPH• assay has resurfaced as a method for the analysis of phenols in plants and plant-derived food products.[196] Several assays emphasized that the mechanism reaction of DPPH with phenol followed the HAT mechanism.[197] On the contrary, another view suggested that the reaction of DPPH with phenols undergoes single electron transfer (SET) mechanism as shown in the following scheme.

DPPH•(Violet at 515 nm) + ArOH → DPPH−(Colorless) +[ArOH]•+(SET)

Scheme 4.4 : Reaction of DPPH radical with phenol under SET mechanism.

Some suggested that this mechanism is a mix between HAT and SET[198] and the steric hindrance of an antioxidant compound determines the type of reaction mechanism. [192] It has been reported that the color interference with samples that include anthocyanines may lead to underestimation of the antioxidant activity.[199] Other limitation of this assay is the bulky antioxidant like BHT protocatechuic acid and will reach the end point of reaction after 3 hours. [197b] Despite this, the method is still widely

used to determine antioxidant ability.[200] It has been known that the medium of reaction has a significant effect on the % inhibitions of DPPH value.[201] The % inhibition of DPPH value can be calculated from the following equation[202]:

$$\%\ \textbf{inhibition of DPPH} = \frac{A_o - A1}{A1} \times 100$$

Where A_0 is the absorbance of a standard that was prepared in the same conditions, but without any sample and A_1 is the absorbance of synthesized sample at 515 nm.

4.3.2 Ferric Reducing Antioxidant Power (FRAP) assay

In 1996, Benzie and Strain[203] developed an assay to measure the ferric reducing power of human plasma. This method was used to quantify the ferric reducing antioxidant power (FRAP) of plant extracts and to determine antioxidant in food as well as other synthetic compound.[204] The assay reaction involves the reduction of Fe^{3+}-TPTZ (iron[III]-2,4,6-tripyridyl-*s*-triazine) to Fe^{2+}–TPTZ through SET with an antioxidant compound. The result of this reaction is an intense blue color at λ_{max}= 595 nm, as demonstrated in Scheme 4.5

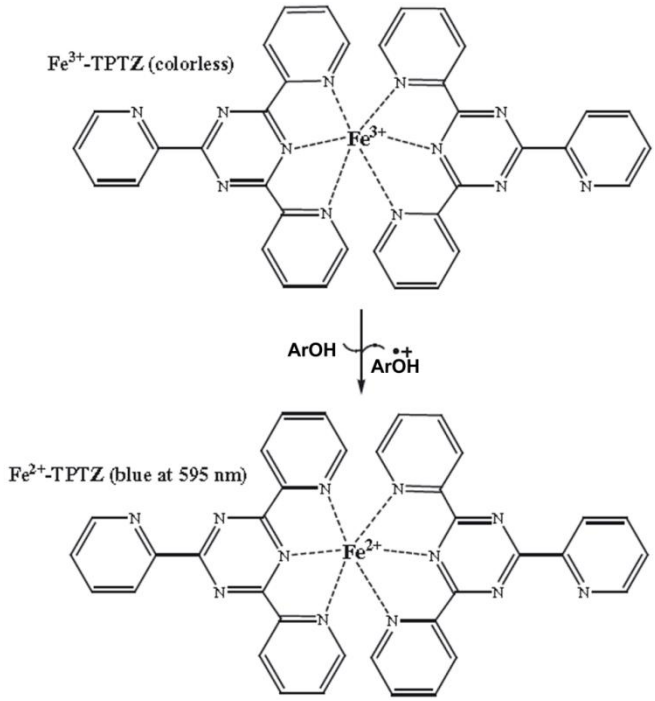

Scheme 4.5 : Reduction of Fe^{3+}–TPTZ to Fe^{2+}–TPTZ in presence of phenol.[205]

This assay appears to be related to the conjugation in phenols as well as the number of hydroxyl constituents.[206] It is also important to note that the results of FRAP assays produce considerably different results depending on the analysis time and the reaction medium used.[192] The assay reaction must be carried out in an acidic inviroment in order to maintain iron solubility. However, this can lower the IP of the reactants and reduce the redox potential of the system.[192] Saliha Esin *et al.*[207] reported that the an interference effect of solvent and the antioxidant in the order of ORAC > ABTS > DPPH > FRAP. This result showed that the FRAP assay was not much effected with solvent. The FRAP value can be calculated from following equation.[208]

$$\textbf{FRAP value} = \frac{0\text{–}4\ min\ \Delta A593nm\ of\ test\ sample}{0\text{–}4\ min\ \Delta A593nm\ of\ standard} \times [standard]\ \ (\mu M) \times Y \times 1000$$

Where Y is the absorbance of the spectrophotometer.

4.4 Results and Discussion

4.4.1 The antioxidant of 2, 6-di-*tert*-butyl-4-(5-Aryl-1,3,4-oxadiazol-2-yl) phenol.

We have successfully synthesized eleven compounds (**2.12-2.22)** that contain DTBP (di-*tert*-butyl phenol) attached with 1,3,4-oxadiazole-5-Aryl DTBP, as shown in Figure 4.10.

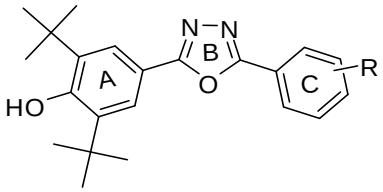

Figure 4.10 : General structure of compounds **2.12-2.22**.

All these compounds have been tested for their antioxidant properties with DPPH assay. The results of their antioxidant properties are presented in Table 4.9.

Table 4.9 : DPPH inhibition % and IC_{50} for 2, 6-di-*tert*-butyl-4-(5-aryl-1,3,4-oxadiazol-2-yl)phenol.

Compound No.	**Substituent at ring C**	**DPPH Inhibition % ± SD [a]**	**IC_{50} ±SEM [b] (100µg/mL)**
2.12	4- CH_3	76.02 ±0.058	41.76 ±0.041
2.13	4- OCH_3	62.03 ±0.018	50.69±0.025
2.14	4- OCH_2CH_3	60.04 ±0.016	54.60±0.011
2.15	4-Br	30.85 ±0.032	> 100
2.16	4-Cl	50.44 ±0.024	99.2±0.017
2.17	4- OH	89.05 ±0.044	15.79±0.031
2.18	3,4-di-Cl	30.35 ±0.038	> 100
2.19	3,5-di-Cl	29.26 ±0.010	> 100
2.20	2,4-di-CH_3	79.22 ±0.037	41.27±0.026
2.21	2-CH_3	87.21 ±0.084	15.9±0.054
2.22	2-Cl	42.14 ±0.078	> 100
BHT	-	66.03 ±0.022	79.835±0.015
Ascorbic acid	-	90.65 ±0.025	22.71±0.020

The results in Table 4.9 showed that some of the compounds have good antioxidant ability. It also indicates that the DPPH % inhibition and IC_{50} values depend on the nature of the substituted group located on the benzene ring (ring C) and their position. The inductive effects of electron donating group (+I), the mesomeric effect (electron releasing group +M or electron withdrawing -M) and the resonance, plays a very important role in the antioxidant ability of the synthesized compound. Ring A and B are maintained in the eleven compounds and differ only on ring C. Compound **2.17** have the highest percentage of inhibition (89.05± 0.044) and lowest IC_{50} (15.79± 0.031) followed by compound **2.21.**

Compound **2.19** gave the lowest of inhibition (29.26 ± 0.010) and IC_{50}>100. Although, they have the same structure in rings **A** and **B**, but they have a different substitute at ring **C**. This is what made the difference when scavenging the free radical. Compound **2.17**, for instance, has a hydroxyl group at *para* position which is known as an electron releasing group in mesomeric effect (+M), while the compound **2.19** have two chloride group in position *meta* where the mesomeric effect for the chloride is less important than their withdrawing inductive effect. The mesomeric effect in position *meta* is also unfavorable. In addition to this, the results are in agreement with literatures that reported the hydroxyl group increase the antioxidant ability. [209] This also indicates that some substitute at ring C can quench the scavenging ability. Compounds **2.17** and **2.21** have excellent antioxidant ability, **2.20, 2.13** and **2.14** are considered good antioxidant, while **2.15**, **2.18** and **2.19** are considered weak antioxidant. Figure 4.11 depicts the inhibition percentage and Figure 4.12 depicts the IC_{50} values.

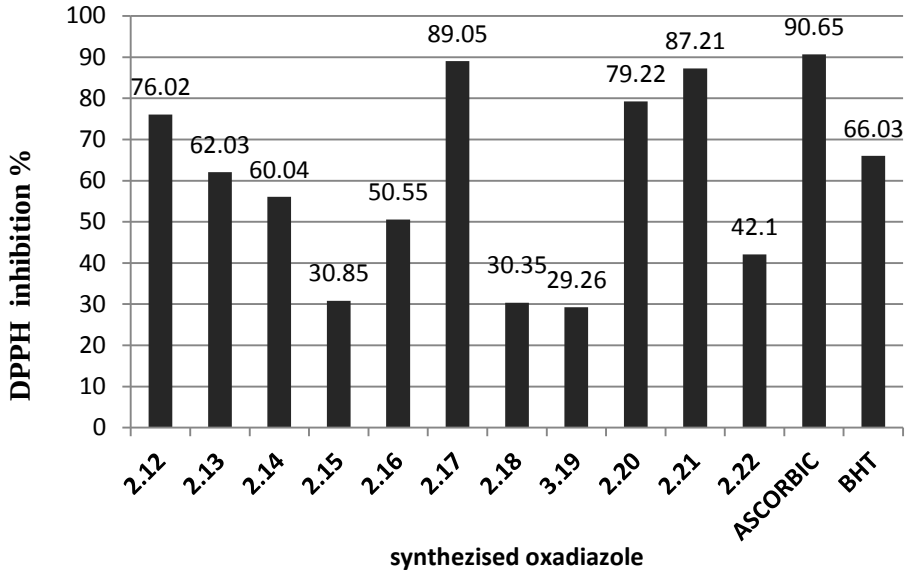

Figure 4.11 : DPPH inhibition % for compounds **2.12-2.22**.

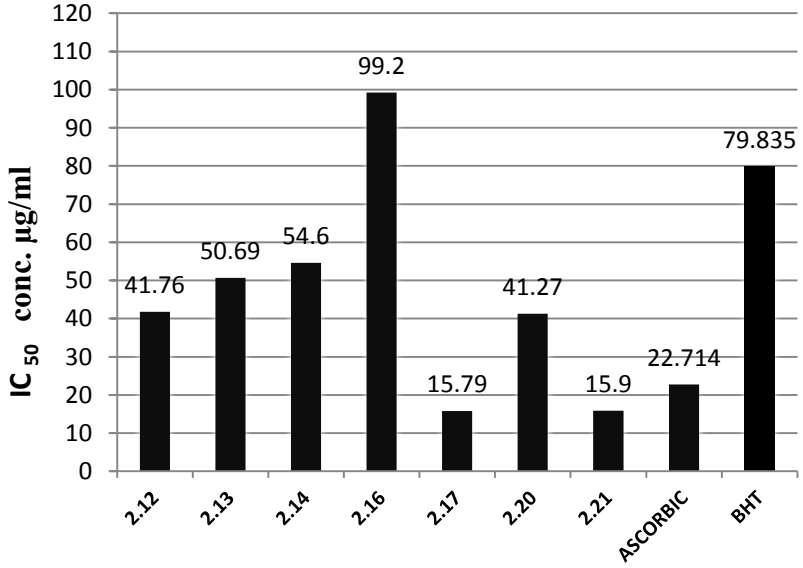

.

Figure 4.12 : IC_{50} values for compounds **2.12-2.22**.

The DPPH inhibition value depends on the concentration of samples tested. Figure 4.13 depicts the relation between the concentration and the DPPH value.

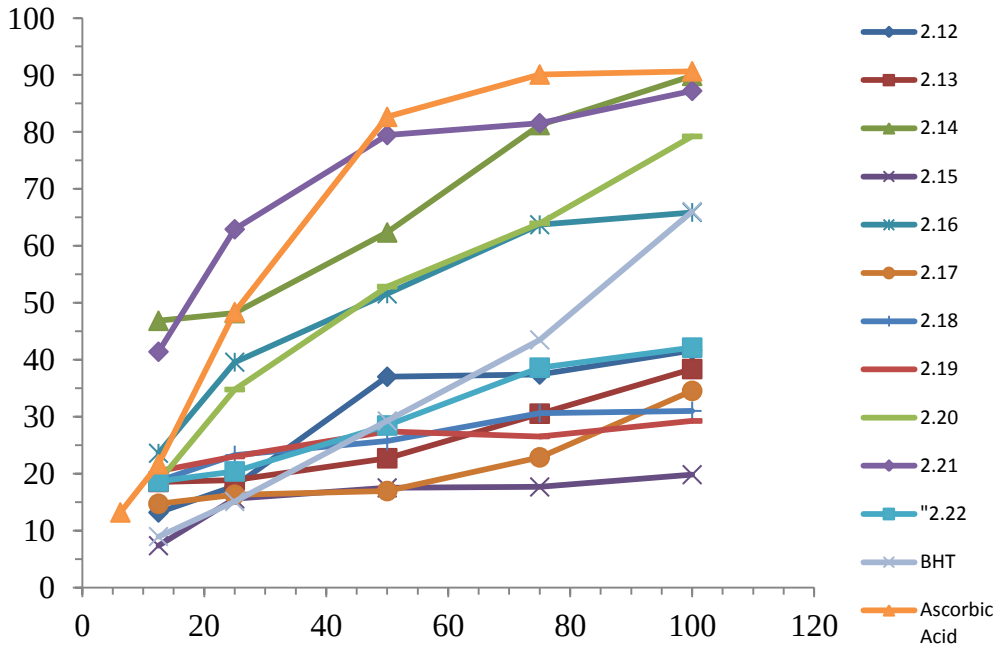

Figure 4.13 : DPPH inhibition with different concentration.

From Table 4.9 and Figure 4.13 we can arrange the sequence for antioxidant ability (inhibition % and the IC_{50} value) of the compound base on the DPPH results as demonstrated in Figure 4.14. From this figure we can recognize the relation between the kind of substituted group and their position on ring C with increasing or decreasing the inhibition.

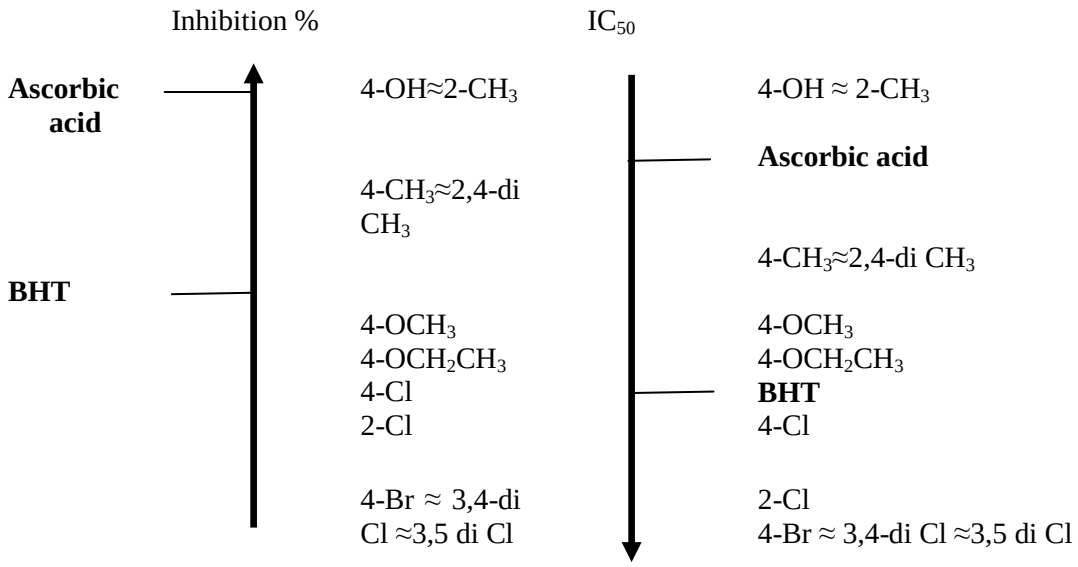

Figure 4.14 : Sequence of substituted group at ring C.

The methyl group in *ortho* position enhances the antioxidant efficiency more than *para* position and this result is in agreement with Rosenwald *et al.*[139] They considered that the *ortho* methyl is more effective when enhancing the antioxidant activity. Furthermore, the DPPH results displayed that the differences between *p*-OMe and *p*-OEt are to small and this observation corresponded with the results reported by Gaspar *et al.*[210] and Rosenwald *et al.*[139] . They reported that the increments of the alkoxy chain are not effective for enhancing the antioxidant values.

All the eleven compounds were tested for their antioxidant properties by FRAP assay. In this assay we used six different standards for comparison. They were BHT, Gallic acid, Ascorbic acid, Rutin, Quercetin and Trolox. The results are tabulated in Figure 4.15.

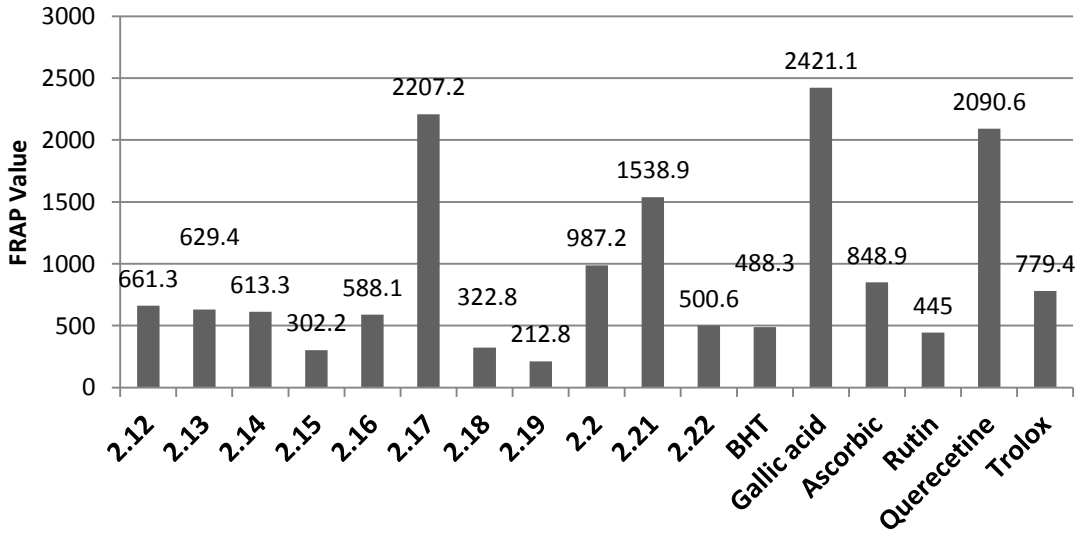

Figure 4.15 : FRAP assay for the eleventh synthesized 2,6-di-*tert*-butyl-4-(5-Aryl-1,3,4-oxadiazol-2-yl)phenol

From Figure 4.15, compound **2.17** (with 4-hydroxyl group in ring C) show strong antioxidant ability with FRAP value of 2207.2, which is higher than the BHT (488.3), Ascorbic acid (848.9.3), Rutin (445), Quercetin (2090.6) and Trolox (779.5) and less than Gallic acid (2421.1). Figure 4.16 illustrated some of these standard structures.

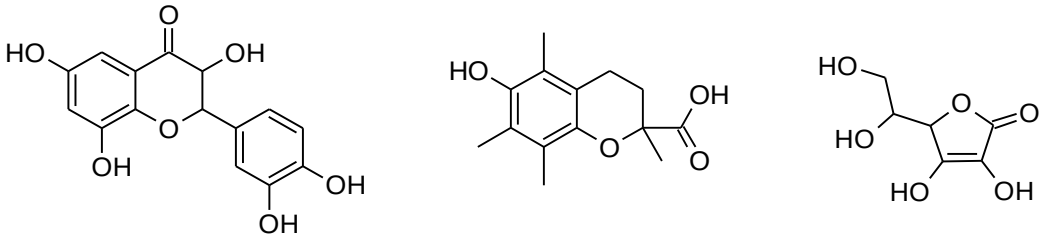

Quercetin Trolox Ascorbic acid

Figure 4.16 : Structures of some standards used in FRAP assay.

The results clearly indicated that the synthesized oxadiazoles enhance the antioxidant ability and the donating groups play an important role in increasing the antioxidant ability. Both compounds **2.17** and **2.21** showed antioxidant ability with DPPH close to Ascorbic acid, while, in FRAP the value is higher than of ascorbic acid. This might be attributed to the differences between the antioxidant mechanisms in each assay. The HAT-mechanism with DPPH assay whereas SET mechanism with FRAP assay.[197b] The FRAP assay show that compound **2.12 (**with donating inductive and hyper-conjugation) have antioxidant ability that is quite similar to **2.13**, **2.14** and **2.16** (4-OMe, 4-OEt and 4-Cl) with donating mesomerism and withdrawal inductive effect. From these results we can conclude that the mesomeric effect has preference over the inductive and these compounds prefer the SET mechanism than HAT mechanism. Whereas, **2.15** (with 4-Br substituent) has low antioxidant ability. Furthermore, the dichloro substituted in compounds **2.18** and **2.19** (with low antioxidant ability) prove that in the *meta* position, inductive effect was more important than the mesomeric effect and are able to quench the antioxidant activity and these results are correspond to the DPPH results.

4.4.2 The 4,4'-(5,5'-(Substitute)bis(1,3,4-oxadiazole-5,2-diyl))bis(2,6-di-*tert*-butyl phenol)

Seven bis DTBP bis oxadiazoles were successfully synthesized. Two groups of hindered phenol in one molecule could increase the antioxidant efficiency.

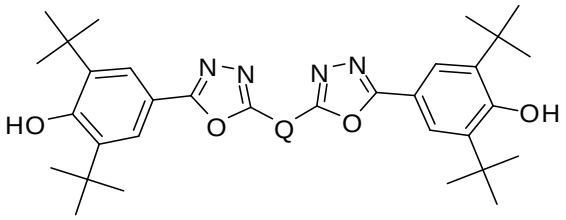

Figure 4.17: General structure of **2.31-2.37**.

The antioxidant properties of these compounds were tested by using DPPH and FRAP assays. The results are demonstrated in Table 4.10 and Figures 4.18- 4.20

Table 4.10 : The DPPH results of compound **2.31-2.37**.

Compound No.	**Q**	**Inhibition % ±SD 100µg/mL**	**IC_{50}± SEM 100µg/mL**
2.31	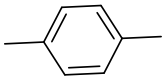	41.65± 0.035	100 >
2.32	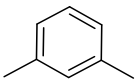	38.37± 0.028	100 >
2.33	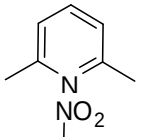	89.848± 0.024	23.15± 0.026
2.34	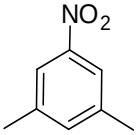	19.82± 0.058	100 >
2.35	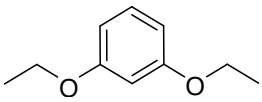	65.87± 0.044	43.421± 0.039
2.36	$-(CH_2)_4$	34.52± 0.027	99.20± 0.025
2.37	$-(CH_2)_0$	31.02± 0.031	100 >
BHT	-	66.03 ±0.022	79.835±0.015
Ascorbic acid	-	90.65 ±0.025	22.71±0.020

Table 4.10 shows that the compound **2.33** possesses better percentage of inhibition than the BHT and almost similar with ascorbic acid. The IC_{50} value for **2.33** was also compared to ascorbic acid. The percentage inhibition of compound **2.35** was quite close to BHT, while the IC_{50} was better than BHT. The rest of the compounds gave poor inhibition and high IC_{50} values. These results demonstrated that having more than one DTBP group in one molecule do not necessarily increase the antioxidant

efficiency. Furthermore, the molecules that have more than one antioxidant group could possess pro-oxidant properties,[211] which can inhibit the antioxidant ability. Figure 4.18 shows the inhibition of these compounds at concentration 100 µg/mL and Figure 4.19 shows the IC_{50} value.

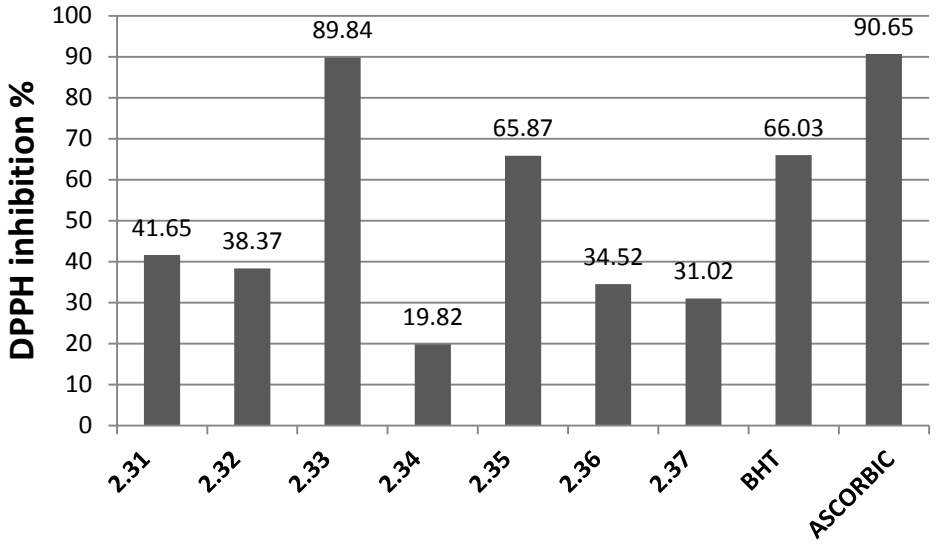

Figure 4.18 : DPPH inhibition for **2.31-2.37**.

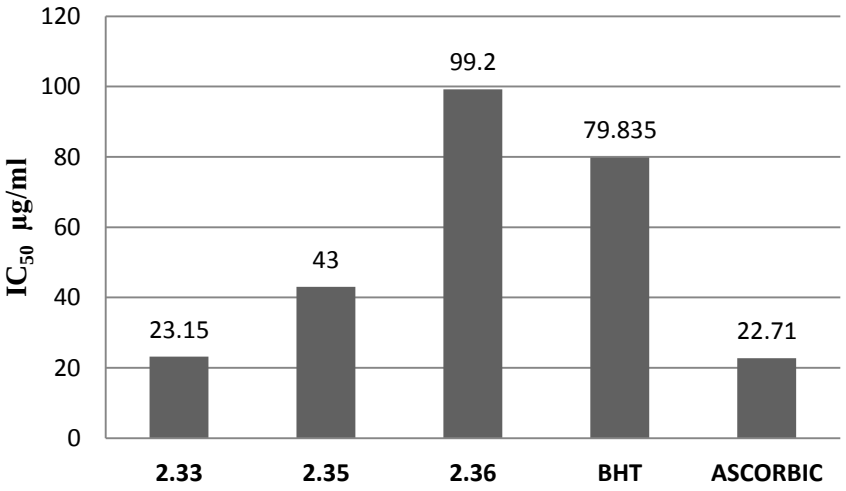

Figure 4.19 : IC_{50} value of **2.33**, **2.35** and **2.36**.

The results of FRAP assay for the bis-1,3,4-oxadiazole derivatives are matched with the DPPH. Compound **2.33** gives the highest activity on this assay, even higher than quercetin. Figure 4.20 depicts the FRAP results.

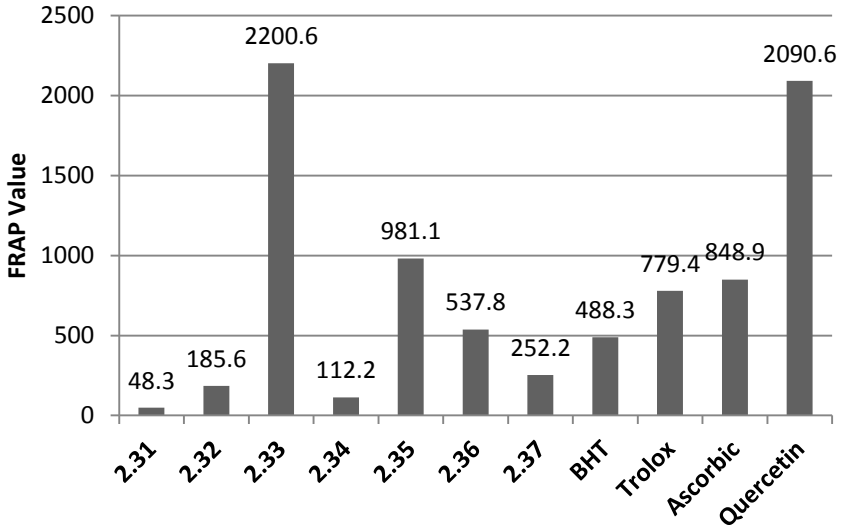

Figure 4.20 : FRAP value for **2.31-2.37.**

Compound **2.35** also demonstrates antioxidant activity higher than ascorbic acid. The same difference has been observed between the DPPH and FRAP results as discussed in Section 4.4.1. For example compound **2.33** in DPPH inhibition was similar to ascorbic acid, whereas, in FRAP **2.33** showed antioxidant ability twice than ascorbic acid as mentioned in Section 4.4.1. Furthermore **2.35** recorded antioxidant activity nearer to BHT in DPPH, while in FRAP it is more than BHT and slightly more than ascorbic acid. The same pattern has been observed with compound **2.37** where it was lower than BHT in DPPH assay, but with FRAP, the assay was to be slightly more than BHT.

4.4.3 The 2,4-di-*tert*-butylphenol derivatives

Apart from the 1,3,4-oxadiazole and bis-oxadiazoles derivative bearing 2,6-di-*tert*-butylphenol group, we successfully prepared different heterocyclic on position six for the semi hindered phenol 2,4-di-*tert*-butylphenol as discussed earlier in Chapter 3. Twenty six new compounds containing heterocyclic and the intermediate compound were tested for their antioxidant properties by DPPH and FRAP assays. These compounds were divided into three groups to make it easier to review the results.

4.4.3.1 Hydrazones, bis hydrazones and their 2,5-substituted 1,3,4-oxadiazoles.

This group consists four hydrazones and two bis hydrazone with four oxadiazole and two bis-oxadiazole. The following Figure 4.21 depict their structures.

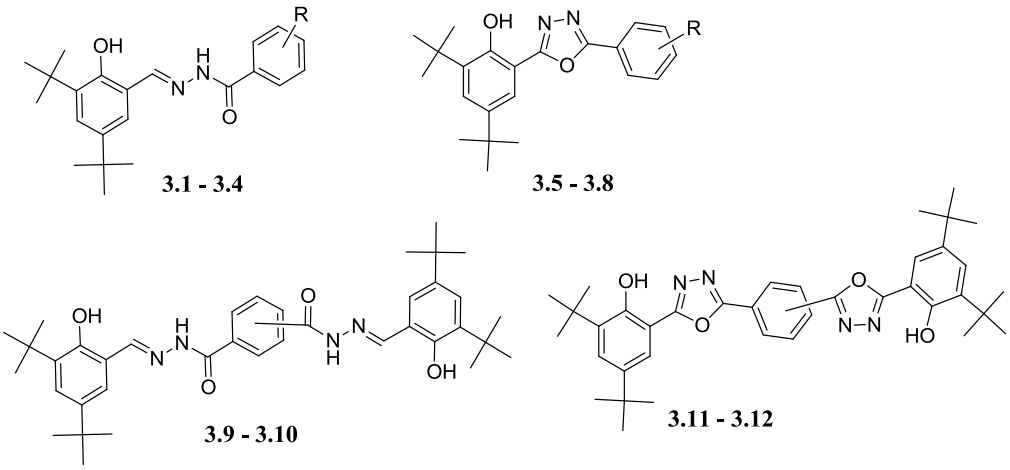

Figure 4.21 : Structures of group one.

The DPPH inhibition percentage and the IC_{50} were presented in Table 4.11.

Table 4.11 : DPPH inhibition and IC_{50} of the Hydrazones, bis hydrazones and their 2,5-substituted 1,3,4-oxadiazoles

Compound	Substituent	Inhibition % ±SD 100µg/mL	IC_{50}± SEM 100µg/mL
3.1	4- Me	61.98±0.061	73.77±0.011
3.2	4-OMe	51.48±0.029	100 >
3.3	4-Br	36.11±0.016	100 >
3.4	2-Cl	48.36±0.013	100 >
3.5	4- Me	61.79±0.038	72.47±0.028
3.6	4-OMe	44.76±0.021	100 >
3.7	4-Br	26.46±0.034	100 >
3.8	2-Cl	54.68±0.065	77.42±0.081
3.9	1,4-C_6H_4	51.40±0.046	100 >
3.10	1,3-C_6H_4	52.52±0.011	88.83±0.034
3.11	1,4-C_6H_4	55.80±0.08	79.63±0.071
3.12	1,3-C_6H_4	56.52±0.053	79.63±0.027
BHT	-	66.03 ±0.022	79.835±0.015
Ascorbic acid	-	90.65 ±0.025	22.71±0.0208

As mentioned earlier, in general the 2,4-di-*tert*-butylphenol exhibited less antioxidant activity from 2,6-di-*tert*-butylphenol and from BHT due to their semi-hindered and the *tert*-butyl group at position *para*, which decrease the antioxidant ability. From Table 4.11 we can observe that the DPPH inhibition of the hydrazones

(**3.1**-**3.4**) are too close to the 1,3,4-oxadiazole (**3.5**-**3.8**). Compounds **3.1** and **3.5** recorded DPPH inhibition less than BHT; however, their IC_{50} was lower than BHT and compound **3.8**. This result showed that we have successfully increased the antioxidant by forming hydrazone at position six and oxadiazole ring at position six. These compounds have one *tert*-butyl group in *ortho* position and are semi-hindered phenolic. In addition to that, the second *tert* -butyl in position *para* have a detrimental effect on antioxidant. The same results were noted with bis-hydrazone and bis-oxadiazole where the DPPH inhibition was less than BHT while the IC_{50} near to BHT. The FRAP value demonstrated that the hydrazone with *para* methyl and their oxadiazole possess antioxidant ability slightly higher than BHT as shown in Figure 4.22.

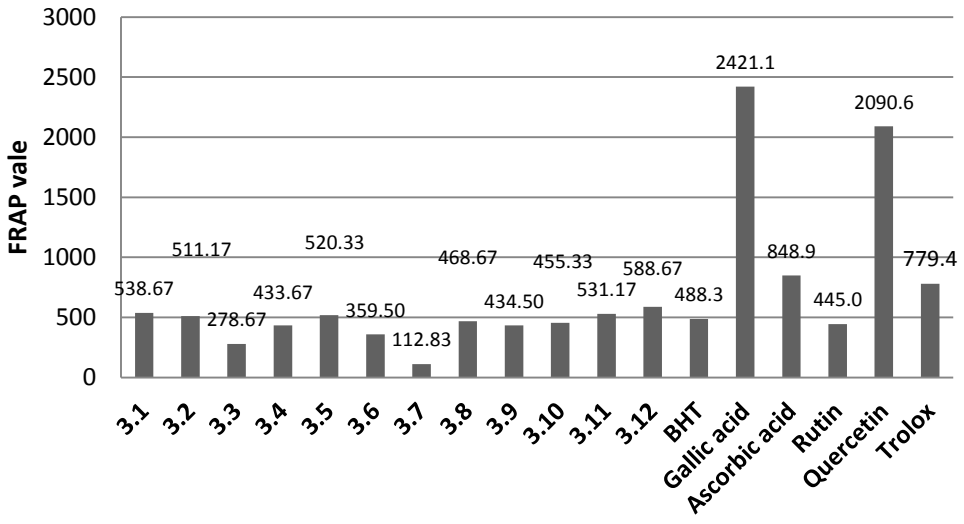

Figure 4.22 : FRAP results of **3.1**-**3.12**.

4.4.3.2 1,3,4-oxadiazole-5- thione and their thio alkyls,5- amino 1,3,4-oxadiazole, thiosemihydrazone and 5-amino-thiadiazole.

The second group consists of seven compounds which have the following structures

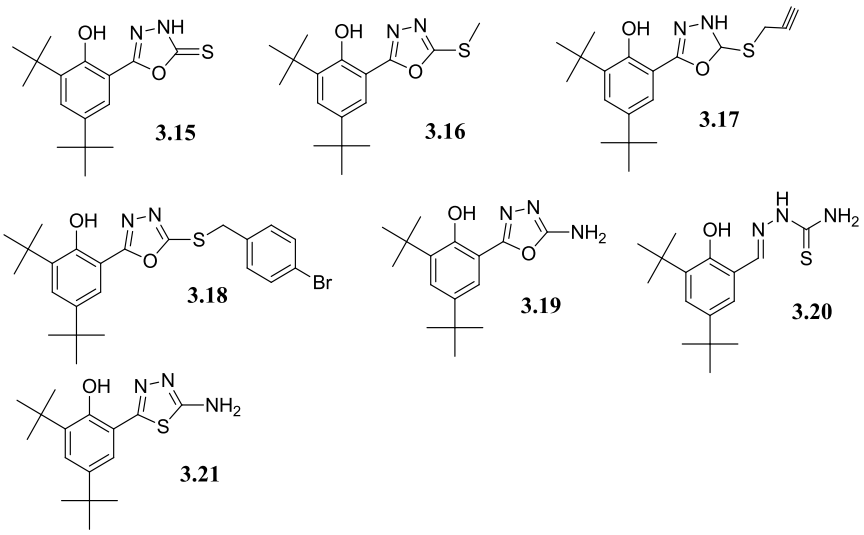

Figure 4.23 : Structures of group two.

These compounds were tested for their antioxidant activity by DPPH and FRAP assays. The DPPH results are presented in Table 4.12

Table 4.12 : The DPPH inhibition and IC_{50} for group two.

Compound	**Inhibition % ±SD 100µg/mL**	**IC_{50}± SEM** 100µg/mL
3.15	91.53±0.017	6.132±0.063
3.16	40.85±0.0101	>100
3.17	37.63±0.0632	>100
3.18	62.59±0.00925	43.622±0.012
3.19	52.32±0.00907	73.657±0.026
3.20	68.59±0.0212	44.063±0.036
3.21	55.32±0.0128	88.389±0.042
BHT	66.03 ±0.022	79.835±0.015
Ascorbic acid	90.65 ±0.025	22.71±0.0208

From the Table 4.12, compound **3.15** displayed the highest inhibition as well the lowest IC_{50} value. This compound showed significant antioxidant properties even at low

concentration as demonstrated within Figure 4.24. For example, at concentration 25µg/mL showed inhibition 70.58, while the ascorbic acid at same concentration shows 48.36.

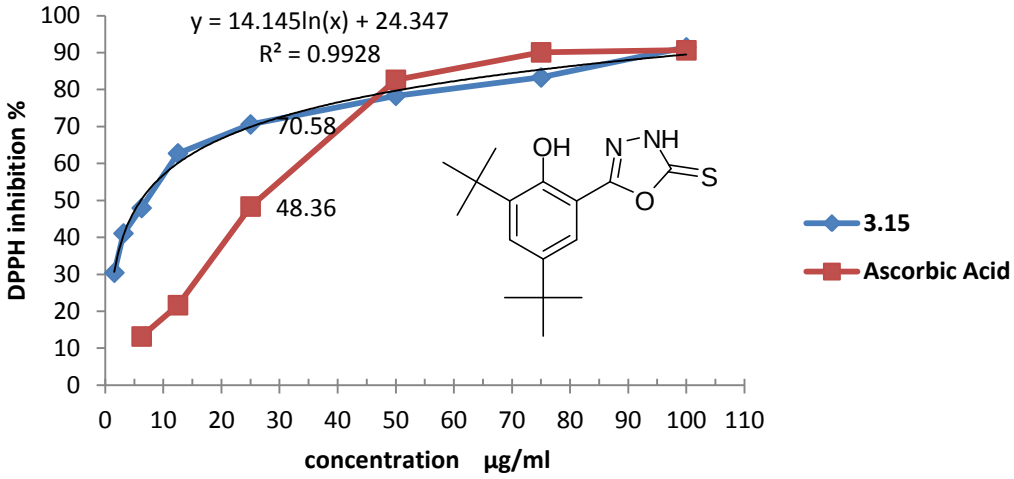

Figure 4.24 : DPPH inhibition of compound **3.15** in different concentrations.

The alkylation of compound **3.15** reduced the antioxidant properties as shown in compounds **3.16**, **3.17** and **3.18**. However, the inhibition percentage of **3.18** is lower than BHT; the IC_{50} value was significant when compared to BHT. The reducing of antioxidant properties of alkyl derivative in compound **3.15** demonstrated that the thioamide group play important role, where they are reported as free radical scavengers.[212] Moreover, the NHCS group is considered as a part of thiourea system which is known as effective antioxidant.[213] Compounds **3.19** and **3.21** exhibited close inhibition value. However, the IC_{50} value of **3.19** was lower than BHT. The following Figure 4.25 depicted the IC_{50} value.

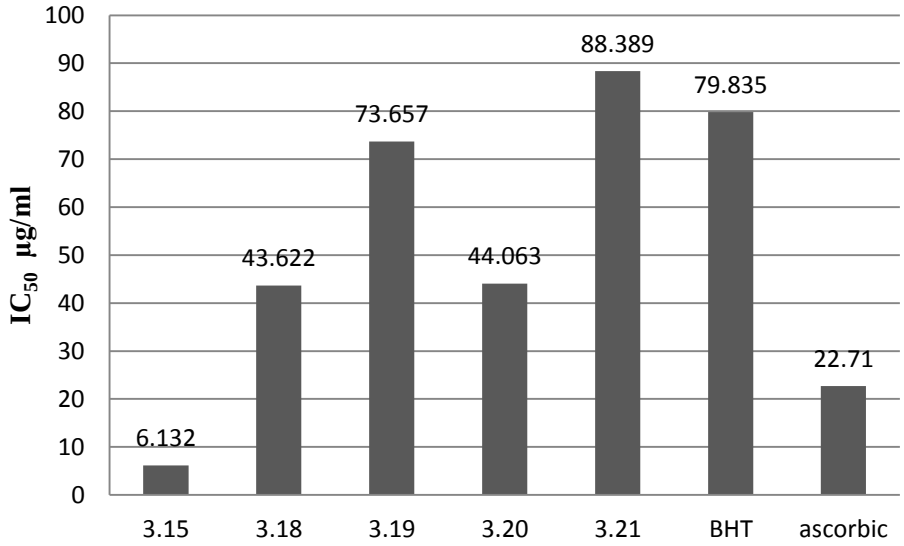

Figure 4.25 : IC_{50} of **3.15-3.21**.

The aromatic amine is known for their antioxidant ability and is considered as primary antioxidant.[214] Thus, the increased in antioxidant ability could be attributed to the aromatic NH_2 group for the oxadiazole **3.19** and in thiadiazole **3.21**. The thiosemicarbazone **3.20** is an intermediate when synthesizing compound **3.21** showed antioxidant better than **3.21**. The thiourea part could increase the antioxidant properties; where the thioruea, propylthiouracil, 1,3-dimethyl thiourea and hydroxyphenyl urea derivatives are branded as effective free radical scavengers.[215] Figure 4.26 depicted the **3.20** structure as a thiourea derivative.

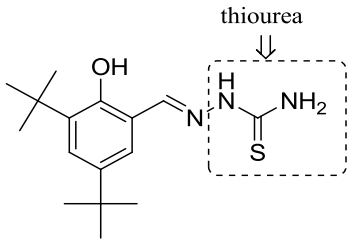

Figure 4.26 : Compound **3.20** as a thiourea derivative.

The FRAP assay results were very similar to the DPPH results when compared to the references BHT (and with others references) mentioned earlier. The Figure 4.27 depicted the FRAP values.

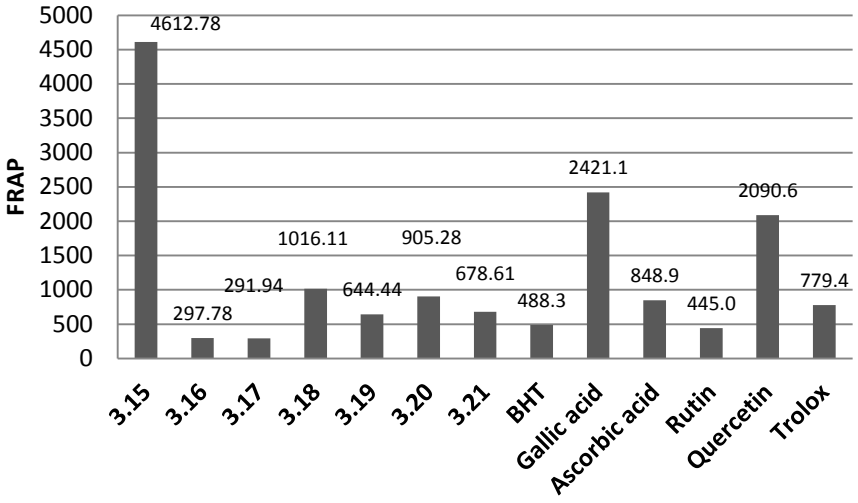

Figure 4.27 : FRAP values of **3.15-3.21**.

The results exhibited that the alkylations of compound **3.15** with *p*-bromobenzyl group gave better antioxidant ability than alkylation with an aliphatic group. Furthermore, the 5-amino-1,3,4-oxadiazole and the 5-amino-1,3,4-thiadiazole possess antioxidant activity higher than BHT.

4.4.3.3 The 2-(3,5-di-*tert*-butyl-2-hydroxybenzoyl)-N-(aryl) hydrazine carbothioamide and the triazoles.

The last group consists of seven compounds and their antioxidant ability were investigated. The structures of this group are shown in the following Figure 4.28.

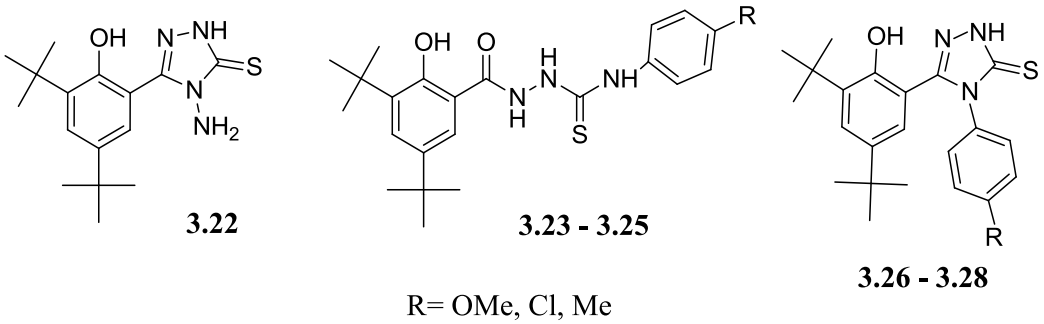

Figure 4.28 : Structures of third group (**3.22-3.28**).

An extraordinary antioxidant behavior was observed in this group. The DPPH result of **3.22** showed an inhibition of 87.29 and the IC_{50} was 6.77 μgm/mL, while the ascorbic acid displayed 90.65 and the IC_{50} was 22.71 μgm/mL. This showed that the

triazole can be considered as a very good antioxidant agent. Furthermore, it has IC_{50} three times less than ascorbic acid as demonstrated in Table 4.13 and Figures 4.29, 4.30 respectively.

Table 4.13 : DPPH inhibition and IC_{50} of 3.22-3.28.

Compound No.	R	Inhibition % ± SD [a]	IC_{50}±SEM [b] (100µg/mL)
3.22	-	87.29±0.013	6.77±0.074
3.23	OMe	91.77±0.017	4.489±0.054
3.24	Cl	91.33±0.062	5.506±0.071
3.25	Me	91.37±0.054	4.646±0.0123
3.26	OMe	74.38±0.023	41.345±0.048
3.27	Cl	76.34±0.025	14.519±0.046
3.28	Me	80.34±0.011	14.517±0.07
BHT	-	66.03 ±0.022	79.835±0.02
Ascorbic acid	-	90.65 ±0.25	22.71±0.208

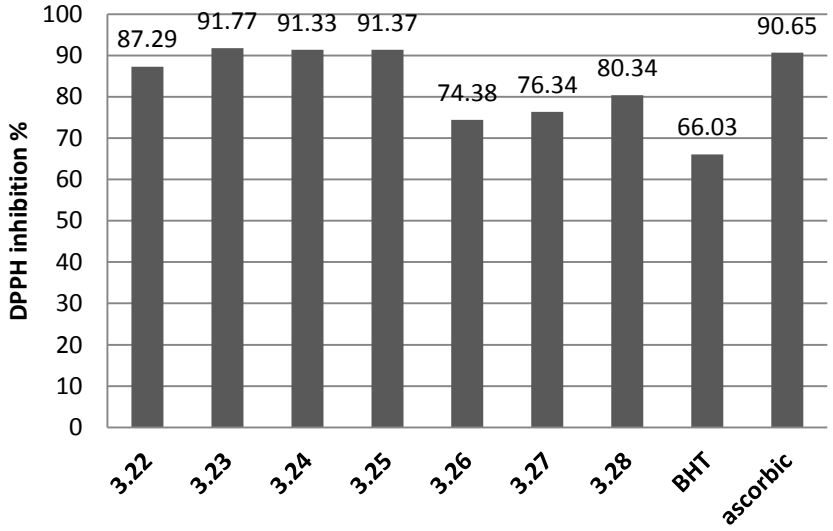

Figure 4.29 : DPPH inhibition of **3.22-3.28**.

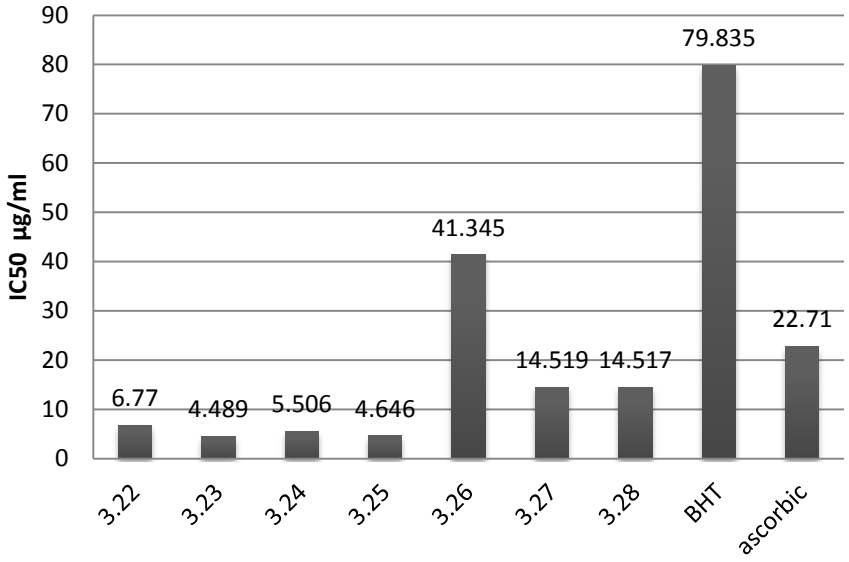

Figure 4.30 : IC_{50} of **3.22-3.28**.

These observations were further supported by the DPPH and FRAP results of the triazoles **3.26-3.28**. The three hydrazinecarbothioamides **3.23-3.25** also show excellent free radical scavenging ability. They have antioxidant ability better than ascorbic acid, while their triazoles derivatives were less than ascorbic acid but higher than BHT.

The similarity of IC_{50} values for compounds **3.23-2.25** support our assumption that the substitute at *the para position* on the phenyl ring did not affect the antioxidant ability. The DPPH results for hydrazinecarbothio amides **3.23-3.25** which are higher than their triazole **3.26-3.28**. This could be explained by their structural differences. The structures of hydrazinecarbothio amides have three primary antioxidant groups, while the trial has just two primary antioxidant group as demonstrated in Figure 4.31.

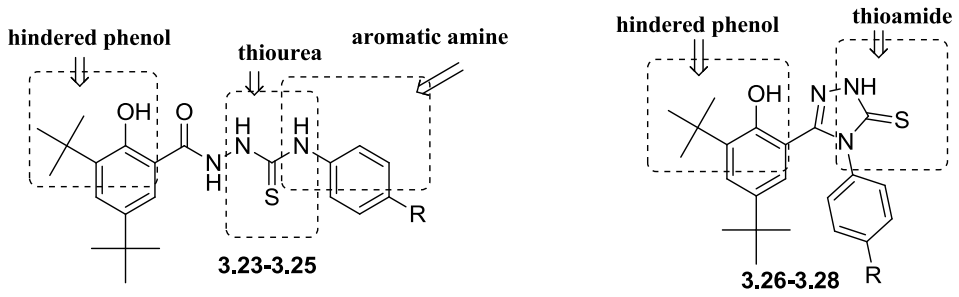

Figure 4.31 : Comparison between hydrazinecarbothio amides structure with triazole.

The FRAP results shows a similar pattern as the DPPH results, which are demonstrated in Figure 4.32.

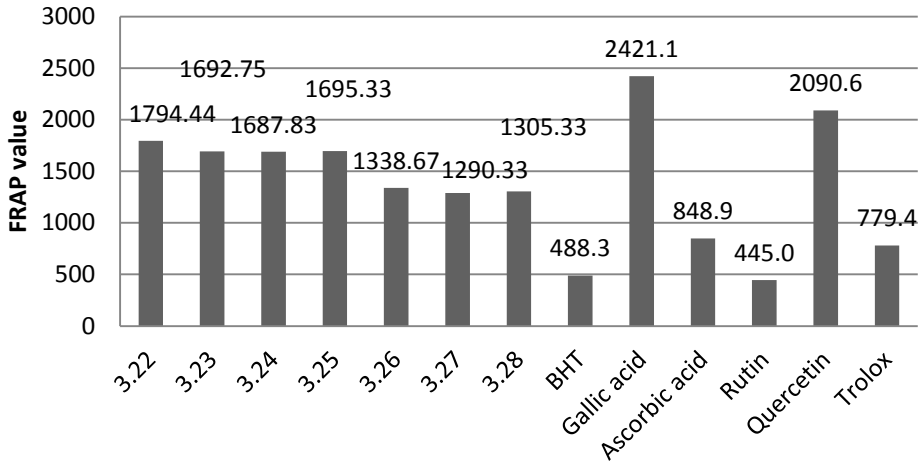

Figure 4.32: The FRAP value of **3.22-3.28**.

All of the compounds have higher antioxidant activity (higher FRAP value) compared to referances compound such as BHT and ascorbic acid. Compound **3.22** has higher FRAP value then the hydrazinecarbothioamide derivatives and even higher antioxidant ability than their triazoles. The FRAP value suggested that the substituted groups on phenyl ring are not effective in promoting antioxidant activity for these structures.

Chapter 5 : Conclusion and future work

5.1 General Conclusion

Eleven compounds of 2,5-disubstituted oxadiazole containing 2,6-di-*tert*-butylphenol were succesfuly synthesized as new antioxidant compounds from reaction of aryl hydrazide and 2,6-di-*tert*-butyl benzoic acid in the presence of $POCl_3$. The antioxidant results indicated that the position and nature of the substituents on the phenyl ring played an important role in influencing the antioxidant properties. Compound with hydroxyl group at the *para* position gave the highest antioxidant activity. High electronegative atoms, such as chlorine or bromine, decreased the antioxidant ability. Seven compounds of bis-oxadiazole bis-2,6-di-*tert*-butylphenol were successfully synthesized and only one of them gave distinctive antioxidant properties, while the other compounds exhibited a pro-oxidative effect.

The antioxidant ability of 2,4-di-*tert*-butylphenol could be promoted by the formation of heterocyclic ring at position six. Furthermore, formation of hydrazone and hydrazinecarbothioamide in the same position enhanced their antioxidant ability. However, the substituted group in hydrazone and hydrazinecarbothioamide was shown to have no effect on the antioxidant ability. Formation of aryl 1,3,4-oxadiazole enhanced the antioxidant ability and the effect of substituted group was similar to the 2,6-di-*tert*-butylphenol oxadiazoles. Formation of oxadiazole-5-thione at position six exhibited interesting antioxidant properties. However, their alkylated derivative exhibited lower antioxidant activity. The 5-amino-oxadiazole and 5-amino-thiadiazole ring enhanced the antioxidant properties and both have quite similar antioxidant activity. The formation of triazole ring at the same position displayed interesting enhancement to the antioxidant ability. However, effect of substituted group at *para* position was not observed.

In general the FRAP assay gives antioxidant ability higher than the DPPH assay in comparison to the standard references. We proposed that the synthesized compounds prefer the SET antioxidant mechanism than the HAT mechanism.

5.2 Future work

The future work can be divided into two parts. The first one is do more biological studies. The synthesized compound will be tested for their toxicity, anti inflammatory and anti cancer's abilities.

The second part, is to synthesize new derivatives of **3.22** as demonstrated in Scheme 5.1 and study their biological activity.

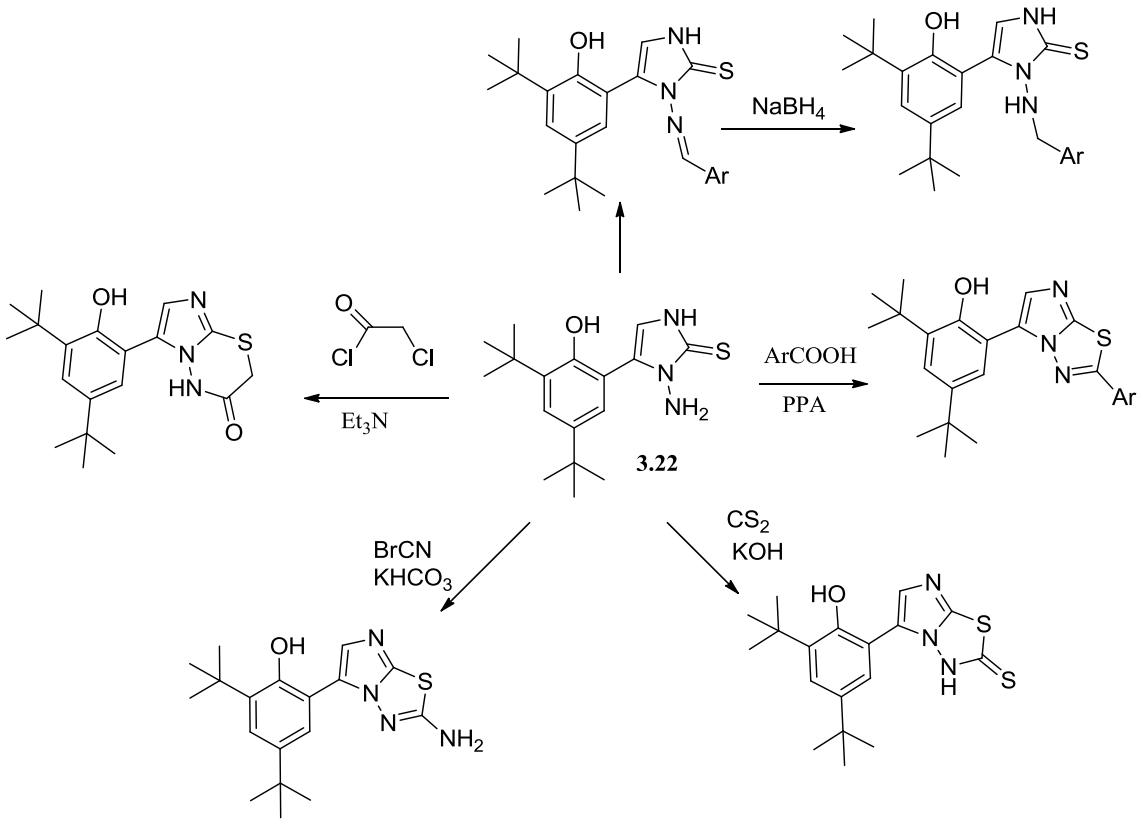

Scheme 5.1 : Outline of future work

Chapter 6 : Experimental Details

6.1 General

The chemicals used for synthesis were purchased from Sigma-Aldrich, Fisher and Merck. Melting point was determined by an open capillary tube method using MEL-TEMP II apparatus and is uncorrected. Purities of compounds were checked with a thin layer chromatography (Silica gel TLC) plate's brand Merck, and the spot located with iodine vapors and UV lights. The IR spectrums were obtained with Perkin Elmer400 Fourier transform infrared (FTIR) Spectrometer.

All NMR spectra were recorded on either JEOL-ECA 400 MHz, JEOL-Lambda 400 MHz spectrometer or Bruker AVN 400 and 600 MHz; $CDCl_3$ and DMSO-d_6 were used as the solvent with TMS as internal standard. The mass spectrum was recorded using Agilent 5975 for EI/MS and Finnigan TSQ7000 for HREIMS (NUS, Singapore). UV spectroscopy Power Wave X340, BIO-TEK instrument INC was used to record the FRAP assay and DPPH assay.

6.1.2 Synthesis of 4-ethoxybenzoic acid

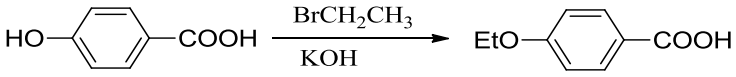

Potassium hydroxide solution (0.2 mole in 10 mL H_2O) and 35 mL ethanol were added into a 100 mL round bottom flask that contains *p*-hydroxy benzoic acid (1.38 g; 0.1mole). The reaction mixture was stirred at room temperature for 1 h. Bromoethane (1.2 mL, 0.15 mole) was added and the mixture was refluxed for 24 h. The excess amount of solvent was removed under reduced pressure and 50 mL of water was added. The solution was acidified with 5% HCl and the resulting precipitate was filtered and crystallized from methanol to give white crystal. Yield 1.43 g (86%), m.p.177-179°C

(lit 176-177 °C)[216]. IR.(KBr, υ_{max}/ cm^{-1}): 3462 (br, O-H), 3062 (w, C-H aromatic), 2982, 2877 (s, C-H aliphatic), 1692 (s, C=O), 1598 (m, C=C); ^{1}H NMR (DMSO-d_6, 400 MHz, ppm): 1.53 (t, 3H, *J*=7.32, $OCH_2\underline{CH_3}$), 4.11 (q, 2H, *J*=8, OCH_2), 7.23(d, 2H, J=8.18,3, H_2), 8.16 (d, 2H, J=8.04, H_4).

6.1.3 General synthesis of hydrazide (2.1-2.11)

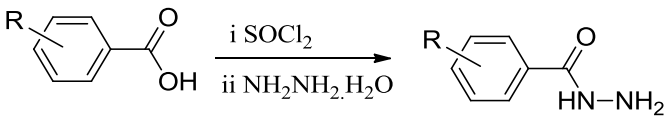

Thionylchloride (3mL) was added in small portions to 1g of aromatic acid. The mixture was refluxed for 3h, the excess of thionyl chloride was removed under reduce pressure. 0.1 mole of acid chloride (without further purification) was dissolved in dry benzene, and it was transferred to an addition funnel. 5 mL hydrazine hydrate (98%) in 10 mL dried benzene was added into a two neck flask that equipped with a condenser. The addition funnel was then fixed onto the flask and secured firmly.The acid chloride was added dropwise at 0°C. After that, the mixture was allowed to stand for 1 h at an ambient temperature. It was then stirred and refluxed for 3h .The excess solvent was removed under reduce pressure and the crude solid was collected, wash with water and recrystallized from suitable solvent. The melting point, IR and ^{1}H NMR were recorded.

4-Methylbenzoic hydrazide (2.1)

Recrystallization of the crude product from ethanol afforded a white crystal. Yield 1.04 g (95%); m.p. 115-118 °C (lit. 116-117 °C)[217]; .(KBr, υ_{max} / cm^{-1}): 3316, 3215 (m, NH, NH_2), 3003 (w, $CH_{aromatic}$), 2945 -2872 (s, $CH_{aliphatic}$), 1669 (s, C=O), 1597 (s, C=C); ^{1}H NMR (DMSO-d_6, 400 MHz, ppm): 2.31 (s, 3H,-CH_3), 4.51(s, 2H ,NH_2), 7.38 (d, 2H, *J*=7.9, 3,5 Ar-H), 7.75(d, 2H, *J*=7.7, 2, 6 Ar-H), 8.84 (bs, 1H, CONH).

4-Methoxybenzoic hydrazide (2.2)

Recrystallization of the crude product from aqueous ethanol afforded a white crystal. Yield 0.93 g (86%); m.p.137-138 $^{\circ}$C (lit. 136-140)[218]; IR.(KBr, υ_{max} / cm^{-1}): 3298, 3210 (m, NH, NH_2), 3083 (s, $CH_{aromatic}$), 2955 -2879 (s, $CH_{aliphatic}$), 1661 (s, C=O), 1598 (m, C=C); ^{1}H NMR (DMSO-d_6, 400 MHz, ppm): 3.72 (s, 3H,-OCH_3), 4,52 (s, 2H, NH_2), 7.15 (d, 2H, *J*=7.8, 2,6 Ar-H),7.88 (d, 2H, J= 8.02, 3, 5 Ar-H), 8.80 (bs, 1H, CONH).

4-Ethoxybenzoic hydrazide (2.3)

Recrystallization of the crude product from ethanol afforded white solid. Yield 0.85 (79%); m.p. 125-127°C (lit. 126-128 $^{\circ}$C)[219]; IR.(KBr, υ_{max} / cm^{-1}): 3352, 3268 (m, NH), 3066 (w, $CH_{aromatic}$), 2923, 2849 (s, $CH_{aliphatic}$), 1658 (s, C=O), 1598, 1495 (s, C=C), 1216 (s, C-O), 1109(s, O-CH_2); ^{1}H NMR (DMSO-d_6, 400 MHz, ppm): 1.32(t, 3H, *J*=7.29, $OCH_2\underline{CH_3}$), 4.18 (q, 2H, *J*=7.9, OCH_2), 4,56 (s, 2H, NH_2), 6.94(d, 2H, *J*=7.3, 2,6 Ar-H), 7.77 (d, 2H, *J*=7.7, 3, 5 Ar-H), 9.58 (bs, 1H, CONH).

4-Bromobenzoic hydrazide (2.4)

Recrystallization of the crude product from methanol afforded white crystal. Yield 0.86 g (82%); m.p. 165-166 ^{0}C (lit. 167 $^{\circ}$C)[219], IR.(KBr, υ_{max} / cm^{-1}): 3364, 3253 (m, NH), 3081 (w, $CH_{aromatic}$), 1662 (s, C=O), 1598,1493 (m, C=C), 1214 (s, C-O); ^{1}H NMR (DMSO-d_6, 400 MHz, ppm): 4.25 (bs, 2H, NH_2), 7.61 (d, 2H *J*=8.2, 2,6 Ar-H), 7.78 (d,2H, *J*=7.8, 3, 5 Ar-H), 10.02(bs, 1H, NH).

4-Chlorobenzoic hydrazide (2.5)

Recrystallization of the crude product from aqueous ethanol afforded off white crystal. Yield 0.98 g (91%); m.p.160-164 $^{\circ}$C (lit. 162-163 $^{\circ}$C)[217]; IR. (KBr, υ_{max} / cm^{-1}): 3367, 3271 (m, NH), 3075 (w, $CH_{aromatic}$), 1659 (s, C=O), 1595,1487 (m, C=C),1212 (s,

C-O); ^{1}H NMR (DMSO-d_6, 400 MHz , ppm): 4.51 (bs, 2H, NH_2), 7.56 (d, 2H , *J*=8.23, H_3, H_5), 8.01(d, 2H, *J*=8.20, H_2, H_6), 10.33 (bs, 1H, NH).

4-hydroxybenzoic hydrazide (2.6)

Recrystallization of the crude product from ethanol afforded white crystal. Yield 0.97 g (89%); m.p. 262-264 dec (lit. 262 dec)[220]; IR (KBr, υ_{max} / cm^{-1}): 3371 (br. OH, NH_2, NH), 3081 (w, $CH_{aromatic}$), 1662 (s, C=O), 1597, 1488 (m, C=C), 1219 (s, C-O); ^{1}H NMR (DMSO-d_6, 400 MHz, ppm): 4.91 (bs, 2H, NH_2), 6.62 (d, 2H, *J*=7.78, H_3, H_5), 7.56 (d, 2H, *J*=7.78, H_2, H_6), 9.80 & 9.87 (bs, NH & OH).

3,4-dichlorobenzoic hydrazide(2.7)

Recrystallization of the crude product from ethanol afforded pale yellow crystal. Yield 0.84 g (79%); m.p.150-152 $^{\circ}$C (lit. 154-160 $^{\circ}$C)[221]; IR (KBr, υ_{max} / cm^{-1}): 3371, 3325, 2279 (br, NH_2, NH), 3090 (w, $CH_{aromatic}$), 1658 (s, C=O), 1595, 1491 (s, C=C), 1220 (s, C-O); ^{1}H NMR (DMSO-d_6, 400 MHz, ppm): 4.23 (bs, 2H, NH_2), 7.44(d, 1H, J=8.2,H_5), 7.65 (d, 1H, J=8.00, H_5), 7.92(s, 1H, H_2),10.03 (bs, 1H, NH).

3,5-dichlorobenzoic hydrazide (2.8)

Recrystallization of the crude product from aqueous ethanol afforded white solid. Yield 0.93 g (87%); m.p. 200-204°C (lit.205-207 $^{\circ}$C)[222]; IR.(KBr, υ_{max} / cm^{-1}): 3366, 3259 (m, NH), 3083 (w, $CH_{aromatic}$), 1660 (s, C=O), 1598, 1490 (m, C=C), 1216 (s, C-O); ^{1}H NMR (DMSO-d_6, 400 MHz, ppm): 4.55 (bs, 2H, NH_2), 7.71 (t, 1H, *J*=1, 84, H**4**), 7.76 (d, 2H, *J*=2.12, H_2, H_6), 10.01(s, 1H, NH).

2,4-di-Methylbenzoic hydrazide (2.9)

Recrystallization of the crude product from ethanol afforded white crystal. Yield 0.95 g (88%); m.p.122-124 $^{\circ}$C (lit. 127-129 $^{\circ}$C)[223]; IR (KBr, υ_{max} / cm^{-1}): 3378, 3320, 2279 (m, NH_2, NH), 3090 (w, $CH_{aromatic}$), 2951, 2847 (s, $CH_{aliphatic}$), 1663 (s, C=O),

1598, 1485 (s, C=C), 1212 (s, C-O); ^{1}H NMR (DMSO-d_6, 400 MHz, ppm): 4.63(bs, 2H, NH_2), 7.07.18(m, 2H, H_3, H_5), 7.91 (d, 1H, *J*=7.78, H_6), 9.62 (bs, 1H, NH).

2-Methylbenzoic hydrazide (2.10)

Recrystallization of the crude product from ethanol afforded white needle .Yield 0.84 g (77%); m.p.120-124 °C (lit. 120-121°C)[217]; IR (KBr, υ_{max} / cm^{-1}): 3355, 3323, 2268 (m, NH_2, NH), 3081 (w, $CH_{aromatic}$), 2949, 2830 (s, $CH_{aliphatic}$), 1659 (s, C=O), 1598, 1490 (s, C=C), 1216 (s, C-O), ^{1}H NMR (DMSO-d ^{6}, 400 MHz, ppm): 4.63 (bs, 2H, NH_2), 7.15-7.18 (m, 2H, H_3, H_5), 7.35-7.38 (m, 1H, H_4), 7.40-7.42 (m, 1H, H_6), 9.55 (bs,1H,NH).

2-Chlorobenzoic hydrazide (2.11)

Recrystallization of the crude product from ethanol afforded white solid. Yield 1.02 g (95%); m.p. 110-114 °C (lit. 118-120 °C) [224]; IR (KBr, υ_{max} / cm^{-1}): 3371, 3328, 2266 (m, NH_2, NH), 3102 (w, $CH_{aromatic}$), 1661 (s, C=O), 1598, 1489 (s, C=C), 1217(s, C-O); ^{1}H NMR (DMSO-d ^{6}, 400 MHz, ppm): 4.48(bs, 2H, NH_2), 7.33-7.38 (m, 1H, H_5),7.46-7.53 (m, 3H, H_3, H_4, H_6), 9.67 (bs, 1H, NH).

6.1.4 General synthesis of 2, 6-di-*tert*-butyl-4-(5-Aryl-1,3,4-oxadiazol-2-yl) phenol (2.12-2.22)

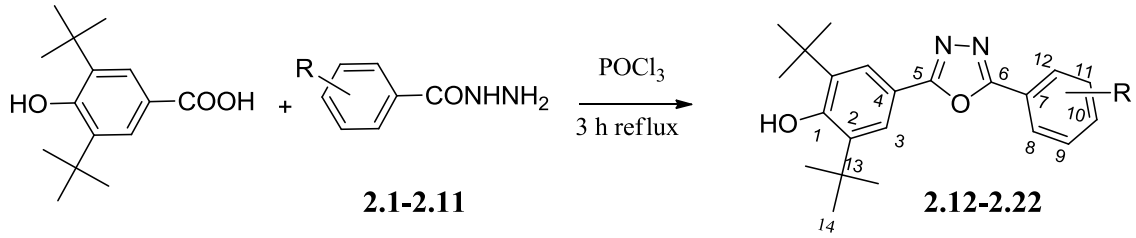

2.1-2.11 **2.12-2.22**

A mixture of 3,5-di-*tert*–butyl-4-hydroxybenzoic acid (0.31g, 1.24 mmol) and aryl acid hydrazide (1.24 mmol) in 50 mL round flask, 5mL of phosphorusoxy chloride was added in a few portions at room temperature. The mixture was stirred and refluxed

for 3 hours in a water bath at 80-90 °C. After cooling, the mixture was poured into 100 mL crushed ice and stirred for 15 minutes. Sodium bicarbonate was added in few portions until the pH adjusted to 7-8. The precipitate was filtered, washed with water and dried. The crude product was purified either from column chromatography or recrystallized from suitable solvent.

2,6-di-tert-butyl-4-(5-(4-methylphenyl)-1,3,4-oxadiazol-2-yl)phenol.

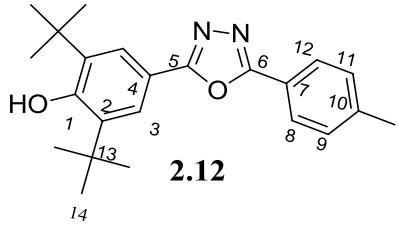

2.12

The product was recrystallized from chloroform-ethanol (1-1) to obtain white crystals. Yield 0.343 g (76.0%); m.p. 196-197 °C; IR.(KBr, υ_{max} / cm^{-1}): 3658(br, OH), 3011 (w, $CH_{aromatic}$), 2962-2947 (s, $CH_{aliphatic}$), 1610(s, C=N), 1585, 1498(s, C=C), 1219(s, C-O); ^{1}H NMR ($CDCl_3$, 400 MHz, ppm): 1.51 (s, 18H, H_{14}, 2×*t*-Bu),2.42(s, 3H, *p*-CH_3-ph), 5.67 (s, 1H, OH), 7.31(d, 2H, *J*=8.28, H_9, H_{11}), 7.94(s, 2H, H_3), 8.01(d, 2H, *J*=8.28, H_8, H_{12});.^{13}C NMR ($CDCl_3$, 100 MHz, ppm): 21.73(*p*-CH_3ph), 30.25(6C, C_{14}, 2×C($\underline{C}H_3)_3$), 34.56 (2C, C_{13}, 2×$\underline{C}(CH_3)_3$), 115.43(C_4), 121.52(C_7), 124.35(C_3), 126.87(2C, C_8 & $_{12}$), 129.77(2C, C_9 & C_{11}), 136.81(C_2), 141.99(C_{10}), 157.12(C_1), 164.22 & 165.21(C_5 & C_6). HREIMs, m/z= 364.2147 [$M^{\cdot+}$] (calc. for $C_{23}H_{28}O_2N_2$, 364.2151).

2,6-di-*tert*-butyl-4-(5-(4-methoxyphenyl)-1,3,4-oxadiazol-2-yl)phenol.

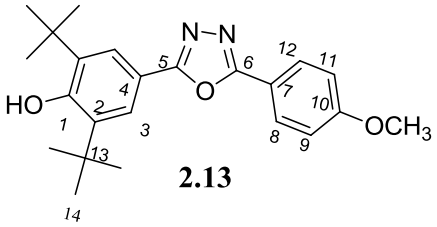

2.13

The solid product was recrystallized from ethyl acetate white crystal to obtain white needle crystal. Yield 0.346 g (73%); m.p. 179-181 °C; IR (KBr, υ_{max} / cm^{-1}): 3625(br, OH_{phenol}), 3006 (w, $CH_{aromatic}$), 2955 (s, $CH_{aliphatic}$), 1611(s, C=N), 1585, 1495 (s, C=C), 1219(s, C-O), 1020(m, O-CH_3); ^{1}H NMR ($CDCl_3$, 400 MHz, ppm): 1.51(s, 18H, H_{14}, 2×C($\underline{CH_3}$)$_3$), 3.89 (s, 3H, OCH_3), 5.63(s, 1H, OH), 7.03 (d, 2H, *J*=9.04, H_9, H_{11}), 7.92(s, 2H, H_3), 8.06 (d, 2H, *J*=8.56, H_8, H_{12}); ^{13}C NMR($CDCl_3$, 100 MHz, ppm): 30.13(6C, C_{14}, 2×C($\underline{CH_3}$)$_3$), 34.45(2C, C_{13}, 2× $\underline{C}(CH_3)_3$), 55.44 (OCH_3), 114.40 (2C, C_8 & C_{12}), 115.37(C_4), 116.72(C_7), 124.19 (C_3), 128.58 (2C, C_9 & C_{11}), 136.68 (C_2), 156.95 (C_1), 162.11(C_{10}), 163.89 & 164.75(C_6 & C_5). HREIMs, m/z=380.2095 [$M^{\cdot+}$] (calc. for $C_{23}H_{28}O_3N_2$, 380.2100).

2,6-di-*tert*-butyl-4-(5-(4-ethoxyphenyl)-1,3,4-oxadiazol-2-yl)phenol.

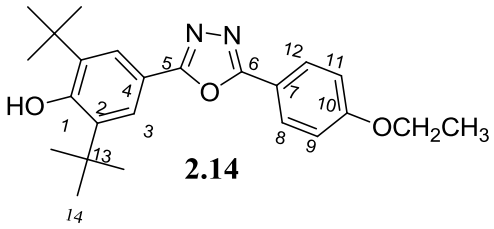

2.14

The crude solid was recrystallized from ethyl acetate-methanol (1-1) to give white amorphous. Yield 0.371 g (76 %), m.p. 176-178 °C, IR(KBr, υ_{max} / cm^{-1}), 3628(br, OH_{phenol}), 3009 (w, $CH_{aromatic}$), 2957 (s, $CH_{aliphatic}$), 1611(m, C=N), 1543, 1495 (s, C=C), 1221(s, C-O), 1111 (m, O-CH_2); ^{1}H NMR ($CDCl_3$,400 MHz, ppm): 1.46 (t, 3H, *J*=7.32, $OCH_2\underline{CH_3}$), 1.51 (s, 18H, H_{14}, 2× C($\underline{CH_3}$)$_3$), 4.11 (q, 2H, *J*=8, OCH_2), 5.64(s, 1H, OH), 7.1(d, 2H, *J*=8.8, H_9 & H_{11}), 7.92 (s, 1H, H_3), 8.05(d, 2H, *J*=8.04, H_8 & H_{12}); ^{13}C NMR ($CDCl_3$, 100 MHz, ppm): 14.71 ($OCH_2\underline{CH_3}$), 30.17(6C, C_{14}, 2×C($\underline{CH_3}$)$_3$), 34.48 (2C, C_{13}, 2×$\underline{C}(CH_3)_3$), 63.73($O\underline{CH_2}$), 114.91(2C, C_8 & C_{12}), 115.50 (C_4), 116.60 (C_7), 124.18(C_3), 128.57(2C, C_9 & C_{11}), 136.69(C_2), 156.93(C_1), 161.52(C_{10}),

164.00&164.90 (C_6 & C_5). HREIMs, m/z=394.2249 [$M^{\cdot+}$] (calc. for $C_{24}H_{30}O_3N_2$, 394.2256).

2,6-di-*tert*-butyl-4-(5-(4-bromophenyl)-1,3,4-oxadiazol-2-yl)phenol.

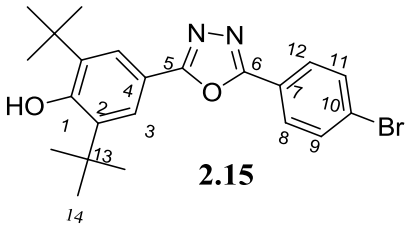

2.15

The solid precipitate was recrystallized from ethyl acetate-methanol (1-1) to give white crystal. Yield 0.447 g (84%); m.p. 168-170 $^{\circ}$C; IR (KBr, υ_{max} /cm^{-1}): 3525 (br, OH_{phenol}), 3005 (w, $CH_{aromatic}$), 2953 (s, $CH_{aliphatic}$), 1602 (s, C=N), 1543, 1495(s, C=C), 1244(s, C-O);^{1}H NMR ($CDCl_3$,400 MHz, ppm): 1.51(s, 18H, H_{14}, 2× C($\underline{CH_3}$)$_3$), 5.66(s, 1H, OH), 7.67(d, 2H, *J*=8.42, H_9 & H_{11}), 7.92(s, 2H, H_3),7.9(d, 2H, *J*=8.54, H_8& H $_{12}$) ;^{13}C NMR ($CDCl_3$, 100 MHz, ppm): 30.23 (6C, C_{14}, 2×C($\underline{CH_3}$)$_3$), 34.56(2C, C_{13}, 2×$\underline{C}(CH_3)_3$), 115.12(C_4) , 123.22(C_7), 124.43(C_3), 126.1(2C, C_8 & C $_{12}$), 128.31 (2C, C_9 & C_{11}), 132.41(C_{10}), 136.87 (C_2), 157.33(C1), 163.37&165.66 (C_5 & C_6) ppm. HREIMs. m/z = 428.1093[$M^{\cdot+}$] (calc. for $C_{22}H_{25}O_2N_2Br$, 428.1099).

2,6-di-*tert*-butyl-4-(5-(4-chlorophenyl)-1,3,4-oxadiazol-2-yl)phenol.

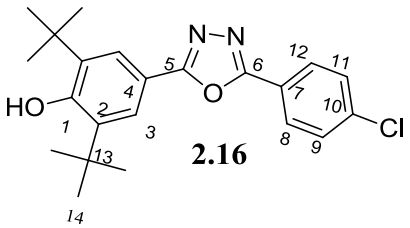

2.16

Crude material was recrystallized from ethyl acetate-methanol (1-1) to obtain white solid. Yield 0.396 g (83%); m.p. 162-164 $^{\circ}$C; IR. (KBr, υ_{max} /cm^{-1}): 3583(br, OH_{phenol}), 3004(w, $CH_{aromatic}$), 2959 (s, $CH_{aliphatic}$), 1607(s, C=N), 1571, 1540(s, C=C), 1239(s, C-O). ^{1}H NMR ($CDCl_3$-400 MHz, ppm): 1.51(s, 18H, H_{14}, 2× C($\underline{CH_3}$)$_3$), 5.67(s,

1H, OH) 7.51(d, 2H, *J*=8.52, H_9 & H_{11}), 7.93 (s, 2H, H_3), 8.07(d, 2H, *J*=8.52, H_8 & H_{12});.^{13}C NMR ($CDCl_3$,100 MHz, ppm): 30.23 (6C, C_{14}, 2×C($\underline{C}H_3$)$_3$), 34.56(2C, C_{13}, 2×$\underline{C}$(CH_3)$_3$), 115(C_4), 122.78(C_7), 124.27 (C_3), 129.46 (2C, C_9 & C_{11}) 128.18(2C, C_8 & C_{12}), 136.87(C_2), 137.71 (C_{10}), 157.32(C_1), 163.29 & 165.64 (C_5 & C_6). HREIMs m/z = 384.1597 [$M^{\cdot+}$] (calc. for $C_{22}H_{25}O_2N_2Cl$, 384.1605).

2,6-di-*tert*-butyl-4-(5-(4-hydroxyphenyl)-1,3,4-oxadiazol-2-yl)phenol.

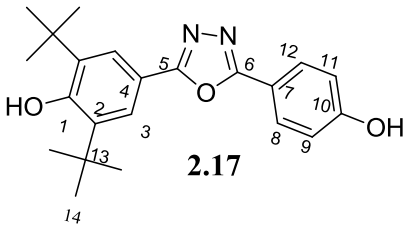

2.17

The mixture was purify by column chromatography using (6-1) hexane ethyl acetate as eluent to give white amorphous solid. Yield 0.318 g (70 %); m.p. 144-146 $^{\circ}$C; IR (KBr, υ_{max} /cm^{-1}): 3617(br, OH_{phenol}), 2958 (s, $CH_{aliphatic}$), 1609(s, C=N), 1546, 1506 (s, C=C), 1250 (s, C-O); ^{1}H NMR ($CDCl_3$, 400 MHz, ppm): 1.51(s, 18H, H_{14}, 2× C($\underline{C}H_3$)$_3$), 5.65(s, 1H, OH), 6.70 (bs, 1H, OH), 7.01 (d, 2H, *J*=8.76, H_9 & H_{11}), 7.92(s, 1H, H_3), 8.01(d, 2H, *J*=8.8, H_8 & H_{12}); ^{13}C NMR ($CDCl_3$, 100 MHz, ppm): 31.06(6C, C_{14}, 2×C($\underline{C}H_3$)$_3$), 34.56(2C, C_{13}, 2×$\underline{C}$(CH_3)$_3$), 115.27(C_4), 115.58 (C_7), 116.40(2C, C_8 & C_{12}), 124.37 (C_3), 128.97(2C, C_9 & C_{11}), 136.85 (C_2), 157.24 (C_1) 159.83(C_{10}), 164.33 & 165.05(C_5 & C_6). HREIMs m/z = 366.1938 [$M^{\cdot+}$] (calc. for $C_{22}H_{26}O_3N_2$, 366.1943).

2,6-di-*tert*-butyl-4-(5-(3,4-dichlorophenyl)-1,3,4-oxadiazol-2-yl)phenol.

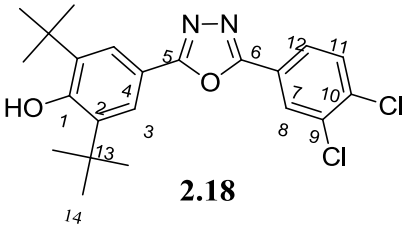

2.18

The crude product was recrystallized from benzene to give white solid. Yield 0.416 g (80 %), m.p. 222-224°C; IR (KBr, υ_{max} /cm^{-1}): 3580 (br, OH_{phenol}), 3003(w, $CH_{aromatic}$), 2952 (s, $CH_{aliphatic}$), 1606 (m, C=N), 1546, 1462 (s, C=C), 1239 (s, C-O). ^{1}H NMR ($CDCl_3$, 400 MHz, ppm) : 1.44 (s, 18H, H_{14}, 2× C($\underline{CH_3}$)$_3$), 5.67 (s, 1H, OH), 7.59 (d, 2H, *J*=8.52, H_{11}), 7.91-7.95 (m, 3H, H_{12} & $H_{3'}$), 8.19 (d, *J*=2.2, 1H, H_8); ^{13}C NMR ($CDCl_3$, 100 MHz, ppm): 30.23(6C, C_{14}, 2×C ($\underline{CH_3}$)$_3$), 34.57 (2C, C_{13}, 2×$\underline{C}$(CH_3)$_3$), 114.89 (C_4), 124.11 (C_7), 124.51 (C_3), 125.95 (C_{12}), 128.53 (C_{11}), 131.28 (C_8), 133.68 (C_9), 135.89 (C_{10}), 136.94 (C_2), 157.50 (C_1), 162.3 & 165.94 (C_5 & C_6). HREIMs m/z = 418.1219[$M^{\cdot+}$] (calc. for $C_{22}H_{24}O_2N_2Cl_2$, 418.1215).

2,6-di-*tert*-butyl-4-(5-(3,5-dichlorophenyl)-1,3,4-oxadiazol-2-yl)phenol.

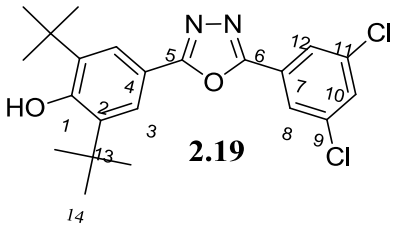

2.19

The crude product was recrystallized from acetonitrile to give white amorphous solid. Yield 0.386g (74.44%); m.p. 195-197 °C; IR (KBr, υ_{max} /cm^{-1}): 3600 (br, OH_{phenol}), 3007 (w, $CH_{aromatic}$), 2961(s, CH $_{aliphatic}$), 1606 (m, C=N), 1574, 1550 (m, C=C), 1240 (s, C-O); ^{1}H NMR ($CDCl_3$, 400 MHz, ppm): 1.52 (s,18H, H_{14}, 2× C($\underline{CH_3}$)$_3$), 5.69 (s,1H, OH), 7.51(t, 1H, *J*=1.24, H_{10}), 7.93 (s, 2H, H_3), 8.01(t, 2H, *J*=1.72, H_8 & H $_{12}$);^{13}C NMR ($CDCl_3$, 100 MHz, ppm):30.39 (6C, C_{14}, 2×C($\underline{CH_3}$)$_3$), 34.50 (2C, C_{13}, 2×$\underline{C}$(CH_3)$_3$), 114.73 (C_4), 124.48 (C_3), 125.02(2C, C_8 & C $_{12}$), 126.87(C_7), 131.24 (C_{10}), 135.92(C_9 & C_{11}), 136.93(C_2), 157.50 (C_1), 161.877 (C_5), 166.05(C6). HREIMs m/z = 418.1210 [$M^{\cdot+}$] (calc. for $C_{22}H_{24}O_2N_2Cl_2$, 418.1215).

2,6-di-*tert*-butyl-4-(5-(2,4-dimethylphenyl)-1,3,4-oxadiazol-2-yl)phenol.

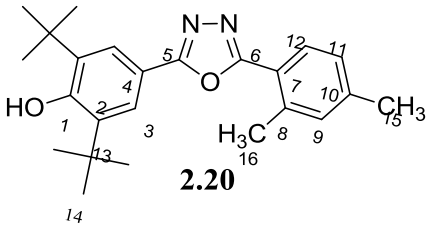

2.20

The crude product was recrystallized from toluene to give white needle crystal. Yield 0.28 (60%); m.p. 170-172 °C. IR (KBr, υ_{max} /cm^{-1}): 3587 (br, OH_{phenol}), 2957 (s, $CH_{aliphatic}$), 1614(s, C=N), 1550, 1536 (s C=C), 1238 (s, C-O); ^{1}H NMR ($CDCl_3$, 400 MHz, ppm): 1.50(s, 18H, H_{14}, 2× C($\underline{CH}_3$)$_3$), 2.39 (s, 3H, H_{15}), 2.70 (s, 3H, H_{16}), 5.64 (s,1H, OH), 7.17-7.14 (m, 2H, H_9 & H_{11}), 7.95-7.90 (m, 3H, H_{12}, $H_{3'}$);^{13}C NMR ($CDCl_3$, 100 MHz, ppm): 21.50 (C_{16}, *o*-CH_3), 22.04 (C_{15}, *p*-CH_3), 30.22 (6C, C_{14}, 2×C($\underline{CH}_3$)$_3$), 34.55 (2C, C_{13}, 2×$\underline{C}$(CH_3)$_3$), 115.40 (C_4) ,12.60 (C_7), 124.38 (C_3), 126.98 (C_{11}), 128.96 (C_{12}), 132.59 (C_9), 136.79 (C_2), 138.19(C_8), 141.43 (C_{10}), 157.11(C_1), 164.49 & 164.81 (C_5 & C_6). HREIMs m/z =378.2301 [$M^{\cdot+}$] (calc. for $C_{24}H_{30}O_2N_2$, 378.2307).

2,6-di-*tert*-butyl-4-(5-o-tolyl-1,3,4-oxadiazol-2-yl)phenol.

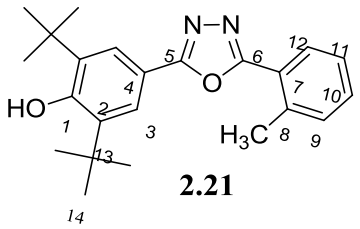

2.21

The crude product was recrystallized from ethyl acetate to give white crystal. Yield 0.308 g (68.5 %); m.p. 132-134 °C, IR (KBr, υ_{max} /cm^{-1}): 3588 (br, OH_{phenol}), 3008 (w, $CH_{aromatic}$), 2963(s, $CH_{aliphatic}$), 1607 (s, C=N), 1592, 1537(s, C=C), 1238(s, C-O); ^{1}H NMR ($CDCl_3$,400 MHz, ppm): 1.52 (s,18H, H_{14}, 2× C($\underline{CH}_3$)$_3$), 5.66 (s, 1H, OH), 7.44-7.34 (m, 3H, H_9, H_{10}, H_{11}), 7.96 (s, 2H, H_3, $H_{3'}$), 8.02 (d, 1H, *J*=7.32, H_{12});^{13}C NMR ($CDCl_3$, 100 MHz, ppm): 2 2.11 (*o*-CH_3), 30.22 (6C, C_{14}, 2× C ($\underline{CH}_3$)$_3$), 34.52 (2C, C_{13},

2 × $\underline{C}(CH_3)_3$), 115.53 (C_4), 123.40 (C_7), 124.37 (C_3), 126.21(C_{11}), 128.96 (C_{12}), 131.03(C_{10}), 131.80(C_9), 136.80(C_2), 138.35(C_8), 157.14 (C_1), 164.32 & 165.04 (C_5 & C_6), HREIMs m/z =364.2144[$M^{\cdot+}$] (calc. for $C_{23}H_{28}O_2N_2$, 364.2151).

2,6-di-*tert*-butyl-4-(5-(2-chlorophenyl)-1,3,4-oxadiazol-2-yl)phenol.

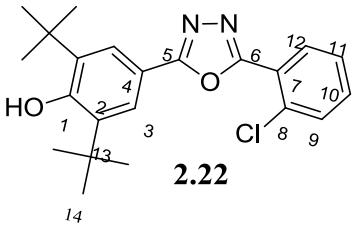

2.22

The precipitated was recrystallized from ethyl acetate to obtain white crystal. Yield 0.386 g (81%); m.p. 113-115 $^{\circ}$C, IR (KBr, υ_{max} /cm^{-1}): 3584(br, OH_{phenol}), 3004 (w, $CH_{aromatic}$), 2959 (s, $CH_{aliphatic}$), 1607(s, C=N), 1570, 1539 (m, C=C), 1239 (s, C-O); ^{1}H NMR ($CDCl_3$, 400 MHz, ppm): 1.48(s, 18H, H_{14}, 2× C($\underline{CH}_3$)$_3$), 5.66 (s, 1H, OH), 7.387.46 (m, 2H, H_{10}, H_{11}), 7.53 (d, 1H, *J*=8.04, H_{12}), 7.95(s, 2H, H_3, H_3'), 8.05(d, 1H, *J*=6.32, H_9); ^{13}C NMR ($CDCl_3$, 100 MHz, ppm): 30.27 (6C, C_{14}, 2× C($\underline{CH}_3$)$_3$), 34.61 (2C, C_{13}, 2× $\underline{C}(CH_3)_3$), 115.18(C_4), 123.65(C_7), 124.61(C_3), 127.21 (C_{11}),131.33(C_{12}), 132.32(C_9), 133.14 (C_8),136.79 (C_9), 136.94 (C_2), 157.28 (C_1), 162.55 & 166.04 (C_5 & C_6). HREIMs m/z =384.1600[$M^{\cdot+}$] (calc. for $C_{22}H_{25}O_2N_2Cl$, 384.1605)

6.1.5 Synthesis of diethyl 2,2'-[benzene-1,3-diylbis(oxy)]diacetate

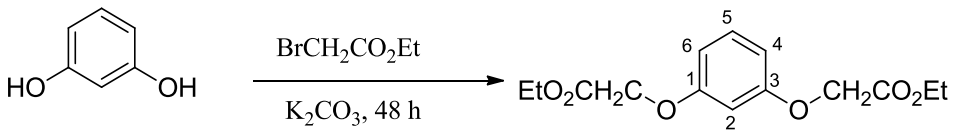

2.23

Resorcinol (1.10 g, 0.1 mole) was dissolved in dry acetone, followed by anhydrous potassium carbonate (2.78 g, 2 mole) and the mixture was allowed to stir at room temperature for 1 hour. Ethyl bromoacetate (3.34 g, 2 mole) was added to the mixture and refluxed for 48 hours. The solvent was removed and the residue was

extracted with ethyl acetate (25 mL ×2). The combined ethyl acetate extracts were then washed with saturated solution of sodium hydrogen carbonate and dried over magnesium sulfate. The oily product, obtained after evaporation under reduced pressure, solidified after three days to give an off white solid. Yield 2.39 g (85%); m.p.42-44 °C; IR (KBr, υ_{max} / cm^{-1}): 3079 (w, $CH_{aromatic}$), 2943-2856 (s, $CH_{aliphatic}$), 1715(s, C=O), 1600, 1581(s, C=C); ^1H NMR ($CDCl_3$, 400 MHz, ppm): 1.42 (t, 6H, *J*=7.8, $2CH_3$), 3.81 (s, 4H, $2(OCH_2)$), 4.33(q, 4H , *J*=8, $2(O\underline{CH_2}CH_3)$, 6.7 (s, 1H, H_2), 7.0-7.41(m, 3H, H_4, H_5, H_6)

6.1.6 General synthesis of dihydrazide (2.24 - 2.30)

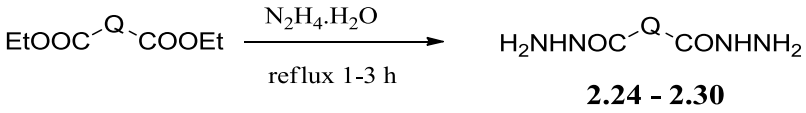

2.24 - 2.30

Excess of hydrazine hydrate (3mL) was added to 1 g of diester in 15 mL ethanol. The mixture was refluxed for (1-3 h), after cooling the precipitate was collected and washed with cold ethanol and recrystallized from suitable solvent. The dihydrazides were characterized by melting point, IR and ^1H NMR.

Terephthalic acid dihydrazides (2.24)

Recrystallization of the crude product from aqueous DMF afforded white solid. Yield 0.80 g (92%); m.p.342-344 °C (lit. 360 °C)[225]; IR (KBr, υ_{max} / cm^{-1}): 3372, 3330, 2271 (br, NH_2, NH), 3082 (w, $CH_{aromatic}$), 1665 (s, C=O), 1601, 1483 (s, C=C), ^1H NMR (DMSO-d_6, 400 MHz, ppm): 4.48 (bs, 4H, $2NH_2$), 8.08(s, 4H, Ar-H), 9.84(bs, 2H, 2NH).

IsoTerephthalic acid dihydrazide (**2.25)**

Recrystallization of the crude product from DMF afforded white powder. Yield 0.75 g (87%); m.p. 302-304 °C (dec.) (lit. >300°C (dec.))[219]; IR (KBr, υ_{max} / cm^{-1}): 3341,

3319, 2271 (m, NH_2, NH), 3090 (w, $CH_{aromatic}$), 1662(s, C=O), 1600, 1871(s, C=C), ^1H NMR (DMSO-d_6, 400 MHz, ppm): 4.51(bs, 4H, $2NH_2$), 7.72-8.22(m, 3H, H_4, H_5,H_6), 8.44(s, 1H, H_2), 9.91(bs, 2H, 2NH).

Pyridine 2,6 acid dihydrazide (2.26)

Recrystallization of the crude product from aqueous ethanol afforded white solid. Yield 0.68 g (79%); m.p.280-284 $^{\circ}$C (lit. 285-286 $^{\circ}$C)[226]; IR (KBr, υ_{max} / cm^{-1}): 3329, 3308, 2265 (NH_2, NH), 3094 ($CH_{aromatic}$), 1668(C=O), 1590, 1882(C=C); ^1H NMR (DMSO-d_6, 400 MHz, ppm): 4.56 (bs, 4H, $2NH_2$), 8.20-8.29(m, 2H, H_3, H_5),8.39(s, 1H, H_4), 9.87(bs, 2H, 2NH).

5-nitro *iso*Terephthalic acid dihydrazide (2.27)

Recrystallization of the crude product from ethanol afforded pale yellow solid. Yield 0.72 g (81%); m.p. 244-246 $^{\circ}$C (lit. 250 $^{\circ}$C)[227]; IR (KBr, υ_{max} / cm^{-1}): 3346, 3288, 2195 (m, NH_2, NH), 3067 (w, $CH_{aromatic}$), 1664 (s, C=O), 1598, 1879 (s, C=C), 1570, 1327 (m, $NO_{2aromatic}$); ^1H NMR (DMSO-d_6, 400 MHz, ppm): 4.51(bs, 4H, $2NH_2$), 8.55-8.43(m, 3H, Ar-H), 9.94(bs, 2H, 2NH).

2,2'-[benzene-1,3-diylbis(oxy)]diacetohydrazide (2.28)

Recrystallization of the crude product from ethanol afforded white solid. Yield 0.64 g (72%); m.p 220-224 $^{\circ}$C (lit. 223-224°C)[228]; IR (KBr, υ_{max} / cm^{-1}): 3363, 3324, 2258 (m, NH_2, NH), 3080 (w, $CH_{aromatic}$), 2950-2834 (s, $CH_{aliphatic}$), 1648(s, C=O), 1590, 1882 (m, C=C), 1215 (C-O); ^1H NMR (DMSO-d_6, 400 MHz, ppm): 4.43 (bs, 4H, $2NH_2$), 4.68(s, 4H, $\underline{OCH_2}$), 6.47 (d,1H, *J*=2.2, H_2), 7.05(dd, 2H, *J*=7.8,1.23, H_4,H_6), 7.31(t, 1H, *J*= 7.68, H_5), 9.91(bs, 2H, 2NH).

Adipic acid dihydrazide (2.29)

Recrystallization of the crude product from aqueous methanol afforded white solid. Yield 0.67 g (79%); mp. 176-178 °C (lit. 180-182 °C)[219]; IR (KBr, υ_{max} / cm^{-1}): 3325, 3292, 2189 (NH_2, NH), 2970-2863 ($CH_{aliphatic}$), 1658(C=O); ^1H NMR (DMSO-d_6, 400 MHz, ppm): 1.57(t, *J*=7.8, 4H, H_2, H_3), 2.41 (t, 4H, *J*=8.2, H_1, H_4), 4.55 (bs, 4H, $2NH_2$), 9.78(bs, 2H, 2NH).

Oxalic acid dihydrazide (2.30)

Recrystallization of the crude product from aqueous ethanol afforded white solid. Yield 0.64 g (81%); m.p. 234-238 °C (lit. 232 °C)[229]; IR (KBr, υ_{max} / cm^{-1}): 3305, 3298, 2219 (m, NH_2, NH), 1673 (s, C=O); ^1H NMR (DMSO-d_6, 400 MHz, ppm): 4.51 (bs, 4H, $2NH_2$), 9.92(bs, 2H, 2NH).

6.1.7 General Synthesis of 4,4'-(5,5'-(Substitute)bis(1,3,4-oxadiazole-5,2-diyl))bis (2,6-di-*tert*-butylphenol)

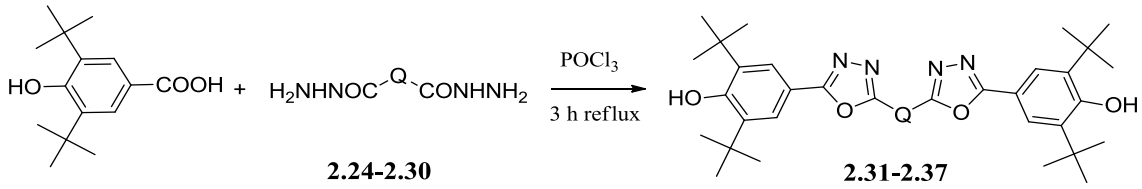

2.24-2.30 **2.31-2.37**

Excess of phosphorusoxy chloride (5 mL) was added dropwise, at room temperature into 3,5-di-*tert*-butyl-4-hydroxybenzoic acid (0.31 g, 1.24 mmol), followed by acid hydrazide (0.155 mmol) in a 250 mL round bottom flask. The mixture was heated up to 80-90 °C and stirred for 3 hours. Upon cooling, 100 mL crushed ice was poured into the mixture and stirred for 15 minutes. pH of the mixture was adjusted to 7-8 by adding a solution of sodium bicarbonate. The precipitate was filtered, washed with

distilled water and dried. Recrystallization of the crude product from suitable solvent afforded the desired product.

4,4'-(5,5'-(1,4-phenylene)bis(1,3,4-oxadiazole-5,2-diyl))bis(2,6-di-*tert*-butylphenol).

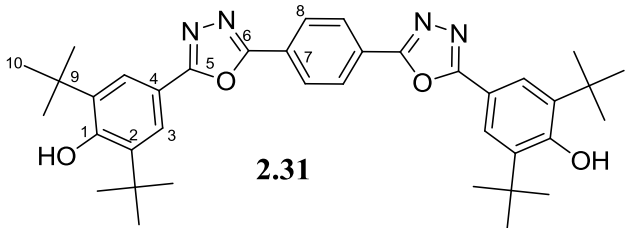

2.31

Recrystallization of the crude product from chloroform-methanol afforded white amorphous solid. Yield 0.290 g (74.0%); m.p. 335-336 $^{\circ}$C; IR (KBr, υ_{max} /cm^{-1}): 3550 (br, OH_{phenol}), 2956 (s, $CH_{aliphatic}$), 1608(m, C=N), 1576, 1542 (s, C=C), 1238 (s, C-O); ^{1}H NMR ($CDCl_3$, 400 MHz, ppm): 1.43(s, 36H, 4× C($\underline{CH_3}$)$_3$), 5.69(s, 2H, 2OH), 7.97(s, 4H, H_3), 8.30(s, 4H, H_2); ^{13}C NMR ($CDCl_3$, 100 MHz, ppm): 30.17(12C, C_{10}, 4×-C($\underline{CH_3}$)$_3$), 34.52(4C, C_9, 4×$\underline{C}$(CH_3)$_3$), 115.02 (2C, C_4), 124.46 (4C, C_3), 126.65(2C, C_7), 127.36 (4C,C_8), 136.87(4C, C_2), 157.37(2C, C_1), 163.25 & 165.85 (4C, C_5 & C_6). HREIMs m/z = 622.3532 [$M^{\cdot+}$] (calc. for $C_{38}H_{46}O_4N_4$, 622.3519).

4,4'-(5,5'-(1,3-phenylene)bis(1,3,4-oxadiazole-5,2-diyl))bis(2,6-di-*tert*-butylphenol) .

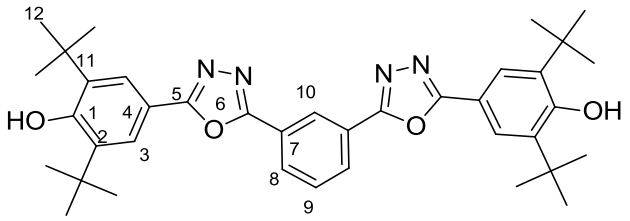

2.32

Recrystallization of the crude product from ethyl acetate afforded white crystal. Yield 0.31 g (78%); m.p. 274-276°C; IR (KBr, υ_{max} /cm^{-1}): 3600 (br, OH_{phenol}), 2956(s, $CH_{aliphatic}$), 1610 (m, C=N), 1535 (s, C=C), 1236 (s, C-O); ^{1}H NMR ($CDCl_3$,400 MHz, ppm): 1.51(s, 36H, 4 × C($\underline{CH_3}$)$_3$), 5.69(s, 2H, OH), 7.70(t, 1H, *J*=7.78, H_9) ,7.97(s, 4H,

H_3), 8.31(d, 2H, *J*=8.02, H_8), 8.82 (s, 1H, H_{10}); ^{13}C NMR ($CDCl_3$, 100 MHz ppm): 30.27(12C, C_{12}, 4×-C($\underline{C}H_3)_3$), 34.58(4C,C_{11}, 4×$\underline{C}(CH_3)_3$), 115.08 (2C, C_4), 124.55(2C, C_7), 124.88 (4C, C_3), 125.34(1C, C_9), 129.60 (2C, C_8), 129.38(1C, C_{10}), 136.94 (4C, C_2), 157.94(2C, C_1), 163.28 & 165.97(4C, C_5 & C_6). HREIMs m/z = 622.3527 [$M^{\cdot+}$] (calc. for $C_{38}H_{46}O_4N_4$, 622.3519).

4,4'-(5,5'-(pyridine-2,6-diyl)bis(1,3,4-oxadiazole-5,2-diyl))bis(2,6-di-*tert*-butylphenol).

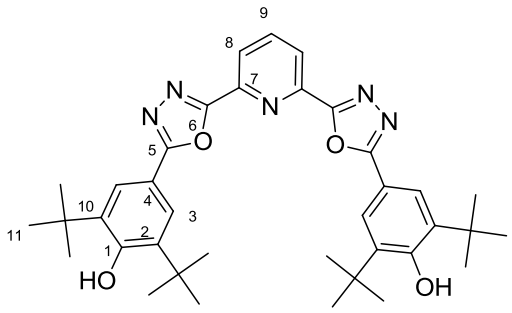

2.33

The solid crude was purified by column chromatography using (9:1) hexane: ethyl acetate as eluent and was then recrystallized from ethyl acetate to give white crystal. Yield 0.275 g (71.0 %); m.p.300-302°C. IR (KBr, υ_{max} /cm^{-1}): 3601(br, OH_{phenol}), 2957 (s, $CH_{aliphatic}$), 1608 (s, C=N), 1589, 1537 (s, C=C), 1239 (s, C-O); ^{1}H NMR ($CDCl_3$, 400 MHz, ppm): 1.51(s, 36H, H_{11}, 4× C($\underline{C}H_3)_3$), 5.7(s, 2H, 2OH), 8.03-8.08 (m, 5H, H_3 & H_9), 8.44(d, 2H, *J*=1.78, H_8); ^{13}C NMR($CDCl_3$, 100 MHz ppm): 30.33(12C, C_{11}, 4×-C($\underline{C}H_3)_3$), 34.58(4C, C_{10}, 4×-$\underline{C}(CH_3)_3$), 114.96 (2C, C_4), 124.90(4C, C_3), 124.98(2C, C_8), 136.88 (1C, C_9), 138.40(4C, C_2), 144.61(2C, C_7), 157.61(2C, C_1), 162.94 & 166.98 (4C, C_5 & C_6). HREIMs m/z = 623.3478 [$M^{\cdot+}$] (calc. for $C_{37}H_{45}O_4N_5$, 623.3472).

4,4'-(5,5'-(5-nitro-1,3-phenylene)bis(1,3,4-oxadiazole-5,2-diyl))bis(2,6-di-*tert*-butylphenol).

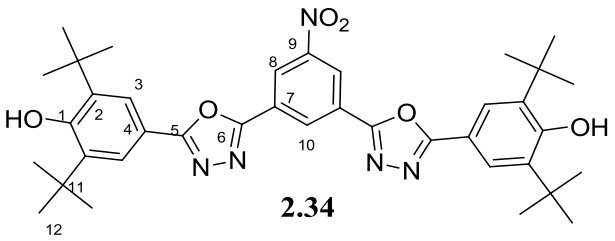

2.34

Recrystallization of the crude product from ethyl acetate afforded white crystal. Yield 0.30 g (70%); m.p. 286-288 °C; IR (KBr, υ_{max} /cm^{-1}): 3621(br, OH_{phenol}), 3094 (w, $CH_{aromatic}$), 2957 (s, $CH_{aliphatic}$), 1606 (m, C=N), 1530 (s, C=C), 1347 (m, Ar-NO_2), 1234 (s, C-O). ^{1}H NMR ($CDCl_3$, 400 MHz, ppm): 1.51(s, 36H, H_{11}, 4× C($\underline{CH_3}$)$_3$), 5.72(s, 2H, 2OH), 7.97(s, 4H, H_3), 9.07(d, 2H, *J*=1.44, H_8), 9.14(s, 1H, H_{10}); ^{13}C NMR($CDCl_3$, 100 MHz, ppm): 30.17(12C, C_{12}, 4×-C($\underline{CH_3}$)$_3$), 34.52(4C, C_{11}, 4×-$\underline{C}$(CH_3)$_3$), 114.44(2C,C_4), 123.46(2C, C_8), 124.66(4C, C_3), 127.06(2C, C_7), 129.59(1C, C_{10}), 137.03(1C, C_2), 149.19(1C, C_9), 157.75 (2C, C_1), 161.50 & 166.62(4C, C_5 & C_6). HREIMs m/z = 667.3372 [$M^{\cdot+}$] (calc. for $C_{38}H_{45}O_6N_5$, 667.3370).

4,4'-(5,5'-(1,3-phenylenebis(oxy))bis(methylene)bis(1,3,4-oxadiazole-5,2-diyl)) bis(2,6-di-*tert*-butylphenol).

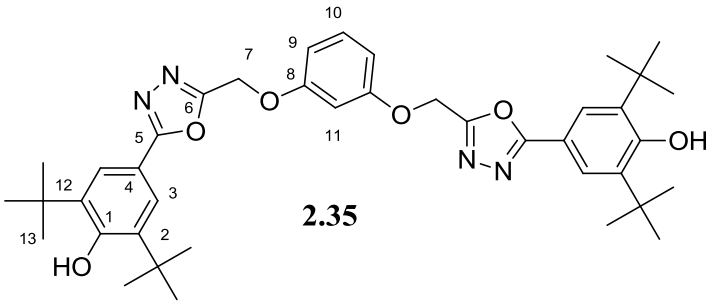

2.35

The crude product was purified by column chromatography using hexane ethyl acetate (9-1) as solvent system. The product was recrystallized from diethyl ether to obtain white crystal. Yield 0.29 g (69%); m.p.98-100 °C; IR (KBr, υ_{max}/ cm^{-1}), 3621 (br, OH_{phenol}), 2958 (s, $CH_{aliphatic}$), 1603(s, C=N), 1539, 1490 (s, C=C), 1236(s, C-O); ^{1}H

NMR($CDCl_3$, 400 MHz, ppm): 1.47(s, 36H, H_{11},4× C($\underline{CH_3}$)$_3$), 5.30(s, 4H, H_7, 2×O-$\underline{CH_2}$), 5.66(2H, 2OH), 6.72-7.25(m, 4H, H_9, H_{10}, H_{11}), 7.87(s, 4H, H_3); ^{13}C NMR($CDCl_3$, 100 MHz, ppm): 30.21(12C, C_{13}, 4×-C($\underline{CH_3}$)$_3$), 34.55(4C, C_{12}, 4×-$\underline{C}$(CH_3)$_3$), 60.10(2C, C_7), 102.77(1C, C_{11}), 108(2C, C_9), 114.84(2C, C_4), 124.60(4C, C_3), 130.50(1C, C_{10}), 136.82(4C, C_2), 157.44(2C, C_1), 158.97(2C, C_8), 161.49 & 166.73(4C, C_5 & C_6). HREIMs m/z = 682.3706 [$M^{\cdot+}$] (calc. for $C_{40}H_{50}O_6N_4$, 682.30).

4,4'-(5,5'-(butane-1,4-diyl)bis(1,3,4-oxadiazole-5,2-diyl))bis(2,6-di-*tert*-butylphenol)

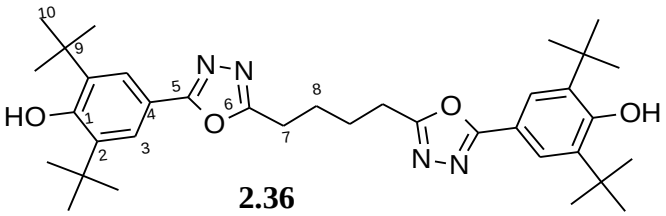

2.36

Recrystallization of the crude product from ethyl acetate afforded white solid. Yield 0.28 g (78%); m.p. 163-165°C; IR ((KBr, υ_{max}/ cm^{-1}): 3621(br, OH_{phenol}), 3097(w, $CH_{aromatic}$), 2958 (s, $CH_{aliphatic}$), 1608 (s, C=N), 1574, 1547(s, C=C), 1234(s, C-O); ^{1}H NMR ($CDCl_3$, 400 MHz, ppm): 1.47(s, 36H, H_{11}, 4× C($\underline{CH_3}$)$_3$), 1.99(t, 2H, *J*=9.6, H_8), 2.97(t, 2H, *J*=11.8, H_7), 5.61(2H, 2OH), 7.80(s, 4H, H_3); ^{13}C NMR($CDCl_3$, 100 MHz, ppm): 25.12(2C, C_8), 26.02(2C, C_7), 30.22 (12C, C_{10}, 4×C($\underline{CH_3}$)$_3$), 34.53(4C, C_9, 4×$\underline{C}$(CH_3)$_3$), 115.36(2C, C_4),124.21(4C, C_3), 157.03 (2C, C_1), 165.59 (2C, C_6). 165.61 (2C, C_5), HREIMs m/z = 602.3840 [$M^{\cdot+}$] (calc. for $C_{36}H_{50}O_4N_4$, 602.3832).

4,4'-(2,2'-bi(1,3,4-oxadiazole)-5,5'-diyl)bis(2,6-di-*tert*-butylphenol).

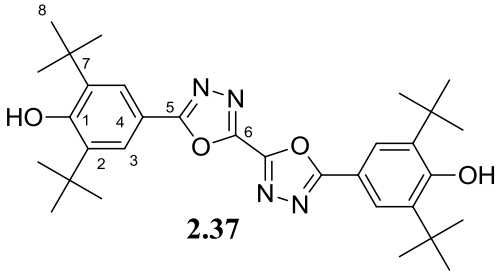

2.37

Recrystallization of the crude product from ethyl acetate afforded white precipitate. Yield 0.24 g (73%); m.p. 272-276 $^{\circ}$C (dec.); IR (KBr, υ_{max}/ cm^{-1}), 3620 (br, OH_{phenol}), 2958 (s, $CH_{aliphatic}$), 1614(s, C=N), 1574, 1547(s, C=C), 1238(s, C-O); ^{1}H NMR ($CDCl_3$, 400 MHz, ppm): 1.53(s, 36H, H_{11}, 4× C($\underline{CH_3}$)$_3$), 5.78(s, 2H, 2OH), 8.03(s, 4H, H_3).^{13}C NMR($CDCl_3$, 100 MHz, ppm): 30.23(12C, C_8, 4×-C($\underline{CH_3}$)$_3$), 34.53(4C, C_7, 4×$\underline{C}$(CH_3)$_3$), 113.95(2C, C_4), 125.23(4C, C_3), 137.12(4C, C_2), 152.71(2C, C_1), 158.19(2C, C_6), 167.15 (2C, C_5). HREIMs m/z = 546.3207 [$M^{\cdot+}$] (calc. for $C_{32}H_{42}O_4N_4$, 602.3832).

6.2 General synthesis of *N′*-[(3,5-di-*tert*-butyl-2-hydroxyphenyl)methylidene]-substituted benzohydrazide.

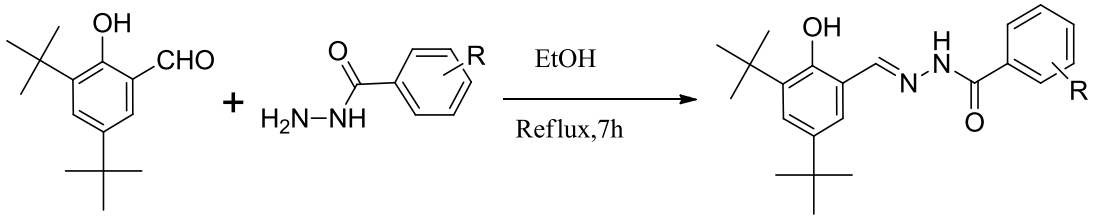

3.1-3.4

R= 4-OMe, 4-Br, 4-Me, 2-Cl

To a warm stirred solution of aryl hydrazide (3 mmol) in 20 mL absolute ethanol, 3,5-di-*tert*-butyl-salicylaldehyde (0.70 g, 3 mmol) was added in small portions, and refluxed for 7h, upon cooling, the mixture was stored overnight in a refrigerator at 5°C. The precipitate was washed with cold ethanol and recrystallized from suitable solvent.

***N′*-[(3,5-di-*tert*-butyl-2-hydroxyphenyl)methylidene]-4-methylbenzohydrazide**

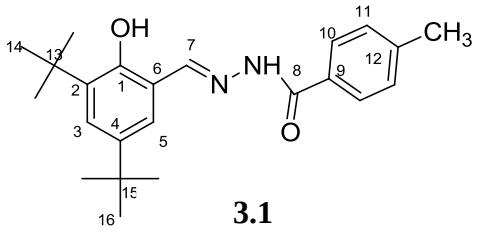

3.1

The crude product was recrystallized from ethanol to obtain white precipitate. Yield 0.95 g (87%); m.p. 314-316 °C, IR (KBr, υ_{max}/ cm^{-1}): 3675(br, OH_{phenol}), 3160(br, NH), 3090 (w, $CH_{aromatic}$), 2955, 2868 (s, $CH_{aliphatic}$), 1651 (s, C=O), 1611(m, C=N), 1595, 1551(s, C=C), 1231(s, C-O); ^{1}H NMR (DMSO-d ^{6}, 400 MHz, ppm): 1.27(s, 9H, H_{14}), 1.40 (s, 9H, H_{16}), 2.38 (s, 3H, *p*-CH_3), 7.20(d, 1H, *J*=2.4, H_3), 7.30(d, 1H, *J*=2.2, H_5), 7.35(d, 2H, *J*=8.1, H_{11}), 7.84(d, 2H, *J*=8.1, H_{10}), 8.56(s, 1H, CH=N), 12.14 (s, 1H, NH), 12.29(s, 1H, OH); ^{13}C NMR (DMSO-d_6, 100 MHz, ppm): 21.61(1C, *p*-CH_3), 29.82(3C, C_{16}), 31.83 (3C, C_{14}), 34.42(1C, C_{13}), 35.19 (1C, C_{15}), 117 (1C, C_6), 126.04(1C, C_5), 126.24(1C, C_3), 128.20(2C, C_{10}), 129.67 (2C, C_{11}), 130.26(1C, C_9), 136.17(1C, C_2), 140.29(1C, C_4), 142.75 (1C, C_{12}), 151.54 (1C, C_7, C=N), 155.54(1C, C_1), 163.16(1C, C_8, C=O) HREIMs m/z = 366.2310 [$M^{\cdot+}$] (calc. for $C_{23}H_{30}N_2O_2$, 366.2307).

_N'_-[(3,5-di-*tert*-butyl-2-hydroxyphenyl)methylidene]-4-methoxybenzohydrazide.

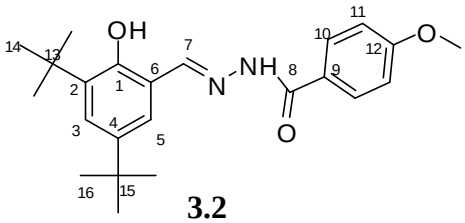

3.2

The crude product was recrystallized from ethanol to obtain white precipitate. Yield 1.08 g (95%); m.p. 258-260 °C, IR (KBr, υ_{max}/ cm^{-1}): 3662(br, OH_{phenol}), 3174(br, NH), 3098($CH_{aromatic}$), 3958(s, $CH_{aliphatic}$), 1662(s, C=O), 1619(s, C=N), 1596, 1572(m, C=C), 1237(s, C-O), 1095(m, Ar-O-CH_3); ^{1}H NMR(DMSO-d_6,400 MHz, ppm): 1.24(s, 9H, H_{14}), 1.37(s, 9H, H_{16}), 3.80(s, 3H, OCH_3), 7.05(d, 2H, *J*=9.1, H_{11}), 7.16(d, 1H, *J*=2.28, H_3), 7.26(d, 1H, *J*=2.28, H_5),7.89 (d, 2H, *J*=8.72, H_{10}), 8.51(s, 1H, CH=N), 12.05(s, 1H, NH), 12.28(s, 1H, OH); ^{13}C NMR (DMSO-d_6, 100 MHz, ppm): 29.30(3C, C_{16}), 31.31 (3C, C_{14}), 33.88(1C, C_{13}), 34.67(1C, C_{15}), 55.52 (1C, OCH_3), 114.00(2C, C_{11}), 117.18(1C, C_6), 124.73(1C, C_9), 125.56(1C, C_5), 125.77(1C, C_3), 129.73(2C, C_{10}),

135.78(1C, C_2), 140.45(1C, C_4), 150.83(1C, C_7), 154(1C, C_1), 162.41(1C, C_{12}), 162.74 & 162.80 (1C, C_8). HREIMs m/z = 382.2256 [M^+] (calc. for $C_{23}H_{30}N_2O_3$, 382.2256).

***N'*-[(3,5-di-*tert*-butyl-2-hydroxyphenyl)methylidene]-4-bromo-benzohydrazide**

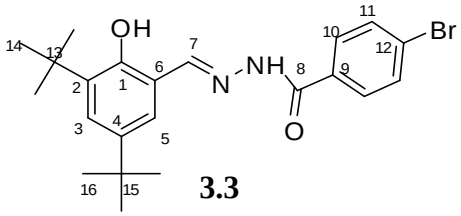

3.3

The crude product was recrystallized from aqueous acetonitrile to obtain white amorphous. Yield 1.22 g (95%); m.p.276-278 °C; IR (KBr, υ_{max}/ cm^{-1}): 3660 (br, OH_{phenol}), 3167 (br, NH), 3089 (w, C-$H_{aromatic}$), 2959, 1871(s, $CH_{aliphatic}$), 1664(s, C=O), 1621(s, C=N), 1995, 1558(s, C=C), 1236(s, C-O); ^{1}H NMR (DMSO-d_6, 400 MHz, ppm): 1.27(s, 9H, H_{14}), 1.40(s, 9H,H_{16}), 7.22(d, 1H, *J*=2.2, H_3), 7.31(d, 1H, *J*=2.2, H_5), 7.78(d, 2H, *J*=8.5, H_{11}), 7.88(d, 2H, *J*=8.5, H_{10}), 8.56(s, 1H, H_7), 12.23(s, 1H, NH), 12.28(s, 1H, OH); ^{13}C NMR (DMSO-d_6, 100 MHz, ppm): 29.81(3C, C_{16}), 31.82(3C, C_{14}), 34.44(1C, C_{13}), 35.18 (1C, C_{15}), 117.38 (1C, C_6), 125.38 (1C, C_5), 126.25 (1C, C_3), 126.44 (1C, C_{12}), 130.22(2C, C_{10}), 132.13(3C, C_{11}, C_9), 136.01(1C, C_2), 140.91(1C, C_4), 152.06(1C, C_7), 155.04(1C, C_1), 162.30(1C, C_8). HREIMs, m/z = 430.1084 [$M^{\cdot+}$] (calc. for $C_{22}H_{27}BrN_2O_3$,430.1256).

***N'*-[(3,5-di-*tert*-butyl-2-hydroxyphenyl) methylidene] 2-chloro-benzohydrazide.**

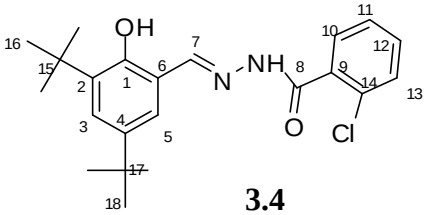

3.4

Recrystallization of the crude product from ethanol afforded white precipitate. Yield 1.03 g (90%); m.p.138-140 °C; IR (KBr, υ_{max}/ cm^{-1}): 3675(br, OH_{phenol}), 3161(br,

NH), 3092 (w, $CH_{aromatic}$), 2955, 2868 (s, $CH_{aliphatic}$), 1651 (s, C=O), 1611 (m, C=N), 1231(s, C-O);. ^{1}H NMR (DMSO-d_6, 400 MHz, ppm): 1.28(s, 9H, H_{16}), 1.42(s, 9H, H_{18}), 7.23 (d, 1H, *J*=2.38, H_3), 7.32(d, 1H, *J*=2.26, H_5), 7.46-7.63(m, 4H, H_{10}, H_{11}, H_{12}, H_{13}), 8.42 (s, 1H, H_7), 10.15(bs, 1H, NH), 12.23(bs, 1H, OH); ^{13}C NMR (DMSO-d_6, 100 MHz, ppm); 29.26(3C, C_{18}), 31.26(3C, C_{16}), 33.87(1C, C_{15}), 34.62(1C, C_{17}), 116.81(1C, C_6), 125.70(1C, C_5), 125.89(1C, C_{11}), 127.30 (1C, C_3), 129.42 (1C, C_{10}), 129.79 (1C, C_{13}), 130.47(1C, C_9), 131.58(1C, C_{12}), 134.69(1C, C_{14}), 135.63 (1C, C_2), 140.41(1C, C_4), 151.42(1C, C_7), 154.78 (1C, C_1), 162.38(1C, C_8), HREIMs, m/z = 386.1763 [$M^{\cdot+}$] (calc. for $C_{22}H_{27}ClN_2O_2$, 386.1761).

6.2.1 General synthesis of 2,4-di-*tert*-butyl-6-[5-aryl-1,3,4-oxadiazol-2-yl]phenol.

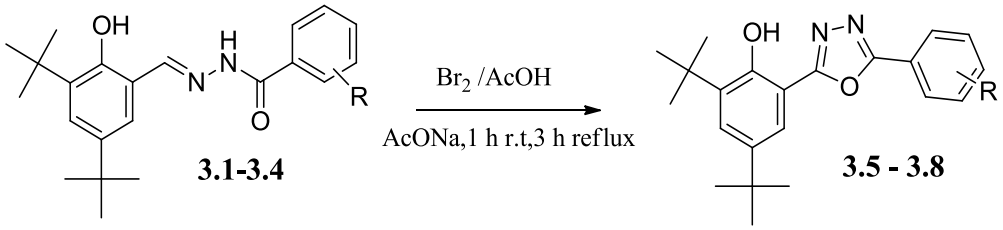

To a solution of *N'*-[(3,5-di-*tert*-butyl-2-hydroxyphenyl) methylidene]-substituted benzohydrazide (2 mmol) in 10 mL glacial acetic acid and anhydrous sodium acetate (2 mmol) in 50 mL round bottom flask, bromine (1 mmol in 3mL ACOH) was added dropwise at ambient temperature with vigorous stirring. The Mixture was allowed to stirre for 1h and then refluxed further for 3 h. Upon cooling, the mixture was poured into 50 mL ice water. The resulting precipitate was collected and washed with distilled water, dried and purified either by column chromatography or recrystallized with suitable solvent.

2,4-di-*tert*-butyl-6-[5-(4-methylphenyl)-1,3,4-oxadiazol-2-yl]phenol.

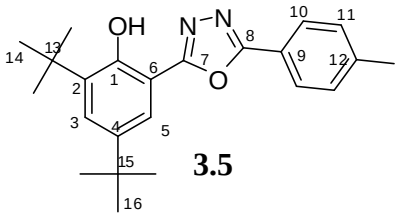

3.5

The crude material was purified by column chromatography using (hexane-ethyl acetate) 6-1 as elute to give a white crystal. Yield 0.50 g (70%) yield; m.p.184-186 $^{\circ}$C; IR(KBr, υ_{max}/ cm^{-1}), 3474 (br, OH_{phenol}), 3082 (w, $CH_{aromatic}$), 2962, 2855 (s, $CH_{aliphatic}$), 1609 (m, C=N), 1590, 1552 (m, C=C), 1219 (s, C-O); ^{1}H NMR ($CDCl_3$,400 MHz, ppm): 1.40 (s, 9H, H_{14},-C(C$\underline{H}_3$)$_3$), 1.44 (s, 9H, H_{16}, C(C$\underline{H}_3$)$_3$), 2.43(s, 3H,-CH_3), 7.33(d, 2H, *J*=8, H_{11}), 7.49(d, 1H, *J*=2.44, H_3), 7.67(d, 2H, *J*=2.44, H_5), 8.02 (d, 2H, *J*=8, H_{10}), 10.57 (bs, 1H, OH); ^{13}C NMR ($CDCl_3$, 100 MHz, ppm): 21.68(1C, *p*-CH_3), 29.41(3C, C_{16}), 31.47(3C, C_{14}), 34.37 (1C, C_{13}), 35.32 (1C, C_{15}), 107.63 (1C, C_6), 120.50(1C, C_5), 120.68 (1C, C_9), 126.99 (2C, C_{11}), 128.37 (1C, C_3), 129.82 (2C, C_{10}), 137.45 (1C, C_2), 141.60(1C, C_4) 142.58(1C, C_{12}), 154.68 (1C, C_1), 163.16, 164.97 (C_7 & C_8). HREIMs, m/z = 364.2162 [M^+] (calc. for $C_{23}H_{28}N_2O_2$, 364.2151).

2,4-di-*tert*-butyl-6-[5-(4-methoxyphenyl)-1,3,4-oxadiazol-2-yl]phenol.

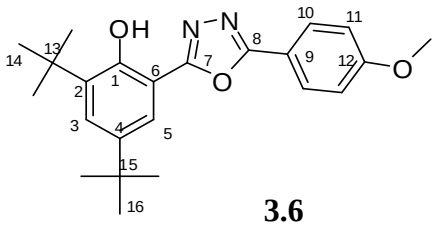

3.6

Recrystallization of the crude product from methanol-chloroform afforded white crystal. Yield 0.56 g (74%); m.p. 170-172 $^{\circ}$C, IR(KBr, υ_{max}/ cm^{-1}), 3470(br, OH_{phenol}), 3090(w, $CH_{aromatic}$), 2959, 2868 (s, $CH_{aliphatic}$), 1610(m, C=N), 1585,1547 (m, C=C), 1222 (s, C-O), 1170(O-CH_3); ^{1}H NMR($CDCl_3$,400 MHz, ppm): 1.37 (s, 9H, H_{14}, C(C$\underline{H}_3$)$_3$), 1.48 (s, 9H, H_{16}, C(C$\underline{H}_3$)$_3$), 3.87(s, 3H, ph-OCH_3), 7.06(d, 2H, *J*=8.8, H_{11}),

7.51 (d, 1H, *J*=2.2, H_3), 7.68(d, 2H, *J*=2.4, H_5), 8.10 (d, 2H, *J*=8.8, H_{10}), 10.58 (s, 1H, OH); ^{13}C NMR ($CDCl_3$, 100 MHz, ppm): 29.42 (3C, C_{16}), 31.48 (3C, C_{14}), 34.38(1C, C_{13}), 35.33 (1C, C_{15}), 3.51(1C, OCH_3), 107.69 (1C, C_6), 114.60(2C, C_{11}), 115.96 (1C, C_5), 120.46 (1C, C_3), 128.30(1C, C_9), 128.87 (2C, C_{10}), 137.44(1C, C_2), 141.58(1C, C_4),154.63 (1C, C_1), 162.62(1C, C_{12}), 162.56, 164.78 (C_7 & C_8), HREIMS. m/z = 380.2102[$M^{\cdot+}$] (calc. for $C_{23}H_{28}N_2O_3$, 380.2100).

2,4-di-*tert*-butyl-6-[5-(4-bromophenyl)-1,3,4-oxadiazol-2-yl]phenol.

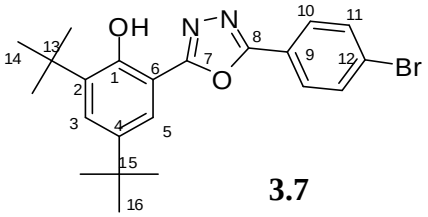

3.7

The crude product was recrystallized from THF to obtain white precipitate. Yield 0.67 g (79%); m.p. 158-160 °C, IR (KBr, υ_{max}/ cm^{-1}), 3462(br, OH_{phenol}), 3088(w, $CH_{aromatic}$), 2955, 2842 (s, $CH_{aliphatic}$), 1608 (m, C=N), 1587, 1552 (m, C=C), 1214 (s, C-O), ^{1}H NMR($CDCl_3$, 400 MHz, ppm): 1.37 (s, 9H, H_{14}, $C(C\underline{H}_3)_3$), 1.48 (s, 9H, H_{16}, -$C(C\underline{H}_3)_3$) , 7.53(d, 1H, *J*=2.2, H_3), 7.67(d, 1H, *J*=2.4, H_5), 7.70 (d, 2H, *J*=8.5, H_{11}), 8.03(d, 2H, *J*=8.5, H_{10}), 10.51 (s, 1H, OH); ^{13}C NMR($CDCl_3$, 100 MHz, ppm): 29.42(3C, C_{16}), 31.47(3C, C_{14}), 34.41(1C, C_{13}), 35.36(1C, C_{15}), 113.50(1C, C_6), 120.51(1C, C_5), 122.41(1C, C_{12}), 126.73(1C, C_9), 128.45(2C, C_{10}), 128.76(1C, C_3), 132.64(2C, C_{11}), 137.64 (1C, C_{13}), 141.77(1C, C_{15}), 154.84(1C, C_1), 162.94 & 165.42 (C_7 & C_8), HREIMs, m/z = 428.1102 [$M^{\cdot+}$] (calc. for $C_{22}H_{25}BrN_2O_2$, 428.1099).

2,4-di-*tert*-butyl-6-[5-(2-chlorophenyl)-1,3,4-oxadiazol-2-yl]phenol

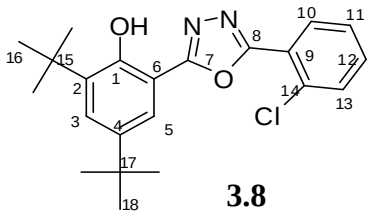

3.8

The crude product was recrystallized from ethanol-chloroform to give white needle crystal. Yield 0.61 g (80%) yield; m.p.138-140 $^{\circ}$C, IR (KBr, υ_{max}/ cm^{-1}), 3475(br, OH $_{phenol}$), 3094(w, $CH_{aromatic}$), 2968, 2857 (s, $CH_{aliphatic}$), 1612(m, C=N), 1585, 1547 (s, C=C), 1221 (s, C-O), ^{1}H NMR($CDCl_3$, 400 MHz, ppm): 1.34 (s, 9H, H_{14}, $C(C\underline{H}_3)_3$), 1.48 (s, 9H, H_{16},-$C(C\underline{H}_3)_3$), 7.70-7.44 (m, 4H, H_{10}, H_{11}, H_{12}), 7.69(d, 1H, J=2.4, H_5), 8.07 (dd, 1H, *J*=7.56, 1.95, H_{13}), 10.46 (s, 1H, OH), ^{13}C NMR ($CDCl_3$, 100 MHz, ppm): 29.46 (1C, C_{18}), 31.47 (1C, C_{16}), 34.41(1C, C_{15}), 35.39(1C, C_{17}), 107.42(1C, C_6), 120.86(1C, C_5), 122.82 (1C, C_9), 127.24(1C, C_3), 128.7 (1C, C_{11}), 131.27(1C,C_{10}), 131.46(1C,C_{12}), 132.67 (1C, C_{13}), 133.39(1C, C_{14}), 137.60(1C, C2), 141.83 (1C, C_4), 154.84(1C, C_1), 161.43(1C,C_8), 165.66(1C, C_7). HREIMs, m/z = 384.1605 [$M^{\cdot +}$] (calc. for $C_{22}H_{25}Cl\ N_2O_2$, 384.1605).

6.2.2 General synthesis of1-*N′*-[(3,5-di-*tert*-butyl-2-hydroxyphenyl)methyl]-X-*N′*-[(3,5-di-*tert*-butyl-2-hydroxyphenyl)methylidene] substituted-dicarbohydrazide.

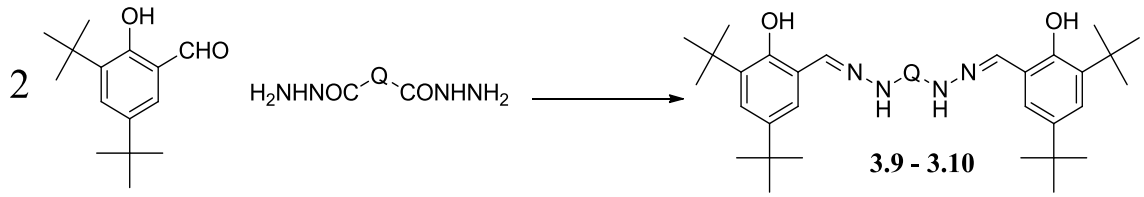

To a suspension of dihydrazide in glacial acetic acid (1.5 mmol.), 3,5-di-*tert*-butyl salicylaldehyde 0.70 g (3 mmol) was added and the mixture was refluxed for 18 h. The solid was filtered and washed with water, followed by absolute ethanol and dried in oven at 80^{0}C.

1-*N'*,4-*N'*-bis[(3,5-di-*tert*-butyl-2-hydroxyphenyl)methylidene]benzene-1,3-dicarbohydrazide.

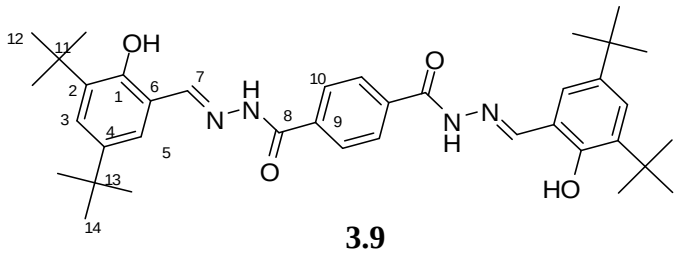

3.9

The crude product was recrystallized from DMF to obtain white precipitate. Yield 0.82 g, (89%) yield; m.p. 344-348 $^{\circ}$C(dec.); IR (KBr, υ_{max}/ cm^{-1}): 3670 (br, OH_{phenol}), 3204(m, NH), 3090(w, $CH_{aromatic}$), 2959, 2865 (s, $CH_{aliphatic}$), 1662 (s, C=O), 1606(m, C=N), 1217(s, C-O).^{1}H NMR (DMSO-d_6-$CDCl_3$, 400 MHz, ppm at 70 $^{\circ}$C), 0.67(s, 18H, H_{12}), 0.80(s, 18H, H_{15}), 6.45 (s, 2H, H_3), 6.70(s, 2H, H_5), 7.47(s, 4H ,H_7, C=N), 11.40(bs, 2H, NH), 11.53(s, 2H, OH); ^{13}C NMR ($CDCl_3$, DMSO-d_6, 100 MHz, ppm): 31.15(6C, C_{14}), 39.00 (6C, C_{12}), 39.21(2C, C_{11}), 39.42(2C, C_{13}), 116.53(2C, C_6), 125.21(2C, C_5), 125.84(2C, C_5), 127.63(4C, C_{10}), 135.58 (2C, C_9), 135.93(2C, C_2), 140.21(2C, C_3), 151.75 (2C, C_7), 162.06(2C, C_8). HREIMs, m/z = 626.3833 [$M^{\cdot +}$] (calc. for $C_{38}H_{50}N_4O_4$, 626.3832).

1-*N'*,3-*N'*-bis[(3,5-di-*tert*-butyl-2-hydroxyphenyl)methylidene]benzene-1,3-dicarbohydrazide.

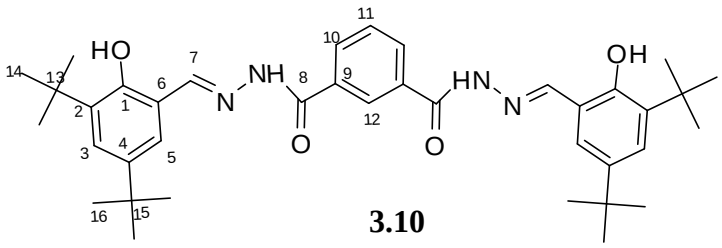

3.10

The crude product was recrystallized from DMSO to give white solid. Yield 0.79 g, (85%); m.p 320-324 °C (dec.); IR (KBr, υ_{max}/ cm^{-1}): 3678(br, OH_{phenol}), 3180(m, NH), 3076 (w, $CH_{aromatic}$), 2955, 2845 (s, $CH_{aliphatic}$), 1658 (s, C=O), 1614(m, C=N),

1228(s, C-O). ^{1}H NMR (DMSO-d_6-$CDCl_3$, 400 MHz, ppm at 70 °C): 1.31(s, 18H, H_{14}), 1.44(s, 18H, H_{16}), 7.1–8.21 (m, 7H, H_3, H_5, H_{10}, H_{11}), 8.50(s, 1H, H_{12}), 8.86 (s, 2H, 2×CH=N), 12.07 & 12.13 (4H, 2OH & 2NH). ^{13}C NMR (DMSO-d_6-$CDCl_3$, 100 MHz, ppm at 70 °C): 29.87 (6C, C_{16}), 31.73(6C, C_{14}), 34.29(2C, C_{13}), 35.12(2C, C_{15}), 117(2C, C_6), 126.08 (2C, C_5), 128.54(2C, C_3), 129.30 (1C, C_{11}) 131.31(1C, C_{12}) 131.31(2C, C_{10}) 133.83 (2C, C_9), 136.45(2C, C_2), 141.09(2C, C_4), 152.51(2C, C=N), 155.25(2C, C_1).HREIMs. m/z = 626.3826[$M^{\cdot+}$] (calc. for $C_{38}H_{50}N_4O_4$, 626.3832).

6.2.3 General synthesis of Bis(1,3,4-oxadiazole) bis(2,4-di–*tert*-butylphenol. (3.11-3.12)

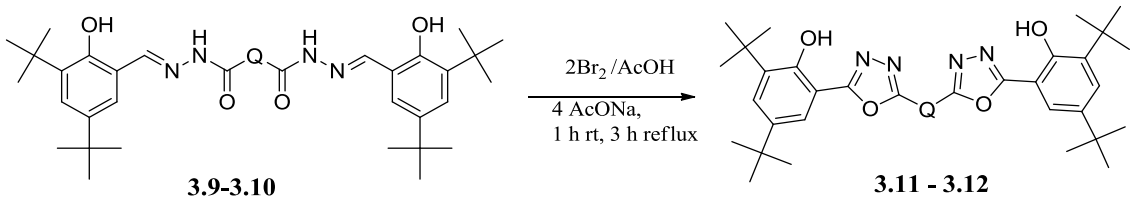

3.9-3.10 **3.11 - 3.12**

To a solution of 1-N'-[(3,5-di-tert-butyl-2-hydroxyphenyl)methyl]-X-N'-[(3,5-di-*tert*-butyl-2-hydroxyphenyl) methylidene]substituted-dicarbohydrazide (2 mmol) in 7 mL glacial acetic acid and anhydrous sodium acetate (4 mmol)was added bromine (2mmol) in glacial acetic acid dropwise at ambient temperature and allow to stir for 1 hour and then refluxed for 2 h. After cooling to room temperature, the mixture was poured onto a 50 mL ice water. The precipitate was collected, washed with water, dried and purified by column chromatography.

6,6'-(5,5'-(1,4-phenylene)bis(1,3,4-oxadiazole-5,2-diyl))bis(2,4-di-*tert*-butylphenol).

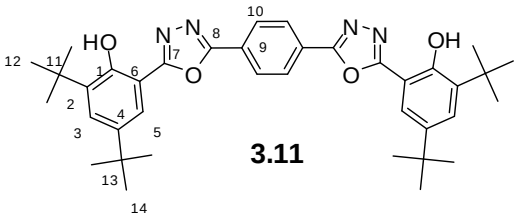

3.11

The crude product was purified by column chromatography using (hexane-ethyl acetate) 6-1 as eluent, then recrystallized from chloroform: ethanol (1:4), white amorphous. Yied 0.86 g (70%); m.p.288-290 $^{\circ}$C, IR (KBr, υ_{max}/ cm^{-1}): 3676(OH_{phenol}), 3091($CH_{aromatic}$), 2966, 2854 ($CH_{aliphatic}$), 1611(C=N), 1219 (C-O); ^{1}H NMR ($CDCl_3$ 400 MHz, ppm): 1.39 (s, 18H,H_{12},2× C($\underline{CH_3}$)$_3$), 1.49 (s,18H, H_{14}, 2× C($\underline{CH_3}$)$_3$), 7.55(d, 2H, *J*=2.4, H_3), 7.72(d, 2H, *J*=2.4, H_5), 8.37 (s, 4H, H_{10});^{13}C NMR($CDCl_3$, 100 MHz, ppm): 29.49 (6C, C_{14}, 2×C($\underline{CH_3}$)$_3$), 31.55(6C, C_{12}, 2×C($\underline{CH_3}$)$_3$), 34.50 (2C, C_{13}, 2×$\underline{C}$(CH_3)$_3$), 35.46(2C, C_{13}, 2×$\underline{C}$(CH_3)$_3$), 107.32(2C, C_6), 120.66(2C, C_5), 126.45 (2C, C_3), 127.80(2C, C_{10}), 129.06 (2C, C_9), 137,78(2C, C_4), 141.96(2C, C_2), 155.02(2C, C_1), 162.19 & 165.81 (C_5 & C_6). HREIMs m/z = 622.3516 [$M^{\cdot +}$] (calc. for $C_{38}H_{46}N_4O_4$, 622.3519).

6,6'-(5,5'-(1,3-phenylene)bis(1,3,4-oxadiazole-5,2-diyl))bis(2,4-di-*tert*-butyl phenol). (5.48)

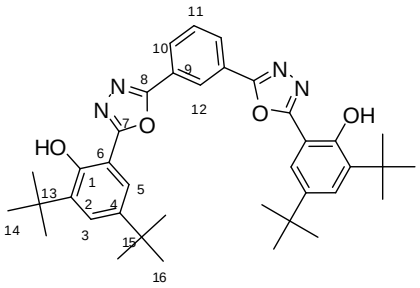

3.12

The crude product was purified by column chromatography using (hexane : ethylacetate) 6:1 as elute, to give white crystals. Yield 0.96 g (78%); m.p.172-174 $^{\circ}$C; IR (KBr, υ_{max}/ cm^{-1}): 3670(br, OH_{phenol}), 3095(w, $CH_{aromatic}$), 2968, 2852 (s, $CH_{aliphatic}$), 1610(m, C=N), 1228(s, C-O); ^{1}H NMR($CDCl_3$, 600 MHz, ppm): 1.32 (s, 9H, H_{14}, C($C\underline{H_3}$)$_3$), 1.42 (s, 9H, H_{16}), 7.48(s, 2H, H_3), 7.67(s, 2H, H_5), 7.72(t, 1H, *J*= 7.81, H_{11}), 8.33(d, 2H, *J*=7.72, H_{10}), 8.81(s, 1H, H_{12}), 10.50(s, 1H, OH); ^{13}C NMR($CDCl_3$, 150MHz, ppm): 29.42(18C, C_{16}), 31.56(18C, C_{14}), 34.46(2C, C_{13}), 35.40(2C, C_{15}),

107.30(2C, C_6), 120.64(2C, C_9), 124.73(2C, C_5), 125.12(1C, C_{12}), 128.94(2C, C_3), 130.21(1C, C_{11}), 130.30 (2C, C_{10}), 137.66(2C, C_2), 141.18(2C, C_4), 154.95(2C, C_1), 162.10(2C, C_8),165.79(2C, C_7). HREIMs m/z = 622.3506 [$M^{\cdot +}$] (calc. for $C_{38}H_{46}N_4O_4$, 622.3519).

6.2.4 Synthesis of methyl 3,5-di-*tert*-butyl-salicylate.

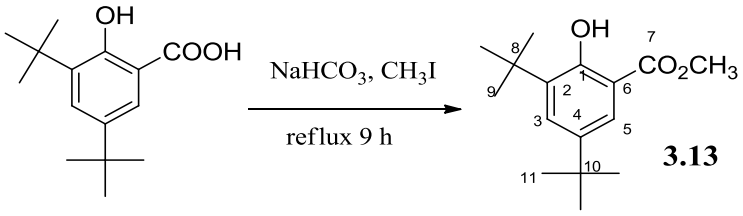

3.13

100 mL round bottom flask was charged with 3,5-di-*tert*-butyl-salcylic acid (3.75 g, 15 mmol) and sodium hydrogen carbonate (1.3 g, 15.5 mmol) in dry DMF (20 mL). Excess of methyl iodide was added. The mixture was refluxed for 9 h and reaction monitored by TLC using (hexane: ethyl acetate, 5:1). The excess of solvent was evaporated under reduced pressure. To the solid residue, 25mL distilled water was added and then extracted with 50 mL ethyl acetate. The organic layer was washed with water and dried under anhydrous magnesium sulfate.The solvent was evaporated under reduced pressure. The crude product was recrystallized from ethanol-hexane afforded pure white solid ester. Yield 3.76 g (94%); m.p.72-74 $^{\circ}$C; IR (KBr, υ_{max}/ cm^{-1}): 3105 (w, $CH_{aromatic}$), 2957, 2908, 2870 (s, $CH_{aliphatic}$), 1727 (s, C=O) 1600, 1559 (s, C=C), 1215 (s, C-O); ^{1}H NMR ($CDCl_3$, 400 MHz, ppm): 1.28 (s, 9H, *o*-C($\underline{CH_3}$)$_3$), 1.41 (s, 9H, *p*-C($\underline{CH_3}$)$_3$), 3.92(s, 3H, OCH_3), 7.57(d, 1H, *J*=2.76, H_3), 7.78(d, 1H, *J*=2.76, H_5), 11.32(s, 1H, OH); ^{13}C NMR ($CDCl_3$, 100 MHz, ppm): 29.47(3C, *p*-(C($\underline{CH_3}$)$_3$), 31.50(3C, *o*-(C($\underline{CH_3}$)$_3$)), 34.38(1C, *o*-($\underline{C}$(CH_3)$_3$, 35.25(1C, *p*-($\underline{C}$(CH_3)$_3$), 52.28(1C, OCH_3), 110.50(1C, C_6), 124.69(1C, C_5), 131(1C, C_3), 137.51 (1C, C_2), 140.96(1C, C_4),

159.79(1C, C_1), 176.05(1C, CO). HREIMs. m/z = 264.1725[$M^{\cdot+}$] (calc. for $C_{16}H_{24}O_3$, 264.1725).

6.2.5 Synthesis of 3,5-di-*tert*-butyl-salcylic hydrazide.

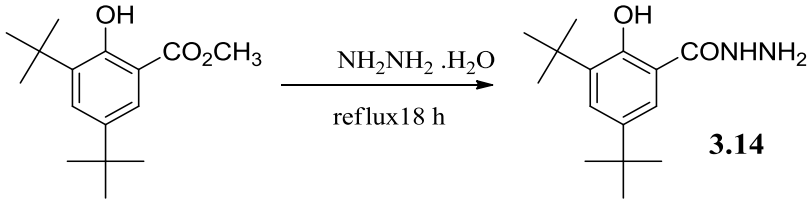

3.14

Method –A

A solution of methyl 3,5-di-*tert*-butyl-salicylate (2.64 g,10 mmol) in 20 mL benzene and 1mL ethanol and excess of hydrazine hydrate 98% 5mL was refluxed for 18 h. The excess solvent and hydrazine was removed under reduced pressure and co-evaporated with (5 mL×2) using toluene. A solid mass was obtained when recrystallized with aqueous ethanol. A white precipitate was obtained. Yield 1.66 g (63%), m.p.192-194 $^{\circ}$C.

Method –B

Methyl 3,5-di-*tert*-butyl-salicylate (2.64 g,10 mmol) was heated to melting point in a 50mL round bottom flask. When the ester has melted, 5mL of hydrazine hydrate was added dropwise and the mixture was heated to 70-75 $^{\circ}$C for 2 h. Absolute ethanol was added until clear solution appears and then further refluxed for 3 h. Upon cooling, the white precipitate was filtered and washed. Recrystallized from aqueous ethanol afforded white precipitate with 96% yield, (2.53 g) m.p.192-194 °C. IR (KBr, υ_{max}/ cm^{-1}): 3675 (br, OH_{phenol}), 3316, 3208, 3192 (br, $NHNH_2$), 2960, 2871(s, $CH_{aliphatic}$), 1626 (s, C=O), 1593(s, C=C), ^{1}H NMR (DMSO-d_6, 400 MHz, ppm):1.26 (s, 9H, H_9, C($\underline{CH_3}$)$_3$), 1.47 (s, 9H, H_{11}, C($\underline{CH_3}$)$_3$), 4.93(bs, 2H, NH_2), 7.35(s, 1H, H_3), 7.83(s, 1H, H_5), 10.28 (bs, 1H, NH), 13.40(s, 1H, OH); ^{13}C NMR(DMSO-d_6,100 MHz, ppm):

29.68(3C, C_{11}), 31.79 (3C, C_9), 34.61(1C, C_8), 35.14(1C, C_{10}), 112.82(1C, C_6), 121.21(1C, C_5), 127.92 (1C, C_3), 136.83(1C, C_2), 140.22(1C, C_4), 157.82(1C, C_1), 170.11(1C, C_7). HREIMs m/z = 264.1838[$M^{\cdot+}$] (calc. for $C_{15}H_{24}O_2N_2$, 264.1838)

6.2.6 Synthesis of 2,4-di-*tert*-butyl-6-(5-thio-4-hydro-1,3,4-oxadiazol-2-yl)phenol.

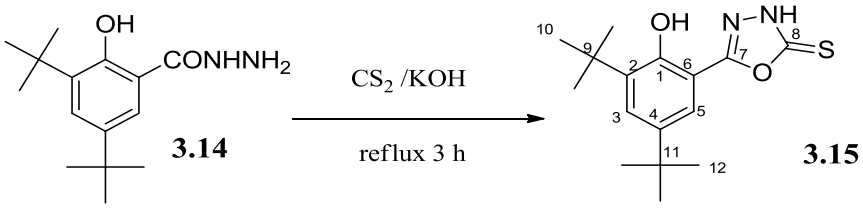

To a solution of hydrazide **3.14** (1g, 3.75 mmol) and excess of carbon disulfide (0.8g, 0.6 mL) in absolute ethanol, potassium hydroxide (0.21 g, 3.75 mmol) was added in one portion at ambient temperatures. The mixture was stirred and refluxed for 3h. After that the solvent was removed under vacuum. Distilled water (25 mL) was added to the residue and stirred for another 15 minutes. It was filtered and the filtrate was acidified with 5% hydrochloric acid and finally re-filter. The white precipitate was washed with water, recrystallized with ethanol. Yield 0.91 g (79%); m.p. 222-224 $^{\circ}$C. IR (KBr, υ_{max}/ cm^{-1}), 3187 (bs, OH, NH), 3092(w, $CH_{aromatic}$), 2956(s, $CH_{aliphatic}$), 1618 (m, C=N), 1594, 1580(s, C=C), 1270(m, C=S), 1218(s, C-O), 1095(m, C-O-C); ^{1}H NMR ($CDCl_3$,400 MHz, ppm): 1.27(s, 9H, H_{10}), 1.38(s, 9H, H_{12}), 7.41(d, 1H, *J*=2.23, H_3), 7.45(d, 1H, *J*=2.20, H_5), 9.1(bs, 1H, OH); ^{13}C NMR($CDCl_3$, 100 MHz, ppm): 29.85(3C, C_{12}), 31.66(3C, C_{10}), 34.61(1C, C9), 35.48(1C, C_{11}), 109.48(1C, C_6), 122.13(1C, C_5), 128.34(1C, C_3), 137.88(1C, C_2), 142.35(1C, C_4), 152.96(1C, C_1), 161.11(1C, C=N), 177.10 (C=S). HREIMs m/z = 306.1402 [$M^{\cdot+}$] (calc. for $C_{16}H_{22}N_2O_2S$, 306.1402).

6.2.7 General alkylation 2,4-di-*tert*-butyl-6-(5-thio-4-hydro-1,3,4-oxadiazol-2-yl) phenol.

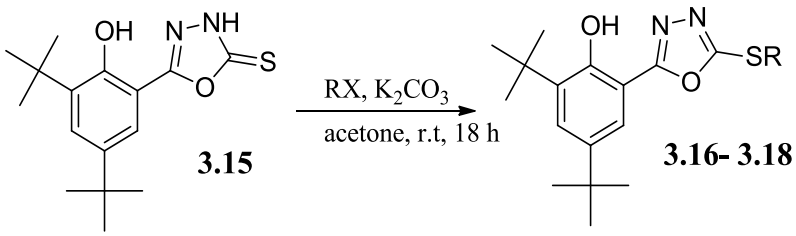

3.15 **3.16- 3.18**

Alkyl halide (1 mmol) was added in small portions to a stirred suspension of 1,3,4-oxadiazole (0.31 g, 1 mmol) in dry acetone and anhydrous potassium carbonate (0.14g, 1mmol). The mixture was left to stand overnight with stirring at ambient temperature. The solvent was evaporated and the residue extracted with 25 mL chloroform. It was dried under anhydrous magnesium sulfate and recrystallized from suitable solvent.

2,4-di-*tert*-butyl-6-(5-methylthio-1,3,4-oxadiazol-2-yl)phenol.

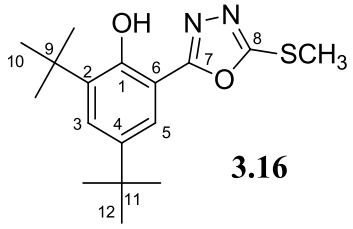

3.16

The crude product was recrystallized from methanol to obtain white needle crystal. Yield 0.26 g (83%); m.p. 100-102 $^{\circ}$C; IR (KBr, υ_{max}/ cm^{-1}): 3163(br, OH), 2950, 2868(s, $CH_{aliphatic}$), 1614 (m, C=N), 1595, 1482 (s, C=C), 1178(s, C-O), 1095(m, C-O-C); ^{1}H NMR($CDCl_3$, 400 MHz, ppm): 1.31(s, 9H, H_{10}), 1.44 (s, 9H, H_{12}), 2.78(s, 3H, SCH_3), 7.46(d, 1H, *J*=2.44, H_3), 7.52(d,1H, *J*=2.44, H_5), 10.21(s, 1H, OH): ^{13}C NMR($CDCl_3$, 100 MHz, ppm): 14.77(1C, S$\underline{CH_3}$), 29.48(3C, C_{12}), 31.53 (3C, C_{10}), 34.46(1C, C_9), 35.39(1C, C_{11}), 107.47(1C, C_6), 120.64 (1C, C_5), 128.46 (1C, C_3),

137.46 (1C, C_2), 141.79(1C, C_4)154.30(1C, C_1), 164.12 & 166.35 (C_7, C_8, C=N). HREIMs m/z = 320.1562 [M^+] (calc. for $C_{17}H_{24}N_2O_2S$, 320.1558).

2,4-di-tert-butyl-6-(5-prop-2-yn-1-ylthio-1,3,4-oxadiazol-2-yl)phenol

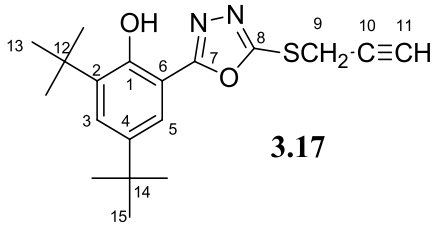

3.17

The crude product was recrystallized from ethanol to obtain white crystal. Yield 0.3 g (86%); mp.108-110 °C, IR (KBr, υ_{max}/ cm^{-1}), 3276 (m, C≡CH), 3153(br, OH_{phenol}), 2951, 2868 (s, $CH_{aliphatic}$), 2164(w, C≡C), 1617(m, C=N), 1995, 1557(s, C=C), 1178 (s, C-O), 1095 (m, C-O-C); ^{1}H NMR (DMSO-d_6, 400 MHz, ppm): 1.29(s, 9H, H_{13}), 1.41 (s, 9H, H_{15}), 3.37 (t, 1H, *J*=2.67, H_{11}), 4.23(d, 2H, *J*=2.68, H_9), 7.48(d, 1H, *J*=2.44, H_3), 7.59 (d, 1H, *J*=2.44, H_5), 10.18(s, 1H, OH); ^{13}C NMR($CDCl_3$,100 MHz, ppm): 20.95 (1C, C_9), 29.21(3C,C_{15}), 31.09(3C, C_{13}), 34.06(1C, C_{12}), 34.88(1C, C_{14}) 75.16 (1C, C_{11}), 78.92 (1C, C_{10}), 107.69 (1C, C_6), 121.13 (1C, C_5), 128.16(1C, C_3), 136.90(1C, C_2), 141.90(1C, C_4), 153.30(1C, C_1), 161.98 & 166.00(C_7 & C_8), HREIMs m/z = 344.1558 [$M^{\cdot +}$] (calc. for $C_{19}H_{24}N_2O_2S$, 344.1558).

2,4-di-tert-butyl-6-(5-(4-bromobenzyl)thio-1,3,4-oxadiazol-2-yl)phenol.

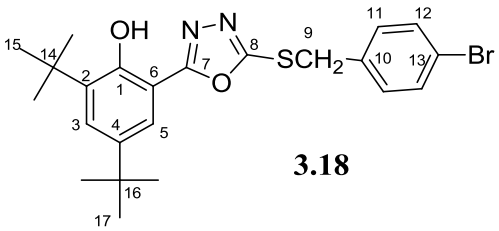

3.18

The solid product was recrystallized from ethanol-ethyl acetate to give white amorphous. Yield 0.37 g (78%); m.p.118-120 °C, IR (KBr, υ_{max}/ cm^{-1}): 3178(br, OH_{phenol}), 3045 (w, $CH_{aromatic}$), 2958, 2845 (s, $CH_{aliphatic}$), 1616 (m, C=N), 1995,1845

(m, C=C), 1265 (s, C-O), 1081 (m, C-O-C); ^{1}H NMR ($CDCl_3$, 400 MHz, ppm): 1.32(s, 9H, H_{15}), 1.45(s, 9H, H_{17}), 4.46(s, 2H, H_9), 7.35(d, 2H, *J*=8.41, H_{11}), 7.36-7.50(m, 4H, H_3, H_5, H_{12}); ^{13}C NMR($CDCl_3$, 100 MHz, ppm): δ; 29.39(3C, C_{17}), 31.44(3C, C_{15}), 34.38(1C, C_9), 35.32(1C, C_{14}), 36.16(1C, C_{16}), 107.27(1C, C_6), 120.57(1C, C_5), 122.26(1C, C_{13}), 128.52(1C, C_3), 130.76(2C, C_{11}), 131.99(2C, C_{12}), 134.64(1C, C_{13}), 137.43(1C, C_2), 141.75(1C, C_5), 154.26(1C, C_1), 162.38 & 166.40 (2C, C=N). HREIMs.m/z = 474.0960 [$M^{\cdot+}$] (calc. for$C_{23}H_{27}BrN_2O_2S$, 474.0956).

6.2.8 Synthesis of 2,4-di-*tert*-butyl-6-(5-amino-1,3,4- oxadiazol-2-yl)phenol.

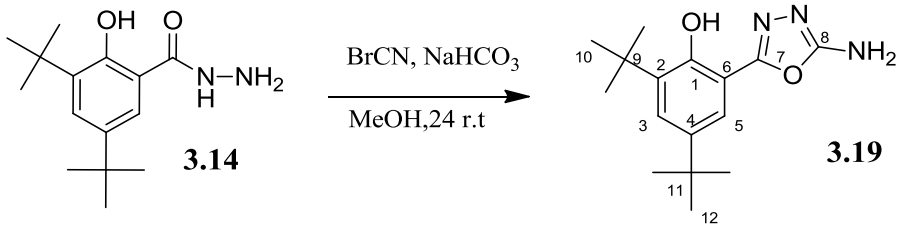

A solution of hydrazide, **3.14** (0.52 g, 2 mmol) in 10 mL methanol and sodium bicarbonate (0.17 g, 2 mmol) was stirred in 50 mL round bottom flask, then (0.22 gm, 2.1 mmol) cyanogene bromide was added. The mixture was left stirring at ambient temperature overnight. After that, 5 mL cold water was added to the mixture and the precipitate was collected and dried at 60 °C. The white solid was recrystallized from aqueous ethanol to give 0.347 g, (61%) yield; m.p. 220-222°C;.IR(KBr, υ_{max}/ cm^{-1}): 3468(br, OH_{phenol}), 3318, 3291 (m, NH_2), 3093(w, $CH_{aromatic}$), 2960, 2870 (s, $CH_{aliphatic}$), 1614(m, C=N), 1600, 1552(s, C=C), 1250(s, C-N), 1203(s, C-O), 1099 (m, C-O-C); ^{1}H NMR (DMSO-d_6, 400 MHz, ppm): 1.23 (s, 9H, H_{10}, C($\underline{CH_3}$)$_3$), 1.35 (s, 9H, H_{12}, C($\underline{CH_3}$)$_3$), 7.34(d, 1H, *J*=1.95, H_3), 7.38(d, 1H, *J*=2.2, H_5), 7.45(s, 2H, NH_2).^{13}C NMR (DMSO-d_6, 100 MHz, ppm): 29.20(3C, C_{12}), 31.28(3C, C_{10}), 108.15(1C, C_6), 119.24(1C, C_5), 126.12 (1C, C_3), 136.13(1C, C_2), 141.09(1C, C_4), 152.58(1C, C_1),

158.27, 162.71(C7, C_8, C=N). HREIMs m/z = 289.1797[$M^{\cdot+}$] (calc.for $C_{16}H_{23}N_3O_2$; 289.1790).

6.2.9 Synthesis of 2-(3,5-di-*tert*-butyl-2-hydroxybenzylidene) hydrazinecarbothioamide

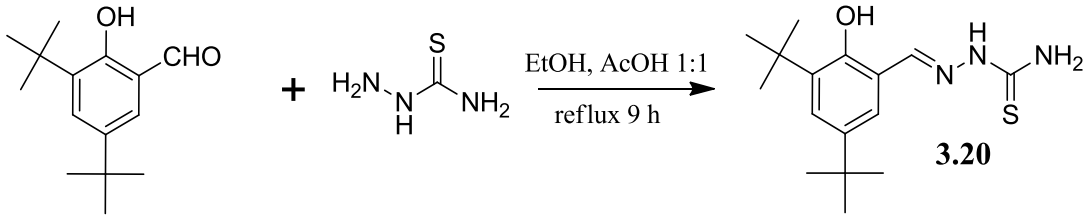

3.20

3,5-di-*tert*-butyl-salicylaldehyde (0.46 g, 2 mmol) was added gradually to a suspension of thiosemicarbazide (0.18 g, 2mmol) in 6 mL of a hot mixture of ethanol and glacial acetic acid. After the addition, the mixture was refluxed for 9 h. Upon cooling, the precipitate was filtered and washed with water, then with cold ethanol and recrystallized from methanol to obtain white crystal. Yield 0.546 g (91%); m.p. 218-220 $^{\circ}$C. IR (KBr, υ_{max}/ cm^{-1}): 3455(br, OH_{phenol}), 3266, 3161, 31042(br, NH, NH_2), 2958, 2868(s, $CH_{aliphatic}$), 1624(m, C=N), 1579, 1506(m, C=C), 1264(m, C=S), 1200(s, C-O), ^{1}H NMR (CD_3OD, 400 MHz, ppm): 1.30(s, 9H, H_{10}), 1.43(s, 9H, H_{12}), 4.59 (s, 2H, NH_2, D_2O exchange), 7.15(d, 1H, *J*=2.44, H_3), 7.39(d, 1H, *J*=2.20, H_5), 8.18(s, 1H, H_7), 10.06(bs, 1H, NH, D_2O exchange), 11.04 (bs, 1H, OH, D_2O exchange); ^{13}C NMR(DMSO-d_6, 100 MHz, ppm): 28.66(3C, C_{12}), 30.53(3C, C_{10}), 33.74(1C, C_9), 34.67(1C, C_{11}), 116.94(1C, C_6), 126.34(1C, C_5), 126.51(1C, C_3), 136.27(1C, C_2), 141.43(1C, C_4). HREIMs m/z =307.1727[$M^{\cdot+}$] (calc for $C_{16}H_{25}N_3O_1S$, 307.1718).

6.2.10 Synthesis of 2,4-di-*tert*-butyl-6-(5-amino-1,3,4-thiadiazol-2-yl) phenol.

Method –A

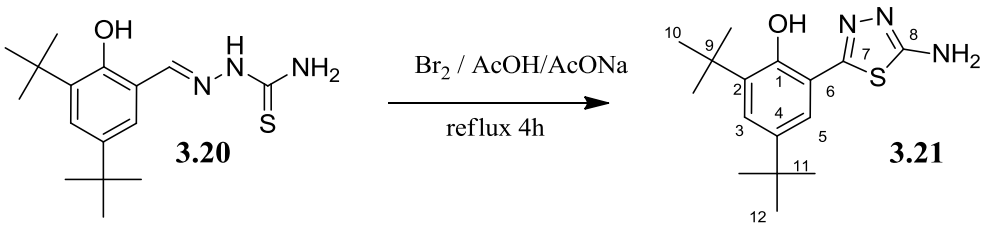

To a suspension of 2-(3,5-di-*tert*-butyl-2-hydroxybenzylidene)hydrazine-carbothioamide (0.3 g, 1 mmol) in 5 mL glacial acetic acid and (0.16 g, 2 mmol) of anhydrous sodium acetate, bromine solution (0.16 g, 0.1 mmol) in 3 mL glacial acetic acid was added dropwise at ambient temperatures. The mixture was refluxed for 4h, and after cooling the mixture was poured into 50 mL ice water and was stirred for another 30 minutes. The precipitates were collected and washed with water, dried and purified by column chromatography using $CHCl_3$-MeOH (99-1) as eluent to afford pale yellow amorphous, 0.243 g with 81% yield; m.p. 248-250 $^{\circ}$C.

Method –B

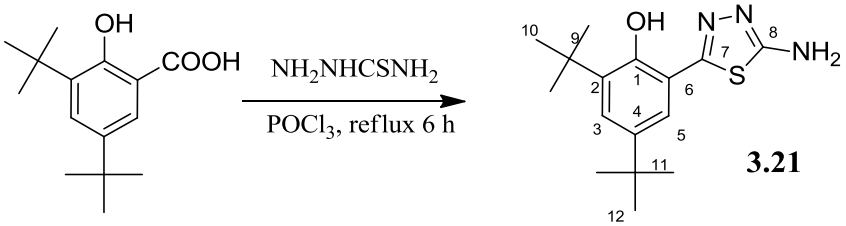

To a mixture of 3,5-di-*tert*–butyl-4-hydroxybenzoic acid (0.25 g, 1 mmol) and thiosemicarbazide (0.09 g, 1 mmol), phosphorusoxychloride 3 mL was added and refluxed for 6 h. The excess of phosphorusoxychloride was removed under vacuum. The oily substance was washed with saturated solution of sodium hydrogen carbonate. The yellow precipitate was filtered and purified by column chromatography using $CHCl_3$:MeOH (99:1) as eluent. A pale yellow amorphous was obtained. Yield 0.147 g

(49%); m.p. 248-250 °C; IR (KBr, υ_{max}/ cm^{-1}): 3266(br, OH, NH_2), 1630(m, C=N), 1601(s, C=C), 1360(s, C-N), 1201(s, C-O); ^{1}H NMR (DMSO-d_6, 400 MHz, ppm): 0.7 (s, 9H, H_{10}, C($\underline{CH}_3$)$_3$), 0.87 (s,9H, H_{12}, C($\underline{CH}_3$)$_3$), 6.52(d, 1H, *J*=1.8, H_3), 6.84(d, 1H, *J*=1.36, H_5), 6.71(s, 2H, NH_2). ^{13}C NMR(DMSO-d_6, 100 MHz, ppm): 29.48(3C, C_{12}, (C($\underline{C}H_3$)$_3$), 31.43(3C, C_{10}, C($\underline{C}H_3$)$_3$), 34.33(1C, C_9, $\underline{C}$(CH_3)$_3$), 35.39(1C, C_{11}, $\underline{C}$(CH_3)$_3$), 112.84(1C, C_6), 122.89 (1C, C_5), 127.95(1C, C_3), 137.94(1C, C_2), 142.19(1C, C_4), 153.46(1C, C_1), 160.44 & 167.33(2C, C_7 & C_8), HREIMs m/z= 305.1563.[$M^{\cdot+}$] (calc. for $C_{16}H_{23}N_3O_1S$, 305.1562).

6.2.11 Synthesis of 2,4-di-*tert*-butyl-6-(4-amino-1,2,4-triazol-3-yl-5-thione)phenol

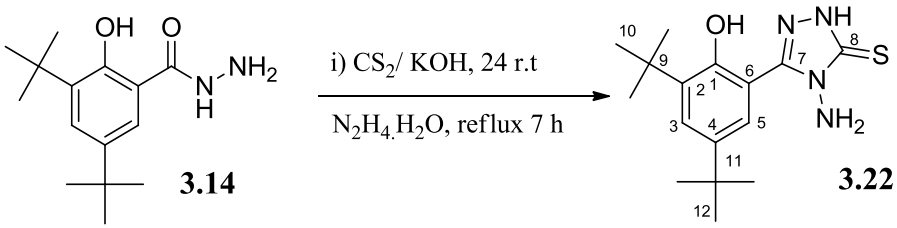

To a solution of 3,5 di-*tert*-butyl salicylic hydrazide (0.52 g, 2 mmol) in 7 mL absolute ethanol was added. Carbon disulphide (0.23 g, 3 mmol) was added and potassium hydroxide (0.11 g, 2 mmol) at room temperature. The mixture was stirred for 24 h, then 25 mL dry ether was added and allow to stir for another 2 h. The precipitated was filtrated and washed with dry ether. The product was dried at 80 °C to give white solid of potassium 2-(3,5-di-*tert*-butyl-2-hydroxybenzoyl)hydrazinecarbodithioate salt (0.34 g, 2 mmol). The resulting product was dissolved in excess of hydrazine hydrate 80%. The mixture was heated and refluxed for 7 h then cooled and poured into ice water. The pH was adjusted to 5 by using 10% HCl. The precipitate was filtrated, washed with water, dried and recrystallized from methanol to obtain 0.2 g (65%) of white precipitate, m.p.140-142 °C; IR(KBr, υ_{max}/ cm^{-1}), 3512(br, OH_{phenol}) 3420, 3300, 3145(m, NH, NH_2), 2956 (s, $CH_{aliphatic}$), 1635 (m, C=N), 1595, 1879 (s, C=C), 1360 (s, C-N), 1252(m, C=S), 1217(s, C-O). ^{1}H NMR (DMSO-d_6, 400 MHz, ppm): 1.26(s, 9H,

H_{10}, C($\underline{CH_3}$)$_3$), 1.35 (s, 9H, H_{12}, C($\underline{CH_3}$)$_3$), 6.21(bs, 1H, NH_2),7.38(d, 1H, *J*=2.2, H_3), 7.63 (d, 1H, J=1.87, H_5), 10.91(bs, 1H, OH), 14.03(bs, 1H, NH).^{13}C NMR (DMSO-d_6, 100 MHz, ppm): 29.50(1C, C_{12}), 31.26(1C,C_{10}), 34.02(1C,C_9), 34.68(1C, C_{11}), 113.02(1C, C_6), 124.73(1C, C_5), 126.24(1C, C_3), 137.34(1C, C_2), 141.08(1C, C_4), 149.78(1C, C_7), 152.14(1C, C_1), 165.74(1C, C_8). HREIMs, m/z=320.1668 [$M^{\cdot+}$] (calc. for $C_{16}H_{24}N_4O_1S$, 320.1671).

6.2.12 General synthesis of 2-(3,5- di-*tert*-butyl -2-hydroxybenzoyl)-*N*-(aryl) hydrazinecarbothioamide.

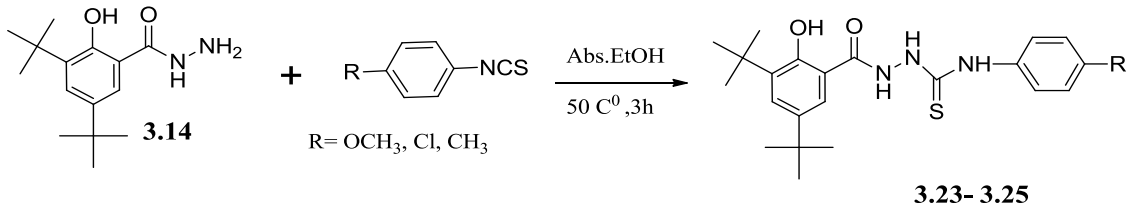

Aryl *iso*thiocyanate (2 mmol) was added dropwise to a stirred solution of 3,5-di-*tert*-butyl-salicylic hydrazide (0.52 g, 2 mmol) in 15 mL absolute ethanol and the mixture was heated to 50 $^{\circ}$C for 3 h. The solid mass was collected after cooling, washed with cold absolute ethanol and then dried under reduced pressure and recrystallized from suitable solvent.

2-(3,5-di-*tert*-butyl-2-hydroxybenzoyl)-*N*-(4-methoxyphenyl)hydrazinecarbothio amide.

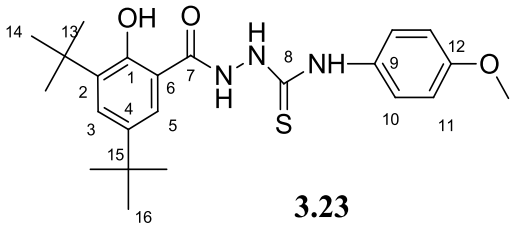

The solid was recrystallized from methanol to afford white crystals. Yield 0.76 g, (94%); m.p.168-170 $^{\circ}$C, IR (KBr, υ_{max}/ cm^{-1}): 3562(br, OH), 3224 (br, NH), 1651(s,

C=O), 1601, 1586 (s, C=C), 1250(m, C=S), 1175(s, C-O). ^{1}H NMR (DMSO-d_6, 600 MHz, ppm): 1.29 (s, 9H, H_{14}, C($\underline{CH_3}$)$_3$), 1.38 (s, 9H, H_{16}, C($\underline{CH_3}$)$_3$), 3.74 (s, 3H, O$\underline{CH_3}$), 6.89(d, 2H, *J*=8.34, H_{10}), 7.27(d, 2H, *J*=8.34, H_{11}), 7.43(s,1H, H_3), 7.75(s, 1H, H_5), 9.70 (bs, 1H, NHCO), 9.84, (s, 1H, NH-Ph), 10.93 (sb,1H, NHCS) 12.97(s, 1H, OH); ^{13}C NMR (DMSO-d_6, 150 MHz, ppm): 29.21(3C, C_{16}, 3×(C($\underline{CH_3}$)$_3$), 31.27(3C,C_{14}, 3×(C($\underline{CH_3}$)$_3$), 34.21 (1C, C_{13}), 34.68 (1C, C_{15}), 55.16(1C, O$\underline{C}H_3$), 112.19(1C, C_6), 113.15(1C, C_{11}), 122.10 (1C, C_5), 127.54(1C, C_3), 128.12(1C, C_{10}), 131.93(1C, C_9), 136(1C, C_2), 139.84(1C, C_4), 156.76(1C, C_1), 158.06(1C, C_{12}), 171.22(1C, C_7), 181.25(1C, C_8). HREIMs m/z = 429.2096[$M^{\cdot+}$] (calc. for $C_{23}H_{31}N_3O_3S$, 429.2086).

2-(3,5-di-*tert*-butyl-2-hydroxybenzoyl)-*N*-(4-chlorophenyl)-hydrazinecarbothio amide.

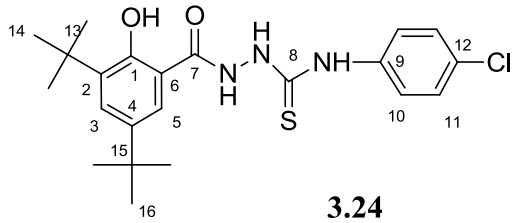

3.24

The crude product was recrystallized from ethanol to obtain white crystals. Yield 0.67 g (95 %); m.p.196-198 $^{\circ}$C, IR (KBr, υ_{max}/ cm^{-1}): 3480 (br, OH), 3217 (br, NH), 1658 (s, C=O), 1600, 1585 (s, C=C), 1239 (m, C=S), 1175(s, C-O); ^{1}H NMR (DMSO-d_6, 600 MHz, ppm): 1.31 (s, 9H, H_{14}), 1.40(s, 9H, H_{16}), 7.39-7.48(m, 5H, H_{11}, H_{12}, H_3), 7.79(s, 1H, H_5), 9.93(bs, 1H, NH ,NHCO), 9.99 (bs, 1H, NH-ph), 10.99 (bs, 1H, NHCS), 12.96 (s, 1H, OH); ^{13}C NMR(DMSO-d_6, 150MHz, ppm): 29.22(3C, C_{16}, 3(C($\underline{CH_3}$)$_3$), 31.29 (3C, C_{14}, 3(C($\underline{CH_3}$)), 34.24 (1C, C_{13}), 34.71 (1C, C_{15}), 112.19(1C, C_6), 122.06(1C, C_5), 127.60(1C, C_3), 127.81(1C, C_{11}), 128.21(1C, C_{10}), 129.12(1C, C_{12}), 136.34 (1C, C_9), 138.13(1C, C_2), 139.52(1C, C_4), 158.13(1C, C_1), 171.20(1C, C_7), 181.08 (1C, C_8). HREIMs, m/z = 433.1595[$M^{\cdot+}$] (calc. for $C_{22}H_{28}ClN_3O_2S$, 433.1591).

2-(3,5-di-*tert*-butyl-2-hydroxybenzoyl)-*N*-(4-methylphenyl)-hydrazinecarbothio-amide.

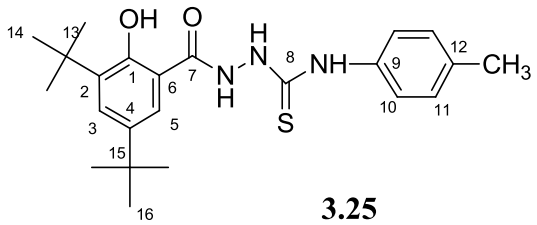

3.25

The solid mass was recrystallized from ethanol to afford white crystal. Yield 0.65 g (96%); m.p.162-164 °C. IR (KBr, υ_{max}/ cm^{-1}), 3250 (br, OH & NH), 1652 (s, C=O), 1595, 1585 (m, C=C), 1221(m, C=S), 1175(s, C-O). ^{1}H NMR ($CDCl_3$,400 MHz, ppm): 1.29 (s, 9H, H_{14}, C($\underline{CH_3}$)$_3$), 1.38 (s, 9H, H_{16}, C($\underline{CH_3}$)$_3$), 2.28 (s, 3H, ph-$\underline{CH_3}$), 7.43-7.71(m, 5H, H_3, H_{10}, H_{11}), 7.75 (s, 1H, H_5), 9.71(bs, 1H, CONH), 9.88 (bs, ph-$\underline{NH}$CS), 10.93 (bs, 1H, CSNH), 12.95(s, 1H, OH); ^{13}C NMR(DMSO-d_6,100 MHz, ppm): 20.50(1C, Ph-CH_3), 29.21(3C, C_{16}), 31.27(3C, C_{14}), 34.21(1C, C_{15}), 34.68(1C, C_{13}), 112.20(1C, C_6), 122.09(1C, C_5), 126.01(1C, C_3), 128.15(2C, C_{10}), 128.44(1C, C_9), 134.32(1C, C_{11}), 136.30(2C, C_{12}), 136.50(1C, C_2), 139.52(1C, C_4), 158.06(1C, C_1), 171.22 (1C, C_7, CO), 181.17(1C, C_8, CS). HREIMs, m/z=413.2122[$M^{\cdot+}$] (calc. for $C_{23}H_{31}N_3O_2S$, 413.2110)

6.2.13 General synthesis of 2,4-di-*tert*-butyl-6-(4-aryl-1,2,4-triazol-3-yl-5-thione) phenol

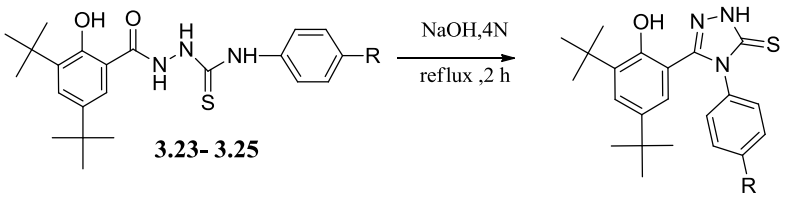

3.23- 3.25 **3.26 - 3.28**

A suspension of 2-(3,5-di-*tert*-butyl-2-hydroxybenzoyl)-*N*-(aryl)hydrazine carbothioamide (1 mmol) in 10 mL sodium hydroxide solution (4N) was refluxed for 2 h. After cooling to room temperature, the mixture was filtered, and the filtrate was

poured into 50 mL ice water. The pH was adjusted to pH 5 using 10% hydrochloric acid. The solid separated, collected and washed with cold water, dried and purified by column chromatograph or recrystallized with suitable solvent.

2,4-di-*tert*-butyl-6-(4-(4-methoxyphenyl)-1,2,4-triazol-3-yl-5-thione)phenol.

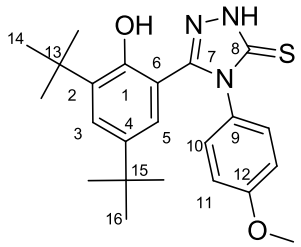

3.26

The solid mass was recrystallized from acetone to obtain white crystals. Yield 0.28 g (69%); m.p.300-302 $^{\circ}$C (dec.). IR (KBr, υ_{max}/ cm^{-1}): 3314 (br, OH), 3194(br, NH), 1612(m, C=N), 1598, 1587 (m, C=C), 1245(m, C=S), 1178(s, C-O); ^{1}H NMR ($CDCl_3$,400 MHz, ppm): 1.03 (s, 9H, H_{14}, C($\underline{C}H_3)_3$), 1.38 (s,9H, H_{16}, C($\underline{C}H_3)_3$), 3.72 (s, 3H ,O$\underline{C}H_3$), 6.83 (s,1H, H_3), 6.94(d, 2H, *J*=8.56, H_{10}), 7.17(s,1H, H_5),7.22 (d, 2H, *J*=8.52, H_{11}), 9.17 (s, 1H, OH), 14.05(s, 1H, NH); ^{13}C NMR($CDCl_3$, 100 MHz, ppm): 29.21 (3C,C_{16}, 3(C($\underline{C}H_3)_3$), 31.27(3C, C_{14}, 3(C($\underline{C}H_3)_3$) , 34.21 (1C, C_{13}), 34.68(1C, C_{15}), 55.16(1C, O$\underline{C}H_3$), 112.80(1C, C_6), 114.48(2C, C_{11}), 125.15(1C, C_5), 125.67(1C, C_3) 127.75(1C, C_9), 129.96(1C, C_{10}), 136.66(1C, C_2), 140.51(1C, C_4), 150.10(1C, C_1), 152.53(1C, C_7), 159.77(1C, C_{12}), 168.50(1C, C_8). HREIMs, m/z =411.1987 [$M^{\cdot+}$] (cal. for $C_{23}H_{29}N_3O_2S$, 411.1980).

2,4-di-*tert*-butyl-6-(4-(4-chlorophenyl)-1,2,4-triazol-3-yl-5-thione)phenol

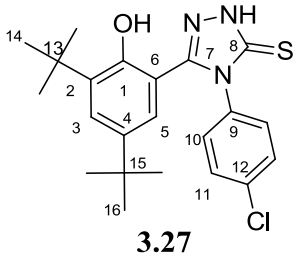

3.27

The solid product was purified by column chromatography using hexane-ethyl acetate (6-1) as eluent to give white precipitate. Yield 0.27 g (66%); m.p. 238-240 °C. IR (KBr, υ_{max}/ cm^{-1}), 3306 (br, OH & NH), 1610(m, C=N) 1594, 1585(s, C=C), 1213(m, C=S), 1170(s, C-O). ^{1}H NMR ($CDCl_3$, 400 MHz, ppm):1.07 (s, 9H, H14), 1.25 (s, 9H, H_{16}), 6.68 (d, 1H, *J*=2.5, H_3), 7.20 (d, *J*=2.5, H_5), 7.32(d, *J*=8.8, 2H, H_{10}), 7.74(d, *J*=8.8, 2H, H_{11}), 9.06 (bs, 1H, OH), 14.10(bs, 1H, NH); ^{13}C NMR($CDCl_3$, 100 MHz, ppm): 29.79(3C , C_{16}), 31.54 (3C, C_{14}), 39.62(1C, C_{13}), 39.83 (1C, C_{15}), 113.24 (1C, C_6) 125.72(1C, C_5), 125.98(1C, C_3), 129.31(2C, C_{11}), 130.74 (2C, C_{10}), 134.09(2C, C_9, C_{12}), 137.06(1C, C_2), 140.97(1C, C_4), 150.12(1C, C_7), 152.47(1C, C_1), 168.28 (1C, C_8, C=S). HREIMS m/z = 415.1488[$M^{\cdot+}$] (calc. for $C_{22}H_{26}ClN_3OS$, 413.2110).

2,4-di-*tert*-butyl-6-(4-(4-methylphenyl)-1,2,4-triazol-3-yl-5-thione)phenol.

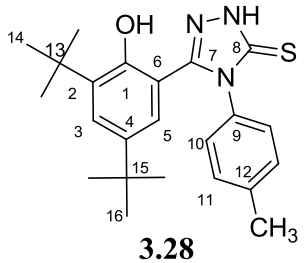

3.28

The solid product was recrystallized from ethanol: ethyl acetate (2:8) to obtain white precipitate. Yield 0.285 g (72%); m.p. 236-238 °C (dec.). IR (KBr, υ_{max}/ cm^{-1}): 3293 (br, OH), 3176(br, NH), 1607(m, C=N), 1595, 1585 (s, C=C), 1233(m, C=S), 1170(s, C-O); ^{1}H NMR ($CDCl_3$, 400 MHz, ppm): 1.02(s, 9H, H_{14}), 1.27 (s, 9H, H_{16}),

2.27(s, 3H, ph-CH_3), 6.80(d, 1H, *J*=2.44, H_3), 7.22-7.16(m, 5H, H_5, H_{10}, H_{11}), 9.18(s, 1H, NH), 14.07(1H, OH). ^{13}C NMR($CDCl_3$, 100 MHz, ppm): 21.18 (1C, ph-CH_3), 29.83(3C, C_{16}), 31.48 (3C, C_{14}), 34.20(1C, C_{13}), 35.29(1C, C_{15}), 112.97 (1C, C_6) 125.38(1C, C_5), 125.83(1C, C_3) , 128.67(2C, C_{11}), 129.84 (2C, C_{10}), 132.72 (1C, C_9), 136.80(1C, C_{12}), 139.04(1C, C_2), 140.65(1C, C_4), 150.133 (1C, C_7, C=N), 152.68(1C, C_1), 168.44(1C, C_8, C=S) , HREIMs m/z =395.2030[$M^{\cdot+}$] (calc. for $C_{23}H_{29}N_3OS$, 395.2031).

References

1. Lin, C. C., Huang, P C., Antioxidant and hepatoprotective effects of *Acathopanax senticosus*. *Phytother Res.* **2000,** *14* (7), 489-494.

2. Halliwell, B., Gutteridge, M C., *Free Radicals in Biology and Medicine*. Oxford: Clarendon Press: **1989**; Vol. 189, p 1-85.

3. Asmus, K.-D., Bonifacic, M., Free radical chemistry. In *Handbook of Oxidants and Antioxidants in Exercise*, Chandan K. Sen, P. D., FACSM, Ed. Elsevier Science B.V. : **2000**; p 52.

4. Mills, R., Wu, G Z., Synthesis and evaluation of novel prodrugs of foscarnet and dideoxycytidine with a universal carrier compound comprising a chemiluminescent and a photochromic conjugate. *J Pharm Sci.* **2004,** *93* (5), 1320-1336.

5. Rotilio, G., *Superoxide and superoxide dismutase in chemistry, biology and medicine*. Amsterdam: Elsevier: **1986**; p 688.

6. Shacter, E., Quantification And Significance Of Protein Oxidation In Biological Samples. *Drug Metabolism Reviews* **2000,** *32* (3-4), 307-326.

7. Chatterjee, R.; Bandyopadhyay, U., Mazumdar, A., Banerjee, R. K., Lactoperoxidase-catalysed oxidation of indomethacin, a nonsteroidal antiinflammatory drug, through the formation of a free radical. *Biochem Pharmacol.* **1996,** *52* (8), 1169-1175.

8. Sangeetha, P., Das, U. N., Koratkar, R., Suryaprabha, P., Increase in free radical generation and lipid peroxidation following chemotherapy in patients with cancer. *Free Radic Biol Med.* **1990,** *8* (1), 15-19.

9. Kar, S., Subbaram, S., Carrico, P M., Melendez, J A., Redox-control of matrix metalloproteinase-1: A critical link between free radicals, matrix remodeling and degenerative disease. *Respir Physiol Neurobiol.* **2010,** *174* (3), 299-306.

10. Khalil, Z., Khodr, B., A role for free radicals and nitric oxide in delayed recovery in aged rats with chronic constriction nerve injury. *Free Radic Biol Med.* **2001,** *31* (4), 430-439.

11. Lee, J., Koo, N., Min, D.B., Reactive Oxygen Species, Aging, and Antioxidative Nutraceuticals. *Comprehensive Reviews In Food Science And Food Safety* **2004,** *3* (1), 21-33.

12. Barclay, L. R. C., Vinqvist, M. R., Chapter 12:.Phenols as Antioxidants. In *The Chemistry of phenols part 2*, Rappoport, Z., Ed. John Wiley &Sons: **2003**, pp 840-902.

13. Minisci, F., *Free Radicals in Biology and Environment*. springer Netherlands: **1997**, Vol. 27, p 516.

14. Ostrea EM Jr., Cepeda, E. E., Fleury, CA., Balun, JE., Red Cell Membrane Lipid Peroxidation and Hemolysis Secondary to Phototherapy. *Acta Paediatrica* **1985,** *74* (3), 378-381.

15. Wright, J. S., Johnson, E. R., DiLabio, G. A., Predicting the Activity of Phenolic Antioxidants: Theoretical Method, Analysis of Substituent Effects, and Application to Major Families of Antioxidants. *J. Am. Chem. Soc.* **2001,** *123* (6), 1173-1183.

16. Pratt, D. E., Hudson, B. J. F., Natural antioxidants not exploited commercially. In *Applied Food Science Series*, Hudson, B. J. F., Ed. Elsevier: Amsterdam., **1990**, pp 171-192.

17. Nivas, D., Gaikwad, D. K., Chavan, P. D., Antiradical Activity Of Medicinally Important *Morinda Pubescens* Fruits. *Int J Pharm. Bio. Sci.* **2010,** *1* (3), 1-4.

18. Ghosal, S., Phenolic antioxidant-chromium complexes for treatment or prevention of type 2 diabetes or glucose intolerance. *United States Patent Application* **2003,** *20050085454*.

19. Weiguang Yi, Fischer, J, Krewer, G, Akoh, C. C., Phenolic Compounds from Blueberries Can Inhibit Colon Cancer Cell Proliferation and Induce Apoptosis. *J. Agric. Food Chem.* **2005,** *53* (18), 7320–7329.

20. Schroeder, H., Adams, M., The Effect Of Tyrosinase On Experimental Hypertension. *J Exp Med.* **1941,** *73* (4), 531-550.

21. Sandoval M, Okuhama NN, Zhang XJ, Condezo LA, Lao J, Angeles' FM, Musah RA, Bobrowski P, MJ., M., Anti-inflammatory and antioxidant activities of cat's claw (*Uncaria tomentosa* and *Uncaria guianensis*) are independent of their alkaloid content. *Phytomedicine.* **2002,** *9* (4), 325-37.

22. (a) Key, T., Allen, N., Spencer, E., Travis, R., The effect of diet on risk of cancer. *Lancet* **2002,** *360* (9336), 861-868, (b) Rimm, E., Stampfer, M., Ascherio, A., Giovannucci, E., Colditz, G., Willett, W., Vitamin E consumption and the risk of coronary heart disease in men. *N Engl J Med.* **1993,** *328* (20), 1450-1456, (c) Zhang, S., Hunter, D. J., Forman, M. R., Rosner, B. A., Speizer, F. E., Colditz, G. A., Manson, J. E., Hankinson, S., E., Willett, W. C., Dietary Carotenoids and Vitamins A, C, and E and Risk of Breast Cancer. *Journal of the National Cancer Institute*, **1999,** *91* (6), 547-556, (d) Dillard, C. J., German, J. B., Phytochemicals: nutraceuticals and human health. *J. Sci. Food Agric.* **2000,** *80* (12), 1744-1756.

23. Osawa, T., Phenolic Antioxidants in Dietary Plants as Antimutagens. In *Phenolic Compounds in Food and Their Effects on Health II*, ACS Symposium Series: **1992**, Vol. 507.chapter 11, pp 135-149.

24. Huxley, R., Ansary-Moghaddam, A., Clifton, P., Czernichow, S., Parr, C., Woodward, M., The impact of dietary and lifestyle risk factors on risk of colorectal cancer: a quantitative overview of the epidemiological evidence. *international journal of cancer* **2009,** *125* (1), 171-180.

25. Schrier, R. W., *Diseases of the Kidney and Urinary Tract*. lippincott William &wilkins: **2007**, Vol. II, p 3776.

26. Bravo, L., Polyphenols: chemistry, dietary sources, metabolism, and nutritional significance. *Nutrition Reviws* **1998,** *56* (11), 317-333.

27. Williams, R. J. P., Baughan, E. C., Willson, R. L., *The Necessary and the Desirable Production of Radicals in Biology [and Discussion]*. Philosophical Transactions of the Royal Society of London. Series B, Biological Sciences: **1985**, Vol. 311, p 593-603.

28. Gluck, M., Ehrhart, J., Jayatilleke, E., Zeevalk, G., Inhibition of brain mitochondrial respiration by dopamine: involvement of H_2O_2 and hydroxyl radicals but not glutathione-protein-mixed disulfides. *J Neurochem.* **2002,** *82* (1), 66-74.

29. Dimitrios, B., Sources of natural phenolic antioxidants. *Trends in Food Science & Technology* **2006,** *17* (9), 505-512.

30. Huang, D., Ou, B., Hampsch-Woodill, M., Flanagan, J., Deemer, E., Development and validation of oxygen radical absorbance capacity assay for lipophilic antioxidants using randomly methylated beta-cyclodextrin as the solubility enhancer. *J Agric Food Chem.* **2002,** *50* (7), 1815-1821.

31. Winterle, J., Dulin, D., Mill, T., Products of stoichiometry of reaction of vitamin E with alkylperoxy radicals. *J Org Chem.* **1984,** *49* (3), 491-495.

32. Shao, H.-B., Chu , L.-Y., Lu , Z.-H., Kan, C.-M., Primary antioxidant free radical scavenging and redox signaling pathways in higher plant cells. *Int J Biol Sci.* **2008,** *4* (1), 8-14

33. Kamal-Eldin, A., Appelqvist, L., The chemistry and antioxidant properties of tocopherols and tocotrienols. *Lipids.* **1996,** *31* (7), 671-701.

34. Bowry, V. W., Ingold, K. U., Extraordinary Kinetic Behavior of the .alpha.-Tocopheroxyl (Vitamin E) Radical. *J Org Chem.* **1995,** *60* (17), 5456-5467.

35. Littarru, G. P., Biomedical and clinical aspects of coenzyme Q. *Journal of Molecular Medicine* **1993,** *71* (8), 587-588.

36. Hilton, J. W., Antioxidants: function, types and necessity of inclusion in pet foods. *The Canadian Veterinary Journal* **1989,** *30* (8), 682-284.

37. Chattopadhyay, M. K., Adverse effects of antoxidants *Current Science* **2003,** *85* (2), 121.

38. Wu, C, Functional design of organic hybrids consisting of polarized polymers and hindered phenol. *J. Mater. Sci. Lett.* **2001,** *20* (15), 1389-1391.

39. Wu, C, Yamagishi, T.-A., Nakamoto, Y., Ishida, S.-I., Kubota, S., Nitta, K.-H., Organic hybrid of chlorinated polyethylene and hindered phenol. II. Influence of the chemical structure of small molecules on viscoelastic properties. *J. Polym. Sci. B Polym. Phys.* **2000,** *38* (11), 1496–1503.

40. Moore, G. G., Swingle, K. F., 2,6-Di-*tert*-butyl-4-(2'-thenoyl)phenol(R-830):a novel nonsteroidal anti-inflammatory agent with antioxidant properties. *Agents Actions.* **1982,** *12* (5-6), 674-683.

41. Katayama, K., Shirota, H., Kobayashi, S., Terato, K., Ikuta, H., Yamatsu, I., In vitro effect of N-methoxy-3-(3,5-di-*tert*-butyl-4-hydroxybenzylidene)-2-pyrrolidone (E-5110), a novel nonsteroidal antiinflammatory agent, on generation of some inflammatory mediators. *Agents Actions.* **1987,** *21* (3-4), :269-271.

42. Shirota, H., Chiba, K., Ono, H., Yamamoto, H., Kobayashi, S., Terato, K., Ikuta, H., Yamatsu, I., Katayama, K., Pharmacological properties of the novel non-steroidal antiinflammatory agent N-methoxy-3-(3,5-di-*tert*-butyl-4-hydroxybenzylidene) pyrrolidin-2 -one. *Arzneimittelforschung.* **1987,** *37* (8), 930-936.

43. Shirota, H., Katayama, K., Ono, H., Chiba, K., Kobayashi, S., Terato, K., Ikuta, H., Yamatsu, I., Pharmacological properties of N-methoxy-3-(3,5-di-*tert*-butyl-4-hydroxybenzylidene)-2-pyrrolidone (E-5110), a novel nonsteroidal antiinflammatory agent. *Agents Actions.* **1987,** *21* (3-4), 250-252.

44. Hidaka, T. Hosoe, K. Yamashita, T. Watanabe, K. Hiramatsu, Y. Fujimura, H., Analgesic and anti-inflammatory activities in rats of alpha-(3,5-di-*tert*-butyl-4-hydroxy benzylidene)- zgamma-butyrolactone (KME-4), and its intestinal damage. *J Pharm Pharmaco* **1986,** *38* (10), 748-753.

45. Hidaka, T. Hosoe, K. Yamashita, T. Watanabe, K. Hiramatsu, Y. Fujimura, H., Effect of alpha-(3,5-di-*tert*-butyl-4-hydroxybenzylidene)-gamma-butyrolactone (KME-4), a new anti-inflammatory drug, on the established adjuvant arthritis in rats. *Jpn J Pharmacol.* **1986,** *42* (2), 181-187.

46. Mullican, M. D., Wilson, M. W., Connor, D. T., Kostlan, C. R., Schrier, D. J., Dyer, R. D., Design of 5-(3,5-Di-*tert*-butyl-4-hydroxyphenyl)-l,3,4-thiadiazoles, -1,3,4-oxadiazoles, and -1,2,4-triazoles as Orally- Active, Nonulcerogenic Antiinflammatory Agents. *J. Med. Chem* **1993,** *36*, 1090-1099.

47. Lombardino, J. G., *Nonsteroidal antiinflammatory drugs*. Willey: New York, **1985** p442.

48. Ziakas, G. N., Rekka, E. A., Gavalas, A. M., Eleftheriou, P. T., Kourounakis, P. N., New analogues of butylated hydroxytoluene as anti-inflammatory and antioxidant agents. *Bioorg Med Chem.* **2006,** *14* (16), 5616-5624.

49. Chang, T. Y., Chang, C. C. Y., Cheng, D., Acyl-coenzyme A: Cholesterol acyltransferase. *Annu Rev Biochem.* **1997,** *66*, 613-638.

50. Lee, R. G., Willingham, M. C., Davis, M. A., Skinner, K. A., Rudel, L. L., Differential expression of ACAT1 and ACAT2 among cells within liver, intestine, kidney, and adrenal of nonhuman primates *J. Lipid Res* **2000,** *41* (12), 1991-2001.

51. Buhman, K. F., Accada, M., Farese Jr, R. V., Mammalian acyl-CoA:cholesterol acyltransferases. *Biochim Biophys Acta* **2000,** *1529* (1-3), 142-154.

52. (a) Jeong, T.-S., Kim, K. S., An, S.-J., Cho, K.-H., Lee, S., Lee, W. S., Novel 3,5-diaryl pyrazolines as human acyl-CoA:cholesterol acyltransferase inhibitors. *Bioorg Med Chem Lett.* **2004,** *14* (11), 2715-2717, (b) Jeong, T.-S., Kim, K. S., Kim, J.-R., Cho, K.-H., Lee, S., Lee, W. S., Novel 3,5-diaryl pyrazolines and pyrazole as low-density lipoprotein (LDL) oxidation inhibitor. *Bioorg Med Chem Lett.* **2004,** *14* (11), 2719-2723.

53. Pontiki, E., Hadjipavlou-Litina, D., Litinas, K., Nicolotti, O., Carotti, A., Design, synthesis and pharmacobiological evaluation of novel acrylic acid derivatives acting as lipoxygenase and cyclooxygenase-1 inhibitors with antioxidant and anti-inflammatory activities. *Eur J Med Chem.* **2011,** *46* (1), 191-200.

54. Duarte, C. D., Tributino, J. L. M., Lacerda, D. I., Martins, M. V., Alexandre-Moreira, M. S., Dutra, F., Bechara, E. J. H., De-Paula, F. S., Goulart, M. O. F., Ferreira, J., Calixto, J. B., Nunes, M. P., Bertho, A. L., Miranda, A. L. P., Barreiro, E. J., Fraga, C. A. M., Synthesis, pharmacological evaluation and electrochemical studies of novel 6-nitro-3,4-methylenedioxyphenyl-N-acylhydrazone derivatives: Discovery of LASSBio-881, a new ligand of cannabinoid receptors. *Bioorg Med Chem.* **2007,** *15* (6), 2421-2433.

55. Howlett, A. C., The cannabinoid receptors. *Prostaglandins Other Lipid Mediat.* **2002,** *68-69*, 619-31.

56. Marnett, L. J., Kalgutkar, A. S., Design of selective inhibitors of cyclooxygenase-2 as nonulcerogenic anti-inflammatory agents. *Current Opinion in Chemical Biology* **1998,** *2* (4), 482-490.

57. Noguchi, N., Niki, E., Phenolic antioxidants:: A rationale for design and evaluation of novel antioxidant drug for atherosclerosis. *Free Radic Biol Med.* **2000,** *28* (10), 1538-1546.

58. Unangst, P. C., Connor, D. T., Cetenko, W. A., Sorenson, R. J., Kostlan, C. R., Sircar, J. C., Wright, C. D., Schrier, D. J., Dyer, R. D., Synthesis and biological evaluation of 5-[[3,5-bis(1,1-dimethylethyl)-4-hydroxyphenyl]methylene]oxazoles, -thiazoles, and -imidazoles: novel dual 5-lipoxygenase and cyclooxygenase inhibitors with antiinflammatory activity. *J Med Chem.* **1994,** *37* (2), 322-328.

59. Wong S, Lee SJ, Frierson MR 3rd, Proch J, Miskowski TA, Rigby BS, Schmolka SJ, Naismith RW, Kreutzer DC, Lindquist, R., Antiarthritic profile of BF-389--a novel anti-inflammatory agent with low ulcerogenic liability. *Agents Actions.* **1992,** *37* (1-2), 90-98.

60. Bendele AM, Benslay DN, Hom JT, Spaethe SM, Ruterbories KJ, Lindstrom TD, Lee, S. J., Naismith, R., Anti-inflammatory activity of BF389, a Di-T-butylphenol, in animal models of arthritis. *J Pharmacol Exp Ther* **1992,** *260* (1), 300-305.

61. Ye, X., Zhou, W., Li, Y., Sun, Y., Zhang, Y., Ji, H., Lai, Y., Darbufelone, a novel anti-inflammatory drug, induces growth inhibition of lung cancer cells both in vitro and in vivo. *Cancer Chemotherapy and Pharmacology* **2010,** *66* (2), 277-285.

62. Kato, T., Ozaki, T., Tamura, K., Suzuki, Y., Akima, M., Ohi, N., Novel Calcium Antagonists with Both Calcium Overload Inhibition and Antioxidant Activity. 1.2-(3,5-Di-*tert*-butyl-4-hydroxyphenyl)-3-(aminopropyl)thiazolidinones. *J. Med. Chem.* **1998,** *41* (22), 4309-4316.

63. Pontiki, E., Hadjipavlou-Litina, D., Synthesis and pharmacochemical evaluation of novel aryl-acetic acid inhibitors of lipoxygenase, antioxidants, and anti-inflammatory agents. *Bioorg Med Chem.* **2007,** *15* (17), 5819-5827.

64. Belostotskaya, I. V., Vol'eva, V. B., Komissarova, N. L, Dekaprilevich, M. D, Khrustalev, A. N, Karmilov, A. YU, Ershov, V. V., Oxidation of 2-dialkylaminomethyl-4,6-di- *tert* -butylphenols. *Russian Chemical Bulletin* **1997,** *46* (7), 1328--1335.

65. Lodyato, V. I., Yurkova, I. L., Sorokin, V. L., Shadyro, O. I., Dolgopalets, V. I., Kisel, M. A., Synthesis and properties of 11-(3,5-Di-*tert*-butyl-2-hydroxyphenylcarbamoyl) undecanoic acid, a new amphiphilic antioxidant. *Bioorg Med Chem Lett.* **2003,** *13* (6), 1179-1182.

66. Lodyato, V. I., Yurkova, I. L., Sorokin, V. L., Shadyro, O. I., Dolgopalets, V. I., Kisel, M. A., Novel (3,5-di-*tert*-butyl-2-hydroxy-phenylcarbamoyl)-alkanoic acids as potent antioxidants. *Bioorg Med Chem Lett.* **2004,** *14* (16), 4253-4256.

67. Ju-Mi Jeong , S.-K. K., In-Hwa Lee, Ji-Yoon Lee, Hyuk Jung, and Cheol-Hee Choi, Antioxidant and Chemosensitizing Effects of Flavonoids with Hydroxy and/or Methoxy Groups and Structure-Activity Relationship. *J Pharm Pharmaceut Sci* **2007,** *10* (4), 537-546.

68. Edge, R., McGarvey, D. J., Truscott, T. G., The carotenoids as anti-oxidants - a review. *J Photoch Photobio B* **1997,** *41* (3), 189-200.

69. (a) Nagalakshmi, G., Synthesis, antimicrobial and antiinflammatory activity of 2,5-disubstituted-1,3,4-oxadiazoles. *Indian J Pharm Sci.* **2008,** *70* (1), 49-55, (b) Rajak, H., Kharya, M. D., Mishra, P., Synthesis of Some Novel Oxadiazole and Oxadiazoline Analogues for Their Antiinflammatory Activity. *Yakugaku zasshi journal of the Pharmaceutical Society of Japan* **2007,** *127* (10), 1757-1764.

70. (a) Jin L., Chen J., Song B., Chen Z., Yang S., Li Q., Hu D., Xu, R., Synthesis, structure, and bioactivity of N′-substituted benzylidene-3,4,5-trimethoxybenzohydrazide and 3-acetyl-2-substituted phenyl-5-(3,4,5-trimethoxyphenyl)-2,3-dihydro-1,3,4-oxadiazole derivatives. *Bioorg Med Chem Lett.* **2006,** *16* (19), 5036-5040. , (b) Tuma MC, Malikzay, A., Ouyang X, Surguladze D, Fleming J, Mitelman S, Camara M, Finnerty B, Doody J, Chekler EL, Kussie P, Tonra, J., Antitumor Activity of IMC-038525, a Novel Oral Tubulin Polymerization Inhibitor. *Translational Oncology* **2010,** *3* (5), 318-325.

71. Banday, M. R., Mattoo, R. H., Rauf., A., Synthesis, characterization and anti-bacterial activity of 5-(alkenyl)-2-amino- and 2-(alkenyl)-5-phenyl-1,3,4-oxadiazoles. *J. Chem. Sci., Indian Academy of Sciences* **2010,** *122* (2), 177–182.

72. Maslat, A. O., Abussaud, M., Tashtoush, H., AL-Talib, M., Synthesis, Antibacterial, Antifungal And Genotoxic Activity Of Bis-1,3,4-Oxadiazole Derivatives. *Polish Journal of Pharmacology* **2002,** *54*, 55-59.

73. Shah, H. P., Shah, B. R., Bhatt, J. J., Desai, N. C., Trivedi, P. B., Undavia, N. K., Synthesis of 2,5-Disubstituted 1,3,4-Oxadiazoles as Potential Antimicrobial, Anticancer and Anti-HIV Agents. *Indian J. Chem* **1998,** *37* (B), 180-182.

74. Maheshwari, R., Chawla, P., Saraf, S., Comparison between antioxidant activity of 2,5-disubstituted 1,3,4-oxadiazoles containing heteroaromatic ring and aromatic ring at 2nd position. *Medicinal Chemistry Research* **2010,** (3), 1-6.

75. Kerimov, I., Ayhan-Kılcıgil, G., Özdamar, E. D., Can-Eke, B., Çoban, T., Özbey, S., Kazak, C., Design and one-pot and microwave-assisted synthesis of 2-amino/5-aryl-1,3,4-oxadiazoles bearing a benzimidazole moiety as antioxidants. *Arch. Pharm. Chem. Life Sci* **2012,** *345* (7), 349–356.

76. Hanif, M., Shoaib, K., Saleem, M., Hasan, R. N., Zaib, S., Iqbal, J., Synthesis, urease inhibition, antioxidant, antibacterial, and molecular docking studies of 1,3,4-oxadiazole derivatives. *ISRN Pharmacology* **2012,** *2012*, 928901.

77. Padmaja, A., Rajasekhar, C., Muralikrishna, A., Padmavathi, V., Synthesis and antioxidant activity of disubstituted 1,3,4-oxadiazoles, 1,3,4- thiadiazoles and 1,2,4-triazoles. *J. Chem. Pharm. Res.* **2012,** *4* (1), 294-302.

78. Rai, G., Kenyon, V., Jadhav, A., Schultz, L., Armstrong, M., Jameson, J. B., Hoobler, E., Leister, W., Simeonov, A., Holman, T. R., Maloney, D. J., Discovery of Potent and Selective Inhibitors of Human Reticulocyte 15-Lipoxygenase-1. *J Med Chem.* **2010,** *53* (20), 7392-7404.

79. Vittal, S., Poojary, B., Bansal, P., Nandagokula, C., Tangavelu, A., Shenoy, S., Synthesis, characterization and antioxidant activity of some 1,3,4-oxadiazoles carrying 4-(methylsulfonyl)benzyl moiety *Der Pharma Chemica* **2011,** *3* (6), 138-146.

80. (a) Shaban, M. A. E., Nasr, A. Z., El-Badry, S. M., Synthesis And Biological Activities Of Some 1,3,4-Oxadiazoles And Bis (1,3,4-Oxadiazoles). *Journal of Islamic Academy of Sciences* **1991,** *4* (3), 184-191, (b) Musad, E. A., Mohamed, R., Ali Saeed, B., Vishwanath, B. S., Lokanatha Rai, K. M., Synthesis and evaluation of antioxidant and antibacterial activities of new substituted bis(1,3,4-oxadiazoles), 3,5-bis(substituted) pyrazoles and isoxazoles. *Bioorg Med Chem Lett.* **2011,** *21* (12), 3536-3540.

81. (a) Wang, X.-L., Li, J., Lin, H.-Y., Hu, H.-L., Chen, B.-K., Mu, B., Synthesis, structures and electrochemical properties of two novel metal-organic coordination complexes based on trimesic acid (H3BTC) and 2,5-bis(3-pyridyl)-1,3,4-oxadiazole (BPO). *Solid State Sciences* **2009,** *11* (12), 2118-2124, (b) Chen, Y., Huang, C.-F., Aromatic polyethers containing distyrylbenzene and 1,3,4-oxadiazole chromophores: synthesis and electrochemical properties. *Synthetic Metals* **2001,** *125* (3), 379-387.

82. Kim, J. H., Synthesis and electro-optical properties of poly(p-phenylenevinylene) derivative with conjugated 1,3,4-oxadiazole pendant and its AC electroluminescence. *Synthetic Metals* **2008,** *158* (21-24), 1028-1036.

83. Huda, M. K., Dolui, S. K., Luminescence property of poly(1,3-bis(phenyl-1,3,4-oxadiazole))s containing polar groups in the main chain. *Journal of Luminescence* **2010,** *130* (11), 2242-2246.

84. (a) Allen, L. B., Boswell, K. H., Khwaja, T. A., Meyer, R. B., Sidwell, R. W., Witkowski, J. T., Christensen, L. F., Robins, R. K., Synthesis and antiviral activity of some phosphates of the broad-spectrum antiviral nucleoside, 1-.*beta*.-D-ribofuranosyl-1,2,4-triazole-3-carboxamide (ribavirin). *J Med Chem.* **1978,** *21* (8), 742-746, (b) Montagu, A. l., Roy, V., Balzarini, J., Snoeck, R., Andrei, G., Agrofoglio, L. A., Synthesis of new C5-(1-substituted-1,2,3-triazol-4 or 5-yl)-2'-deoxyuridines and their antiviral evaluation. *Eur J Med Chem.* **2011,** *46* (2), 778-786.

85. Marino, J. P., Fisher, P. W., Hofmann, G. A., Kirkpatrick, R. B., Janson, C. A., Johnson, R. K., Ma, C., Mattern, M., Meek, T. D., Ryan, M. D., Schulz, C., Smith, W. W., Tew, D. G., Tomazek, T. A., Veber, D. F., Xiong, W. C., Yamamoto, Y., Yamashita, K., Yang, G., Thompson, S. K., Highly Potent Inhibitors of Methionine Aminopeptidase-2 Based on a 1,2,4-Triazole Pharmacophore. *J Med Chem.* **2007,** *50* (16), 3777-3785.

86. Wilkinson, B. L., Bornaghi, L. F., Houston, T. A., Innocenti, A., Vullo, D., Supuran, C. T., Poulsen, S.-A., Carbonic Anhydrase Inhibitors: Inhibition of Isozymes I, II, and IX with Triazole-Linked O-Glycosides of Benzene Sulfonamides. *J Med Chem.* **2007,** *50* (7), 1651-1657.

87. Xia, Y., Liu, Y., Wan, J., Wang, M., Rocchi, P., Qu, F., Iovanna, J. L., Peng, L., Novel Triazole Ribonucleoside Down-Regulates Heat Shock Protein 27 and Induces Potent Anticancer Activity on Drug-Resistant Pancreatic Cancer. *J Med Chem.* **2009,** *52* (19), 6083-6096.

88. Abdel-Megeed, A. M., Abdel-Rahman, H. M., Alkaramany, G.-E. S., El-Gendy, M. A., Design, synthesis and molecular modeling study of acylated 1,2,4-triazole-3-acetates with potential anti-inflammatory activity. *Eur J Med Chem.* **2009,** *44* (1), 117-123.

89. De La Rosa, M., Kim, H. W., Gunic, E., Jenket, C., Boyle, U., Koh, Y.-h., Korboukh, I., Allan, M., Zhang, W., Chen, H., Xu, W., Nilar, S., Yao, N., Hamatake, R., Lang, S. A., Hong, Z., Zhang, Z., Girardet, J.-L., Tri-substituted triazoles as potent non-nucleoside inhibitors of the HIV-1 reverse transcriptase. *Bioorg Med Chem Lett.* **2006,** *16* (17), 4444-4449.

90. Wang, X.-L., Wan, K., Zhou, C.-H., Synthesis of novel sulfanilamide-derived 1,2,3-triazoles and their evaluation for antibacterial and antifungal activities. *Eur J Med Chem.* **2010,** *45* (10), 4631-4639.

91. Hussein, M. A., Shaker, R. M., Ameen, M. A., Mohammed, M. F., Synthesis, anti-inflammatory, analgesic, and antibacterial activities of some triazole, triazolothiadiazole, and triazolothiadiazine derivatives. *Archives of Pharmacal Research* **2011,** *43* (8), 1239-1250.

92. Khan, I., Ali, S., Hameed, S., Rama, N. H., Hussain, M. T., Wadood, A., Uddin, R., Ul-Haq, Z., Khan, A., Ali, S., Choudhary, M. I., Synthesis, antioxidant activities and urease inhibition of some new 1,2,4-triazole and 1,3,4-thiadiazole derivatives. *Eur J Med Chem.* **2010,** *45* (11), 5200-5207.

93. El-Naggar, S. A., El-Barbary, A. A., Mansour, M. A., Abdel-Shafy, F., Talat, S., Anti-tumor Activity of Some 1,3,4-thiadiazoles and 1,2,4-triazine Derivatives against Ehrlichs Ascites Carcinoma. *International Journal of Cancer Research* **2011,** *7* (4), 278-288.

94. Schenone, S., Brullo, C., Bruno, O., Bondavalli, F., Ranise, A., Filippelli, W., Rinaldi, B., Capuano, A., Falcone, G., New 1,3,4-thiadiazole derivatives endowed with analgesic and anti-inflammatory activities. *Bioorg Med Chem.* **2006,** *14* (6), 1698–1705.

95. Thomasco, L. M., Gadwood, R. C., Weaver, E. A., Ochoada, J. M., Ford, C. W., Zurenko, G. E., Hamel, J. C., Stapert, D., Moerman, J. K., Schaadt, R. D., Yagi, B. H., The synthesis and antibacterial activity of 1,3,4-Thiadiazole phenyl oxazolidinone analogues. *Bioorg Med Chem Lett.* **2003,** *13* (23), 4193–4196.

96. Camoutsis C, G. A., Ciric A, Soković M, Zoumpoulakis P, Zervou M., Sulfonamide-1,2,4-thiadiazole derivatives as antifungal and antibacterial agents: synthesis, biological evaluation, lipophilicity, and conformational studies. *Chem Pharm Bull (Tokyo).* **2010,** *58* (2), 160-167.

97. Yusuf, M., Khan, R. A., Ahmed, B., Syntheses and anti-depressant activity of 5-amino-1, 3, 4-thiadiazole-2-thiol imines and thiobenzyl derivatives. *Bioorg Med Chem.* **2008,** *16* (17), 8029-8034.

98. Cressier, D., Prouillac, C., Hernandez, P., Amourette, C., Diserbo, M., Lion, C., Rima, G., Synthesis, antioxidant properties and radioprotective effects of new benzothiazoles and thiadiazoles. *Bioorg. Med. Chem.* **2009,** *17* (14), 5275-5284.

99. Yehye, W. A., Abdul Rahman, N., Alhadi, A A., Khaledi, H. , Seik Weng Ng and Ariffin, A. , Butylated Hydroxytoluene Analogs: Synthesis and Evaluation of Their Multipotent Antioxidant Activities. *Molecules* **2012,** *17* (7), 17077645.

100. Gökçe, M., Utku, S., Küpeli, E., Synthesis and analgesic and anti-inflammatory activities 6-substituted-3(2H)-pyridazinone-2-acetyl-2-(p-substituted/nonsubstituted benzal)hydrazone derivatives. *Eur J Med Chem.* **2009,** *44* (9), 3760-3764.

101. Sondhi, S. M., Dinodia, M., Kumar, A., Synthesis, anti-inflammatory and analgesic activity evaluation of some amidine and hydrazone derivatives. *Bioorg Med Chem.* **2006,** *14* (13), 4657-4663.

102. Angelusiu, M. V., Barbuceanu, S.-F., Draghici, C., Almajan, G. L., New Cu(II), Co(II), Ni(II) complexes with aroyl-hydrazone based ligand. Synthesis, spectroscopic characterization and in vitro antibacterial evaluation. *Eur J Med Chem.* **2010,** *45* (5), 2055-2062.

103. Terzioglu, N., Gürsoy, A., Synthesis and anticancer evaluation of some new hydrazone derivatives of 2,6-dimethylimidazo[2,1-b][1,3,4]thiadiazole-5-carbohydrazide. *Eur J Med Chem.* **2003,** *38* (7-8), 781-786.

104. Wang, Q., Yang, Z.-Y., Qi, G.-F., Qin, D.-D., Synthesis, crystal structure, antioxidant activities and DNA-binding studies of the Ln(III) complexes with 7-methoxychromone-3-carbaldehyde-(4'-hydroxy) benzoyl hydrazone. *Eur J Med Chem.* **2009,** *44* (6), 2425-2433.

105. Hruskova, K., Kovarikova, P., Bendova, P., Haskova, P., Mackova, E., Stariat, J., Vavrova, A., Vavrova, K., Simunek, T., Synthesis and Initial in Vitro Evaluations of Novel Antioxidant Aroylhydrazone Iron Chelators with Increased Stability against Plasma Hydrolysis. *Chem. Res. Toxicol.* **2011,** *24* (3), 290-302.

106. (a) Müller, E., Ludsteck, D., Untersuchungen an Diazomethanen, V. Mitteil.1): Reaktives Verhalten von Diazomethyllithium. *Chemische Berichte* **1955,** *88* (7), 921–933, (b) Ainsworth, C., The Condensation of Aryl Carboxylic Acid Hydrazides with Orthoesters. *J. Am. Chem. Soc* **1955,** *77* (5), 1148–1150.

107. Ainsworth, C., Hackler, R. E., Alkyl-1,3,4-oxadiazoles. *J Org Chem.* **1966,** *31* (10), 3442-3444.

108. Tandon, V., K., Chhor, R. B., An Efficient One Pot Synthesis of 1,3,4-Oxadiazoles. *Synthetic Communications* **2001,** *31* (11), 1727–1732.

109. Bentiss, F., Lagrene´e , M., Barbry, D., Rapid Synthesis of 2,5-Disubstituted1,3,4-Oxadiazoles Under Microwave Irradiation. *Synthetic Communications* **2001,** *31* (6), 935–938.

110. Mashraqui, S. H., Ghadigaonkar, S. G., Kenny, R. S., An Expeditious and Convenient One Pot Synthesis of 2,5-Disubstituted-1,3,4-oxadiazoles. *Synthetic Communications* **2003,** *33* (14), 2541–2545.

111. Shang, Z., Oxidative Cyclization of Aromatic Aldehyde N-Acylhydrazones by bis(Trifluoroacetoxy)iodobenzene. *Synthetic Communications* **2006,** *36*, 2927–2937.

112. Dabiri, M., Salehi, P., Baghbanzadeh, M., Zolfigol, M. A., Bahramnejad, M., Silica Sulfuric Acid: An Efficient and Versatile Acidic Catalyst for the Rapid and Ecofriendly Synthesis of 1,3,4-Oxadiazoles at Ambient Temperature. *Synthetic Communications* **2007,** *37*, 1201–1209.

113. Pardeshi, S. P., Patil, S. S., Bobade, V. D., N-Chlorosuccinimide/1,8-Diazabicyclo[5.4.0]Undec-7-Ene (Dbu)–Mediated Synthesis of 2,5-Disubstituted 1,3,4-Oxadiazoles. *Synthetic Communications* **2010,** *40*, 1601–1606.

114. Kidwai, M., Bhatnagar, D., Mishra, N. K., Polyethylene glycol (PEG) mediated green synthesis of 2,5-disubstituted 1,3,4-oxadiazoles catalyzed by ceric ammonium nitrat (CAN). *Green Chemistry Letters and Reviews* **2010,** *3* (1), 55 59.

115. Mohammed, I. A., Chloramine-T mediated synthesis of 1,3,4-Oxadiazole as antibacterial agents. *Der Pharmacia Sinica* **2011,** *2* (6), 102-106.

116. Rostamizadeh, S., Ghamkhar, S., A mild and facile method for one pot synthesis of 2,5-di-substituted 1,3,4-oxadiazoles at room temperature. *Chinese Chem Lett.* **2008,** *19* (6), 639-642.

117. Rostamizadeh, S., Housaini, S. A. G., Microwave assisted syntheses of 2,5-disubstituted 1,3,4-oxadiazoles. *Tetrahedron Letters* **2004,** *45* (47), 8753-8756.

118. (a) Amr, A. E.-G. E., Mohamed, S. F., Abdel-Hafez, N. A., Abdalla, M. M., Antianexiety activity of pyridine derivatives synthesized from 2-chloro-6-hydrazino-isonicotinic acid hydrazide. *Monatshefte für Chemie* **2008,** *139* (12), 1491-1498, (b) Shaban MA, Iskander, M., El-Badry, S., Synthesis of acyclo-C-nucleosides: 2-(alditol-1-yl)-5-methylthio- and -5-benzylthio-1,3,4-thiadiazoles. *Pharmazie* **1997,** *52* (5), 350-357, (c) Shawali, A. S., Gomha, S. M., Regioselectivity in 1,5-electrocyclization of N-[as-triazin-3-yl]nitrilimines.Synthesis of s-triazolo[4,3-b]-as-triazin-7(8H)-ones. *Tetrahedron* **2002,** *58*, 8559–8564, (d) Taha, M. A. M., El-Badry, S. M., Synthesis of 1,3,4-Oxadiazole Acyclo C-Nucleosides Bearing 5-Methylthio{7-substituted-1,2,4-triazolo[1,5-d]tetrazol-6-yl}moieties. *Jnl Chinese Chemical Soc.* **2006,** *53*, 1181-1188.

119. (a) Akhter, M., Husain, A., Azad, B., Ajmal, M., Aroylpropionic acid based 2,5-disubstituted-1,3,4-oxadiazoles: Synthesis and their anti-inflammatory and analgesic activities. *Eur J Med Chem.* **2009,** *44* (6), 2372-2378, (b) Pattan, S. R., Rabara, P. A., Pattan, J. S., Bukitagar, A. A., Wakale, V. S., Musmade, D. S., Synthesis and evaluation of some novel substituted 1,3,4-oxadiazole and pyrazole derivatives for antitubercular activity. *IJC-B* **2009,** *48* (B), 1453-1456.

120. Hung, C.-Y., Yen, G.-C., Antioxidant Activity of Phenolic Compounds Isolated from Mesona procumbens Hemsl. *J. Agric. Food Chem.* **2002,** *50* (10), 2993-2997.

121. Nonhebel, D. C., Walton, J. C., *Free-radical chemistry, structure and mechanism*. cambridge university press: cambridge, **1974**, p 477.

122. Selverstein, R., Webster, F., *Spectromeetric Identification Of Organic Compounds*. Jon Wiley & Sons Inc. : New York, **1998**, p 90-91.

123. Delen, Z., Xie, C., Hill, P. J., Choi, J., Lahti, P. M., Hindered Hydrogen Bonding in 2,6-Di-tert-butylphenols with Para Aza-Heterocyclic Rings. *Crystal Growth & Design* **2005,** *5* (5), 1867-1873.

124. Litwinienko, G., Megiel, E., Wojnicz, M., Hydrogen Bonding between Phenols and Fatty Acid Esters: 1H NMR Study and ab Initio Calculations*Organic Letters* **2002,** *4* (14), 2425-2428.

125. Breitmaier, E., *Structure Elucidatio by Nmr In Organic Chemistry A Practical Guide*. John Wiley & Sons, Ltd: **2002**, p 271.

126. (a) Frański, R., Eitner, K., Schroeder, G., Mass Spectrometric Study of Some Protonated and Lithiated 2,5-Disubstituted-1,3,4-Oxadiazoles. *J Am Soc Mass Spectrom* **2003,** *14* (4), 289–294, (b) Frański, R., Schroeder, G., Rybachenko, V., Szwajka, O. P., Loss of *iso*cyanic acid from the internal oxadiazole ring of protonated molecules of some 2,5-diaryl-1,3,4-oxadiazoles. *Rapid Commun. Mass Spectrom.* **2002,** *16* (5), 390–395, (c) Frański, R., Gierczyk, B., Schroeder, G., Mass spectrometric fragmentation

pathways of isotope labeled 2,5-disubstituted-1,3,4-oxadiazoles and thiadiazoles. *Int J Mass Spectrom.* **2004,** *231* (1), 47-49.

127. Raied M. Shakir, Azhar Ariffin, Mahmood Ameen Abdulla, Synthesis of New 2,5-Di-substituted 1,3,4-Oxadiazoles Bearing 2,6-Di-tert-butylphenol Moieties and Evaluation of Their Antioxidant Activity. *Molecules* **2014,** *19* (3), 3436-3449.

128. (a) Hayes, F. N., Rogers, B. S., Ott, D. G., 2,5-Diaryloxazoles and 2,5-Diaryl-1,3,4-oxadiazoles. *J. Am. Chem. Soc.* **1955,** *77* (7), 1850-1852, (b) Nesynov, E. P., Grekov, A. P., The Chemistry of 1,3,4-Oxadiazole Derivatives. *Russian Chemical Reviews* **1964,** *33* (10), 508-514.

129. Levin, Y. A., Skorobogatova, M. S., The closure mechanism of the 1,3,4-oxadiazole ring by means of phosphorus oxychloride. *Chemistry of Heterocyclic Compounds* **1969,** *5* (1), 142-142.

130. Venkatapuram Padmavathi, G. S. R., Annaji Venkata Nagendra Mohan, and Konda Mahesh, Synthesis of symmetrical and unsymmetrical 1,3,4-oxadiazoles and their interconversion to 1,3,4-thiadiazoles and 1,2,4-triazoles. *Arkivoc* **2008,** *xvii*, 48-60.

131. (a) March, J., Smith, M. B., *March's advanced organic chemistry: reactions, mechanisms, and structure*. 6th ed., John willy &sons.Inc.: **2007**, p 2384, (b) McMurry, J., *Organic Chemistry: With Biological Applications*. Brooks/Cole, Cengage Learning ed., Mary Finch: 2007, p 1044.

132. Ahluwalia, V. K., Aggarwal, R., *Comprehensive Practical Organic Chemistry: Preparations And Quantitative Analysis*. universities press (India): **2004**.

133. Sarker, S. D., Nahar, L., *Chemistry for pharmacy students: general, organic and natural product chemistry*. Jone Wiley: **2007**, p 383.

134. Bentiss, F., Lagrenée, M., A new synthesis of symmetrical 2,5-disubstituted 1,3,4-oxadiazoles. *Journal of Heterocyclic Chemistry* **1999,** *36* (4), 1029–1032,.

135. Effenberger, F., Konig, G., Klenkc, H., Mixed Carboxylic-Dichlorophosphoric Anhydrides-Reactive Intermediates in Acyl Chloride Synthesis with $POCl_3$. *Angew. Chem. Int . Ed. Engl.* **1978,** *17* (9), 695-696.

136. smith, j. g., Alkyl Halides & Nucleophilic Substitution. In *Organic Chemistry* second edition ed., Mc,Graw Hill: **2007**, pp 230-279.

137. (a) Saunders RD, Dugan, L., Demediuk P, Means ED, Horrocks LA, Anderson, D., Effects of methylprednisolone and the combination of alpha-tocopherol and selenium on arachidonic acid metabolism and lipid peroxidation in traumatized spinal cord tissue. *J Neurochem* **1987,** *49* (1), 24-31, (b) Marcinik, G., Petty, M. A., Design and biological

evaluation of new antioxidants for use in cerebrovascular disorder. *Drugs of the Future* **1996,** *21* (10), 1037.

138. Özyürek, M., Güngör, N., Baki, S., Güçlü, K., Apak, R., Development of a Silver Nanoparticle-Based Method for the Antioxidant Capacity Measurement of Polyphenols. *Anal. Chem.* **2012,** *84* (18), 8052-8059.

139. Rosenwald, R. H., Hoatson, J. R., Chenicek, J. A., Alkyl Phenols as Antioxidants. *Ind. Eng. Chem.* **1950,** *42* (1), 162-165.

140. Bakhshandeh, G. R., Khorasani, M. T., Preparation and Activity of Sterically Hindered Phenol Antioxidants for NR and SBR. *Iranian Journal of Polymer Scince &Technology* **1992,** *1* (2), 62-68.

141. Indroisena, W. M., Barrow, C. J., oxidation and stability of food-grade fish oil:Role of antioxidants In *Handbook of Seafood Quality, Safety and Health Applications*, cesarettin Alasalvar, F. S., Kazuo Miyashita, Udaya Wanasundara, Ed. John Wiley & Sons: **2010**, pp 317-335.

142. (a) Bailey, J., Synthesis of 1H-pyrazolo[3,2-c]-s-triazoles and derived azamethine dyes. *J. Chem. Soc., Perkin Trans. 1* **1977**, 2047-2052, (b) Csunderlik, C., Bercean, V., Peter, F., Badea, V., Facile bromination of the benzene ring during the cyclisation of the 1H-3-methyl-4-ethoxycarbonyl-5-arylidenehydrazonopyrazoles to the 3-substituted-aryl-1H-6-methyl-7-ethoxycarbonyl--pyrazolo[3,2-c]-s-triazoles. .*Arkivoc* **2002,** *ii*, 133-141

143. (a) Cyrański, M. K., Schleyer, P. v. R., Krygowski, T. M., Jiao, H., Hohlneicher, G., Facts and artifacts about aromatic stability estimation. *Tetrahedron* **2003,** *59* (10), 1657-1665, (b) Ramaprasad, G. C., Kalluraya, B., Kumar, B. S., Hunnur, R. K., Synthesis and biological property of some novel 1,3,4-oxadiazoles. *Eur J Med Chem.* **2010,** *45* (10), 4587-4593.

144. (a) Enchev, V., Angelova, S., Ab initio study of the tautomerism of 2,5-substituted diazoles. *Structural Chemistry* **2010,** *21* (5), 1053-1060, (b) Shtefan, E. D., Vvedenskii, V. Y., The tautomerism of heterocyclic thiols. Five-membered heterocycles. *Russian Chemical Reviews* **1996,** *65* (4), 307 - 314.

145. (a) Balci, M., Spin Systems: Analysis of the 1H-NMR Spectra. In *Basic 1H- and 13C-NMR Spectroscopy*, Elsevier Science: Amsterdam, **2005**, pp 159-197, (b) Sohàr, P., *Nuclear Magnetic Resonance Spectroscopy*. Boca Raton: : **1983**., Vol. 2.

146. Chattaway, F. D., Walker, A. J., Compounds Formed by the Action of Bromine on Benzaldehydephenylhydrazone. *J. Chenz. Soc.* **1925,** *127*, 975-984.

147. (a) Gibson, M. S., Hydrazones—IV: The bromination of benzylidene 2-pyridylhydrazone. *Tetrahedron* **1963,** *19* (11), 1587-1589, (b) Tobin, J. C., Hegarty, A. F., Scott, F. L., The mechanism of bromination of heterocyclic hydrazones. syn-anti-

Isomerisation of 5-(arymethylenehydrazino)-1- and -2-benzyltetrazoles. *J. Chem. Soc. B* **1971**, 2198-2202.

148. Ainsworth, C., The Condensation of Carboxylic Acid Hydrazides with Carbon Disulfide. *J. Am. Chem. Soc.* **1956,** *78* (17), 4475-4478.

149. Young, R. W., Wood, K. H., The Cyclization of 3-Acyldithiocarbazate Esters1. *J. Am. Chem. Soc.* **1955,** *77* (2), 400-403.

150. Gross, E., Witkop, B., Nonenzymatic Cleavage of Peptide Bonds: The Methionine Residues in Bovine Pancreatic Ribonuclease. *J Biol Chem.* **1962,** *237* (6), 1856-1869.

151. Shaw, J. T., Adams, R., Synthesis of Some N-Cyano and N,N'-Dicyanobenzamidines Using Cyanogen Bromide. *J. Chem. Eng. Data* **1968,** *13* (1), 142-143.

152. Vinod, K., Cyanogen Bromide (CNBr). *SYNLETT* **2005,** *10* (1), 1638–163917.

153. Arnold, R. T., Campos, M. d. M., Lindsay, K. L., Participation of a Neighboring Carboxyl Group in Addition Reactions. I. The Mechanism of the Reaction of Bromine with γ,δ-Unsaturated Acids and Esters1. *J. Am. Chem. Soc.* **1953,** *75* (5), 1044-1047.

154. Parfitt, R. T., The reaction of tetralones and their enamines with cyanogen halides: a new synthesis of 2-naphthylamines. *J Chem Soc C* **1967,** (0), 140-142.

155. Kandeel, Z. E.-S., Abdelrazek, F. M., Salah Eldin, N. E. M., Elnagdi, M. H., Activated Nitriles in Heterocyclic Synthesis: Reaction of Cyanogen Bromide with some Functionally Substituted Enamines. *J. Chem. Soc. Perkin, trans. I* **1985**, 1499-1501.

156. Dewick, P. M., *Essentials of Organic Chemistry: For Students of Pharmacy, Medicinal Chemistry and Biological Chemistry*. wiley: **2006**.

157. (a) Singh, R. J., Antibactericidal Effect of Some Substituted-1, 2, 4-Triazole Derivatives. *J.Chem.Soc.Pak.* **2011,** *33* (4), 485-489, (b) Foroughifar, N., Mobinikhaledi, A., Ebrahimi, S., Fard, M. A. B., Moghanian, H., A Simple and Efficient Procedure for Synthesis of Optically Active 1,2,4-Triazolo-[3,4-b]-1,3,4-thiadiazole Derivatives Containing L-Amino Acid Moieties. *Jnl Chinese Chemical Soc.* **2009,** *56* (5), 1043-1047.

158. Cretu, O. D., Barbuceanu, S. F., Saramet, G., Draghici, C., Synthesis and characterization of some 1,2,4-triazole-3-thiones obtained from intramolecular cyclization of new 1-(4-(4-X-phenylsulfonyl) benzoyl)-4-(4-iodophenyl)-3-thiosemicarbazides. *J. Serb. Chem. Soc.* **2010,** *75* (11), 1463-1471.

159. Akkz, C., Tekeli, Y., Dogan, H. H., In vitro Antioxidant Activity of Enteromorpha intestinalis (Linnaeus) Nees. *Asian J. Chem.* **2009,** *21* (8), 6525 - 6528

160. Hertog, M. G. L., Kromhout, D., Aravanis, C., Blackburn, H., Buzina, R., Fidanza, F., Giampaoli, S., Jansen, A., Menotti, A., Nedeljkovic, S., Pekkarinen, M., Simic, B. S., Toshima, H., Feskens, E. J. M., Hollman, P. C. H., Katan, M. B., Flavonoid Intake and Long-term Risk of Coronary Heart Disease and Cancer in the Seven Countries Study. *Arch Intern Med.* **1995,** *155* (4), 381-386. .

161. Middleton Jr, E., Kandaswami, C., Effects of flavonoids on immune and inflammatory cell functions. *Biochemical Pharmacology* **1992,** *43* (6), 1167-1179.

162. Aruoma, O. I., Nutrition and health aspects of free radicals and antioxidants. *Food Chem Toxicol* **1994,** *32* (7), 671-683.

163. Javanmardi, J., Stushnoff, C., Locke, E., Vivanco, J. M., Antioxidant activity and total phenolic content of Iranian Ocimum accessions. *Food Chemistry* **2003,** *83*, 547–550.

164. Harman, D., Free radical theory of aging: Effect of free radical reaction inhibitors on the mortality rate of male LAF1 mice. *Journal of Gerontology* **1968,** *23* (4), 476-482.

165. Donaldson, T., a guide to anti aging drugs. In *chapter 2, Antioxidants As Drugs Against Aging*, Donaldson, T., Ed. Periastron: usa, **1994**.

166. Deichmann WB, Rakoczy, R., Toxicity and mechanism of action of systox. *AMA Arch. Ind. Health* **1955,** *11* (4), 324-331. .

167. Wasson, J. I., Smith, W. M., Effect of Alkyl Substitution on Antioxidant Properties of Phenols. *Ind. Eng. Chem.* **1953,** *45* (1), 197-200.

168. Burton, G. W., Doba, T., Gabe, E., Hughes, L., Lee, F. L., Prasad, L., Ingold, K. U., Autoxidation of biological molecules. 4. Maximizing the antioxidant activity of phenols. *J. Am. Chem. Soc.* **1985,** *107* (24), 7053-7065.

169. Barclay, L. R. C., Baskin, K. A., Dakin, K. A., Locke, S. J., Vinqvist, M. R., The antioxidant activities of phenolic antioxidants in free radical peroxidation of phospholipid membranes. *Can. J. Chem.* **1990,** *68* (12), 2258-2269.

170. Ohshima, H., *Electrical Phenomena at Interfaces and Biointerfaces: Fundamentals and Applications in Nano-, Bio-, and Environmental Sciences*. John Wiley & son Inc.: **2012**.

171. (a) Klein, E., Lukeš, V., DFT/B3LYP study of O–H bond dissociation enthalpies of para and meta substituted phenols: Correlation with the phenolic C–O bond length. *Journal of Molecular Structure: THEOCHEM* **2006,** *767* (1–3), 43-50, (b) Najafi, M., Mood, K. H., Zahedi, M., Klein, E., DFT/B3LYP study of the substituent effect on the reaction enthalpies of the individual steps of single electron transfer–proton transfer and sequential proton loss electron transfer mechanisms of chroman derivatives antioxidant action. *Computational and Theoretical Chemistry* **2011,** *969* (1–3), 1-12, (c) Najafi, M., Nazarparvar, E., Mood, K. H., Zahedi, M., Klein, E., DFT/B3LYP study of the

substituent effects on OH bond dissociation enthalpies of chroman derivatives in the gas phase and solvent environment. *Computational and Theoretical Chemistry* **2011,** *965* (1), 114-122.

172. Jovanovic, S. V., Tosic, M., Simic, M. G., Use of the Hammett correlation and .delta.+ for calculation of one-electron redox potentials of antioxidants. *The Journal of Physical Chemistry* **1991,** *95* (26), 10824-10827.

173. Wayner, D. D. M., Lusztyk, E., Ingold, K. U., Mulder, P., Application of Photoacoustic Calorimetry to the Measurement of the O-H Bond Strength in Vitamin E (α- and δ-Tocopherol) and Related Phenolic Antioxidants1. *J Org Chem.* **1996,** *61* (18), 6430-6433.

174. (a) Brigati, G., Lucarini, M., Mugnaini, V., Pedulli, G. F., Determination of the Substituent Effect on the O-H Bond Dissociation Enthalpies of Phenolic Antioxidants by the EPR Radical Equilibration Technique. *J Org Chem.* **2002,** *67* (14), 4828-4832, (b) Lucarini, M., Pedulli, G. F., Cipollone, M., Bond Dissociation Enthalpy of .alpha.-Tocopherol and Other Phenolic Antioxidants. *J Org Chem.* **1994,** *59* (17), 5063-5070, (c) Lucarini, M., Pedrielli, P., Pedulli, G. F., Cabiddu, S., Fattuoni, C., Bond Dissociation Energies of O-H Bonds in Substituted Phenols from Equilibration Studies. *J Org Chem.* **1996,** *61* (26), 9259-9263.

175. Burton, G. W., Ingold, K. U., Autoxidation of biological molecules. 1. Antioxidant activity of vitamin E and related chain-breaking phenolic antioxidants in vitro. *J. Am. Chem. Soc.* **1981,** *103* (21), 6472-6477.

176. Kajiyama, T., Ohkatsu, Y., Effect of para-substituents of phenolic antioxidants. *Polymer Degradation and Stability* **2001,** *71* (3), 445-452.

177. Lawandy, S. N., Shehata, A. B., Younan, A. F., Acrylamides as Phenolic Antioxidants for Acrylqnitrile-Butadiene Rubber Compounds. *Polymer-Plastics Technology and Engineering* **1996,** *35* (6), 813-825.

178. Amorati, R., Fumo, M. G., Menichetti, S., Mugnaini, V., Pedulli, G. F., Electronic and Hydrogen Bonding Effects on the Chain-Breaking Activity of Sulfur-Containing Phenolic Antioxidants. *J Org Chem.* **2006,** *71* (17), 6325-6332.

179. Barclay, L. R. C., Xi, F., Norris, J. Q., Antioxidant Properties of Phenolic Lignin Model Compounds. *Journal of Wood Chemistry and Technology* **1997,** *17* (1-2), 73-90.

180. de Heer, M. I., Korth, H.-G., Mulder, P., Poly Methoxy Phenols in Solution: O-H Bond Dissociation Enthalpies, Structures, and Hydrogen Bonding. *J Org Chem.* **1999,** *64* (19), 6969-6975.

181. de Heer, M. I., Mulder, P., Korth, H.-G., Ingold, K. U., Lusztyk, J., Hydrogen Atom Abstraction Kinetics from Intramolecularly Hydrogen Bonded Ubiquinol-0 and Other (Poly)methoxy Phenols. *J. Am. Chem. Soc.* **2000,** *122* (10), 2355-2360.

182. Foti, M., Ruberto, G., Kinetic Solvent Effects on Phenolic Antioxidants Determined by Spectrophotometric Measurements. *J Agric Food Chem.* **2000,** *49* (1), 342-348.

183. Kajiyama, T., Ohkatsu, Y., Effect of meta-substituents of phenolic antioxidants-proposal of secondary substituent effect. *Polymer Degradation and Stability* **2002,** *75* (3), 535-542.

184. (a) Das, P. K., Encinas, M. V., Steenken, S., Scaiano, J. C., Reaction of *tert*-butoxy radicals with phenols. Comparison with the reactions of carbonyl triplets. *J. Am. Chem. Soc.* **1981,** *103* (14), 4162-4166, (b) Snelgrove, D. W., Lusztyk, J., Banks, J. T., Mulder, P., Ingold, K. U., Kinetic Solvent Effects on Hydrogen-Atom Abstractions: Reliable, Quantitative Predictions via a Single Empirical Equation1. *J. Am. Chem. Soc.* **2000,** *123* (3), 469-477.

185. Litwinienko, G., Ingold, K. U., Solvent Effects on the Rates and Mechanisms of Reaction of Phenols with Free Radicals. *Accounts of Chemical Research* **2007,** *40* (3), 222-230.

186. Avila, D. V., Brown, C. E., Ingold, K. U., Lusztyk, J., Solvent effects on the competitive .beta.-scission and hydrogen atom abstraction reactions of the cumyloxyl radical. Resolution of a long-standing problem. *J. Am. Chem. Soc.* **1993,** *115* (2), 466-470.

187. Lucarini, M., Pedulli, G. F., Valgimigli, L., Do Peroxyl Radicals Obey the Principle That Kinetic Solvent Effects on H-Atom Abstraction Are Independent of the Nature of the Abstracting Radical? *J Org Chem.* **1998,** *63* (13), 4497-4499.

188. Valgimigli, L., Ingold, K. U., Lusztyk, J., Solvent Effects on the Reactivity and Free Spin Distribution of 2,2-Diphenyl-1-picrylhydrazyl Radicals. *J Org Chem.* **1996,** *61* (22), 7947-7950.

189. Koner, A. L., Pischel, U., Nau, W. M., Kinetic Solvent Effects on Hydrogen Abstraction Reactions. *Organic Letters* **2007,** *9* (15), 2899-2902.

190. (a) Serce, S., Özgen, M., Torun, A. A., Ercişli , S., Chemical composition, antioxidant activities and total phenolic content of Arbutus andrachne L. (Fam. Ericaceae) (the Greek strawberry tree) fruits from Turkey. *J Food Compos Anal.* **2010,** *23* (6), 619-623, (b) Zhenbao, J., Fei, T., Ling, G., Guanjun, T., Xiaolin, D., Antioxidant properties of extracts from juemingzi (Cassia tora L.) evaluated in vitro. *LWT - Food Science and Technology* **2007,** *40* (6), 1072-1077, (c) Laus, M. N., Tozzi, D., Soccio, M., Fratianni, A., Panfili, G., Pastore, D., Dissection of antioxidant activity of durum wheat (Triticum durum Desf.) grains as evaluated by the new LOX/RNO method. *Journal of Cereal Science* **2012,** *56* (2), 214-222.

191. Turrens, J. F., Topical Review, Mitochondrial formation of reactive oxygen species. *J. Physiology* **2003,** *552* (2), 335–344.

192. Huang, D., Ou, B., Prior, R. L., The Chemistry behind Antioxidant Capacity Assays. *J Agric Food Chem.* **2005,** *53* (6), 1841-1856.

193. Jayaprakasha, G. K., Girennavar, B., Patil, B. S., Antioxidant capacity of pummelo and navel oranges: Extraction efficiency of solvents in sequence. *LWT - Food Science and Technology* **2008,** *41* (3), 376-384.

194. Braude , E. A., Brook, A. G., Linstead, R. P., Hydrogen transfer. Part V. Dehydrogenation reactions with diphenylpicrylhydrazyl. *J. Chem. Soc* **1954**, 3574-3578.

195. Blois, M. S., Antioxidant Determinations by the Use of a Stable Free Radical. *Nature* **1958,** *181*, 1199 - 1200.

196. Sánchez-Moreno, C., Larrauri, J. A., Saura-Calixto, F., A procedure to measure the antiradical efficiency of polyphenols. *J. Sci. Food Agric.* **1998,** *76* (2), 270–276.

197. (a) Bondet, V., Brand-Williams, W., Berset, C., Kinetics and Mechanisms of Antioxidant Activity using the DPPH.Free Radical Method. *LWT - Food Science and Technology* **1997,** *30* (6), 609-615, (b) Brand-Williams, W., Cuvelier, M. E., Berset, C., Use of a free radical method to evaluate antioxidant activity. *LWT - Food Science and Technology* **1995,** *28* (1), 25-30, (c) Silva FA, Borges F, Guimarães C, Lima JL, Matos C, S., R., Phenolic acids and derivatives: studies on the relationship among structure, radical scavenging activity, and physicochemical parameters. *J Agric Food Chem.* **2000,** *48* (6), 2122-2126.

198. Schaich, K. M., Developing A Rational Basis For Selection Of Antioxidant Screening And Testing Methods. *Acta Hort* **2006,** *709*, 79-94.

199. Cano A, Acosta M, MB., A., A method to measure antioxidant activity in organic media: application to lipophilic vitamins. *Redox Report* **2000,** *5* (6), 365-370.

200. (a) Jord'n, M. J., Lax, V., Rota, M. C., Lorán, S., Sotomayor, J. A., Relevance of Carnosic Acid, Carnosol, and Rosmarinic Acid Concentrations in the in Vitro Antioxidant and Antimicrobial Activities of Rosmarinus officinalis (L.) Methanolic Extracts. *J Agric Food Chem.* **2012,** *60* (38), 9603-9608, (b) Tsantili, E., Konstantinidis, K., Christopoulos, M. V., Roussos, P. A., Total phenolics and flavonoids and total antioxidant capacity in pistachio (Pistachia vera L.) nuts in relation to cultivars and storage conditions. *Scientia Horticulturae* **2011,** *129* (4), 694-701, (c) Hussain, H. H., Babic, G., Durst, T., Wright, J. S., Flueraru, M., Chichirau, A., Chepelev, L. L., Development of Novel Antioxidants: Design, Synthesis, and Reactivity. *J Org Chem.* **2003,** *68* (18), 7023-7032.

201. (a) Foti, M. C., Daquino, C., DiLabio, G. A., Ingold, K. U., Kinetics of the Oxidation of Quercetin by 2,2-Diphenyl-1-picrylhydrazyl (dpph$^{\cdot}$). *Organic Letters* **2011,** *13* (18), 4826-4829, (b) Ordoudi, S. A., Tsimidou, M. Z., Vafiadis, A. P., Bakalbassis, E. G., Structure-DPPH$^{\cdot}$ Scavenging Activity Relationships: Parallel Study of Catechol and Guaiacol Acid Derivatives. *J Agric Food Chem.* **2006,** *54* (16), 5763-5768, (c)

Litwinienko, G., Ingold, K. U., Abnormal Solvent Effects on Hydrogen Atom Abstraction. 3. Novel Kinetics in Sequential Proton Loss Electron Transfer Chemistry. *J Org Chem.* **2005,** *70* (22), 8982-8990.

202. Puoci, F., Iemma, F., Curcio, M., Parisi, O. I., Cirillo, G., Spizzirri, U. G., Picci, N., Synthesis of Methacrylic-Ferulic Acid Copolymer with Antioxidant Properties by Single-Step Free Radical Polymerization. *J Agric Food Chem.* **2008,** *56* (22), 10646-10650.

203. Benzie, I. F., Strain, J. J., The Ferric Reducing Ability of Plasma (FRAP) as a Measure of ‘‘Antioxidant Power’’: The FRAP Assay. *Analytical Biochemistry* **1996,** *239*, 70–76.

204. Fındık, E., Mustafa Ceylan, Elmastaş, M., Isoeugenol-based novel potent antioxidants: Synthesis and reactivity. *Eur J Med Chem.* **2011,** *46* (9), 4618-4624.

205. Craft, B. D., Kerrihard, A. L., Amarowicz, R., Pegg, R. B., Phenol-Based Antioxidants and the In Vitro Methods Used for Their Assessment. *Comprehensive Reviews in Food Science and Food Safety* **2012,** *11* (2), 148–173.

206. Prior RL, Wu X, Schaich, K., Standardized methods for the determination of antioxidant capacity and phenolics in foods and dietary supplements. *J Agric Food Chem.* **2005,** *53* (10), 4290-4302.

207. Celik S.E, Ozyürek M, Güçlü K, Apak, R., Solvent effects on the antioxidant capacity of lipophilic and hydrophilic antioxidants measured by CUPRAC, ABTS/persulphate and FRAP methods. *Talanta* **2010,** *81* (4-5), 1300-1309.

208. Rustaiyan, A., Javidnia, K., Farjam, M H., Aboee-Mehrizi, F., Ezzatzadeh, E., Antimicrobial and antioxidant activity of the Ephedra sarcocarpa growing in Iran. *J Med Plants Res.* **2011,** *5* (17), 4251-4255.

209. (a) Shahidi, F., *Natural Antioxidants: Chemistry, Health Effects, and Applications*. ACOS,: USA 1997, p p:18, (b) Simić, A., Manojlović, D., Šegan, D., Todorović, M., Electrochemical Behavior and Antioxidant and Prooxidant Activity of Natural Phenolics. *Molecules* **2007,** *12*, 2327-2340, (c) Moalin, M., Strijdonck, G. P. F., Beckers, M., Hagemen, G. J., Borm, P. J., Bast, A., Haenen, G. R. M. M., A Planar Conformation and the Hydroxyl Groups in the B and C Rings Play a Pivotal Role in the Antioxidant Capacity of Quercetin and Quercetin Derivatives. *Molecules* **2011,** *16* (11), 9636-9650, (d) Torres, R., Urbina, F., Morales, C., Modak, B., Monache, F D., Antioxidant Properties Of Lignans And Ferulic Acid From The Resinous Exudate Of Larrea Nitida *J. Chil. Chem. Soc.* **2003,** *48* (3), 0717-9324.

210. Gaspar A, Martins M, Silva P, Garrido EM, Garrido J, Firuzi O, Miri R, Saso L, F., B., Dietary Phenolic Acids and Derivatives. Evaluation of the Antioxidant Activity of Sinapic Acid and Its Alkyl Esters. *J. Agric. Food Chem.* **2010,** *58* (21), 11273–11280.

211. Sergedien, E., Jönsson, K., Szymusiak, H., Tyrakowska, B., Rietjens, I. M. C. M., Čenas, N., Prooxidant toxicity of polyphenolic antioxidants to HL-60 cells: description of quantitative structure-activity relationships. *FEBS letters* **1999,** *462* (3), 392-396.

212. Velkov, Z., Balabanova, E., Tadjer, A., Radical scavenging activity prediction of o-coumaric acid thioamide. *Journal of Molecular Structure: THEOCHEM* **2007,** *821* (1-3), 133-138.

213. Ozdem S, Alicigüzel Y, Ozdem, S. S., Karayalçin, U., Effects of propylthiouracil treatment on antioxidant activities in blood of toxic multinodular goiter patients. *Pharmacology* **2000,** *61* (1), 31-36.

214. (a) Varatharajan, K., Cheralathan, M., Effect of aromatic amine antioxidants on NOx emissions from a soybean biodiesel powered DI diesel engine. *Fuel Processing Technology* **2013,** *106*, 526-532, (b) Nishiyama, T., Suzuki, T., Hashiguchi, Y., Shiotsu, S., Fujioka, M., Antioxidant activity of aromatic cyclic amine derivatives. *Polym. Degrad. Stab.* **2002,** *75* (3), 549-554.

215. (a) Hicks M, Wong LS, Day, R., Antioxidant activity of propylthiouracil. *Biochem Pharmacol.* **1992,** *43* (3), 439-444, (b) Reid, L. C., Effect of thiourea and thyroxine on oxygen uptake of tissue homogenates. *Arch. Exper. Path.U. Pharmakol.* **1953,** *219* (5), 467-468, (c) Lewis CP, Dinsdale D, B., N., Potentiation of oxidant-induced toxicity in hamster lung slices by dimethylthiourea. *Free Radic Biol Med.* **1994,** *16* (5), 561-569, (d) Nakao K, Kubota H, Yasuhara M, Saito K, Suzuki T, Ohmizu H, R., S., Novel hydroxyphenylurea dual inhibitor against acyl-CoA: cholesterol acyltransferase (ACAT) and low density lipoprotein (LDL) oxidation as antiatherosclerotic agent. *Bioorg Med Chem* **2001,** *9* (4), 853-861.

216. Salih, N., Salimon, J., Hameed, A., Yousif, E., Synthesis, characterization and antimicrobial evaluation of some 1,3,4-oxadiazole derivatives. *International Journal of PharmTech Research* **2011,** *3* (2), 1097-1102.

217. Vogel, A. I., Tatchell, A. R., Furnis, B. S., Hannaford, A. J., Smith, P. W. G., *Vogel 's Textbook of practical organic chemistry*. 5 th ed., Longman Scientific and Tacnical: Essex England: **1989** p841.

218. Toda , F., Hyoda , S., Okada, K., Hirotsu, K., Isolation of anhydrous hydrazine as stable inclusion complexes with hydroquinone and p-methoxyphenol, and their solid state reaction with esters which gives pure hydrazides. *J. Chem. Soc., Chem. Commun.* **1995,** *15*, 1531-1532.

219. Qian, X., Zhang, R., Syntheses and Insecticidal Activities of Novel 2,5Disubstituted-1,3,4-0xadiazoles. *J . Chem. Tech. Biotechnol.* **1996,** *67*, 124-130.

220. Fox, H. H., Giras, J. T., synthetic Tuberculostats. iv. Pyridine Carboxylic Acid Hydrazides and Benzoic Acid Hydrazides. *J. Org. Chem.* **1952,** *17* (12), 1653–1660.

221. 3,4-Dichlorobenzene-1-carbohydrazide .http://www.chemexper.com/search/cas/28036911.html (accessed 2012).

222. 3,5-dichlorobenzene-1-carbohydrazide. http://www.chemexper.com/search/cas/62899789.html.

223. 2,4-dimethylbenzohydrazide. http://www.chemspider.com/Chemical-Structure.4031636.html?rid=a58b5b26-fe35-4d1d-8d9a-a2c36ed85d4f.

224. Kaushik, D., Khan, S. A., Chawla, G., Design & synthesis of 2-(substituted aryloxy)-5-(substituted benzylidene)-3-phenyl-2,5-dihydro-1H-[1,2,4] triazin-6-one as potentialantico nvulsant agents. *Eur J Med Chem.* **2010,** *45*, 3960-3969.

225. Acierno, D., Concilio, S., Diodati, A., Iannelli, P., Piotto, S. P., Scarfato, P., Synthesis and liquid crystalline properties of low molecularmass compounds containing the1,4-bis(5-phenyl-1,3,4-oxadiazolyl)benzene unit. *Liquid Crystals*, **2002,** *29* (11), 1383-1392.

226. Vadavi, R. S., Shenoy, R. V., Badiger, D. S., Gudasi, K. B., Devi, L. G., Nethaji, M., Crystal structure of nonadentate tricompartmental ligand derived from pyridine-2,6-dicarboxylic acid: Spectroscopic, electrochemical and thermal investigations of its transition metal(II) complexes. *Spectrochimica Acta Part A* **2011,** *79*, 348-355.

227. Yoneno, M., Bito, T., Iizuka, S., Namba, K., Nitro Compound having two function group.II *Kogyo Kagaku Zasshi* **1969,** *69* (3), 457-460.

228. Mei, Q., Yang, J., Peng, Y., Zhao, Z., Synthesis and characterisation of novel 1,3-bis{(6-aryl-1,2,4-triazolo [3,4-b][1,3,4]thiadiazol-3-yl)-methoxy}benzenes under microwave irradiation. *Journal of Chemical Research* **2011,** *35* (7), 368-389.

229. Narang, K. K., Pandey, J. P., Singh, V. P., Synthesis, characterization and physicochemical studies of some Copper(II) tetrathiocyanato dithallate(I) complexes with hydrazides and hydrazones. *Polyhedron* **1994,** *13* (4), 529-538.

Appendix A NMR

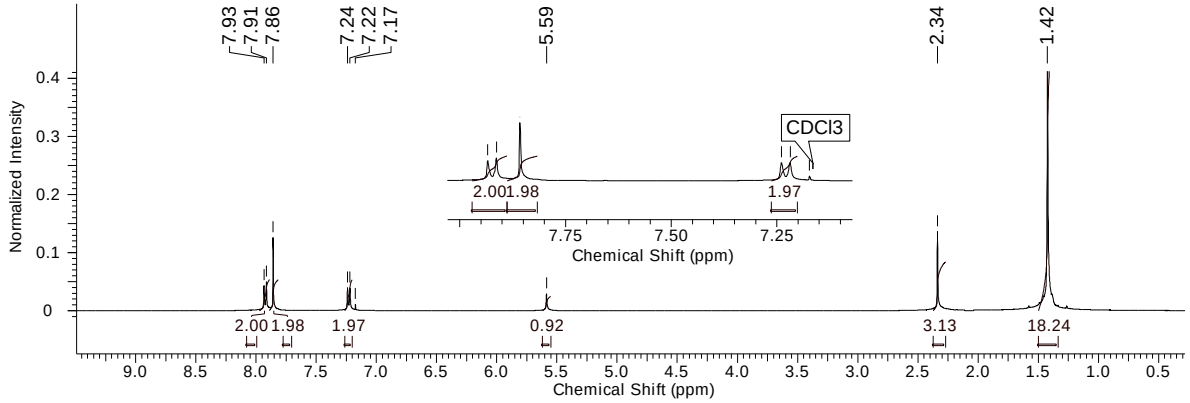

Figure A- 1 : ^{1}H NMR (400 MHz, $CDCl_3$) of compound **2.12**

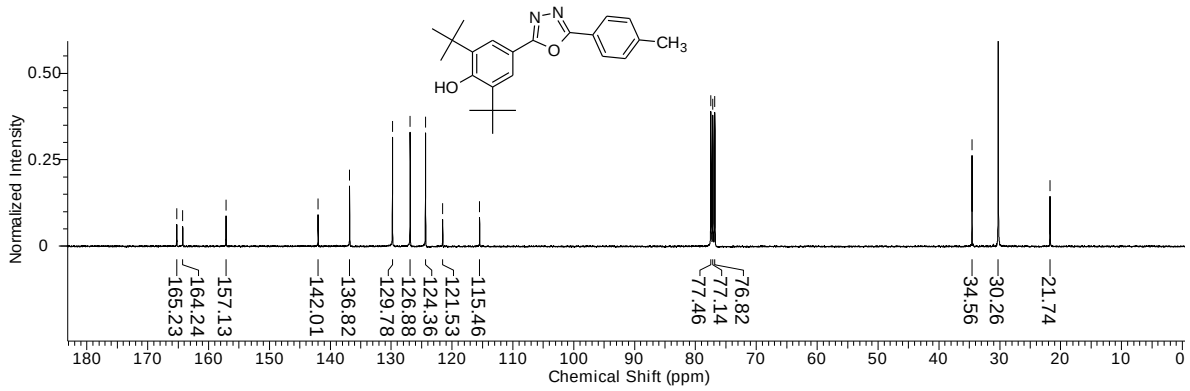

Figure A- 2 : ^{13}C NMR (100 MHz, $CDCl_3$) of compound **2.12**

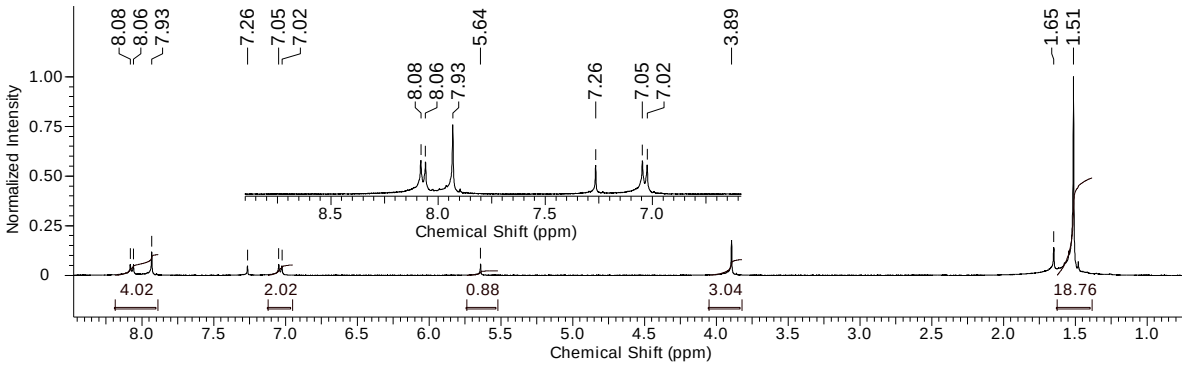

Figure A- 3 : ^{1}H NMR (400 MHz, $CDCl_3$) of compound **2.13**

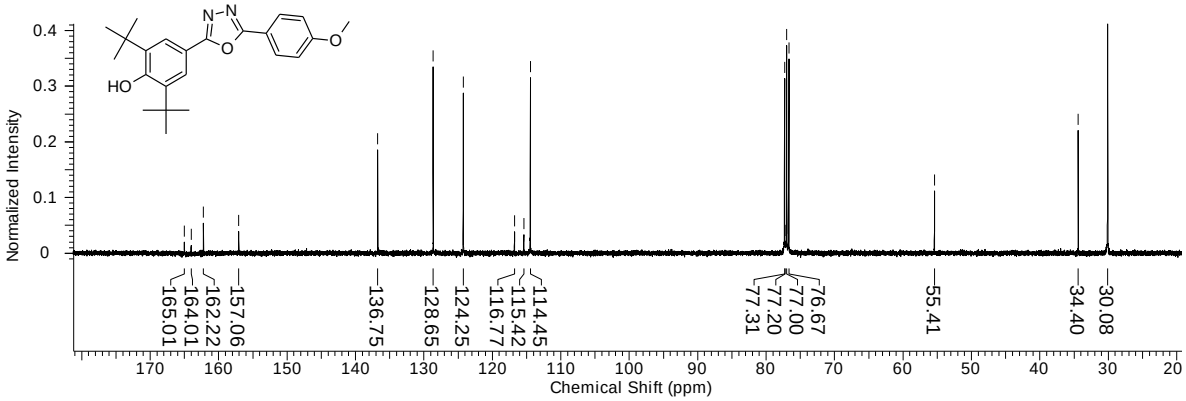

Figure A- 4 : ^{13}C NMR (100 MHz, $CDCl_3$) of compound **2.13**

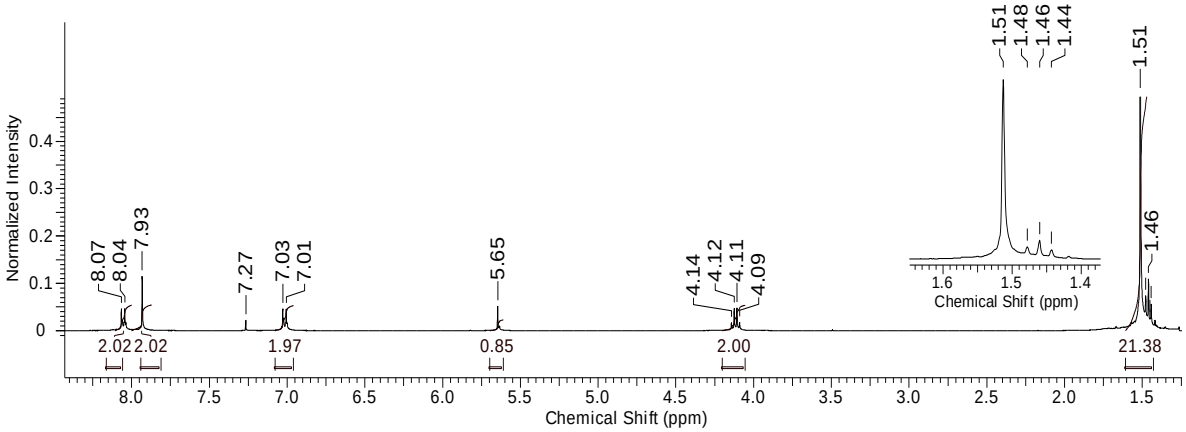

Figure A- 5 :^{1}H NMR (400 MHz, $CDCl_3$) of compound **2.14**

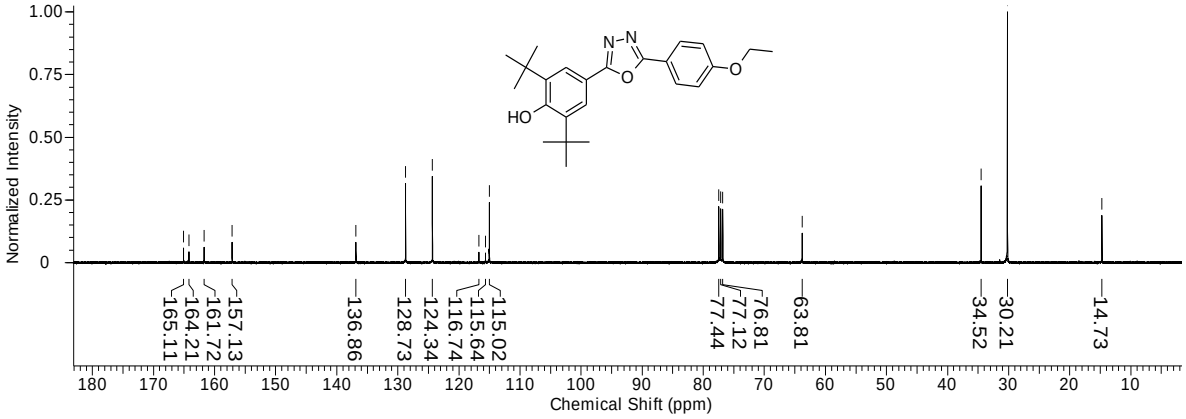

Figure A- 6 : ^{13}C NMR (100 MHz, $CDCl_3$) of compound **2.14**

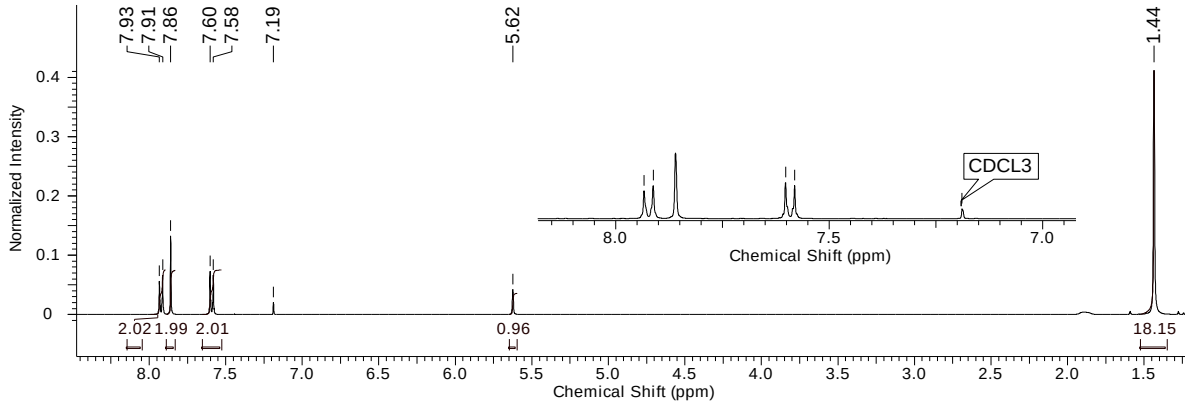

Figure A- 7 : ^{1}H NMR (400 MHz, $CDCl_3$) of compound **2.15**

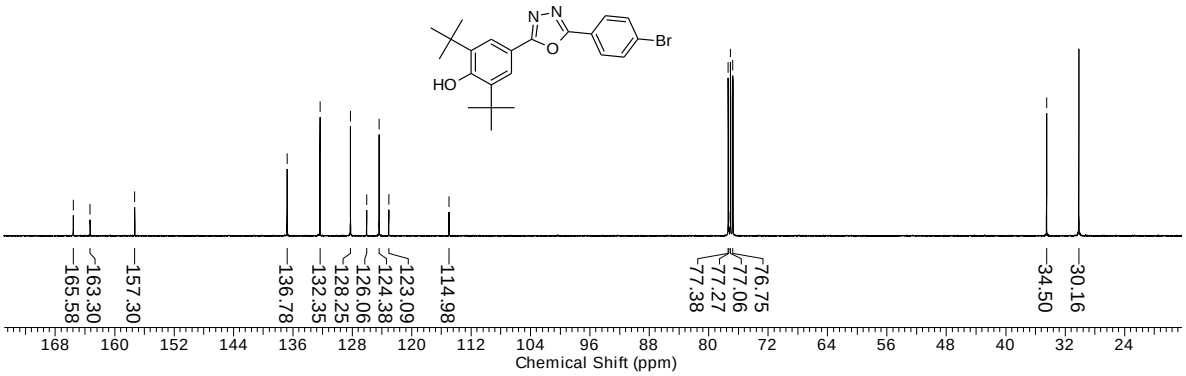

Figure A- 8 : ^{13}C NMR (100 MHz, CDCl3) of compound **2.15**

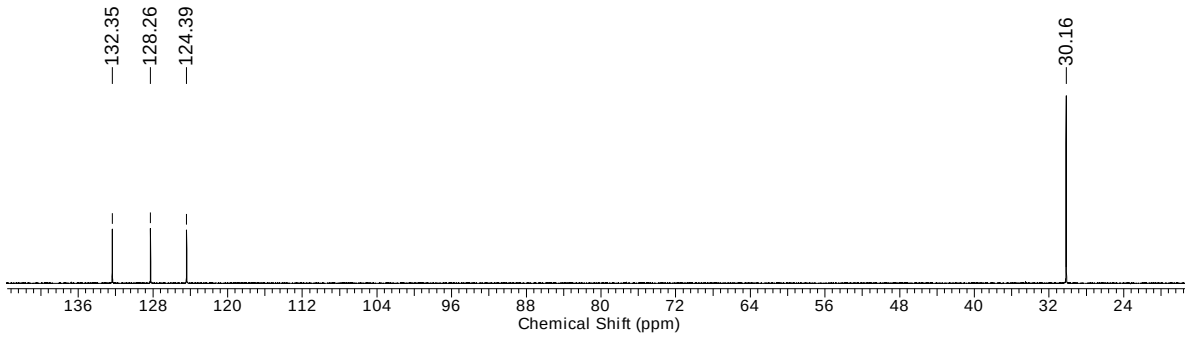

Figure A- 9 : DEPT-135 of compound **2.15**

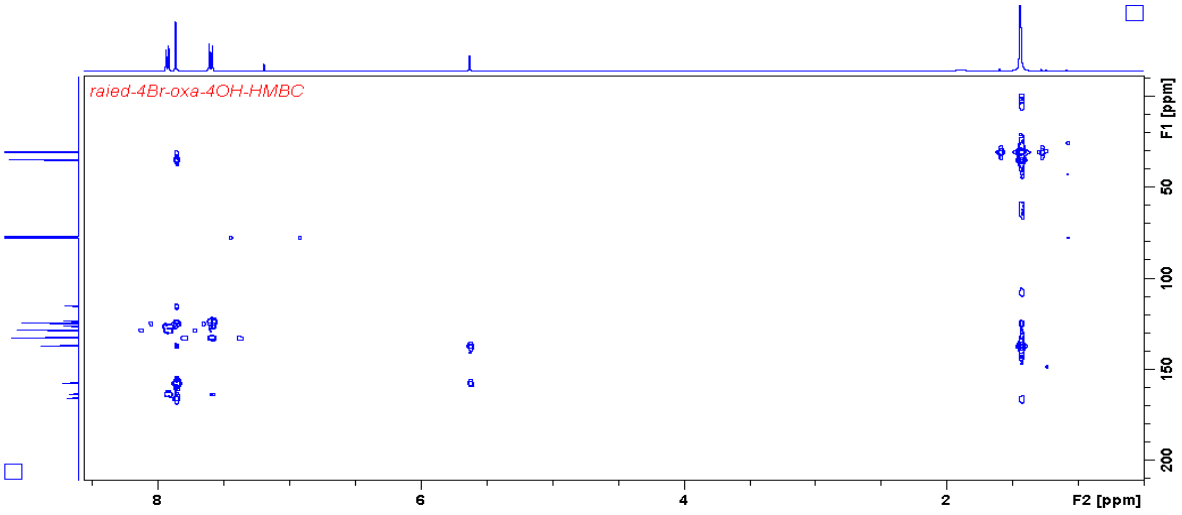

Figure A- 10 : HMBC of compound **2.15**

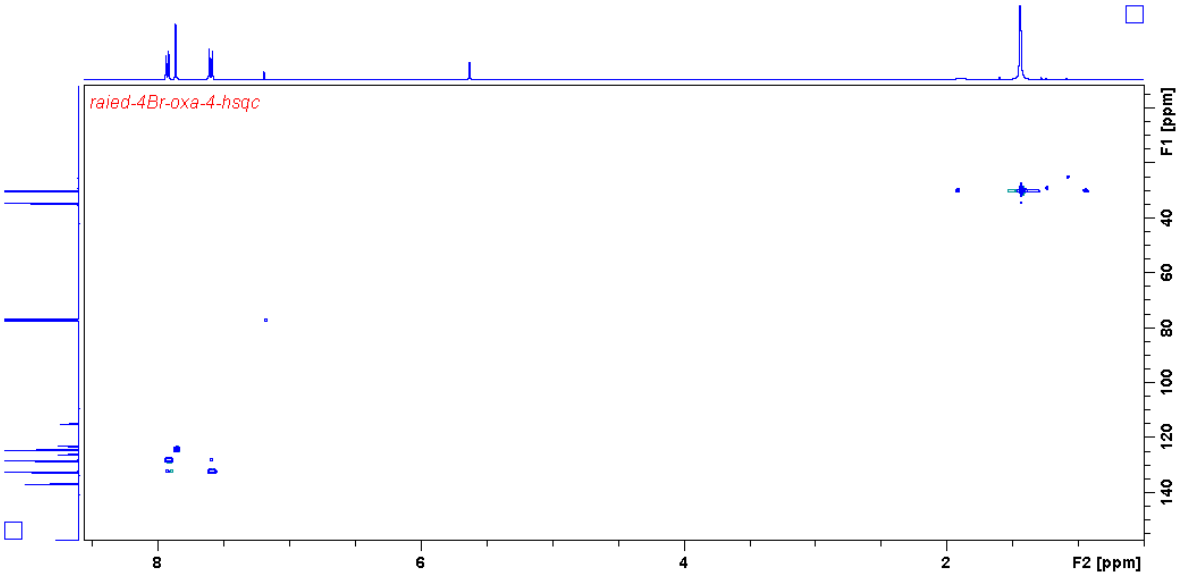

Figure A- 11 : HSQC of compound **2.15**

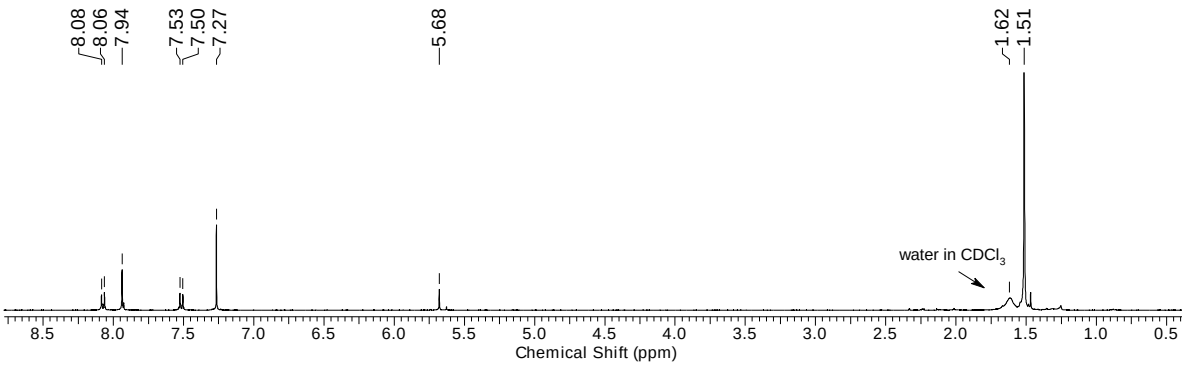

Figure A- 12 : ^{1}H NMR (400 MHz, $CDCl_3$) of compound **2.16**

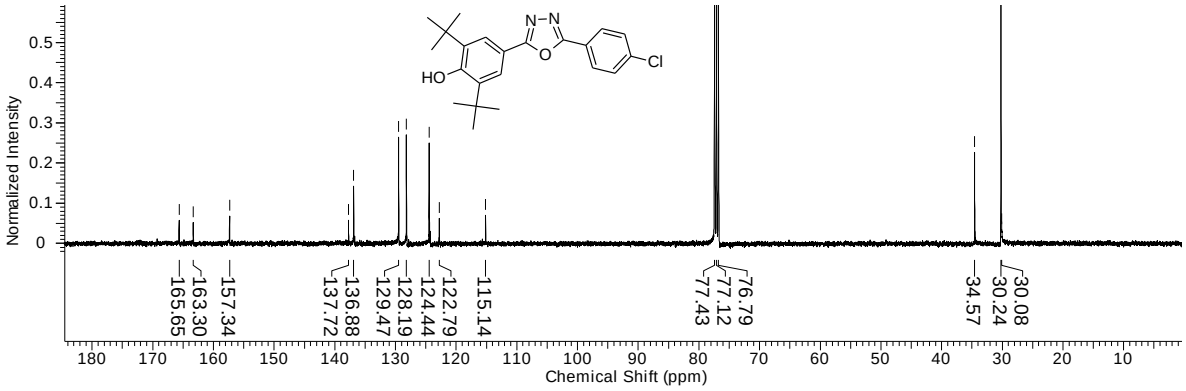

Figure A- 13 : ^{13}C NMR (100 MHz, $CDCl_3$) of compound **2.16**

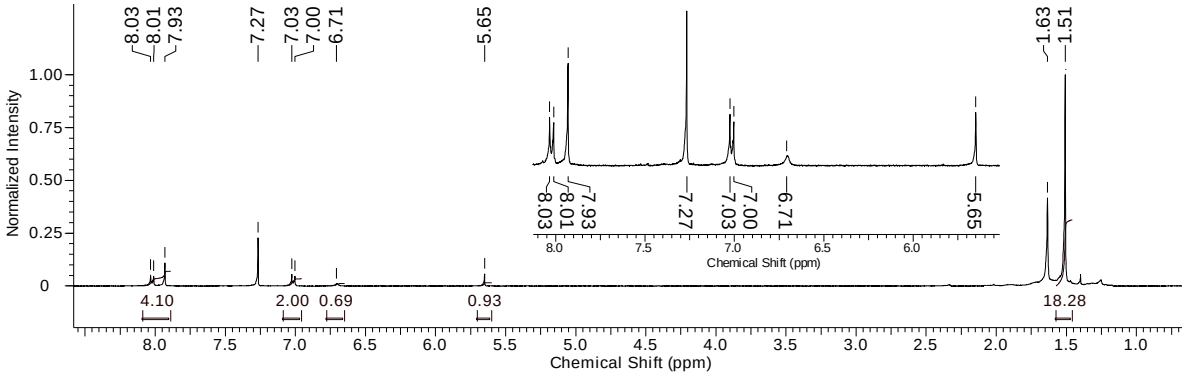

Figure A- 14 : ^{1}H NMR (400 MHz, $CDCl_3$) of compound **2.17**

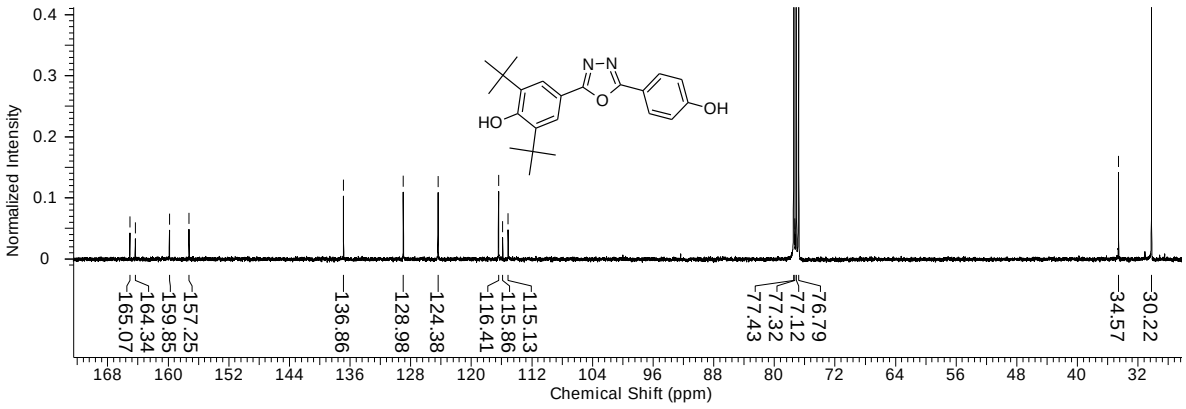

Figure A- 15 : ^{13}C NMR (100 MHz, $CDCl_3$) of compound **2.17**

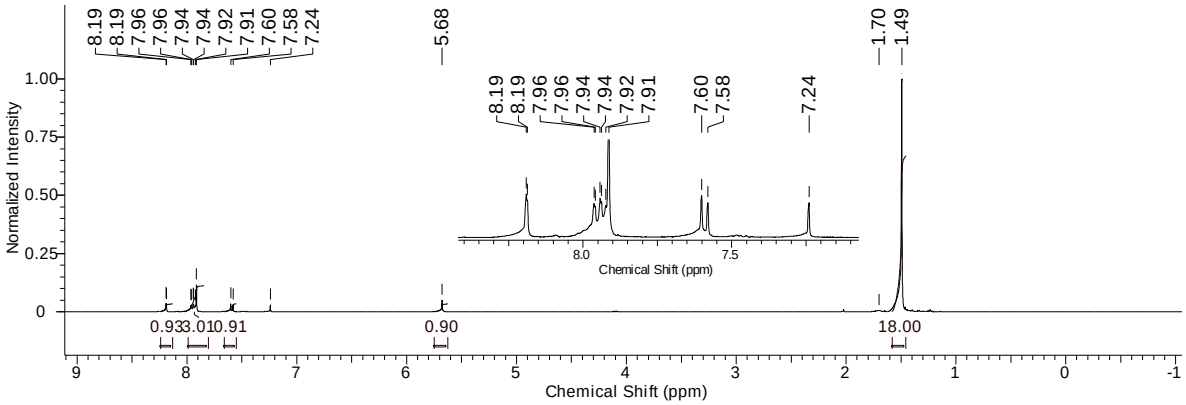

Figure A- 16 : ^{1}H NMR (400 MHz, $CDCl_3$) of compound **2.18**

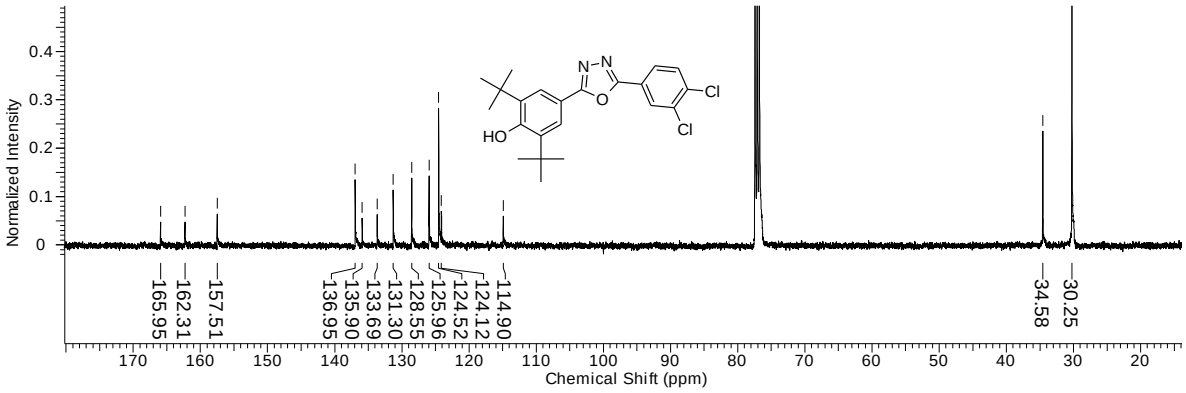

Figure A- 17 : ^{13}C NMR (100 MHz, $CDCl_3$) of compound **2.18**

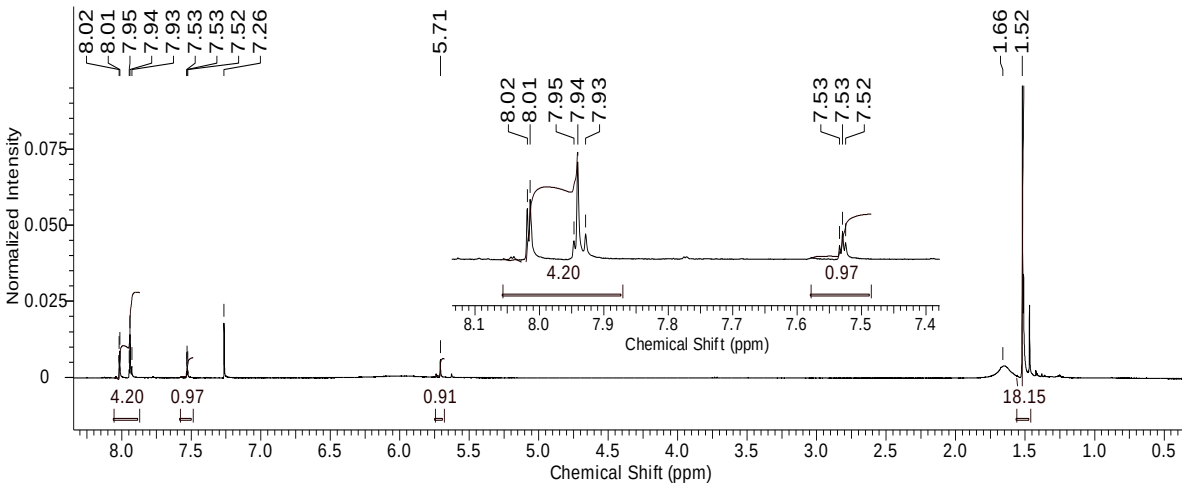

Figure A- 18 : ^{1}H NMR (400 MHz, $CDCl_3$) of compound **2.19**

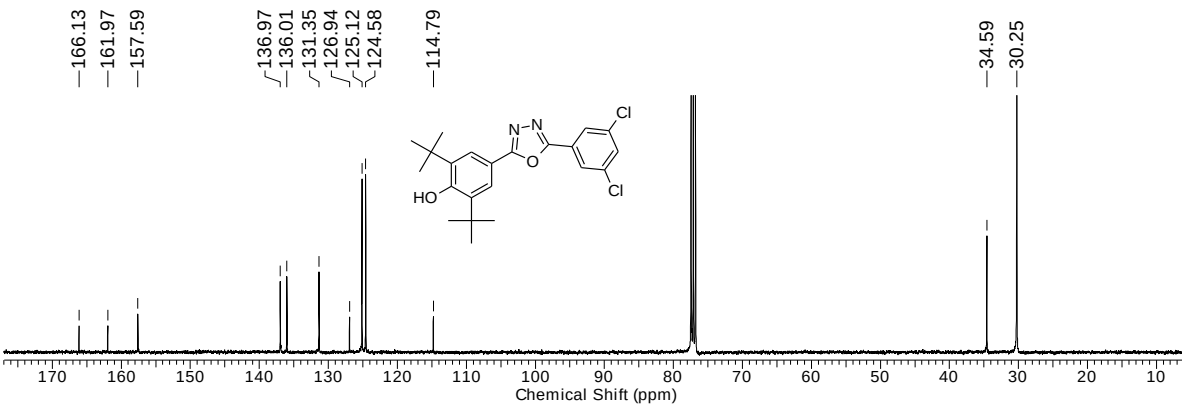

Figure A- 19 : ^{13}C NMR (100 MHz, $CDCl_3$) of compound **2.19**

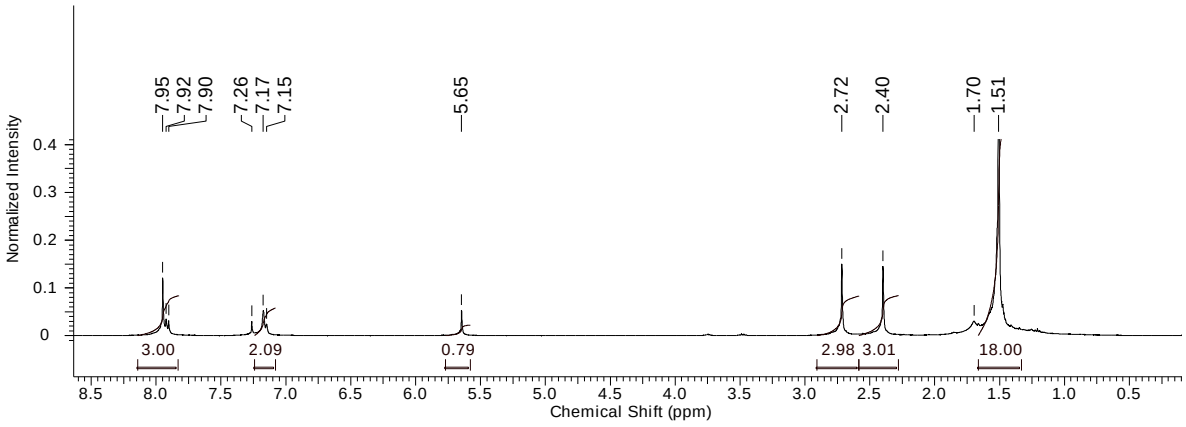

Figure A- 20 : ^{1}H NMR (400 MHz, $CDCl_3$) of compound **2.20**

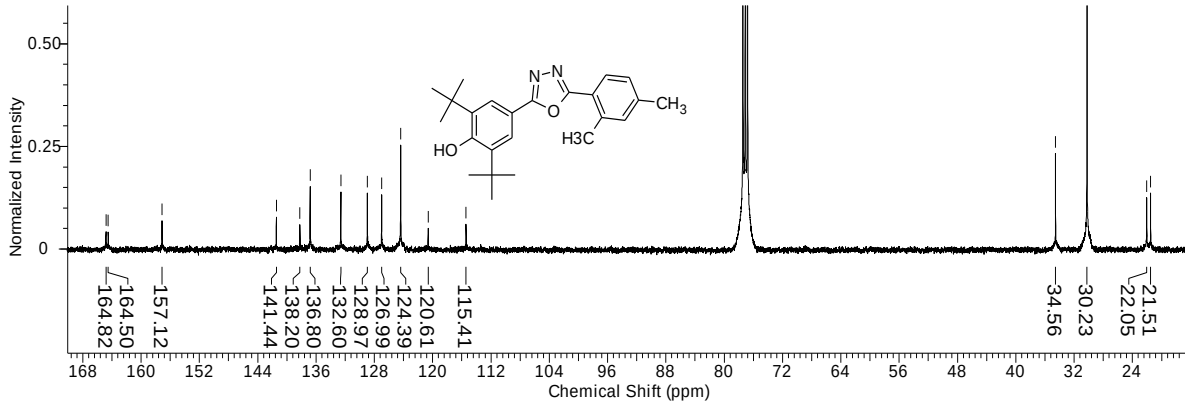

Figure A- 21 : ^{13}C NMR (100 MHz, $CDCl_3$) of compound **2.20**

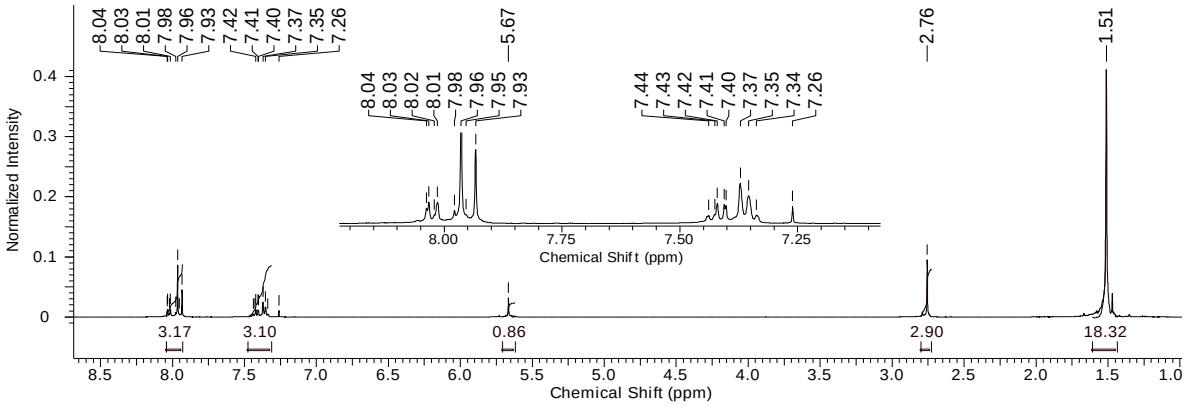

Figure A- 22 : ^{1}H NMR (400 MHz, $CDCl_3$) of compound **2.21**

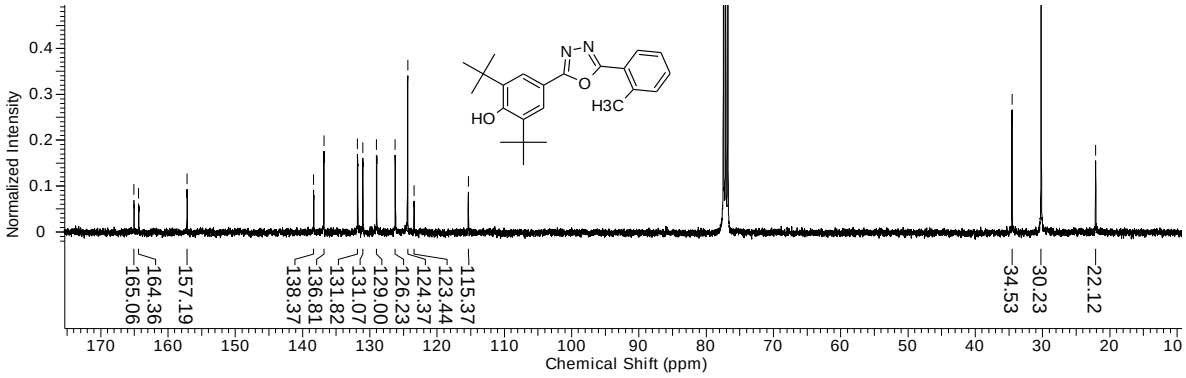

Figure A- 23 : ^{13}C NMR (100 MHz, $CDCl_3$) of compound **2.21**

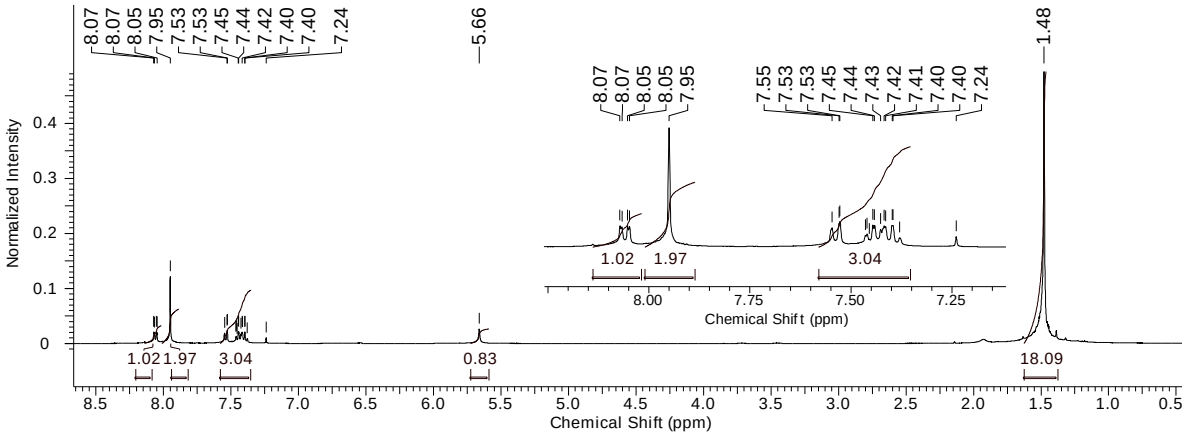

Figure A- 24 : ^{1}H NMR (400 MHz, $CDCl_3$) of compound **2.22**

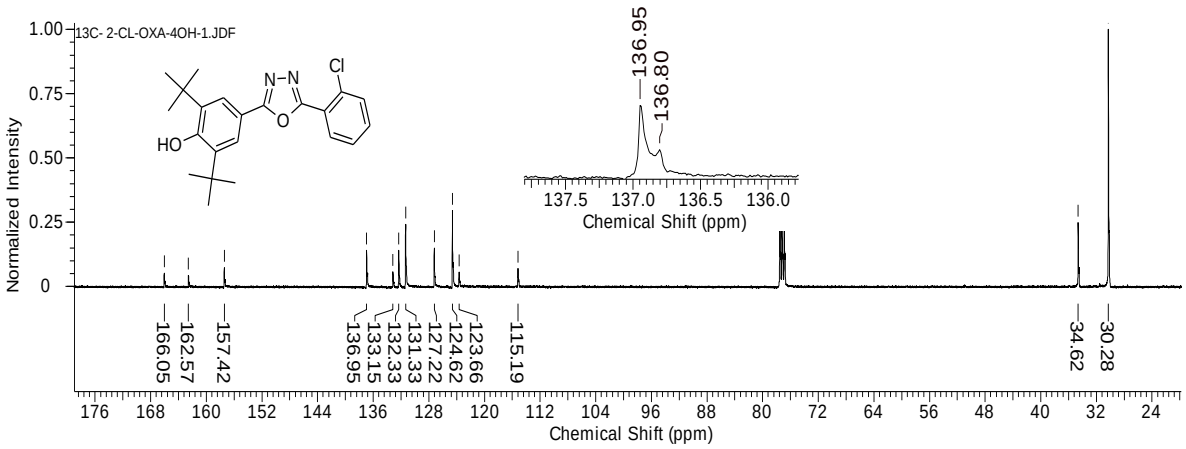

Figure A- 25 : ^{13}C NMR (100 MHz, $CDCl_3$) of compound **2.22**

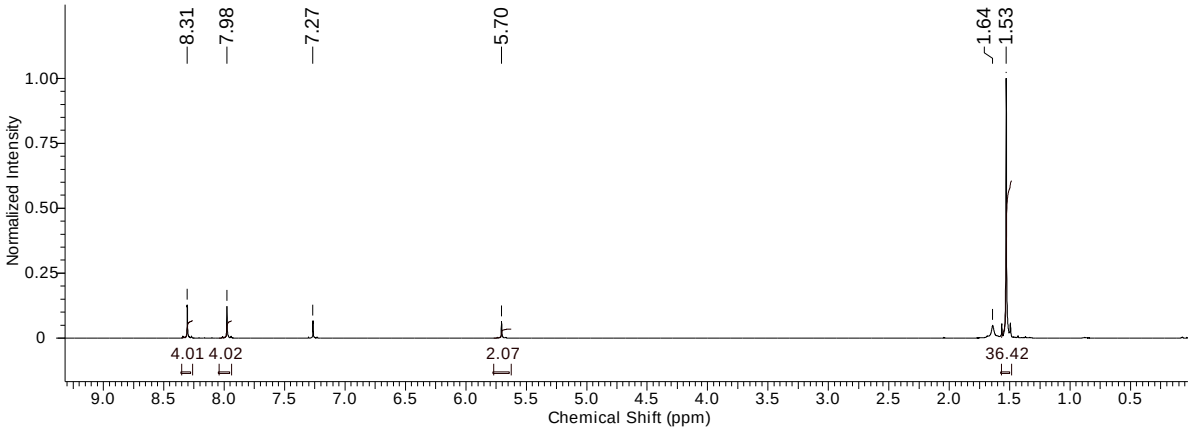

Figure A- 26 : ^{1}H NMR (400 MHz, $CDCl_3$) of compound **2.31**

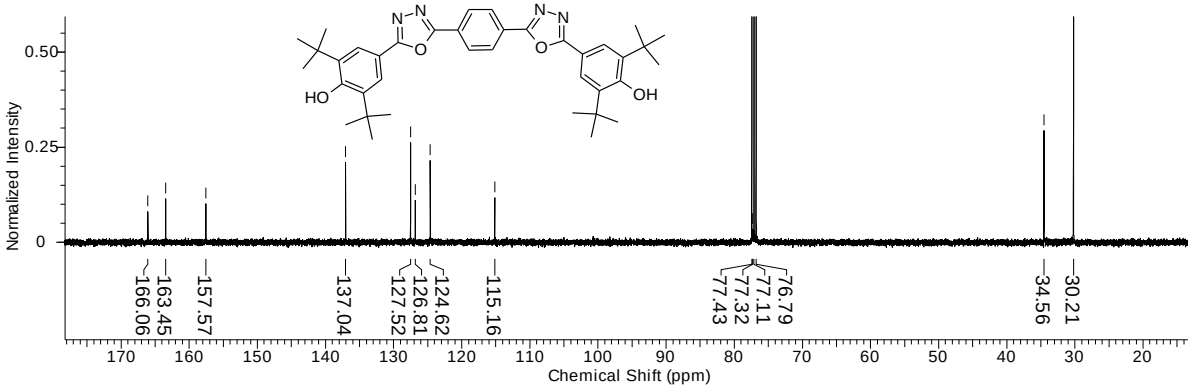

Figure A- 27 : ^{13}C NMR (100 MHz, $CDCl_3$) of compound **2.31**

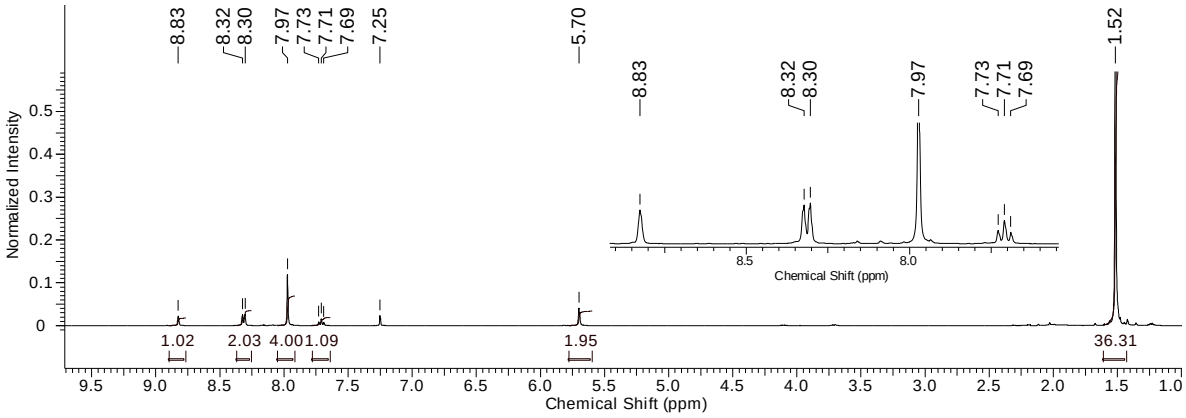

Figure A- 28 : ^{1}H NMR (400 MHz, $CDCl_3$) of compound **2.32**

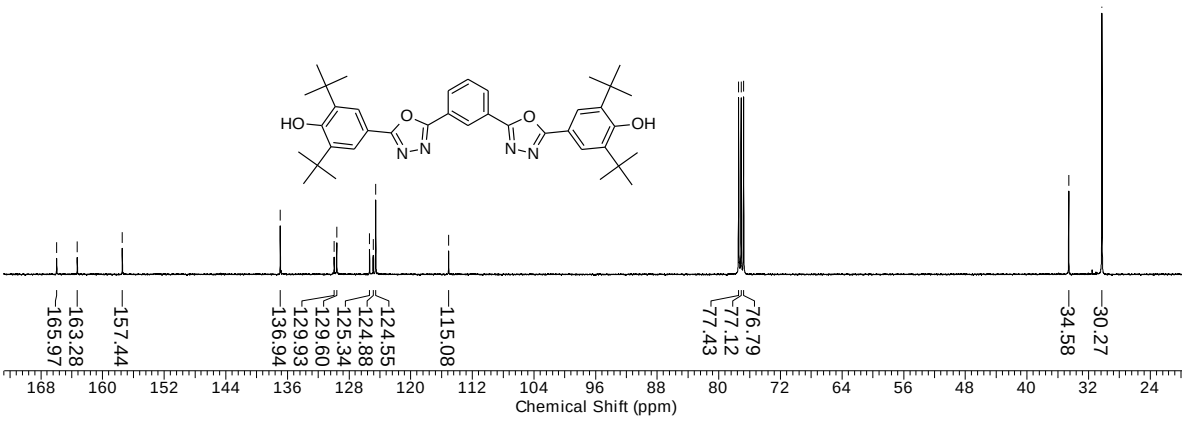

Figure A- 29 : ^{13}C NMR (100 MHz, $CDCl_3$) of compound **2.32**

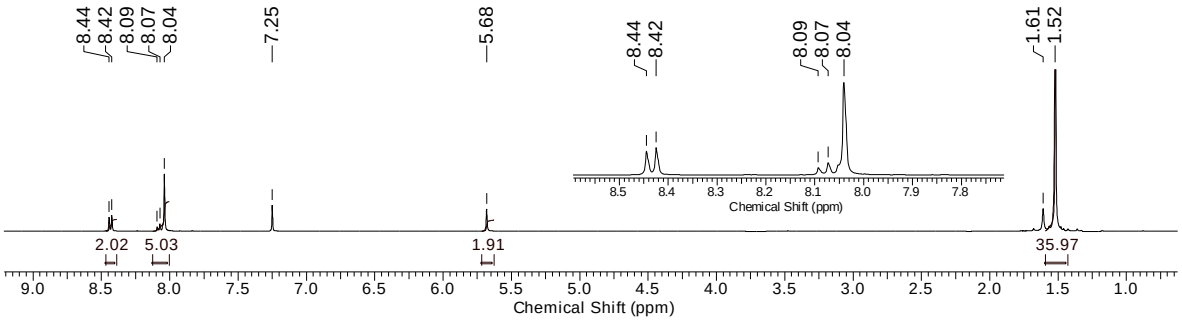

Figure A- 30 : ^{1}H NMR (400 MHz, CDCl3) of compound **2.33**

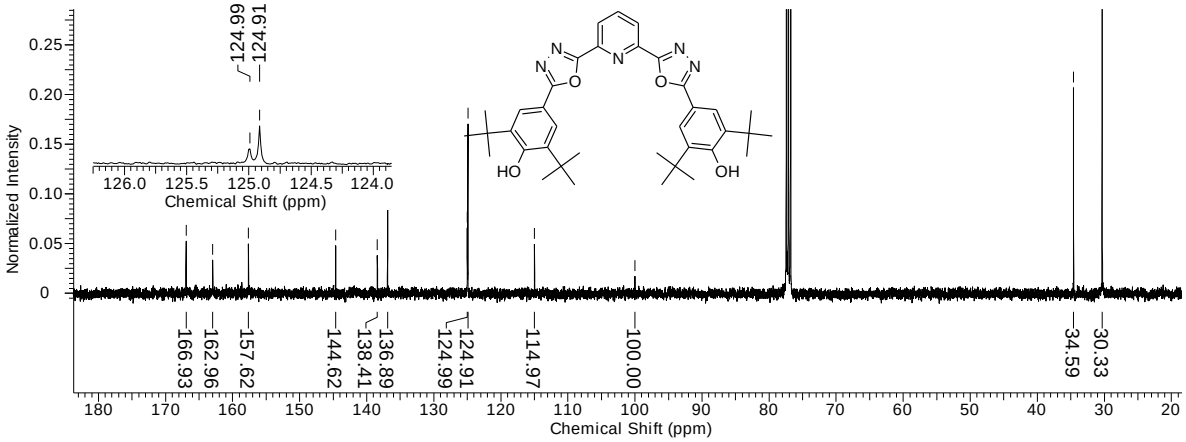

Figure A- 31 : ^{13}C NMR (100 MHz, $CDCl_3$) of compound **2.33**

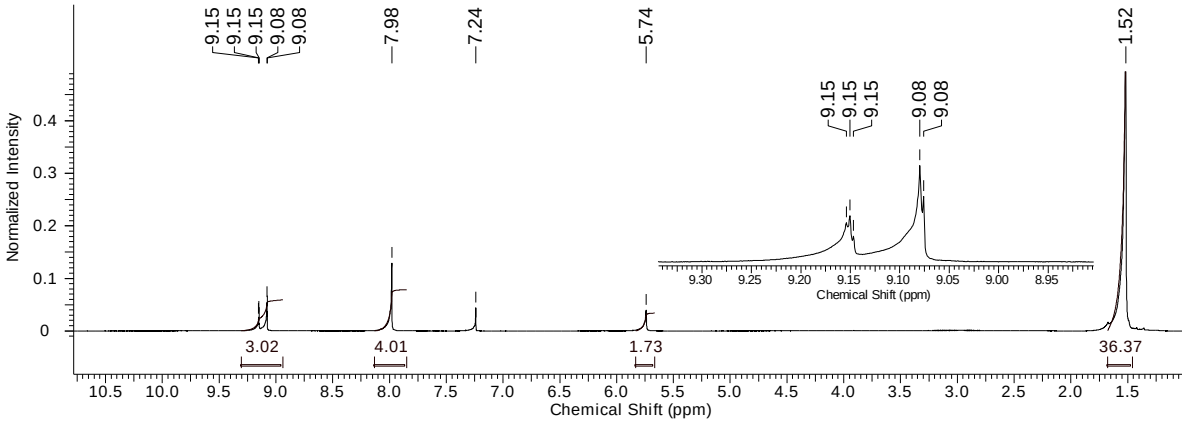

Figure A- 32 : ^{1}H NMR (400 MHz, CDCl3) of compound **2.34**

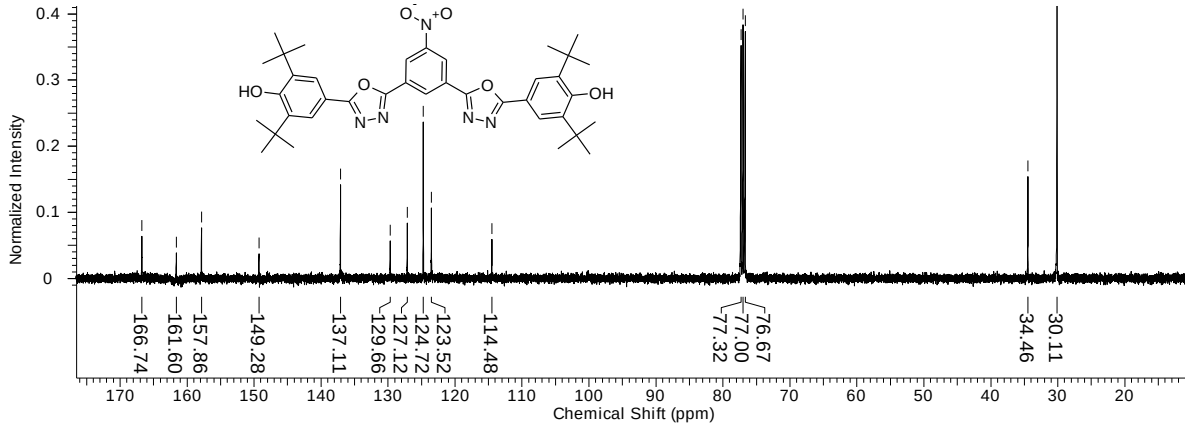

Figure A- 33 : ^{13}C NMR (100 MHz, $CDCl_3$) of compound **2.34**

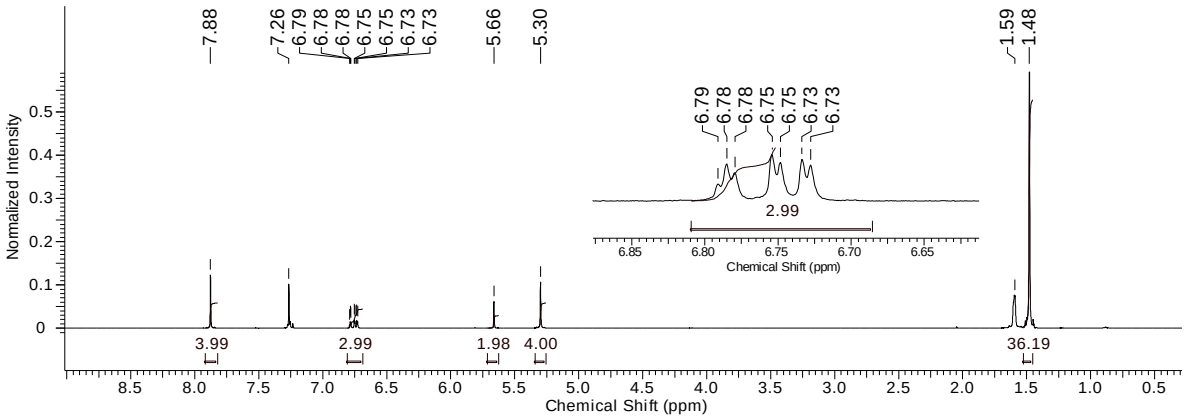

Figure A- 34 : ^{1}H NMR (400 MHz, CDCl3) of compound **2.35**

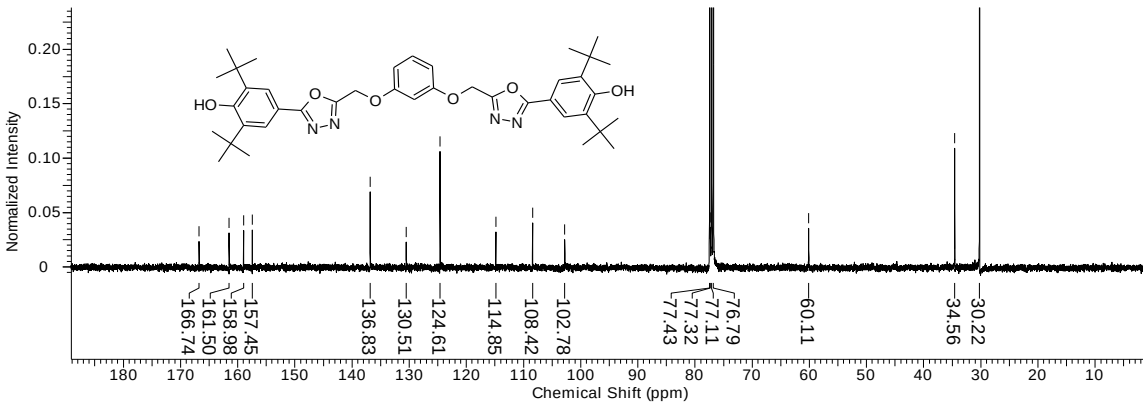

Figure A- 35 : ^{13}C NMR (100 MHz, $CDCl_3$) of compound **2.35**

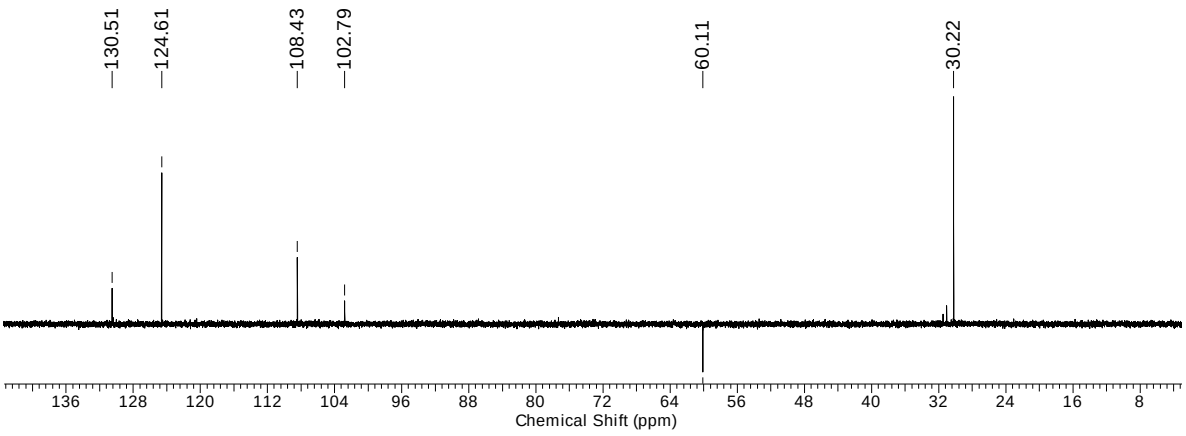

Figure A- 36 : Dept-135 of compound **2.35**

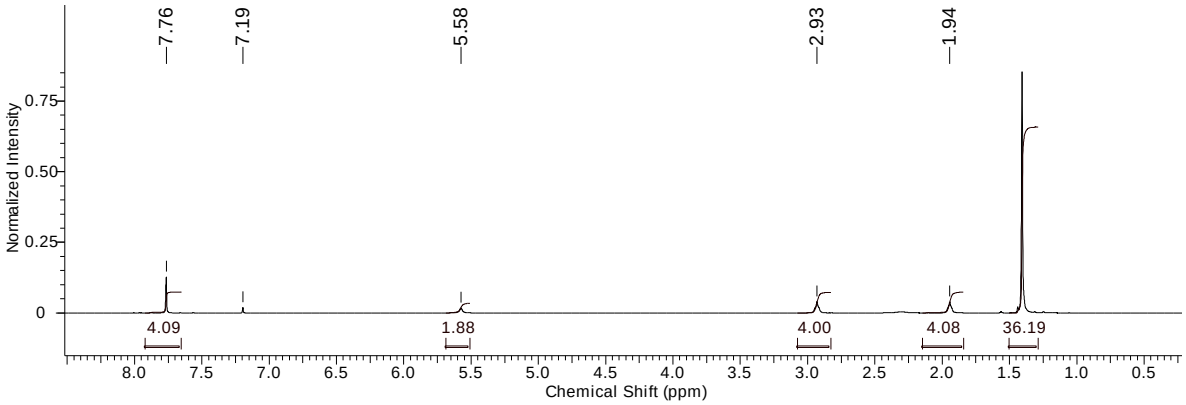

Figure A- 37 : ^{1}H NMR (400 MHz, CDCl3) of compound **2.36**

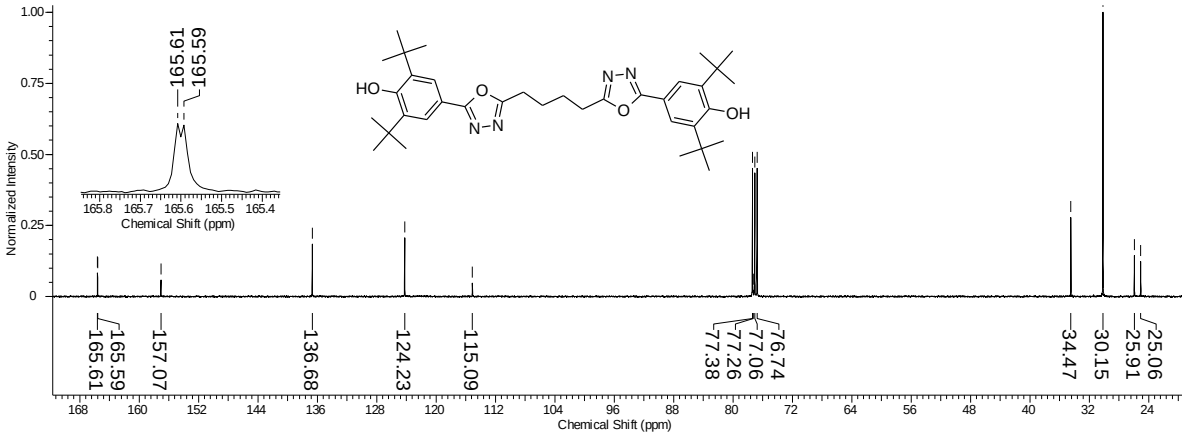

Figure A- 38 : ^{13}C NMR (100 MHz, $CDCl_3$) of compound **2.36**

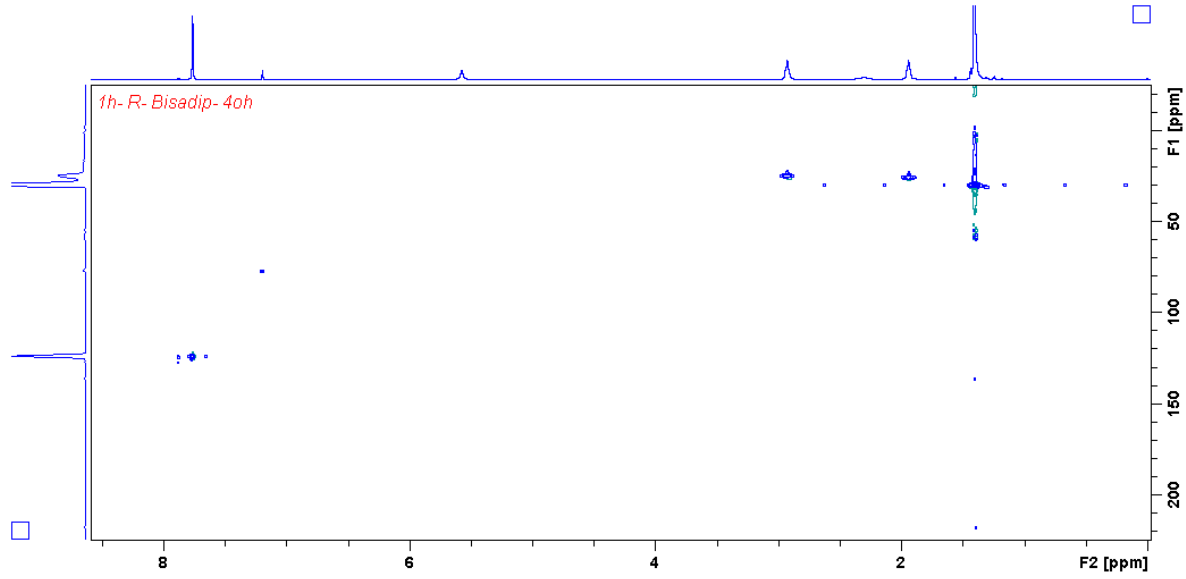

Figure A- 39 : HSQC of compound **2.36**

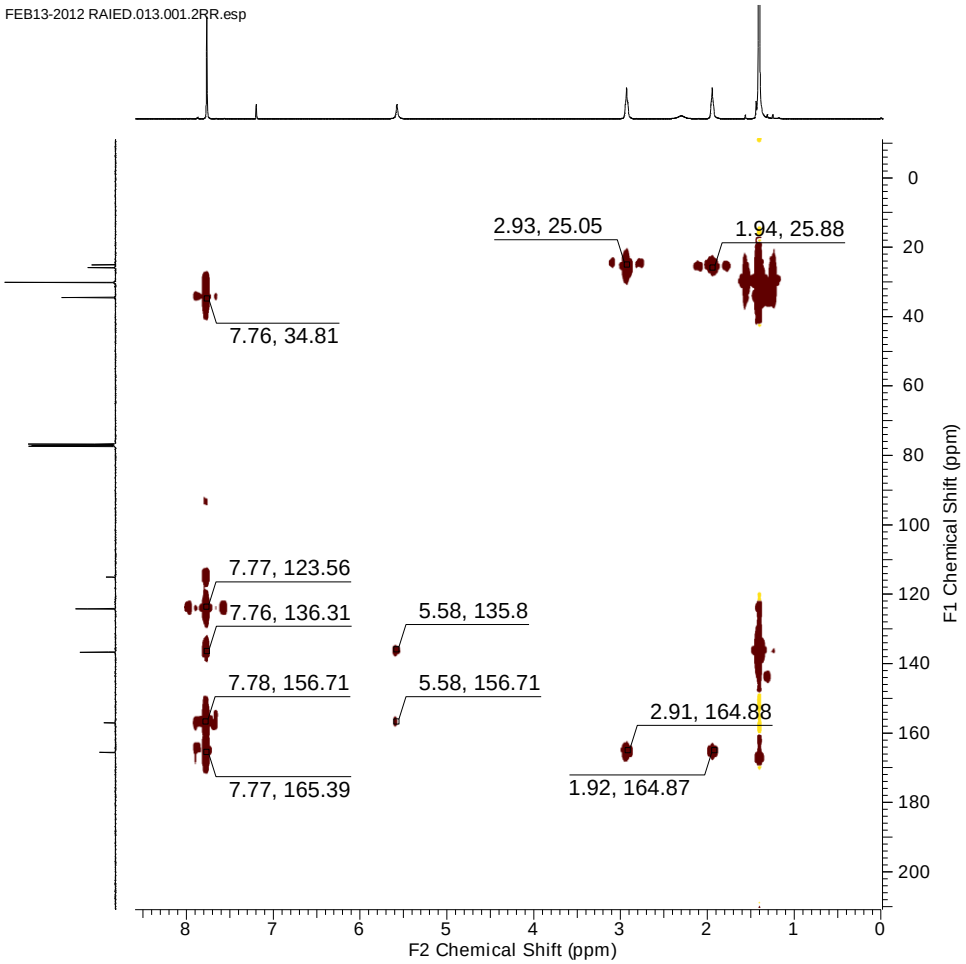

Figure A- 40: HMBC of compound **2.36**

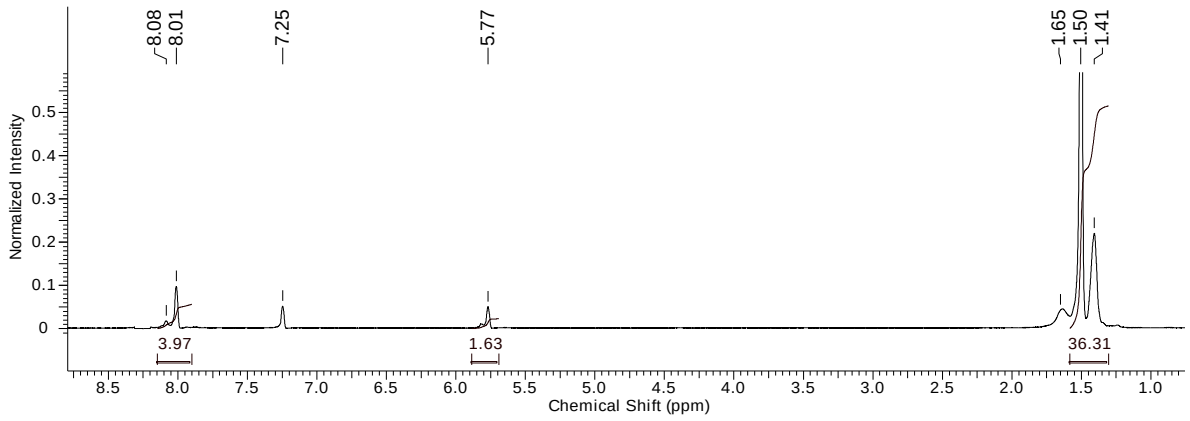

Figure A- 41 : ^{1}H NMR (400 MHz, $CDCl_3$) of compound **2.37**

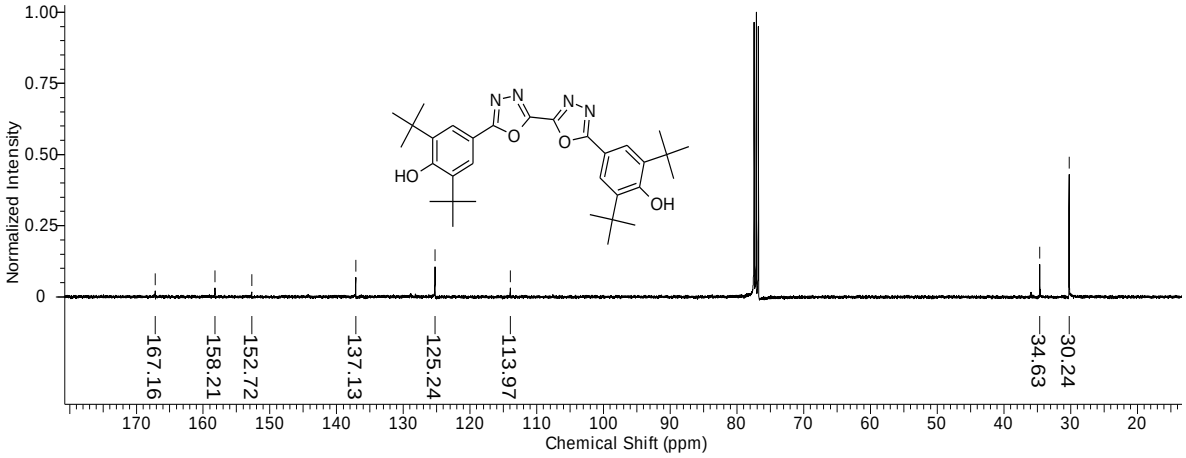

Figure A- 42 : ^{13}C NMR (100 MHz, $CDCl_3$) of compound **2.37**

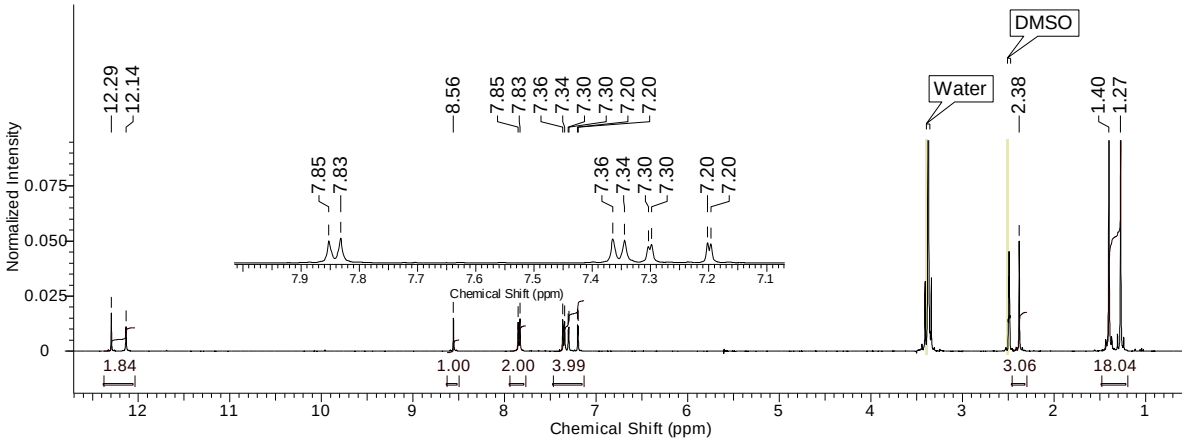

Figure A- 43 : ^{1}H NMR (400 MHz, DMSO-d_6) of compound **3.1**

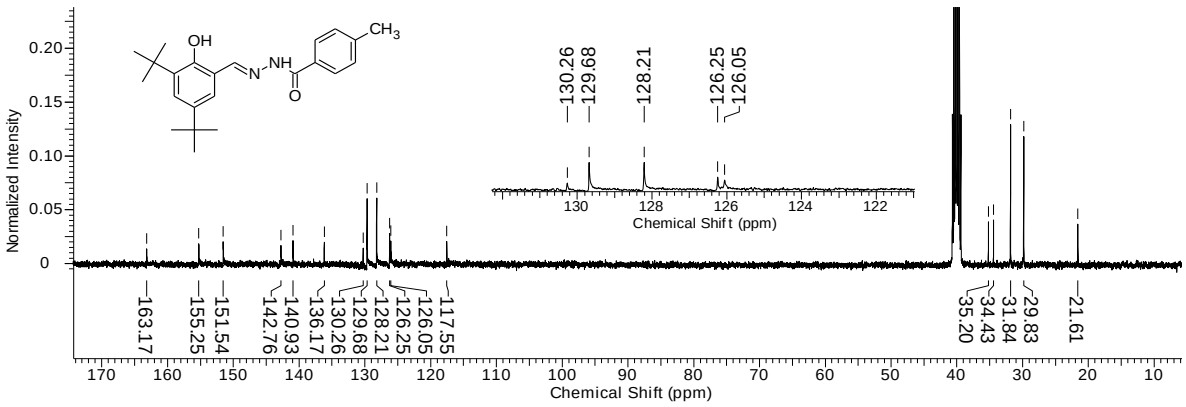

Figure A- 44 : ^{13}C NMR (100 MHz, DMSO-d_6) of compound **3.1**

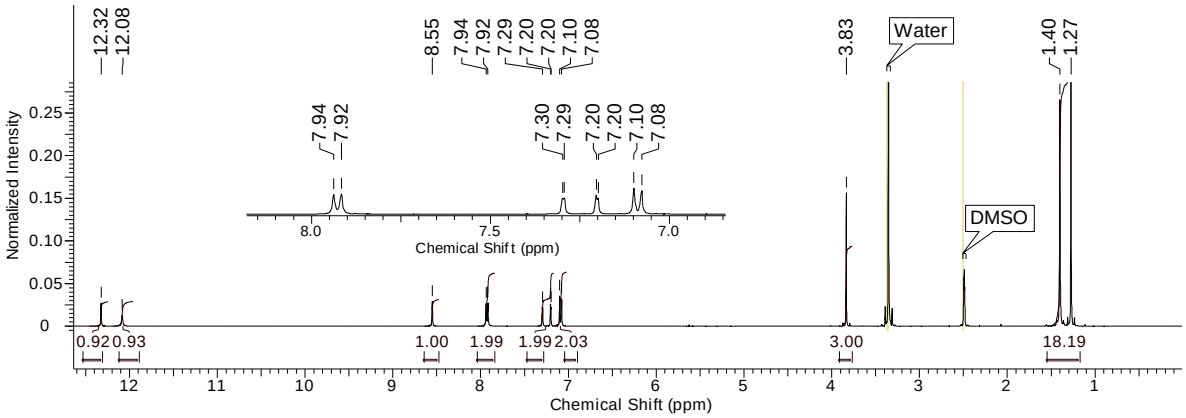

Figure A- 45 : ^{1}H NMR (400 MHz, DMSO-d_6) of compound **3.2**

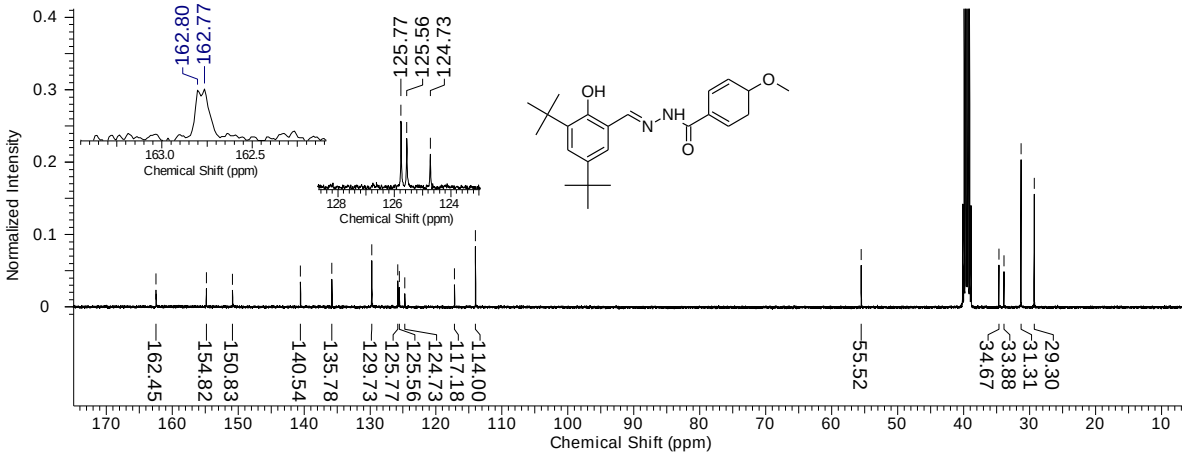

Figure A- 46 : ^{13}C NMR (100 MHz, DMSO-d_6) of compound 3.2

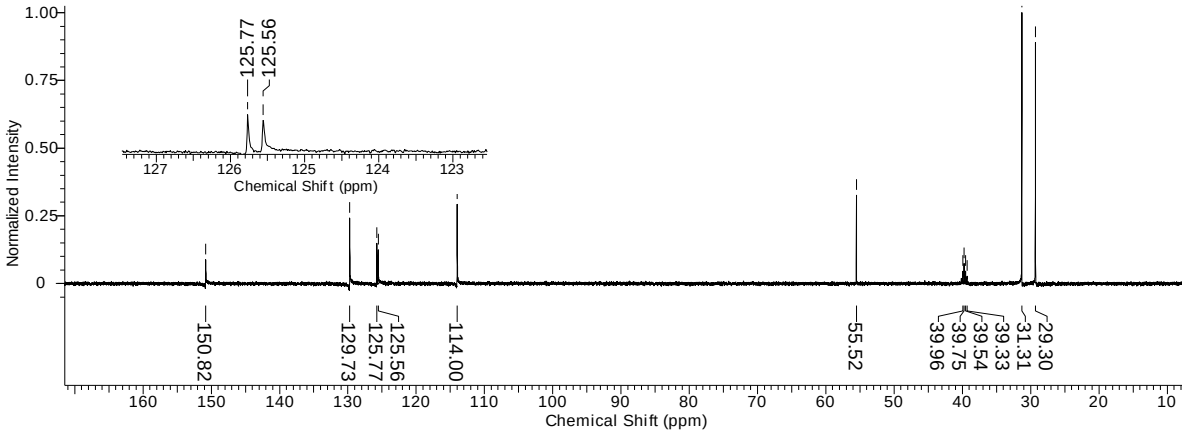

Figure A- 47 : Dept-135 of compound 3.2

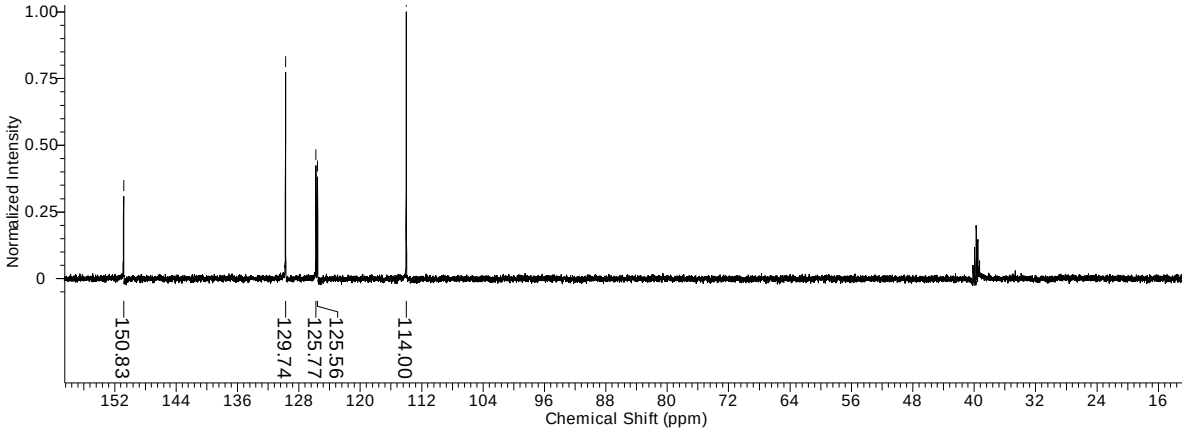

Figure A- 48 : Dept-90 of compound **3.2**

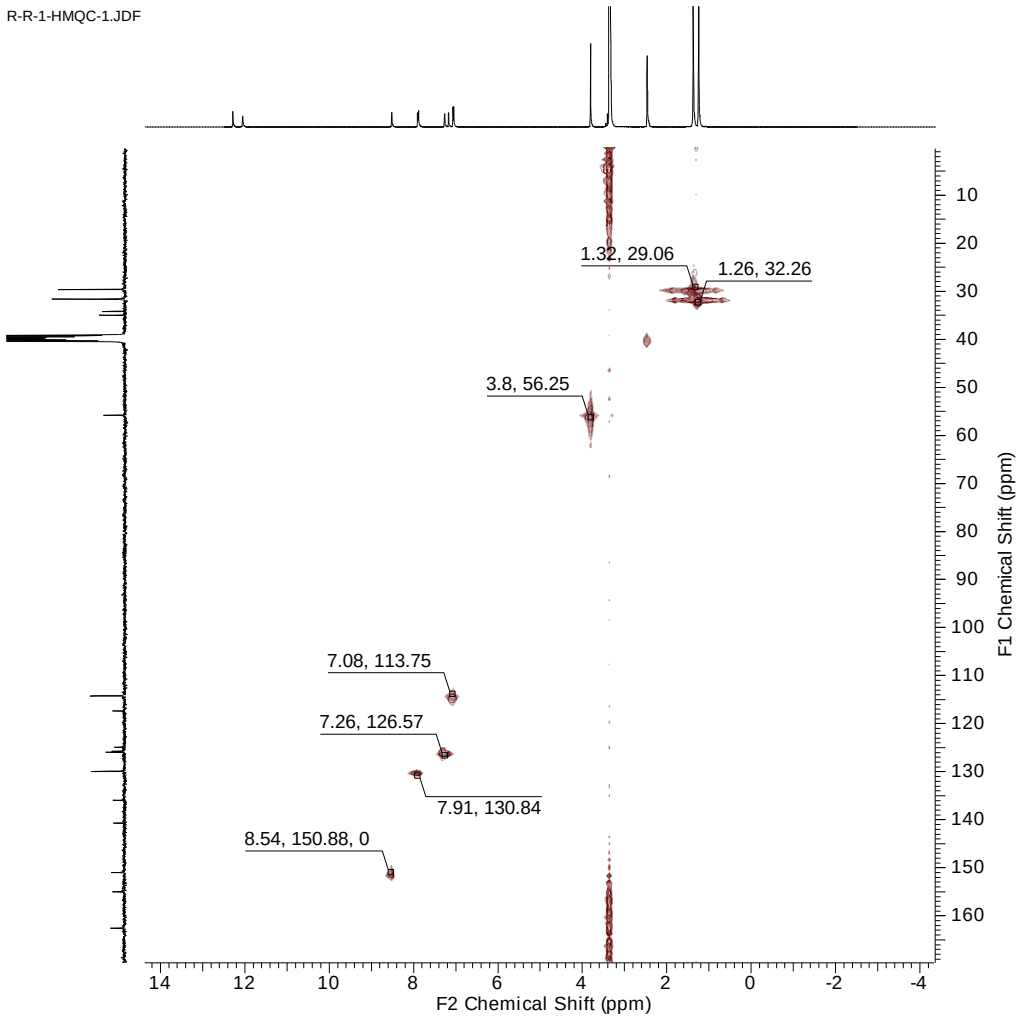

Figure A- 49 : HMQC of compound **3.2**

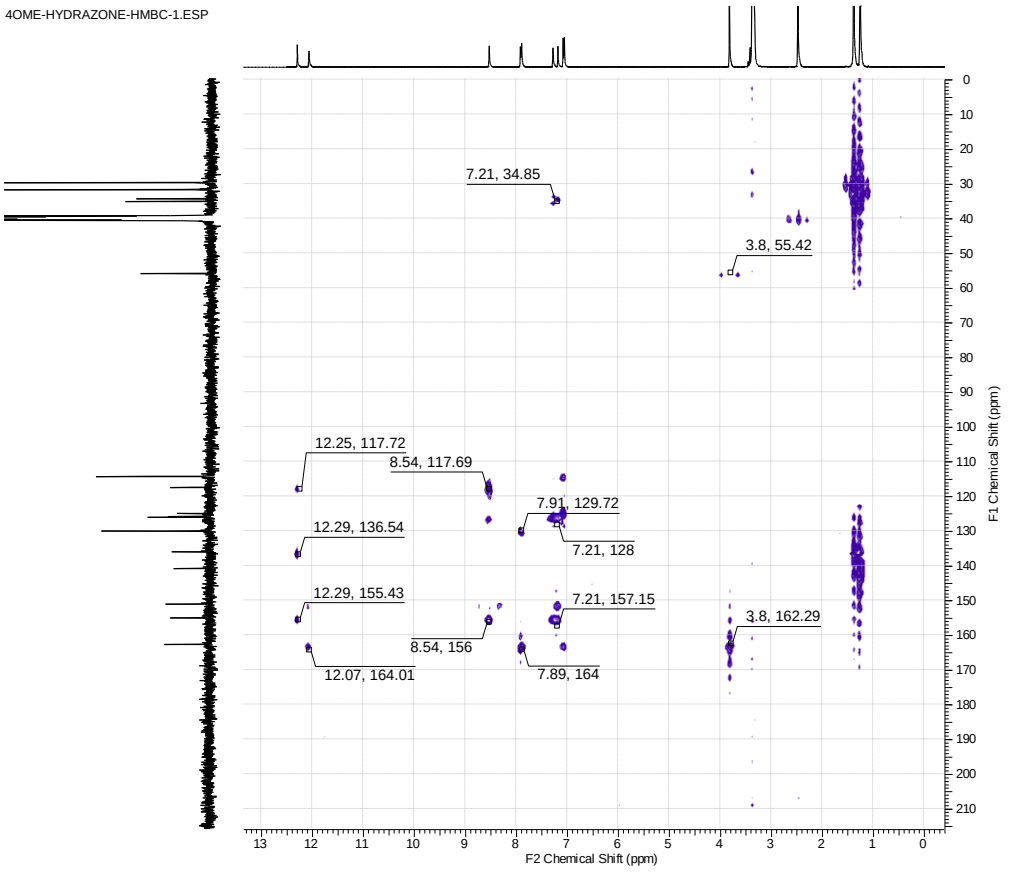

Figure A- 50 : HMBC of compound **3.2**

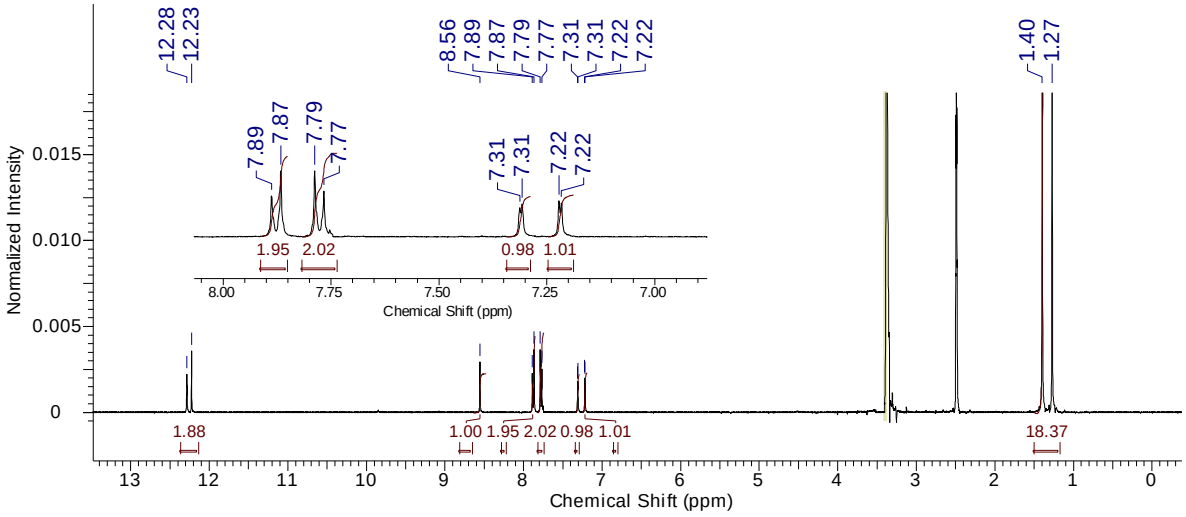

Figure A- 51 : ^{1}H NMR (400 MHz, DMSO-d_6) of compound **3.3**

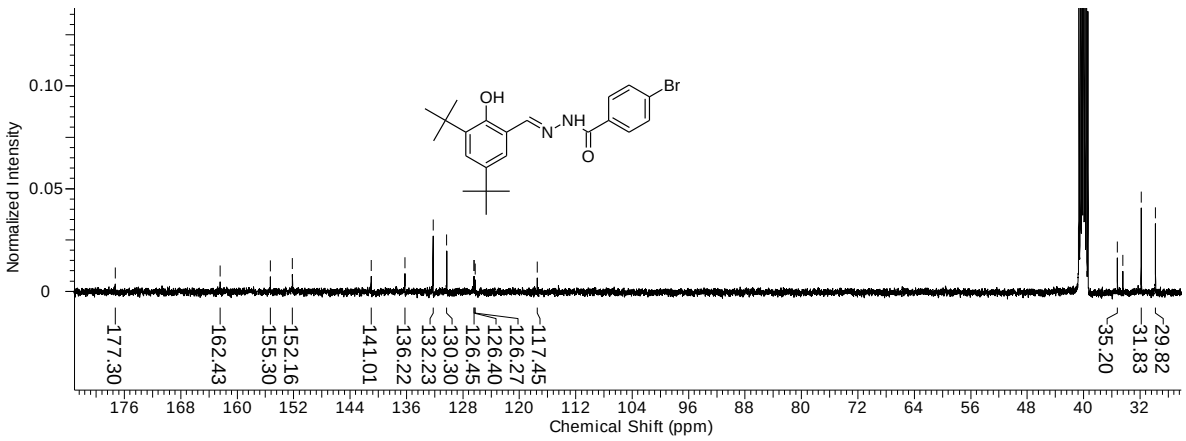

Figure A- 52 : ^{13}C NMR (100 MHz, DMSO-d_6) of compound **3.3**

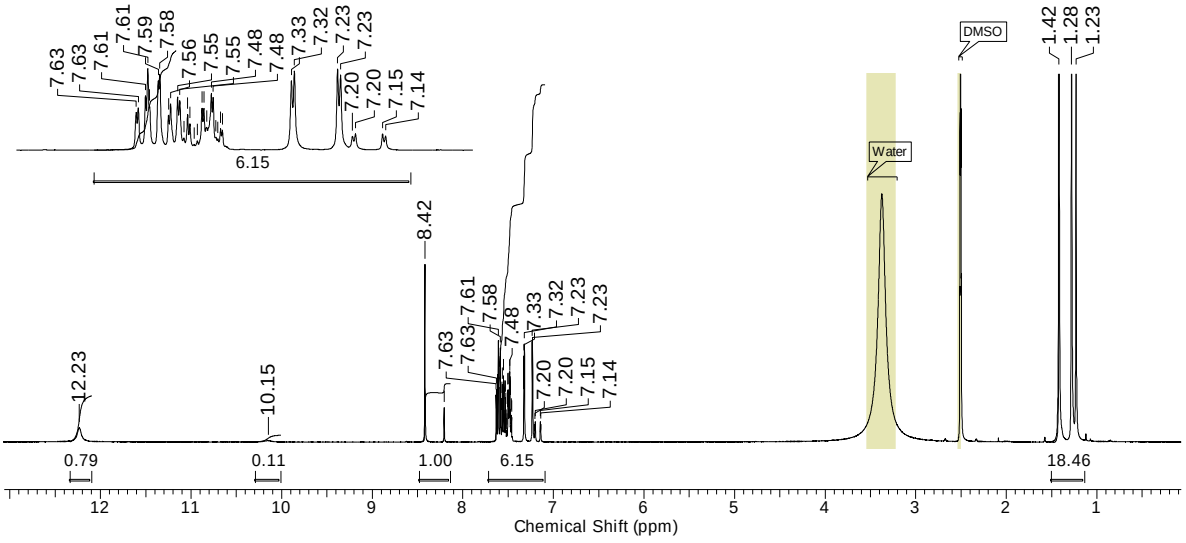

Figure A- 53 : ^{1}H NMR (400 MHz, DMSO-d_6) of compound **3.4**

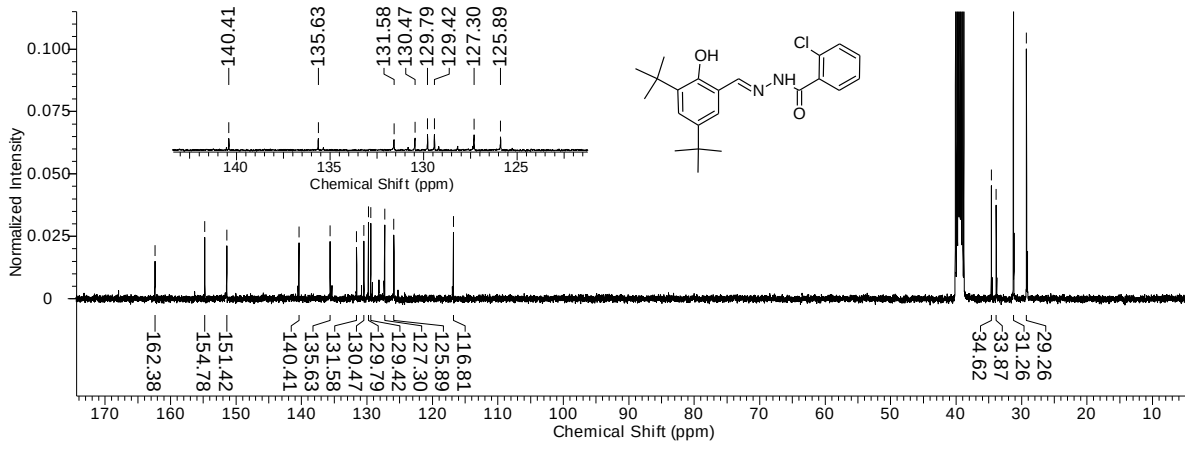

Figure A- 54 : ^{13}C NMR (100 MHz, DMSO-d_6) of compound **3.4**

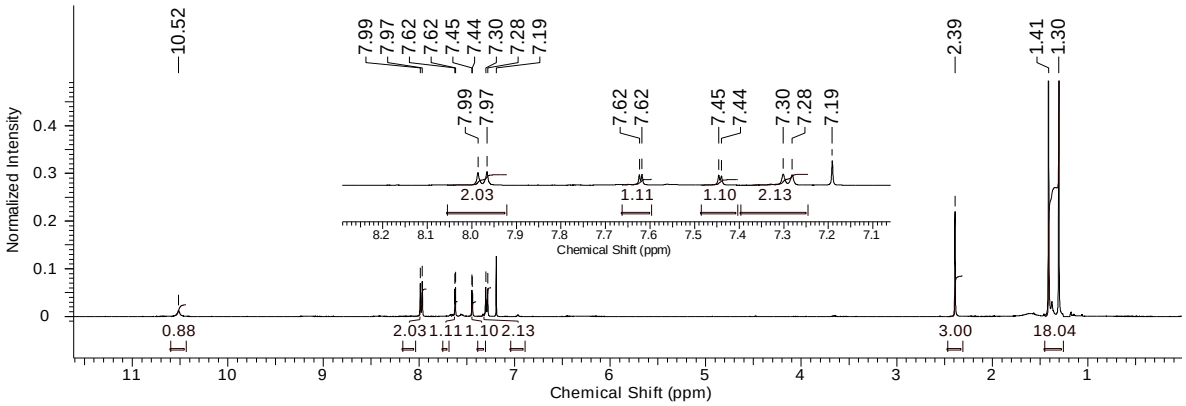

Figure A- 55 : ^{1}H NMR (400 MHz, $CDCl_3$) of compound **3.5**

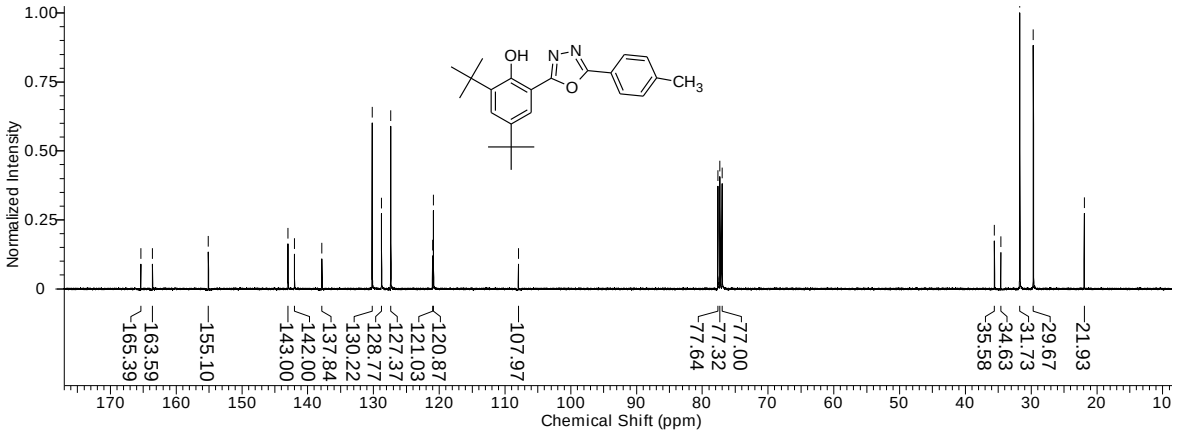

Figure A- 56 : ^{13}C NMR (100 MHz, $CDCl_3$) of compound **3.5**

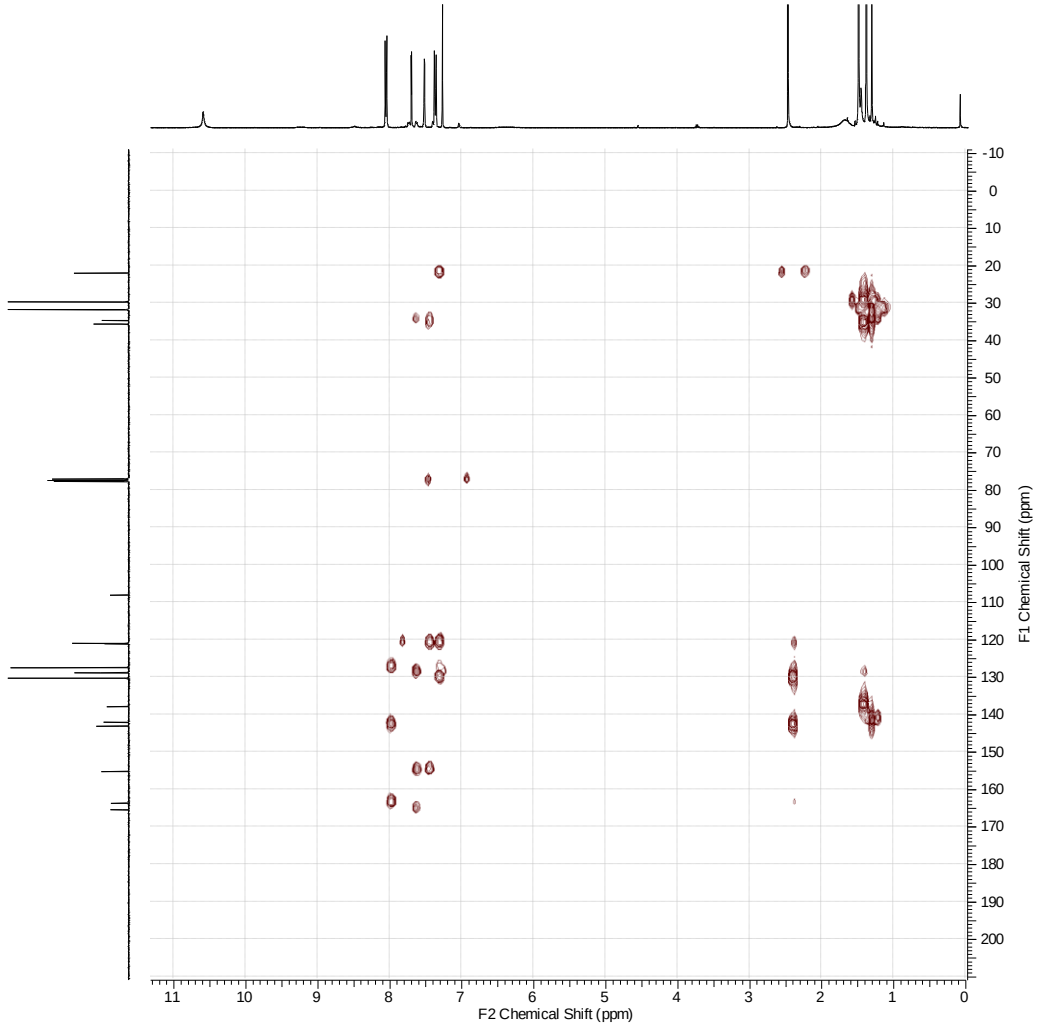

Figure A- 57 : HMBC of compound **3.5**

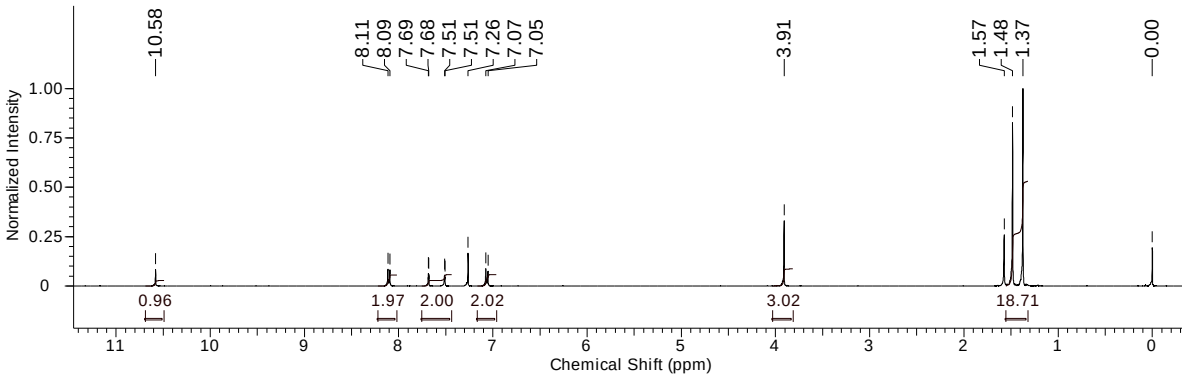

Figure A- 58 : ^{1}H NMR (400 MHz, DMSO-d_6) of compound **3.6**

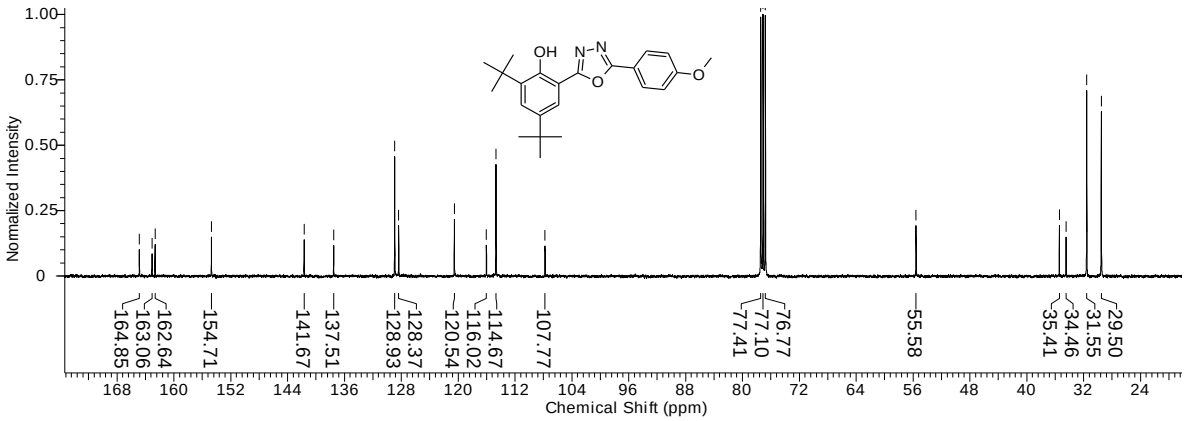

Figure A- 59 : ^{13}C NMR (100 MHz, $CDCl_3$) of compound **3.6**

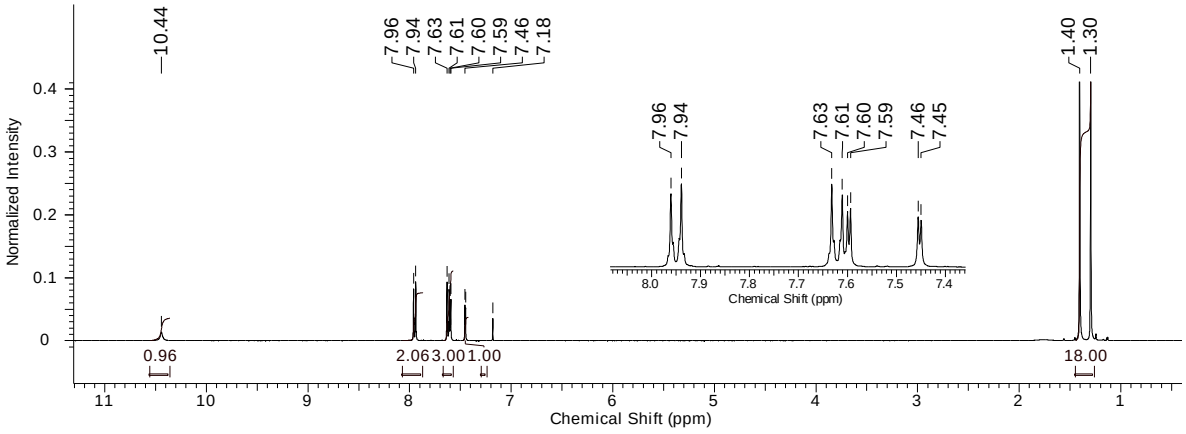

Figure A- 60 : ^{1}H NMR (400 MHz, DMSO-d_6) of compound **3.7**

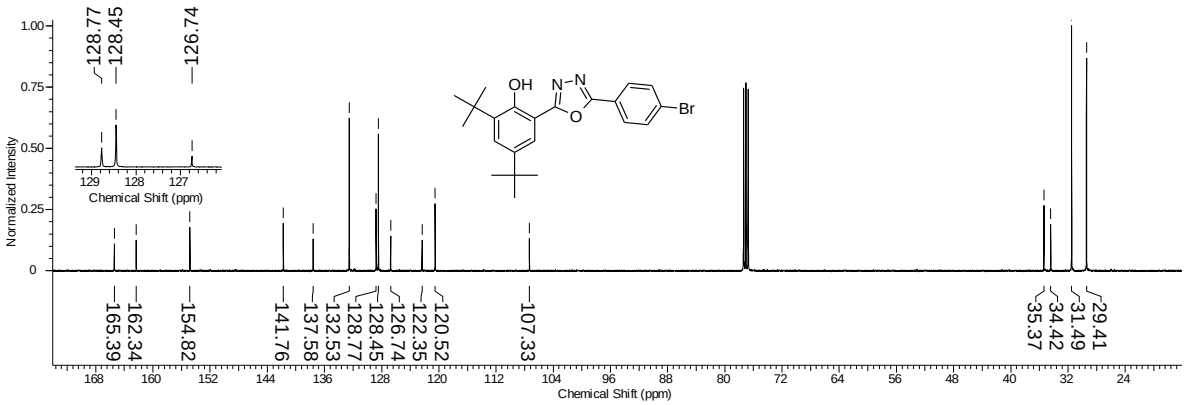

Figure A- 61 : ^{13}C NMR (100 MHz, $CDCl_3$) of compound **3.7**

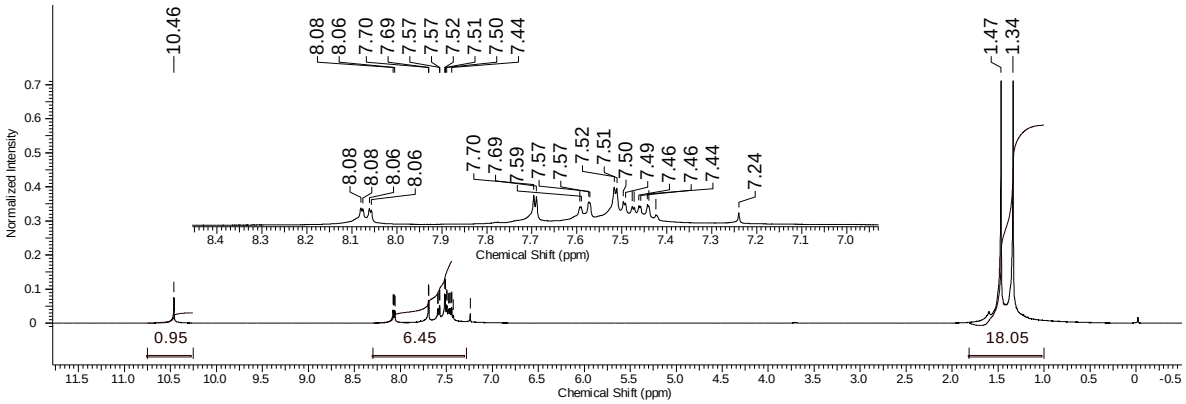

Figure A- 62 : ^{1}H NMR (400 MHz, $CDCl_3$) of compound **3.8**

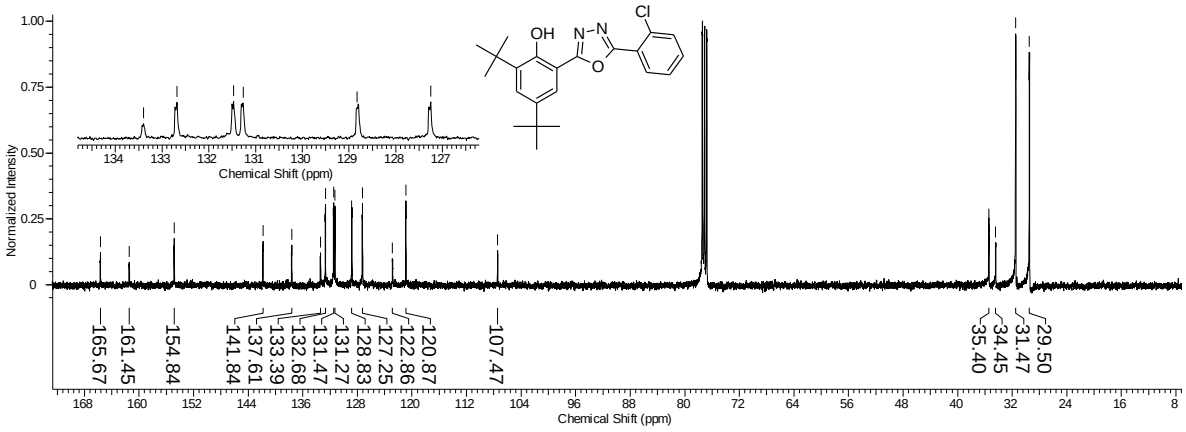

Figure A- 63 : ^{13}C NMR (100 MHz, $CDCl_3$) of compound **3.8**

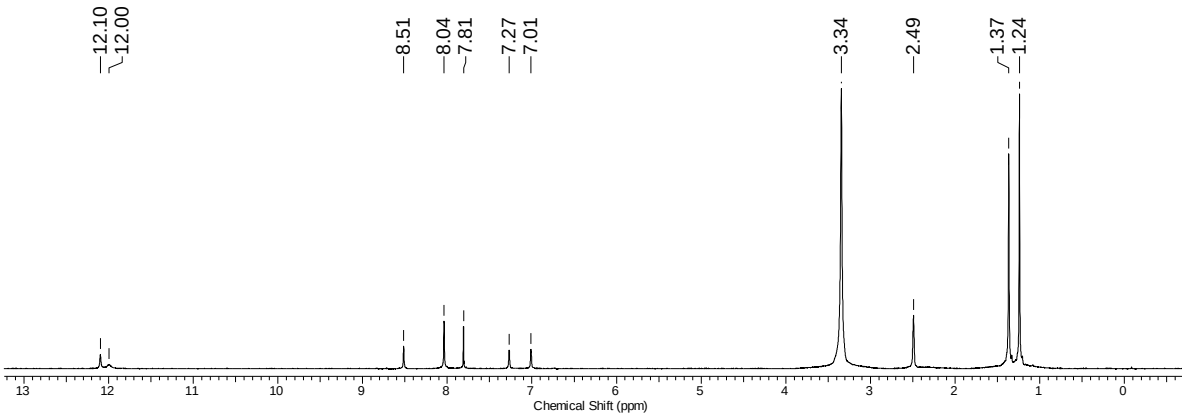

Figure A- 64 : ^{1}H NMR (400 MHz, $CDCl_3$+DMSO-d_6) of compound **3.9**

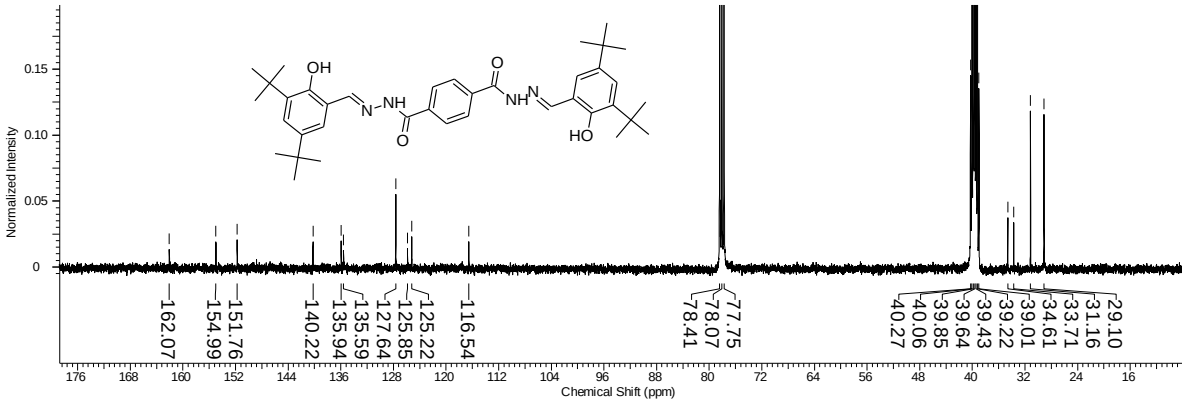

Figure A- 65 : ^{13}C NMR (100 MHz, $CDCl_3$+DMSO-d_6) of **3.9**

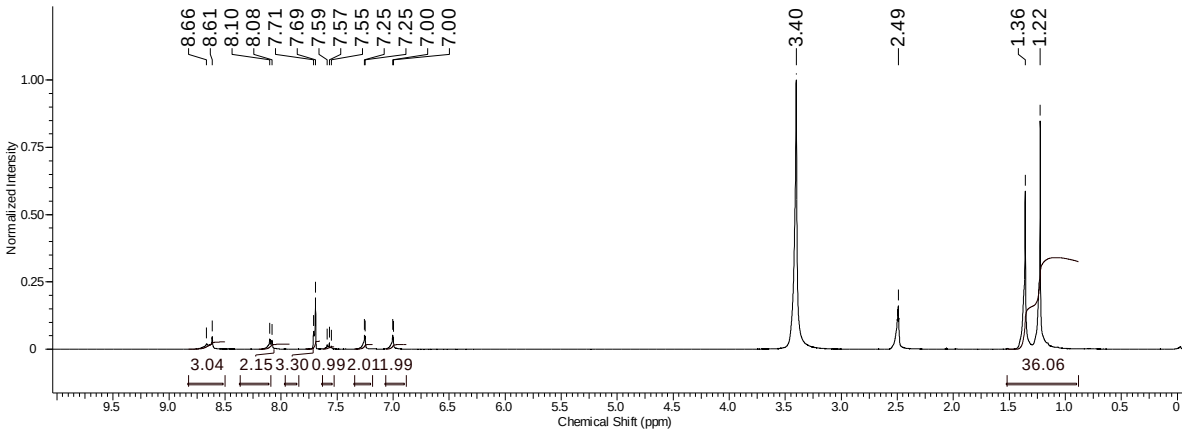

Figure A- 66 : ^{1}H NMR (400 MHz, $CDCl_3$+DMSO-d_6) of 3.**10**

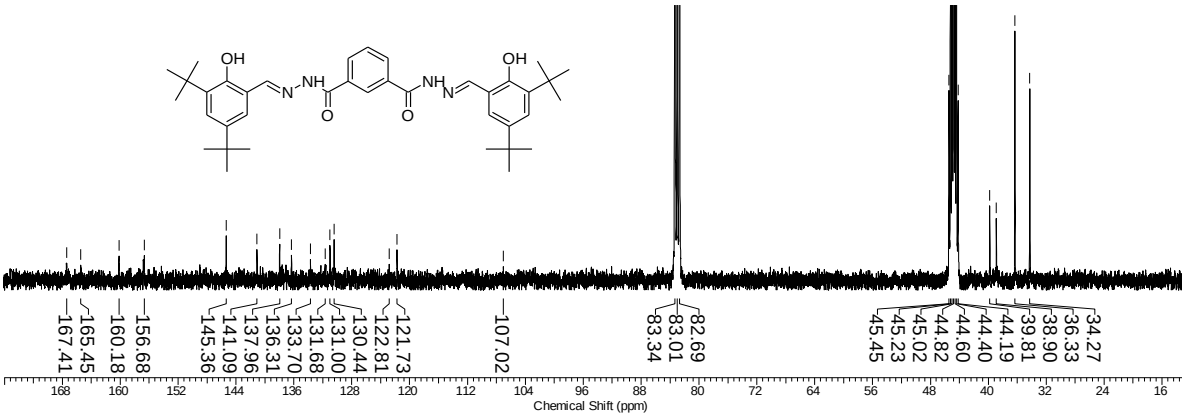

Figure A- 67 : ^{13}C NMR (100 MHz, $CDCl_3$+DMSO-d_6) of **3.10**

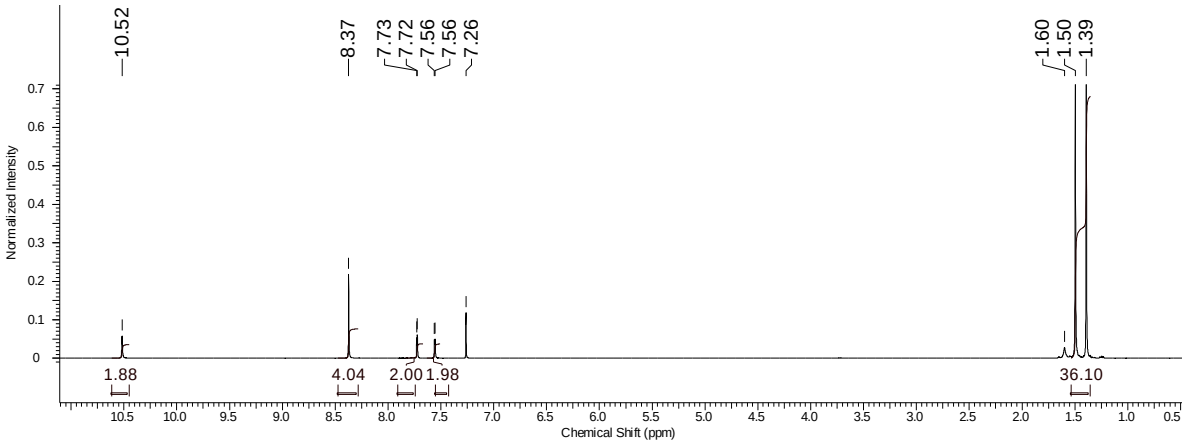

Figure A- 68 : ^{1}H NMR (400 MHz, $CDCl_3$) of compound **3.11**

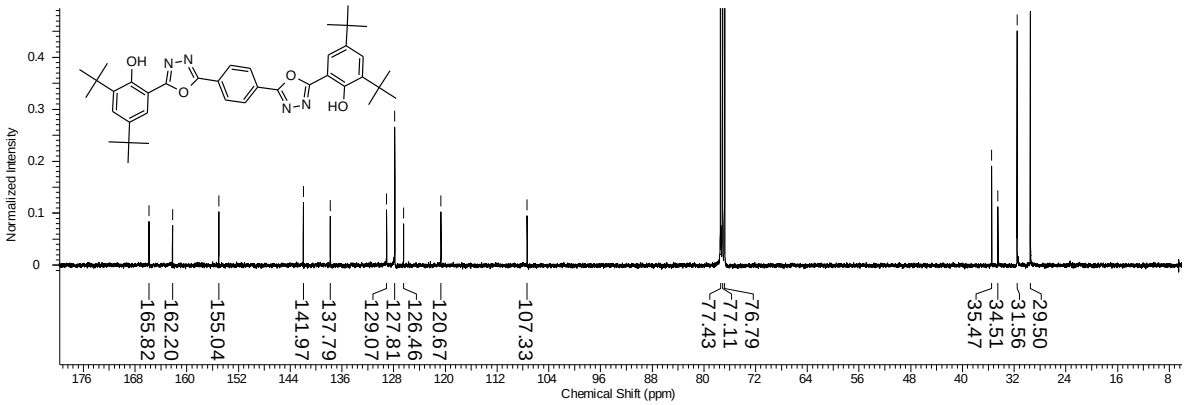

Figure A- 69 : ^{13}C NMR (100 MHz, $CDCl_3$) of **3.11**

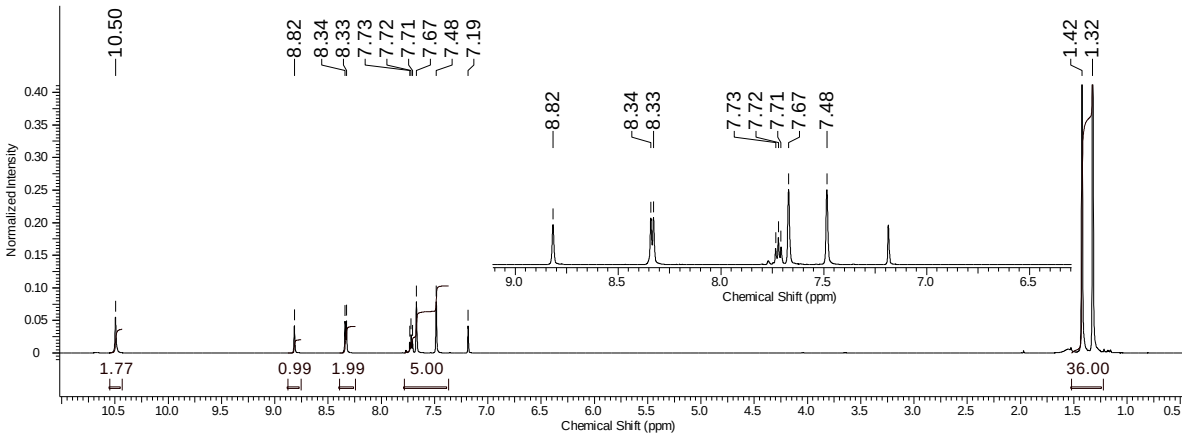

Figure A- 70 : ^{1}H NMR (400 MHz, $CDCl_3$) of compound **3.12**

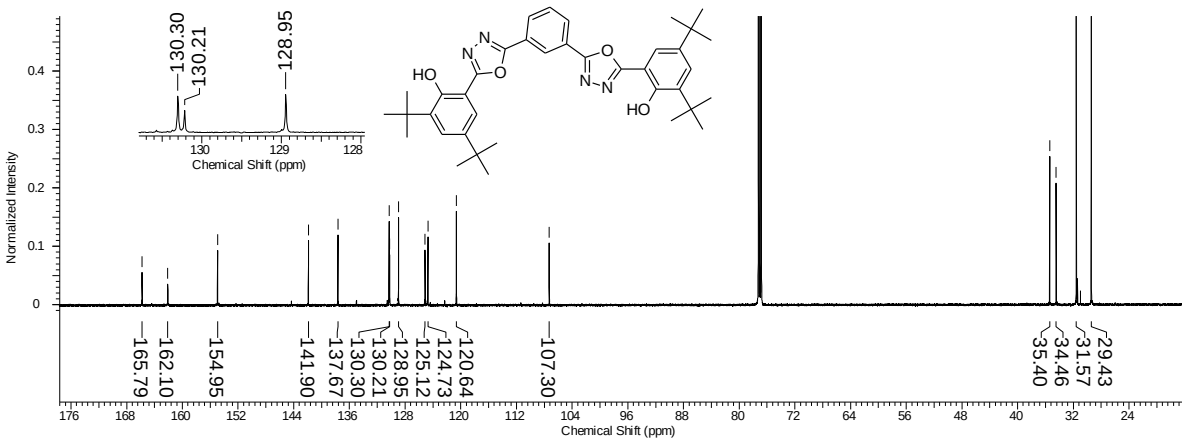

Figure A- 71 : ^{13}C NMR (100 MHz, $CDCl_3$) of **3.12**

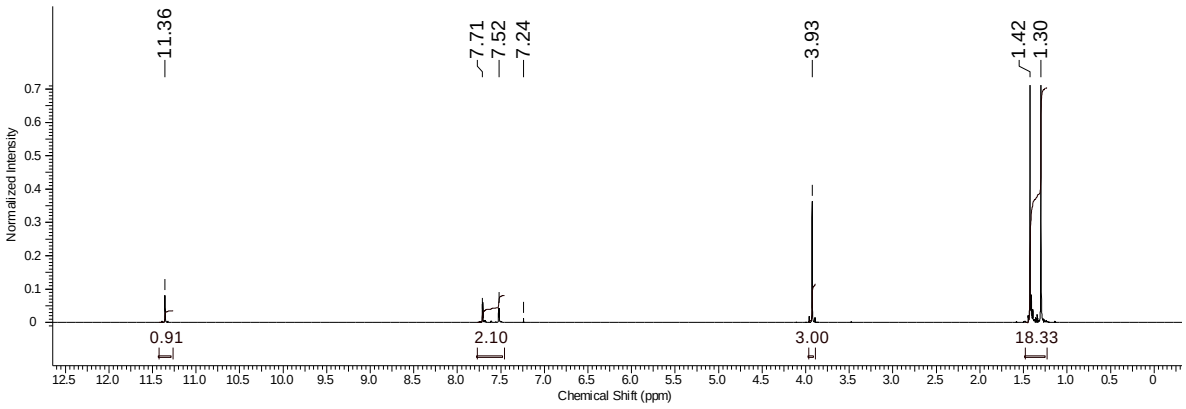

Figure A- 72 : ^{1}H NMR (400 MHz, $CDCl_3$) of compound **3.13**

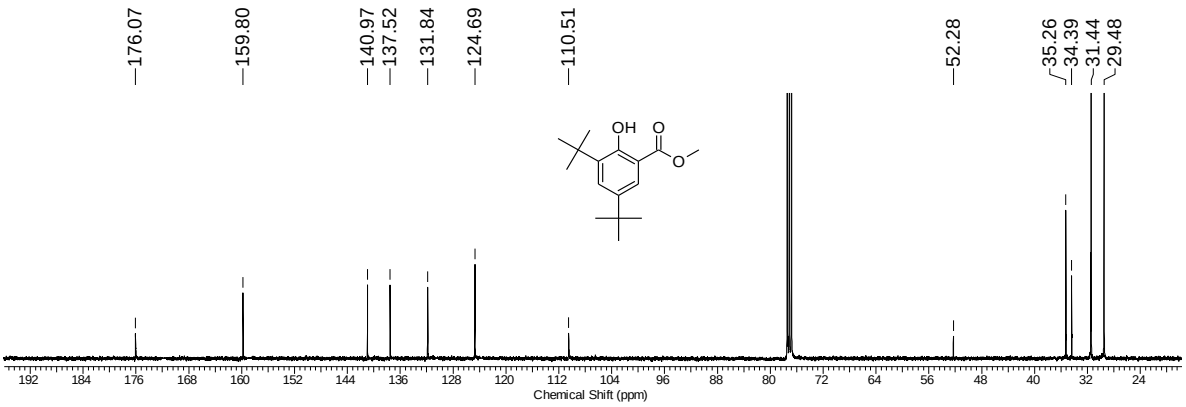

Figure A- 73 : ^{13}C NMR (100 MHz, $CDCl_3$) of compound **3.13**

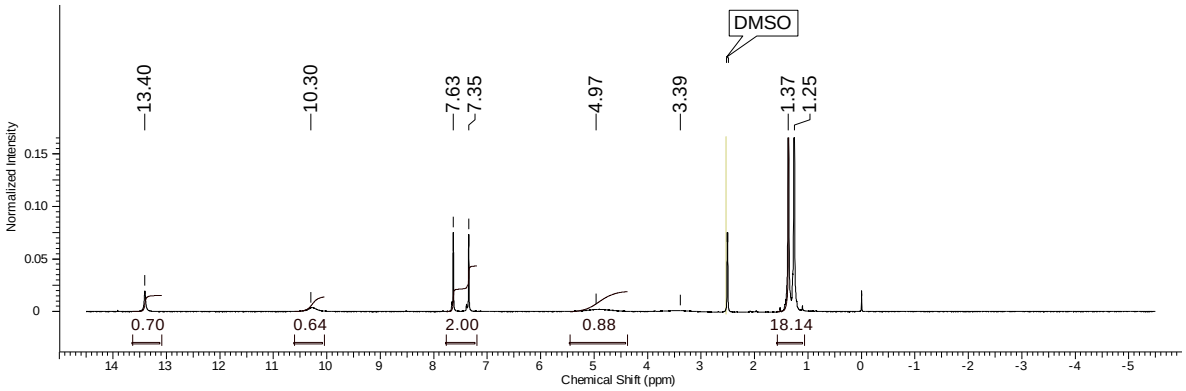

Figure A- 74 : ^{1}H NMR (400 MHz, $CDCl_3$) of compound **3.14**

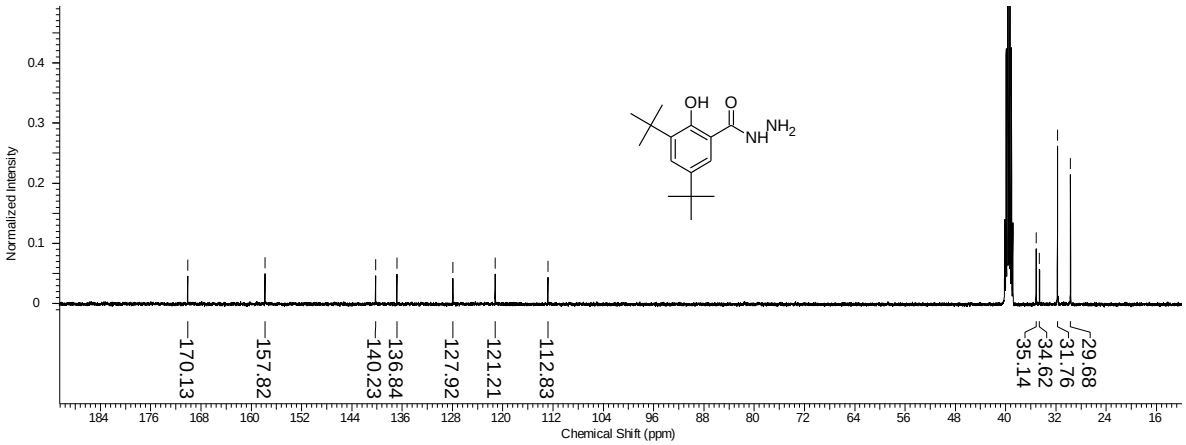

Figure A- 75 : ^{13}C NMR (100 MHz, $CDCl_3$) of compound **3.14**

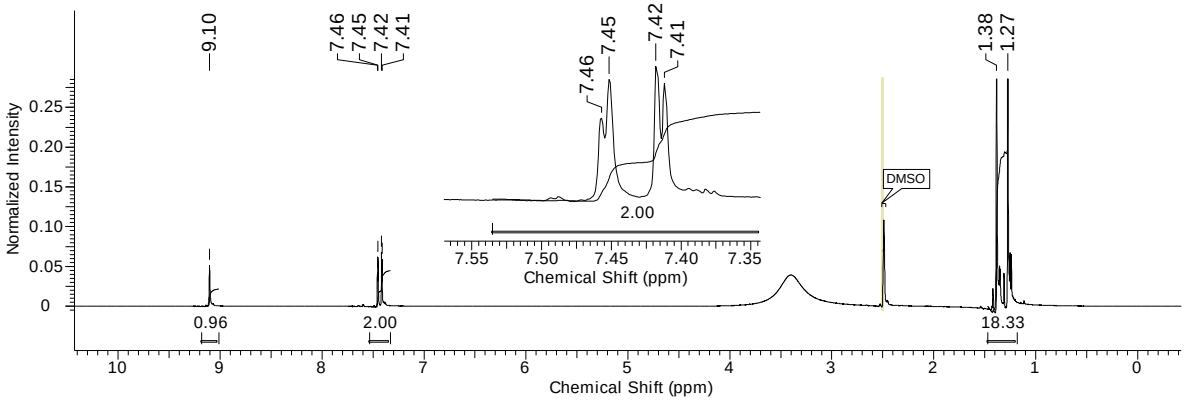

Figure A- 76 : ^{1}H NMR (400 MHz, DMSO-d_6) of **3.15**

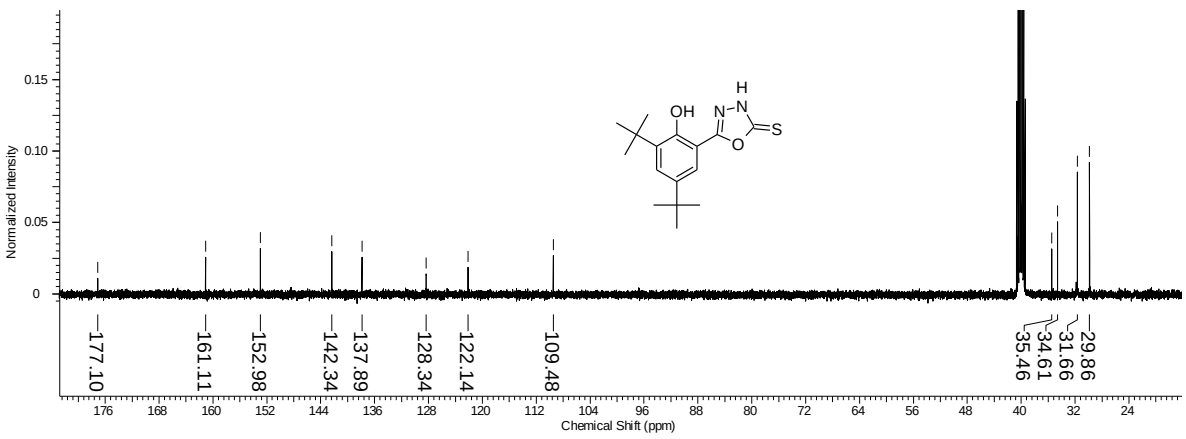

Figure A- 77 : ^{13}C NMR (100 MHz, DMSO-d_6) of **3.14**

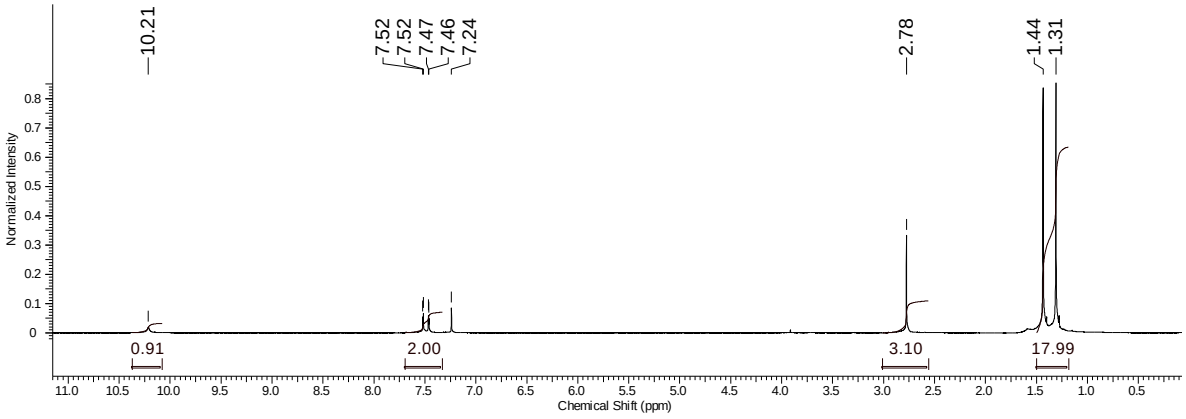

Figure A- 78 : ^{1}H NMR (400 MHz, $CDCl_3$) of **3.16**

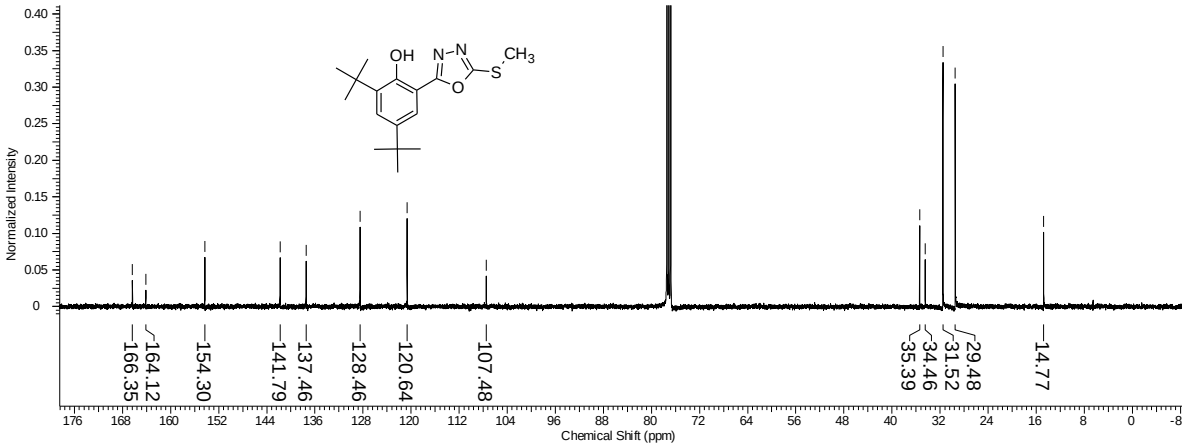

Figure A- 79 : ^{13}C NMR (100 MHz, $CDCl_3$) of **3.16**

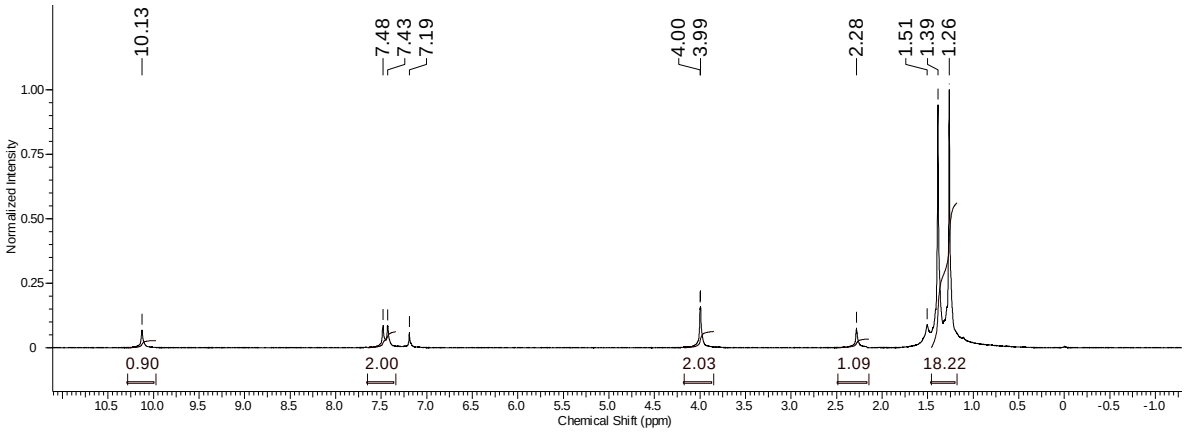

Figure A- 80 : ^{1}H NMR (400 MHz, $CDCl_3$) of **3.17**

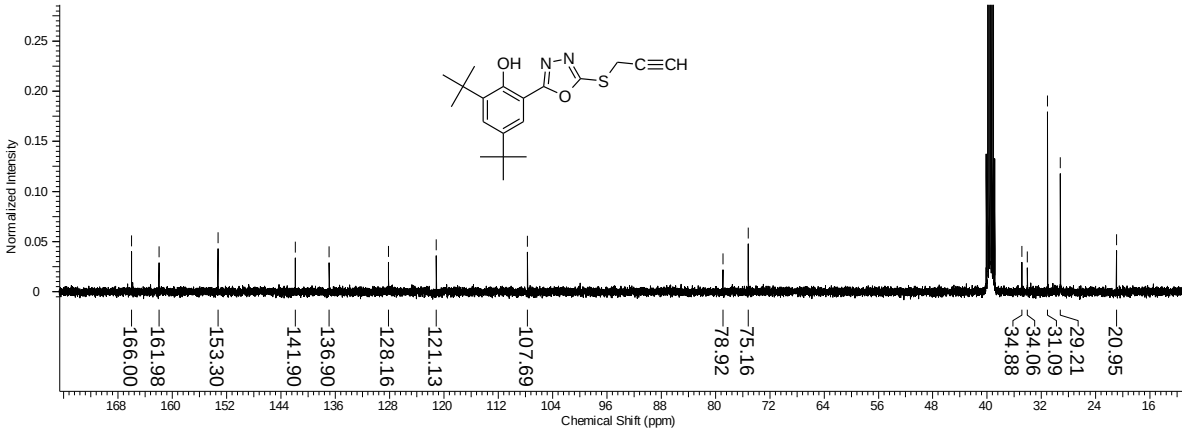

Figure A- 81 : ^{13}C NMR (100 MHz, DMSO-d_6) of **3.17**

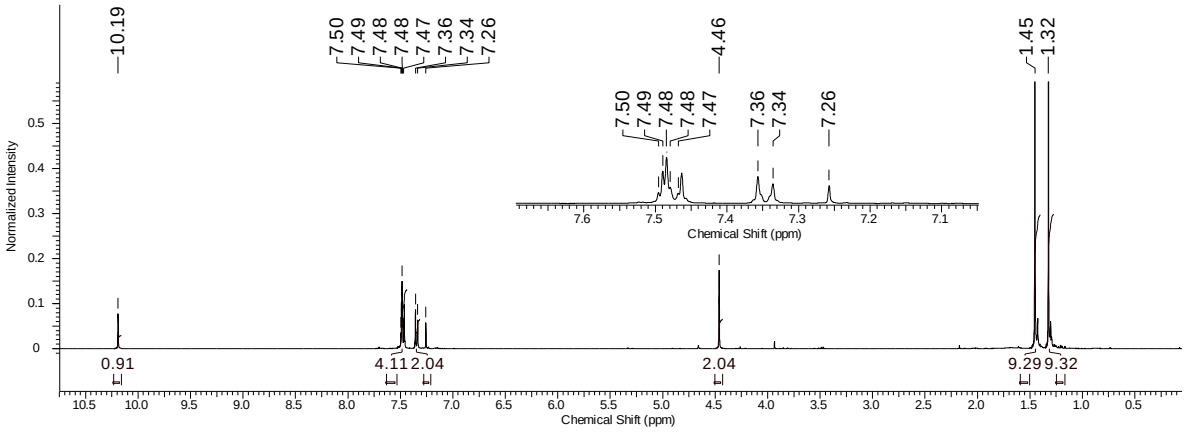

Figure A- 82 : ^{1}H NMR (400 MHz, $CDCl_3$) of **3.18**

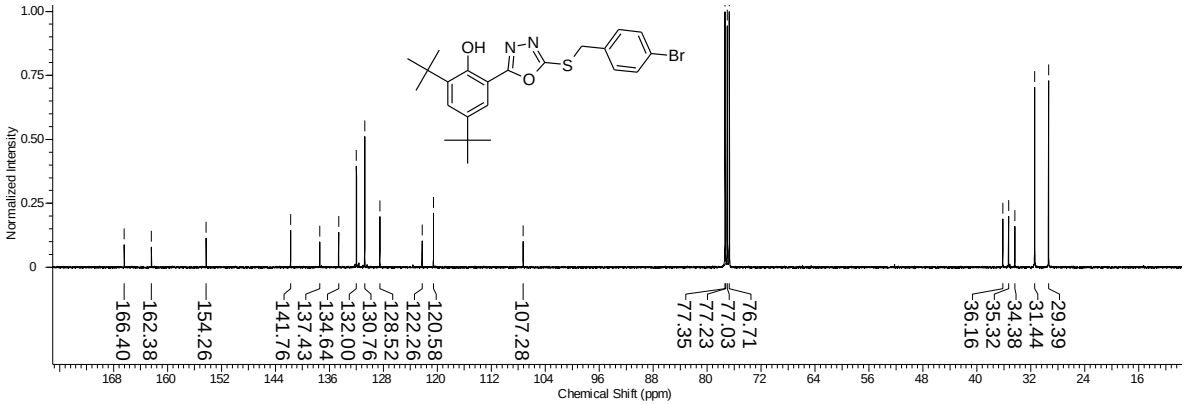

Figure A- 83 : ^{13}C NMR (100 MHz, $CDCl_3$) of **3.18**

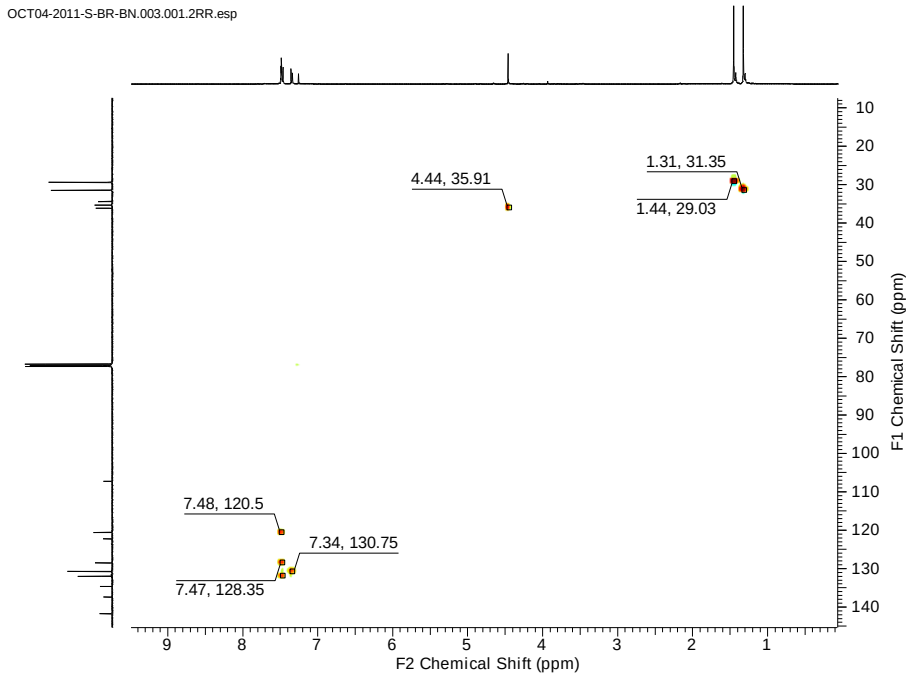

Figure A- 84 : HSQC of compound **3.18**

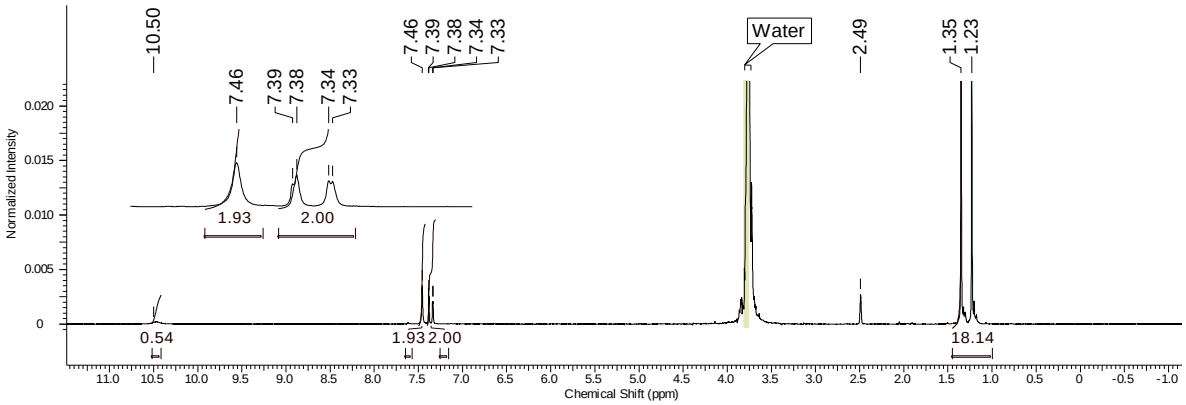

Figure A- 85 : ^{1}H NMR (400 MHz, DMSO-d_6) of **3.19**

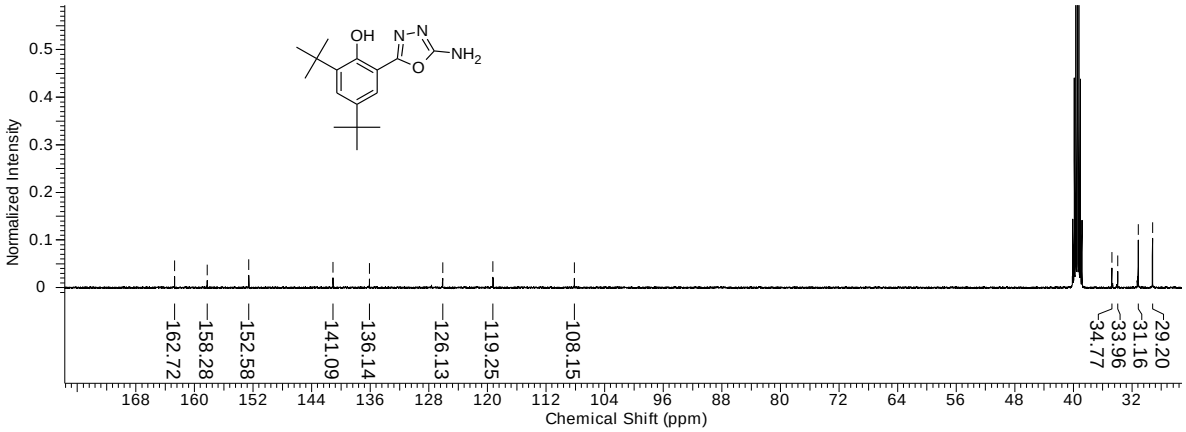

Figure A- 86 : ^{13}C NMR (100 MHz, DMSO-d_6) of **3.19**

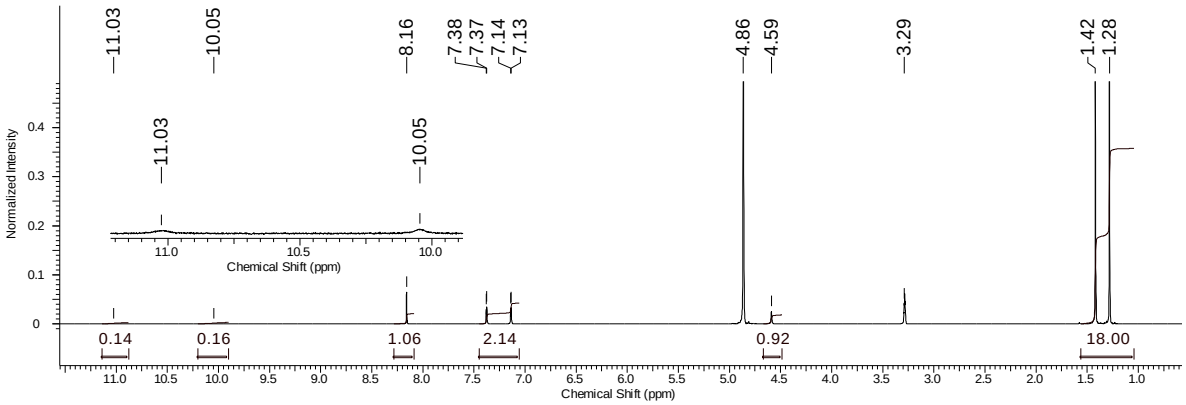

Figure A- 87 : ^{1}H NMR (400 MHz, DMSO-d_6) of **3.20**

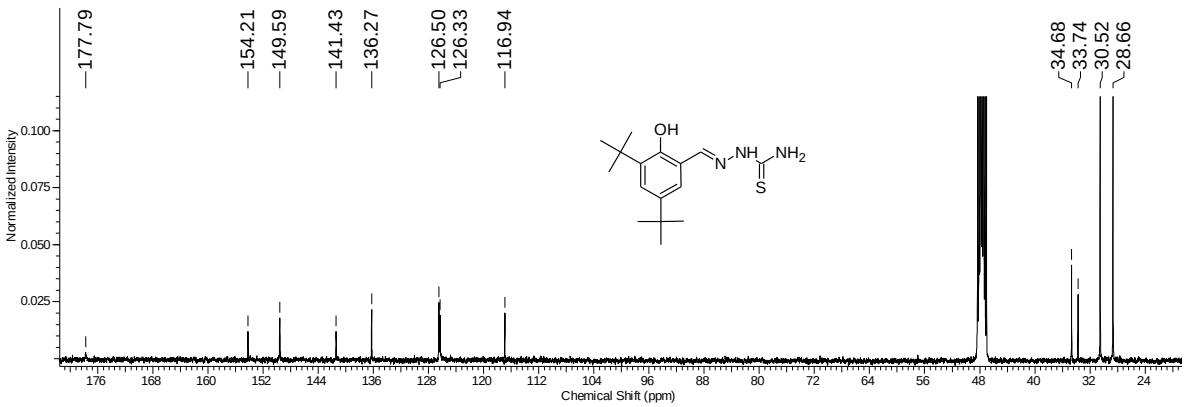

Figure A- 88 : ^{13}C NMR (100 MHz, DMSO-d_6) of **3.20**

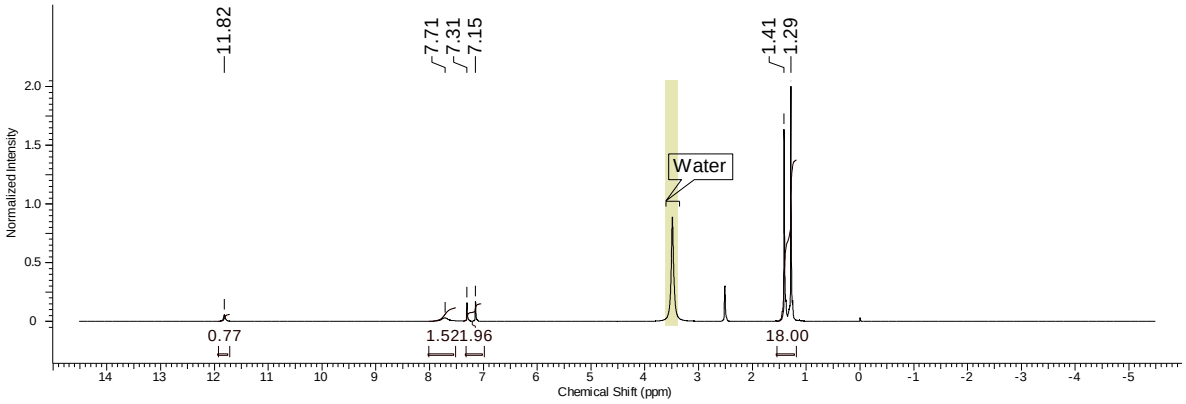

Figure A- 89 : ^{1}H NMR (400 MHz, DMSO-d_6) of **3.21**

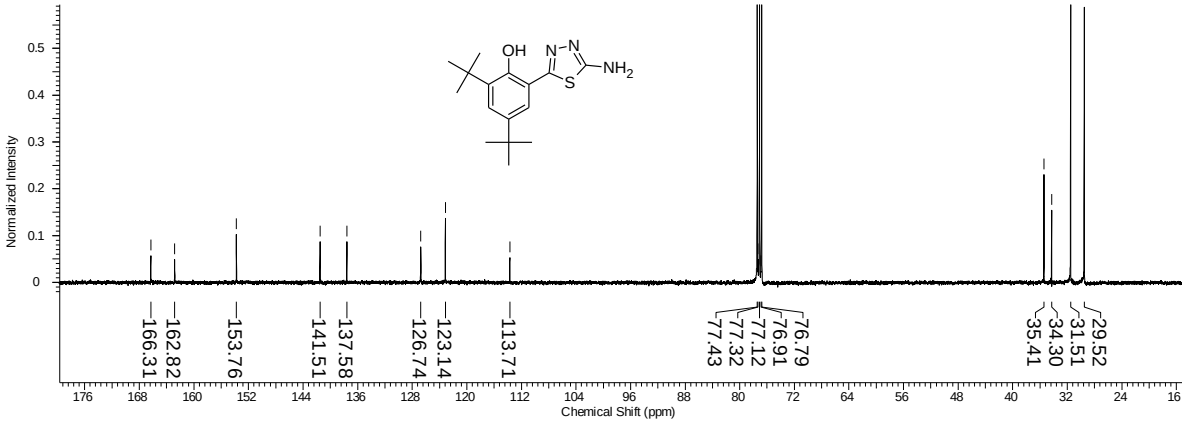

Figure A- 90 : ^{13}C NMR (100 MHz, $CDCl_3$) of **3.21**

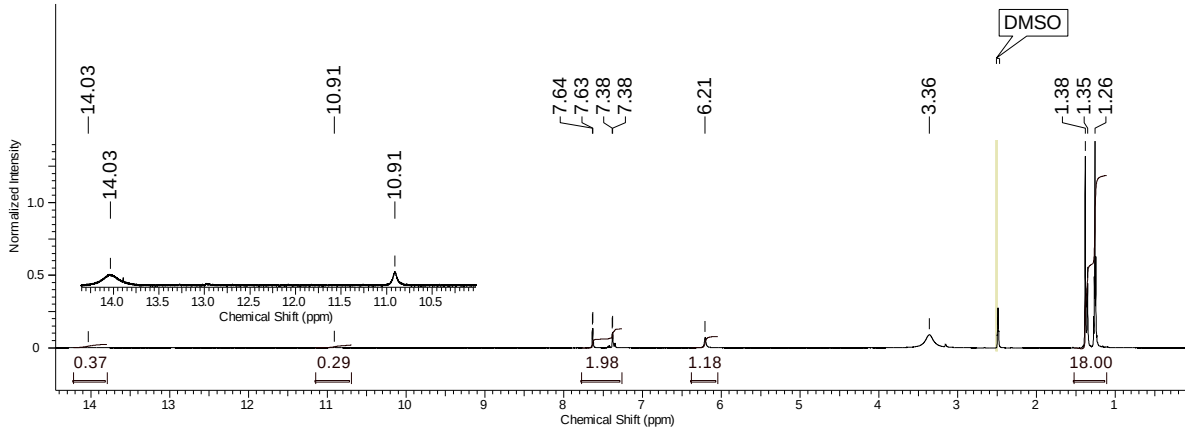

Figure A- 91 : ^{1}H NMR (400 MHz, DMSO-d_6) of **3.22**

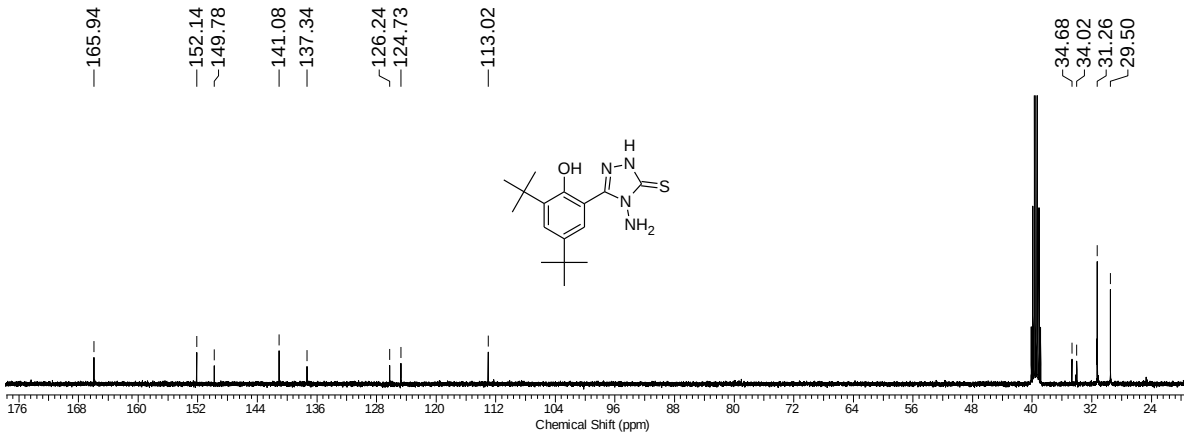

Figure A- 92 : ^{13}C NMR (100 MHz, DMSO-d_6) of **3.22**

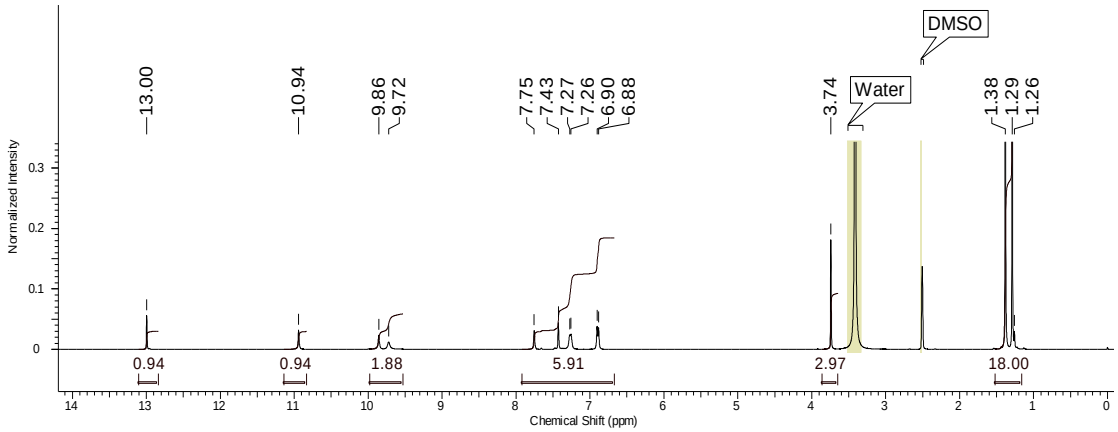

Figure A- 93 : ^{1}H NMR (600 MHz, DMSO-d_6) of **3.23**

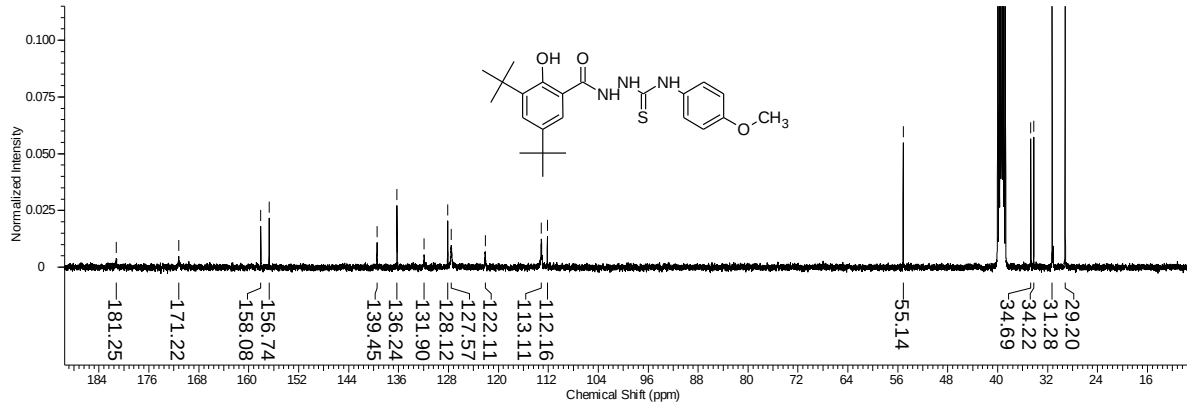

Figure A- 94 : ^{13}C NMR (150 MHz, DMSO-d_6) of **3.23**

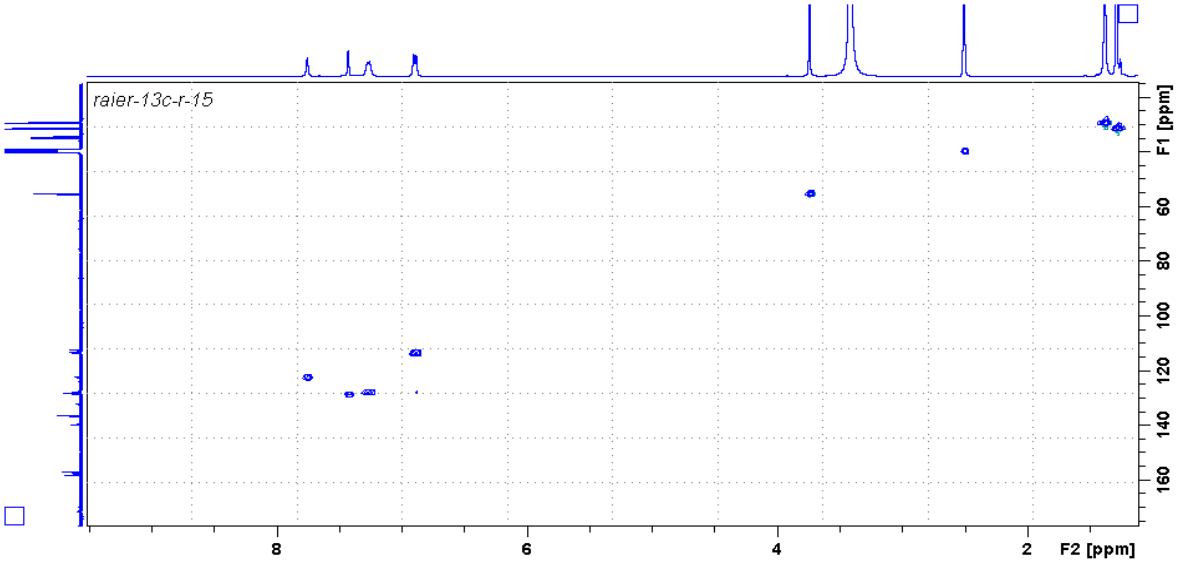

Figure A- 95 : HSQC of **3.23**

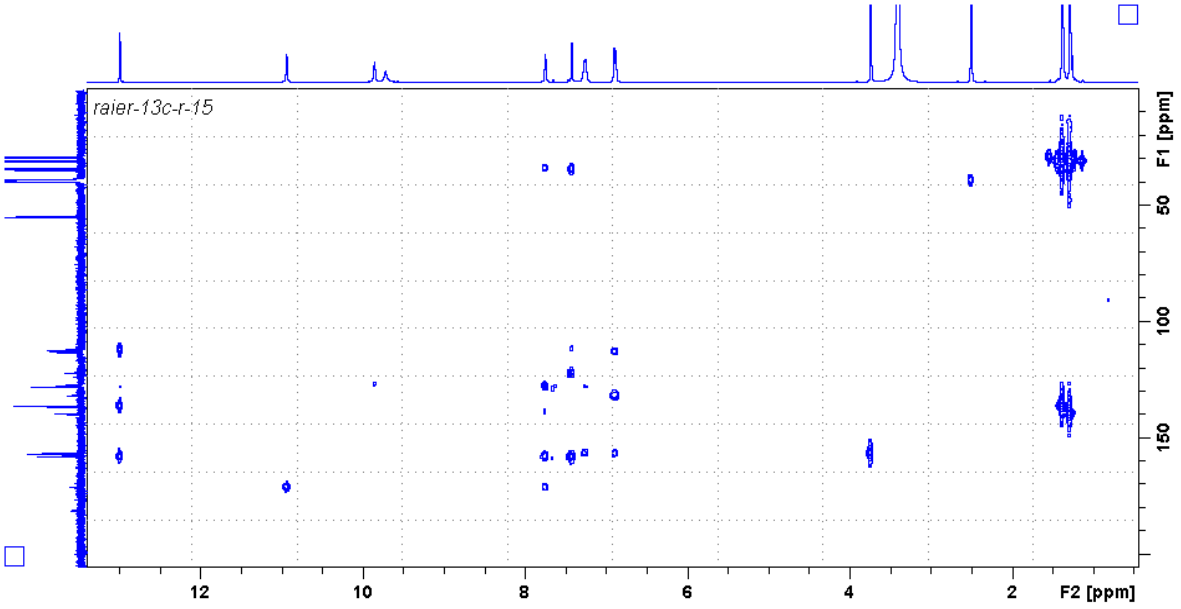

Figure A- 96 : HMBC of **3.23**

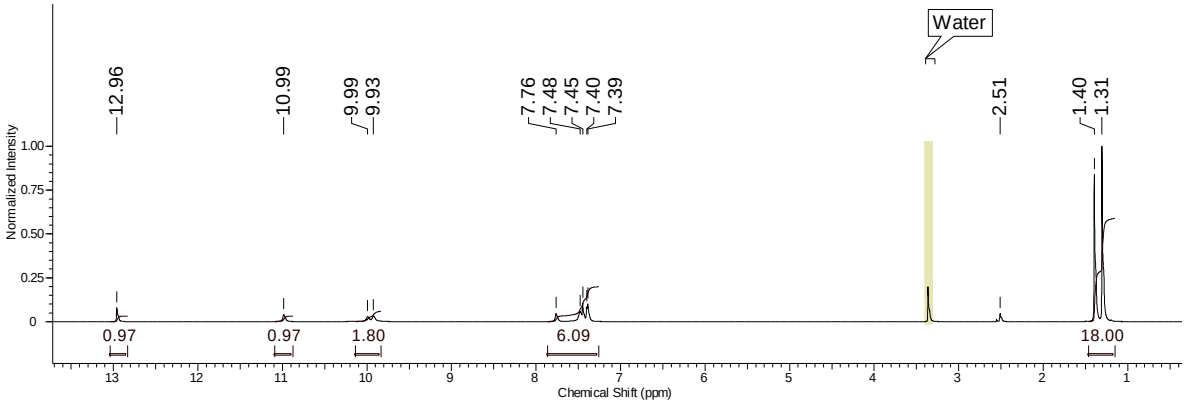

Figure A- 97 : ^{1}H NMR (600 MHz, DMSO-d_6) of **3.24**

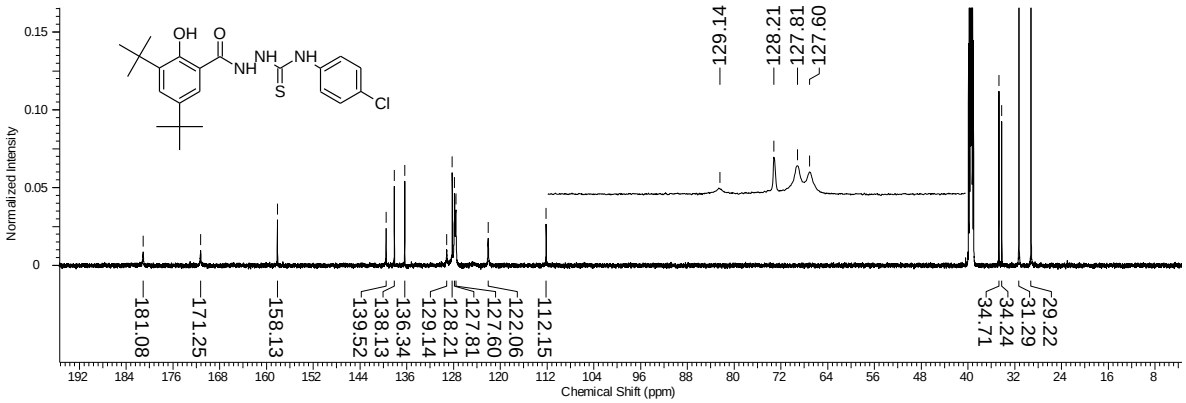

Figure A- 98 : ^{13}C NMR (150 MHz, DMSO-d_6) of **3.24**

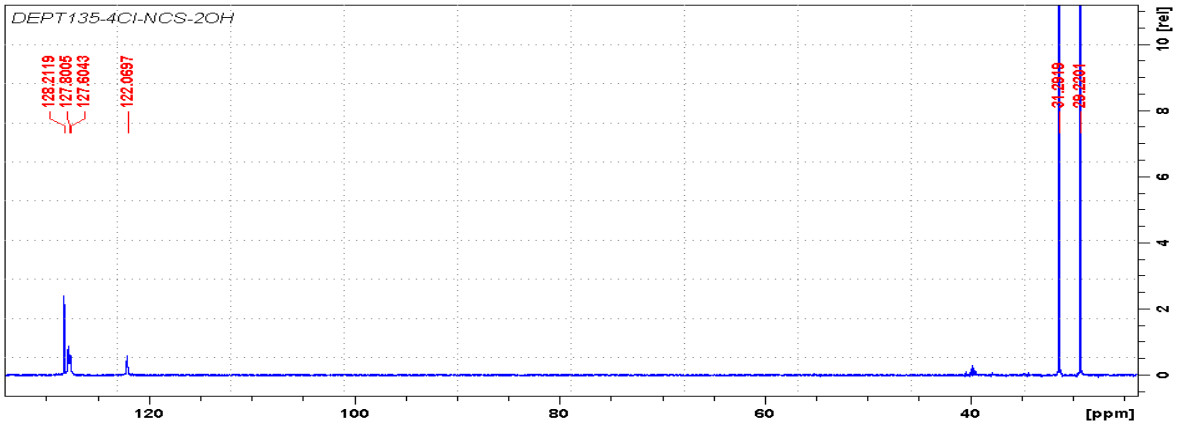

Figure A- 99 : Dept-135 of **3.24**

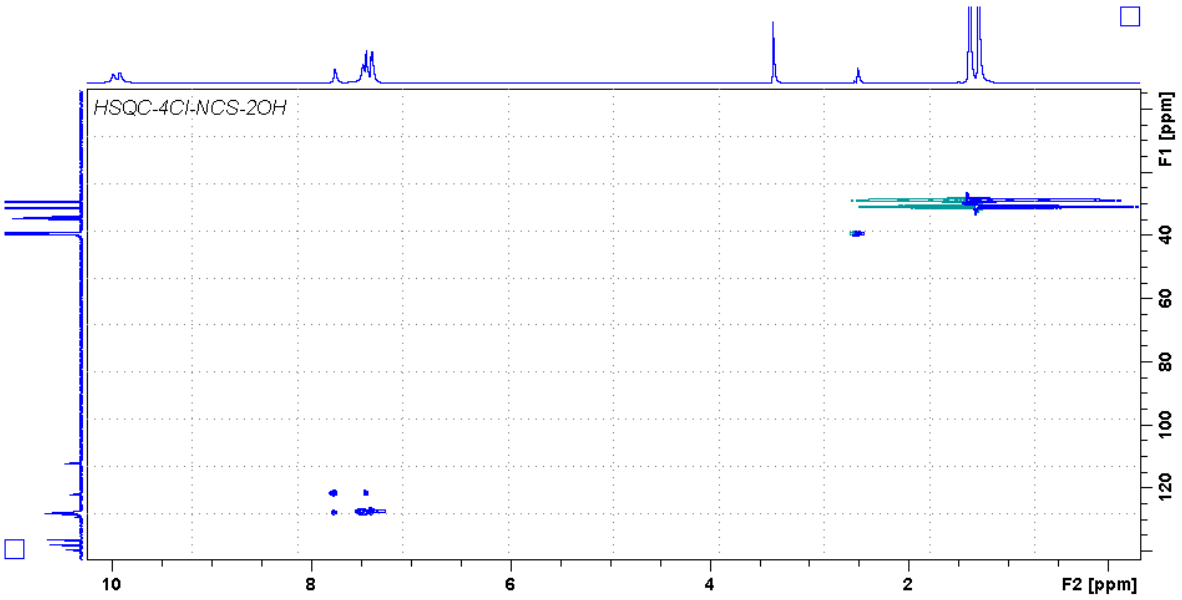

Figure A- 100 : HSQC of **3.24**

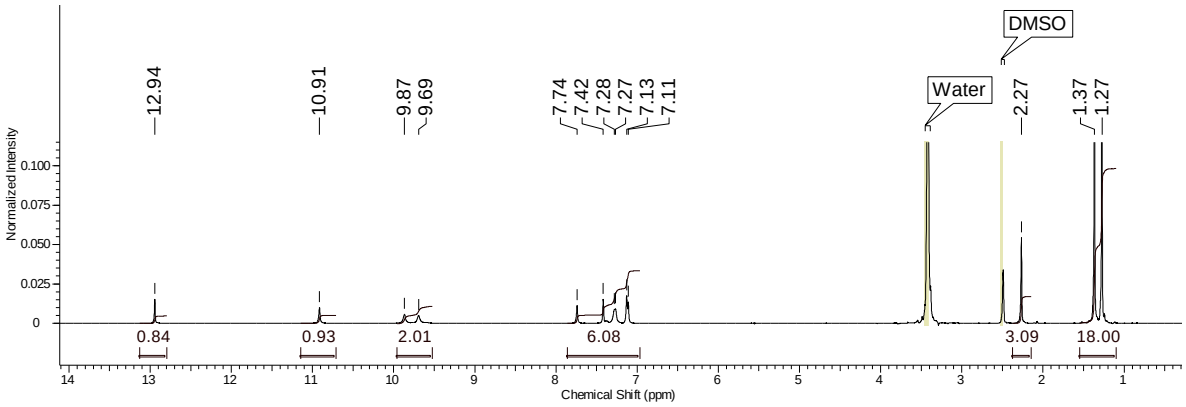

Figure A- 101 : ^{1}H NMR (600 MHz, DMSO-d_6) of **3.25**

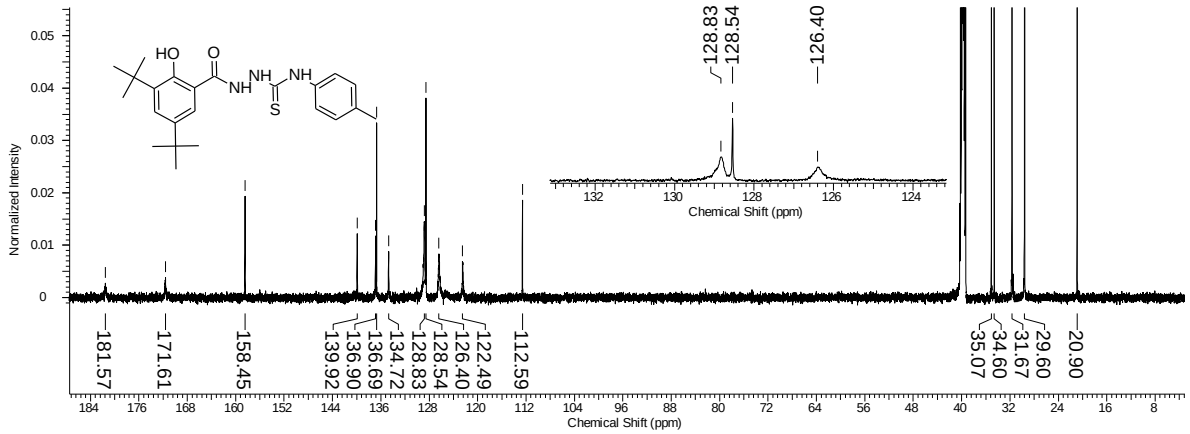

Figure A- 102 : ^{13}C NMR (150 MHz, DMSO-d_6) of **3.25**

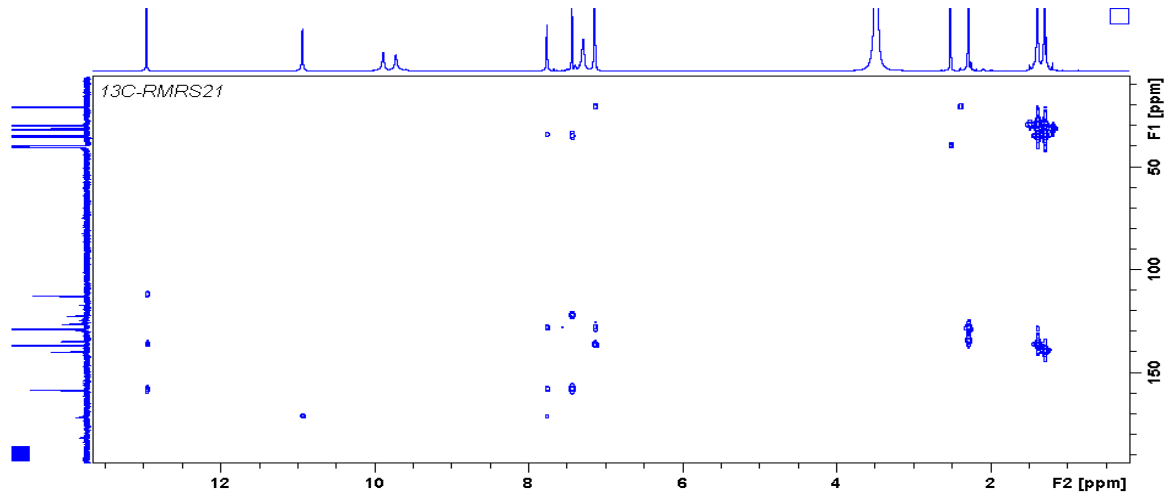

Figure A- 103 : HMBC of **3.25**

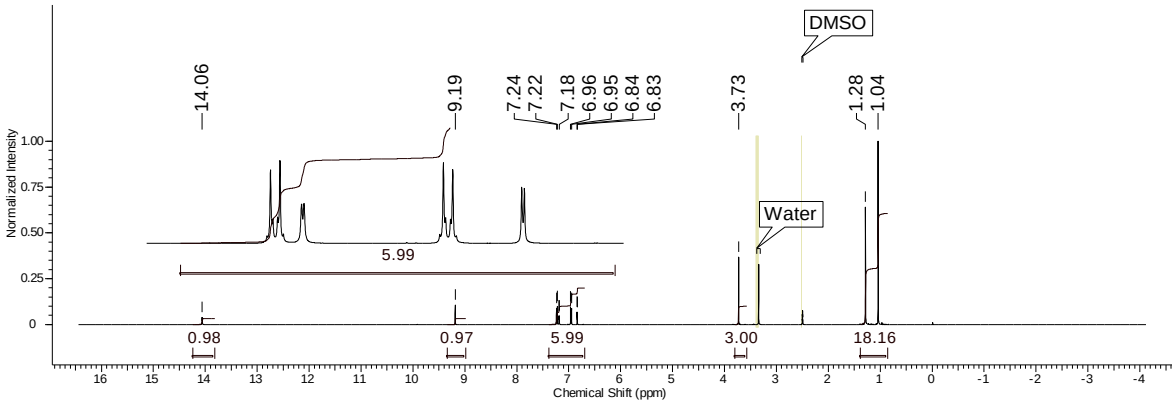

Figure A- 104 : ^{1}H NMR (600 MHz, DMSO-d_6) of **3.26**

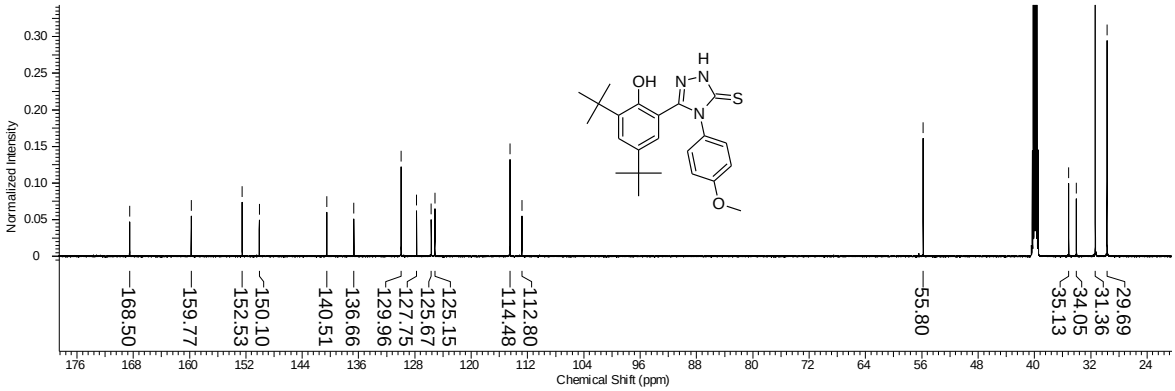

Figure A- 105 : ^{13}C NMR (150 MHz, DMSO-d_6) of **3.26**

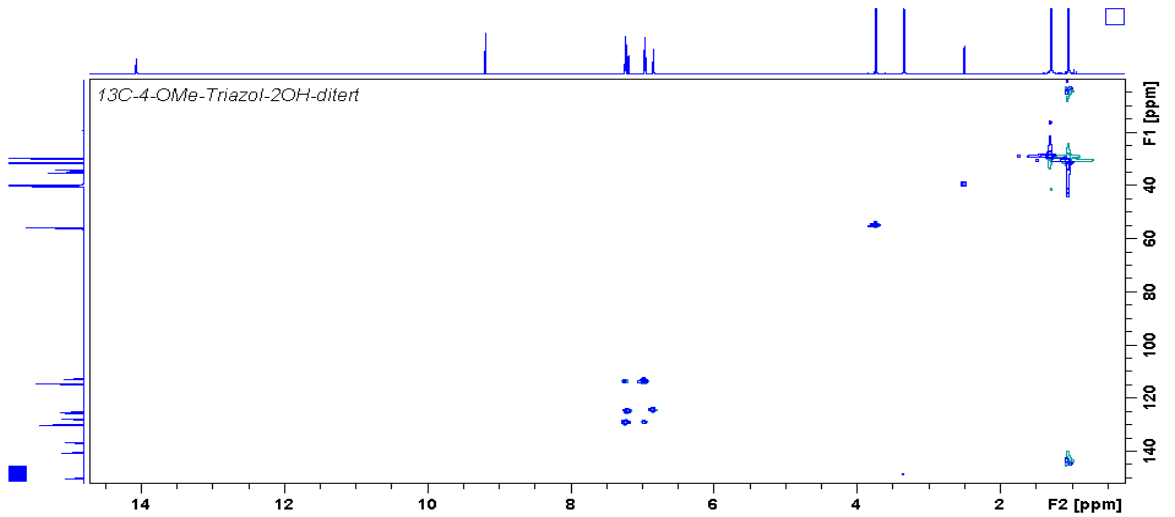

Figure A- 106 : HSQC of **3.26**

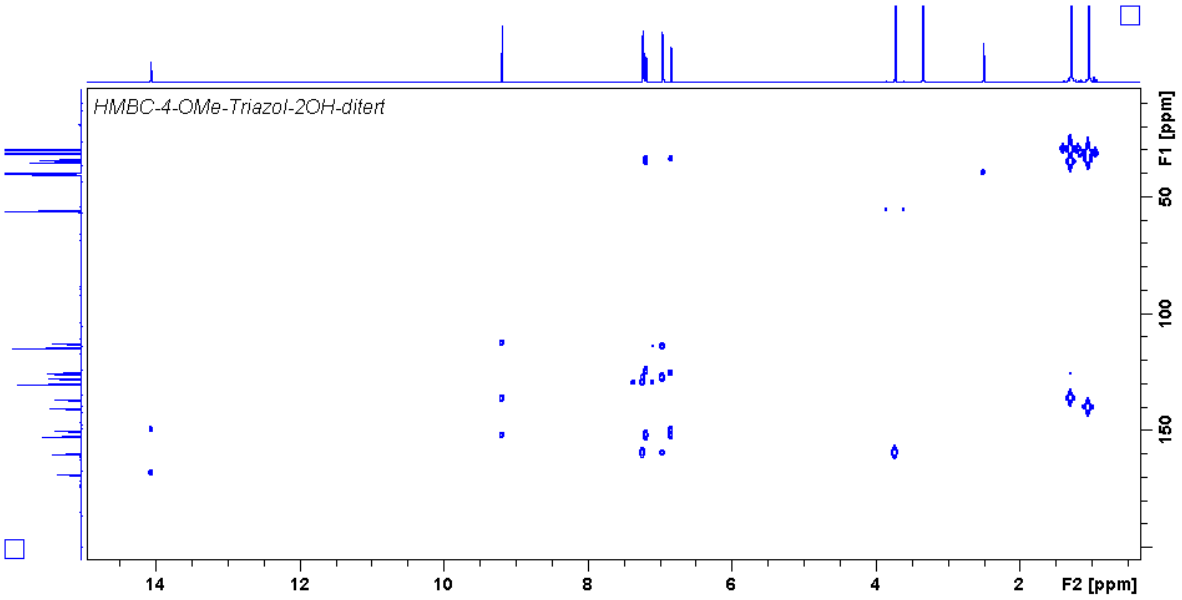

Figure A- 107 : HMBC of **3.26**

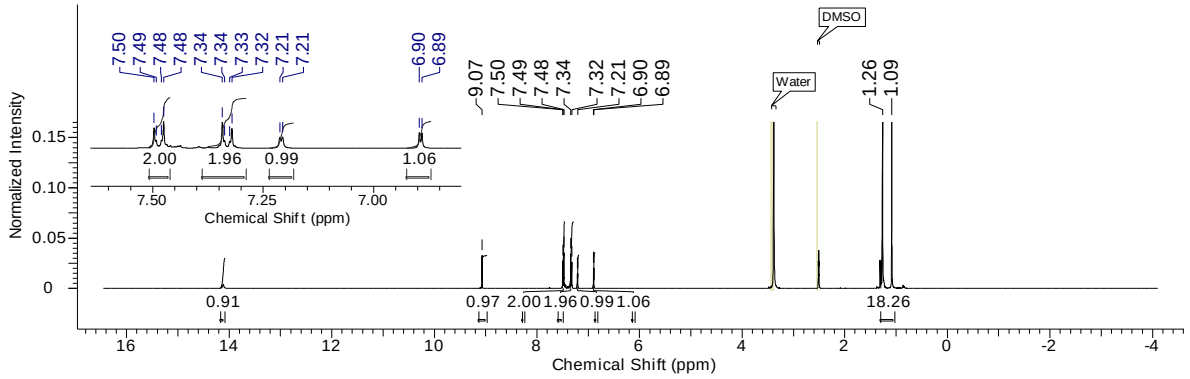

Figure A- 108 : ^{1}H NMR (400 MHz, DMSO-d_6) of **3.27**

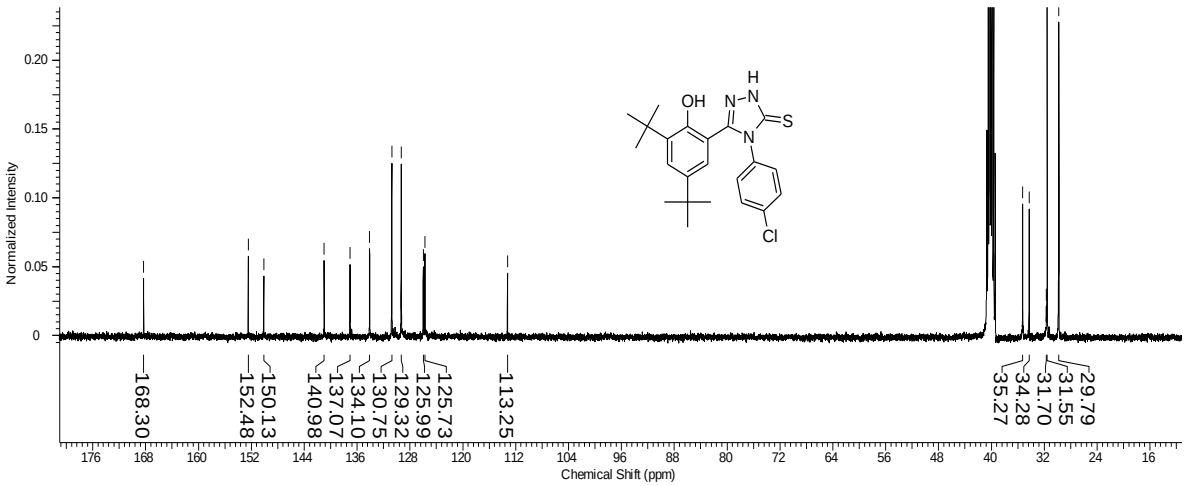

Figure A- 109 : ^{13}C NMR (100 MHz, DMSO-d_6) of **3.27**

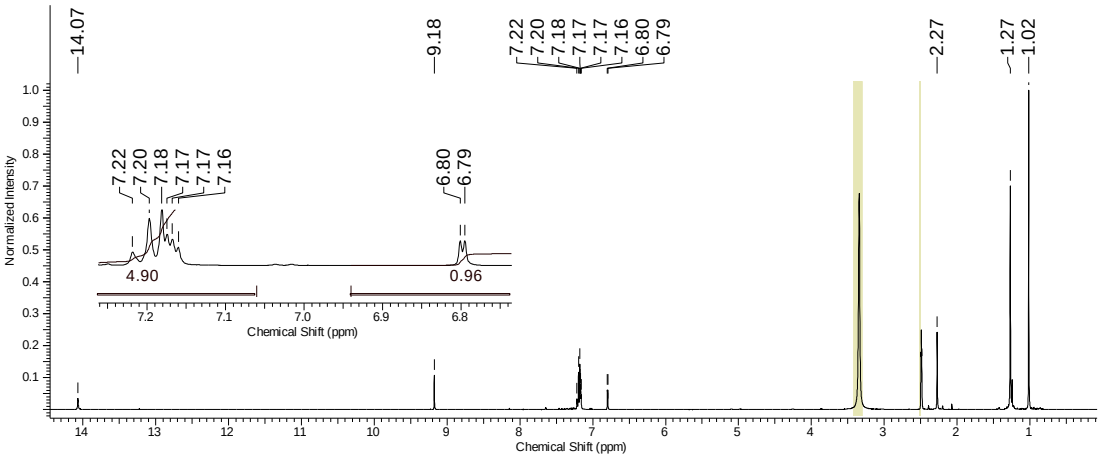

Figure A- 110 : ^{1}H NMR (400 MHz, DMSO-d_6) of **3.28**

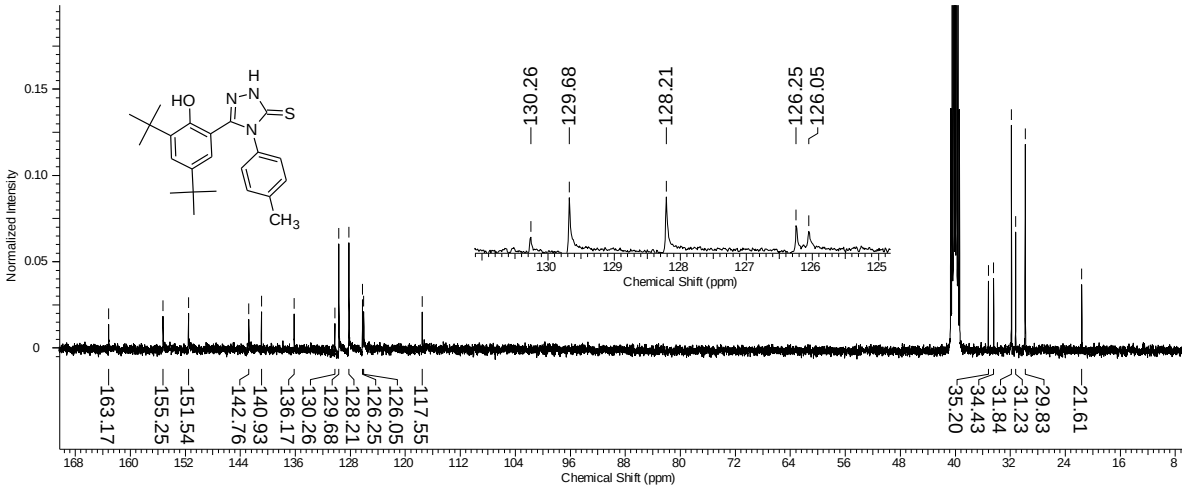

Figure A- 111 : ^{13}C NMR (100 MHz, DMSO-d_6) of **3.28**

Appendix B Selective Mass Spectroscopy

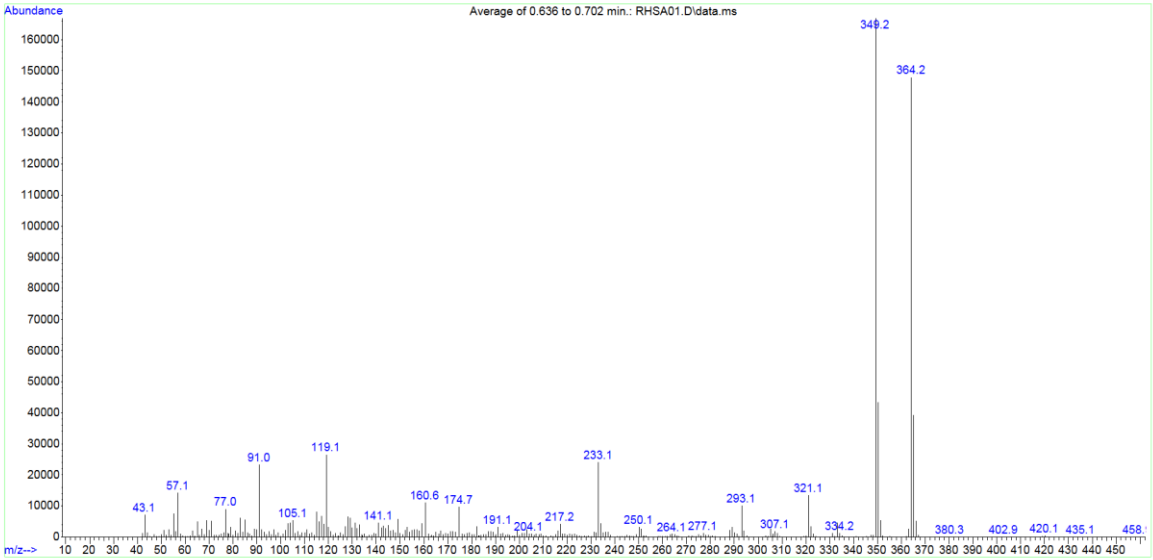

Figure B- 1 : EIMs spectrum of **2.12**

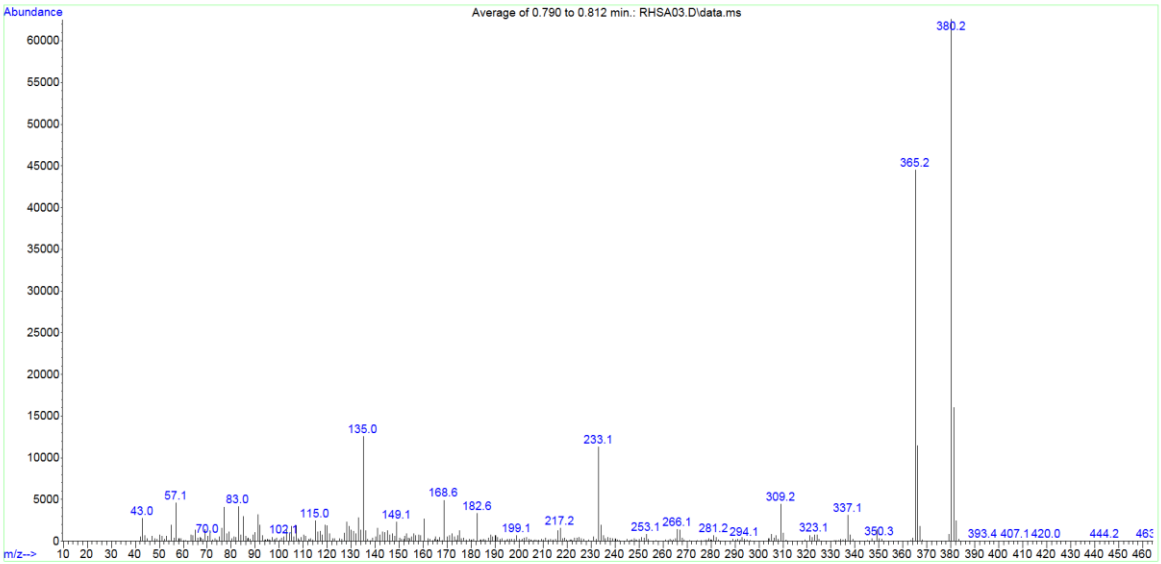

Figure B- 2 : EIMS spectrum of **2.13**

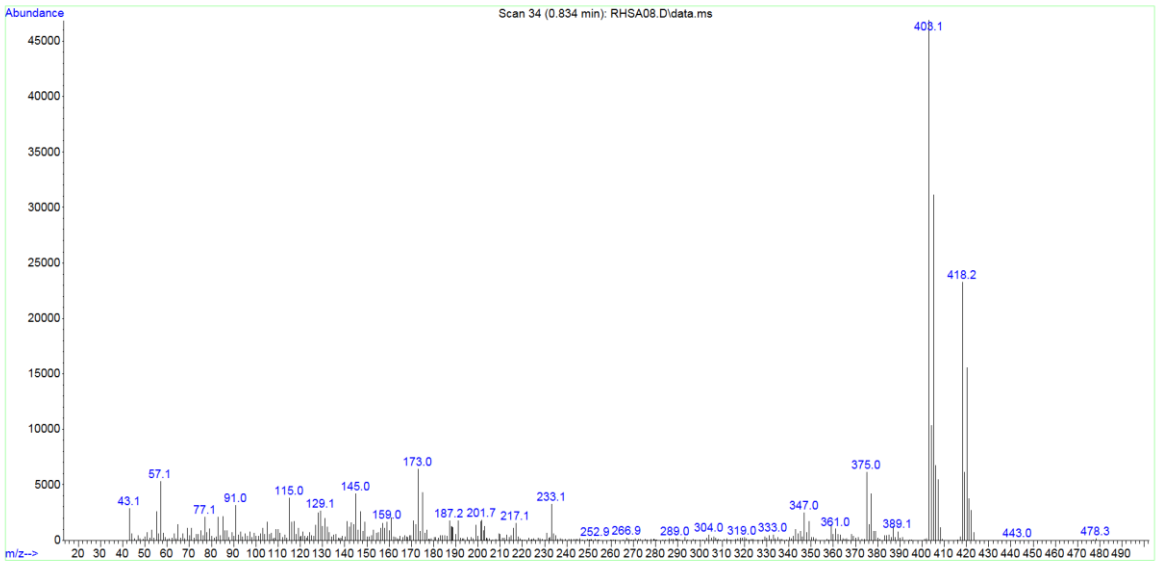

Figure B- 3 : EIMS spectrum of **2.18**

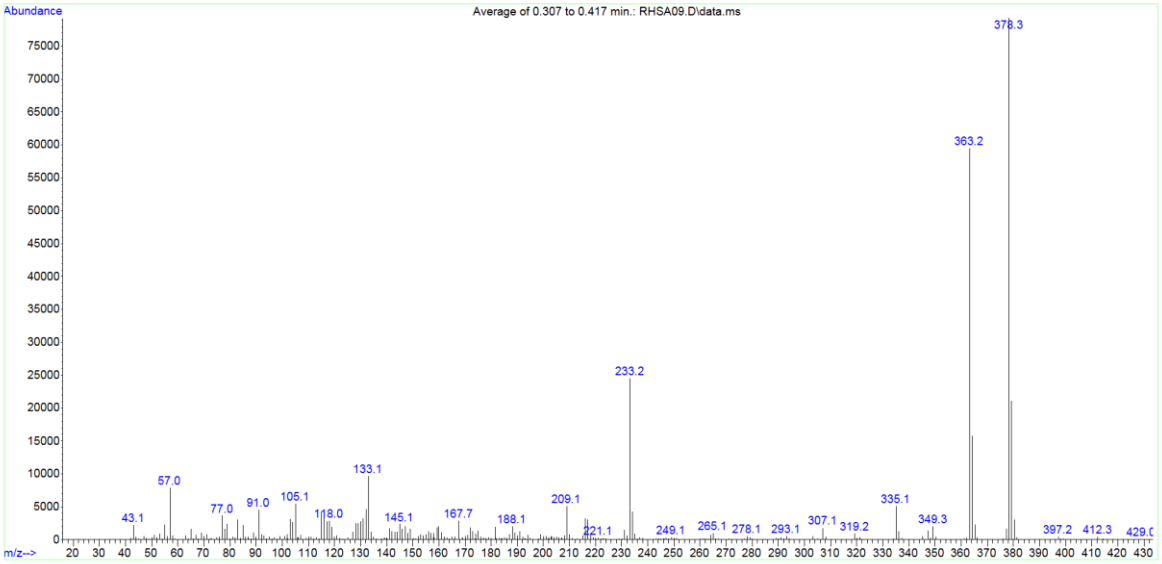

Figure B- 4 : EIMS spectrum of **2.20**

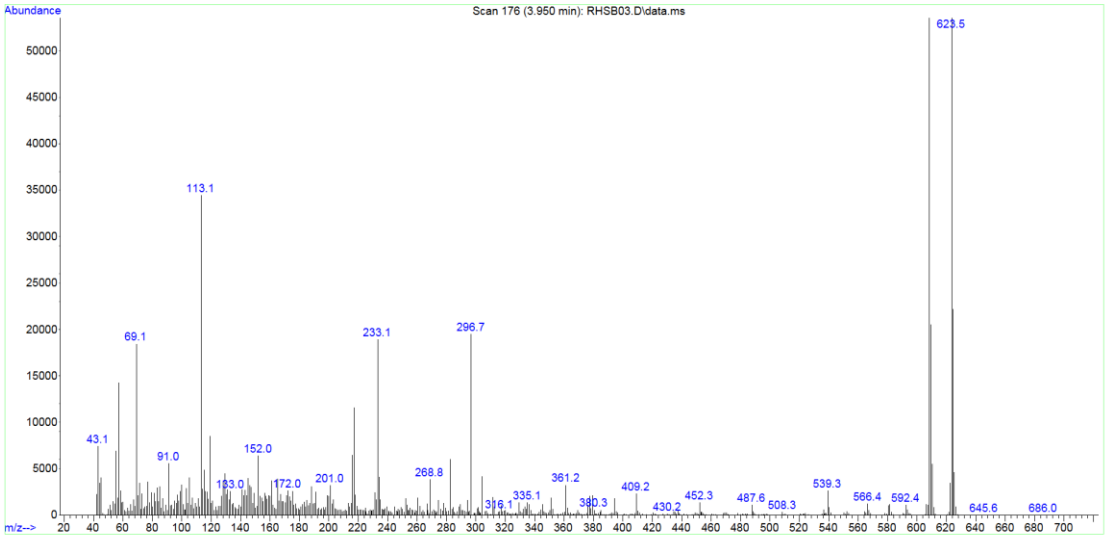

Figure B- 5 : EIMS spectrum of **2.20**

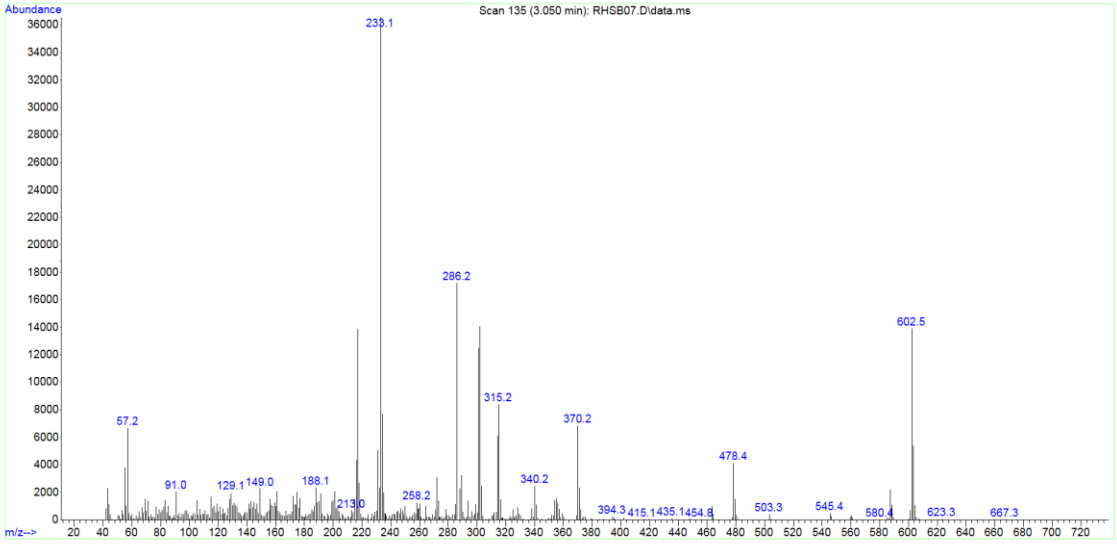

Figure B- 6 : EIMS spectrum of **2.20**

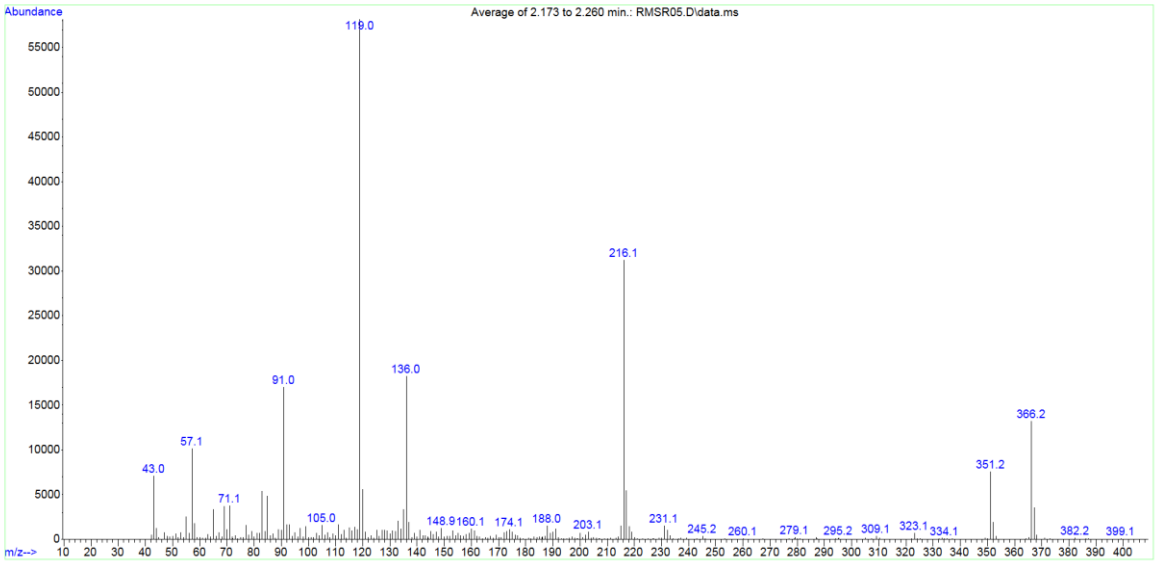

Figure B- 7 : EIMS spectrum of **3.1**

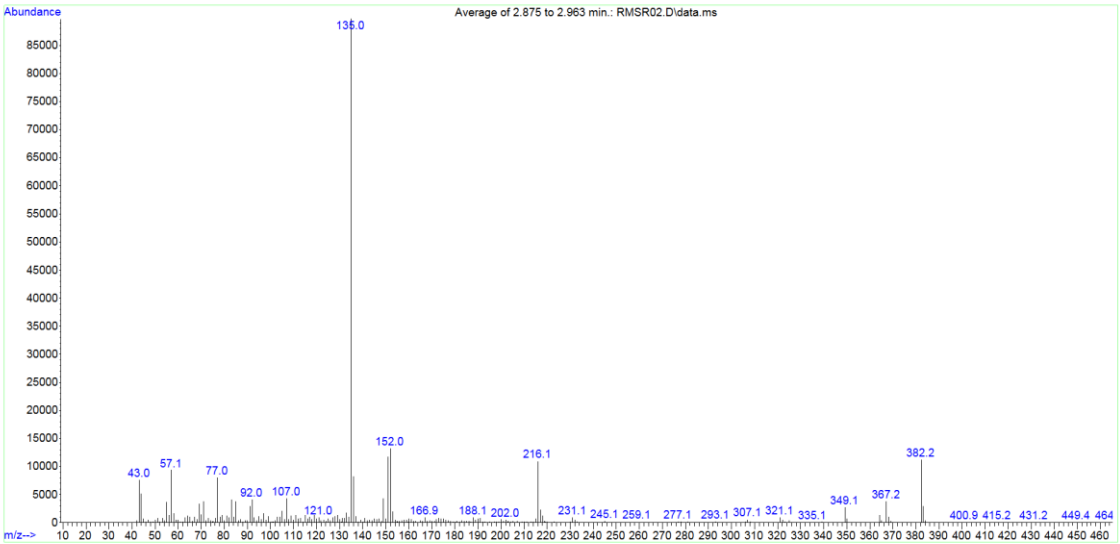

Figure B- 8 : EIMS spectrum of **3.2**

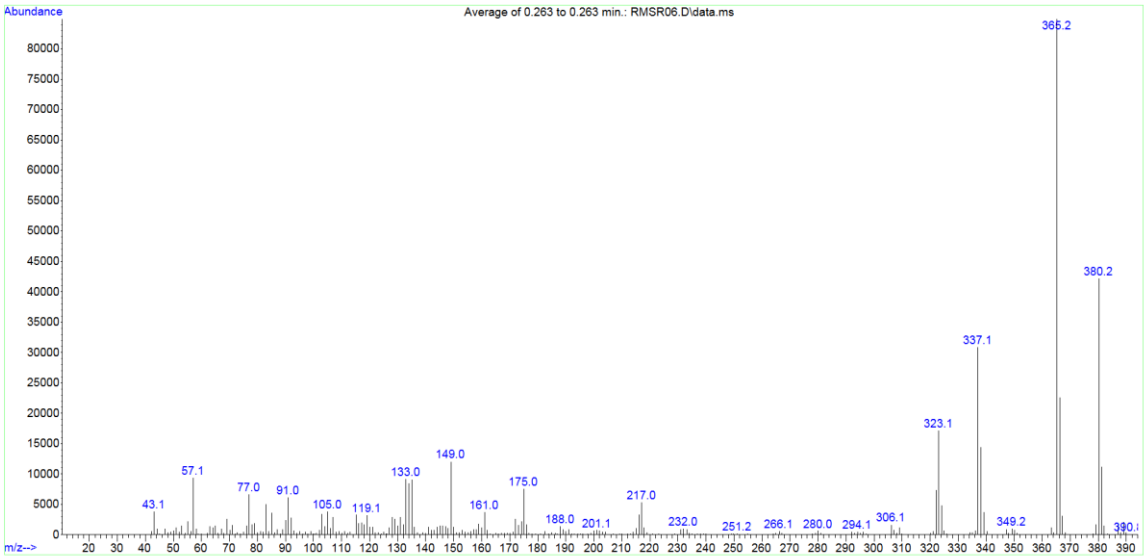

Figure B- 9 : EIMS spectrum of **3.6**

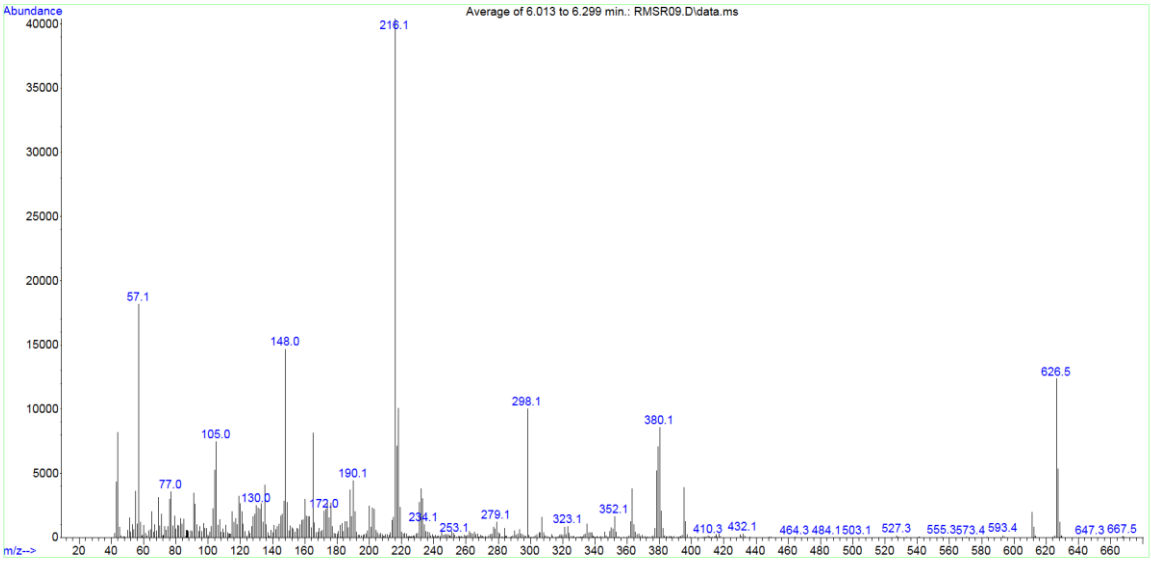

Figure B-10 : EIMS spectrum of **3.10**

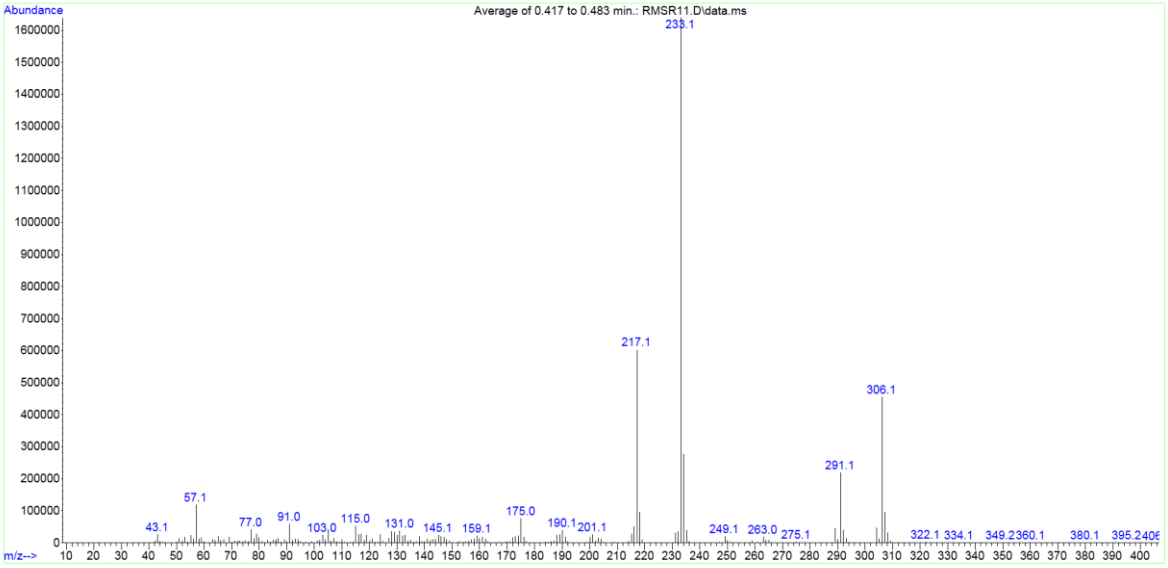

Figure B- 11 : EIMS spectrum of **3.15**

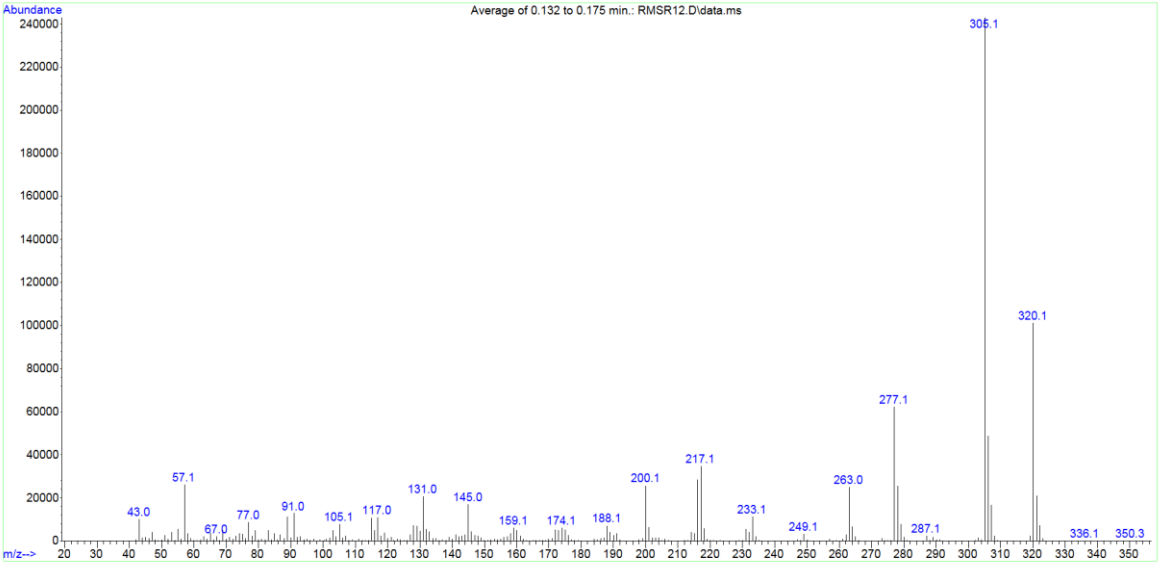

Figure B- 12 : EIMS spectrum of **3.16**

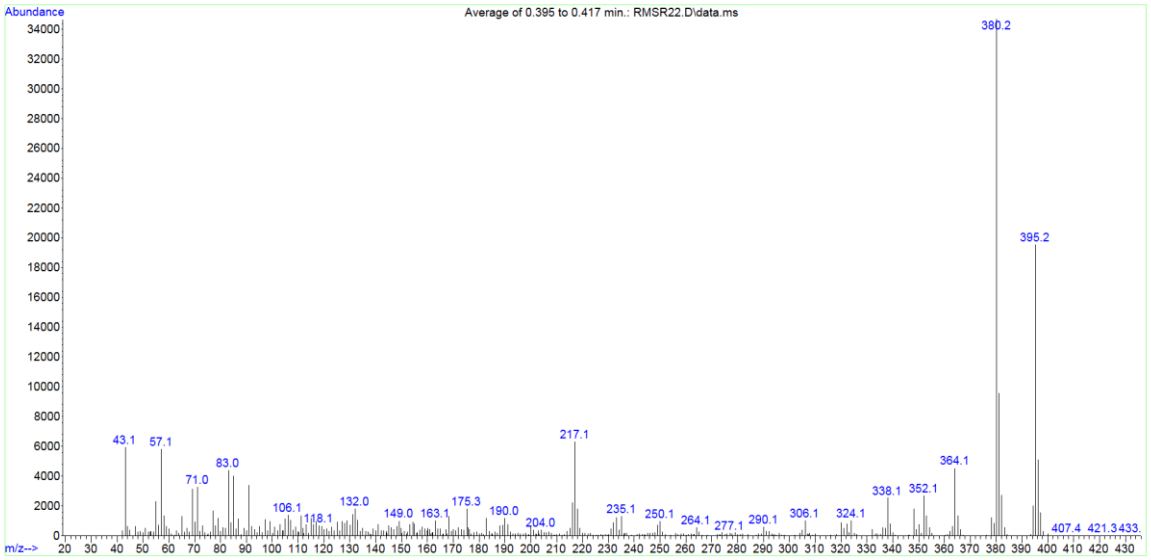

Figure B- 5 : EIMS spectrum of **3.28**

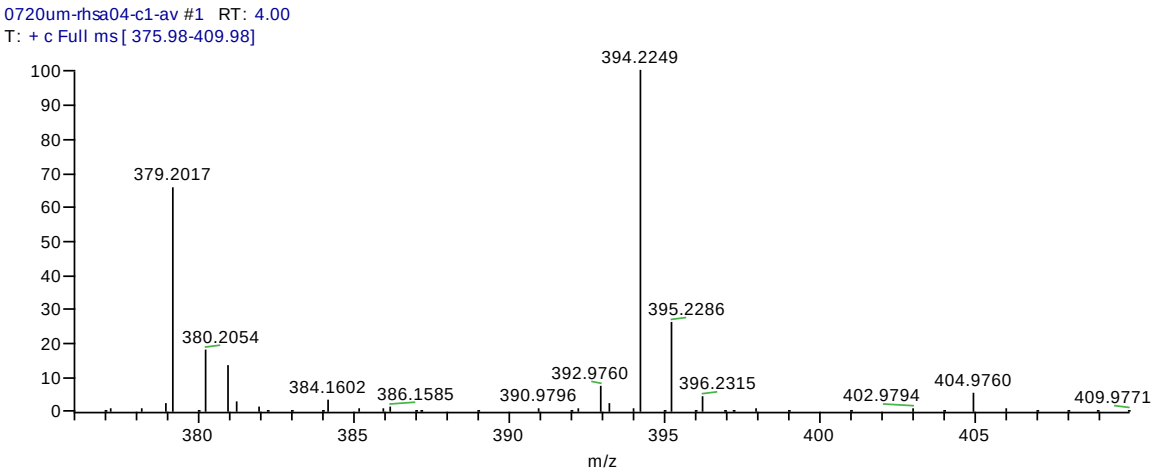

0720um-rhsa04-c1-av#1 RT: 4.00
T: + c Full ms [375.98-409.98]
m/z= 393.98-394.31

m/z	Intensity	Relative	Theo. Mass	Delta (ppm)	RDB equiv.	Composition
394.2249	8951296.0	100.00	394.2256	-1.89	11.0	$C_{24}H_{30}O_3N_2$

Figure B- 6 : HREIMS spectrum of **2.14**

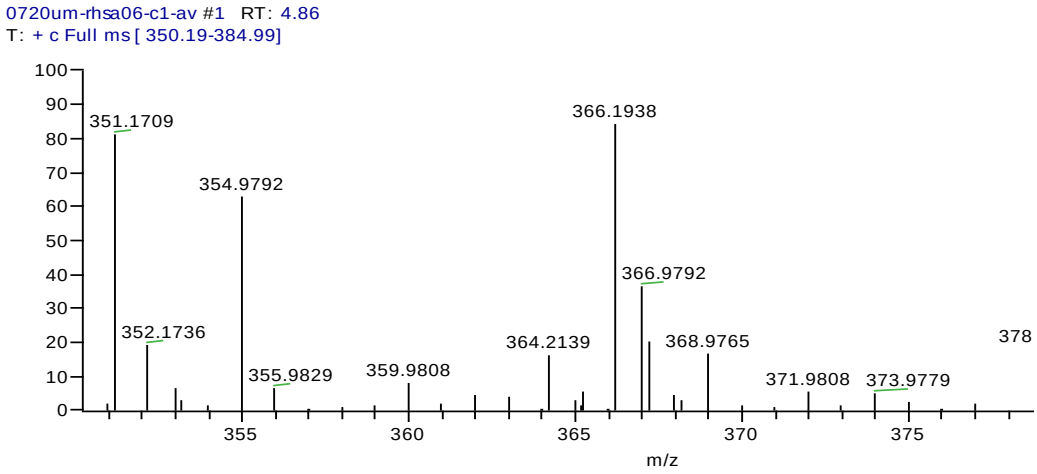

0720um-rhsa06-c1-av#1 RT: 4.86
T: + c Full ms [350.19-384.99]
m/z= 365.94-366.28

m/z	Intensity	Relative	Theo. Mass	Delta (ppm)	RDB equiv.	Composition
366.1938	881428.0	100.00	366.1943	-1.52	11.0	$C_{22}H_{26}O_3N_2$

Figure B- 7 : HREIMS spectrum of **2.17**

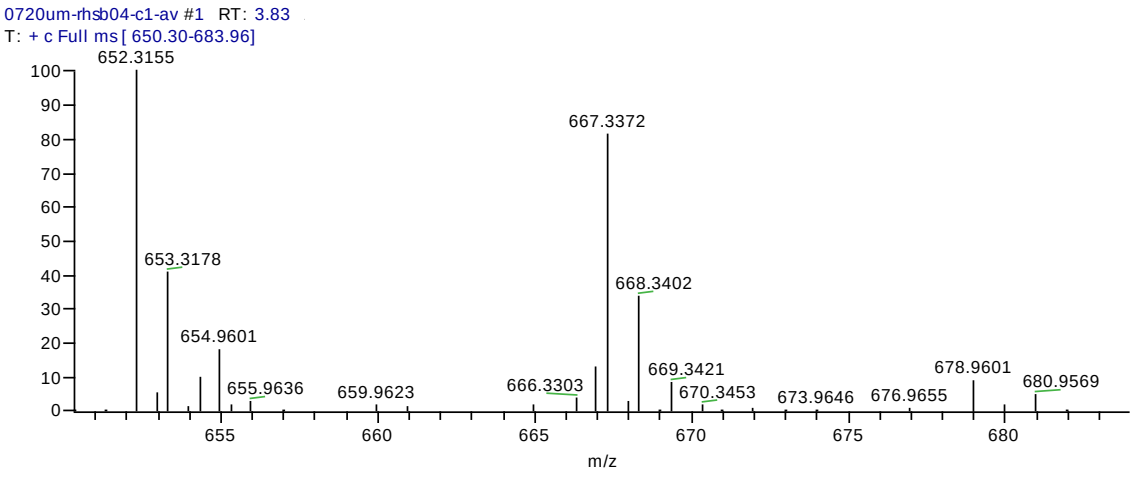

0720um-rhsb04-c1-av#1 RT: 3.83
T: + c Full ms [650.30-683.96]
m/z= 667.13-667.63

m/z	Intensity	Relative	Theo. Mass	Delta (ppm)	RDB equiv.	Composition
667.3372	1050452.0	100.00	667.3370	0.37	19.0	$C_{38}H_{45}O_6N_5$
			667.3365	1.14	31.5	$C_{52}H_{43}$

Figure B- 8 : HREIMS spectrum of **2.34**

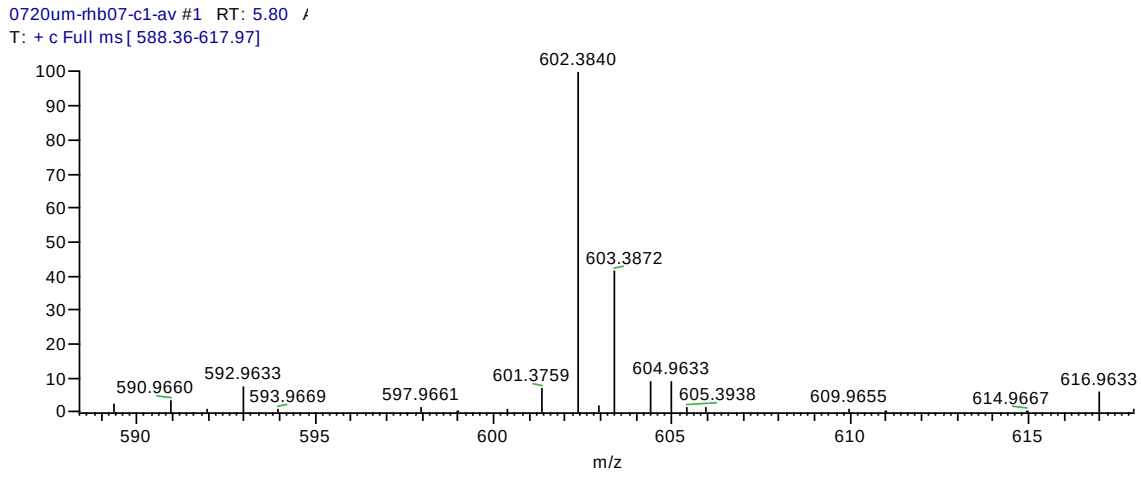

0720um-rhb07-c1-av#1 RT: 5.80
T: + c Full ms [588.36-617.97]
m/z= 602.05-602.63

m/z	Intensity	Relative	Theo. Mass	Delta (ppm)	RDB equiv.	Composition
602.3840	3734423.0	100.00	602.3845	-0.93	13.5	$C_{38}H_{52}O_5N_1$
			602.3832	1.30	14.0	$C_{36}H_{50}O_4N_4$

Figure B- 9 : HREIMS spectrum of **2.36**

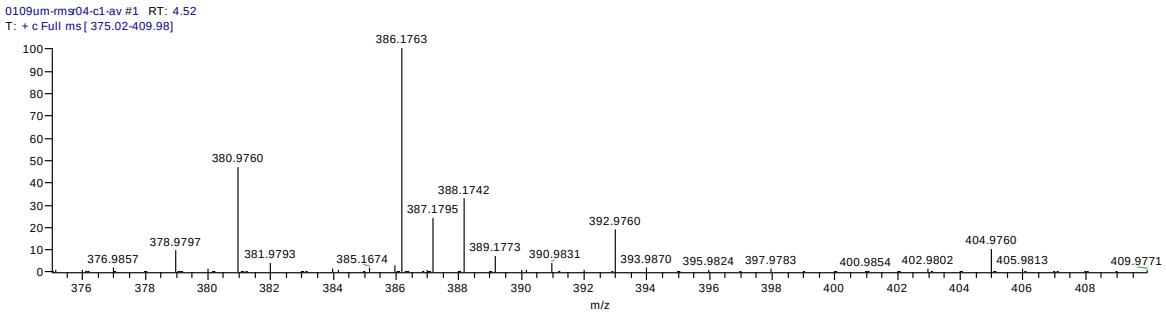

0109um-rmsr04-c1-av#1 RT: 4.52
T: + c Full ms [375.02-409.98]
m/z= 385.70-386.50

m/z	Intensity	Relative	Theo. Mass	Delta (ppm)	RDB equiv.	Composition
386.1763	907627.0	100.00	386.1761	0.42	10.0	$C_{22}H_{27}O_2N_2{}^{35}Cl_1$

Figure B- 10 : HREIMS spectrum of **3.4**

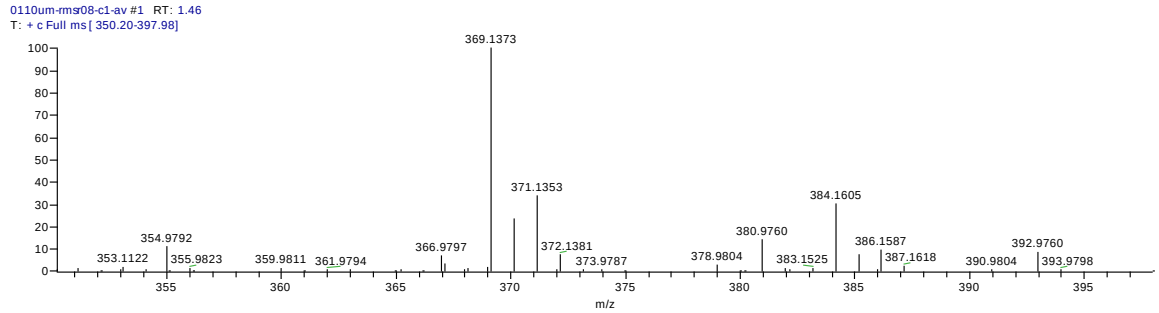

0110um-rmsr08-c1-av#1 RT: 1.46
T: + c Full ms [350.20-397.98]
m/z= 368.15-384.47

m/z	Intensity	Relative	Theo. Mass	Delta (ppm)	RDB equiv.	Composition
369.1373	7310125.0	100.00	369.1370	0.94	11.5	$C_{21}H_{22}O_2N_2{}^{35}Cl_1$
			369.1365	2.26	16.0	$C_{24}H_{19}O_3N_1$
384.1605	2229705.0	30.50	384.1605	0.09	11.0	$C_{22}H_{25}O_2N_2{}^{35}Cl_1$

Figure B- 19: HREIMS spectrum of **3.8**

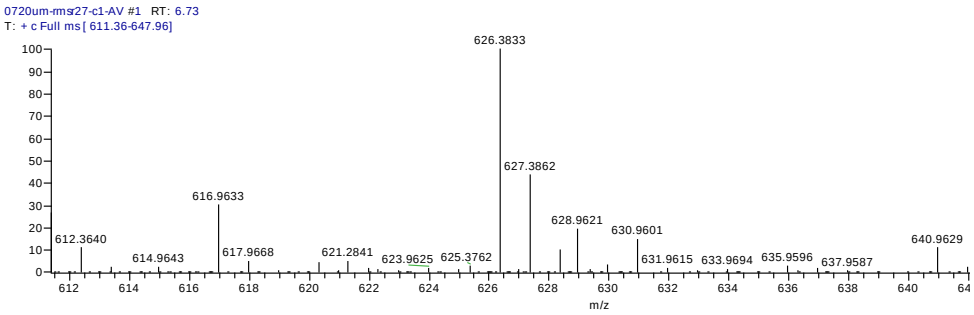

0720um-rmsr27-c1-AV#1 RT: 6.73
T: + c Full ms [611.36-647.96]
m/z= 626.23-626.62

m/z	Intensity	Relative	Theo. Mass	Delta (ppm)	RDB equiv.	Composition
626.3833	1340677.0	100.00	626.3832	0.17	16.0	$C_{38}H_{50}O_4N_4$

Figure B- 20 : HREIMS spectrum of **3.9**

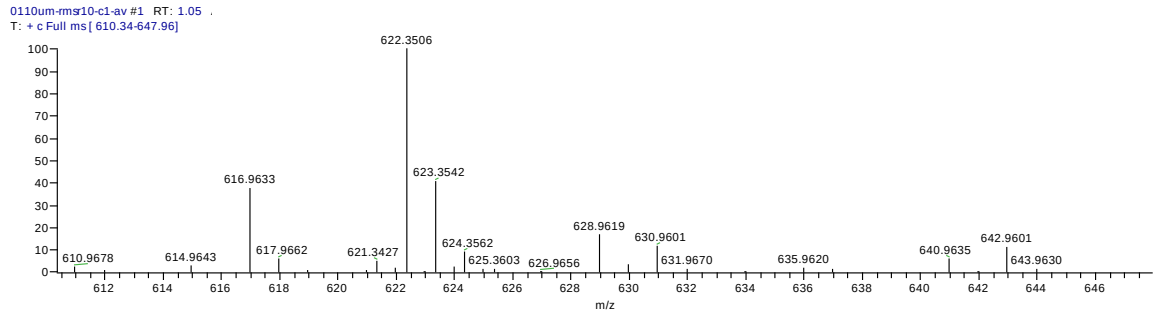

0110um-rmsr10-c1-av#1 RT: 1.05
T: + c Full ms [610.34-647.96]
m/z= 621.71-622.57

m/z	Intensity	Relative	Theo. Mass	Delta (ppm)	RDB equiv.	Composition
622.3506	3170632.0	100.00	622.3519	-2.15	18.0	$C_{38}H_{46}O_4N_4$
			622.3532	-4.30	17.5	$C_{40}H_{48}O_5N_1$

Figure B- 21: HREIMS spectrum of **3.11**

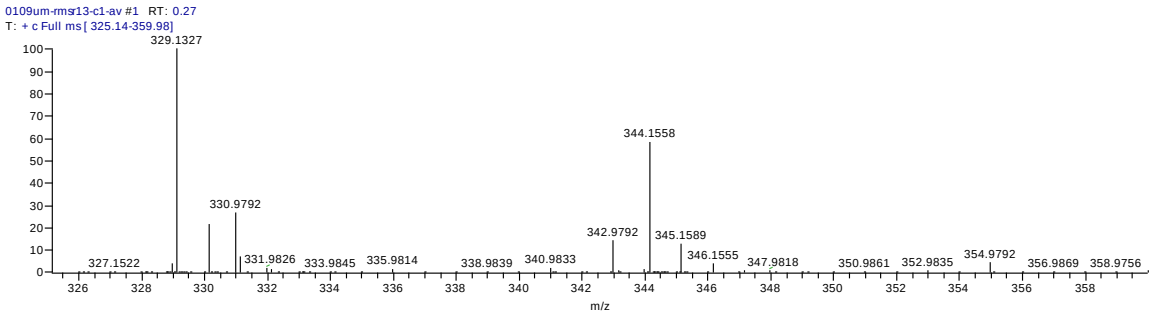

0109um-rmsr13-c1-av#1 RT: 0.27
T: + c Full ms [325.14-359.98]
m/z= 343.92-344.49

m/z	Intensity	Relative	Theo. Mass	Delta (ppm)	RDB equiv.	Composition
344.1558	1423495.0	100.00	344.1558	-0.26	9.0	$C_{19}H_{24}O_2N_2{}^{32}S_1$

Figure B- 22 : HREIMS spectrum of **3.17**

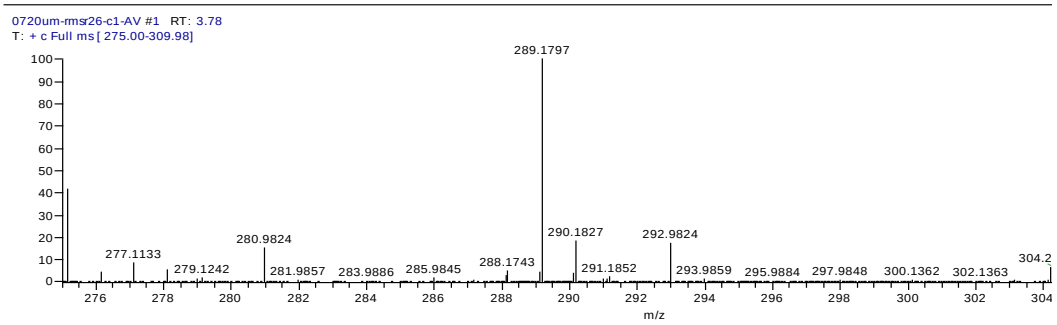

0720um-rmsr26-c1-AV#1 RT: 3.78
T: + c Full ms [275.00-309.98]
m/z= 289.10-289.36

m/z	Intensity	Relative	Theo. Mass	Delta (ppm)	RDB equiv.	Composition
289.1797	23275776.0	100.00	289.1804	-2.31	6.5	$C_{18}H_{25}O_3$
			289.1790	2.34	7.0	$C_{16}H_{23}O_2N_3$

Figure B- 11 : HREIMS spectrum of **3.19**

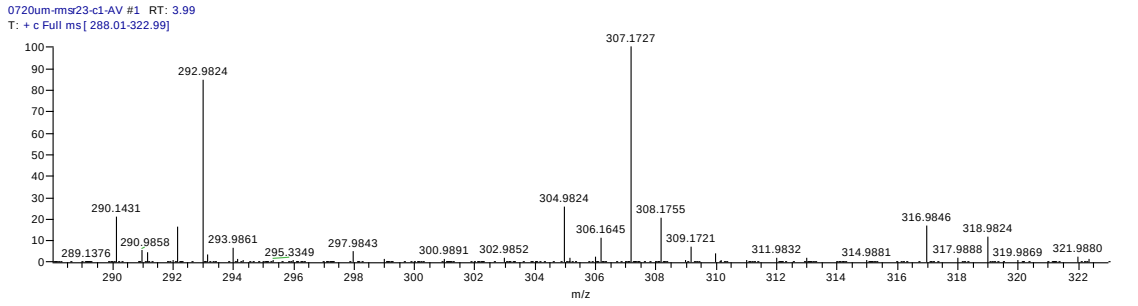

0720um-rmsr23-c1-AV#1 RT: 3.99
T: + c Full ms [288.01-322.99]
m/z= 306.87-307.56

m/z	Intensity	Relative	Theo. Mass	Delta (ppm)	RDB equiv.	Composition
307.1727	5137225.0	100.00	307.1732	-1.66	5.5	$C_{18}H_{27}O_2{}^{32}S_1$
			307.1718	2.72	6.0	$C_{16}H_{25}O_1N_3{}^{32}S_1$

Figure B- 12: HREIMS spectrum of **3.20**

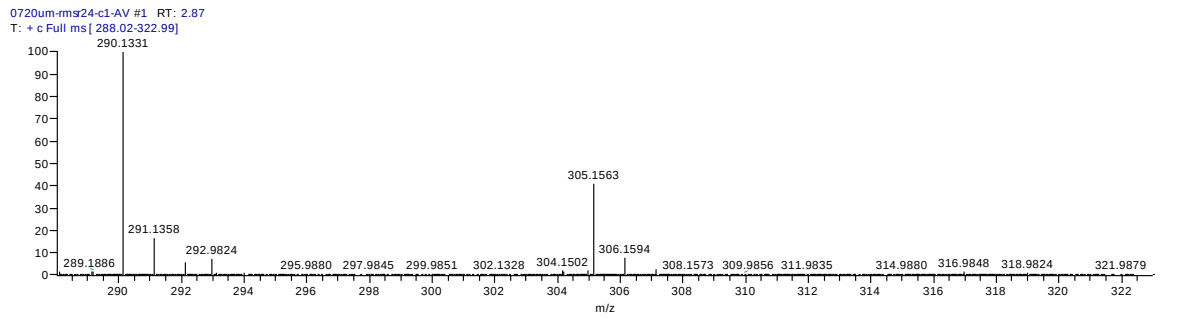

0720um-rmsr24-c1-AV#1 RT: 2.87
T: + c Full ms [288.02-322.99]
m/z= 304.93-305.28

m/z	Intensity	Relative	Theo. Mass	Delta (ppm)	RDB equiv.	Composition
305.1563	22585856.0	100.00	305.1562	0.47	7.0	$C_{16}H_{23}O_1N_3{}^{32}S_1$
			305.1575	-3.93	6.5	$C_{18}H_{25}O_2{}^{32}S_1$

Figure B- 13: HREIMS spectrum of **3.21**

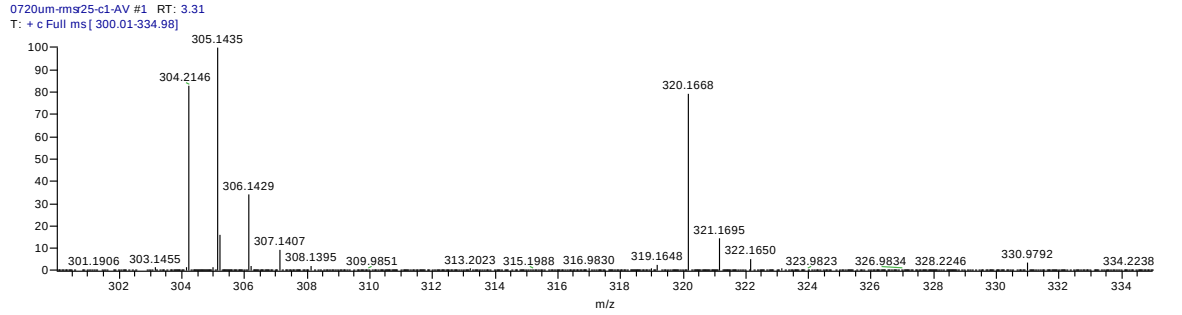

0720um-rmsr25-c1-AV#1 RT: 3.31
T: + c Full ms [300.01-334.98]
m/z= 320.04-320.48

m/z	Intensity	Relative	Theo. Mass	Delta (ppm)	RDB equiv.	Composition
320.1668	41676288.0	100.00	320.1671	-0.86	7.0	$C_{16}H_{24}O_1N_4{}^{32}S_1$

Figure B- 14 : HREIMS spectrum of **3.22**

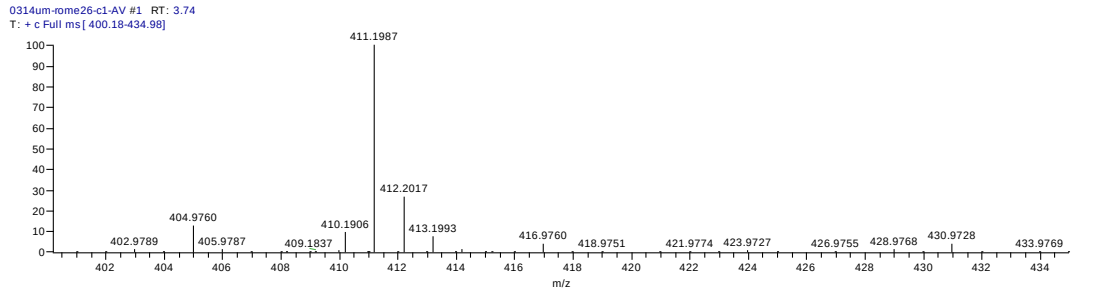

0314um-rome26-c1-AV#1 RT: 3.74
T: + c Full ms [400.18-434.98]
m/z= 410.82-411.56

m/z	Intensity	Relative	Theo. Mass	Delta (ppm)	RDB equiv.	Composition
411.1987	6441255.0	100.00	411.1987	-0.04	20.0	$C_{31}H_{25}N_1$
			411.1980	1.55	11.0	$C_{23}H_{29}O_2N_3{}^{32}S_1$

Figure B- 15 : HREIMS spectrum of **3.26**

Appendix C X-Ray Data

Table 1 : Crystal data and structure refinement for **2.20**

Empirical formula	$C_{24}H_{30}N_2O_2$	Crystal size/mm^3	0.35 × 0.15 × 0.05
Formula weight	378.50	2Θ range for data collection	6.92 to 153.1°
Temperature/K	100(2)	Index ranges	$-23 \le h \le 23$, $-8 \le k \le 5$, $-21 \le l \le 21$
Crystal system	orthorhombic	Reflections collected	11568
Space group	Pnma	Independent reflections	2544[R(int) = 0.0357]
a/Å	18.6820(6)	Data/restraints/parameters	2544/66/215
b/Å	6.8630(2)	Goodness-of-fit on F^2	1.033
c/Å	17.4936(5)	Final R indexes [I>=2σ (I)]	R_1 = 0.0465, wR_2 = 0.1290
α/°	90.00	Final R indexes [all data]	R_1 = 0.0567, wR_2 = 0.1419
β/°	90.00	Largest diff. peak/hole / e Å^{-3}	0.19/-0.26
γ/°	90.00		
Volume/Å^3	2242.93(12)		
Z	4		
ρ_{calc}mg/mm^3	1.121		
m/mm^{-1}	0.558		
F(000)	816.0		

Table 2 : Fractional Atomic Coordinates (×10^4) and Equivalent Isotropic Displacement Parameters (Å^2×10^3) for **2.20**. U_{eq} is defined as 1/3 of of the trace of the orthogonalised U_{IJ} tensor.

Atom	*x*	*y*	*z*	U(eq)
O1	2498.6(7)	2500	1302.7(7)	42.0(3)
O2	4668.6(6)	2500	4130.1(7)	37.6(3)
N1	5458.1(8)	2500	3188.5(10)	47.3(4)
N2	5827.2(9)	2500	3885.2(11)	50.6(4)
C1	4176.8(9)	2500	2842.8(10)	34.3(4)
C2	4298.4(9)	2500	2057.9(10)	35.9(4)
C3	3739.2(10)	2500	1536.9(9)	35.5(4)
C4	3032.5(9)	2500	1836.3(9)	34.4(4)
C5	2896.4(9)	2500	2632.5(9)	33.1(4)
C6	3484.8(9)	2500	3120.6(9)	33.3(4)
C7	4697.1(12)	2500	504.8(12)	55.1(5)
C8	3888.7(11)	2500	672(1)	44.8(5)
C9	3575.2(9)	664(2)	298.8(8)	58.2(4)
C10	1738.2(7)	623.6(19)	2731.9(8)	43.5(3)
C11	2135.6(9)	2500	2969.1(10)	37.2(4)
C12	2148.3(11)	2500	3846.6(11)	47.4(5)
C13	4784.9(9)	2500	3360(1)	36.7(4)
C14	5347.9(10)	2500	4419.7(12)	43.7(4)
C15	5505(3)	2500	5194(3)	36.6(10)
C16	6224(2)	2500	5414.1(19)	41.6(7)

C17	6419.8(18)	2500	6174.0(17)	46.1(8)
C18	5897(3)	2500	6745(4)	45.8(15)
C19	5181.2(19)	2500	6526.0(18)	43.6(7)
C20	4968(3)	2500	5758(3)	37.8(9)
C21	4166.1(17)	2500	5592.6(16)	42.2(7)
C22	6114(2)	2500	7576.2(16)	53.6(9)
C15'	5322(4)	2500	5384(5)	27(2)
C16'	4673(4)	2500	5775(5)	34(2)
C17'	4657(4)	2500	6567(3)	46.2(15)
C18'	5291(4)	2500	6987(4)	47.0(16)
C19'	5943(5)	2500	6600(6)	45(4)
C20'	5970(3)	2500	5799(4)	39.3(14)
C21'	6700(4)	2500	5418(4)	56.7(18)
C22'	5258(4)	2500	7852(3)	54.2(18)

Table 3 : Anisotropic Displacement Parameters ($Å^2 \times 10^3$) for **2.20**. The Anisotropic displacement factor exponent takes the form: $-2\pi^2[h^2a^{*2}U_{11}+...+2hka \times b \times U_{12}]$

Atom	**U_{11}**	**U_{22}**	**U_{33}**	**U_{23}**	**U_{13}**	**U_{12}**
O1	37.1(7)	53.6(8)	35.2(6)	0	-2.1(5)	0
O2	34.2(6)	34.6(6)	44.2(7)	0	-7.7(5)	0
N1	31.9(8)	48.5(9)	61.4(10)	0	-2.0(7)	0
N2	32.3(8)	47.2(9)	72.4(12)	0	-8.4(8)	0
C1	33.2(8)	28.9(7)	40.9(9)	0	0.6(7)	0
C2	33.2(8)	31.4(8)	43.1(9)	0	7.0(7)	0
C3	39.0(9)	31.7(8)	35.8(8)	0	5.1(7)	0
C4	35.9(9)	32.7(8)	34.4(8)	0	-2.0(7)	0
C5	30.6(8)	31.8(7)	36.8(8)	0	3.3(6)	0
C6	34.3(8)	31.7(7)	33.9(8)	0	1.0(7)	0
C7	55.4(13)	62.5(12)	47.5(11)	0	17.5(10)	0
C8	50.4(11)	48.4(10)	35.7(9)	0	7.8(8)	0
C9	68.2(10)	64.0(9)	42.4(7)	-13.5(7)	8.1(7)	-4.8(8)
C10	34.5(6)	41.7(7)	54.3(8)	4.6(5)	1.1(5)	-1.7(5)
C11	29.8(8)	41.9(9)	40.0(9)	0	3.5(7)	0
C12	37.8(10)	63.2(12)	41.3(10)	0	8.4(8)	0
C13	33.8(9)	30.4(8)	45.9(9)	0	-0.8(7)	0
C14	37.5(10)	30.1(8)	63.4(12)	0	-16.2(9)	0
C15	41(2)	29.3(14)	40(2)	0	-1.8(18)	0
C16	41.9(19)	37.3(13)	45.7(17)	0	-10.9(15)	0
C17	52.5(18)	35.2(13)	50.5(16)	0	-19.1(15)	0
C18	65(4)	28(2)	43.5(19)	0	-15.2(19)	0
C19	59(2)	30.6(12)	40.8(16)	0	-7.8(14)	0
C20	43(3)	31.8(14)	38.9(19)	0	-6(2)	0
C21	45.3(18)	40.1(13)	41.1(14)	0	0.2(12)	0
C22	80(2)	37.8(13)	42.9(15)	0	-20.7(15)	0
C15'	26(5)	28(3)	29(4)	0	-7(4)	0
C16'	35(5)	32(3)	37(3)	0	-3(4)	0
C17'	48(4)	42(3)	49(3)	0	-2(3)	0
C18'	60(4)	33(3)	48(4)	0	-17(3)	0
C19'	47(6)	35(5)	52(6)	0	-16(4)	0

C20'	40(3)	33(3)	45(3)	0	-6(3)	0
C21'	47(4)	65(4)	58(4)	0	-11(3)	0
C22'	73(4)	42(3)	48(3)	0	-7(3)	0

Table 4 : Bond Lengths for **2.20**

Atom	Atom	Length/Å	Atom	Atom	Length/Å
O1	C4	1.366(2)	C11	C12	1.535(2)
O2	C13	1.364(2)	C14	C15	1.386(5)
O2	C14	1.366(2)	C14	C15'	1.687(8)
N1	N2	1.400(2)	C15	C16	1.397(6)
N1	C13	1.293(2)	C15	C20	1.407(5)
N2	C14	1.295(3)	C16	C17	1.379(4)
C1	C2	1.392(2)	C17	C18	1.397(6)
C1	C6	1.381(2)	C18	C19	1.391(6)
C1	C13	1.452(2)	C18	C22	1.509(7)
C2	C3	1.386(2)	C19	C20	1.402(5)
C3	C4	1.420(2)	C20	C21	1.526(5)
C3	C8	1.539(2)	C15'	C16'	1.392(8)
C4	C5	1.416(2)	C15'	C20'	1.412(8)
C5	C6	1.392(2)	C16'	C17'	1.386(8)
C5	C11	1.539(2)	C17'	C18'	1.394(7)
C7	C8	1.538(3)	C18'	C19'	1.394(8)
C8	C9	1.5354(18)	C18'	C22'	1.514(8)
C8	C9[1]	1.5354(18)	C19'	C20'	1.402(9)
C10	C11	1.5433(16)	C20'	C21'	1.519(7)
C11	C10[1]	1.5433(16)			

[1]+X,1/2-Y,+Z

Table 5 : Bond Angles for **2.20**

Atom	Atom	Atom	Angle/°	Atom	Atom	Atom	Angle/°
C13	O2	C14	102.61(14)	N1	C13	C1	128.04(17)
C13	N1	N2	106.08(16)	O2	C14	C15	124.0(3)
C14	N2	N1	106.73(15)	O2	C14	C15'	110.1(3)
C2	C1	C13	119.14(15)	N2	C14	O2	112.00(18)
C6	C1	C2	120.00(16)	N2	C14	C15	124.0(3)
C6	C1	C13	120.86(15)	N2	C14	C15'	137.9(3)
C3	C2	C1	121.70(16)	C14	C15	C16	118.3(4)
C2	C3	C4	117.26(15)	C14	C15	C20	122.3(4)
C2	C3	C8	120.64(16)	C16	C15	C20	119.5(4)
C4	C3	C8	122.10(16)	C17	C16	C15	121.4(4)
O1	C4	C3	115.26(14)	C16	C17	C18	120.3(4)
O1	C4	C5	122.75(15)	C17	C18	C22	120.1(4)
C5	C4	C3	121.99(15)	C19	C18	C17	118.4(5)
C4	C5	C11	122.85(15)	C19	C18	C22	121.6(5)
C6	C5	C4	117.49(15)	C18	C19	C20	122.5(4)
C6	C5	C11	119.66(15)	C15	C20	C21	124.6(4)
C1	C6	C5	121.56(15)	C19	C20	C15	118.0(4)
C7	C8	C3	111.42(16)	C19	C20	C21	117.4(4)
C9	C8	C3	110.42(10)	C16'	C15'	C14	121.1(6)
C9[1]	C8	C3	110.42(10)	C16'	C15'	C20'	119.7(7)

C9[1]	C8	C7	107.07(11)	C20'	C15'	C14	119.3(6)
C9	C8	C7	107.07(11)	C17'	C16'	C15'	120.6(7)
C9	C8	C9[1]	110.34(18)	C16'	C17'	C18'	120.6(6)
C5	C11	C10[1]	109.96(9)	C17'	C18'	C22'	119.5(6)
C5	C11	C10	109.96(9)	C19'	C18'	C17'	119.1(7)
C10	C11	C10[1]	113.12(15)	C19'	C18'	C22'	121.4(7)
C12	C11	C5	111.62(15)	C18'	C19'	C20'	121.1(8)
C12	C11	C10	106.04(10)	C15'	C20'	C21'	123.0(6)
C12	C11	C10[1]	106.04(10)	C19'	C20'	C15'	118.9(7)
O2	C13	C1	119.38(15)	C19'	C20'	C21'	118.1(6)
N1	C13	O2	112.58(16)				

[1]+X,1/2-Y,+Z

Table 6 : Torsion Angles for **2.20**

A	B	C	D	Angle/°	A	B	C	D	Angle/°
O1	C4	C5	C6	180.0	C8	C3	C4	C5	180.0
O1	C4	C5	C11	0.0	C11	C5	C6	C1	180.0
O2	C14	C15	C16	180.0	C13	O2	C14	N2	0.0
O2	C14	C15	C20	0.0	C13	O2	C14	C15	180.0
O2	C14	C15'	C16'	0.000(1)	C13	O2	C14	C15'	180.0
O2	C14	C15'	C20'	180.0	C13	N1	N2	C14	0.0
N1	N2	C14	O2	0.0	C13	C1	C2	C3	180.0
N1	N2	C14	C15	180.0	C13	C1	C6	C5	180.0
N1	N2	C14	C15'	180.000(1)	C14	O2	C13	N1	0.0
N2	N1	C13	O2	0.0	C14	O2	C13	C1	180.0
N2	N1	C13	C1	180.0	C14	C15	C16	C17	180.0
N2	C14	C15	C16	0.0	C14	C15	C20	C19	180.0
N2	C14	C15	C20	180.0	C14	C15	C20	C21	0.0
N2	C14	C15'	C16'	180.000(1)	C14	C15'	C16'	C17'	180.000(1)
N2	C14	C15'	C20'	0.000(1)	C14	C15'	C20'	C19'	180.000(2)
C1	C2	C3	C4	0.0	C14	C15'	C20'	C21'	0.000(1)
C1	C2	C3	C8	180.0	C15	C14	C15'	C16'	180.000(3)
C2	C1	C6	C5	0.0	C15	C14	C15'	C20'	0.000(3)
C2	C1	C13	O2	180.0	C15	C16	C17	C18	0.000(1)
C2	C1	C13	N1	0.0	C16	C15	C20	C19	0.0
C2	C3	C4	O1	180.0	C16	C15	C20	C21	180.0
C2	C3	C4	C5	0.0	C16	C17	C18	C19	0.000(1)
C2	C3	C8	C7	0.0	C16	C17	C18	C22	180.0
C2	C3	C8	C9[1]	-118.85(12)	C17	C18	C19	C20	0.000(1)
C2	C3	C8	C9	118.85(12)	C18	C19	C20	C15	0.000(1)
C3	C4	C5	C6	0.0	C18	C19	C20	C21	180.0
C3	C4	C5	C11	180.0	C20	C15	C16	C17	0.0
C4	C3	C8	C7	180.0	C22	C18	C19	C20	180.000(1)
C4	C3	C8	C9	-61.15(12)	C15'	C14	C15	C16	180.000(2)
C4	C3	C8	C9[1]	61.15(12)	C15'	C14	C15	C20	0.000(2)
C4	C5	C6	C1	0.0	C15'	C16'	C17'	C18'	0.000(2)
C4	C5	C11	C10[1]	-62.60(10)	C16'	C15'	C20'	C19'	0.000(2)
C4	C5	C11	C10	62.60(10)	C16'	C15'	C20'	C21'	180.000(1)
C4	C5	C11	C12	180.0	C16'	C17'	C18'	C19'	0.000(2)

C6	C1	C2	C3	0.0	C16'	C17'	C18'	C22'	180.000(1)
C6	C1	C13	O2	0.0	C17'	C18'	C19'	C20'	0.000(2)
C6	C1	C13	N1	180.0	C18'	C19'	C20'	C15'	0.000(2)
C6	C5	C11	C10	-117.40(10)	C18'	C19'	C20'	C21'	180.000(2)
C6	C5	C11	C10[1]	117.40(10)	C20'	C15'	C16'	C17'	0.000(2)
C6	C5	C11	C12	0.0	C22'	C18'	C19'	C20'	180.000(1)
C8	C3	C4	O1	0.0					

[1]+X,1/2-Y,+Z

Table 7 : Hydrogen Atom Coordinates (Å×10^4) and Isotropic Displacement Parameters (Å^2×10^3) for **2.20**

Atom	***x***	***y***	***z***	**U(eq)**	**Atom**	***x***	***y***	***z***	**U(eq)**
H1	2110	2195	1512	63	H19	4823	2500	6912	52
H2	4777	2500	1874	43	H21A	4033	3725	5342	63
H6	3409	2500	3657	40	H21B	3901	2371	6074	63
H7A	4917	3658	734	83	H21C	4049	1404	5256	63
H7B	4775	2516	-49	83	H22A	6493	3466	7657	80
H7C	4915	1326	723	83	H22B	6291	1205	7717	80
H9A	3779	-496	543	87	H22C	5699	2829	7894	80
H9B	3692	656	-247	87	H16'	4236	2500	5496	41
H9C	3054	658	363	87	H17'	4210	2500	6826	55
H10A	1254	635	2948	65	H19'	6377	2500	6884	54
H10B	1999	-514	2924	65	H21D	6812	1184	5236	85
H10C	1709	559	2173	65	H21E	7064	2913	5788	85
H12A	1656	2500	4041	71	H21F	6697	3403	4984	85
H12B	2398	3666	4029	71	H22D	4889	1585	8022	81
H12C	2398	1334	4029	71	H22E	5142	3813	8033	81
H16	6586	2500	5032	50	H22F	5723	2102	8059	81
H17	6912	2500	6310	55					

Table 1 : Crystal data and structure refinement for **2.33**

Empirical formula	$C_{37}H_{45}N_5O_4$	Crystal size/mm^3	0.4 × 0.1 × 0.02
Formula weight	623.78	2Θ range for data collection	6.06 to 55.12°
Temperature/K	100(2)	Index ranges	$-20 \le h \le 19$, $-13 \le k \le 12$, $-26 \le l \le 27$
Crystal system	monoclinic	Reflections collected	20850
Space group	$P2_1/n$	Independent reflections	7867[R(int) = 0.0443]
a/Å	16.0299(7)	Data/restraints/parameters	7867/36/445
b/Å	10.0744(6)	Goodness-of-fit on F^2	1.042
c/Å	21.1344(9)	Final R indexes [I>=2σ (I)]	R_1 = 0.0564, wR_2 = 0.1223
α/°	90.00	Final R indexes [all data]	R_1 = 0.0865, wR_2 = 0.1413
β/°	92.946(4)	Largest diff. peak/hole / e Å^{-3}	0.36/-0.28
γ/°	90.00		
Volume/Å^3	3408.5(3)		
Z	4		
ρ_{calc}mg/mm^3	1.216		
m/mm^{-1}	0.080		

F(000)
1336.0

Table 2 : Fractional Atomic Coordinates ($\times 10^4$) and Equivalent Isotropic Displacement Parameters ($Å^2 \times 10^3$) for **2.33**. U_{eq} is defined as 1/3 of of the trace of the orthogonalised U_{IJ} tensor.

Atom	***x***	***y***	***z***	**U(eq)**
O1	2776.2(9)	770(2)	8442.7(6)	45.8(5)
O2	5588.6(7)	3893.8(13)	6968.7(5)	21.7(3)
O3	5710.4(7)	3975.1(13)	4644.1(5)	20.8(3)
O4	3471.4(8)	134.8(14)	2819.6(6)	28.2(3)
N1	6204.3(10)	3681.7(18)	7927.2(7)	29.1(4)
N2	6748.5(10)	4342.8(18)	7535.0(7)	27.0(4)
N3	6307.5(9)	4778.0(16)	5857.4(7)	20.2(3)
N4	6453.1(10)	5532.4(18)	4193.7(7)	26.9(4)
N5	6011.6(10)	4820.2(18)	3714.3(7)	26.9(4)
C1	4772.7(11)	2801(2)	7770.2(8)	23.2(4)
C2	4642.1(12)	2731(2)	8416.9(8)	26.1(4)
C3	3963.1(12)	2072(2)	8640.8(8)	27.4(4)
C4	3414.2(11)	1450(2)	8190.5(9)	26.6(4)
C5	3523.5(11)	1500(2)	7532.3(8)	23.6(4)
C6	4210.4(12)	2209(2)	7338.6(8)	23.5(4)
C7	3836.4(13)	1969(3)	9359.4(9)	36.5(5)
C8	4516.8(17)	2735(3)	9742.7(10)	60.2(8)
C9	2986.7(16)	2565(3)	9517.4(10)	51.6(7)
C10	3884.7(14)	526(3)	9575(1)	43.9(6)
C11	2966.5(12)	736(2)	7039.8(9)	28.3(5)
C12	2086(2)	1248(7)	7039(2)	55.3(14)
C13	3028(3)	-749(4)	7218(2)	45.7(12)
C14	3270(3)	891(4)	6387.2(15)	39.5(11)
C12'	2061(4)	303(9)	7182(3)	35.6(17)
C13'	3423(4)	-477(7)	6820(4)	49(2)
C14'	2792(5)	1659(8)	6417(3)	44(2)
C15	5529.7(12)	3449(2)	7577.6(8)	23.0(4)
C16	6359.8(11)	4446(2)	6982.0(8)	22.5(4)
C17	6682.0(11)	5087.6(19)	6423.7(8)	21.6(4)
C18	7355.8(11)	5941(2)	6504.9(9)	24.2(4)
C19	7683.9(12)	6496(2)	5974.4(9)	26.3(4)
C20	7314.9(11)	6204(2)	5385.3(9)	24.0(4)
C21	6630.8(11)	5342(2)	5350.3(8)	21.3(4)
C22	6262.3(11)	5001(2)	4721.9(8)	21.4(4)
C23	5586.9(11)	3923(2)	3997.8(8)	20.9(4)
C24	5031.5(11)	2919(2)	3709.2(8)	20.9(4)
C25	4597.5(11)	2027(2)	4069.3(8)	21.6(4)
C26	4065.9(11)	1079.5(19)	3785.9(8)	21.6(4)
C27	3976.5(11)	1080(2)	3118.1(9)	23.0(4)
C28	4422.5(11)	1957(2)	2740.3(8)	22.2(4)
C29	4943.5(11)	2878(2)	3049.9(8)	22.1(4)
C30	3635.4(12)	33(2)	4189.7(9)	27.3(4)
C31	3776.1(13)	300(2)	4900.1(9)	31.9(5)
C32	2680.5(13)	3(3)	4062.0(11)	41.2(6)

C33	4001.9(17)	-1336(2)	4049.4(11)	46.8(6)
C34	4340.3(12)	1917(2)	2008.4(8)	26.2(4)
C35	3446.7(12)	2283(2)	1778.0(9)	29.3(5)
C36	4571.3(13)	537(2)	1762.3(9)	34.1(5)
C37	4927.8(14)	2924(3)	1717.0(9)	39.6(6)

Table 3 : Anisotropic Displacement Parameters ($Å^2 \times 10^3$) for **2.33**. The Anisotropic displacement factor exponent takes the form: $-2\pi^2[h^2a^{*2}U_{11}+...+2hka \times b \times U_{12}]$

Atom	**U_{11}**	**U_{22}**	**U_{33}**	**U_{23}**	**U_{13}**	**U_{12}**
O1	28.2(8)	83.7(15)	25.9(8)	6.4(8)	5.1(6)	-12.1(8)
O2	24.0(7)	22.7(7)	18.0(6)	0.7(5)	-1.7(5)	0.4(5)
O3	22.4(6)	22.7(7)	16.9(6)	-2.3(5)	-2.0(5)	-1.7(5)
O4	31.2(7)	25.9(8)	26.3(7)	-5.8(6)	-8.9(6)	0.2(6)
N1	32.3(9)	31.8(10)	22.7(8)	3.3(7)	-2.0(7)	-1.5(8)
N2	29.0(9)	30.3(10)	21.3(8)	2.5(7)	-2.4(6)	-1.5(7)
N3	20.4(8)	20.5(9)	19.6(7)	-1.9(6)	-1.2(6)	2.1(6)
N4	28.4(9)	31.2(10)	20.8(8)	-1.8(7)	-2.4(6)	-4.3(7)
N5	25.6(9)	35.3(11)	19.3(8)	-1.3(7)	-2.6(6)	-3.2(7)
C1	26.7(10)	22.2(10)	20.7(9)	1.0(8)	1.3(7)	4.6(8)
C2	31.3(11)	27.4(11)	19.1(9)	-1.4(8)	-2.0(7)	4.5(8)
C3	28.8(10)	34.0(12)	19.5(9)	3.3(9)	2.7(7)	9.7(9)
C4	21.9(10)	33.5(12)	24.8(10)	5.9(9)	5.6(7)	7.7(8)
C5	25.5(10)	24.8(11)	20.5(9)	1.1(8)	1.6(7)	5.6(8)
C6	30.8(10)	23.4(11)	16.4(9)	0.8(8)	1.3(7)	3.7(8)
C7	37.2(12)	54.3(16)	18.4(10)	3.6(10)	4.2(8)	6.4(11)
C8	69.9(18)	92(2)	18.4(11)	-1.0(13)	0.6(11)	-21.4(16)
C9	58.9(16)	71(2)	26.3(11)	1.4(12)	15.8(10)	23.0(14)
C10	39.9(13)	63.0(18)	29.6(11)	15.8(12)	8.1(9)	7.4(12)
C11	26.3(10)	31.1(12)	27.4(10)	-0.2(9)	2.4(8)	-1.9(9)
C12	30(2)	91(4)	44(2)	-17(3)	-7.7(16)	8(2)
C13	55(3)	38(2)	44(2)	4.5(19)	-6.1(19)	-19.4(19)
C14	52(2)	43(3)	23.1(17)	-4.9(16)	1.2(15)	-21(2)
C12'	30(3)	48(4)	29(3)	-4(3)	4(2)	-12(3)
C13'	46(4)	38(4)	62(5)	-21(4)	-7(3)	13(3)
C14'	52(4)	49(4)	29(3)	-1(3)	-14(3)	-15(3)
C15	30.1(10)	22.2(10)	16.5(9)	0.2(8)	-0.8(7)	3.4(8)
C16	22.7(9)	22(1)	22.4(9)	-3.5(8)	-1.7(7)	1.3(8)
C17	23.5(9)	20.5(10)	20.5(9)	-1.5(8)	-2.3(7)	3.7(8)
C18	23.5(10)	24.2(11)	24.3(9)	-3.3(8)	-6.0(7)	0.4(8)
C19	22.8(10)	26.2(11)	29.7(10)	-2.4(9)	-1.7(7)	-3.7(8)
C20	23.8(10)	24.8(11)	23.5(9)	0.2(8)	2.1(7)	-2.2(8)
C21	20.8(9)	21.9(10)	20.9(9)	-3.2(8)	-0.9(7)	2.4(7)
C22	18.9(9)	22.2(10)	22.8(9)	-1.9(8)	0.2(7)	0.3(7)
C23	20.0(9)	26.2(11)	16.6(8)	-2.6(8)	0.0(7)	2.4(8)
C24	18.0(9)	24.6(11)	19.9(9)	-4.0(8)	-2.1(7)	5.1(7)
C25	21.6(9)	24.6(11)	18.3(9)	-1.8(8)	-3.1(7)	5.2(8)
C26	22.9(9)	18.9(10)	22.5(9)	-1.9(8)	-3.7(7)	4.1(7)
C27	22.0(9)	22.1(10)	24.1(9)	-5.2(8)	-6.5(7)	5.1(8)
C28	23.0(9)	25.0(11)	18.4(9)	-3.1(8)	-2.8(7)	7.9(8)
C29	20.9(9)	25.6(11)	19.9(9)	-1.3(8)	0.3(7)	5.0(8)

C30	34.0(11)	22.5(11)	24.6(10)	2.3(8)	-6.4(8)	-2.8(8)
C31	34.3(11)	34.7(13)	26.1(10)	4.4(9)	-3.5(8)	-8.0(9)
C32	38.5(12)	41.4(14)	42.2(13)	14.6(11)	-12.9(10)	-19.3(11)
C33	80.0(18)	25.3(13)	34.2(12)	1.6(11)	-7.0(11)	8.8(12)
C34	29.8(10)	31.7(12)	16.8(9)	-4.2(8)	-3.4(7)	4.5(9)
C35	34.1(11)	31.8(12)	21.0(9)	-0.1(9)	-6.8(8)	6.2(9)
C36	37.3(12)	40.4(14)	24.1(10)	-10.4(10)	-4.3(8)	13.1(10)
C37	44.6(13)	56.7(17)	17.4(10)	-3.3(10)	1.0(8)	-9.1(11)

Table 4 : Bond Lengths for **2.33**

Atom	Atom	Length/Å	Atom	Atom	Length/Å	Atom	Atom	Length/Å	Atom	Atom	Length/Å
O1	C4	1.362(2)	C11	C13	1.545(5)	N5	C23	1.296(2)	C24	C29	1.394(2)
O2	C15	1.370(2)	C11	C14	1.494(4)	C1	C2	1.395(2)	C25	C26	1.394(3)
O2	C16	1.355(2)	C11	C12'	1.559(6)	C1	C6	1.384(3)	C26	C27	1.411(2)
O3	C22	1.365(2)	C11	C13'	1.509(7)	C1	C15	1.454(3)	C26	C30	1.542(3)
O3	C23	1.371(2)	C11	C14'	1.623(7)	C2	C3	1.380(3)	C27	C28	1.410(3)
O4	C27	1.381(2)	C16	C17	1.463(3)	C3	C4	1.409(3)	C28	C29	1.389(3)
N1	N2	1.402(2)	C17	C18	1.384(3)	C3	C7	1.546(3)	C28	C34	1.546(2)
N1	C15	1.299(2)	C18	C19	1.381(3)	C4	C5	1.412(2)	C30	C31	1.530(3)
N2	C16	1.300(2)	C19	C20	1.382(3)	C5	C6	1.391(3)	C30	C32	1.541(3)
N3	C17	1.348(2)	C20	C21	1.398(3)	C5	C11	1.542(3)	C30	C33	1.534(3)
N3	C21	1.340(2)	C21	C22	1.466(2)	C7	C8	1.533(3)	C34	C35	1.534(3)
N4	N5	1.403(2)	C23	C24	1.460(3)	C7	C9	1.541(3)	C34	C36	1.537(3)
N4	C22	1.289(2)	C24	C25	1.387(3)	C7	C10	1.525(4)	C34	C37	1.534(3)
						C11	C12	1.502(4)	C24	C29	1.394(2)

Table 5 : Bond Angles for **2.33**

Atom	Atom	Atom	Angle/°	Atom	Atom	Atom	Angle/°
C16	O2	C15	102.80(13)	N2	C16	O2	112.37(16)
C22	O3	C23	102.03(14)	N2	C16	C17	126.01(17)
C15	N1	N2	105.92(15)	N3	C17	C16	117.04(17)
C16	N2	N1	106.59(15)	N3	C17	C18	124.27(17)
C21	N3	C17	116.04(16)	C18	C17	C16	118.68(16)
C22	N4	N5	106.24(16)	C19	C18	C17	118.57(17)
C23	N5	N4	106.26(14)	C18	C19	C20	118.79(18)
C2	C1	C15	117.78(17)	C19	C20	C21	118.57(17)
C6	C1	C2	119.90(18)	N3	C21	C20	123.75(16)
C6	C1	C15	122.25(16)	N3	C21	C22	118.07(16)
C3	C2	C1	121.41(19)	C20	C21	C22	118.15(16)
C2	C3	C4	117.30(17)	O3	C22	C21	120.99(16)
C2	C3	C7	121.00(19)	N4	C22	O3	113.04(15)
C4	C3	C7	121.64(18)	N4	C22	C21	125.79(17)
O1	C4	C3	114.49(16)	O3	C23	C24	119.75(16)
O1	C4	C5	122.50(18)	N5	C23	O3	112.43(16)
C3	C4	C5	123.00(18)	N5	C23	C24	127.81(16)
C4	C5	C11	123.39(17)	C25	C24	C23	122.12(16)
C6	C5	C4	116.65(18)	C25	C24	C29	120.07(17)
C6	C5	C11	119.80(16)	C29	C24	C23	117.81(17)
C1	C6	C5	121.71(17)	C24	C25	C26	121.37(16)
C8	C7	C3	111.08(18)	C25	C26	C27	117.25(17)
C8	C7	C9	107.6(2)	C25	C26	C30	120.78(16)

C9	C7	C3	110.44(17)	C27	C26	C30	121.89(17)
C10	C7	C3	110.50(19)	O4	C27	C26	118.93(17)
C10	C7	C8	107.3(2)	O4	C27	C28	118.41(16)
C10	C7	C9	109.8(2)	C28	C27	C26	122.55(17)
C5	C11	C13	106.9(2)	C27	C28	C34	122.04(17)
C5	C11	C12'	121.5(3)	C29	C28	C27	117.50(16)
C5	C11	C14'	109.3(3)	C29	C28	C34	120.45(17)
C12	C11	C5	109.9(2)	C28	C29	C24	121.22(18)
C12	C11	C13	112.4(3)	C31	C30	C26	112.04(16)
C14	C11	C5	111.5(2)	C31	C30	C32	105.68(17)
C14	C11	C12	108.2(3)	C31	C30	C33	108.00(17)
C14	C11	C13	107.9(3)	C32	C30	C26	112.66(16)
C12'	C11	C14'	101.2(4)	C33	C30	C26	108.74(17)
C13'	C11	C5	109.8(3)	C33	C30	C32	109.59(19)
C13'	C11	C12'	107.6(4)	C35	C34	C28	109.98(15)
C13'	C11	C14'	106.3(4)	C35	C34	C36	110.31(17)
O2	C15	C1	120.55(16)	C35	C34	C37	107.24(17)
N1	C15	O2	112.31(16)	C36	C34	C28	110.64(16)
N1	C15	C1	127.14(17)	C37	C34	C28	111.22(16)
O2	C16	C17	121.62(15)	C37	C34	C36	107.37(17)

Table 6 : Torsion Angles for **2.33**

A	B	C	D	Angle/°	A	B	C	D	Angle/°
O1	C4	C5	C6	-178.78(19)	C6	C5	C11	C14'	-43.8(4)
O1	C4	C5	C11	-3.5(3)	C7	C3	C4	O1	0.2(3)
O2	C16	C17	N3	-19.2(3)	C7	C3	C4	C5	-178.55(19)
O2	C16	C17	C18	162.25(17)	C11	C5	C6	C1	-173.64(18)
O3	C23	C24	C25	2.0(3)	C15	O2	C16	N2	0.9(2)
O3	C23	C24	C29	-178.12(16)	C15	O2	C16	C17	-178.42(17)
O4	C27	C28	C29	-178.38(16)	C15	N1	N2	C16	-0.4(2)
O4	C27	C28	C34	1.9(3)	C15	C1	C2	C3	-176.50(18)
N1	N2	C16	O2	-0.3(2)	C15	C1	C6	C5	174.79(18)
N1	N2	C16	C17	178.94(18)	C16	O2	C15	N1	-1.2(2)
N2	N1	C15	O2	1.0(2)	C16	O2	C15	C1	178.80(17)
N2	N1	C15	C1	-178.97(18)	C16	C17	C18	C19	176.97(17)
N2	C16	C17	N3	161.58(19)	C17	N3	C21	C20	0.1(3)
N2	C16	C17	C18	-17.0(3)	C17	N3	C21	C22	178.01(16)
N3	C17	C18	C19	-1.5(3)	C17	C18	C19	C20	1.5(3)
N3	C21	C22	O3	-11.3(3)	C18	C19	C20	C21	-0.9(3)
N3	C21	C22	N4	174.06(18)	C19	C20	C21	N3	0.1(3)
N4	N5	C23	O3	-0.1(2)	C19	C20	C21	C22	-177.89(17)
N4	N5	C23	C24	-179.40(18)	C20	C21	C22	O3	166.75(17)
N5	N4	C22	O3	-0.7(2)	C20	C21	C22	N4	-7.9(3)
N5	N4	C22	C21	174.33(17)	C21	N3	C17	C16	-177.80(16)
N5	C23	C24	C25	-178.68(19)	C21	N3	C17	C18	0.7(3)
N5	C23	C24	C29	1.2(3)	C22	O3	C23	N5	-0.3(2)
C1	C2	C3	C4	1.1(3)	C22	O3	C23	C24	179.09(16)
C1	C2	C3	C7	178.40(19)	C22	N4	N5	C23	0.4(2)
C2	C1	C6	C5	-2.1(3)	C23	O3	C22	N4	0.6(2)
C2	C1	C15	O2	-161.04(18)	C23	O3	C22	C21	-174.66(16)

C2	C1	C15	N1	18.9(3)	C23	C24	C25	C26	179.62(17)
C2	C3	C4	O1	177.42(18)	C23	C24	C29	C28	-179.56(17)
C2	C3	C4	C5	-1.3(3)	C24	C25	C26	C27	-1.1(3)
C2	C3	C7	C8	3.0(3)	C24	C25	C26	C30	175.70(17)
C2	C3	C7	C9	122.3(2)	C25	C24	C29	C28	0.3(3)
C2	C3	C7	C10	-116.1(2)	C25	C26	C27	O4	178.42(16)
C3	C4	C5	C6	-0.2(3)	C25	C26	C27	C28	2.4(3)
C3	C4	C5	C11	175.15(19)	C25	C26	C30	C31	7.5(3)
C4	C3	C7	C8	-179.9(2)	C25	C26	C30	C32	126.47(19)
C4	C3	C7	C9	-60.6(3)	C25	C26	C30	C33	-111.8(2)
C4	C3	C7	C10	61.1(3)	C26	C27	C28	C29	-2.3(3)
C4	C5	C6	C1	1.9(3)	C26	C27	C28	C34	178.00(17)
C4	C5	C11	C12	64.5(3)	C27	C26	C30	C31	-175.93(17)
C4	C5	C11	C13	-57.8(3)	C27	C26	C30	C32	-56.9(2)
C4	C5	C11	C14	-175.4(3)	C27	C26	C30	C33	64.8(2)
C4	C5	C11	C12'	23.9(5)	C27	C28	C29	C24	0.9(3)
C4	C5	C11	C13'	-102.8(4)	C27	C28	C34	C35	64.5(2)
C4	C5	C11	C14'	141.0(4)	C27	C28	C34	C36	-57.6(2)
C6	C1	C2	C3	0.5(3)	C27	C28	C34	C37	-176.88(18)
C6	C1	C15	O2	22.1(3)	C29	C24	C25	C26	-0.2(3)
C6	C1	C15	N1	-158.0(2)	C29	C28	C34	C35	-115.2(2)
C6	C5	C11	C12	-120.3(3)	C29	C28	C34	C36	122.67(19)
C6	C5	C11	C13	117.4(3)	C29	C28	C34	C37	3.4(2)
C6	C5	C11	C14	-0.3(3)	C30	C26	C27	O4	1.7(3)
C6	C5	C11	C12'	-160.9(4)	C30	C26	C27	C28	-174.36(17)
C6	C5	C11	C13'	72.4(4)	C34	C28	C29	C24	-179.37(17)

Table 7 : Hydrogen Atom Coordinates (Å×10^4) and Isotropic Displacement Parameters (Å^2×10^3) for **2.33**

Atom	***x***	***y***	***z***	**U(eq)**	**Atom**	***x***	***y***	***z***	**U(eq)**
H1	2423	559	8153	69	H13F	3076	-937	6494	73
H4	2977	412	2790	42	H14D	2531	2493	6541	66
H2	5029	3147	8709	31	H14E	2419	1191	6111	66
H6	4296	2288	6899	28	H14F	3322	1851	6224	66
H8A	4500	3672	9618	90	H18	7588	6140	6917	29
H8B	5065	2363	9660	90	H19	8155	7069	6014	32
H8C	4420	2660	10195	90	H20	7522	6581	5012	29
H9A	2963	3497	9384	77	H25	4664	2063	4518	26
H9B	2920	2509	9975	77	H29	5246	3490	2808	27
H9C	2537	2068	9293	77	H31A	4377	330	5011	48
H10A	3809	479	10032	66	H31B	3519	-411	5139	48
H10B	4432	159	9484	66	H31C	3522	1152	5005	48
H10C	3445	12	9348	66	H32A	2438	-676	4329	62
H12A	1829	960	7426	83	H32B	2550	-208	3615	62
H12B	1765	897	6669	83	H32C	2446	873	4160	62
H12C	2092	2220	7020	83	H33A	4609	-1316	4132	70
H13A	3128	-835	7678	69	H33B	3874	-1565	3604	70
H13B	3491	-1156	7004	69	H33C	3757	-2003	4322	70
H13C	2505	-1197	7087	69	H35A	3307	3163	1939	44
H14A	3715	246	6322	59	H35B	3056	1626	1934	44

H14B	3488	1792	6336	59	H35C	3406	2293	1314	44
H14C	2807	738	6075	59	H36A	4203	-131	1938	51
H12D	2074	-213	7575	53	H36B	5153	336	1893	51
H12E	1829	-244	6832	53	H36C	4505	525	1299	51
H12F	1712	1092	7228	53	H37A	4795	3818	1864	59
H13D	3538	-1074	7181	73	H37B	4856	2888	1254	59
H13E	3951	-207	6644	73	H37C	5508	2708	1847	59

Table 1 : Crystal data and structure refinement for **2.35**

Empirical formula	$C_{40}H_{50}N_4O_6$	F(000)	732.0
Formula weight	682.84	Crystal size/mm^3	0.3 × 0.3 × 0.15
Temperature/K	100(2)	2Θ range for data collection	6.14 to 153.4°
Crystal system	triclinic	Index ranges	$-10 \le h \le 14$, $-14 \le k \le 12$, $-18 \le l \le 17$
Space group	P-1	Reflections collected	14333
a/Å	11.5105(4)	Independent reflections	7724[R(int) = 0.0238]
b/Å	11.6129(4)	Data/restraints/parameters	7724/0/453
c/Å	14.9858(6)	Goodness-of-fit on F^2	1.016
α/°	91.529(3)	Final R indexes [I>=2σ (I)]	R_1 = 0.0534, wR_2 = 0.1405
β/°	105.651(3)	Final R indexes [all data]	R_1 = 0.0609, wR_2 = 0.1485
γ/°	102.036(3)	Largest diff. peak/hole / e Å^{-3}	0.78/-0.74
Volume/Å^3	1879.15(12)		
Z	2		
ρ_{calc}mg/mm^3	1.207		
m/mm^{-1}	0.654		

Table 2 : Fractional Atomic Coordinates (×10^4) and Equivalent Isotropic Displacement Parameters (Å^2×10^3) for **2.35**U_{eq} is defined as 1/3 of of the trace of the orthogonalised U_{IJ} tensor.

Atom	***x***	***y***	***z***	**U(eq)**
O1	2922.5(11)	9051.5(11)	1881.6(8)	25.4(3)
O2	1400.5(10)	4759.7(10)	4195.0(8)	23.0(2)
O3	1195.7(12)	2139.2(11)	4495.1(8)	26.8(3)
O4	1847.2(11)	-127.2(11)	7108.0(8)	26.2(3)
O5	3650.6(10)	409.2(10)	8952.6(8)	23.0(2)
O6	6601(2)	4553.3(14)	12148.8(12)	71.1(7)
N1	-490.1(14)	4982.7(13)	3512.1(12)	30.7(3)
N2	-574.9(14)	4006.8(14)	4052.5(12)	32.2(3)
N3	2221.8(13)	-1035.1(14)	9198.3(10)	28.0(3)
N4	2791.6(13)	-300.8(14)	10029.5(10)	27.1(3)
C1	1272.7(15)	6383.4(14)	3204.8(11)	20.8(3)
C2	2553.5(14)	6800.6(14)	3462.6(11)	20.1(3)
C3	3105.4(14)	7736.2(13)	3048.1(10)	18.9(3)
C4	2321.9(15)	8209.4(14)	2319.9(10)	19.8(3)
C5	1021.0(15)	7864.2(14)	2091.3(11)	20.7(3)
C6	525.1(14)	6938.2(14)	2546.5(11)	21.1(3)
C7	4510.9(15)	8259.8(15)	3390.6(11)	22.6(3)
C8	5118.6(16)	7702.5(19)	4261.0(13)	33.6(4)

C9	4750.6(16)	9593.0(16)	3665.2(13)	29.7(4)
C10	5151.0(15)	8050.7(16)	2641.8(12)	26.8(4)
C11	140.6(15)	8421.7(16)	1350.9(12)	25.8(3)
C12	527.2(19)	9780.4(18)	1428.0(15)	38.1(4)
C13	66.2(17)	7900.8(18)	378.9(12)	31.1(4)
C14	-1174.5(17)	8132.7(19)	1462.4(13)	34.4(4)
C15	683.3(15)	5390.9(14)	3620.1(12)	22.7(3)

Table 3 : Anisotropic Displacement Parameters ($Å^2×10^3$) for **2.35**The Anisotropic displacement factor exponent takes the form: $-2\pi^2[h^2a^{*2}U_{11}+2hka×b×U_{12}]$

Atom	**U_{11}**	**U_{22}**	**U_{33}**	**U_{23}**	**U_{13}**	**U_{12}**
O1	26.0(6)	28.2(6)	21.0(6)	11.6(5)	6.8(5)	2.7(5)
O2	25.0(6)	18.2(5)	26.7(6)	8.8(4)	8.6(5)	3.7(4)
O3	36.4(6)	24.0(6)	23.3(6)	9.0(5)	11.1(5)	9.6(5)
O4	33.8(6)	30.0(6)	18.9(6)	8.9(5)	8.2(5)	14.3(5)
O5	26.3(6)	24.8(6)	20.3(5)	7.3(4)	9.0(4)	7.2(5)
O6	142(2)	29.0(8)	40.5(9)	-10.5(7)	45.9(11)	-9.4(10)
N1	27.0(7)	25.3(7)	42.5(9)	17.5(7)	12.9(7)	6.0(6)
N2	29.2(8)	25.3(7)	44.5(9)	18.1(7)	13.4(7)	5.6(6)
N3	27.1(7)	34.8(8)	22.7(7)	11.0(6)	6.8(6)	7.0(6)
N4	27.2(7)	33.5(8)	22.5(7)	10.9(6)	7.8(6)	8.9(6)
C1	25.0(8)	17.0(7)	21.4(7)	3.9(6)	8.4(6)	4.1(6)
C2	24.8(8)	18.9(7)	17.6(7)	4.7(6)	6.1(6)	6.4(6)
C3	22.5(7)	18.1(7)	16.0(7)	2.4(6)	5.5(6)	4.1(6)
C4	24.8(7)	18.4(7)	16.2(7)	3.2(6)	7.1(6)	3.0(6)
C5	24.2(8)	21.0(7)	16.8(7)	3.2(6)	4.8(6)	5.9(6)
C6	20.2(7)	19.9(7)	21.7(7)	2.4(6)	4.5(6)	3.2(6)
C7	22.0(7)	26.3(8)	17.2(7)	4.9(6)	4.5(6)	1.1(6)
C8	23.4(8)	46.9(11)	25.3(9)	12.8(8)	1.8(7)	2.1(8)
C9	27.9(8)	29.3(9)	26.5(9)	-4.2(7)	6.1(7)	-2.5(7)
C10	24.0(8)	31.3(9)	24.8(8)	3.5(7)	8.1(6)	3.8(7)
C11	24.9(8)	31.6(9)	22.7(8)	10.2(7)	6.1(6)	9.6(7)
C12	40.7(10)	32.2(10)	41.3(11)	13.2(8)	5.2(9)	15.2(8)
C13	28.3(8)	44.8(11)	20.4(8)	10.3(7)	5.7(7)	9.3(8)
C14	28.8(9)	50.3(12)	30.4(9)	17.3(8)	10.4(7)	18.2(8)
C15	24.5(8)	19.0(7)	25.8(8)	6.5(6)	7.6(6)	6.6(6)
C16	27.9(8)	18.4(8)	30.1(8)	8.1(6)	11.5(7)	2.7(6)
C17	30.6(8)	19.7(8)	26.2(8)	7.4(6)	9.8(7)	5.5(6)
C18	21.7(7)	21.1(8)	21.4(8)	5.2(6)	5.7(6)	3.5(6)
C19	25.1(8)	28.0(8)	18.7(7)	1.2(6)	6.6(6)	3.5(6)
C20	24.0(8)	24.3(8)	25.2(8)	-2.4(6)	7.3(6)	4.6(6)
C21	21.0(7)	19.9(7)	27.0(8)	3.4(6)	4.7(6)	4.5(6)
C22	19.5(7)	24.0(8)	19.1(7)	4.1(6)	5.2(6)	3.2(6)
C23	20.8(7)	20.9(7)	20.3(7)	1.3(6)	5.3(6)	4.2(6)
C24	29.8(8)	24.8(8)	23.8(8)	9.3(6)	7.3(7)	8.3(7)
C25	22.7(7)	26.3(8)	23.8(8)	10.2(6)	5.8(6)	7.6(6)
C26	27.3(8)	28.4(8)	20.8(8)	11.3(6)	10.2(6)	14.6(7)
C27	36.4(9)	23.3(8)	22.6(8)	8.0(6)	11.5(7)	14.5(7)
C28	38.9(9)	23.3(8)	21.1(8)	4.9(6)	11.5(7)	11.6(7)

C29	60.3(12)	21.8(8)	24.2(9)	3.1(7)	17.1(8)	6.2(8)
C30	93.6(18)	20.6(9)	29.4(10)	0.8(8)	27.8(11)	6.7(10)
C31	85.5(16)	24.5(9)	29.8(10)	9.3(8)	31.8(10)	20.9(10)
C32	52.5(11)	26.4(9)	29.1(9)	13.0(7)	23.2(8)	19.1(8)
C33	56.0(12)	23.8(9)	26.2(9)	0.4(7)	12.2(8)	-4.1(8)
C34	37(1)	30.0(9)	28.7(9)	1.8(7)	10.6(8)	-2.1(8)
C35	87.1(18)	24.4(10)	50.0(13)	5.1(9)	40.4(13)	1.7(10)
C36	67.3(16)	43.6(13)	33.1(11)	-0.6(9)	-0.3(10)	-15.2(11)
C37	111(2)	27(1)	37.7(11)	10.8(9)	46.0(13)	24.9(12)
C38	187(4)	37.8(13)	64.4(17)	19.2(12)	81(2)	52.0(19)
C39	117(2)	44.8(13)	32.7(12)	2.1(10)	37.9(14)	5.9(14)
C40	100(2)	44.0(12)	45.8(13)	16.3(10)	49.6(14)	36.4(13)

Table 4 : Bond Lengths for **2.35**

Atom	Atom	Length/Å	**Atom**	**Atom**	**Length/Å**	**Atom**	**Atom**	**Length/Å**	**Atom**	**Atom**	**Length/Å**
O1	C4	1.3650(19)	C7	C10	1.538(2)	N3	C25	1.285(2)	C27	C32	1.402(2)
O2	C15	1.3651(19)	C11	C12	1.540(3)	N4	C26	1.300(2)	C28	C29	1.395(3)
O2	C16	1.3625(19)	C11	C13	1.536(2)	C1	C2	1.394(2)	C29	C30	1.409(3)
O3	C17	1.428(2)	C11	C14	1.536(2)	C1	C6	1.391(2)	C29	C33	1.539(3)
O3	C18	1.3739(19)	C16	C17	1.489(2)	C1	C15	1.455(2)	C30	C31	1.414(3)
O4	C22	1.3744(19)	C18	C19	1.393(2)	C2	C3	1.390(2)	C31	C32	1.390(3)
O4	C24	1.4326(19)	C18	C23	1.384(2)	C3	C4	1.419(2)	C31	C37	1.548(3)
O5	C25	1.362(2)	C19	C20	1.380(2)	C3	C7	1.541(2)	C33	C34	1.526(3)
O5	C26	1.3633(19)	C20	C21	1.398(2)	C4	C5	1.409(2)	C33	C35	1.549(3)
O6	C30	1.380(3)	C21	C22	1.381(2)	C5	C6	1.393(2)	C33	C36	1.542(3)
N1	N2	1.413(2)	C22	C23	1.398(2)	C5	C11	1.544(2)	C37	C38	1.544(3)
N1	C15	1.298(2)	C24	C25	1.487(2)	C7	C8	1.533(2)	C37	C39	1.536(4)
N2	C16	1.283(2)	C26	C27	1.457(3)	C7	C9	1.539(2)	C37	C40	1.533(4)
N3	N4	1.406(2)	C27	C28	1.389(2)						

Table 5 : Bond Angles for **2.35**

Atom	**Atom**	**Atom**	**Angle/°**	**Atom**	**Atom**	**Atom**	**Angle/°**
C16	O2	C15	102.38(12)	O3	C18	C23	123.88(15)
C18	O3	C17	116.70(12)	C23	C18	C19	120.49(15)
C22	O4	C24	117.81(13)	C20	C19	C18	119.18(15)
C25	O5	C26	102.98(13)	C19	C20	C21	121.74(15)
C15	N1	N2	106.00(14)	C22	C21	C20	117.83(15)
C16	N2	N1	106.07(14)	O4	C22	C21	124.56(15)
C25	N3	N4	106.04(15)	O4	C22	C23	113.74(14)
C26	N4	N3	106.58(14)	C21	C22	C23	121.70(15)
C2	C1	C15	121.80(14)	C18	C23	C22	119.04(15)
C6	C1	C2	119.69(14)	O4	C24	C25	105.22(13)
C6	C1	C15	118.50(14)	O5	C25	C24	118.76(14)
C3	C2	C1	121.17(14)	N3	C25	O5	112.77(15)
C2	C3	C4	117.49(14)	N3	C25	C24	128.39(16)
C2	C3	C7	120.93(14)	O5	C26	C27	118.75(14)
C4	C3	C7	121.55(14)	N4	C26	O5	111.62(15)
O1	C4	C3	114.96(14)	N4	C26	C27	129.56(15)
O1	C4	C5	122.68(14)	C28	C27	C26	120.71(15)

C5	C4	C3	122.32(14)	C28	C27	C32	119.51(17)
C4	C5	C11	123.72(14)	C32	C27	C26	119.73(16)
C6	C5	C4	116.92(14)	C27	C28	C29	122.06(16)
C6	C5	C11	119.32(14)	C28	C29	C30	117.01(19)
C1	C6	C5	121.91(15)	C28	C29	C33	120.88(16)
C8	C7	C3	111.31(13)	C30	C29	C33	122.04(18)
C8	C7	C9	106.80(14)	O6	C30	C29	121.0(2)
C8	C7	C10	107.63(14)	O6	C30	C31	116.48(18)
C9	C7	C3	109.61(13)	C29	C30	C31	122.4(2)
C10	C7	C3	111.42(13)	C30	C31	C37	121.3(2)
C10	C7	C9	109.94(14)	C32	C31	C30	117.81(17)
C12	C11	C5	112.92(14)	C32	C31	C37	120.9(2)
C12	C11	C14	105.54(15)	C31	C32	C27	121.05(18)
C13	C11	C5	109.17(14)	C29	C33	C35	108.92(18)
C13	C11	C12	110.69(15)	C29	C33	C36	111.99(17)
C13	C11	C14	107.49(15)	C34	C33	C29	111.44(15)
C14	C11	C5	110.87(14)	C34	C33	C35	106.20(17)
O2	C15	C1	119.35(14)	C34	C33	C36	105.65(19)
N1	C15	O2	112.35(14)	C36	C33	C35	112.48(19)
N1	C15	C1	128.29(15)	C38	C37	C31	109.43(17)
O2	C16	C17	118.97(14)	C39	C37	C31	110.2(2)
N2	C16	O2	113.21(15)	C39	C37	C38	110.2(2)
N2	C16	C17	127.81(15)	C39	C37	C40	108.36(19)
O3	C17	C16	106.64(13)	C40	C37	C31	111.4(2)
O3	C18	C19	115.61(14)	C40	C37	C38	107.2(2)

Table 6 : Hydrogen Bonds for **2.35**

D	H	A	d(D-H)/Å	d(H-A)/Å	d(D-A)/Å	D-H-A/°
O1	H1	N4[1]	0.84	2.20	2.8678(18)	136.4

[1]+X,1+Y,-1+Z

Table 7 : Torsion Angles for **2.35**

A	B	C	D	Angle/°	A	B	C	D	Angle/°
O1	C4	C5	C6	175.69(14)	C15	O2	C16	N2	0.08(19)
O1	C4	C5	C11	-2.1(2)	C15	O2	C16	C17	179.46(15)
O2	C16	C17	O3	-81.39(18)	C15	N1	N2	C16	0.0(2)
O3	C18	C19	C20	179.92(14)	C15	C1	C2	C3	178.85(15)
O3	C18	C23	C22	-179.08(14)	C15	C1	C6	C5	-177.46(15)
O4	C22	C23	C18	178.98(13)	C16	O2	C15	N1	-0.09(19)
O4	C24	C25	O5	-71.12(18)	C16	O2	C15	C1	-179.31(15)
O4	C24	C25	N3	105.37(19)	C17	O3	C18	C19	177.07(14)
O5	C26	C27	C28	-12.9(2)	C17	O3	C18	C23	-4.4(2)
O5	C26	C27	C32	164.31(15)	C18	O3	C17	C16	-170.38(13)
O6	C30	C31	C32	-179.3(2)	C18	C19	C20	C21	-0.7(2)
O6	C30	C31	C37	1.7(3)	C19	C18	C23	C22	-0.6(2)
N1	N2	C16	O2	0.0(2)	C19	C20	C21	C22	-0.7(2)
N1	N2	C16	C17	-179.35(17)	C20	C21	C22	O4	-178.32(14)
N2	N1	C15	O2	0.1(2)	C20	C21	C22	C23	1.5(2)
N2	N1	C15	C1	179.20(17)	C21	C22	C23	C18	-0.8(2)

N2	C16	C17	O3	97.9(2)	C22	O4	C24	C25	163.34(13)
N3	N4	C26	O5	-1.17(18)	C23	C18	C19	C20	1.3(2)
N3	N4	C26	C27	175.75(16)	C24	O4	C22	C21	18.9(2)
N4	N3	C25	O5	0.04(18)	C24	O4	C22	C23	-160.93(14)
N4	N3	C25	C24	-176.63(15)	C25	O5	C26	N4	1.17(17)
N4	C26	C27	C28	170.35(17)	C25	O5	C26	C27	-176.13(14)
N4	C26	C27	C32	-12.4(3)	C25	N3	N4	C26	0.69(18)
C1	C2	C3	C4	-3.2(2)	C26	O5	C25	N3	-0.71(18)
C1	C2	C3	C7	174.98(14)	C26	O5	C25	C24	176.31(14)
C2	C1	C6	C5	3.8(2)	C26	C27	C28	C29	178.70(16)
C2	C1	C15	O2	-7.9(2)	C26	C27	C32	C31	-177.92(17)
C2	C1	C15	N1	173.02(17)	C27	C28	C29	C30	0.5(3)
C2	C3	C4	O1	-174.26(13)	C27	C28	C29	C33	-176.68(17)
C2	C3	C4	C5	7.9(2)	C28	C27	C32	C31	-0.7(3)
C2	C3	C7	C8	-5.6(2)	C28	C29	C30	O6	-179.8(2)
C2	C3	C7	C9	-123.53(16)	C28	C29	C30	C31	-3.4(3)
C2	C3	C7	C10	114.55(16)	C28	C29	C33	C34	-2.7(3)
C3	C4	C5	C6	-6.7(2)	C28	C29	C33	C35	114.2(2)
C3	C4	C5	C11	175.59(15)	C28	C29	C33	C36	-120.8(2)
C4	C3	C7	C8	172.50(15)	C29	C30	C31	C32	4.1(3)
C4	C3	C7	C9	54.57(19)	C29	C30	C31	C37	-174.9(2)
C4	C3	C7	C10	-67.35(19)	C30	C29	C33	C34	-179.7(2)
C4	C5	C6	C1	0.7(2)	C30	C29	C33	C35	-62.9(3)
C4	C5	C11	C12	-45.1(2)	C30	C29	C33	C36	62.2(3)
C4	C5	C11	C13	78.5(2)	C30	C31	C32	C27	-2.0(3)
C4	C5	C11	C14	-163.25(16)	C30	C31	C37	C38	59.2(4)
C6	C1	C2	C3	-2.5(2)	C30	C31	C37	C39	-62.2(3)
C6	C1	C15	O2	173.39(14)	C30	C31	C37	C40	177.5(2)
C6	C1	C15	N1	-5.7(3)	C32	C27	C28	C29	1.5(3)
C6	C5	C11	C12	137.25(17)	C32	C31	C37	C38	-119.8(3)
C6	C5	C11	C13	-99.17(17)	C32	C31	C37	C39	118.8(2)
C6	C5	C11	C14	19.1(2)	C32	C31	C37	C40	-1.5(3)
C7	C3	C4	O1	7.6(2)	C33	C29	C30	O6	-2.7(4)
C7	C3	C4	C5	-170.23(14)	C33	C29	C30	C31	173.8(2)
C11	C5	C6	C1	178.54(15)	C37	C31	C32	C27	177.04(19)

Table8 : Hydrogen Atom Coordinates (Å×10^4) and Isotropic Displacement Parameters (Å^2×10^3) for **2.35**

Atom	***x***	***y***	***z***	**U(eq)**	**Atom**	***x***	***y***	***z***	**U(eq)**
H1	2486	9054	1333	38	H20	1910	-1386	4289	30
H6	7179	4879	11935	107	H21	2043	-1698	5853	28
H2	3058	6439	3930	24	H23	1408	1576	6226	25
H6A	-349	6678	2403	25	H24A	3231	-985	7417	31
H8A	4982	6848	4117	50	H24B	1919	-1778	7448	31
H8B	4752	7851	4760	50	H28	5498	2080	9598	32
H8C	6010	8052	4462	50	H32	3525	1409	11463	38
H9A	4366	9983	3128	45	H34	7413	2850	9499	50
H9B	5645	9928	3868	45	H34B	7794	4168	9220	50
H9C	4394	9716	4175	45	H34C	6364	3511	8981	50
H10A	4982	7201	2463	40	H35A	6744	5679	10804	77

H10B	6046	8359	2890	40	H35B	5980	5214	9752	77
H10C	4833	8459	2096	40	H35C	7419	5841	9997	77
H12A	1372	10023	1374	57	H36A	8457	4530	11660	83
H12B	497	10099	2032	57	H36B	9039	4750	10806	83
H12C	-41	10085	928	57	H36C	8630	3434	11078	83
H13A	896	8060	290	47	H38A	4146	4756	13250	124
H13B	-478	8265	-94	47	H38B	3610	4499	12144	124
H13C	-266	7045	321	47	H38C	5048	5080	12603	124
H14A	-1465	7274	1440	52	H39A	5510	3518	14162	95
H14B	-1731	8441	957	52	H39B	6442	3817	13535	95
H14C	-1167	8498	2061	52	H39C	5855	2470	13643	95
H17A	1733	3401	5552	30	H40A	3290	2694	13445	81
H17B	323	2680	5360	30	H40B	3599	1629	12918	81
H19	1533	370	3693	29	H40C	2742	2433	12340	81

Table 1 : Crystal data and structure refinement for **3.5**

Empirical formula	$C_{23}H_{28}N_2O_2$	F(000)	784.0
Formula weight	364.47	Crystal size/mm^3	0.3 × 0.15 × 0.1
Temperature/K	100(2)	2Θ range for data collection	4.88 to 55.12°
Crystal system	orthorhombic	Index ranges	$-23 \le h \le 12$, $-8 \le k \le 8$, $-15 \le l \le 21$
Space group	Pnma	Reflections collected	8308
a/Å	18.2298(10)	Independent reflections	2602[R(int) = 0.0298]
b/Å	6.8289(3)	Data/restraints/parameters	2602/1/152
c/Å	16.7227(7)	Goodness-of-fit on F^2	0.991
α/°	90.00	Final R indexes [I>=2σ (I)]	R_1 = 0.0626, wR_2 = 0.1617
β/°	90.00	Final R indexes [all data]	R_1 = 0.0772, wR_2 = 0.1746
γ/°	90.00	Largest diff. peak/hole / e Å^{-3}	0.61/-0.65
Volume/Å^3	2081.80(17)		
Z	4		
ρ_{calc}mg/mm^3	1.163		
m/mm^{-1}	0.074		

Table 2 : Fractional Atomic Coordinates (×10^4) and Equivalent Isotropic Displacement Parameters (Å^2×10^3) for **3.5**. U_{eq} is defined as 1/3 of of the trace of the orthogonalised U_{IJ} tensor.

Atom	***x***	***y***	***z***	**U(eq)**	**Atom**	***x***	***y***	***z***	**U(eq)**
O1	7689.8(10)	2500	6764.6(10)	22.2(4)	C9	9917.4(14)	2500	5773.0(16)	20.6(5)
O2	5872.4(9)	2500	5243.5(10)	16.3(4)	C10	8615.3(11)	676(3)	3165.9(12)	29.1(5)
N1	6269.6(12)	2500	6487.6(13)	20.8(5)	C11	8170.6(14)	2500	3386.3(14)	19.3(5)
N2	5499.1(12)	2500	6507.3(13)	22.5(5)	C12	7462.3(17)	2500	2898.1(19)	31.7(7)
C1	7798.3(14)	2500	5961.4(14)	15.8(5)	C13	6461.1(14)	2500	5741.9(14)	16.3(5)
C2	8524.5(13)	2500	5661.8(14)	15.4(5)	C14	5293.2(14)	2500	5765.7(14)	17.7(5)
C3	8604.8(14)	2500	4834.2(14)	16.5(5)	C15	4542.6(14)	2500	5459.5(15)	17.8(5)
C4	8018.4(14)	2500	4287.5(14)	15.7(5)	C16	3964.3(15)	2500	6007.3(15)	22.3(6)
C5	7316.8(13)	2500	4598.4(14)	15.1(5)	C17	3247.2(15)	2500	5736.2(16)	22.9(6)
C6	7202.4(13)	2500	5428.5(14)	15.7(5)	C18	3085.6(14)	2500	4922.3(16)	19.3(5)
C7	9175.9(10)	644(3)	6753.1(11)	24.3(4)	C19	3667.5(15)	2500	4383.2(15)	20.7(5)

C8	9188.5(14)	2500	6228.2(15)	17.1(5)	C20	4392.2(14)	2500	4643.3(15)	19.8(5)
					C21	2297.7(14)	2500	4650.1(17)	23.3(6)

Table 3 : Anisotropic Displacement Parameters ($Å^2×10^3$) for **3.5** The Anisotropic displacement factor exponent takes the form: $-2\pi^2[h^2a^{*2}U_{11}+...+2hka×b×U_{12}]$

Atom	U_{11}	U_{22}	U_{33}	U_{23}	U_{13}	U_{12}
O1	17.9(10)	35.0(11)	13.8(8)	0	0.1(7)	0
O2	13.6(8)	18.5(9)	16.9(8)	0	-0.2(6)	0
N1	16.8(11)	27.4(11)	18.2(10)	0	0.0(8)	0
N2	15.6(11)	33.4(12)	18.5(10)	0	0.1(8)	0
C1	19.7(12)	14.1(11)	13.7(11)	0	-0.3(9)	0
C2	17.0(12)	13.0(11)	16.1(11)	0	-2.5(9)	0
C3	15.9(12)	16.4(11)	17.2(11)	0	0.2(9)	0
C4	18.4(12)	14.3(11)	14.3(11)	0	-1.1(9)	0
C5	17.0(12)	14.1(11)	14.3(11)	0	-3.4(9)	0
C6	15.1(12)	15.0(11)	17.1(11)	0	-0.6(9)	0
C7	22.8(9)	25.5(10)	24.5(9)	7.9(8)	-5.4(7)	-0.3(8)
C8	17.9(12)	17.3(12)	16.1(11)	0	-2.7(9)	0
C9	17.9(12)	23.2(13)	20.8(12)	0	-4.1(10)	0
C11	20.0(13)	23.5(13)	14.3(11)	0	0.2(9)	0
C13	18.2(12)	14.4(11)	16.4(11)	0	-2.9(9)	0
C14	16.7(12)	19.1(12)	17.3(11)	0	2.9(9)	0
C15	18.3(13)	15.6(11)	19.4(12)	0	-0.1(10)	0
C16	22.1(13)	27.8(14)	17.0(11)	0	0.4(10)	0
C17	19.3(13)	26.9(13)	22.5(13)	0	2.5(10)	0
C18	18.3(13)	14.2(11)	25.2(13)	0	-2.3(10)	0
C19	23.4(13)	20.2(12)	18.6(12)	0	-2.9(10)	0
C20	18.4(13)	22.3(12)	18.6(12)	0	1.4(10)	0
C21	18.9(13)	22.7(13)	28.5(13)	0	-4.3(11)	0

Table 4 : Bond Lengths for **3.5**

Atom	Atom	Length/Å	Atom	Atom	Length/Å	Atom	Atom	Length/Å	Atom	Atom	Length/Å
O1	C1	1.358(3)	C7	C8	1.542(2)	C2	C3	1.392(3)	C15	C20	1.392(3)
O2	C13	1.359(3)	C8	$C7^1$	1.542(2)	C2	C8	1.537(3)	C16	C17	1.384(4)
O2	C14	1.370(3)	C8	C9	1.531(4)	C3	C4	1.407(3)	C17	C18	1.393(4)
N1	N2	1.405(3)	C10	C11	1.531(3)	C4	C5	1.381(3)	C18	C19	1.392(4)
N1	C13	1.295(3)	C11	$C10^1$	1.531(3)	C4	C11	1.532(3)	C18	C21	1.507(4)
N2	C14	1.296(3)	C11	C12	1.528(4)	C5	C6	1.404(3)	C19	C20	1.391(4)
C1	C2	1.415(3)	C14	C15	1.461(3)	C6	C13	1.449(3)			
C1	C6	1.405(3)	C15	C16	1.397(4)						

^{1}+X,1/2-Y,+Z

Table 5 : Bond Angles for**3.5**

Atom	Atom	Atom	Angle/°	Atom	Atom	Atom	Angle/°
C13	O2	C14	102.58(19)	$C10^1$	C11	C4	109.42(14)
C13	N1	N2	107.0(2)	C10	C11	C4	109.42(14)
C14	N2	N1	105.5(2)	$C10^1$	C11	C10	108.9(2)
O1	C1	C2	119.1(2)	$C10^1$	C11	C12	108.60(15)

O1	C1	C6	121.0(2)	C10	C11	C12	108.60(15)
C6	C1	C2	119.9(2)	C12	C11	C4	111.9(2)
C1	C2	C8	121.2(2)	O2	C13	C6	121.0(2)
C3	C2	C1	116.8(2)	N1	C13	O2	112.2(2)
C3	C2	C8	122.0(2)	N1	C13	C6	126.8(2)
C2	C3	C4	124.5(2)	O2	C14	C15	119.9(2)
C3	C4	C11	120.1(2)	N2	C14	O2	112.8(2)
C5	C4	C3	117.3(2)	N2	C14	C15	127.4(2)
C5	C4	C11	122.6(2)	C16	C15	C14	118.5(2)
C4	C5	C6	120.7(2)	C16	C15	C20	119.6(2)
C1	C6	C13	119.4(2)	C20	C15	C14	121.9(2)
C5	C6	C1	120.8(2)	C17	C16	C15	119.9(2)
C5	C6	C13	119.7(2)	C16	C17	C18	121.3(2)
C7[1]	C8	C2	109.82(14)	C17	C18	C19	118.1(2)
C7	C8	C2	109.82(14)	C17	C18	C21	119.8(2)
C7[1]	C8	C7	110.6(2)	C19	C18	C21	122.1(2)
C9	C8	C2	112.1(2)	C20	C19	C18	121.4(2)
C9	C8	C7	107.21(14)	C19	C20	C15	119.6(2)
C9	C8	C7[1]	107.21(14)				

[1]+X,1/2-Y,+Z

Table 6:Hydrogen Bonds for**3.5**

D	H	A	d(D-H)/Å	d(H-A)/Å	d(D-A)/Å	D-H-A/°
O1	H1	N1	0.843(10)	1.87(2)	2.630(3)	150(3)

Table 7: Torsion Angles for **3.5**

A	B	C	D	Angle/°	A	B	C	D	Angle/°
O1	C1	C2	C3	180.0	C3	C4	C11	C12	180.0
O1	C1	C2	C8	0.0	C4	C5	C6	C1	0.0
O1	C1	C6	C5	180.0	C4	C5	C6	C13	180.0
O1	C1	C6	C13	0.0	C5	C4	C11	C10	-120.39(15)
O2	C14	C15	C16	180.0	C5	C4	C11	C10[1]	120.39(15)
O2	C14	C15	C20	0.0	C5	C4	C11	C12	0.0
N1	N2	C14	O2	0.0	C5	C6	C13	O2	0.0
N1	N2	C14	C15	180.0	C5	C6	C13	N1	180.0
N2	N1	C13	O2	0.0	C6	C1	C2	C3	0.0
N2	N1	C13	C6	180.0	C6	C1	C2	C8	180.0
N2	C14	C15	C16	0.0	C8	C2	C3	C4	180.0
N2	C14	C15	C20	180.0	C11	C4	C5	C6	180.0
C1	C2	C3	C4	0.0	C13	O2	C14	N2	0.0
C1	C2	C8	C7[1]	-60.90(15)	C13	O2	C14	C15	180.0
C1	C2	C8	C7	60.90(14)	C13	N1	N2	C14	0.0
C1	C2	C8	C9	180.0	C14	O2	C13	N1	0.0
C1	C6	C13	O2	180.0	C14	O2	C13	C6	180.0
C1	C6	C13	N1	0.0	C14	C15	C16	C17	180.0
C2	C1	C6	C5	0.0	C14	C15	C20	C19	180.0
C2	C1	C6	C13	180.0	C15	C16	C17	C18	0.0

C2	C3	C4	C5	0.0	C16	C15	C20	C19	0.0
C2	C3	C4	C11	180.0	C16	C17	C18	C19	0.0
C3	C2	C8	C7[1]	119.10(15)	C16	C17	C18	C21	180.0
C3	C2	C8	C7	-119.10(14)	C17	C18	C19	C20	0.0
C3	C2	C8	C9	0.0	C18	C19	C20	C15	0.0
C3	C4	C5	C6	0.0	C20	C15	C16	C17	0.0
C3	C4	C11	C10	59.61(15)	C21	C18	C19	C20	180.0
C3	C4	C11	C10[1]	-59.61(15)					

[1]+X,1/2-Y,+Z

Table 8 : Hydrogen Atom Coordinates (Å×10^4) and Isotropic Displacement Parameters (Å^2×10^3) for **3.5**

Atom	***x***	***y***	***z***	**U(eq)**	**Atom**	***x***	***y***	***z***	**U(eq)**
H1	7236(7)	2500	6860(20)	37(10)	H10C	8719	684	2591	44
H3	9089	2500	4624	20	H12A	7178	3680	3022	48
H5	6907	2500	4247	18	H12B	7173	1336	3032	48
H7A	8715	596	7055	36	H12C	7582	2484	2327	48
H7B	9590	675	7126	36	H16	4063	2500	6565	27
H7C	9214	-518	6412	36	H17	2857	2500	6113	28
H9A	10325	2500	6155	31	H19	3567	2500	3826	25
H9B	9947	3672	5436	31	H20	4782	2500	4266	24
H9C	9947	1328	5436	31	H21A	1974	2500	5118	35
H10A	8334	-500	3302	44	H21B	2203	1328	4328	35
H10B	9078	676	3464	44	H21C	2203	3672	4328	35

Table 1 : Crystal data and structure refinement for **3.8**

Empirical formula	$C_{22}H_{25}ClN_2O_2$	Crystal size/mm3	0.3 × 0.15 × 0.05
Formula weight	384.89	2Θ range for data collection	6.2 to 153.68°
Temperature/K	100(2)	Index ranges	-11 ≤ h ≤ 13, -8 ≤ k ≤ 8, -16 ≤ l ≤ 17
Crystal system	monoclinic	Reflections collected	9198
Space group	$P2_1$	Independent reflections	5379[R(int) = 0.0430]
a/Å	10.5449(3)	Data/restraints/parameters	5379/45/244
b/Å	6.6433(2)	Goodness-of-fit on F2	1.044
c/Å	14.2530(4)	Final R indexes [I>=2σ (I)]	R1 = 0.0499, wR2 = 0.1394
α/°	90.00	Final R indexes [all data]	R1 = 0.0571, wR2 = 0.1473
β/°	91.737(3)	Largest diff. peak/hole / e Å-3	0.54/-0.56
γ/°	90.00	Flack parameter	0.41(5)
Volume/Å^3	998.01(5)		
Z	2		
ρ_{calc}mg/mm^3	1.281		
m/mm^{-1}	1.841		
F(000)	408.0		

Table 2 : Fractional Atomic Coordinates ($\times 10^4$) and Equivalent Isotropic Displacement Parameters ($Å^2 \times 10^3$) for **3.8**. U_{eq} is defined as 1/3 of of the trace of the orthogonalised U_{IJ} tensor.

Atom	*x*	*y*	*z*	U(eq)	Atom	*x*	*y*	*z*	U(eq)
Cl1	-2773.4(4)	5037(3)	4168.8(3)	25.56(16)	C13	5809(5)	6879(9)	6437(5)	42.6(15)
O1	583.1(11)	5045(8)	8420.3(8)	24.3(3)	C14	6642.0(17)	5019(19)	7822.4(15)	45.3(6)
O2	1123.3(11)	5039(8)	5530.9(8)	21.2(3)	C15	933.6(15)	5029(10)	6470.8(11)	19.9(3)
N1	-266.4(13)	5038(9)	6655.5(10)	21.3(3)	C16	-90.8(16)	5038(10)	5155.1(12)	20.9(4)
N2	-938.6(14)	5024(9)	5792.5(10)	23.6(3)	C17	-176.9(11)	5026(9)	4114.1(6)	19.6(4)
C1	2003.3(15)	5038(10)	7131.3(12)	20.0(4)	C18	946.8(8)	5024(9)	3628.9(8)	21.2(4)
C2	1784.7(15)	5033(10)	8095.0(12)	20.5(3)	C19	910.9(9)	5024(9)	2653.2(8)	23.8(4)
C3	2812.0(16)	5028(11)	8748.9(12)	21.0(4)	C20	-248.7(11)	5026(10)	2162.8(6)	25.8(5)
C4	4029.2(16)	5018(12)	8382.0(12)	22.7(4)	C21	-1372.4(9)	5028(9)	2648.0(8)	24.2(4)
C5	4277.7(15)	5033(11)	7421.1(12)	21.5(4)	C22	-1336.6(8)	5028(9)	3623.6(8)	20.4(4)
C6	3240.8(16)	5046(10)	6804.2(12)	21.3(4)	Cl1'	1684(4)	5252(11)	3538(3)	25.56(16)
C7	2598.8(14)	5062(11)	9841.2(12)	20.5(4)	C17'	-709(8)	5030(40)	4162(5)	19.6(4)
C8	1826(4)	6942(6)	10073(4)	26.8(10)	C18'	-2014(8)	4860(40)	4018(6)	21.2(4)
C9	3846.8(17)	5051(15)	10386.5(13)	31.1(4)	C19'	-2539(6)	4900(40)	3112(7)	23.8(4)
C10	1911(5)	3164(8)	10068(3)	38.4(14)	C20'	-1760(9)	5120(40)	2350(5)	25.8(5)
C11	5620.0(15)	5037(12)	7039.3(12)	23.4(4)	C21'	-455(9)	5300(30)	2494(6)	24.2(4)
C12	5807(5)	3137(9)	6438(5)	39.5(14)	C22'	71(6)	5250(30)	3400(7)	20.4(4)

Table 3 : Anisotropic Displacement Parameters ($Å^2 \times 10^3$) for **3.8**. The Anisotropic displacement factor exponent takes the form: $-2\pi^2[h^2a^{*2}U_{11}+...+2hka\times b\times U_{12}]$

Atom	U_{11}	U_{22}	U_{33}	U_{23}	U_{13}	U_{12}
Cl1	15.4(2)	37.2(3)	24.0(2)	-0.7(7)	-1.03(15)	-0.8(6)
O1	14.9(5)	37.6(7)	20.4(6)	-2(2)	1.7(4)	-1(2)
O2	19.2(5)	26.5(6)	18.1(6)	3(2)	1.5(4)	1.5(19)
N1	16.5(6)	29.5(8)	17.8(6)	-2(2)	-2.1(5)	2(2)
N2	20.1(7)	30.7(8)	19.6(7)	-6(2)	-3.5(5)	3(2)
C1	17.0(7)	22.2(8)	21.0(8)	5(2)	2.6(6)	2(2)
C2	16.9(7)	23.1(8)	21.8(8)	2(3)	3.7(6)	2(2)
C3	19.9(8)	24.5(8)	18.7(8)	-3(3)	1.2(6)	0(2)
C4	18.1(8)	28.8(9)	21.1(8)	2(3)	0.1(6)	4(2)
C5	17.4(7)	23.8(8)	23.5(8)	3(3)	2.9(6)	2(2)
C6	19.9(8)	24.8(9)	19.5(7)	3(3)	2.9(6)	6(2)
C7	10.2(6)	29.0(9)	22.4(8)	3(3)	3.2(6)	2(3)
C8	25.9(19)	23.6(18)	32(2)	-7.6(17)	11.4(16)	12.3(16)
C9	22.5(8)	48.4(12)	22.4(8)	2(3)	-0.5(7)	0(3)
C10	38(3)	61(3)	16(2)	-1(2)	-9.8(17)	6(2)
C11	16.0(7)	31.7(9)	22.7(8)	0(3)	3.0(6)	0(3)
C12	24(2)	41(3)	54(4)	-20(3)	19(2)	4(2)
C13	27(3)	40(3)	62(4)	6(3)	11(3)	5(2)
C14	16.4(8)	90(2)	29.9(10)	-3(5)	3.0(7)	-1(4)
C15	21.0(8)	21.4(8)	17.6(7)	0(2)	4.4(6)	-1(2)
C16	21.3(7)	21.4(8)	19.7(8)	3(3)	-2.3(6)	1(3)
C17	18.4(9)	21.1(9)	19.2(8)	2(3)	0.2(7)	-1(3)

C18	17.2(9)	24.8(10)	21.6(9)	-2(3)	-0.9(7)	-2(3)
C19	22.0(9)	30.4(10)	19.2(9)	-1(3)	1.9(7)	-1(3)
C20	31.7(10)	26.7(11)	19.0(9)	-5(3)	-1.1(8)	0(3)
C21	23.8(9)	26.7(10)	21.7(9)	1(3)	-6.6(7)	3(3)
C22	17.9(8)	21.4(9)	21.8(9)	-2(3)	0.1(7)	-1(3)
Cl1'	15.4(2)	37.2(3)	24.0(2)	-0.7(7)	-1.03(15)	-0.8(6)
C17'	18.4(9)	21.1(9)	19.2(8)	2(3)	0.2(7)	-1(3)
C18'	17.2(9)	24.8(10)	21.6(9)	-2(3)	-0.9(7)	-2(3)
C19'	22.0(9)	30.4(10)	19.2(9)	-1(3)	1.9(7)	-1(3)
C20'	31.7(10)	26.7(11)	19.0(9)	-5(3)	-1.1(8)	0(3)
C21'	23.8(9)	26.7(10)	21.7(9)	1(3)	-6.6(7)	3(3)
C22'	17.9(8)	21.4(9)	21.8(9)	-2(3)	0.1(7)	-1(3

Table 4 : Bond Lengths for **3.8**

Atom	**Atom**	**Length/Å**	**Atom**	**Atom**	**Length/Å**
Cl1	C22	1.7236	C11	C12	1.542(8)
O1	C2	1.3624(19)	C11	C13	1.511(9)
O2	C15	1.3605(19)	C11	C14	1.528(3)
O2	C16	1.3727(19)	C16	C17	1.4837(18)
N1	N2	1.4009(18)	C16	C17’	1.540(6)
N1	C15	1.300(2)	C17	C18	1.3900
N2	C16	1.294(2)	C17	C22	1.3900
C1	C2	1.400(2)	C18	C19	1.3900
C1	C6	1.399(2)	C19	C20	1.3900
C1	C15	1.447(2)	C20	C21	1.3900
C2	C3	1.407(2)	C21	C22	1.3900
C3	C4	1.401(2)	Cl1’	C22’	1.706(7)
C3	C7	1.580(2)	C17’	C18’	1.3900
C4	C5	1.402(2)	C17’	C22’	1.3900
C5	C6	1.382(2)	C18’	C19’	1.3900
C5	C11	1.532(2)	C19’	C20’	1.3900
C7	C8	1.533(7)	C20’	C21’	1.3900
C7	C9	1.508(2)	C21’	C22’	1.3900
C7	C10	1.495(8)			

Table 5 : Bond Angles for **3.8**

Atom	**Atom**	**Atom**	**Angle/°**	**Atom**	**Atom**	**Atom**	**Angle/°**
C15	O2	C16	102.77(12)	O2	C15	C1	120.36(14)
C15	N1	N2	106.97(13)	N1	C15	O2	111.86(14)
C16	N2	N1	105.93(13)	N1	C15	C1	127.77(15)
C2	C1	C6	120.67(15)	O2	C16	C17	114.73(13)
C2	C1	C15	119.34(15)	O2	C16	C17'	136.3(4)
C6	C1	C15	119.99(15)	N2	C16	O2	112.46(14)
O1	C2	C1	121.10(14)	N2	C16	C17	132.80(15)
O1	C2	C3	118.66(15)	N2	C16	C17'	111.3(4)
C1	C2	C3	120.23(15)	C18	C17	C16	118.05(10)
C2	C3	C7	121.53(14)	C18	C17	C22	120.0
C4	C3	C2	116.64(15)	C22	C17	C16	121.95(10)

C4	C3	C7	121.83(14)	C17	C18	C19	120.0
C3	C4	C5	124.41(15)	C18	C19	C20	120.0
C4	C5	C11	123.31(15)	C21	C20	C19	120.0
C6	C5	C4	116.98(15)	C20	C21	C22	120.0
C6	C5	C11	119.71(15)	C17	C22	Cl1	123.04(7)
C5	C6	C1	121.06(16)	C21	C22	Cl1	116.96(7)
C8	C7	C3	108.4(5)	C21	C22	C17	120.0
C9	C7	C3	111.09(14)	C18'	C17'	C16	121.7(6)
C9	C7	C8	110.7(5)	C18'	C17'	C22'	120.0
C10	C7	C3	106.6(5)	C22'	C17'	C16	118.3(6)
C10	C7	C8	112.07(16)	C19'	C18'	C17'	120.0
C10	C7	C9	107.8(5)	C18'	C19'	C20'	120.0
C5	C11	C12	109.3(4)	C19'	C20'	C21'	120.0
C13	C11	C5	110.0(4)	C22'	C21'	C20'	120.0
C13	C11	C12	109.00(17)	C17'	C22'	Cl1'	121.4(6)
C13	C11	C14	108.6(6)	C21'	C22'	Cl1'	118.3(6)
C14	C11	C5	112.30(14)	C21'	C22'	C17'	120.0
C14	C11	C12	107.5(6)				

Table 6 : Hydrogen Bonds for**3.8**

D	H	A	d(D-H)/Å	d(H-A)/Å	d(D-A)/Å	D-H-A/°
O1	H1	N1	0.84	1.91	2.645(2)	145

Table 7 : Torsion Angles for **3.8**

A	B	C	D	Angle/°	A	B	C	D	Angle/°
O1	C2	C3	C4	-179.9(6)	C6	C5	C11	C14	-179.9(8)
O1	C2	C3	C7	-0.7(10)	C7	C3	C4	C5	-178.5(6)
O2	C16	C17	C18	-0.2(7)	C11	C5	C6	C1	179.9(6)
O2	C16	C17	C22	-179.8(4)	C15	O2	C16	N2	-0.2(7)
O2	C16	C17'	C18'	174.4(10)	C15	O2	C16	C17	-179.4(6)
O2	C16	C17'	C22'	-7(3)	C15	O2	C16	C17'	-179.6(17)
N1	N2	C16	O2	0.7(7)	C15	N1	N2	C16	-0.9(7)
N1	N2	C16	C17	179.7(7)	C15	C1	C2	O1	-0.8(10)
N1	N2	C16	C17'	-179.7(12)	C15	C1	C2	C3	179.6(6)
N2	N1	C15	O2	0.9(7)	C15	C1	C6	C5	-179.3(6)
N2	N1	C15	C1	-180.0(7)	C16	O2	C15	N1	-0.5(7)
N2	C16	C17	C18	-179.3(6)	C16	O2	C15	C1	-179.7(6)
N2	C16	C17	C22	1.1(10)	C16	C17	C18	C19	-179.7(5)
N2	C16	C17'	C18'	-5.1(18)	C16	C17	C22	Cl1	-0.2(5)
N2	C16	C17'	C22'	173.6(11)	C16	C17	C22	C21	179.6(6)
C1	C2	C3	C4	-0.3(10)	C16	C17'	C18'	C19'	179(2)
C1	C2	C3	C7	178.9(7)	C16	C17'	C22'	Cl1'	7.1(18)
C2	C1	C6	C5	0.5(10)	C16	C17'	C22'	C21'	-179(2)
C2	C1	C15	O2	179.8(6)	C17	C16	C17'	C18'	174(4)
C2	C1	C15	N1	0.8(11)	C17	C16	C17'	C22'	-7.5(18)
C2	C3	C4	C5	0.7(12)	C17	C18	C19	C20	0.0
C2	C3	C7	C8	-58.0(8)	C18	C17	C22	Cl1	-179.8(4)
C2	C3	C7	C9	-180.0(6)	C18	C17	C22	C21	0.0
C2	C3	C7	C10	62.8(8)	C18	C19	C20	C21	0.0
C3	C4	C5	C6	-0.4(12)	C19	C20	C21	C22	0.0

C3	C4	C5	C11	179.5(6)	C20	C21	C22	Cl1	179.8(4)
C4	C3	C7	C8	121.1(6)	C20	C21	C22	C17	0.0
C4	C3	C7	C9	-0.8(10)	C22	C17	C18	C19	0.0
C4	C3	C7	C10	-118.0(6)	C17'	C16	C17	C18	179(3)
C4	C5	C6	C1	-0.2(10)	C17'	C16	C17	C22	0(3)
C4	C5	C11	C12	119.3(7)	C17'	C18'	C19'	C20'	0.0
C4	C5	C11	C13	-121.0(7)	C18'	C17'	C22'	Cl1'	-174.2(17)
C4	C5	C11	C14	0.1(11)	C18'	C17'	C22'	C21'	0.0
C6	C1	C2	O1	179.4(6)	C18'	C19'	C20'	C21'	0.0
C6	C1	C2	C3	-0.2(10)	C19'	C20'	C21'	C22'	0.0
C6	C1	C15	O2	-0.3(9)	C20'	C21'	C22'	Cl1'	174.3(16)
C6	C1	C15	N1	-179.4(7)	C20'	C21'	C22'	C17'	0.0
C6	C5	C11	C12	-60.7(8)	C22'	C17'	C18'	C19'	0.0
C6	C5	C11	C13	59.0(8)					

Table 8 : Hydrogen Atom Coordinates (Å×10^4) and Isotropic Displacement Parameters (Å^2×10^3) for **3.8**

Atom	***x***	***y***	***z***	**U(eq)**	**Atom**	***x***	***y***	***z***	**U(eq)**
H1	65	4782	7978	36	H13A	5699	8093	6816	64
H4	4734	5000	8813	27	H13B	5183	6876	5914	64
H6	3371	5060	6148	26	H13C	6666	6862	6190	64
H8A	1699	6999	10751	40	H14A	6537	6196	8227	68
H8B	1000	6883	9740	40	H14B	7482	5060	7547	68
H8C	2285	8147	9877	40	H14C	6563	3788	8195	68
H9A	3689	5108	11060	47	H18	1739	5023	3964	25
H9B	4350	6223	10208	47	H19	1679	5023	2322	29
H9C	4312	3816	10246	47	H20	-273	5026	1496	31
H10A	1748	3128	10741	58	H21	-2165	5030	2313	29
H10B	2430	2002	9902	58	H18'	-2547	4709	4539	25
H10C	1103	3119	9710	58	H19'	-3431	4785	3014	29
H12A	5169	3113	5923	59	H20'	-2119	5155	1731	31
H12B	5712	1936	6829	59	H21'	78	5449	1973	29
H12C	6657	3154	6179	59					

Table 1 : Crystal data and structure refinement for **3.16**

Empirical formula	$C_{17}H_{24}N_2O_2S$	m/mm^{-1}	1.751
Formula weight	320.44	F(000)	688.0
Temperature/K	100(2)	Crystal size/mm^3	0.3 × 0.3 × 0.15
Crystal system	monoclinic	2Θ range for data collection	10.66 to 153.12°
Space group	$P2_1/c$	Index ranges	$-7 \le h \le 13$, $-11 \le k \le 12$, $-20 \le l \le 19$
a/Å	10.9518(2)	Reflections collected	6988
b/Å	9.7025(2)	Independent reflections	3509[R(int) = 0.0156]
c/Å	16.5567(3)	Data/restraints/parameters	3509/0/203
α/°	90.00	Goodness-of-fit on F^2	1.023
β/°	104.082(2)	Final R indexes [I>=2σ (I)]	R_1 = 0.0338, wR_2 = 0.0930
γ/°	90.00	Final R indexes [all data]	R_1 = 0.0358, wR_2 = 0.0947
Volume/Å^3	1706.44(6)	Largest diff. peak/hole / e Å^{-3}	0.27/-0.34

Z	4	m/mm^{-1}	1.751
ρ_{calc}mg/mm^3	1.247		

Table 2 : Fractional Atomic Coordinates (×10^4) and Equivalent Isotropic Displacement Parameters (Å^2×10^3) for **3.16**. U_{eq} is defined as 1/3 of of the trace of the orthogonalised U_{IJ} tensor.

Atom	***x***	***y***	***z***	**U(eq)**
S1	9118.2(3)	12617.1(3)	3730.92(19)	19.24(11)
O1	8243.9(8)	6219.5(9)	4411.7(5)	19.16(19)
O2	8343.1(8)	10531.1(9)	4493.4(5)	16.32(18)
N1	8762.4(11)	8667.8(11)	3846.0(7)	20.9(2)
N2	9175(1)	9824.2(11)	3464.0(7)	21.1(2)
C1	7742(1)	8345.7(12)	5010.5(7)	14.9(2)
C2	7759.6(10)	6893.7(12)	4981.0(7)	14.9(2)
C3	7285.2(10)	6122.8(12)	5558.6(7)	14.8(2)
C4	6772.3(10)	6858.3(12)	6122.0(7)	15.3(2)
C5	6716.2(10)	8298.1(12)	6153.4(7)	15.1(2)
C6	7224.5(11)	9027.2(12)	5593.3(7)	15.6(2)
C7	7361.0(11)	4540.2(12)	5580.5(7)	16.9(2)
C8	8747.9(11)	4091.0(13)	5746.1(8)	19.5(3)
C9	6608.5(12)	3928.6(13)	4749.8(8)	22.2(3)
C10	6817.0(13)	3934.8(13)	6273.6(9)	23.1(3)
C11	6138.5(11)	9071.3(13)	6778.6(7)	17.9(2)
C12	5664.0(14)	8090.0(15)	7360.1(9)	27.6(3)
C13	5022.0(12)	9939.6(15)	6296.2(9)	25.1(3)
C14	7131.1(13)	10022.4(14)	7315.6(8)	22.5(3)
C15	8286.6(11)	9124.8(12)	4437.2(7)	16.0(2)
C16	8901.1(11)	10877.9(13)	3865.2(7)	16.2(2)
C17	9900.2(12)	12517.5(13)	2892.8(8)	20.6(3)

Table 3 : Anisotropic Displacement Parameters (Å^2×10^3) for **3.16** The Anisotropic displacement factor exponent takes the form: $-2\pi^2[h^2a^{*2}U_{11}+...+2hka\times b\times U_{12}]$

Atom	**U_{11}**	**U_{22}**	**U_{33}**	**U_{23}**	**U_{13}**	**U_{12}**
S1	24.71(18)	14.82(16)	20.45(17)	1.28(10)	9.86(12)	-0.34(10)
O1	25.0(4)	16.5(4)	18.5(4)	-1.8(3)	10.3(3)	1.3(3)
O2	19.4(4)	14.4(4)	16.5(4)	0.7(3)	7.0(3)	0.1(3)
N1	29.6(6)	15.4(5)	21.2(5)	2.0(4)	13.2(4)	-0.5(4)
N2	28.6(6)	15.7(5)	21.9(5)	2.5(4)	12.3(4)	-0.6(4)
C1	14.9(5)	15.6(6)	14.0(5)	0.8(4)	3.3(4)	0.1(4)
C2	14.2(5)	15.8(6)	14.4(5)	-1.1(4)	3.1(4)	1.5(4)
C3	13.1(5)	14.8(5)	16.0(5)	0.0(4)	2.1(4)	-0.1(4)
C4	14.0(5)	16.2(6)	15.6(5)	0.3(4)	3.4(4)	-0.7(4)
C5	13.5(5)	16.7(6)	14.9(5)	-1.4(4)	2.8(4)	0.1(4)
C6	15.9(5)	13.4(5)	17.1(5)	-0.2(4)	3.0(4)	1.1(4)
C7	17.6(5)	13.6(5)	20.2(6)	-0.4(4)	5.9(4)	0.2(4)
C8	19.7(6)	16.6(6)	22.1(6)	1.6(5)	4.8(5)	3.5(4)
C9	20.1(6)	18.5(6)	27.0(6)	-5.5(5)	3.8(5)	-2.0(5)
C10	27.6(6)	15.1(6)	30.2(7)	2.7(5)	13.9(5)	1.1(5)
C11	20.4(6)	16.9(6)	17.7(5)	-1.5(5)	7.2(5)	0.6(5)
C12	36.8(7)	23.7(7)	29.4(7)	-3.8(5)	21.7(6)	-2.8(6)

C13	21.7(6)	26.5(7)	27.1(6)	-5.9(5)	6.2(5)	6.1(5)
C14	27.3(6)	22.9(6)	17.3(6)	-4.1(5)	5.3(5)	-1.5(5)
C15	16.9(5)	13.5(5)	17.1(5)	1.4(4)	3.0(4)	0.8(4)
C16	16.0(5)	18.9(6)	14.5(5)	2.7(4)	4.9(4)	0.5(4)
C17	21.7(6)	22.6(6)	18.9(6)	1.5(5)	7.6(5)	-3.4(5)

Table 4 : Bond Lengths for **3.16**

Atom	**Atom**	**Length/Å**	**Atom**	**Atom**	**Length/Å**
S1	C16	1.7260(13)	C3	C4	1.3964(16)
S1	C17	1.8019(14)	C3	C7	1.5377(16)
O1	C2	1.3568(14)	C4	C5	1.3998(17)
O2	C15	1.3680(14)	C5	C6	1.3861(16)
O2	C16	1.3703(14)	C5	C11	1.5341(16)
N1	N2	1.4150(15)	C7	C8	1.5393(16)
N1	C15	1.2940(16)	C7	C9	1.5400(17)
N2	C16	1.2936(16)	C7	C10	1.5329(17)
C1	C2	1.4099(17)	C11	C12	1.5320(17)
C1	C6	1.3985(16)	C11	C13	1.5387(17)
C1	C15	1.4504(16)	C11	C14	1.5340(17)
C2	C3	1.4092(16)			

Table 5 : Bond Angles for **3.16**

Atom	**Atom**	**Atom**	**Angle/°**	**Atom**	**Atom**	**Atom**	**Angle/°**
C16	S1	C17	98.80(6)	C3	C7	C8	109.40(10)
C15	O2	C16	102.38(9)	C3	C7	C9	110.46(10)
C15	N1	N2	107.31(10)	C8	C7	C9	109.90(10)
C16	N2	N1	104.95(10)	C10	C7	C3	111.82(10)
C2	C1	C15	119.13(10)	C10	C7	C8	107.73(10)
C6	C1	C2	120.51(11)	C10	C7	C9	107.45(10)
C6	C1	C15	120.36(11)	C5	C11	C13	108.88(10)
O1	C2	C1	121.12(10)	C12	C11	C5	112.26(10)
O1	C2	C3	119.11(11)	C12	C11	C13	108.56(11)
C3	C2	C1	119.76(10)	C12	C11	C14	108.09(10)
C2	C3	C7	121.28(10)	C14	C11	C5	109.56(10)
C4	C3	C2	117.18(11)	C14	C11	C13	109.45(10)
C4	C3	C7	121.52(11)	O2	C15	C1	119.62(10)
C3	C4	C5	124.28(11)	N1	C15	O2	111.92(10)
C4	C5	C11	122.83(10)	N1	C15	C1	128.45(11)
C6	C5	C4	117.13(11)	O2	C16	S1	116.02(9)
C6	C5	C11	120.03(11)	N2	C16	S1	130.55(10)
C5	C6	C1	121.09(11)	N2	C16	O2	113.43(11)

Table 6 : Hydrogen Bonds for**3.16**

D	**H**	**A**	**d(D-H)/Å**	**d(H-A)/Å**	**d(D-A)/Å**	**D-H-A/°**
O1	H1	N1	0.88(2)	1.85(2)	2.665(1)	153(2)

Table 7 : Torsion Angles for **3.16**

A	B	C	D	Angle/°	A	B	C	D	Angle/°
O1	C2	C3	C4	-178.71(10)	C4	C5	C11	C13	-119.23(12)
O1	C2	C3	C7	2.80(16)	C4	C5	C11	C14	121.10(12)
N1	N2	C16	S1	-179.21(10)	C6	C1	C2	O1	179.13(10)
N1	N2	C16	O2	0.43(13)	C6	C1	C2	C3	-1.84(16)
N2	N1	C15	O2	-0.11(13)	C6	C1	C15	O2	2.92(16)
N2	N1	C15	C1	-179.78(11)	C6	C1	C15	N1	-177.44(12)
C1	C2	C3	C4	2.23(15)	C6	C5	C11	C12	-178.28(11)
C1	C2	C3	C7	-176.26(10)	C6	C5	C11	C13	61.50(14)
C2	C1	C6	C5	-0.10(17)	C6	C5	C11	C14	-58.18(14)
C2	C1	C15	O2	-176.08(10)	C7	C3	C4	C5	177.67(10)
C2	C1	C15	N1	3.56(18)	C11	C5	C6	C1	-179.18(10)
C2	C3	C4	C5	-0.82(16)	C15	O2	C16	S1	179.21(8)
C2	C3	C7	C8	59.25(14)	C15	O2	C16	N2	-0.49(13)
C2	C3	C7	C9	-61.86(14)	C15	N1	N2	C16	-0.19(13)
C2	C3	C7	C10	178.52(10)	C15	C1	C2	O1	-1.87(16)
C3	C4	C5	C6	-1.05(16)	C15	C1	C2	C3	177.16(10)
C3	C4	C5	C11	179.65(10)	C15	C1	C6	C5	-179.09(10)
C4	C3	C7	C8	-119.17(11)	C16	O2	C15	N1	0.35(13)
C4	C3	C7	C9	119.72(12)	C16	O2	C15	C1	-179.95(10)
C4	C3	C7	C10	0.10(15)	C17	S1	C16	O2	178.09(9)
C4	C5	C6	C1	1.50(16)	C17	S1	C16	N2	-2.27(13)
C4	C5	C11	C12	1.00(16)					

Table 8 : Hydrogen Atom Coordinates ($Å \times 10^4$) and Isotropic Displacement Parameters ($Å^2 \times 10^3$) for **3.16**

Atom	*x*	*y*	*z*	U(eq)
H1	8490(20)	6860(20)	4108(14)	52(6)
H4	6440	6348	6509	18
H6	7221	10006	5606	19
H8A	9218	4472	6279	29
H8B	9110	4432	5298	29
H8C	8798	3083	5766	29
H9A	6640	2920	4781	33
H9B	6975	4241	4298	33
H9C	5731	4235	4642	33
H10A	7328	4235	6816	35
H10B	6827	2926	6243	35
H10C	5949	4256	6204	35
H12A	4945	7563	7039	41
H12B	5403	8624	7792	41
H12C	6341	7455	7622	41
H13A	4375	9330	5968	38
H13B	5313	10577	5923	38
H13C	4667	10465	6690	38
H14A	7372	10732	6963	34
H14B	7874	9480	7584	34

H14C	6781	10462	7742	34
H17A	10023	13449	2698	31
H17B	9383	11981	2433	31
H17C	10720	12068	3092	31

Table 1 : Crystal data and structure refinement for**3.26**

Empirical formula	$C_{23}H_{29}N_3O_2S$
Formula weight	411.55
Temperature/K	100(2)
Crystal system	monoclinic
Space group	$P2_1/c$
a/Å	16.6446(3)
b/Å	6.3602(1)
c/Å	20.7088(3)
α/°	90.00
β/°	92.931(2)
γ/°	90.00
Volume/Å^3	2189.43(6)
Z	4
ρ_{calc}mg/mm^3	1.249
m/mm^{-1}	1.495
F(000)	880.0
Crystal size/mm^3	0.4 × 0.3 × 0.1
2Θ range for data collection	9.84 to 153.62°
Index ranges	$-18 \le h \le 20$, $-7 \le k \le 6$, $-25 \le l \le 25$
Reflections collected	8793
Independent reflections	4489[R(int) = 0.0182]
Data/restraints/parameters	4489/0/270
Goodness-of-fit on F^2	1.019
Final R indexes [I>=2σ (I)]	R_1 = 0.0344, wR_2 = 0.0922
Final R indexes [all data]	R_1 = 0.0375, wR_2 = 0.0950
Largest diff. peak/hole / e Å^{-3}	0.32/-0.42

Table 2 : Fractional Atomic Coordinates (×10^4) and Equivalent Isotropic Displacement Parameters (Å^2×10^3) for **3.26**. U_{eq} is defined as 1/3 of of the trace of the orthogonalised U_{IJ} tensor.

Atom	***x***	***y***	***z***	**U(eq)**
S1	5167.15(18)	5669.4(5)	3214.12(13)	15.84(10)
O1	2649.7(6)	2498.5(16)	1081.2(4)	21.3(2)
O2	3805.6(6)	-591.9(15)	5223.5(4)	22.8(2)
N1	4084.8(7)	5992.3(18)	2191.7(5)	17.1(2)
N2	3388.1(7)	5118.3(18)	1928.9(5)	17.7(2)
N3	3722.8(6)	3739.1(16)	2885.7(5)	14.5(2)
C1	2514.7(8)	2239(2)	2235.7(6)	15.9(2)
C2	2289.7(8)	1647(2)	1597.5(6)	16.2(3)
C3	1694.0(8)	100(2)	1476.2(6)	16.8(3)
C4	1340.7(8)	-768(2)	2009.5(6)	17.1(3)
C5	1535.3(8)	-178(2)	2651.8(6)	16.3(3)

C6	2121.3(8)	1339(2)	2753.6(6)	16.2(2)
C7	1457.2(8)	-635(2)	784.7(6)	19.6(3)
C8	2188.3(9)	-1679(2)	493.1(6)	23.7(3)
C9	1153.8(9)	1217(3)	359.4(6)	26.4(3)
C10	782.3(9)	-2280(3)	776.6(7)	28.6(3)
C11	1130.1(8)	-1272(2)	3208.6(6)	18.2(3)
C12	210.6(8)	-1216(2)	3098.2(6)	22.9(3)
C13	1346.6(10)	-223(3)	3860.2(6)	28.7(3)
C14	1411(1)	-3572(2)	3235.9(7)	29.4(3)
C15	3180.0(8)	3716(2)	2353.8(6)	15.8(2)
C16	4315.9(8)	5165(2)	2764.8(6)	15.3(2)
C17	3722.2(8)	2525.6(19)	3475.0(5)	14.8(2)
C18	3396.4(8)	3415(2)	4017.0(6)	16.7(3)
C19	3413.0(8)	2299(2)	4591.3(6)	18.3(3)
C20	3774.1(8)	317(2)	4627.2(6)	16.7(3)
C21	4085.9(8)	-582(2)	4080.2(6)	17.7(3)
C22	4055.6(8)	541(2)	3501.0(6)	17.1(3)
C23	4226.6(9)	-2536(2)	5294.2(7)	25.9(3)

Table 3 : Anisotropic Displacement Parameters ($Å^2×10^3$) for **3.26**. The Anisotropic displacement factor exponent takes the form: $-2\pi^2[h^2a^{*2}U_{11}+...+2hka×b×U_{12}]$

Atom	**U_{11}**	**U_{22}**	**U_{33}**	**U_{23}**	**U_{13}**	**U_{12}**
S1	19.00(17)	13.68(16)	15.13(15)	-0.41(10)	3.70(11)	-0.22(11)
O1	28.0(5)	23.8(5)	12.4(4)	1.3(4)	5.5(4)	-8.1(4)
O2	33.1(5)	21.6(5)	14.0(4)	4.7(3)	3.5(4)	-1.6(4)
N1	21.1(5)	15.3(5)	15.3(5)	2.3(4)	3.1(4)	-3.4(4)
N2	20.8(5)	16.8(5)	15.6(5)	1.2(4)	2.4(4)	-3.1(4)
N3	18.6(5)	13.0(5)	12.2(5)	0.6(4)	4.6(4)	-0.5(4)
C1	18.1(6)	14.8(6)	15.1(6)	1.1(4)	4.0(4)	-0.4(5)
C2	19.3(6)	16.5(6)	13.4(5)	2.2(4)	6.1(4)	1.5(5)
C3	18.1(6)	18.3(6)	14.1(6)	-0.4(5)	3.3(5)	1.8(5)
C4	17.8(6)	17.2(6)	16.5(6)	0.1(5)	3.6(5)	-0.9(5)
C5	18.3(6)	16.6(6)	14.5(5)	2.2(5)	5.1(5)	2.2(5)
C6	19.1(6)	17.0(6)	12.9(5)	1.1(4)	4.5(4)	1.0(5)
C7	21.1(6)	23.7(7)	14.3(6)	-1.7(5)	4.0(5)	-3.2(5)
C8	27.8(7)	23.8(7)	20.2(6)	-4.7(5)	8.3(5)	-2.4(6)
C9	27.7(7)	34.1(8)	17.1(6)	1.3(6)	0.0(5)	2.9(6)
C10	28.7(8)	39.2(9)	18.1(6)	-6.1(6)	4.2(5)	-13.4(7)
C11	20.0(6)	19.5(6)	15.6(6)	3.6(5)	5.3(5)	-1.3(5)
C12	20.6(7)	27.7(7)	21.3(6)	1.4(5)	8.3(5)	-1.8(6)
C13	34.8(8)	37.0(8)	14.7(6)	3.0(6)	6.4(5)	-11.9(7)
C14	32.7(8)	24.8(8)	31.5(7)	11.1(6)	9.1(6)	4.7(6)
C15	19.5(6)	14.9(6)	13.4(5)	-0.3(4)	4.9(4)	0.6(5)
C16	20.4(6)	11.6(6)	14.5(5)	-1.0(4)	6.6(5)	1.3(5)
C17	18.5(6)	14.6(6)	11.5(5)	1.7(4)	3.9(4)	-2.2(5)
C18	19.6(6)	14.5(6)	16.3(6)	-0.8(5)	4.6(4)	1.2(5)
C19	22.7(6)	19.5(6)	13.3(5)	-2.0(5)	6.3(5)	-0.2(5)
C20	18.4(6)	17.5(6)	14.2(6)	2.7(5)	2.6(4)	-4.3(5)
C21	21.3(6)	12.9(6)	19.3(6)	1.8(5)	4.7(5)	0.6(5)
C22	21.2(6)	15.1(6)	15.7(6)	-1.1(4)	7.5(5)	-0.6(5)

C23	32.1(8)	20.7(7)	24.3(6)	8.4(5)	-4.0(6)	-3.1(6)

Table 4 : Bond Lengths for **3.26**

Atom	Atom	Length/Å	Atom	Atom	Length/Å
S1	C16	1.6856(13)	C4	C5	1.4038(17)
O1	C2	1.3643(14)	C5	C6	1.3804(18)
O2	C20	1.3619(14)	C5	C11	1.5323(16)
O2	C23	1.4254(17)	C7	C8	1.5367(18)
N1	N2	1.3731(15)	C7	C9	1.5403(19)
N1	C16	1.3368(16)	C7	C10	1.5346(19)
N2	C15	1.3116(16)	C11	C12	1.5364(18)
N3	C15	1.3885(16)	C11	C13	1.5315(18)
N3	C16	1.3729(16)	C11	C14	1.5362(19)
N3	C17	1.4441(15)	C17	C18	1.3914(16)
C1	C2	1.4065(17)	C17	C22	1.3784(18)
C1	C6	1.4068(16)	C18	C19	1.3837(17)
C1	C15	1.4632(18)	C19	C20	1.3973(19)
C2	C3	1.4099(18)	C20	C21	1.3926(17)
C3	C4	1.3918(17)	C21	C22	1.3949(17)
C3	C7	1.5387(17)			

Table 5 : Bond Angles for **3.26**

Atom	Atom	Atom	Angle/°	Atom	Atom	Atom	Angle/°
C20	O2	C23	117.22(10)	C10	C7	C8	107.15(11)
C16	N1	N2	113.04(11)	C10	C7	C9	107.27(12)
C15	N2	N1	104.83(10)	C5	C11	C12	110.54(10)
C15	N3	C17	129.52(10)	C5	C11	C14	108.37(11)
C16	N3	C15	107.88(10)	C13	C11	C5	111.88(11)
C16	N3	C17	122.60(10)	C13	C11	C12	107.98(11)
C2	C1	C6	119.68(12)	C13	C11	C14	108.96(12)
C2	C1	C15	119.47(11)	C14	C11	C12	109.06(12)
C6	C1	C15	120.79(11)	N2	C15	N3	109.98(11)
O1	C2	C1	121.56(12)	N2	C15	C1	123.22(11)
O1	C2	C3	118.06(11)	N3	C15	C1	126.54(11)
C1	C2	C3	120.36(11)	N1	C16	S1	127.65(10)
C2	C3	C7	121.48(11)	N1	C16	N3	104.18(11)
C4	C3	C2	117.22(11)	N3	C16	S1	128.09(9)
C4	C3	C7	121.29(12)	C18	C17	N3	118.80(11)
C3	C4	C5	124.01(12)	C22	C17	N3	120.31(10)
C4	C5	C11	120.17(12)	C22	C17	C18	120.88(11)
C6	C5	C4	117.29(11)	C19	C18	C17	119.57(12)
C6	C5	C11	122.48(11)	C18	C19	C20	119.86(11)
C5	C6	C1	121.40(11)	O2	C20	C19	115.32(11)
C3	C7	C9	111.14(11)	O2	C20	C21	124.37(12)
C8	C7	C3	109.07(11)	C21	C20	C19	120.29(11)
C8	C7	C9	110.42(11)	C20	C21	C22	119.37(12)
C10	C7	C3	111.71(10)	C17	C22	C21	119.96(11)

Table 6: Hydrogen Bonds for **3.26**

D	H	A	d(D-H)/Å	d(H-A)/Å	d(D-A)/Å	D-H-A/°
O1	H1	N2	0.88(2)	1.91(2)	2.674(2)	145(2)
N1	H2	S1[1]	0.93(2)	2.45(2)	3.349(1)	164(2)

[1]1-X,1/2+Y,1/2-Z

Table 7 : Torsion Angles for **3.26**

A	B	C	D	Angle/°	A	B	C	D	Angle/°
O1	C2	C3	C4	179.24(11)	C6	C5	C11	C12	130.10(13)
O1	C2	C3	C7	0.60(19)	C6	C5	C11	C13	9.72(18)
O2	C20	C21	C22	-176.75(12)	C6	C5	C11	C14	-110.43(14)
N1	N2	C15	N3	1.61(13)	C7	C3	C4	C5	179.46(12)
N1	N2	C15	C1	-172.93(11)	C11	C5	C6	C1	176.56(12)
N2	N1	C16	S1	174.92(9)	C15	N3	C16	S1	-174.04(9)
N2	N1	C16	N3	-2.07(14)	C15	N3	C16	N1	2.94(13)
N3	C17	C18	C19	-178.03(11)	C15	N3	C17	C18	-96.20(16)
N3	C17	C22	C21	177.06(12)	C15	N3	C17	C22	85.23(16)
C1	C2	C3	C4	0.83(19)	C15	C1	C2	O1	-3.42(19)
C1	C2	C3	C7	-177.81(12)	C15	C1	C2	C3	174.93(12)
C2	C1	C6	C5	2.3(2)	C15	C1	C6	C5	-174.92(12)
C2	C1	C15	N2	26.64(19)	C16	N1	N2	C15	0.32(14)
C2	C1	C15	N3	-146.97(12)	C16	N3	C15	N2	-2.95(14)
C2	C3	C4	C5	0.8(2)	C16	N3	C15	C1	171.37(12)
C2	C3	C7	C8	63.25(16)	C16	N3	C17	C18	84.76(15)
C2	C3	C7	C9	-58.73(16)	C16	N3	C17	C22	-93.81(15)
C2	C3	C7	C10	-178.49(12)	C17	N3	C15	N2	177.90(11)
C3	C4	C5	C6	-0.9(2)	C17	N3	C15	C1	-7.8(2)
C3	C4	C5	C11	-178.24(12)	C17	N3	C16	S1	5.19(17)
C4	C3	C7	C8	-115.34(13)	C17	N3	C16	N1	-177.83(10)
C4	C3	C7	C9	122.69(13)	C17	C18	C19	C20	1.6(2)
C4	C3	C7	C10	2.92(18)	C18	C17	C22	C21	-1.5(2)
C4	C5	C6	C1	-0.75(19)	C18	C19	C20	O2	175.91(12)
C4	C5	C11	C12	-52.66(16)	C18	C19	C20	C21	-2.84(19)
C4	C5	C11	C13	-173.04(12)	C19	C20	C21	C22	1.9(2)
C4	C5	C11	C14	66.80(16)	C20	C21	C22	C17	0.3(2)
C6	C1	C2	O1	179.28(11)	C22	C17	C18	C19	0.5(2)
C6	C1	C2	C3	-2.37(19)	C23	O2	C20	C19	-175.03(12)
C6	C1	C15	N2	-156.09(12)	C23	O2	C20	C21	3.67(19)
C6	C1	C15	N3	30.30(19)					

Table 8 : Hydrogen Atom Coordinates (Å×10^4) and Isotropic Displacement Parameters (Å^2×10^3) for**3.26**

Atom	x	y	z	U(eq)	Atom	x	y	z	U(eq)
H4	944	-1825	1934	20	H13B	1090	-990	4205	43
H6	2262	1784	3182	19	H13C	1156	1235	3851	43
H8A	2376	-2848	770	35	H14A	1997	-3619	3308	44
H8B	2621	-643	463	35	H14B	1256	-4269	2826	44

H8C	2034	-2212	60	35	H14C	1159	-4296	3591	44
H9A	1568	2312	359	40	H18	3164	4778	3993	20
H9B	663	1795	532	40	H19	3179	2881	4960	22
H9C	1037	723	-84	40	H21	4317	-1948	4101	21
H10A	954	-3481	1046	43	H22	4265	-60	3125	21
H10B	663	-2755	332	43	H23A	4219	-3008	5744	39
H10C	299	-1654	947	43	H23B	4785	-2344	5176	39
H12A	28	249	3076	34	H23C	3965	-3594	5011	39
H12B	-39	-1928	3457	34	H1	2938(13)	3590(30)	1204(10)	42(6)
H12C	56	-1931	2692	34	H2	4315(11)	7150(30)	2002(9)	32(5)
H13A	1932	-244	3942	43					